Main Group and Transition Metal Complexes Supported by Carbon, Sulfur, and Selenium Donor Ligands

Patrick J. Quinlivan

Submitted in partial fulfillment of the
requirements for the degree of
Doctor of Philosophy
in the Graduate School of Arts and Sciences

Columbia University
2018

© 2018

Patrick Quinlivan

All rights reserved

ABSTRACT

Main Group and Transition Metal Complexes Supported by Carbon, Sulfur, and Selenium Donor Ligands

Patrick J. Quinlivan

This thesis explores the synthesis, characterization, and reactivity of main group and transition metal complexes that feature ligands with carbon, sulfur, and selenium donor atoms. Specifically, the carbon donor ligands explored include the carbodiphosphorane, $(Ph_3P)_2C$, and the analytical reagent, nitron, which behaves like an *N*-heterocyclic carbene in solution. The sulfur ligands include the amino acids cysteine and glutathione, and the tripodal *tris*(2-mercapto-1-t-butylimidazolyl)hydroborato ligand, of which the latter provides an $[S_3]$ coordination environment. Finally, the selenium donor ligands explored comprise the phenylselenolate, $[PhSe]^-$, and the selenobenzimidazole, $H(sebenzim^{Me})$.

Chapter 1 investigates the chemistry of two-coordinate mercury alkyl complexes supported by sulfur and selenium ligands. The first part of Chapter 1 examines the structure of the amino acid complexes, (Cys)HgMe and (GS)HgMe, which indicate that both complexes possess linear geometries. Additionally, ^1H NMR studies confirm the labile nature of the cysteinato ligand in (Cys)HgMe. More specifically, in the presence of excess cysteine, exchange is observed, a result that is of relevance to mercury toxicity and detoxification. The second part of Chapter 1 examines the exchange reactions of the phenylselenolate mercury alkyl complexes, PhSeHgR (R = Me, Et), as well as their propensity to undergo protolytic Hg–C bond cleavage. The results from these

experiments indicate that coordination by selenium promotes protolytic cleavage of Hg–C bonds more rapidly than compared to the sulfur analogues.

Expanding the metal centers to include the lighter group 12 metals, Chapter 2 investigates ligand exchange between zinc, cadmium, and mercury in a sulfur-rich coordination environment as provided by the [S_3] *tris*(2-mercapto-1-t-butylimidazolyl)hydroborato ligand. Similar to the Schlenk equilibrium, alkyl group exchange between the same metal center is observed as demonstrated by the formation of [Tm^{Bu^t}]MMe *via* treatment of [Tm^{Bu^t}]$_2$M with Me_2M (M = Zn, Cd). Additionally, alkyl group exchange between different metals centers is also possible. For example, a mixture of [Tm^{Bu^t}]ZnMe and Me_2Cd form an equilibrium mixture with [Tm^{Bu^t}]CdMe and Me_2Zn. Furthermore, transfer of the [Tm^{Bu^t}] ligand between the metal centers is possible too. This is demonstrated by the transfer of [Tm^{Bu^t}] from mercury to zinc in the methyl system, [Tm^{Bu^t}]HgMe/Me_2Zn. Additionally, transfer of [Tm^{Bu^t}] from zinc to mercury is also observed upon treatment of [Tm^{Bu^t}]$_2$Zn with HgI_2 to afford [Tm^{Bu^t}]HgI and [Tm^{Bu^t}]ZnI, thereby indicating that the nature of the co-ligand has a profound effect on the thermodynamics of ligand exchange.

Chapter 3 explores the coordination chemistry of the selenium donor ligand, H(sebenzim^{Me}). H(sebenzim^{Me}) is able to coordinate metal centers through the selenium atom in a dative fashion, and, depending upon the metal center, up to four H(sebenzim^{Me}) ligands can coordinate the same metal. Additionally, H(sebenzim^{Me}) can be deprotonated to form [sebenzim^{Me}]$^-$, allowing for the potential of an LX coordination mode, which results in bridging complexes for the metal compounds investigated. In regards to the metal centers investigated in Chapter 3, H(sebenzim^{Me}) has been demonstrated to be an effective ligand for Pd, Ni, Zn and Cd.

Chapter 4 investigates the various structural polymorphs of the carbodiphosphorane, $(Ph_3P)_2C$. More specifically, previous crystal structures of $(Ph_3P)_2C$ have demonstrated that the P–C–P bond angle is highly bent. This is consistent with simple VSEPR theory, which predicts a bent geometry for compounds possessing a coordination number of two and two lone pairs of electrons. However, Chapter 4 details the characterization of a new *linear* form of $(Ph_3P)_2C$. DFT calculations indicate that the energy required to bend the P–C–P bonds of $(Ph_3P)_2C$ over the range of 130°-180° is less than 1.0 kcal mol^{-1}. Analysis of the Natural Localized Molecular Orbitals (NLMOs) indicates that upon bending of the P–C–P bond angle, the σ-type lone pair NLMO on the central carbon atom is stabilized, while the two P–C bonding orbitals NLMOs are destabilized. The differential behavior of the lone-pair and bonding orbitals upon bending is one component that provides a simple rationalization for the flexibility of $(Ph_3P)_2C$.

In view of the fact that carbodiphosphoranes possess two lone pairs of electrons on the central carbon atom, $(Ph_3P)_2C$ is an effective ligand for a variety of metals and nonmetals. Chapter 5 investigates the reactivity of $(Ph_3P)_2C$ towards the main group alkyl metal complexes, Me_3E (E = Al, Ga), Me_2M (M = Mg, Zn, Cd), and MeHgI, as well as $Mg[N(TMS)_2]_2$. Additionally, the reactivity of $(Ph_3P)_2C$ towards transition metal complexes was also investigated. $(Ph_3P)_2C$ is capable of coordinating in several different ways, a couple of which include forming a Lewis acid/base adduct, and ortho metalation of one of the phenyl groups.

Lastly, Chapter 6 expands the coordination chemistry of nitron. Nitron, which is used as a quantitative analytical reagent, has recently been shown to behave like an NHC in solution. This is attributed to the presence of the carbenic tautomer of nitron when

placed in solution. Thus, nitron effectively coordinates metal centers through the central carbon atom. Chapter 6 outlines (*i*) the synthesis and structural characterization of nickel, palladium, and iridium complexes that feature nitron as a ligand, and (*ii*) the ability of the corresponding iridium complexes to serve as catalysts for the dehydrogenation of formic acid and the hydrosilylation of aldehydes.

TABLE OF CONTENTS

LIST OF FIGURES AND SCHEMES

Chapter 1.

Chapter 2.

Chapter 3.

Chapter 5.

Chapter 6.

LIST OF TABLES

Chapter 1.

Chapter 3.

Chapter 4.

Chapter 5.

Chapter 6.

ACKNOWLEDGEMENTS

The past 5 years have been a wonderful NY adventure for this Irish southern boy who was actually born in the Bronx. I have had the pleasure of pursing my PhD in chemistry at Columbia University where I have also had the opportunity to take classes and conduct research in one of the most diverse, multidisciplinary educational environments in the entire world.

The number of individuals who have helped me along this journey are almost too many to count, however I cannot go any further without first thanking my mentor, boss and PI, Gerard Parkin. For anyone who personally knows Ged, he is quite the character. I'm pretty sure 70-80% of everything that comes out of his mouth is sarcastic, which can be frustrating at times, however his comical nature provides for a pleasant laboratory environment to conduct research. Ged is also a very accomplished magician himself, and I was often times a test subject for him when he was testing out a new trick…where else can you get that at work?

The skills I have learned while working in the Parkin lab are absolutely invaluable. After 5 years, I have been able to further my knowledge of inorganic, organometallic, and organic synthesis, have learned the fine and intricate details of NMR spectroscopy, and have become an experienced and accomplished crystallographer. But perhaps, the most important skill I have learned while working for Ged is to how to really think like a scientist. Ged is one of the most talented scientists I have ever met. His inquisitive nature makes him one of the top researchers in the field of inorganic chemistry, and my hope is that I take that I have learned and can live up to what he has taught me.

My five years of research would not be possible without my committee members, Jack Norton and Jonathon Owen. I am thankful for all the conversations we have had about my research and I am grateful for your 24- hour open door policy. Thank you for your differing perspectives and all the knowledge that you have passed down to me. I would also like to recognize the 4th and 5th members of my thesis committee, Xavier Roy and Mike Campbell. I hope you enjoy reading all 400 plus pages of my thesis I look forward to our discussion, although I am not sure outside of this committee, anyone else will even look at this manuscript cover to cover, so please enjoy your time with my scientific work of art.

I would also like to personally thank my undergraduate research advisor at UNCC, Daniel Rabinovich. Daniel was the first person who helped me realize the passion I had for inorganic chemistry, and through his encouragement and mentorship, steered me to attend graduate school at Columbia University. I want to thank you for looking out for me during my years at UNCC, and your continued scientific support! I cannot forget to thank my other UNCC mentor who also helped pave my career path in inorganic chemistry, Dr. Richard Jew. Thank you for all your encouragement during my undergraduate career.

Over the course of my graduate career, I have had the pleasure of working with several talented lab members. In this regard, I would like to thank a few of the former members of the Parkin lab. First and foremost a special thank you to Dr. Josh Palmer, for taking time out of your busy schedule to help train me when I was a first year. I truly learned a lot from you, and miss the energy you brought to the lab. Also, a huge thank you to Dr. Ava Kreider-Mueller for your training during my first year as well. It was a pleasure to take over and finish up some of your projects, and I am extremely honored to be co-

authors with you on several scientific articles. Also, a special shout out to Dr. Yi Rong, Dr. Ahmed Al-Harbi, Dr. Neena Chakrabarti, and Dr. Ashley Zuzek whom I had the pleasure of overlapping time with in the Parkin lab. I enjoyed spending time with each one of you in the lab day in and day out.

Next, I would like to thank both Dr. Serge Ruccolo and Dr. Michelle Neary, who defended two years ahead of me. Both of you are brilliant scientists and I learned so much about chemical synthesis and crystallography from both of you. But above all, both of you are great friends of mine, and with any hope, we will still be around the NYC area in the near future!

As for the current members of the Parkin lab as I finish up, Mike Rauch and I have overlapped the longest together. Mike is one of the most talented chemists I know. He is super-efficient with his lab time and has performed some incredible chemical transformations during my time there. But more than that, we have become incredible friends. Hanging out with you at your summer BBQs, nights out, and St. Patrick's days are some of my fondest memories of graduate school. I knew from the minute I met you at visit weekend you would fit right into the Parkin lab. Next is Dave Sambade. Dave is also a very talented chemist who has pursued very interesting projects during my time in the lab and I am excited to read your future papers. I also learned a lot from you Dave, as you were the first one I turned to when something broke…the contraption we made to evacuate the cold-head was a thing of beauty. Both of you have been amazing friends and I have appreciated

I would also like to wish the two youngest members of the Parkin lab, Matthew Hammond and Daniel Shlian the best of luck with their PhD research. I have enjoyed

getting to know both of you and I know you both have the makings to be successful graduate students and good luck with your projects in the future (Also Matthew, work on your handwriting! And Danny, focus on the carbodiphosphoranes!).

Additionally, during my graduate research work I had the opportunity to work with several talented visiting students, undergraduates, and high school students. It was great getting to work with each of you, and I want to personally thank Mahnaz, Walid, Iffat, Joan, Natalie, and Melanie.

I would like to acknowledge the U.S. National Science Foundation, the U.S. Department of Energy (Office of Basic Energy Sciences) and the U.S. National Institutes of Health for supporting the research described in this thesis.

I would also like to thank all of the support staff at Columbia. Thank you Socky and Daisy for always having a smile on your faces when I walked into the main office and helping me out with things I needed all throughout my PhD! Thank you to Dani and Alison for all your logistical help and Carlos and Vivian for all your help with reimbursements in the financial office. Also, thank you to the guys in the stock room, Chris and Danny, for everything you do, and to John Decatur and Michael Appel for all your help in the NMR rooms. Lastly, thank you to Luis Avila, Tudor Spataru, and Joseph Ulichny for helping with various things throughout the years when I was teaching.

During my time at Columbia, I have also had the pleasure of being a graduate teaching assistant for general chemistry, organometallics, NMR spectroscopy, and X-ray crystallography classes. I TA'ed at least one class every fall and spring with the

exception of my last semester. I thoroughly enjoyed teaching everyone that passed through one of my recitation sections and I hope I was able to get you excited about some aspect of chemistry! Also, thanks again to Ged for running one of the most fantastic introductory chemistry classes I have ever seen. I really enjoyed setting up and helping you perform all those demos we did in class and I hope I lived up to the VERY prestigious title of Head TA for the last 3 years of my PhD.

At Columbia, not only do we work hard, but we also know how to play hard too. I had the pleasure of serving as a Happy Hour chair with Leslie Hamachi my second year and had so much fun planning all of those events! I hope everyone enjoyed them as much as I did! Our Wintershows were so much fun every year (from what I remember), and our BBQs, visit weekends, and STAT weeks were all awesome!

And perhaps most importantly, I have made life-long friends at Columbia. I want to personally thank everyone in my year defending with me. It has been an honor to be at Columbia with all of you and wish everyone good luck with your future endeavors! Also, thank you to everyone I have overlapped with in years above and below me. There are too many people for me to thanks personally, but you know who you are.

Special shout-out to all the Spicy Boyz out there too! I have had the pleasure of being your fearless softball coach the past 3 years. We have played some of the most amazing games and have had some incredible come from behind wins, and have made the playoffs every year! I wish the team the best of luck and I hope you keep up the tradition for years to come.

I also need to thank the Panther crew too! Spending Sundays at the Turkeys Nest in Brooklyn was one of my favorite past times, thank you guys for all the memories!

As most people know, when I am not doing research, I am in the dance studio teaching Irish dance. Since moving up to New York, I have had the pleasure of joining the teaching staff at the Lynn O'Grady Quinlan Academy of Irish dance. We have enjoyed much success at regional, national, and international level over the past 3 years, highlighted by our schools first World Champion, numerous top 5s and 10s at Nationals, and amazing Oireachtaisí. Additionally, our ceili program is just starting to take off and I am super excited to see what the future holds. I have enjoyed every moment I had teaching all the kids on the weekends, as it provided me with a nice break from lab. Personally, I want to thank Mary Lynn and her family for all their support and help in Tarrytown over the last 3 years. Mary Lynn, all of your kids are amazing in their own way, and they are a please to teach.

Also, I want to personally thank the owner of Lynn Academy, Maureen. I have had an amazing time teaching with you and getting to know you over the last few years. But more importantly, thank you for being such a great friend. I look forward to going to many more majors with you and bringing home even more trophies! Thank you for all your support and guidance as well, you definitely had a big part in getting me through my thesis.

And last but certainly not least…I need to thank all my family for their support over the past 5 years. Thank you Uncle Sean and Aunt Betty for always having a place for me to crash when I come up to Pearl River and for always having a fresh bottle of ketchup in the fridge. Uncle Kevin, Aunt Barbra, Aunt Terry, Uncle George, and Grandma it was

great getting to see all of you on the weekends now that I am up this area! Also, thank you to all my cousins Timmy, Ciara, and Shannon, and their wonderful significant others, Taylor and Tommy for being such good friends! We always have a great time when we go out in Pearl River or the city and I can't wait for us to go to each other's weddings! Thank you to all my family over in Ireland as well! Now that I am done with school I should be able to sneak over more often! Love you all, especially my Nana, miss you so much.

Congratulations to my sister and brother in law, Anna and Mitchell on the birth of their second child! Brian and Luke are the most adorable kids and I wish I could see your family more. But now that I am done with school maybe I can take a few more trips! Conor you are my favorite brother! It was so good to see you up here a few months ago and go to a Rangers game with you. You are such a talented and caring person and I know that you can do anything if you set your mind to it! And my youngest sister Caroline is the sweetest person you could meet! Good luck finishing up high school and I hope you pursue your dreams when you go to college! The world is your oyster, go out there and make a difference in the world! I love all 3 of you so dearly, and it breaks my heart that I can't see you in person more often, but there will definitely be way more sibling retreats as we get older! Thank you all for your support, I would not be the person I am today without your help.

And speaking of support, probably the two most important people I need to thank are my Mother and Stepfather, Trish and Wrennie. Both of you have provided me with everything I ever needed over the past 5 years and your constant love and encouragement have meant everything to me. There is no way I would have been able to get through this PhD without both of you. Thank you and love you both.

And last but not least, thank you Dad. None of this would have been possible without you. Even though you have moved on from this life, I still feel your presence every single day. Enjoy reading this WHOLE thesis from Heaven, because you have inspired me to be the best person I can be. Love you, and can't wait to see you again.

For you Dad. None of this would be possible without you.

CHAPTER 1

Mercury Alkyl Complexes Which Feature Cysteinate, Glutathionate, Phenylthiolate, and Phenylselenolate Ligands: Structural Characterization, Exchange Reactions, and Mercury–Carbon Bond Cleavage

Table of Contents

Reproduced in part from Yurkerwich, K.; Quinlivan, P. J.; Rong, Y.; Parkin, G. *Polyhedron* **2016**, 103, 307-314.

1.1 Introduction

Mercury alkyl complexes display potent toxicity.[1,2] Exposure to these compounds can result in neurotoxicity and, depending upon the type, length, and magnitude of exposure, can cause mild to severe cognitive and neuromotor impairment and even death.[2-5] Of the organomercurials, methylmercury species, $[MeHg]^+$, are considered the most dangerous due to their lipophilicities and abilities to cross cellular membranes, including the blood-brain barrier and placental barrier.[4,6,7] The devastating after-effects of methylmercury poisonings in Minamata[8] and Iraq[9] illustrate just how deleterious contact with the heavy metal can be. Consequently, efforts have been made to reduce the large-scale use of mercury where possible.[2] However, chronic, low-dose exposure to organomercurials is not as well studied compared to acute organomercury poisoning and still remains a global concern.[10,11] The most common way humans are exposed to organomercury is through consumption of contaminated seafood which results from the bio-accumulation of mercury in the food chain.[12,13] Other forms of mercury exposure can result from dental amalgam fillings, vaccines, and contaminated water and air samples.[2,5,14] Due to all these concerns, studies that examine the coordination chemistry of mercury alkyl complexes and their detoxification still warrant attention.

On a molecular level, it is well known that organomercury complexes effectively bind sulfur-containing amino acids and cofactors, such as cysteine (Cys) and glutathione (GSH) (Figure 1), which in turn perturbs their functions.[15-18] However, in addition to the thiophilicity of mercury, it has also become evident that its selenophilicity[19] also plays an important role in toxicity. With regards to its biological function, selenium is considered an essential trace element in the human body due to its important antioxidant properties.[19,20] Furthermore, selenium deficiency has been linked to cancer and neurodegenerative diseases.[19,21] Consequently, organomercurials are capable of

binding to selenium-containing amino acids, such as selenocysteine, and selenium-containing active sites of proteins, which in turn reduces the overall bioavailability of selenium and inhibits their functions.[7,19-24] As such, it is therefore evident that the toxic effects of organomercury and selenium are intertwined.

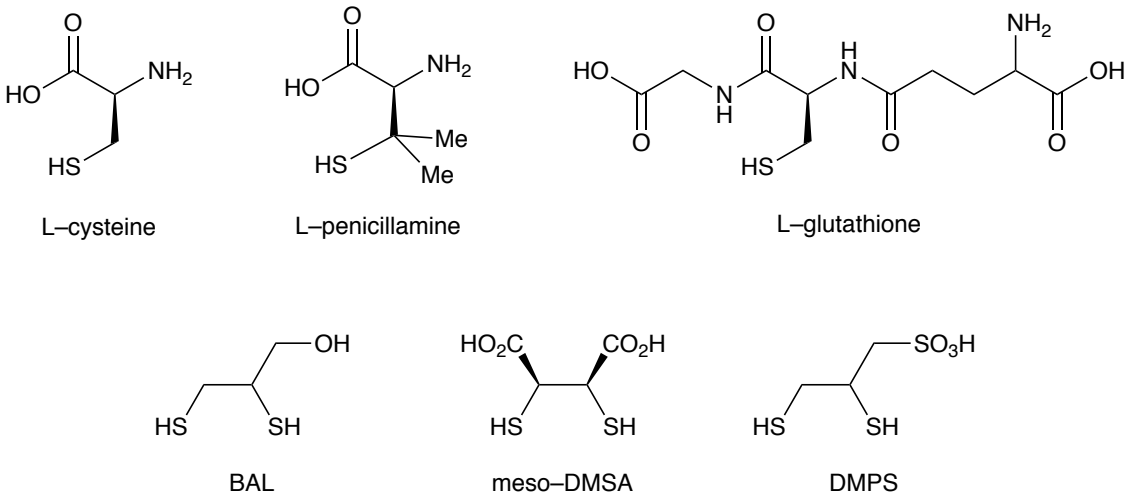

Figure 1. Structures of L-cysteine, L-penicillamine, L-glutathione, 2,3-dimercaptopropanol (British anti-Lewisite, BAL), dimercaptosuccinic acid (DMSA), and dimercaptopropanesulfonic acid (DMPS) in their neutral forms.

The treatment for mercury poisoning in humans is usually chelation therapy, with some of the most commonly employed drugs being 2,3-dimercaptopropanol (British anti-Lewisite, BAL), dimercaptosuccinic acid (DMSA), and dimercaptopropanesulfonic acid (DMPS) (Figure 1).[25,26] The aim of chelation therapy is to rid the body of mercury by forming a chelated complex with the heavy metal, which can then be safely excreted. While success in removing mercury *via* urinary excretion with DMSA and DMPS has been achieved, evidence suggests that a true chelate is not actually formed.[27] Furthermore, depending upon the type of mercury exposure and patient profile, a cocktail of drugs may be necessary to remove significant amounts of mercury.[28]

Despite all the issues and drawbacks that are associated with mercury poisoning and chelation therapy, Nature has been able to develop its own detoxification system. More specifically, certain strains of bacteria are able to survive in environments contaminated with methylmercury by acquiring the *mer* operon, which codes for two enzymes, organomercurial lyase (MerB) and mercurial reductase (MerA).[29,30] MerB first facilitates the cleavage of the Hg–C bond to form methane and Hg^{2+}, which is then reduced to less toxic Hg^0 by MerA, and subsequently expelled by the cell. The mechanism of action of MerB is of great interest because dealkylation of mercury to less toxic forms could aid in remediation efforts of sites contaminated by organomercurials.[31]

Previous research in the Parkin group has shown that the ability to cleave Hg–C bonds of linear mercury alkyl complexes is dependent upon the ability of the metal center to access higher coordination modes.[32] This was demonstrated by the rapid generation of methane upon treatment of [κ^1-Tm^{Bu^t}]HgMe with PhSH to form the [κ^3-Tm^{Bu^t}]HgSPh complex (Scheme 1), whereas elevated temperatures were required for the generation of methane and ethane with the phenylthiolate mercury compounds, PhSHgR (R = Me, Et). However, a detailed study comparing the reactivity of the phenylselenolate analogues, PhSeHgR, towards protolytic Hg–C bond cleavage had not been completed. Given that selenium coordination is an important contributor to mercury toxicity,[19-24] an investigation into selenium's role in Hg–C bond cleavage was in order.

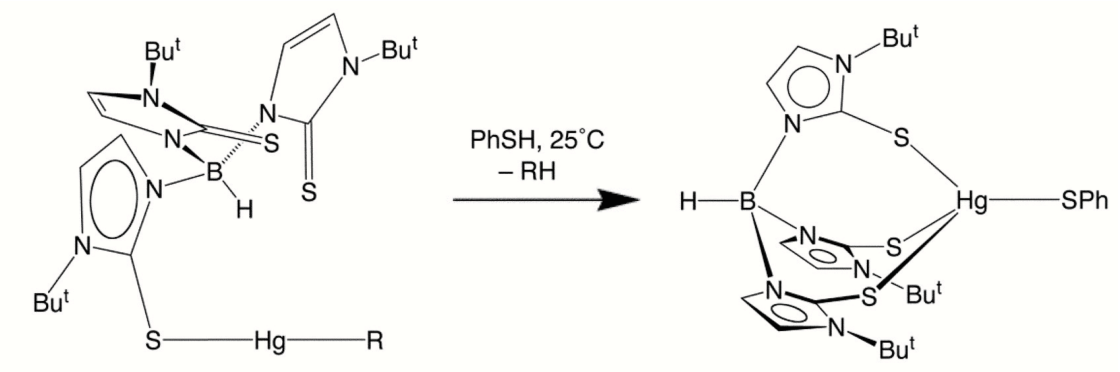

Scheme 1. Synthesis of [κ^3-Tm$^{Bu^t}$]HgSPh *via* reaction of [κ^1-Tm$^{Bu^t}$]HgMe and PhSH.

This chapter discusses (i) the coordination chemistry of cysteine and glutathione towards methylmercury, (ii) the synthesis and characterization of the phenyselenolate mercury alkyl compounds, PhSeHgR (R = Me, Et), and (iii) exchange reactions of PhSeHgR, and their susceptibility towards protolytic Hg–C bond cleavage.

1.2 Synthesis and Characterization of (Cys)HgMe and (GS)HgMe

1.2.1 Synthesis and Structural Characterization of (Cys)HgMe

The structural characterization of cysteine-mercury compounds is of great interest due to their role in biological systems. In this regard, although the synthesis and molecular structure of (Cys)HgMe has previously been reported,[33] the data were obtained at room temperature and no hydrogen atoms were able to be located, thus preventing a thorough discussion of hydrogen bonding interaction. The X-ray crystal structure of (Cys)HgMe has been re-examined and is discussed herein this section.

(Cys)HgMe was synthesized according to the procedure put forth by Taylor *et. al.*[33] Specifically, L-cysteine reacts with MeHgOH in a mixture of H_2O and EtOH (1:1) to yield (Cys)HgMe (Scheme 2), which can be recrystallized from H_2O to afford crystals suitable for X-ray diffraction.

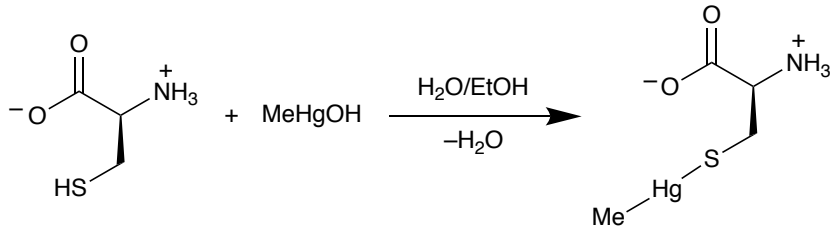

Scheme 2. Synthesis of (Cys)HgMe from L-cysteine and MeHgOH.

The molecular structure of (Cys)HgMe reveals that cysteine is bound to mercury in a unidentate fashion through the deprotonated thiol group with a bond distance of 2.361(3) Å. As expected for two-coordinate mercury alkyl complexes, the S–Hg–Me bond angle is nearly linear (178.7(4)°).[34-36] A secondary interaction is also observed between the Hg center and one of the carboxylate oxygens, O2, having a Hg···O distance of 2.821(7) Å. While this distance is certainly longer than the sum of the covalent radii for a Hg–O bond (1.98 Å),[37] it is well within the sum of the crystallographic van der Waals radii (3.6 Å).[38] Although the reported values for Hg–O bond lengths in the Cambridge Structural Database (CSD)[39] span the range 1.797–3.621 Å, with an average of 2.614 Å,[33,40-42] analysis of the molecular orbitals of (Cys)HgMe does not reveal any significant Hg–O overlap. Given this data, the Hg–O interaction can be considered weak. In addition to the (Cys)HgMe unit in the crystal structure, a water molecule is present and hydrogen bonding interactions are discussed below.

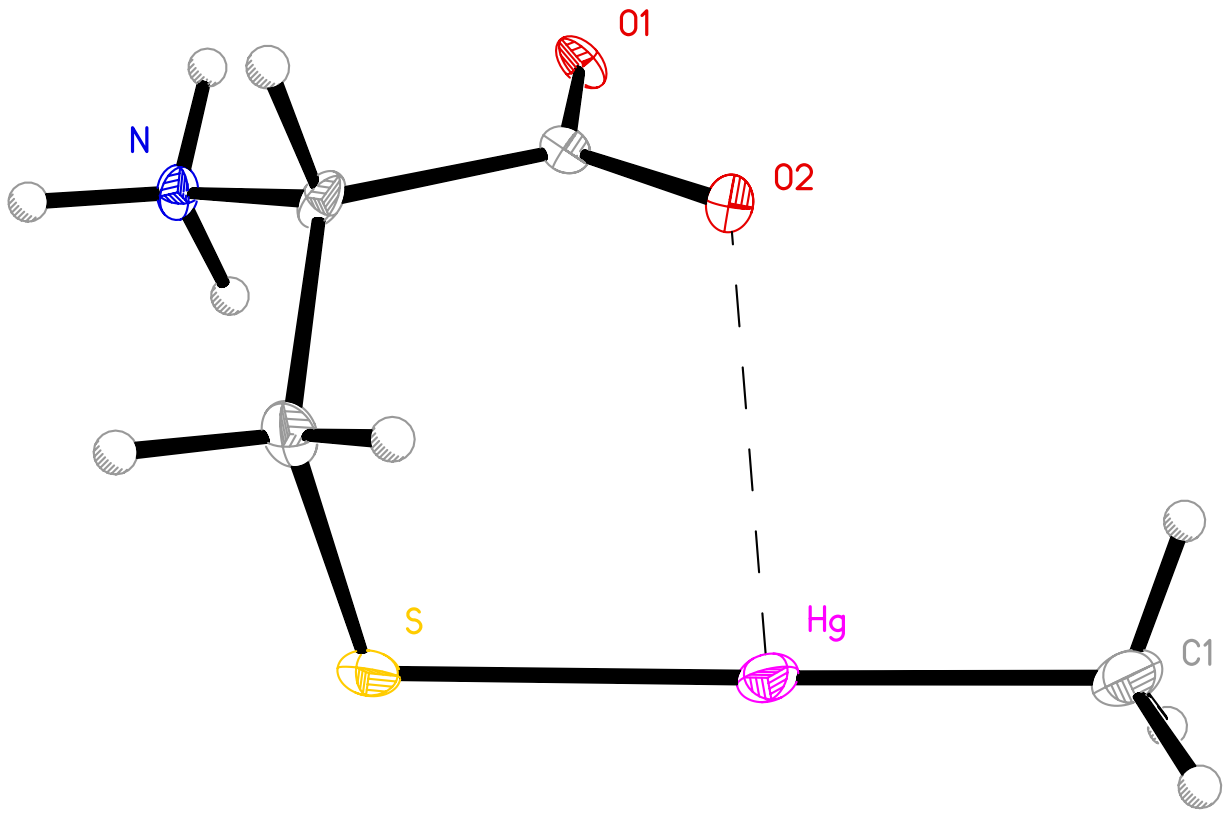

Figure 2. Molecular structure of [(Cys)HgMe]•H_2O.

Comparing the structure of (Cys)HgMe with the one that was previously reported by Taylor *et al.*,[33] the bond distances and angles are similar (Table 1). Additionally, in the newly determined solution, all hydrogen atoms on heteroatoms were located, which allows for a more detailed analysis of the hydrogen bonding pattern in the crystal structure as illustrated in Figure 3. Namely, both hydrogen atoms of the H_2O molecule hydrogen bond with carboxylate oxygens of adjacent molecules, having O···H distances of 2.05(12) Å and 2.04(9) Å (O···O distances are 2.719(10) Å and 2.757(11) Å respectively). Additionally, one hydrogen of the $[NH_3]^+$ group hydrogen bonds to an adjacent H_2O molecule with N···H and N···O distances of 1.85(5) Å and 2.713(10) Å, and a different hydrogen atom of the $[NH_3]^+$ group hydrogen bonds to an adjacent carboxylate oxygen with N···H and N···O distances of 2.01(8) Å and 2.808(12) Å. The

new structure also benefits from a lower R-value of 3.7% compared to 6.5% reported by Taylor *et al.*

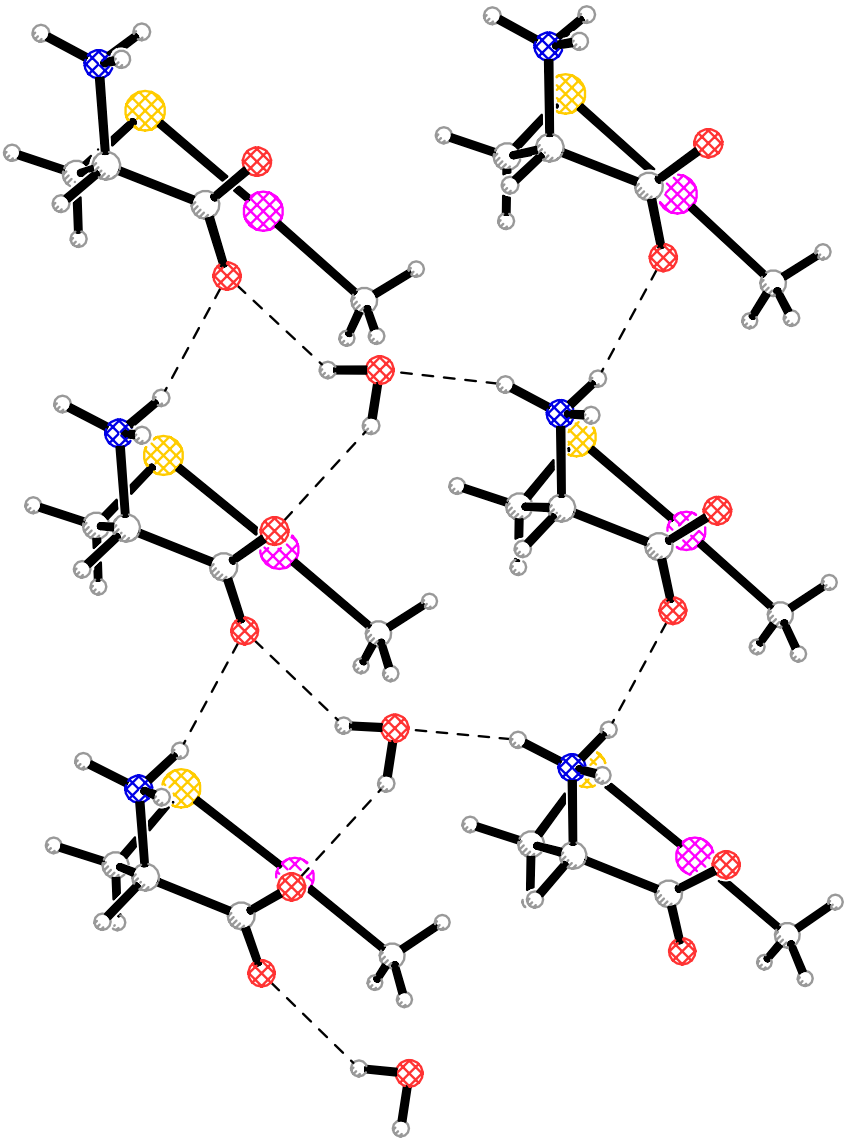

Figure 3. Intermolecular hydrogen bonding interactions (shown as dashed lines) for [(Cys)HgMe]•H_2O.

Table 1. Selected bond distances and angles for [(Cys)HgMe]•H_2O and [(pen)HgMe]•H_2O.

	Hg–CH_3 /Å	**Hg–S /Å**	**Hg–O_2C /Å**	**S–Hg–CH_3 /°**	**Hg–S–(β–C) /°**	**Ref**
[(Cys)HgMe]•H_2O	2.10(4)	2.352(12)	2.85(2)	177.6(0.9)	100.4(0.9)	33
[(Cys)HgMe]•H_2O	2.101(14)	2.361(3)	2.821(7)	178.7(4)	100.1(4)	this work
[(pen)HgMe]•H_2O	2.07(6) 2.09(5)	2.38(1) 2.36(1)	2.88(3) 2.89(3)	175(2) 175(2)	107(1) 111(1)	43

pen = DL-penicillamine

The structure of the $[MeHg]^+$ adduct of the closely related sulfur-containing amino acid, DL-penicillamine (pen), where the β-hydrogens of cysteine are replaced by methyl groups (Figure 1), has also been reported.[43] A linear structure is also observed with very similar Hg–Me (2.07(6) Å and 2.09(5) Å) and Hg–S (2.38(1) Å and 2.36(1) Å) bond lengths.[44] However, the Hg–S–(β–C) bond angles are larger, likely due to the increased steric demands of the methyl groups relative to the hydrogen atoms. An extended hydrogen bonding network similar to (Cys)HgMe is also observed.

1.2.2 Spectroscopic Characterization of (Cys)HgMe

Spectroscopically, (Cys)HgMe is characterized by a singlet at 0.82 ppm in the ^{1}H NMR spectrum corresponding to the methyl protons. Due to the presence of the magnetically active ^{199}Hg nucleus (16.9% abundant, spin = ½),[23] satellite peaks are also observed flanking the methyl peak, having a $^2J_{Hg–H}$ of 177 Hz.[45] Furthermore, the α-hydrogen is characterized as a broad peak at 4.12 ppm and the diastereotopic β-hydrogens are displayed as a second-order pattern centered at 3.55 ppm (Figure 4).

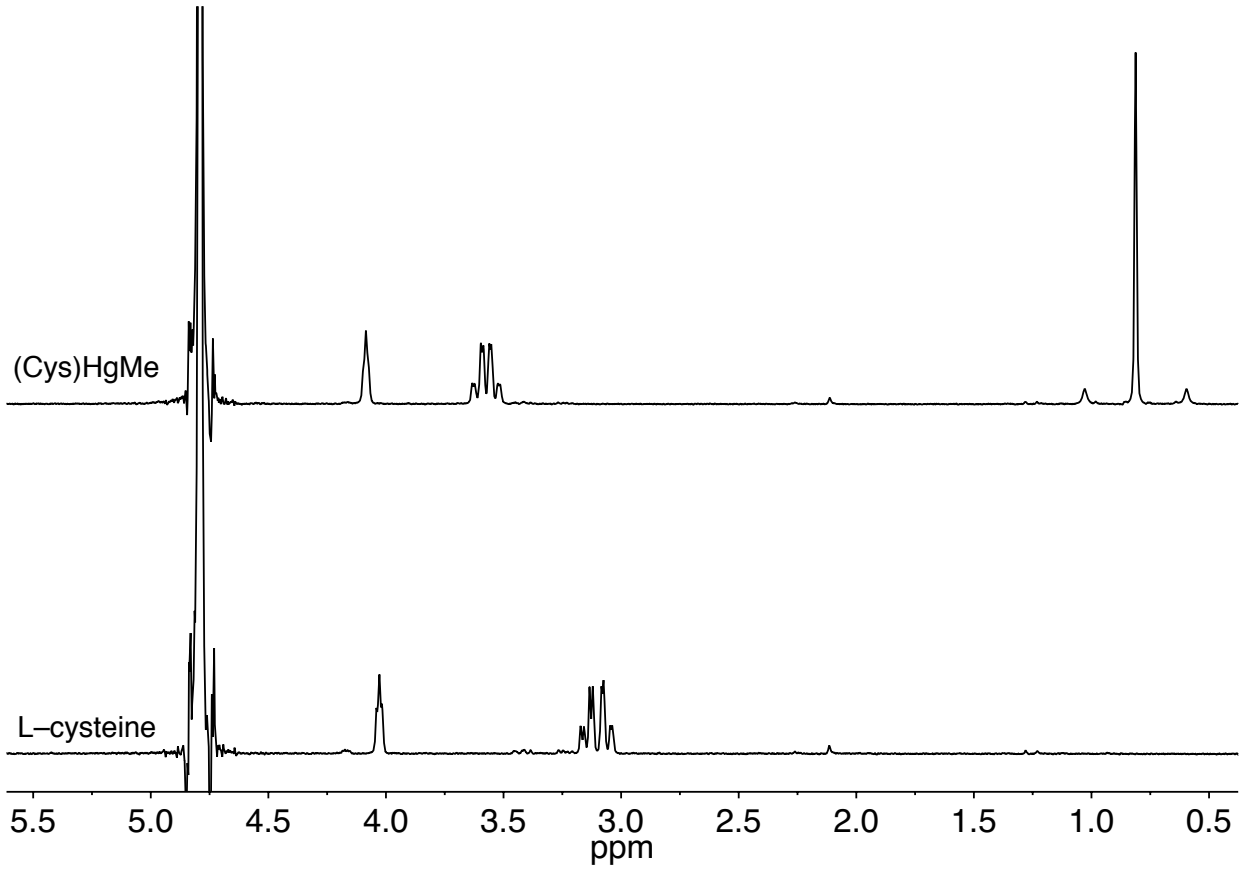

Figure 4. ^{1}H NMR spectra of L-cysteine (bottom) and (Cys)HgMe (top).

1.2.3 Degenerate Exchange of Cysteine with (Cys)HgMe

In the presence of excess cysteine, exchange between free cysteine and bound cysteine in (Cys)HgMe can be observed. For example, in a 1:1 mixture of cysteine and (Cys)HgMe, broadened peaks are observed for the α and β-hydrogens, demonstrating the labile nature of the cysteine ligand (Figure 5).[46] The methyl peak does not show any significant broadening, reinforcing the fact that exchange of alkyl groups in mercury alkyl complexes is not facile.[23,47] An associative mechanism that involves an incoming cysteine replacing a dissociating cysteinato ligand through a 4-atom-centered transition state has been proposed for this exchange reaction as illustrated in Figure 6.[46-48] The exchange of cysteine, as well as other thiols, has also been found to be pH

dependent.[49-51] Consistent with these spectroscopic data, it is reasonable to suggest that $[MeHg]^+$ travels through cells and cellular membranes in such a way that it is constantly exchanged from one thiol to the next.[46]

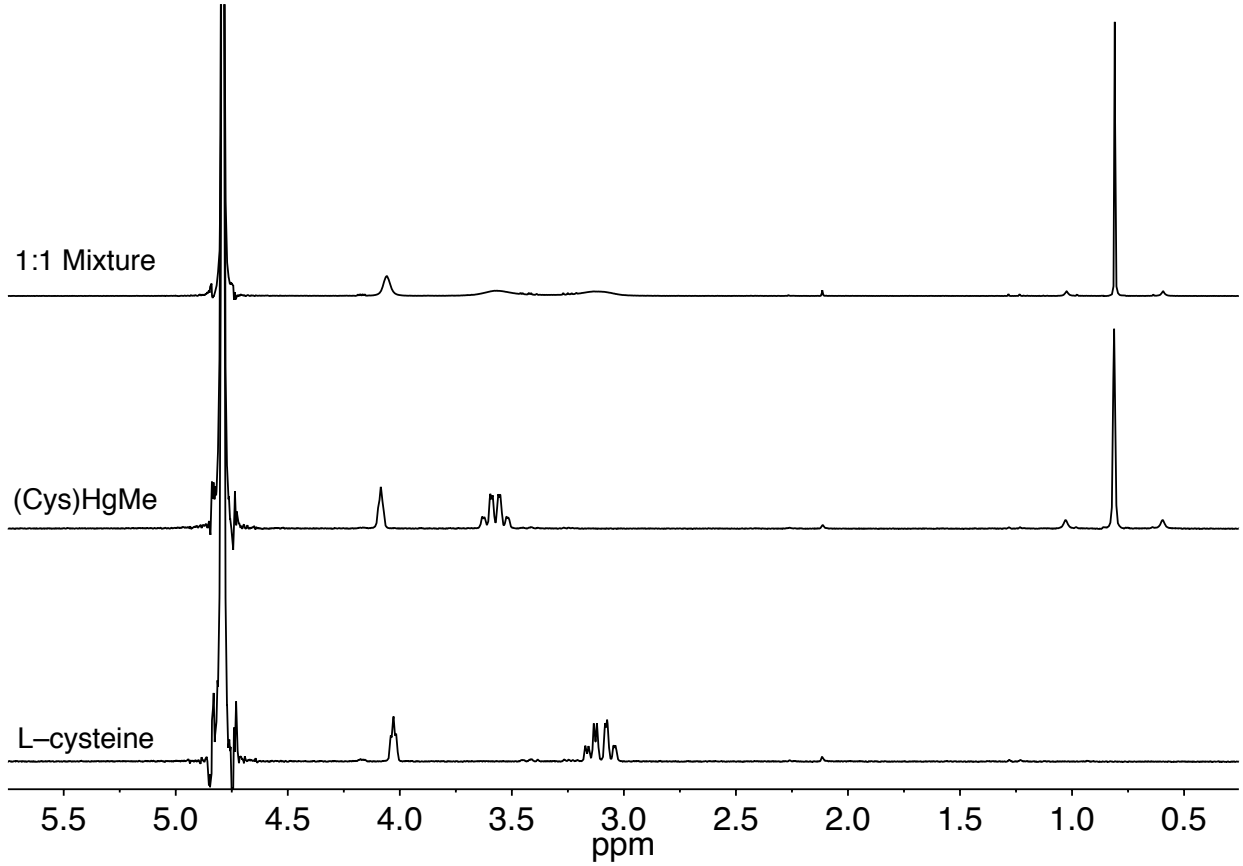

Figure 5. ^{1}H NMR spectra of L-cysteine (bottom), (Cys)HgMe (middle), and a 1:1 mixture of L-cysteine and (Cys)HgMe.

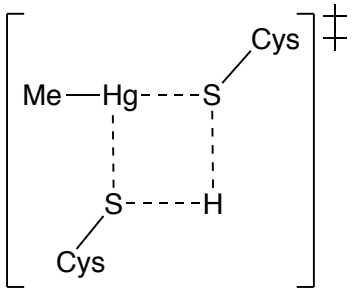

Figure 6. Proposed 4-atom-centered transition state for exchange of an incoming cysteine replacing a dissociating cysteinato ligand.

1.2.4 Synthesis and Characterization of (GS)HgMe

The coordination of glutathione (a tri-peptide consisting of glutamic acid, cysteine, and glycine residues) with $[MeHg]^+$ is of great interest due to its biological relevance during mercury poisoning.[52-55] To this end, (GS)HgMe can be synthesized through the reaction of L-glutathione with MeHgCl in a mixture of EtOH and H_2O (1:1) (Scheme 3).

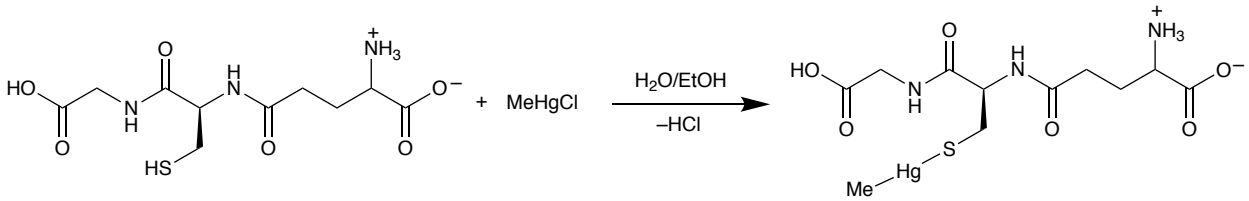

Scheme 3. Synthesis of (GS)HgMe from L-glutathione and MeHgCl.

Several attempts were made to crystallize (GS)HgMe, but crystals suitable for X-ray diffraction could not be isolated. In fact, in the CSD,[39] there are only two coordination complexes of glutathione that have been characterized by X-ray diffraction, namely the copper complex $[CuGSSGCu]Na_4 \bullet 6H_2O$,[56] which features reduced glutathione, and the cobalt complex glutathionylcobalamin[57] (vitamin B_{12}, coordinated by glutathione).

In view of the fact that the structure of (GS)HgMe could not be determined by X-ray diffraction, the geometry optimized structure in the gas phase was determined (Figure 7). Similar to (Cys)HgMe, unidentate coordination is observed through the deprotonated thiol of the cysteine residue. Additionally, the geometry optimized Hg–S (2.554 Å) and Hg–C (2.228 Å) bond lengths are very similar to the geometry optimized bond lengths for (Cys)HgMe (2.550 Å and 2.226 Å respectively). Also, the S–Hg–C geometry optimized bond angle (170.8˚) of (GS)HgMe is comparable to that of the geometry optimized S–Hg–C bond angle in (Cys)HgMe (172.4˚). Interestingly, there is

also a Hg–O secondary interaction of 2.761 Å from the cysteine oxygen residue. Similar to (Cys)HgMe, this distance is much longer than the sum of the covalent radii for a Hg–O bond (1.98 Å),[37] but is well within the sum of the crystallographic van der Waals radii (3.6 Å).[38] Analysis of the molecular orbitals of (GS)HgMe does not reveal any significant Hg–O overlap, and therefore this interaction can be considered weak.

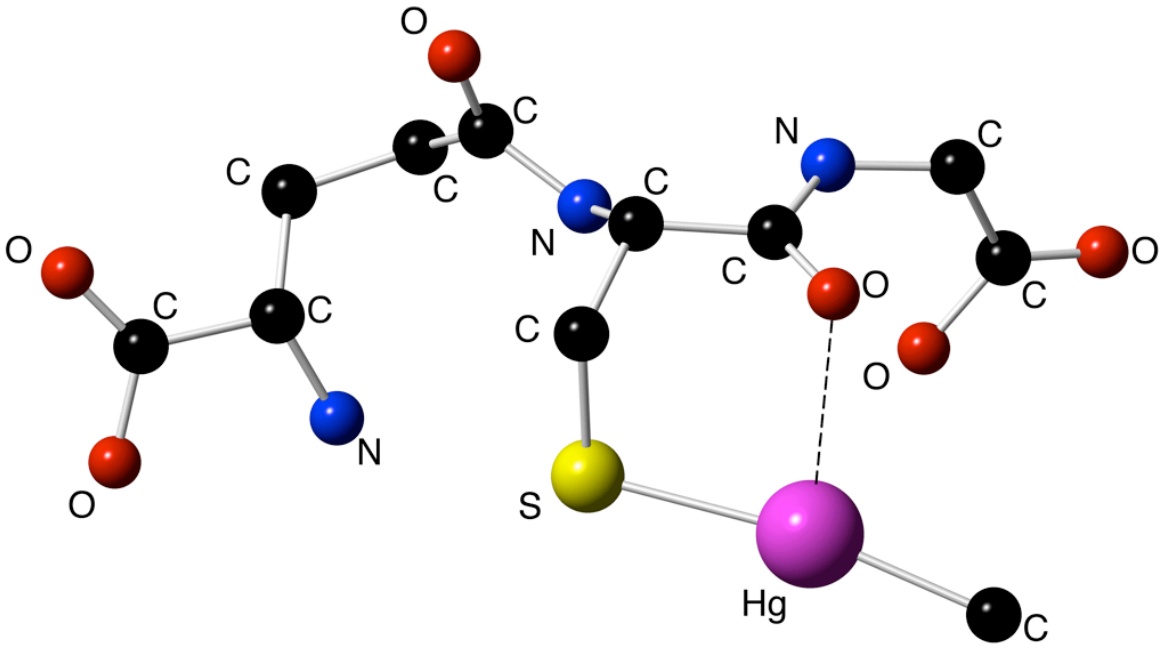

Figure 7. Geometry optimized structure of (GS)HgMe in the gas phase (hydrogen atoms are omitted for clarity).

Spectroscopically, (GS)HgMe is characterized by a singlet at 0.75 ppm in the ^{1}H NMR spectrum, which corresponds to the methyl protons (Figure 8). Due to the presence of the magnetically active ^{199}Hg nucleus (16.9% abundant, spin = ½),[23] satellite peaks on both sides of the methyl peak are also observed, with a $^{2}J_{Hg-H}$ of 172 Hz.[58] A significant shift in the diastereotopic β-hydrogens of the cysteine residue is observed, moving from a multiplet centered around 2.96 ppm in free glutathione to 3.37 ppm in (GS)HgMe.

Additionally, the broadened methyl satellites are due to chemical shift anisotropy.[59] In the $^{13}C\{^{1}H\}$ NMR, the peak corresponding to the methyl carbon appears at 9.19 ppm.

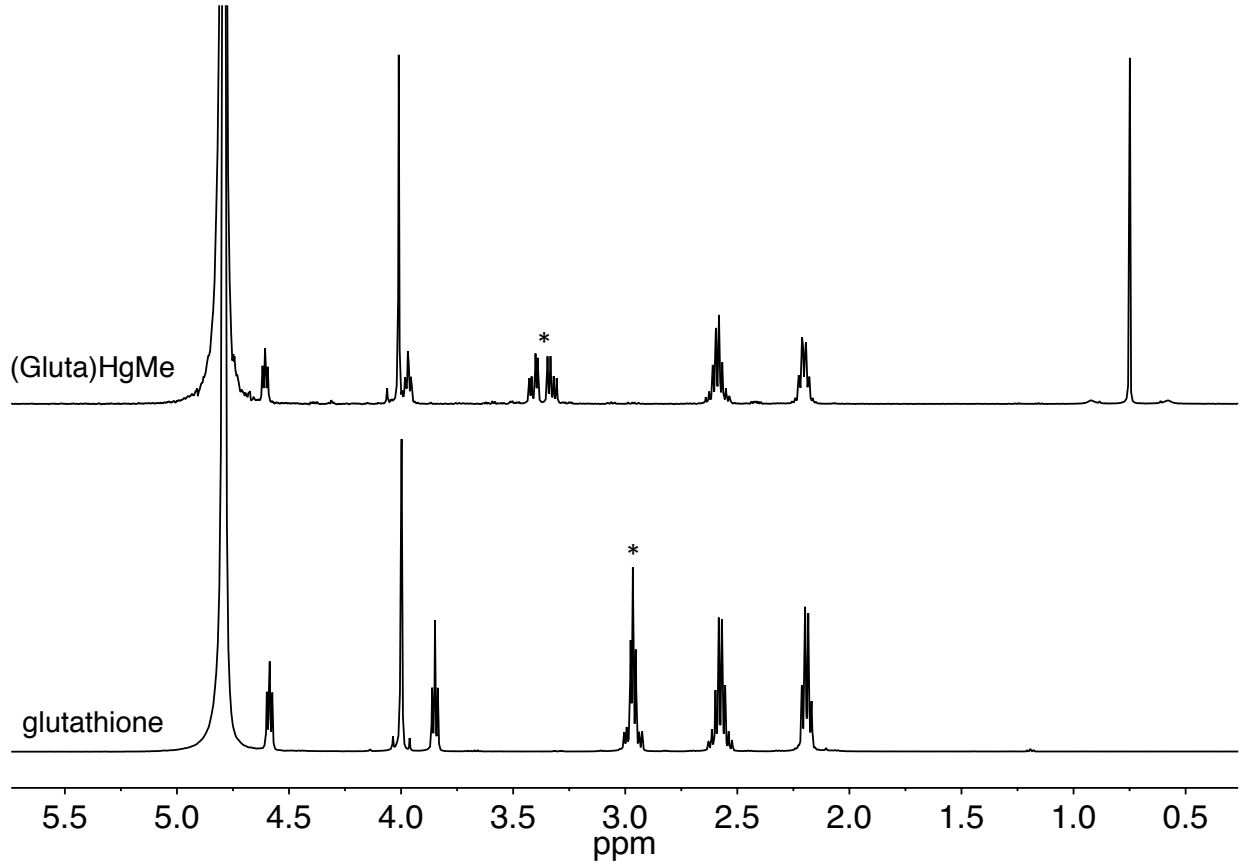

Figure 8. ^{1}H NMR spectra of glutathione (bottom) and (GS)HgMe(* indicates the β-hydrogens of glutathione and (GS)HgMe.

The spectroscopic and computational data collected for (GS)HgMe suggest that glutathione coordinates to $[MeHg]^{+}$ in a unidentate fashion through the deprotonted thiol group. Support for this structure is provided by nearly identical chemical shifts in the ^{1}H NMR for all protons on (GS)HgMe, compared to free glutathione, except for the β-hydrogens on the cysteine residue (Figure 8) and geometry optimization calculations (Figure 7). Furthermore, NMR spectroscopic studies by Rabenstein *et. al.* also suggests

that glutathione coordinates to $[MeHg]^+$ through the deprotonated thiol when mixed in a 1:1 ratio.[53-55]

1.3 Synthesis and Characterization of PhSeHgR (R = Me, Et)

Examples of arylthiolate mercury ethyl complexes have previously been structurally characterized by X-ray diffraction, including the mercury ethyl vaccine preservative, thimerosal.[32b,60-62] Additionally, the arylthiolate mercury complexes, PhSHgR (R = Me, Et), have also been synthesized and structurally characterized, and have been shown to release methane and ethane when treated with PhSH at high temperatures.[32] However, there are no examples of selenolate analogues listed in the CSD.[39] Considering this absence, it is noteworthy that the Parkin lab has previously synthesized and characterized the phenylselenolate mercury alkyl complexes, PhSeHgR (R = Me, Et).[23,63]

1.3.1 Synthesis of PhSeHgR (R = Me, Et)

According to a procedure developed by Dr. Kevin Yurkerwich, the synthesis of PhSeHgR (R = Me, Et) can be achieved *via* the treatment of diphenyldiselenide, Ph_2Se_2, with $NaBH_4$ in EtOH, followed by addition of the corresponding mercury alkyl chloride, RHgCl (R = Me, Et) (Scheme 4).[23,63]

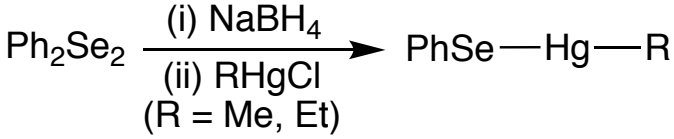

Scheme 4. Synthesis of PhSeHgR.

1.3.2 Structural Characterization of PhSeHgR (R = Me, Et)

The molecular structures of both PhSeHgMe and PhSeHgEt have been previously determined by X-ray diffraction (Figure 9 and Figure 10) by Dr. Kevin Yurkerwich.[63] Both complexes possess approximately linear coordination geometries (Table 2), which is common for two-coordinate mercury alkyl complexes.[34,35] While two-coordinate mercury complexes are well precedented, there are only four other two-coordinate mercury alkyl complexes that feature a [Se–Hg–C] motif listed in the CSD.[39,64-66] For reference, their relevant bond lengths and angles are listed in Table 2.

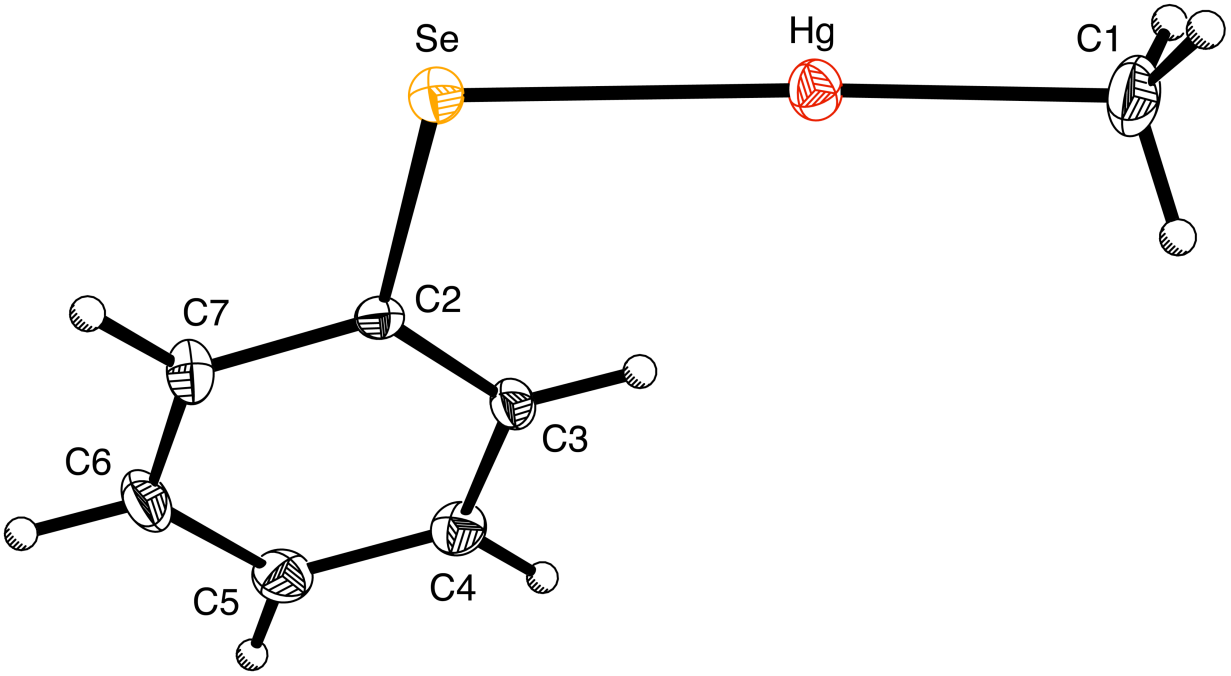

Figure 9. Molecular structure of PhSeHgMe.

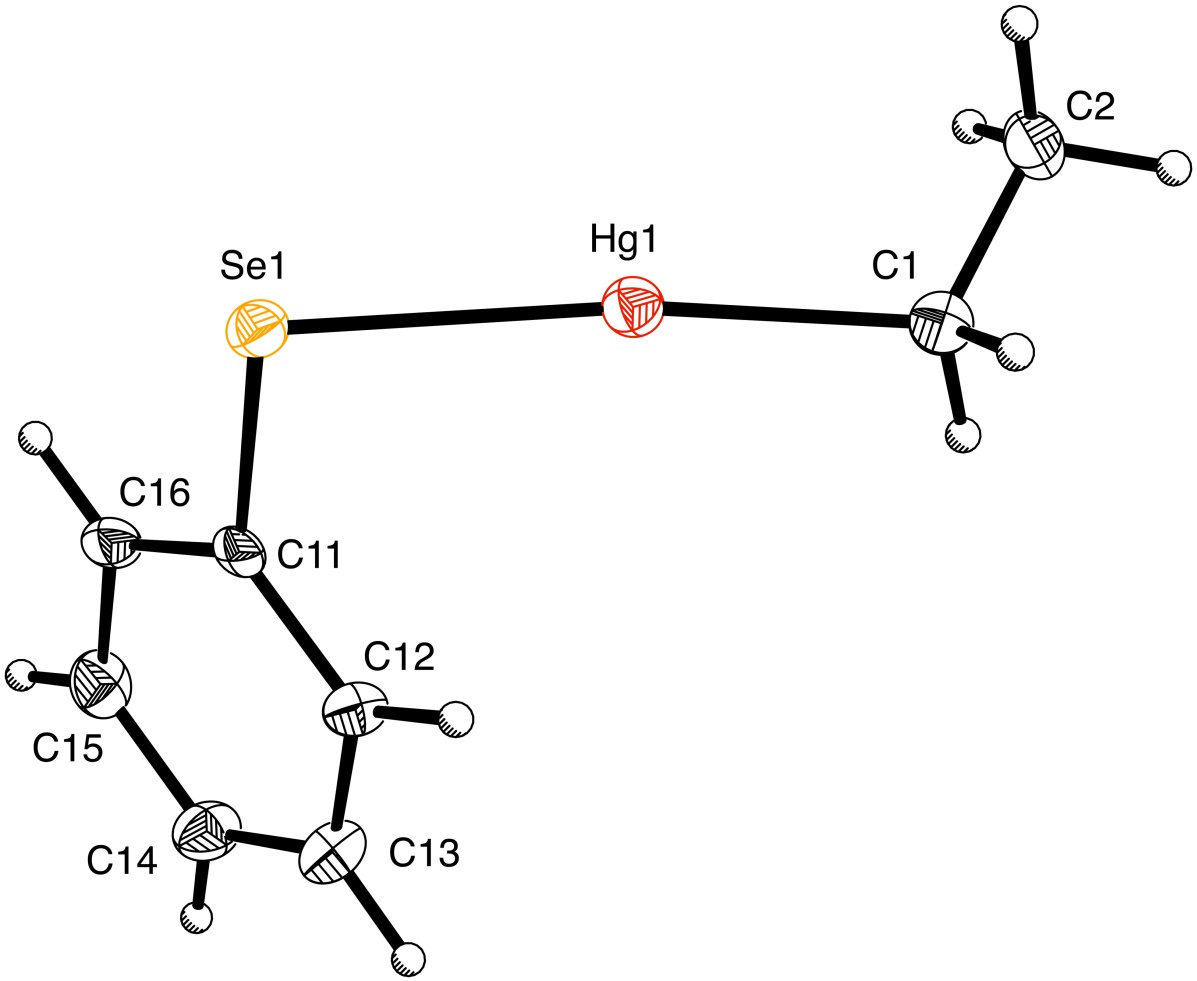

Figure 10. Molecular structure of PhSeHgEt (only one of the crystallographically independent molecules is shown).

Table 2. Bond length and angle data for selected two coordinate mercury alkyl compounds with selenium co-ligands.

	Hg–C/Å	Hg–Se/Å	Se–Hg–C/°	Reference
$PhSeHgCH_3$	2.087(6)	2.4990(13)	177.03(19)	this work
$PhSeHgCH_2CH_3$	2.083(9) 2.111(10)	2.4955(14) 2.4940(14)	173.6(2) 174.7(3)	this work
$(2,4,6\text{-}Pr^i_3C_6H_2)SeHgMe$	2.039(35)	2.460(3)	175.7(9)	64
$\{(H_2N)_2CSeHgMe\}[NO_3]$	2.13(3)	2.477(3)	177.0(8)	65
$[O_2C(H_3N)CHCH_2Se]HgMe$	2.10(4)	2.469(4)	177.8(11)	66

The Hg–C and Hg–SePh bond lengths of PhSeHgMe and PhSeHgEt are comparable to the other derivatives listed in Table 2. Additionally, the Hg–SePh bond lengths are similar to those of the two-coordinate homoleptic compound, $Hg(SePh)_2$ [2.4802(2) Å],[67] and the four-coordinate complex, $[Tm^{Bu^t}]HgSePh$ [2.5244(4) Å].[68] However, it is worth noting that significantly longer Hg–Se bond lengths have been observed for complexes that feature Hg–Se dative covalent L-type interactions.[69] For example, the benzimidazole-2-selone derivative, $[H(sebenzim^{Me})]_2HgCl_2$, has bond lengths of 2.5732(5) Å and 2.6090(5) Å,[70] while those in $[Hg_2(SePh_2)_4][ClO_4]_2$ range from 2.65 Å to 2.92 Å.[71] This variability in bond lengths is not unique to Hg–Se interactions, as it is a common feature of dative covalent bonds.[72]

1.3.3 Spectroscopic Characterization of PhSeHgR (R = Me, Et)

Spectroscopically, PhSeHgMe is characterized by a ^{199}Hg NMR signal at –658 ppm which is comparable to the values for other two-coordinate mercury alkyl complexes with a sulfur or selenium co-ligand (Table 3). The presence of the ^{199}Hg nucleus is also

evident in the ^{1}H and $^{13}C\{^{1}H\}$ NMR spectra as indicated by flanking satellite peaks[23] for the methyl group. For example, in the ^{1}H NMR spectrum, the methyl group is characterized by a singlet at 0.21 ppm which is flanked by ^{199}Hg satellite peaks with $^{2}J_{Hg-H}$ of 155 Hz.

Similarly, PhSeHgEt is characterized by a ^{199}Hg NMR signal at –815 ppm, which is in the range for other two-coordinate mercury alkyl complexes with a sulfur or selenium co-ligand (Table 3). The presence of ^{199}Hg satellite peaks[23] is also observed in the ^{1}H and $^{13}C\{^{1}H\}$ NMRs for the ethyl group of PhSeHgEt. Interestingly, while $^{1}J_{Hg-C}$ (1145 Hz) is considerably larger than $^{2}J_{Hg-C}$ (63 Hz), $^{2}J_{Hg-H}$ (159 Hz) is significantly smaller than $^{3}J_{Hg-H}$ (232 Hz).[73] This trend of $^{2}J_{Hg-H}$ being smaller than $^{3}J_{Hg-H}$ has been observed for a variety of other EtHgX compounds.[60,61,74]

Table 3. ^{199}Hg NMR data for two-coordinate mercury alkyl complexes with sulfur or selenium co-ligands.

	δ/ppm	**Reference**
PhSeHgMe	–688[a]	75
	–658[b]	this work
PhSeHgEt	–815[b]	this work
$[O_2C(H_3N)CHCH_2Se]HgMe$	–644[c]	75,66
PhSHgMe	–620[a]	75
	–557[b]	32b
PhSHgEt	–730[b]	32b
$[(Ar^{CO_2})SHgEt]Na$ (thimerosal)	–784[c]	53
$(Ar^{CO_2H})SHgEt$	–788[d]	61
$(3\text{-}H_2NC_6H_4S)HgMe$	–613[d]	62c
$(4\text{-}H_2NC_6H_4S)HgMe$	–645[d]	62c

(a) DMF, (b) Benzene, (c) D_2O, (d) DMSO

Furthermore, the ^{1}H NMR spectrum of PhSeHgEt displays another interesting spectroscopic feature. Specifically, rather than exhibit just a first-order triplet and quartet associated with an A_2X_3 spin system, additional coupling is observed due to second-order effects. Varying degrees of second order-effects can be seen as a function of magnetic field strengths (Figure 11). These second order-effects can be simulated using the following spectral parameters: $\delta(CH_2) = 0.86$ ppm, $\delta(CH_3) = 1.00$ ppm, and $|^3J_{H-H}| = 7.8$ Hz.[76]

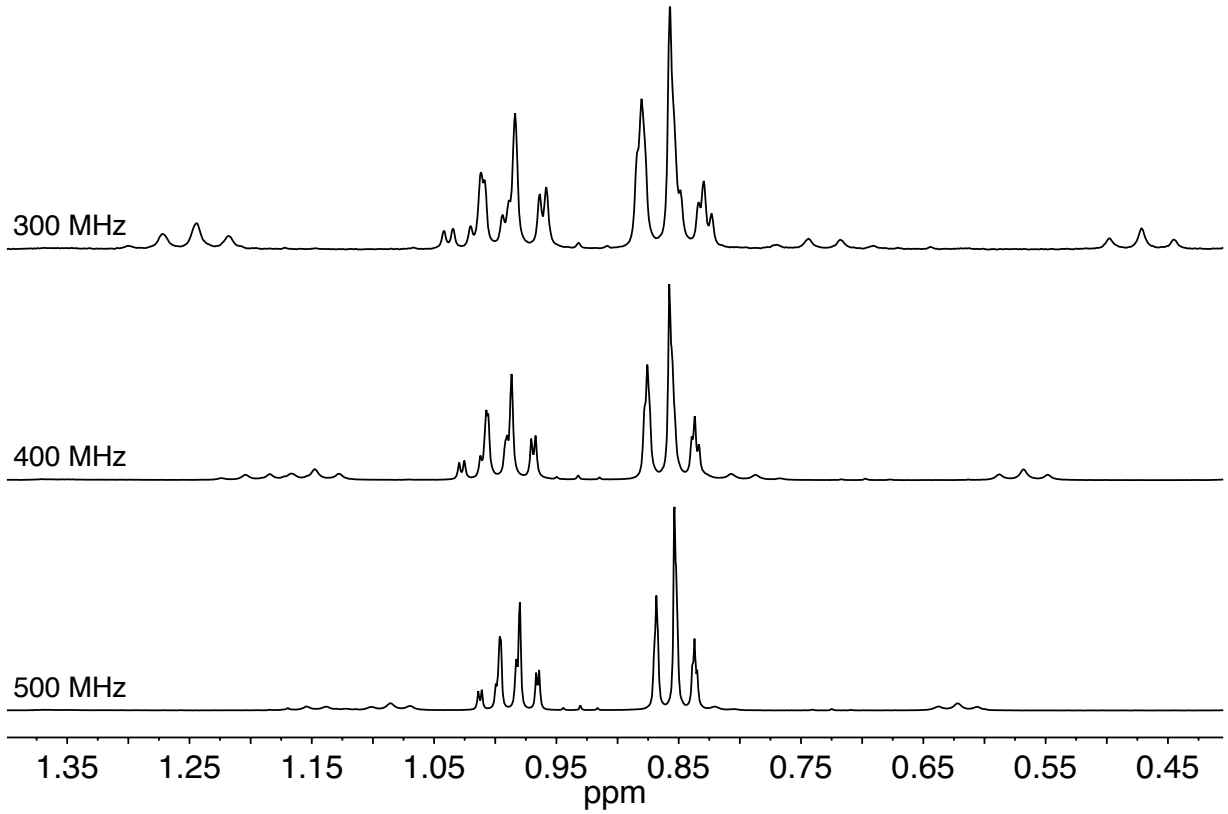

Figure 11. Non first-order ^{1}H NMR spectra of the ethyl group of PhSeHgEt in benzene: 300 MHz (top), 400 MHz (middle) and 500 MHz (bottom).

While the principal NMR signals for the ethyl group of PhSeHgEt are not first-order, the outer ^{199}Hg Satellite signals exhibit a first order-pattern. For example, at 500 MHz, the outer quartet and outer triplet (which are associated with the same ^{199}Hg spin state)[77] are separated by 0.52 ppm (*i.e.* 260 Hz), which is significantly greater than the $^{3}J_{H–H}$ coupling constant (7.8 Hz) and is therefore consistent with a first-order appearance. The inner satellite quartet and triplet are separated by 0.26 ppm (*i.e.* 129 Hz) and would therefore also be expected to display a first-order pattern, however the quartet overlaps with the primary triplet signal, thus obscuring the peak. The observation of a first-order pattern for the satellite peaks of PhSeHgEt is distinctly different from that of EtHgCl at 400 MHz.[61] More specifically, the inner satellite peaks of

EtHgCl appear as a singlet due to the CH_2 and CH_3 groups being coincidentally equivalent in chemical shift at this field.[61]

1.4 Reactivity of PhSeHgR (R = Me, Et)

The reactivity of PhSeHgR (R = Me, Et) towards exchange reactions and protolytic Hg–C bond cleavage was investigated. Specifically, degenerate exchange reactions between PhSeHgR and RHgCl (R = Me, Et), as well as PhSeHgR and PhSHgR, were investigated. Additionally, the reactivity of PhSeHgR towards protolytic cleavage with PhEH (E = O, S, Se) was also investigated.

1.4.1 Degenerate Exchange reactions of PhSeHgR (R = Me, Et)

The compounds PhSeHgR (R = Me, Et) are capable of undergoing degenerate exchange reactions with RHgCl (R = Me, Et) and PhSHgR. For example, only a single resonance for the methyl groups is observed in the ^{1}H NMR spectrum of both a 1:1 mixture of PhSeHgMe and MeHgCl (Figure 12) and a 1:1 mixture of PhSeHgMe and PhSHgMe (Figure 13). Similarly, only one set of ethyl resonances are observed for a 1:1 mixture of PhSeHgEt and EtHgCl in the ^{1}H NMR (Figure 14). The observation of a single set of resonances for the alkyl groups indicates that the exchange processes are in the fast exchange regime.[78] Additionally, only a single ^{199}Hg{^{1}H} NMR spectroscopic signal is observed for both a 1:1 mixture of PhSeHgMe and MeHgCl (Figure 15), and a 1:1 mixture of PhSeHgEt and EtHgCl (Figure 16).

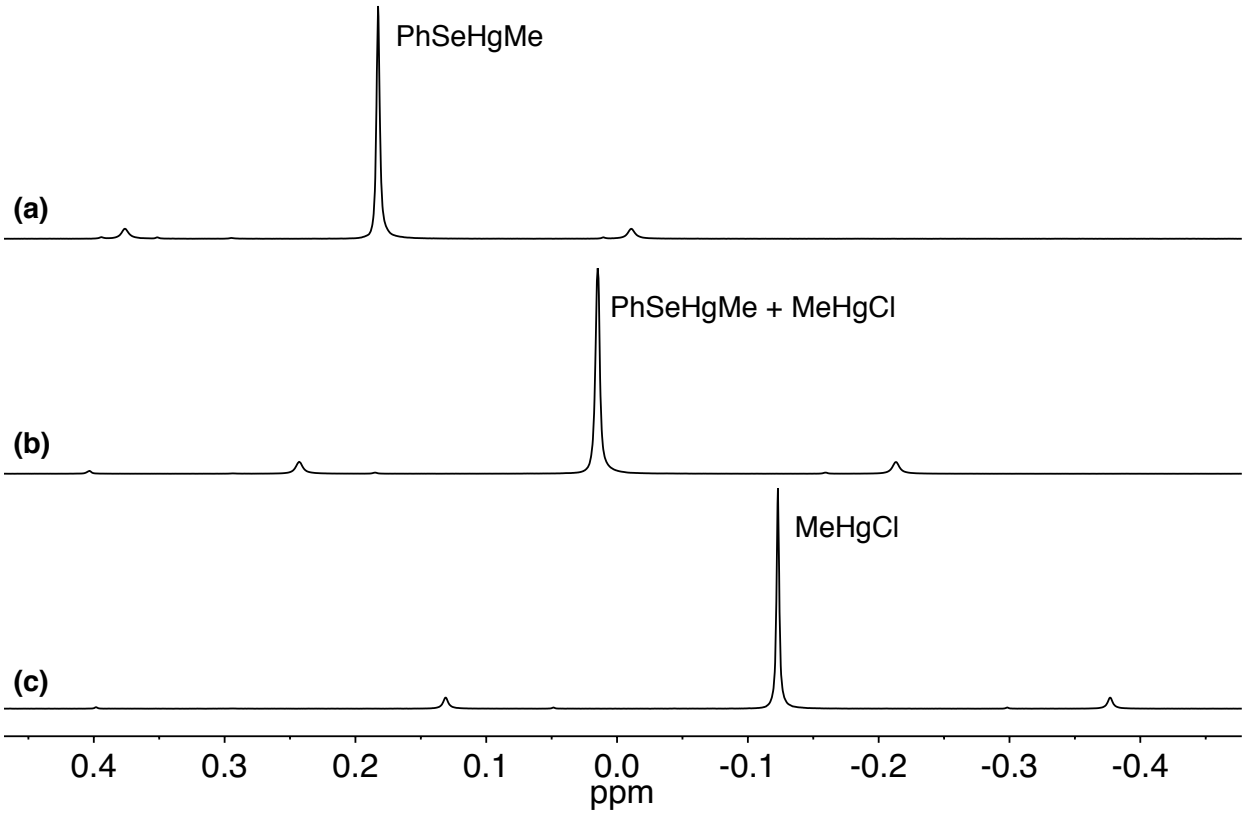

Figure 12. ^{1}H NMR spectra of the methyl region of (a) PhSeHgMe, (b) a mixture of PhSeHgMe and MeHgCl, and (c) MeHgCl.

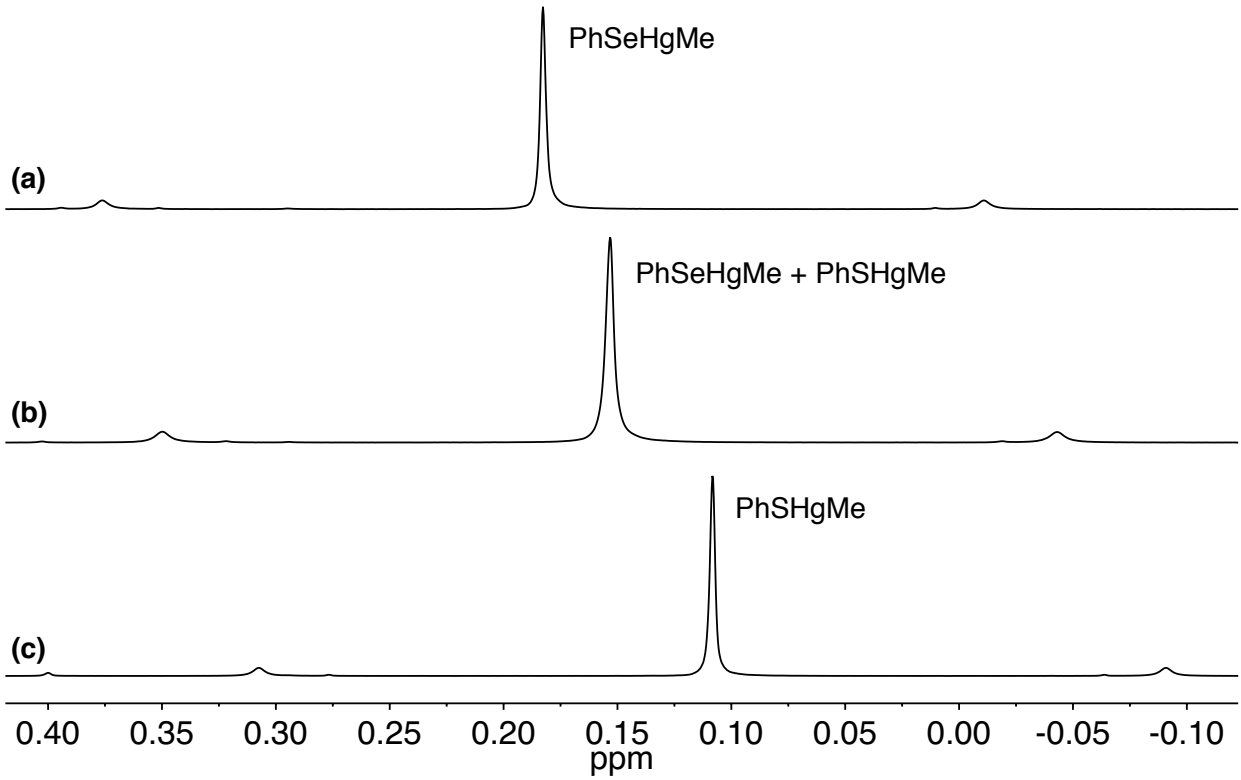

Figure 13. ^{1}H NMR spectra of the methyl region of (a) PhSeHgMe, (b) a mixture of PhSeHgMe and PhSHgMe, and PhSHgMe.

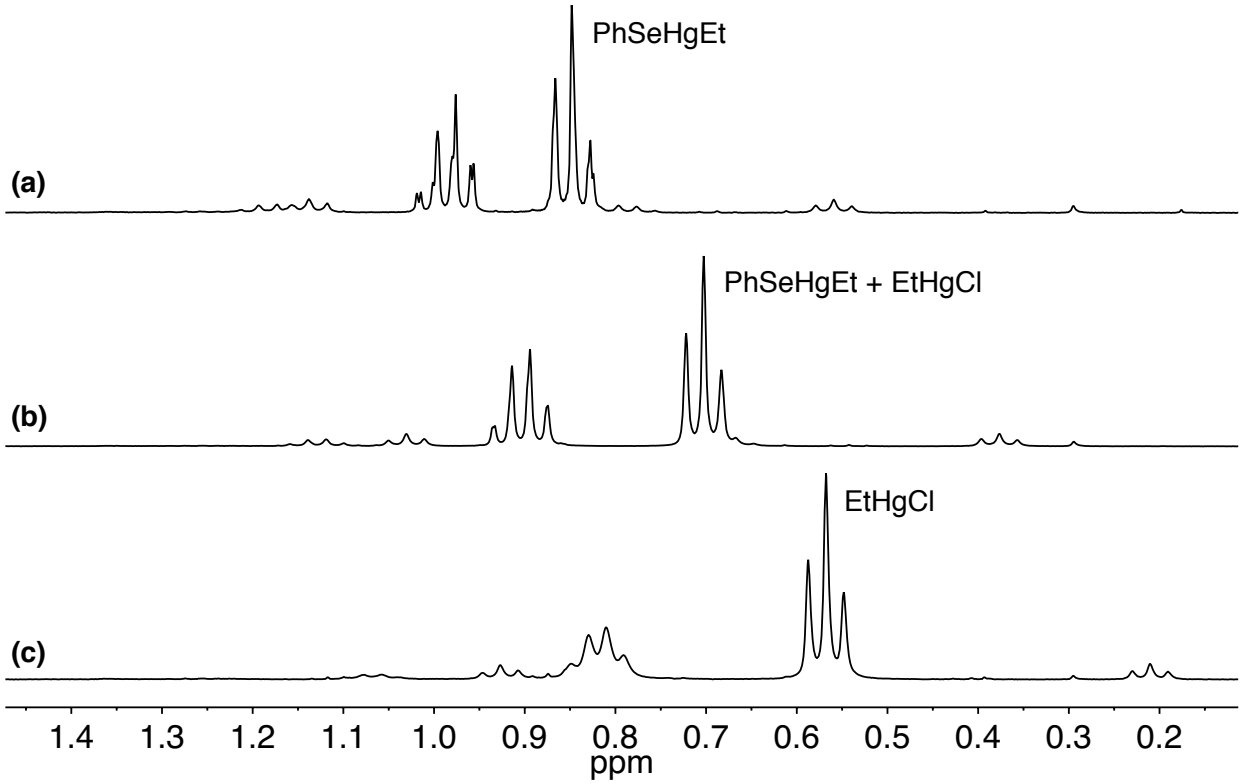

Figure 14. ^{1}H NMR spectra (400 MHz) of the ethyl region of (a) PhSeHgEt, (b) a mixture of PhSeHgEt and EtHgCl, and (c) EtHgCl.

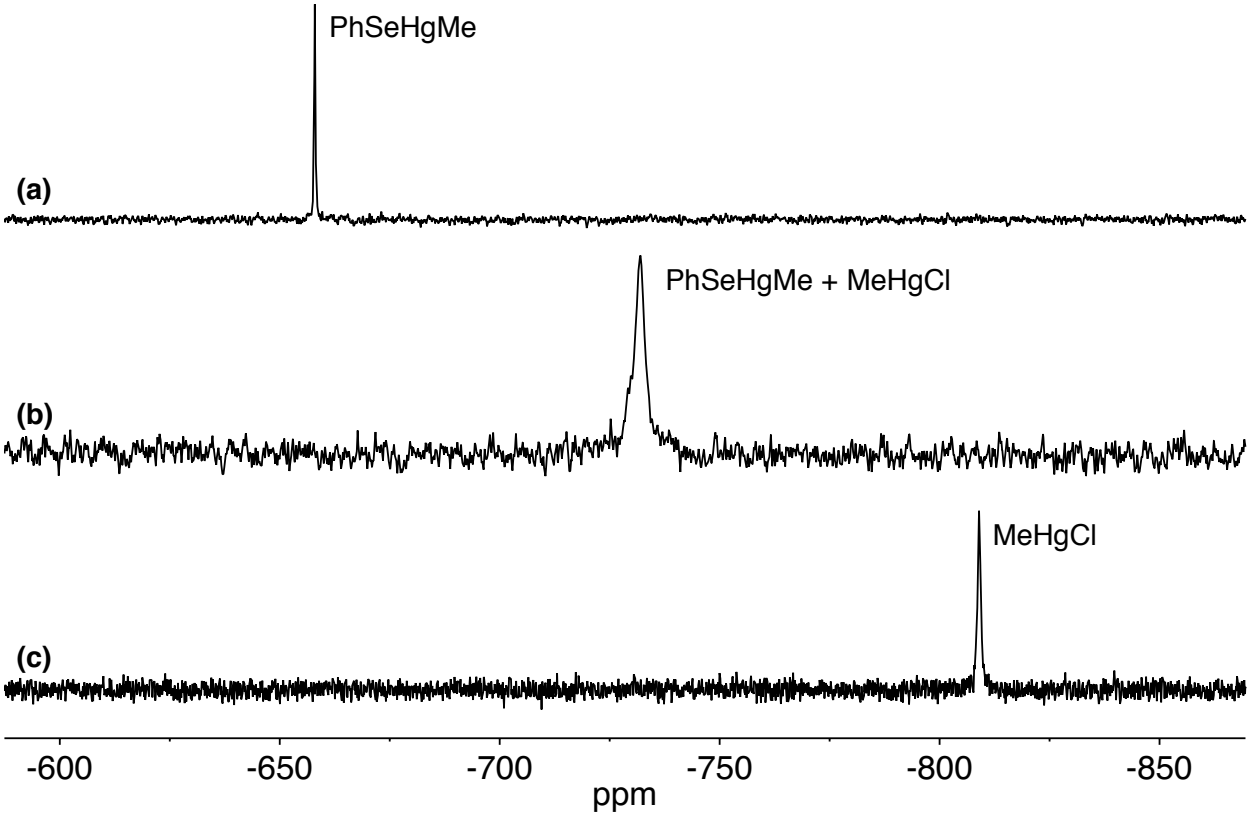

Figure 15. ^{199}Hg NMR spectra of (a) PhSeHgMe, (b) a mixture of PhSeHgMe and MeHgCl, and (c) MeHgCl.

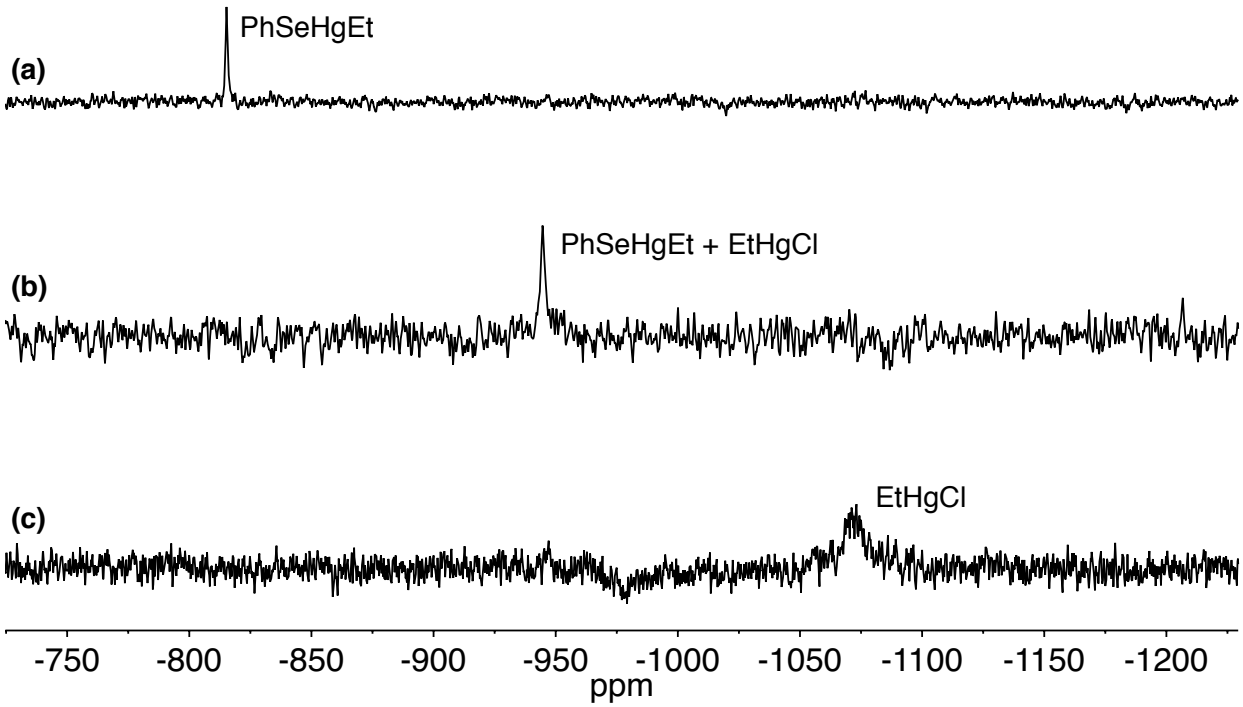

Figure 16. ^{199}Hg NMR spectra of (a) PhSeHgEt, (b) a mixture of PhSeHgEt and EtHgCl, and (c) EtHgCl.

Two possible mechanisms for the degenerate exchange reactions described above can be envisioned. As illustrated in Scheme 5, one involves Hg–R/Hg–R metathesis while the other involves Hg–SePh/Hg–X metathesis.[79] Of these, the latter option appears more consistent with the NMR spectroscopic data. For example, in a mixture of PhSeHgR and RHgCl, the exchange-averaged alkyl signals in the ^{1}H NMR spectrum retain ^{199}Hg coupling (albeit a weighted average of the exchanging species), indicating that Hg–C bond cleavage does not occur on the timescale associated with the exchange process.[80,81] Furthermore, the ^{199}Hg{^{1}H} NMR spectrum of a mixture of PhSeHgMe and PhSeHgEt exhibits two distinct spectroscopic signals, rather than a single signal which would be expected if the alkyl groups were exchanging (Figure 17).

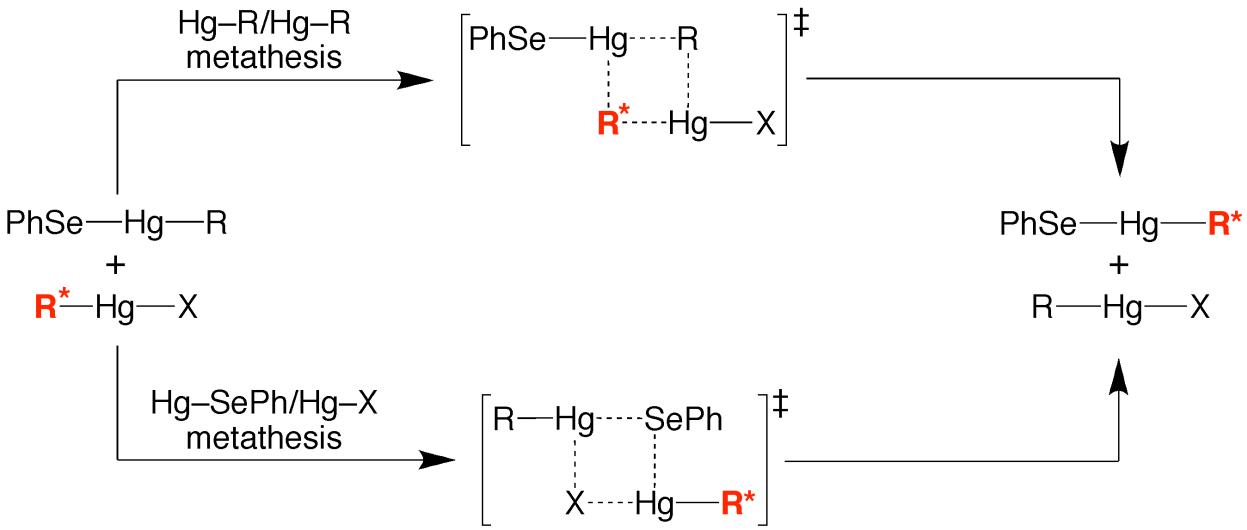

Scheme 5. Two possible mechanisms for degenerate exchange reactions involving PhSeHgR and RHgCl.

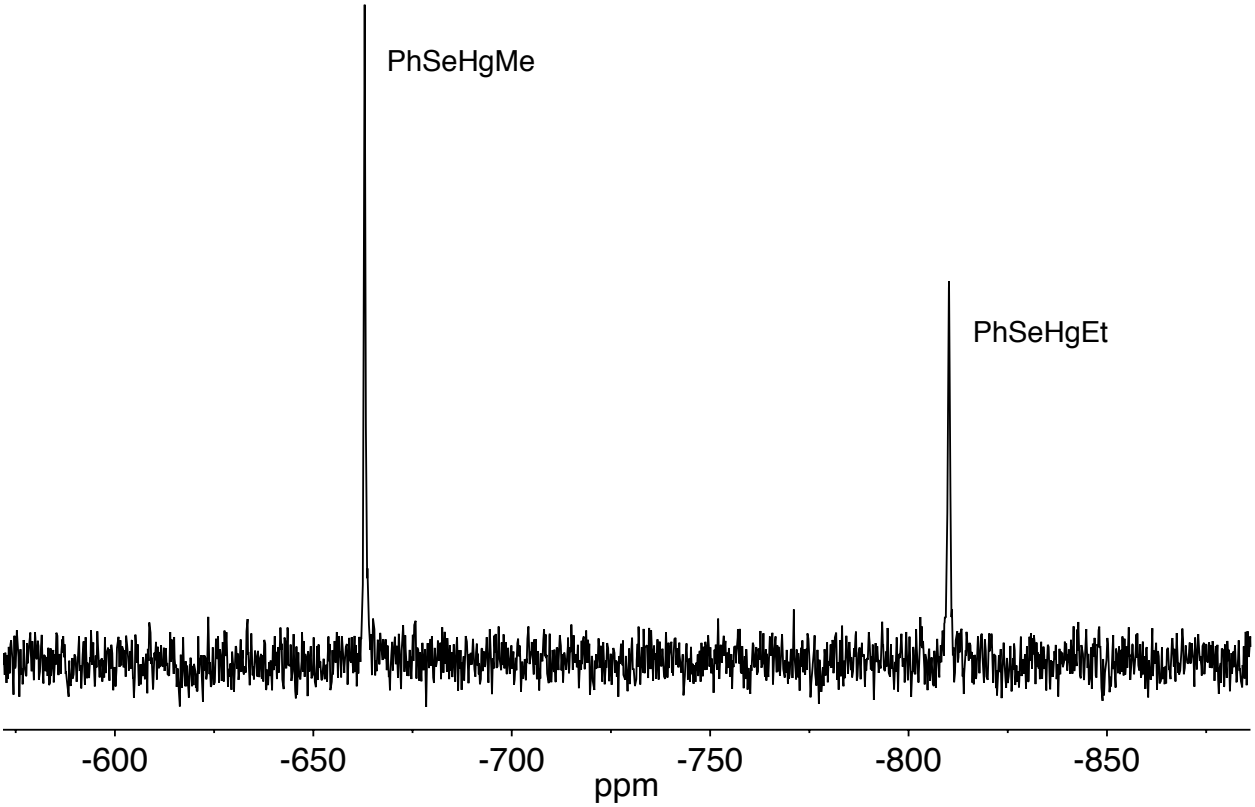

Figure 17. $^{199}Hg\{^{1}H\}$ NMR spectrum of a mixture of PhSeHgMe and PhSeHgEt.

Previous studies involving RHgX compounds also indicate that metathesis involving Hg–X bonds is more facile than those involving Hg–R bonds, likely due to the availability of the lone pairs on X that favor a 4-centered transition state as depicted in Scheme 5.[82,83] It is noteworthy that a previous investigation proposed Hg–R/Hg–R metathesis as a means to explain the greater linewidth of ^{199}Hg satellite peaks in the ^{1}H NMR spectra of RHgX compounds (*e.g.* MeHgI)[84]. However, this result was later proposed to be due to quadrupolar relaxation of the adjacent ^{127}I nucleus inducing relaxation of the ^{199}Hg nucleus, thereby increasing the linewidth of the satellite signals relative to the central signal[85] (i.e. scalar relaxation of the second kind[86]). In addition, it

is also possible that relaxation due to chemical shift anisotropy could also contribute to the width of the satellites.

1.4.2 Cleavage of the Hg–C bond in PhSeHgR (R = Me, Et)

Previously, the Parkin group examined the propensity of PhSHgR to undergo protolytic Hg–C bond cleavage with PhSH.[32b] To further study factors that promote Hg–C bond cleavage, in particular, how the coordination of selenium ligands to mercury affects cleavage, the reactivity of PhSeHgR (R = Me, Et) towards the acids ArEH (Ar = Ph, C_6F_5; E = O, S, Se) was investigated and their results compared to that of the thiolate derivatives.

Scheme 6. Reactivity of PhEHgR with ArEH.

The phenylselenolate compound, PhSeHgEt, reacts readily with PhSH at room temperature to generate ethane over the course of one day.[87] However, the reaction of PhSHgEt with PhSH requires elevated temperatures or longer reaction times at room temperature to efficiently liberate ethane.[32b] The use of PhSeH in place of PhSH has an even more profound effect on the rate of ethane generation, with the reaction of PhSeHgEt and PhSeH essentially going to completion in approximately 20 minutes. Interestingly, when PhSHgEt is treated with PhSeH, ligand exchange occurs to produce PhSeHgEt and PhSH, which then slowly produces ethane over the course of several days. It is apparent that coordination of selenium to mercury and the use of selenium-containing acids promotes Hg–C bond cleavage more effectively than the sulfur counterparts.

Also of note, the protolytic cleavage of a Hg–Et bond in this system appears to be more facile than the cleavage of a Hg–Me bond. For example, while the generation of ethane from the reaction of PhSeHgEt and PhSH is complete after a period of 1 day at room temperature, only negligible amounts of methane are produced from a mixture of PhSeHgMe and PhSH under identical conditions. For comparison, the reaction of PhSHgMe and PhSH requires heating at 145˚C for extended periods to release considerable amounts of methane.[32b] Similar to the ethyl complexes, the reaction of PhSeHgMe with PhSeH, instead of PhSH, results in more efficient release of methane, and the reaction of PhSHgMe with PhSeH results in redistribution to PhSeHgMe and PhSH, followed by the slow release of methane. The more facile Hg–Et versus Hg–Me bond cleavage in this system is contrary to what has been observed in the protonolysis of RHgI by $HClO_4$ and H_2SO_4, where the Hg–Me bond is more reactive.[88,89] This result suggests that the nature of the X ligand can have a profound effect on protolytic Hg–C bond cleavage and that there is still much to learn regarding the factors that influence the dealkylation of mercury compounds, and consequently, mercury detoxification.

To further explore Hg–C bond cleavage in the PhEHgR system, the use of PhOH as a protic reagent was investigated. However, mixtures of PhEHgR and PhOH do not yield any detectable quantities of methane or ethane at room temperature over the course of 1 week. One possible rationalization for the increase in activity towards Hg–C bond cleavage along the series PhSeH > PhSH > PhOH could involve increased acidity (pK_a's PhSeH = 5.9, PhSH = 6.6, PhOH = 10).[90] To test this hypothesis, the use of a more acidic, oxygen-containing protic reagent (pentafluorophenol, C_6F_5OH, $pK_a = 5.5$)[91] was utilized. However, when PhEHgR was treated with C_6F_5OH, no detectable quantities of

methane or ethane were produced over the course of 1 week at room temperature. Thus, a reliance on relative acidities to explain this behavior is not entirely satisfactory.

As with any metathesis reaction, all bonds being broken and formed must be considered. With regards to the PhSeHgR/PhSeH system, the formation of a new Hg–Se bond, in conjunction with the cleavage of an Se–H bond, provides a better thermodynamic driving force for the production of methane and ethane versus the use of PhSH. As a result, it can be concluded that in this system mercury complexes coordinated by selenium ligands tend to promote Hg–C bond cleavage more rapidly than their sulfur analogues. Additionally, the use of a selenium-containing acid, such as PhSeH, permits more efficient protolytic Hg–C bond cleavage than PhSH, PhOH, or C_6F_5OH.

As a result of these studies, it can be concluded that in this system mercury complexes that are already coordinated by selenium ligands tend to promote Hg–C bond cleavage more rapidly than their sulfur analogues, and that the use of a selenium-containing acid, which is accompanied by the formation of a new Hg–Se bond, permits more efficient protolytic Hg–C bond activation.

1.5 Summary and Conclusions

Sulfur–containing amino acid complexes of $[MeHg]^+$, namely (Cys)HgMe and (GS)HgMe, have been synthesized and characterized. An improved X–ray crystal structure of (Cys)HgMe reveals unidentate coordination through the deprotonated thiol group to $[MeHg]^+$ thereby resulting in a linear geometry. Additionally, ^1H NMR studies confirm cysteine coordination, and in the presence of excess cysteine, exchange is observed, a result that is of relevance to mercury chemistry and detoxification.

(GS)HgMe is proposed to coordinate to $[MeHg]^+$ *via* only the deprotonated thiol group in a unidentate fashion, similar to (Cys)HgMe, on the basis of ^1H NMR experiments, geometry optimizations, and previous literature investigation.

The phenylselenolate mercury alkyl complexes, PhSeHgR (R = Me, Et), have also been synthesized and characterized. X–ray crystal structures of PhSeHgR reveal a linear geometry with ^1H and ^{199}Hg NMR experiments confirming mercury coordination. PhSeHgR undergoes degenerate exchange reactions with RHgCl and various PhEHgR complexes which involves the metathesis of Hg–SePh/Hg–X bonds as indicated by NMR data. Additionally, the propensity of PhSeHgR to undergo protolytic Hg–C bond cleavage has been investigated. The coordination of selenium to mercury promotes protolytic cleavage of Hg–C bonds, and the use of selenium containing acids, such as PhSeH, also promotes Hg–C bond cleavage.

1.6 Experimental Details

1.6.1 General Considerations

All manipulations were performed in air unless otherwise stated, in which case a combination of glovebox, high vacuum and Schlenk techniques under a nitrogen or argon atmosphere were used.[92] Solvents were purified and degassed by standard procedures. NMR spectra were measured on Bruker 300 DRX, Bruker 400 Avance III, Bruker 400 DRX, and Bruker Avance 500 DMX spectrometers. ^1H NMR spectra are reported in ppm relative to $SiMe_4$ ($\delta = 0$) and were referenced internally with respect to the protio solvent impurity ($\delta = 7.26$ for $CDCl_3$, $\delta = 7.16$ for C_6D_5H, $\delta = 4.74$ for D_2O, $\delta = 2.50$ for Me_2SO-d_5).[93] ^{13}C NMR spectra are reported in ppm relative to $SiMe_4$ ($\delta = 0$) and were referenced internally with respect to the solvent ($\delta = 128.06$ for C_6D_6 and $\delta = 77.16$ for $CDCl_3$).[94] For ^{13}C NMR spectra reported in D_2O, spectra are reported in ppm relative

to DSS ($\delta = 0$) and were obtained by using the $\Xi/100\%$ value of 25.144953.[93] ^{199}Hg{^{1}H} NMR spectra are reported in ppm relative to Me_2Hg ($\delta = 0$) and were obtained by using the $\Xi/100\%$ value of 17.910822.[95] Coupling constants are reported in hertz. IR spectra were recorded as KBr pellets on a Nicolet iS10 FT-IR spectrometer (ThermoScientific), and the data are reported in reciprocal centimeters (cm^{-1}). Mass spectra were obtained on a JEOL JMS-HX110HF tandem mass spectrometer using fast atom bombardment (FAB). Ph_2Se_2 was purchased from Strem Chemicals, EtHgCl was purchased from Alfa Aesar, and all other chemicals were purchased from Sigma-Aldrich. *CAUTION: All mercury compounds are toxic and appropriate safety precautions must be taken in handling these compounds*.

1.6.2 X-ray Structure Determinations

X-ray diffraction data were collected on a Bruker Apex II diffractometer. Crystal data, data collection, and refinement parameters are summarized in Table 4. The structures were solved using direct methods and standard difference map techniques, and were refined by full-matrix least-squares procedures on F^2 with SHELXTL (Versions 2008/4 and 2014/7).[96]

1.6.3 Computational Details

Calculations were carried out using DFT as implemented in the Jaguar 8.9 (release 15) suite of *ab initio* quantum chemistry programs.[97] Geometry optimizations were performed with the B3LYP density functional using the LACVP** basis sets.[98] Cartesian coordinates and energies of the geometry optimized structures are provided in Table 6.

1.6.4 Synthesis of (Cys)HgMe

(Cys)HgMe was prepared by modifying a previous literature method.[33] To a suspension of L-cysteine (274 mg, 2.03 mmol) in a 50/50 mixture of EtOH/H_2O (150 mL), MeHgOH (2 mL of a 1 M solution in H_2O, 2.00 mmol) was added dropwise. The white suspension was stirred for 3 hours, filtered, and the filtrate pumped to dryness on a rotary evaporator to yield (Cys)HgMe as a white solid (412 mg, 61%). Colorless crystals of (Cys)HgMe suitable for X-ray diffraction were obtained by slow evaporation of a solution in H_2O. Anal. calcd for (Cys)HgMe: C, 14.3; H, 2.7; N, 4.2. Found: C, 14.0; H, 2.8; N, 4.0. ^{1}H NMR (D_2O): 0.82 [s, $^2J_{Hg-H}$ = 173, 3 H of [$(NH_3)CH(CO_2)CH_2S$]Hg$C\underline{H}_3$], 3.55 [m, 2 H of [$(NH_3)CH(CO_2)C\underline{H}_2S$]Hg$CH_3$], 4.12 [broad t, 1 H of [$(NH_3)C\underline{H}(CO_2)C\underline{H}_2S$]Hg$CH_3$].

1.6.5 NMR spectroscopic investigation of degenerate exchange involving (CysHgMe) and cysteine

A solution of (Cys)HgMe (10.1 mg, 0.030 mmol) and cysteine (3.6 mg, 0.030 mmol) in D_2O (0.7 mL) was transferred to an NMR tube equipped with a J. Young valve. The sample was examined by ^{1}H NMR spectroscopy, thereby demonstrating broad peaks for the alpha and beta hydrogens of (Cys)HgMe and cysteine at room temperature.

1.6.6 Synthesis of (GS)HgMe

To a suspension of MeHgCl (80 mg, 0.32 mmol) in a 50/50 mixture of EtOH/H_2O (5 mL), a solution of glutathione (98 mg, 0.32 mmol) in the same solvent was added dropwise bringing the total volume of the reaction to 10 mL. This was then stirred for 18 hours resulting in a colorless solution. The reaction mixture was then pumped to dryness to yield (GS)HgMe as a white solid (81 mg, 49%). Anal. calcd for (GS)HgMe: C, 25.3; H, 3.7; N, 8.1. Found: C, 25.0; H, 3.8; N, 8.0. ^{1}H NMR (D_2O): 0.75 [s, $^2J_{Hg-H}$ = 172, 3 H of (GS)Hg$C\underline{H}_3$], 2.20 [m, 2 H of (GS)HgCH_3], 2.58 [m, 2 H of (GS)HgCH_3], 3.37 [m, 2 β-H

of (GS)$HgCH_3$], 3.97 [m, 1 H of (GS)$HgCH_3$], 4.01 [m, 2 H of (GS)$HgCH_3$], 4.61 [m, 1 H of (GS)$HgCH_3$]. $^{13}C\{^1H\}$ NMR (D_2O): 9.19 [s, 1 C of (GS)$HgCH_3$], 25.63 [s, 1 C of (GS)$HgCH_3$],28.26 [s, 1 C of (GS)$HgCH_3$], 31.04 [s, 1 C of (GS)$HgCH_3$], 41.11 [s, 1 C of (GS)$HgCH_3$], 52.84 [s, 1 C of (GS)$HgCH_3$], 56.62 [s, 1 C of (GS)$HgCH_3$], 172.38 [s, 1 C of (GS)$HgCH_3$], 172.77 [s, 1 C of (GS)$HgCH_3$], 173.02 [s, 1 C of (GS)$HgCH_3$], 174.52 [s, 1 C of (GS)$HgCH_3$].

1.6.7 Synthesis of PhSeHgMe

PhSeHgMe was synthesized by a method related to that in the literature.[75] An ethanol solution (50 mL) of diphenyl diselenide (264 mg, 0.85 mmol) was treated with an ethanol solution (20 mL) of sodium borohydride (65 mg, 1.7 mmol). The yellow solution slowly turned colorless over a period of several minutes, and the resulting solution was treated with an ethanol solution (30 mL) of MeHgCl (423 mg, 1.7 mmol). The suspension was stirred for 2.5 hours, allowed to settle, and filtered. The volatile components of the filtrate were removed *in vacuo* leaving PhSeHgMe as a yellow powder (395 mg, 63%). Anal. calcd for PhSeHgMe: C, 22.6; H, 2.2. Found: C, 22.7; H, 2.0. ^1H NMR (C_6D_6): 0.21 [s, $^2J_{Hg-H}$ = 155, 3 H of $C_6H_5SeHgCH_3$], 6.93 [m, 3 H of $C_6H_5SeHgMe$], 7.59 [m, 2 H of $C_6H_5SeHgMe$]; ^1H NMR ($CDCl_3$): 0.95 [s, $^2J_{Hg-H}$ = 155, 3 H of $C_6H_5SeHgCH_3$], 7.17 [m, 3 H of $C_6H_5SeHgMe$], 7.56 [m, 2 H of $C_6H_5SeHgMe$]. $^{13}C\{^1H\}$ NMR ($CDCl_3$): 16.4 [$^1J_{Hg-C}$ 1080 Hz, 1 C of PhSeHgCH_3], 126.2 [1 C of C_6H_5Hg], 126.3 [1 C of C_6H_5Hg], 129.1 [2 C of C_6H_5Hg], 135.9 [2 C of C_6H_5Hg]. ^{199}Hg NMR (C_6D_6): –658. IR Data (KBr pellet, cm^{-1}): 3059 (w), 2990 (w), 2905 (m), 1658 (w), 1572 (s), 1471 (vs), 1431 (s), 1322 (w), 1292 (w), 1263 (w), 1179 (w), 1159 (w), 1067 (s), 1018 (s), 996 (m), 889 (w), 767 (m), 726 (vs), 687 (vs), 663 (s). FAB-MS m/z = 372.0 $[M]^+$, M = PhSeHgMe.

1.6.8 Synthesis of PhSeHgEt

An ethanol solution (60 mL) of diphenyl diselenide (274 mg, 0.88 mmol) was treated with an ethanol solution (15 mL) of sodium borohydride (66 mg, 1.7 mmol). The yellow solution slowly turned colorless over a period of several minutes and the resulting solution was treated with an ethanol solution (25 mL) of EtHgCl (466 mg, 1.76 mmol). The suspension was stirred for 10 hours, allowed to settle, and filtered. The volatile components of the filtrate were removed *in vacuo* leaving PhSeHgEt as a yellow powder (488 mg, 72%). Anal. calcd for PhSeHgEt: C, 24.9; H, 2.6. Found: C, 25.0; H, 1.6. ^{1}H NMR (C_6D_6, 500 MHz): 0.85 [t, $^{3}J_{H-H}$ = 8, 3 H of PhSeHgCH$_2$C$\underline{H}_3$], 0.99 [q, $^{3}J_{H-H}$ = 8, 2 H of PhSeHgC$\underline{H}_2$CH$_3$], 6.92 [m, 3 H of C$_6\underline{H}_5$SeHgEt], 7.59 [m, 2 H of C$_6\underline{H}_5$SeHgEt]; ^{1}H NMR ($CDCl_3$, 500 MHz): 1.37 [t, $^{3}J_{H-H}$ = 8, 3 H of PhSeHgCH$_2$C$\underline{H}_3$], 1.80 [q, $^{3}J_{H-H}$ = 8, 2 H of PhSeHgC$\underline{H}_2$CH$_3$], 7.17 [m, 3 H of C$_6\underline{H}_5$SeHgEt], 7.55 [m, 2 H of C$_6\underline{H}_5$SeHgEt]. ^{13}C{^{1}H} NMR (C_6D_6): 13.6 [$^{2}J_{Hg-C}$ = 63 Hz, 1 C of PhSeHgCH$_2\underline{C}$H$_3$], 31.8 [$^{1}J_{Hg-C}$ 1145 Hz, 1 C of PhSeHg$\underline{C}$H$_2$CH$_3$], 126.1 [1 C of $\underline{C}_6$H$_5$HgEt], 129.2 [2 C of $\underline{C}_6$H$_5$HgEt], 136.1 [2 C of $\underline{C}_6$H$_5$HgEt] (note: the *ipso* carbon is obscured by the solvent); ^{13}C{^{1}H} NMR ($CDCl_3$): 14.0 [$^{2}J_{Hg-C}$ = 63 Hz, 1 C of PhSeHgCH$_2\underline{C}$H$_3$], 32.4 [$^{1}J_{Hg-C}$ 1145 Hz, 1 C of PhSeHg$\underline{C}$H$_2$CH$_3$], 126.3 [1 C of $\underline{C}_6$H$_5$HgEt], 126.4 [1 C of $\underline{C}_6$H$_5$HgEt], 129.1 [2 C of $\underline{C}_6$H$_5$HgEt], 135.9 [2 C of $\underline{C}_6$H$_5$HgEt]. ^{199}Hg{^{1}H} NMR (C_6D_6): –815. IR Data (KBr pellet, cm^{-1}): 3066 (w), 3053 (w), 2965 (m), 2942 (m), 2919 (w), 2855 (m), 1573 (s), 1471 (s), 1433 (s), 1372 (w), 1295 (w), 1172 (m), 1066 (m), 1017 (s), 997 (m), 960 (w), 896 (w), 730 (vs), 690 (vs), 663 (s), 672 (m), 615 (w). FAB-MS m/z = 386.0 $[M]^+$, M = PhSeHgEt.

1.6.9 NMR spectroscopic investivation of degenerate exchange involving PhSeHgMe and MeHgCl

A solution of PhSeHgMe (6 mg, 0.016 mmol) and MeHgCl (4 mg, 0.016 mmol) in C_6D_6 (0.7 mL) was transferred to an NMR tube equipped with a J. Young valve. The sample was examined by ^{1}H NMR spectroscopy, thereby demonstrating a single resonance

attributable to the mercury methyl groups. Similarly, a solution consisting of PhSeHgMe (7 mg, 0.019 mmol) and MeHgCl (5 mg, 0.020 mmol) in C_6D_6 (0.7 mL) was examined by $^{199}Hg\{^1H\}$ NMR, thereby demonstrating a single resonance.

1.6.10 NMR spectroscopic investigation of degenerate exchange involving PhSeHgMe and PhSHgMe

A solution of PhSeHgMe (6 mg, 0.016 mmol) and PhSHgMe (5 mg, 0.015 mmol) in C_6D_6 (0.7 mL) was transferred to an NMR tube equipped with a J. Young valve. The sample was examined by ^1H NMR spectroscopy, thereby demonstrating a single resonance attributable to the mercury methyl groups.

1.6.11 NMR spectroscopic investigation of degenerate exchange involving PhSeHgEt and EtHgCl

A solution of PhSeHgEt (5 mg, 0.013 mmol) and EtHgCl (3 mg, 0.011 mmol) in C_6D_6 (0.7 mL) was transferred to an NMR tube equipped with a J. Young valve. The sample was examined by ^1H NMR spectroscopy, thereby demonstrating a single resonance attributable to the mercury ethyl groups. Similarly, a solution consisting of PhSeHgEt (15 mg, 0.039 mmol) and EtHgCl (10 mg, 0.038 mmol) in C_6D_6 (1.5 mL) was examined by $^{199}Hg\{^1H\}$ NMR, thereby demonstrating a single resonance.

1.6.12 NMR spectroscopic investigation of exchange involving PhSeHgMe and PhSeHgEt

A solution of PhSeHgMe (6 mg, 0.016 mmol) and PhSeHgEt (6 mg, 0.016 mmol) in C_6D_6 (0.7 mL) was examined by $^{199}Hg\{^1H\}$ NMR spectroscopy, which showed independent signals for PhSeHgMe and PhSeHgEt, thereby indicating that exchange of methyl and ethyl groups is not facile on the NMR timescale.

1.6.13 Reactivity of PhSeHgEt towards PhSH

A solution of PhSeHgEt (10 mg, 0.026 mmol) in C_6D_6 (0.7 mL) was treated with PhSH (2.7 μL, 0.026 mmol) and transferred to an NMR tube equipped with a J. Young valve. The reaction was monitored by ^1H NMR spectroscopy, thereby demonstrating the release of C_2H_6 over a period of 1 day at room temperature, accompanied by the formation of a precipitate which is assigned as a rapidly interconverting mixture of (PhS)Hg(SePh), $(PhS)_2Hg$ and $(PhSe)_2Hg$ in solution.

1.6.14 Reactivity of PhSeHgEt towards PhSeH

A solution of PhSeHgEt (10 mg, 0.026 mmol) in C_6D_6 (0.7 mL) was treated with PhSeH (2.8 μL, 0.026 mmol) and transferred to an NMR tube equipped with a J. Young valve. The reaction was monitored by ^1H NMR spectroscopy, thereby demonstrating the release of C_2H_6 over a period of 20 minutes, accompanied by the precipitation of $(PhSe)_2Hg$.

1.6.15 Reactivity of PhSHgEt towards PhSeH

A solution of PhSHgEt (10 mg, 0.030 mmol) in C_6D_6 (0.7 mL) was treated with PhSeH (3.2 μL, 0.030 mmol) and transferred to an NMR tube equipped with a J. Young valve. The reaction was monitored by ^1H NMR spectroscopy, thereby demonstrating the formation of PhSeHgEt, PhSH, and a small amount of C_2H_6 which is slowly produced over the course of 1 day. The reaction is also accompanied by the formation of a precipitate which is assigned as a rapidly interconverting mixture of (PhS)Hg(SePh), $(PhS)_2Hg$ and $(PhSe)_2Hg$ in solution.

1.6.16 Reactivity of PhSeHgMe towards PhSH

A solution of PhSeHgMe (10 mg, 0.027 mmol) in C_6D_6 (0.7 mL) was treated with PhSH (2.8 μL, 0.027 mmol) and transferred to an NMR tube equipped with a J. Young valve. The sample was monitored by ^1H NMR spectroscopy, thereby demonstrating that there is negligible formation of CH_4 over a period of 1 day at room temperature.

1.6.17 Reactivity of PhSeHgMe towards PhSeH

A solution of PhSeHgMe (10 mg, 0.027 mmol) in C_6D_6 (0.7 mL) was treated with PhSeH (2.8 μL, 0.027 mmol) and transferred to an NMR tube equipped with a J. Young valve. The sample was monitored by ^1H NMR spectroscopy, thereby demonstrating that CH_4 is formed over a period of 1 week at room temperature.

1.6.18 Reactivity of PhSHgMe towards PhSeH

A solution of PhSeHgMe (10 mg, 0.031 mmol) in C_6D_6 (0.7 mL) was treated with PhSeH (3.2 μL, 0.030 mmol) and transferred to an NMR tube equipped with a J. Young valve. The sample was monitored by ^1H NMR spectroscopy, thereby demonstrating the formation of PhSeHgMe and PhSH which produces negligible amounts of CH_4 over the course of 1 day at room temperature.

1.6.19 Reactivity of PhSeHgEt towards PhOH

A solution of PhSeHgEt (10 mg, 0.026 mmol) in C_6D_6 (0.7 mL) was treated with PhOH (2.2 mg, 0.023 mmol) and transferred to an NMR tube equipped with a J. Young valve. The sample was monitored by ^1H NMR spectroscopy, thereby demonstrating no detectable amount of C_2H_6 after 1 week.

1.6.20 Reactivity of PhSeHgMe towards PhOH

A solution of PhSeHgMe (10 mg, 0.027 mmol) in C_6D_6 (0.7 mL) was treated with PhOH (2.3 mg, 0.024 mmol) and transferred to an NMR tube equipped with a J. Young valve. The sample was monitored by ^1H NMR spectroscopy, thereby demonstrating no detectable amount of CH_4 after 1 week.

1.6.21 Reactivity of PhSHgEt towards PhOH

A solution of PhSHgEt (9.0 mg, 0.027 mmol) in C_6D_6 (0.7 mL) was treated with PhOH (2.6 mg, 0.028 mmol) and transferred to an NMR tube equipped with a J. Young valve. The sample was monitored by ^1H NMR spectroscopy, thereby demonstrating no detectable amount of C_2H_6 after 1 week.

1.6.22 Reactivity of PhSHgMe towards PhOH

A solution of PhSeHgMe (9.0 mg, 0.028 mmol) in C_6D_6 (0.7 mL) was treated with PhOH (2.7 mg, 0.029 mmol) and transferred to an NMR tube equipped with a J. Young valve. The sample was monitored by ^1H NMR spectroscopy, thereby demonstrating no detectable amount of CH_4 after 1 week.

1.6.23 Reactivity of PhSHgEt towards C_6F_5OH

A solution of PhSeHgEt (6.2 mg, 0.016 mmol) in C_6D_6 (0.7 mL) was treated with C_6F_5OH (3.5 mg, 0.019 mmol) and transferred to an NMR tube equipped with a J. Young valve. The sample was monitored by ^1H NMR spectroscopy, thereby demonstrating no detectable amount of C_2H_6 after 1 week.

1.6.24 Reactivity of PhSHgEt towards C_6F_5OH

A solution of PhSeHgMe (9.2 mg, 0.025 mmol) in C_6D_6 (0.7 mL) was treated with C_6F_5OH (4.9 mg, 0.026 mmol) and transferred to an NMR tube equipped with a J. Young valve. The sample was monitored by ^1H NMR spectroscopy, thereby demonstrating no detectable amount of CH_4 after 1 week.

1.7 Crystallographic Data

Table 4. Crystal, intensity collection, and refinement data.

	[(Cys)HgMe]•H_2O	**PhSeHgMe**
lattice	Orthorhombic	Orthorhombic
formula	$C_4H_{11}HgNO_3S$	C_7H_8HgSe
formula weight	353.79	371.68
space group	$P2_12_12_1$	*Pbcn*
a / Å	5.2506(11)	24.803(12)
b / Å	6.3712(13)	9.758(5)
c / Å	25.700(5)	7.041(3)
α / °	90	90
β / °	90	90
γ / °	90	90
V / Å^3	859.7(3)	1704.2(14)
Z	4	8
temperature (K)	130(2)	200(2)
radiation (λ, Å)	0.71073	0.71073
ρ (calcd.) g cm^{-3}	2.733	2.897
μ (Mo Kα), mm^{-1}	18.100	22.249
θ max, deg.	32.019	30.71
no. of data collected	14376	24879
no. of data	2989	2631
no. of parameters	108	82
R_1 [$I > 2\sigma(I)$]	0.0379	0.0297
wR_2 [$I > 2\ \sigma(I)$]	0.0936	0.0549
R_1 [all data]	0.0401	0.0682
wR_2 [all data]	0.0946	0.0653
GOF	1.109	1.008
R_{int}	0.0476	0.0836

Table 4. Crystal, intensity collection, and refinement data.

	PhSeHgEt
lattice	Monoclinic
formula	$C_8H_{10}HgSe$
formula weight	385.71
space group	$P2_1/c$
a / Å	14.275(5)
b / Å	17.858(7)
c / Å	7.239(3)
α / °	90
β / °	91.743(6)
γ / °	90
V / Å^3	1844.7(12)
Z	8
temperature (K)	200(2)
radiation (λ, Å)	0.71073
ρ (calcd.) g cm^{-3}	2.778
μ (Mo Kα), mm^{-1}	20.559
θ max, deg.	29.61
no. of data collected	27354
no. of data	5165
no. of parameters	181
R_1 [$I > 2\sigma(I)$]	0.0372
wR_2 [$I > 2\ \sigma(I)$]	0.0570
R_1 [all data]	0.1059
wR_2 [all data]	0.0726
GOF	1.007
R_{int}	0.0653

1.8 Computational Data

Table 5. Cartesian Coordiantes for Geometry Optimized (Cys)HgMe

(Cys)HgMe -804.008156198035 Hartrees			
atom	**x**	**y**	**z**
Hg	-6.563526129	4.208244633	97.88265464
S	-5.195404572	6.351447897	98.07294047
N	-3.457774444	6.238091632	100.8246125
H	-3.558805443	4.506749648	101.431545
H	-3.103617263	7.10594803	101.21491
H	-3.181439849	6.202012682	99.84093107
O	-4.343732498	3.899036665	101.3737614
O	-6.436907012	4.277904194	100.6742266
C	-7.725465868	2.365166284	97.4245885
H	-7.15912744	1.510014744	97.7948147
H	-7.875829739	2.286803523	96.34740142
H	-8.683251701	2.434505719	97.94115613
C	-5.674525611	6.914296402	99.76761883
H	-5.434177443	7.980831648	99.81765476
H	-6.749313992	6.808771871	99.92498736
C	-4.925619206	6.180281262	100.8881376
H	-5.23689742	6.610708974	101.8515259
C	-5.32574293	4.692183663	100.9593887

Table 6. Cartesian Coordinates for Geometry Optimized (GS)HgMe

(GS)HgMe -1487.23051067954 Hartrees			
atom	**x**	**y**	**z**
S	5.542023983	6.057801611	12.72051454
C	2.586268983	3.567964975	10.98967945
C	1.881773825	4.040736393	9.705977987
C	2.50399299	5.285860768	9.046983257
C	2.450181664	6.509095921	9.956947162
C	1.818126836	2.362754394	11.5926248
C	3.808229172	7.930213444	11.45548374
C	4.092009017	7.20905931	12.78272266
C	4.867305257	9.008351858	11.17016917
C	5.970154015	10.34924083	9.444252128
C	7.311697381	9.785725463	8.982869704
N	4.010595995	3.214244758	10.85796578
N	3.688332584	7.006487393	10.33346769
N	4.988575536	9.380504677	9.872416171
O	2.624156664	1.403037989	12.05765877
O	0.610501905	2.314099572	11.64969314
O	1.400398195	7.020535038	10.31532371
O	5.541351555	9.520563455	12.07097452
O	8.10465601	10.41082956	8.32050822
O	7.542189118	8.522080305	9.417221559
H	8.427194095	8.285273256	9.089802717
H	3.533040424	1.729126667	11.83324761

H	4.62970892	3.938982603	11.21491557
H	4.267113026	2.990451801	9.901033664
H	2.510628353	4.359761973	11.74601121
H	2.836238137	8.434938074	11.53580101
H	0.836958122	4.238464537	9.955971661
H	1.88048763	3.221710789	8.974947396
H	3.533859526	5.083135788	8.729336835
H	1.929010291	5.527011595	8.146687769
H	4.22828278	7.948286415	13.57254884
H	3.222379644	6.598184734	13.03833999
H	5.580728662	10.96356328	8.628859336
H	6.179930491	11.00995505	10.2917528
H	4.475213159	6.368693158	10.25789823
H	4.480857115	8.833549667	9.190046973
Hg	7.484148064	7.71232724	12.83074482
C	9.367590916	8.881251666	13.05429562
H	10.19396778	8.317691366	12.61907231
H	9.548183355	9.049803031	14.11640364
H	9.238854414	9.832405977	12.53702872

1.9 References and Notes

(1) Cardiano, P. Falcone, G.; Foti, C.; Giuffre, O.; Sammartano, S. *New J. Chem.* **2011**, *35*, 800-806.

(2) Ariya, P. A. Amyot, M.; Dastoor, A.; Deeds, D.; Feinberg, A.; Kos, G. Poulain, A.; Ryjkov, A.; Semeniuk, K. Subir, M. Toyota, K. *Chem. Rev.* **2015**, *115*, 3760–3802.

(3) Branco, V.; Coppo, L.; Sola, S.; Lu, J.; Rodrigues, M. P.; Holmgren, A.; Carvalho, C. *Redox Biol.* **2017**, *13*, 278–287.

(4) Yin, Z.; Jiang, H.; Syversen, T.; Rocha, J. B. T.; Farina, M.; Aschner, M. *J. Neurochem.* **2008**, *107*, 1083–1090.

(5) Bernhoft, R. A. *J. Enviro. Public Health.* **2012**, 460508.

(6) Korbas, M.; O'Donoghue, J. L. Watson, G. E.; Pickering, I. J.; Singh, S. P. Myers, G. J.; Clarkson, T. W.; George, G. N. *ACS Chem. Neurosci.* **2010**, *1*, 810–818.

(7) Khan, M. A. K.; Asaduzzaman, A. Md.; Schreckenbach, G.; Wang, F. *Dalton Trans.* **2009**, 5766–5772.

(8) Harada, M. *Crit. Rev. Toxicol.* **1995**, *25*, 1–24.

(9) Bakir, F.; Damluji, S. F.; Amin-Zaki, L.; Murtadha, M.; Khalidi, A.; Al-Rawi, N. Y.; Tikriti, S.; Dhahir, H. I.; Clarkson, T. W.; Smith, J. C.; Doherty, R. A. *Science* **1973**, *181*, 230–241.

(10) Simoes, M. R.; Azevedo, B. F.; Fiorim, J.; Freire Jr., D. D.; Covre, E. P.; Vassallo, D. V.; dos Santos, L. *Clin. Exp. Pharmacol. Physiol.* **2016**, *43*, 1038–1045.

(11) Laks, D. R. *Biometals.* **2009**, *22*, 1103–1114.

(12) Alderighi, L.; Gans, P.; Midollini, S.; Vacca, A. *Inorganica Chimica Acta.* **2003**, *356*, 8–18.

(13) Lemes, M.; Wang, F.; Stern, G.; Ostertag, S. K.; Chan, H. M. *Environ. Toxicol. Chem.* **2011**, *30*, 2733–2738.

(14) Martinez, C. S.; Torres, J. G. D.; Pecanha, F. M.; Anselmo-Franci, J. A.; Vassallo, D. V.; Salaices, M.; Alonso, M. J.; Wiggers, G. A. *PLoS ONE* **2014**, *9*, e111202.

(15) Arnold, A. P.; Canty, A. J. *Environ. Toxicol. Chem.* **2011**, *30*, 2733–2738.

(16) Rabenstein, D. L.; Evans, C. A. *Bioinorg. Chem.* **1978**, *8*, 107–114.

(17) Rabenstein, D. L.; Fairhurst, M. T. *J. Am. Chem. Soc.* **1975**, *97*, 2086–2092.

(18) Casas, J. S.; Couce, M. D.; Garcia-Vega, M.; Sanchez, A.; Sordo, J.; Lopez, E. M. V. *New J. Chem.* **2016**, *40*, 6735–6744.

(19) Melnick, J. G.; Yurkerwich, K.; Parkin, G. *J. Am. Chem. Soc.* **2010**, *132*, 647–655.

(20) (a) Kohrle, J. *Biochimie* **1999**, *81*, 527-533.
(b) Reddy, C. C.; Massaro, E. J. *Fundam. Appl. Toxicol.* **1983**, *3*, 431-436.
(c) Frost, D. V.; Lish, P. M. *Annu. Rev. Pharmacol. Toxicol.* **1975**, *15*, 259-284.

(21) (a) Prince, R. C.; Gailer, J.; Gunson, D. E.; Turner, R. J.; George, G. N.; Pickering, I. J. *J. Inorg. Biochem.* **2007**, *101*, 1891-1893.
(b) Gailer, J. *Appl. Organometal. Chem.* **2002**, *16*, 701-707.
(c) Yang, D.-Y.; Chen, Y.-W.; Gunn, J. M.; Belzile, N. *Environ. Rev.* **2008**, *16*, 71-92.
(d) Magos, L.; Webb, M.; Clarkson, T. W. *Crit. Rev. Toxicol.* **1980**, *8*, 1-42.
(e) Seppanen, K.; Soininen, P.; Salonen, J. T.; Lotjonen, S.; Laatikainen, R. *Biol. Trace Elem. Res.* **2004**, *101*, 117-132.
(f) Ralston, N. V. C.; Ralston, C. R.; Blackwell III, J. L.; Raymond, L. J. *Neurotoxicology* **2008**, *29*, 802-811.

(22) Sugiura, Y.; Tamai, Y.; Tanaka, H. *Bioinorg Chem.* **1978**, *9*, 167–180.

(23) Yurkerwich, K.; Quinlivan, P. J.; Rong, Y.; Parkin, G. *Polyhedron* **2016**, *103*, 307–314 and references therein.

(24) Palmer, H. J.; Parkin, G. *J. Am. Chem. Soc.* **2015**, *137*, 4503–4516.

(25) Arnold, A. P.; Canty, A. J.; Moors, P. W.; Deacon, G. B *J. Inorg. Biochem* **1983**, *19*, 319–327.

(26) George, G. N.; Prince, R. C.; Gailer, J.; Buttigieg, G. A.; Denton, M. B. Harris, H. H.; Pickering, I. J. *Chem. Res Toxicol.* **2004**, *17*, 999–1006.

(27) Sattler, W.; Palmer, J. H.; Bridges, C. C.; Joshee, L.; Zalups, R. K.; Parkin, G. *Polyhedron* **2013**, *64*, 268–279 and references therein.

(28) Aaseth, J.; Ajsuvakova, O. P.; Skalny, A. V.; Skalnaya, M. G.; Tinkov, A. A. *Coord. Chem. Rev.* **2018**, *358*, 1–12.

(29) Richmond, M. H.; John, M. *Nature* **1964**, *202*, 1360–1361.

(30) Wahba, H. M.; Lecoq, L.; Stevenson, M.; Mansour, A.; Cappadocia, L.; Lafrance-Vanasse, J.; Wilkinson, K. J.; Sygusch, J.; Wilcox, D. E. *Biochemistry* **2016**, *55*, 1070–1081.

(31) Karri, R.; Banerjee, M.; Chalana, A.; Jha, K. K.; Roy, G. *Inorg. Chem.* **2018**, *56*, 12102–12115.

(32) (a) Melnick, J. G.; Parkin, G. *Science* **2007**, *317*, 225–227.
(b) Melnick, J. G.; Yurkerwich, K.; Parkin, G. *Inorg. Chem.* **2009**, 48, 6763-6772.

(33) Taylor, N. J.; Wong, Y. S.; Chieh, P. C.; Carty, A. J. *J. C. S. Dalton* **1975**, 438–442.

(34) Rabenstein, D. L. *Acc. Chem. Res.* **1978**, *11*, 100–107.

(35) Casas, J. S.; Garcia-Tasende, M. S.; Sordo, J. *Coord. Chem. Rev.* **1999**, *193-195*, 283–3593.

(36) The preference of mercury alkyl complexes to be two-coordinate has been attributed to relativistic effects, although other explanations and factors have been suggested. See reference 23 and: Tossell, J. A.; Vaughan, D. J. *Inorg. Chem.* **1981**, *20*, 3333–3340.

(37) Cordero, B.; Gomez, V.; Platero-Prats, A. E.; Reves, M.; Echeverria, J.; Cremades, E.; Barragan, F.; Alvarez, S. *Dalton Trans.* **2008**, 2832-2838.

(38) Batsanov, S. S.; *Inorg. Mater.* **2001**, *37*, 871–885.

(39) Cambridge Structural Database, CSD version 5.39

(40) Lundberg, D.; Persson, I. *Z. Kristallogr.* **2012**, *227*, 683–687.

(41) Williams, N. J.; Hancock, R. D.; Riebenspies, J. H.; Fernandes, M.; de Sousa, A. S. *Inorg. Chem.* **2009**, *48*, 11724–11733.

(42) Holloway, C. E.; Melnik, M. *J. Organomet. Chem.* **1995**, *495*, 1–31.

(43) Wong, Y. S.; Carty, A. J.; Chieh, C. *J. C. S. Dalton Chem.* **1977**, 1801–1808.

(44) Note: there are two independent molecules in the unit cell for [(pen)HgMe]•H_2O.

(45) For reference, the $^2J_{Hg–H}$ coupling constant for MeHgOH is 203 Hz. See: Robert, J. M.; Rabenstein, D. L. *Anal. Chem.* **1991**, *63*, 2674–2679.

(46) Rabenstein D. L.; Reid, R. S. *Inorg. Chem.* **1984**, *23*, 1246–1250.

(47) Simpson, P. G.; Hopkins, T. E.; Haque, R. *J. Phys. Chem.* **1973**, *77*, 2282–2285.

(48) Bach, R. D.; Weibel, A. T. *J. Am. Chem. Soc.* **1976**, *98*, 6241–6249.

(49) Cheesman, B. V.; Arnold, A. P.; Rabenstein, D. L. *J. Am. Chem. Soc.* **1988**, *110*, 6359–6364.

(50) Arnold, A. P.; Canty, A. J. *Can. J. Chem.* **1983**, *61*, 1428–1434.

(51) Rabenstein, D. L.; Evans, C. A. *Bioinorg. Chem.* **1978**, *8*, 107–114.

(52) Rabenstein, D. L.; Isab, A. A.; Reid, R. S. *Biochim. Biophys. Acta.* **1982**, *696*, 53–64.

(53) Rabenstein, D. L. Metal Complexes of Glutathione and their biological Significance. In *Coenzymes and Cofactors*; Wiley: New York, 1986; Vol. 3, pp 147-186

(54) Rabenstein, D. L. *J. Am. Chem. Soc.* **1973**, *95*, 2797–2803.

(55) Rabenstein, D. L.; Fairhurst, M. T. *J. Am. Chem. Soc.* **1975**, *97*, 2086–2092.

(56) Miyoshi, K.; Sugiura, Y.; Ishizu, K.; Iitaka, Y.; Nakamura, H. *J. Am. Chem. Soc.* **1980**, *102*, 6130–6136.

(57) Hannibal, L.; Smith, C. A.; Jacobsen, D. W. *Inorg. Chem.* **2010**, *49*, 9921–9927.

(58) For reference, the $^{2}J_{Hg-H}$ coupling constant of MeHgCl is 204 Hz.

(59) Hore, P. J. *Nuclear Magnetic Resonance*, 1st ed.; Oxford University Press Inc.: New York, 1995

(60) Melnick, J. G.; Yurkerwich, K.; Buccella, D.; Sattler, W.; Parkin, G. *Inorg. Chem.* **2008**, *47*, 6421-6426.

(61) Sattler, W.; Yurkerwich, K.; Parkin, G. *Dalton Trans.* **2009**, 4327-4333.

(62) For some structurally characterized arylthiolate mercury methyl and related compounds, see reference 60 and

(a) Chieh, C. *Can. J. Chem.* **1978**, *56*, 560-563.
(b) Castiñeiras, A.; Hiller, W.; Strähle, J.; Bravo, J.; Casas, J. S.; Gayoso, M.; Sordo, J. *J. Chem. Soc. Dalton Trans.* **1986**, 1945-1948.
(c) Almagro, X.; Clegg, W.; Cucurull-Sánchez, L.; González-Duarte, P.; Traveria, M. *J. Organomet. Chem.* **2001**, *623*, 137-148.
(d) Aupers, J. H.; Howie, R. A.; Wardell, J. L. *Polyhedron* **1997**, *16*, 2283-2289.

(63) The phenylselenolate mercury alkyl complexes, PhSeHgR (R = Me, Et) have been synthesized and structurally characterized previously by Kevin Yurkerwich. See: Yurkerwich, K., The Chemistry of Gallium, Indium, and Mercury Supported by a Sulfur-Rich Coordination Environment. Ph.D. Dissertation, Columbia University, New York City, NY, 2010.

(64) Bochmann, M.; Coleman, A. P.; Powell, A. K. *Polyhedron* **1992**, *11*, 507-512.

(65) Carty, A. J.; Malone, S. F.; Taylor, N. J. *J. Organomet. Chem.* **1979**, *172*, 201-211.

(66) Carty, A. J.; Malone, S. F.; Taylor, N. J.; Canty, A. J. *J. Inorg. Biochem.* **1983**, *18*, 291-300.

(67) Emge, T. J.; Romanelli, M. D.; Moore, B. F.; Brennan, J. G. *Inorg. Chem.* **2010**, *49*, 7304–7312.

(68) Melnick, J. G.; Yurkerwich, K.; Parkin, G. *J. Am. Chem. Soc.* **2010**, *132*, 647-655.

(69) (a) Green, M. L. H. *J. Organomet. Chem.* **1995**, *500*, 127-148.
(b) Parkin, G. in *Comprehensive Organometallic Chemistry III*, Volume 1, Chapter 1.01; Crabtree, R. H. and Mingos, D. M. P. (Eds), Elsevier, Oxford, 2007.
(c) Green, J. C.; Green, M. L. H.; Parkin, G. *Chem. Commun.* **2012,** *48*, 11481−11503.
(d) Green, M. L. H.; Parkin, G. *J. Chem. Educ.* **2014**, *91*, 807-816.

(70) (a) Palmer, J. H.; Parkin, G. *Polyhedron* **2013**, *52*, 658-668.
(b) Palmer, J. H.; Parkin, G. *J. Am. Chem. Soc.* **2015,** 137, 4503−4516.

(71) (a) Brodersen, K.; Liehr, G.; Rosenthal, M.; Thiele, G. *Z. Naturforsch. (B)* **1978**, *33*, 1227-1230.
(b) Brodersen, K.; Liehr, G.; Rosenthal, M. *Chem. Ber.-Recl.* **1977**, *110*, 3291-3296.

(72) Haaland, A. *Angew. Chem. Int. Ed. Engl.* **1989**, *28*, 992-1007.

(73) In cases where the signs of the coupling constants for mercury ethyl compounds have been measured, $^{2}J_{\text{Hg-H}}$ are negative, whereas $^{3}J_{\text{Hg-H}}$ are positive. See: Anet, F. A. L.; Sudmeier, J. L. *J. Magn. Reson.* **1969**, *1*, 124-138.

(74) (a) Evans, D. F.; Maher, J. P. *J. Chem. Soc.* **1962**, 5125-5128
(b) Narasimhan, P. T.; Rogers, M. T. *J. Am. Chem. Soc*. **1960**, *82*, 34-40.
(c) Dessy, R. E.; Flautt, T. J.; Jaffé, H. H.; Reynolds, G. F. *J. Chem. Phys*. **1959**, *30*, 1422-1425.

(75) Canty, A. J.; Carty, A. J.; Malone, S. F. *J. Inorg. Biochem.* **1983**, *19*, 133-142.

(76) We note, however, that the ^{1}H NMR chemical shifts of PhSeHgEt are concentration dependent. Similar variations are also observed for MeHgCl and EtHgCl and could possibly indicate the existence of an equilibrium with a dimeric form. In this regard, it is worth noting that PhHgOMe is dimeric in benzene, while other PhHgOR derivatives exist as an equilibrium mixture of monomer and dimers. See: Bloodworth, A. J. *J. Chem. Soc. (C)* **1970**, 2051-2056.

(77) The observation that the outer satellite signals (and likewise the inner satellite signals) are associated with the same ^{199}Hg spin state is a consequence of the fact that $^{2}J_{\text{Hg-H}}$ and $^{3}J_{\text{Hg-H}}$ have opposite signs.

(78) Bryant, R. G. *J. Chem. Educ.* **1983**, *60*, 933-935.

(79) While the Hg–SePh/Hg–X metathesis illustrated in Scheme 5 is depicted as bimolecular, other exchange mechanisms are possible, including those that are dissociative in nature.

(80) Faller, J. W. "Dynamic NMR Spectroscopy in Organometallic Chemistry" in *Comprehensive Organometallic Chemistry III*, Volume 1, Chapter 1.15; Crabtree, R. H. and Mingos, D. M. P. (Eds), Elsevier, Oxford, 2007.

(81) Furthermore, the observation of ^{199}Hg satellites in the ^{1}H NMR spectra of individual samples of PhSeHgR and RHgX also indicates that degenerate Hg–R/Hg–R metathesis does not occur. We also note that neither ^{199}Hg–^{77}Se coupling nor long range ^{199}Hg–^{1}H coupling involving the phenyl group are observed in the ^{1}H NMR spectra of PhSeHgR. Since long range ^{199}Hg–^{1}H coupling has been observed in mercury alkyl and aryl compounds,[a-d] the absence of these couplings may be associated with facile exchange of the phenylselenolate ligand.
(a) Singh, G.; Reddy, G. S. *J. Organomet. Chem.* **1972**, *42*, 267-275.
(b) Banney, P. J.; Wells, P. R. *Aust. J. Chem.* **1971**, *24*, 317-324.
(c) Wrackmeyer, B.; Contreras, R. *Annu. Rep. NMR Spectrosc.* **1992**, *24*, 267-329.
(d) Bebout, D. C.; Garland, M. M.; Murphy, G. S.; Bowers, E. V.; Abelt, C. J.; Butcher, R. J. *Dalton Trans.* **2003**, 2578-2584.

(82) (a) Bach, R. D.; Weibel, A. T. *J. Am. Chem. Soc.* **1976**, *98*, 6241-6249.
(b) Bach, R. D.; Weibel, A. T. *J. Am. Chem. Soc.* **1975**, *97*, 2575-2576.

(83) Murrell, L. L.; Brown, T. L. *J. Organomet. Chem.* **1968**, *13*, 301-311.

(84) Hatton, J. V.; Schneider, W.G.; Siebrand, W. *J. Chem. Phys.* **1963**, *39*, 1330-1336.

(85) Simpson, R. B. *J. Chem. Phys.* **1967**, *46*, 4775-4783.

(86) Bruch, M. *NMR Spectroscopy Techniques* (2nd Ed). Marcel Dekker, New York, 1996.

(87) The mercury product is tentatively identified as heteroleptic (PhS)Hg(SePh), which undergoes redistribution to form a mixture with $(PhS)_2Hg$ and $(PhSe)_2Hg$.

(88) Kreevoy, M. M.; Hansen, R. L. *J. Am. Chem. Soc.* **1961**, *83*, 626-630.

(89) Nugent, W. A.; Kochi, J. K. *J. Am. Chem. Soc.* **1976**, *98*, 5979-5988.

(90) Physical Constants of Organic Compounds. In *CRC Handbook of Chemistry and Physics*. 98th ed.; [Online]; Rumble, J. R., Ed.; CRC Press: Boca Raton, FL, 2017; RN 110-82-7; http://hbcponline.com/faces/contents/ContentsSearch.xhtml (accessed Feb, 2018)

(91) Han, J.; Tao, F. *J. Phys. Chem. A* **2006**, *110*, 257–263.

(92) (a) McNally, J. P.; Leong, V. S.; Cooper, N. J. in *Experimental Organometallic Chemistry*, Wayda, A. L.; Darensbourg, M. Y., Eds.; American Chemical Society: Washington, DC, 1987; Chapter 2, pp 6-23.
(b) Burger, B.J.; Bercaw, J. E. in *Experimental Organometallic Chemistry*; Wayda, A. L.; Darensbourg, M. Y., Eds.; American Chemical Society: Washington, DC, 1987; Chapter 4, pp 79-98.
(c) Shriver, D. F.; Drezdzon, M. A.; *The Manipulation of Air-Sensitive Compounds*, 2nd Edition; Wiley-Interscience: New York, 1986.

(93) Fulmer, G. R.; Miller, A. J. M.; Sherden, N. H.; Gottlieb, H. E.; Nudelman, A.; Stoltz, B. M.; Bercaw, J. E.; Goldberg, K. I. *Organometallics* **2010**, *29*, 2176-2179.

(94) Gottlieb, R. B. *J. Org. Chem.* **1997**, *62*, 7512–7515.

(95) (a) Harris, R. K.; Becker, E. D.; De Menezes, S. M. C.; Goodfellow, R.; Granger, P. *Pure Appl. Chem.* **2001**, *73*, 1795-1818.
(b) Harris, R. K.; Becker, E. D.; De Menezes, S. M. C.; Granger, P.; Hoffman, R. E.; Zilm, K. W. *Pure Appl. Chem.* **2008**, *80*, 59-84.

(96) (a) Sheldrick, G. M. SHELXTL, An Integrated System for Solving, Refining, and Displaying Crystal Structures from Diffraction Data; University of Göttingen, Göttingen, Federal Republic of Germany, 1981.
(b) Sheldrick, G. M. *Acta Cryst.* **2008**, *A64*, 112-122.
(c) Sheldrick, G. M. *Acta Cryst.* **2015**, *A71*, 3–8.

(97) (a) Jaguar, version 8.9, Schrodinger, Inc., New York, NY, 2015.
(b) Bochevarov, A. D.; Harder, E.; Hughes, T. F.; Greenwood, J. R.; Braden, D. A.; Philipp, D. M.; Rinaldo, D.; Halls, M. D.; Zhang, J.; Friesner, R. A. *Int. J. Quantum Chem.* **2013**, *113*, 2110–2142.

(98) (a) Becke, A. D. *J. Chem. Phys.* **1993**, *98*, 5648-5652.
(b) Becke, A. D. *Phys. Rev. A* **1988**, *38*, 3098-3100.
(c) Lee, C. T.; Yang, W. T.; Parr, R. G. *Phys. Rev. B* **1988**, *37*, 785-789.
(d) Vosko, S. H.; Wilk, L.; Nusair, M. *Can. J. Phys.* **1980**, *58*, 1200-1211.
(e) Slater, J. C. *Quantum Theory of Molecules and Solids, Vol. 4: The Self-Consistent Field for Molecules and Solids*; McGraw-Hill: New York, 1974.

CHAPTER 2

Exchange of Alkyl and Tris(2-mercapto-1-t-butylimidazolyl)hydroborato Ligands Between Zinc, Cadmium, and Mercury

Table of Contents

Reproduced in part from Kreider-Mueller, A.; Quinlivan, P. J.; Rong, Y.; Owen, J. S.; Parkin, G. *J. Organomet. Chem.* **2015**, *792*, 177-183.

2.1 Introduction

2.1.1 Alkyl Group Exchange

The exchange of alkyl, aryl, and cyclopentadienyl groups between metal centers is one of the most important reactions in organometallic chemistry, as it allows for the synthesis of a variety of compounds.[1,2] For example, transition metal alkyl complexes are often synthesized *via* metathesis of a transition metal halide with a main group alkyl compound such as RMgX, RLi, or R_2Zn.[3] Main group alkyl compounds have found several other applications as well. For example, Et_2Zn[4] is an important chain transfer agent in olefin polymerization for control of molecular weight distributions;[5] furthermore, the zinc alkyl allows for the synthesis of novel block copolymers, as it is capable of shuttling growing polymer chains between different catalyst centers.[6] Additionally, Me_2Mg has been employed by the Parkin group for the synthesis of a terminal magnesium methyl carbatrane complex, which can be utilized as a pre-catalyst for hydrosilylation and hydroboration reactions.[7] Also, Me_2Cd has found applications in the synthesis of cadmium chalcogenide nanocrystals.[8]

While zinc[5,6,9,10] and, to a lesser extent, cadmium[9,11,12] dialkyls have important synthetic applications, the mercury analogues have found little utility due to their extreme toxicity.[13] One of the factors that is responsible for the high toxicity of mercury alkyl complexes is the affinity of mercury for sulfur. Mercury is known to effectively bind to sulfur-containing amino acids and cofactors such as cysteine and glutathione.[14-16] Additionally, mercury is capable of displacing zinc from cysteine-rich structural and catalytic sites in enzymes.[17,18] Therefore, in addition to examining alkyl group exchange between zinc, cadmium, and mercury, it is also pertinent to examine exchange reactions involving sulfur ligands with these main group metals.

2.1.2 Tris(mercaptoimidazolyl)hydroborato Ligands [Tm^R]

The *tris*(mercaptoimidazolyl)hydroborato ligand, [Tm^R] (Figure 1), first reported by Reglinski and Spicer in 1996,[19] has been demonstrated to be a useful L_2X[20] [S_3] donor array that provides a sulfur-rich coordination environment.[21-25] The [Tm^R] ligand provides a complement to the commonly employed [N_3] tripodal ligand, *tris*(pyrazolyl)hydroborato, [Tp$^{R,R'}$] (Figure 1).[26] The t-butyl derivative, [Tm$^{Bu^t}$], has been used to synthesize a variety of zinc,[27-29] cadmium[28,30] and mercury[28,31] complexes, which provides a basis to investigate the exchange of alkyl and sulfur ligands between these metals, the results of which are described in this chapter.[32]

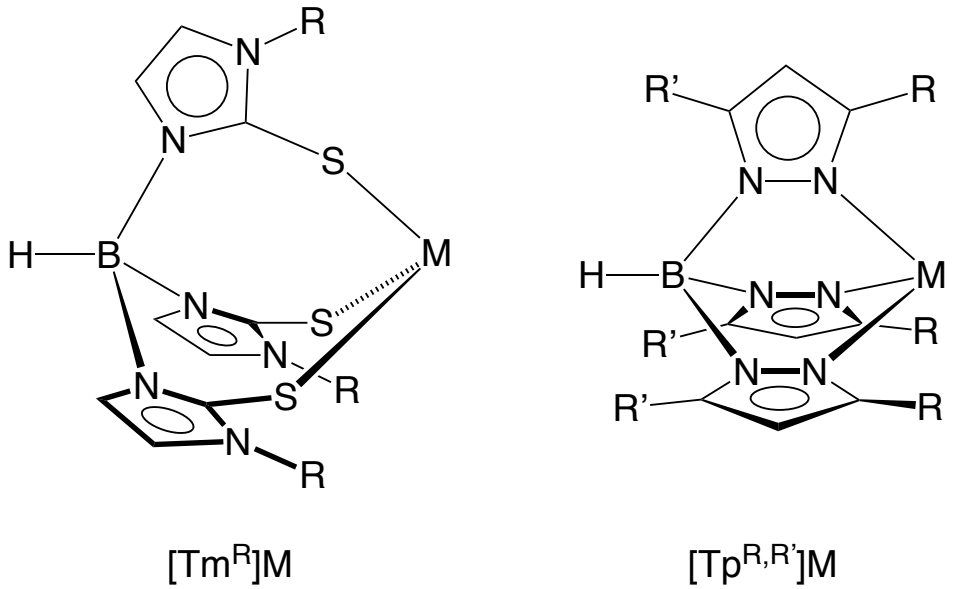

Figure 1. [Tm^R] and [Tp$^{R,R'}$] ligands, as illustrated in their κ^3-coordination modes.

2.2 Alkyl Exchange Between the Same Metals

While the primary synthetic use of main group alkyl compounds involves exchange of alkyl ligands between two different metals, alkyl transfer between the same metal centers is also possible. An example illustrating this is the Schlenk equilibrium, which

involves the interconversion of Grignard reagents and the corresponding dialkyl magnesium compounds.[33]

Previous work done by Dr. Ava Kreider-Mueller in the Parkin group has shown that a similar type of transformation also exists between [Tm^{But}]MMe and [Tm^{But}]$_2$M/Me$_2$M (M = Zn, Cd), however the equilibrium lies heavily in favor of the heteroleptic compound, [Tm^{But}]MMe.[34] Thus, treatment of [Tm^{But}]$_2$Zn[29] with Me$_2$Zn results in the rapid formation of [Tm^{But}]ZnMe[27a] as illustrated in Scheme 1. Likewise, [Tm^{But}]CdMe[30] is rapidly obtained by mixing [Tm^{But}]$_2$Cd[30] and Me$_2$Cd.

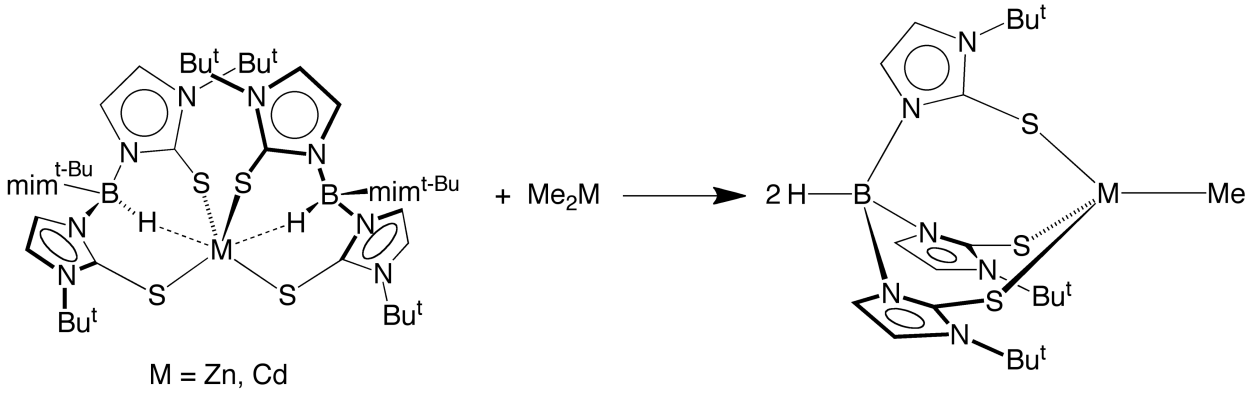

Scheme 1. Formation of [Tm^{But}]MMe by treatment of [Tm^{But}]$_2$M with Me$_2$M (M = Zn, Cd)

The formation of [Tm^{But}]MMe (M = Zn, Cd) by these reactions provides a useful method of synthesis from the sodium complex, [Tm^{But}]Na,[24,35] because [Tm^{But}]$_2$M may be generated via the reactions of [Tm^{But}]Na with the corresponding MCl$_2$ (Scheme 2). More specifically, and developed by Dr. Ava Kreider-Mueller,[34] [Tm^{But}]MMe can be directly synthesized in a one-pot, two-step reaction that involves (*i*) the reaction of 2 equivalents of [Tm^{But}]Na with the appropriate MCl$_2$ to generate [Tm^{But}]$_2$M, followed by (*ii*) treatment with Me$_2$M to yield [Tm^{But}]MMe (Scheme 3).

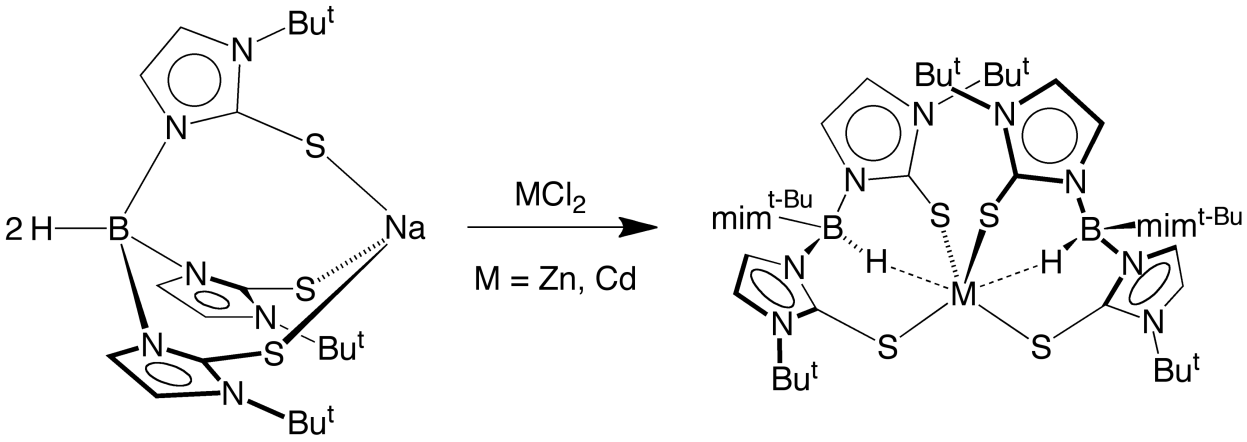

Scheme 2. Formation of $[Tm^{Bu^t}]_2M$ from MCl_2 (M = Zn, Cd) and $[Tm^{Bu^t}]Na$

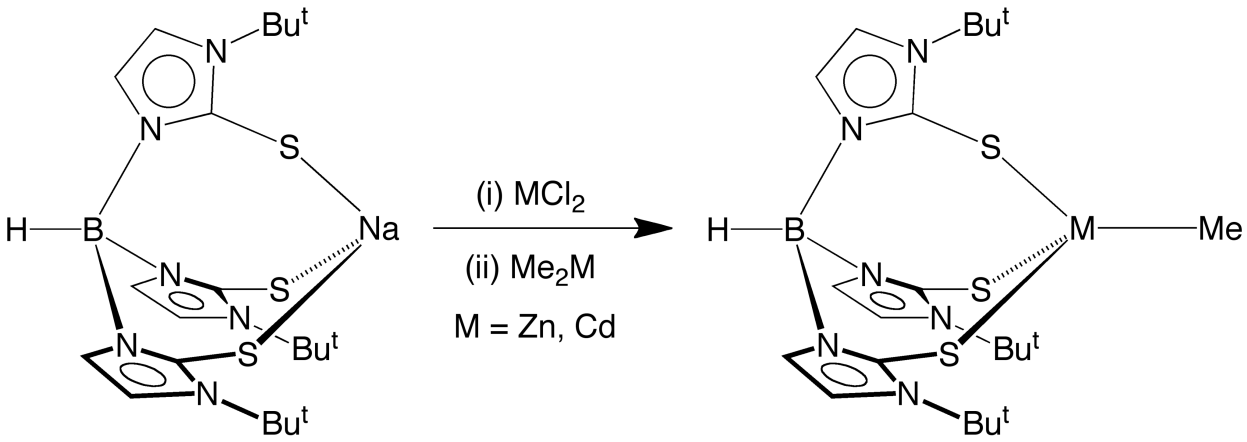

Scheme 3. Synthesis of $[Tm^{Bu^t}]MMe$ from $[Tm^{Bu^t}]Na$ by sequential reaction with MCl_2 and Me_2M (M = Zn, Cd)

An advantage of this synthetic route is that it does not require the use of the thallium reagent, $[Tm^{Bu^t}]Tl$.[35] Thus, although $[Tm^{Bu^t}]MMe$ can be synthesized directly from the reaction of $[Tm^{Bu^t}]Tl$ with Me_2M,[35] $[Tm^{Bu^t}]Tl$ is also synthesized from $[Tm^{Bu^t}]Na$ by treatment with Tl(OAc).[35] Therefore, the method as shown in Scheme 3 for the synthesis of $[Tm^{Bu^t}]MMe$ from $[Tm^{Bu^t}]Na$ is more direct and excludes the use of thallium reagents.

Also of note, the Schlenk-type redistribution reaction illustrated in Scheme 1 is observed for [$Tp^{R,R'}$] systems, as developed by Dr. Yi Rong in the Parkin group. More specifically, [Tp^{Me2}]$_2$Zn[36] rapidly reacts with Me_2Zn to form the heteroleptic compound [Tp^{Me2}]ZnMe,[36] as illustrated in Scheme 4. Similar to the [Tm^{Bu^t}] system, the equilibrium lies greatly in favor of the heteroleptic compound.

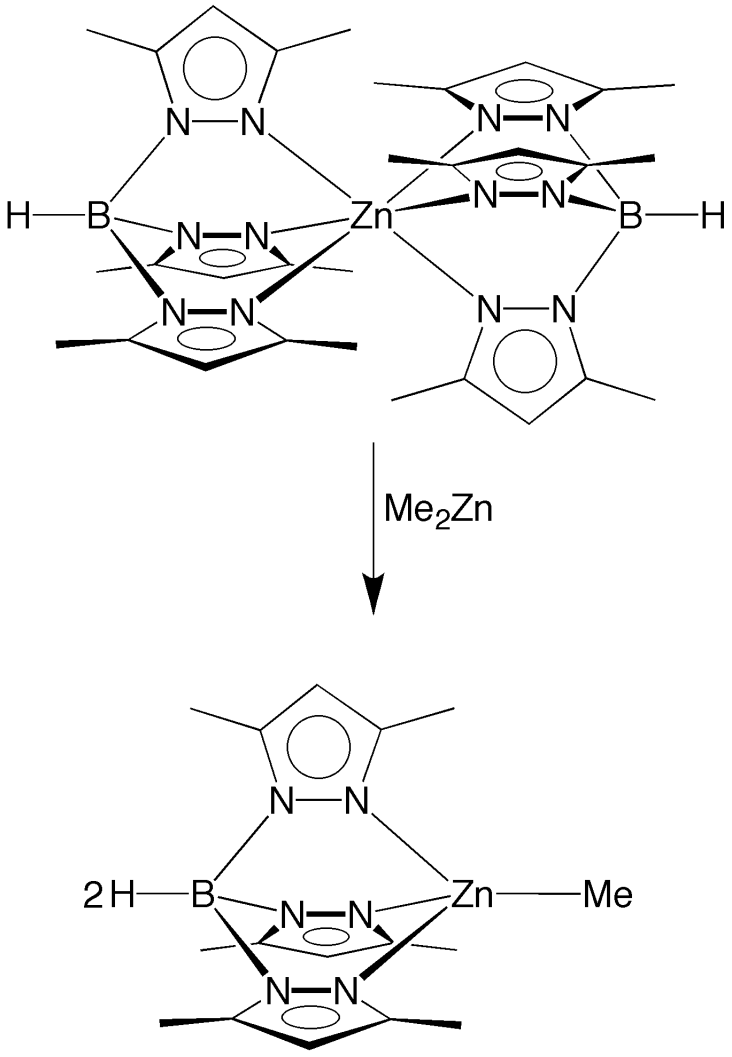

Scheme 4. Formation of [Tp^{Me2}]ZnMe from [Tp^{Me2}]$_2$Zn and Me_2Zn.

2.3 Exchange Between Different Metal Centers

2.3.1 Exchange of Alkyl and Sulfur Ligands Between Zinc and Cadmium

In addition to the Schlenk-type equilibria studied above involving the [Tm$^{Bu^t}$]MMe complexes, exchange of alkyl groups between two different metal centers was also investigated. For example, the treatment of [Tm$^{Bu^t}$]ZnMe with Me_2Cd results in the rapid formation of [Tm$^{Bu^t}$]CdMe and Me_2Zn. However, this reaction does not go to completion. Rather, an equilibrium mixture is obtained, as confirmed by studying the reverse reaction of [Tm$^{Bu^t}$]CdMe and Me_2Zn (Scheme 5).

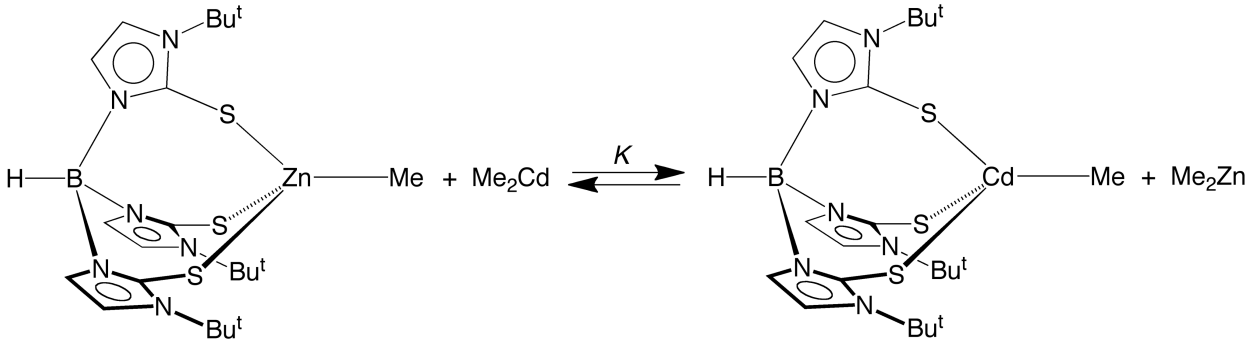

Scheme 5. [Tm$^{Bu^t}$] ligand transfer between zinc and cadmium

The equilibrium constant for the reaction between [Tm$^{Bu^t}$]ZnMe and Me_2Cd, as determined by ^{1}H NMR spectroscopy, is 7.0(5) × 10^{-2} at 300 K [ΔG = 1.6(1) kcal mol^{-1}]. Furthermore, measurement of the equilibrium constant at variable temperatures allows for the construction of a van't Hoff plot (Figure 2) and the determination of the thermodynamic paramters, ΔH [1.82(7) kcal mol^{-1}] and ΔS [0.9(3) e.u.]. A value close to zero for ΔS is typical for a redistribution reaction of this type.[37]

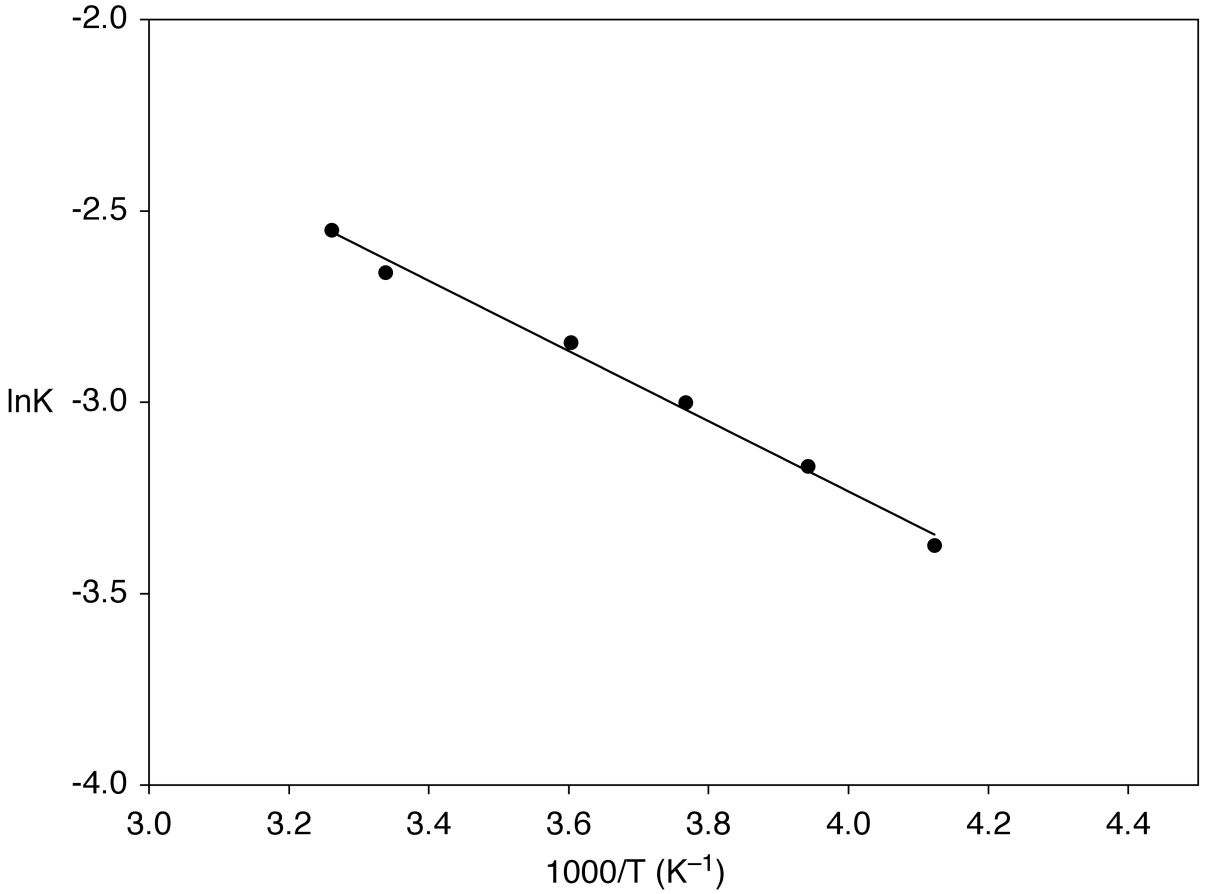

Figure 2. van't Hoff plot for the reaction of [Tm^{But}]ZnMe with Me_2Cd.

This thermodynamic data suggests that there is a phenomenological preference for the [Tm^{But}] ligand to coordinate to zinc, rather than cadmium in this system. However, this observation does not, *per se,* mean that the Zn–[Tm^{But}] bond dissociation energy (BDE, *D*) is greater than the Cd–[Tm^{But}] BDE because it is also necessary to take into account the M–Me BDEs in [Tm^{But}]MMe and Me_2M.

More specifically, ΔH for the reaction may be expressed by equation (1), where L = [Tm^{But}]:

$$\Delta H = [2D(\text{Cd–Me})_{Me_2Cd} + D(\text{Zn–Me})_{LZnMe} + D(\text{Zn–L})_{LZnMe}] -$$

$$[2D(\text{Zn–Me})_{\text{Me}_2\text{Zn}} + D(\text{Cd–Me})_{\text{LCdMe}} + D(\text{Cd–L})_{\text{LCdMe}}] \qquad (1)$$

Rearranging, ΔH may be expressed in the form shown in equation (2):

$$\begin{aligned}\Delta H = \; & [D(\text{Zn–L})_{\text{LZnMe}} - D(\text{Cd–L})_{\text{LCdMe}}] + \\ & [2D(\text{Cd–Me})_{\text{Me}_2\text{Cd}} - D(\text{Cd–Me})_{\text{LCdMe}}] - \\ & [2D(\text{Zn–Me})_{\text{Me}_2\text{Zn}} - D(\text{Zn–Me})_{\text{LZnMe}}] \qquad (2)\end{aligned}$$

Thus, ΔH will only directly correspond to the difference in Zn–[Tm$^{\text{Bu}^t}$] and Cd–[Tm$^{\text{Bu}^t}$] BDEs if the combined term, $\{[2D(\text{Cd–Me})_{\text{Me}_2\text{Cd}} - D(\text{Cd–Me})_{\text{LCdMe}}] - [2D(\text{Zn–Me})_{\text{Me}_2\text{Zn}} - D(\text{Zn–Me})_{\text{LZnMe}}]\}$, is coincidentally zero, *i.e.* $2[D(\text{Zn–Me})_{\text{Me}_2\text{Zn}} - D(\text{Cd–Me})_{\text{Me}_2\text{Cd}}] = [D(\text{Zn–Me})_{\text{LZnMe}} - D(\text{Cd–Me})_{\text{LCdMe}}]\}$.

Employing the literature values for the average M–Me BDEs of Me_2Zn (42.0 kcal mol^{-1}) and Me_2Cd (33.3 kcal mol^{-1}),[38,39] and the experimental value of 1.8 kcal mol^{-1} determined for ΔH, the difference in Zn–[Tm$^{\text{Bu}^t}$] and Cd–[Tm$^{\text{Bu}^t}$] BDEs may be expressed in the form shown in equation (3), which clearly indicates that the value is dependent on the difference in Zn–Me and Cd–Me BDEs.

$$[D(\text{Zn–L})_{\text{LZnMe}} - D(\text{Cd–L})_{\text{LCdMe}}] = 19.2 - [D(\text{Zn–Me})_{\text{LZnMe}} - D(\text{Cd–Me})_{\text{LCdMe}}] \quad (3)$$

Therefore, a difference of less than 19.2 kcal mol^{-1} between the Zn–Me and Cd–Me BDEs corresponds to a Zn–[Tm$^{\text{Bu}^t}$] interaction that is stronger than the Cd–[Tm$^{\text{Bu}^t}$] interaction. Alternatively, a greater difference would correspond to a Cd–[Tm$^{\text{Bu}^t}$] interaction that is stronger than the Zn–[Tm$^{\text{Bu}^t}$] interaction.[40] Although there are few comparisons between Zn–X and Cd–X BDEs found in the literature, it is worth noting that the Zn–N

BDE of $Zn[N(SiMe_3)_2]_2$ is 15.6 kcal mol^{-1} stronger than the corresponding Cd–N bond in $Cd[N(SiMe_3)_2]_2$.[41] Additionally the Zn–C BDE of Me_2Zn is 8.7 kcal mol^{-1} stronger than the corresponding Cd–C bond in Me_2Cd.[38] Thus, if the difference between the Zn–Me and Cd–Me BDEs of $[Tm^{Bu^t}]MMe$ were to be similar to these comparable examples, the Zn–$[Tm^{Bu^t}]$ interaction would be predicted to be stronger than the Cd–$[Tm^{Bu^t}]$ interaction.

2.3.2 Exchange of Alkyl and Sulfur Ligands from Mercury to Zinc and Cadmium

Transfer of the $[Tm^{Bu^t}]$ ligand from mercury to zinc and cadmium can also be accomplished. Namely, the reaction of $[Tm^{Bu^t}]HgMe$[31a] with Me_2Zn or Me_2Cd affords $[Tm^{Bu^t}]ZnMe$ and $[Tm^{Bu^t}]CdMe$ respectively, along with concomitant formation of Me_2Hg as illustrated in Scheme 6.

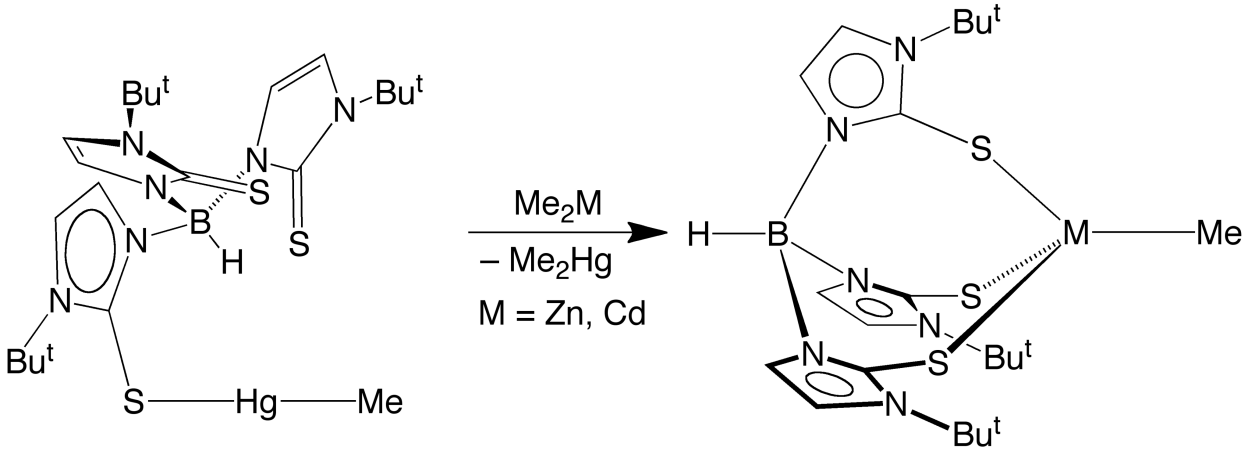

Scheme 6. $[Tm^{Bu^t}]$ ligand transfer from mercury to zinc or cadmium

The transfer of $[Tm^{Bu^t}]$ from mercury to zinc or cadmium is certainly unexpected, given the high thiophilicity of mercury.[14-16,31] However, it is important to emphasize that the thermodynamics of exchange reactions require consideration of *all* bonds being broken and formed. As such, a contributing factor to the observed exchange reaction may be

that [Tm$^{Bu^t}$]HgMe exhibits κ^1-coordination to the [Tm$^{Bu^t}$] ligand,[31a] whereas both the zinc and cadmium counterparts exhibit κ^3-coordination.

2.4 Transfer of [Tm$^{Bu^t}$] from Zinc and Cadmium to Mercury

In contrast to the above reaction involving the transfer of the [Tm$^{Bu^t}$] ligand from mercury to zinc or cadmium, it is noteworthy that in the presence of different co-ligands, the transfer of [Tm$^{Bu^t}$] from zinc or cadmium to mercury can be accomplished. Specifically, treatment of [Tm$^{Bu^t}$]$_2$M (M = Zn, Cd) with HgI_2 affords a 1:1 mixture of [Tm$^{Bu^t}$]MI (M = Zn,[27a] Cd[30]) and [Tm$^{Bu^t}$]HgI,[31a] as illustrated in Scheme 7. Thus, it is evident that in this system, the nature of the co-ligand has a profound effect on the thermodynamics of ligand exchange.

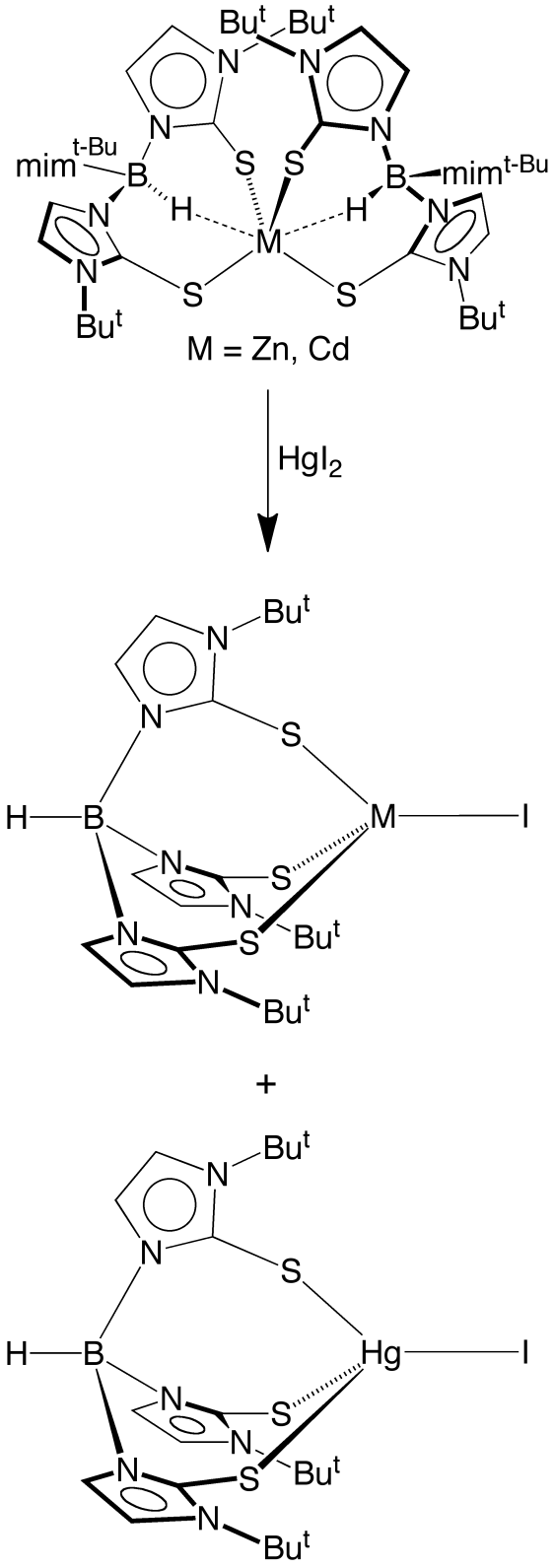

Scheme 7. [Tm^{Bu^t}] ligand transfer from zinc to cadmium to mercury

2.5 Summary and Conclusions

In summary, a variety of ligand exchange reactions between zinc, cadmium, and mercury centers have been investigated for compounds of the type [Tm^{But}]MMe (M = Zn, Cd, Hg). For example, the formation of [Tm^{But}]MMe can be accomplished by treatment of [Tm^{But}]$_2$M with Me_2M (M = Zn, Cd). This allows for the convenient synthesis of [Tm^{But}]CdMe, which was developed by Dr. Ava Kreider-Mueller, due to the fact that this Schlenk-type equilibrium lies heavily in favor of the heteroleptic compound. Ligand exchange between different metal centers was also observed. For example, [Tm^{But}]ZnMe and Me_2Cd form an equilibrium mixture with [Tm^{But}]CdMe and Me_2Zn. Likewise, [Tm^{But}]HgMe reacts with Me_2Cd to also form an equilibrium mixture with [Tm^{But}]CdMe and Me_2Hg. In contrast to the transfer of the [Tm^{But}] ligand from mercury to zinc in the methyl system, [Tm^{But}]HgMe/Me_2Zn, transfer from zinc to mercury is observed upon treatment of [Tm^{But}]$_2$Zn with HgI_2 to afford [Tm^{But}]HgI and [Tm^{But}]ZnI. These observations demonstrate that the phenomenological preference for the [Tm^{But}] ligand to bind mercury or zinc is strongly influenced by the nature of the co-ligands, which is a reflection of the fact that *all* bond energies need to be considered when predicting the thermodynamics of exchange reactions.

2.6 Experimental Details

2.6.1 General Considerations

All manipulations were performed using a combination of glovebox, high-vacuum, and Schlenk techniques under a nitrogen or argon atmosphere,[42] except where otherwise stated. Solvents were purified and degassed by standard procedures. NMR solvents were purchased from Cambridge Isotope Labs and stored over 3 Å molecular sieves.

NMR spectra were measured on Bruker 300 DPX, Bruker 400 Avance III, Bruker 400 Cyber-enabled Avance III, and Bruker 500 DMX spectrometers. ^{1}H NMR chemical shifts are reported in ppm relative to $SiMe_4$ ($\delta = 0$) and were referenced internally with respect to the protio solvent impurity ($\delta = 7.16$ for C_6D_6, 2.08 for C_7D_8, and 1.94 for CD_3CN).[43] Me_2Cd and Me_2Zn were obtained from Strem, while $[Tm^{Bu^t}]Na$,[24,44] $[Tm^{Bu^t}]_2Zn$,[29] $[Tm^{Bu^t}]_2Cd$,[30] $[Tp^{Me_2}]_2Zn$[36] and $[Tm^{Bu^t}]HgMe$[31a] were prepared by literature methods. *CAUTION: Mercury and cadmium compounds are toxic, and appropriate safety precautions must be taken in handling these compounds*.

2.6.2 Formation of $[Tm^{Bu^t}]_2Zn$ Upon Treatment of $[Tm^{Bu^t}]Na$ with $ZnCl_2$

A mixture of $[Tm^{Bu^t}]Na$ (31 mg, 0.0619 mmol) and $ZnCl_2$ (4.0 mg, 0.0293 mmol) in C_6D_6 (1.5 mL) in an NMR tube equipped with a J. Young valve was heated at 80°C for 20 hours and monitored by ^{1}H NMR spectroscopy, thereby demonstrating the formation of $[Tm^{Bu^t}]_2Zn$.[29]

2.6.3 Formation of $[Tm^{Bu^t}]_2Cd$ Upon Treatment of $[Tm^{Bu^t}]Na$ with $CdCl_2$

A mixture of $[Tm^{Bu^t}]Na$ (19 mg, 0.0380 mmol) and $CdCl_2$ (3.3 mg, 0.0180 mmol) in C_6D_6 (1.5 mL) in an NMR tube equipped with a J. Young valve was heated at 80°C for 20 hours and monitored by ^{1}H NMR spectroscopy, thereby demonstrating the formation of $[Tm^{Bu^t}]_2Cd$.[29]

2.6.4 Reaction of $[Tm^{Bu^t}]_2Zn$ with Me_2Zn

A solution of $[Tm^{Bu^t}]_2Zn$ (2.7 mg, 0.0026 mmol) in C_6D_6 (0.7 mL) in an NMR tube equipped with a J. Young valve was treated with Me_2Zn (150 μL of a 0.082 M solution in

C_6D_6, 0.0123 mmol). The reaction was monitored by ^{1}H NMR spectroscopy, which demonstrated the immediate formation of [Tm$^{Bu^t}$]ZnMe.[27a]

2.6.5 Reaction of [Tm$^{Bu^t}$]$_2$Cd with Me$_2$Cd

A solution of [Tm$^{Bu^t}$]$_2$Cd (2.4 mg, 0.0022 mmol) in C_6D_6 (1 mL) in an NMR tube equipped with a J. Young valve was treated with Me_2Cd (60 μL of a 0.111 M solution in C_6D_6, 0.0067 mmol). The reaction was monitored by ^{1}H NMR spectroscopy, which demonstrated the immediate formation of [Tm$^{Bu^t}$]CdMe.[30]

2.6.6 Reaction of [Tp^{Me_2}]$_2$Zn with Me$_2$Zn

A solution of [Tp^{Me_2}]$_2$Zn (4 mg, 0.006 mmol) in C_6D_6 (1 mL) in an NMR tube equipped with a J. Young valve was treated with excess Me_2Zn. The reaction was monitored by ^{1}H NMR spectroscopy, which demonstrated the immediate formation of [Tp^{Me_2}]ZnMe.[36] The sample was then lyophilized to remove solvent and excess Me_2Zn and allowed to crystallize by slow evaporation at room temperature to afford [Tp^{Me_2}]ZnMe as a white solid (3.2 mg, yield 71%).

2.6.7 Reaction of [Tm$^{Bu^t}$]ZnMe with Me$_2$Cd

(a) A solution of [Tm$^{Bu^t}$]ZnMe (5.8 mg, 0.0104 mmol) in C_6D_6 (0.7 mL) in an NMR tube equipped with a J. Young valve was treated with Me_2Cd (50 μL of a 0.111 M solution in C_6D_6, 0.0056 mmol). The reaction was monitored by ^{1}H NMR spectroscopy, which demonstrated the immediate formation of an equilibrium mixture with [Tm$^{Bu^t}$]CdMe[30] and Me_2Zn.

(b) A solution of [Tm$^{Bu^t}$]ZnMe (3.8 mg, 0.0068 mmol) in C_7D_8 (1 mL) in an NMR tube equipped with a J. Young valve was treated with Me_2Cd (50 μL of a 0.111 M solution in

C_6D_6, 0.0056 mmol). The reaction was monitored by ^{1}H NMR spectroscopy, which demonstrated the immediate formation of an equilibrium mixture with [Tm$^{Bu^t}$]CdMe[30] and Me_2Zn. The equilibrium constant was measured as a function of temperature, thereby allowing determination of ΔH and ΔS.

2.6.8 Reaction of [Tm$^{Bu^t}$]CdMe with Me_2Zn

A solution of Me_2Zn (1 mL of a 0.0143 M solution in C_6D_6, 0.0143 mmol) was added to an NMR tube equipped with a J. Young valve that contained [Tm$^{Bu^t}$]CdMe (6.1 mg, 0.0101 mmol). The reaction was monitored by ^{1}H NMR spectroscopy, which demonstrated the immediate formation of [Tm$^{Bu^t}$]ZnMe[27a] and Me_2Cd.

2.6.9 Reaction of [Tm$^{Bu^t}$]HgMe with Me_2Zn

A solution of [Tm$^{Bu^t}$]HgMe (2.4 mg, 0.0035 mmol) in C_6D_6 (0.7 mL) in an NMR tube equipped with a J. Young valve was treated with Me_2Zn (100 μL of a 0.082 M solution in C_6D_6, 0.0082 mmol). The reaction was monitored by ^{1}H NMR spectroscopy, which demonstrated the immediate formation of [Tm$^{Bu^t}$]ZnMe[27a] and Me_2Hg.

2.6.10 Reaction of [Tm$^{Bu^t}$]HgMe with Me_2Cd

A solution of [Tm$^{Bu^t}$]HgMe (2.7 mg, 0.0039 mmol) in C_7D_8 (0.7 mL) in an NMR tube equipped with a J. Young valve was treated with Me_2Cd (85 μL of a 0.111 M solution in C_6D_6, 0.0094 mmol). The reaction was monitored by ^{1}H NMR spectroscopy, which demonstrated the immediate formation of [Tm$^{Bu^t}$]CdMe[30] and Me_2Hg.

2.6.11 Reaction of $[Tm^{Bu^t}]_2Zn$ with HgI_2

A solution of $[Tm^{Bu^t}]_2Zn$ (1.5 mg, 0.0015 mmol) in CD_3CN (1 mL) was added to HgI_2 (0.7 mg, 0.0015 mmol) and the solution was transferred to an NMR tube equipped with a J. Young valve. The reaction was monitored by ^1H NMR spectroscopy, which demonstrated the immediate formation of a 1:1 mixture of $[Tm^{Bu^t}]HgI$[31a] and $[Tm^{Bu^t}]ZnI$.[27a]

2.6.12 Reaction of $[Tm^{Bu^t}]_2Cd$ with HgI_2

A solution of $[Tm^{Bu^t}]_2Cd$ (4.4 mg, 0.0041 mmol) in CD_3CN (1 mL) was added to HgI_2 (1.8 mg, 0.0040 mmol) and the solution was transferred to an NMR tube equipped with a J. Young valve. The reaction was monitored by ^1H NMR spectroscopy, which demonstrated the immediate formation of a *ca*. 1:1 mixture of $[Tm^{Bu^t}]HgI$[31a] and $[Tm^{Bu^t}]CdI$.[30]

2.6.13 Synthesis of $[Tm^{Bu^t}]CdMe$

$[Tm^{Bu^t}]CdMe$ was prepared by following the method developed by Dr. Ava Kreider-Mueller:[34] A suspension of $[Tm^{Bu^t}]Na$ (1.110 g, 2.22 mmol) in benzene (*ca*. 30 mL) was treated with $CdCl_2$ (193.5 mg, 1.06 mmol) and heated at 125˚C with stirring in a pressure vessel for 19 hours. After this period, the reaction mixture was allowed to cool to room temperature, thereby depositing a white precipitate. Me_2Cd (120 μL, 1.67 mmol) was added and the mixture was stirred at room temperature for 1 hour and filtered. The white precipitate was extracted with benzene (*ca*. 2 × 5 mL), and the extracts were combined with the filtrate from the reaction. A white precipitate started to form and was redissolved by addition of benzene (*ca*. 10 mL). The solution was transferred to a Schlenk flask and the volatile components removed *in vacuo* to yield $[Tm^{Bu^t}]CdMe$ as a white solid (984 mg, 77 %) which was identified by ^1H NMR spectroscopy.[30]

2.6.14 Synthesis of [Tm$^{Bu^t}$]ZnMe

[Tm$^{Bu^t}$]ZnMe was prepared by following the method developed by Dr. Ava Kreider-Mueller:[34] A suspension of [Tm$^{Bu^t}$]Na (384.5 mg, 0.768 mmol) in benzene (*ca*. 10 mL) was treated with $ZnCl_2$ (51.2 mg, 0.376 mmol) and stirred vigorously at room temperature for 2 days, resulting in the formation of a thick white suspension. Me_2Zn (157.8 mg, 1.65 mmol) was added and the mixture was stirred at room temperature for 1 day. After this period, the reaction mixture was centrifuged and the mother liquor was filtered. The solid isolated from the centrifugation was extracted into benzene (8 mL) and the extract was combined with the above filtrate. The volatile components were removed *in vacuo* to yield [Tm$^{Bu^t}$]ZnMe as a white solid (235.0 mg, 56 %), which was identified by ^{1}H NMR spectroscopy.[27a]

2.7 References and Notes

(1) Puddephat, R. J. in *The Chemistry of the Metal-Carbon Bond*, Hartley, F. R.; Patai, S. (Eds) John Wiley & Sons, 1982, Chapter 6.

(2) Vedernikov, A. N.; Caulton, K. G. *Angew. Chem. Int. Ed.* **2002**, *41*, 4101-4104.

(3) Hartwig, J. F. *Organotransition Metal Chemistry: From Bonding to Catalysis*, University Science Books, 2010.

(4) Seyferth, D. *Organometallics*, **2001**, *20*, 2940-2955.

(5) (a) Mazzolini, J.; Espinosa, E.; D'Agosto, F.; Boisson, C. *Polym. Chem.* **2010**, *1*, 793-800.
(b) Gibson, V. C. *Science* **2006**, *312*, 703-704.

(6) (a) Arriola, D. J.; Carnahan, E. M.; Hustad, P. D.; Kuhlman, R. L.; Wenzel, T. T. *Science* **2006**, *312*, 714-719.
(b) Hustad, P. D.; Kuhlman, R. L.; Arriola, D. J.; Carnahan, E. M.; Wenzel, T. T. *Macromolecules* **2007**, *40*, 7061-7064.
(c) Wenzel, T. T.; Arriola, D. J.; Carnahan, E. M.; Hustad, P. D.; Kuhlman, R. L. *Top. Organomet. Chem.* **2009**, *26*, 65-104.

(7) (a) Rauch, M.; Ruccolo, S.; Parkin, G. *J. Am. Chem. Soc.* **2017**, *139*, 13264-13267.
(b) Ruccolo, S.; Rauch, M.; Parkin, G. *Chem. Sci.* **2017**, *8*, 4465-4474.

(8) Peng, Z. A.; Peng, X. *J. Am. Chem. Soc.* **2001**, *123*, 183-184.

(9) Knochel, P. "Diethylzinc" in *e-EROS Encyclopedia of Reagents for Organic Synthesis* (2001).

(10) Talapin, D. V.; Mekis, I.; Go1tzinger, S.; Kornowski, A.; Benson, O.; Weller, H. *J. Phys. Chem. B* **2004**, *108*, 18826-18831.

(11) Murray, C. B.; Norris, D. J.; Bawendi, M. G. *J. Am. Chem. Soc.* **1993**, *115*, 8706–8715.

(12) Chen, P. E.; Anderson, N. C.; Norman, Z. M.; Owen, J. S. *J. Am. Chem. Soc.* **2017**, *139*, 3227-3236.

(13) (a) Clarkson, T. W.; Magos, L. *Crit. Rev. Toxicol.* **2006**, *36*, 609-662.
(b) Dorea, J. G.; Farina, M.; Rocha, J. B. T. *J. Appl. Toxicol.* **2013**, *33*, 700-711.
(c) Syversen, T.; Kaur, P. *J. Trace Elem. Med. Biol.* **2012**, *26*, 215-226.

(14) Arnold, A. P.; Canty, A. J. *Environ. Toxicol. Chem.* **2011**, *30*, 2733–2738.

(15) Rabenstein, D. L.; Evans, C. A. *Bioinorg. Chem.* **1978**, *8*, 107–114.

(16) Rabenstein, D. L.; Fairhurst, M. T. *J. Am. Chem. Soc.* **1975**, *97*, 2086–2092.

(17) (a) Lippard, S. J.; Berg, J. M. "Principles of Bioinorganic Chemistry", University Science Books, Mill Valley, California (1994).
(b) Fraústo da Silva, J. J. R.; Williams, R. J. P. "The Biological Chemistry of the Elements", Oxford University Press, Oxford (1991).
(c) Dudev, T.; Lim, C. *Annu. Rev. Biophys.* **2008**, *37*, 97–116.
(d) Dudev, T.; Lim, C. *Chem. Rev.* **2003,** *103,* 773-787.
(e) Roesijadi, G. *Cell. Mol. Biol.* **2000**, *46*, 393-405.

(18) (a) Asmuss, M.; Mullenders, L. H. F.; Eker, A.; Hartwig, A. *Carcinogenesis* **2000**, *21*, 2097-2104.
(b) O'Connor, T. R.; Graves, R. J.; de Murcia, G.; Castaing, B.; Laval, J. *J. Biol. Chem.* **1993**, *268*, 9063-9070.
(c) Hartwig, A.; Asmuss, M.; Blessing, H.; Hoffmann, S.; Jahnke, G.; Khandelwal, S.; Pelzer, A.; Bürkle, A. *Food Chem. Toxicol.* **2002**, *40*, 1179-1184.

(19) (a) Barner, M.; Reglinski, J.; Cassidy, I.; Spicer, M. D.; Kennedy, A. R. *Chem. Commun.* **1996,** 1975-1976.
(b) Reglinski, J.; Garner, M.; Cassidy, I. D.; Slavin, P. A.; Spicer, M. D.; Armstrong, D. R. *J. Chem. Soc., Dalton Trans.* **1999,** 2119-2126.

(20) (a) Green, M. L. H. *J. Organomet. Chem.* **1995**, *500*, 127-148.
(b) Parkin, G. in *Comprehensive Organometallic Chemistry III*, Volume 1, Chapter 1.01; Crabtree, R. H. and Mingos, D. M. P. (Eds), Elsevier, Oxford, 2006.
(c) Green, J. C.; Green, M. L. H.; Parkin, G. *Chem Commun.* **2012**, *48*, 11481-11503.
(d) Green, M. L. H.; Parkin, G. *J. Chem. Educ.* **2014**, *91*, 807-816.

(21) (a) Spicer, M. D.; Reglinski, J. *Eur. J. Inorg. Chem.* **2009**, 1553-1574.
(b) Smith, J. M. *Comm. Inorg. Chem.* **2008**, *29*, 189-233.
(c) Soares, L. F.; Silva, R. M. *Inorg. Synth.* **2002**, *33*, 199-202.
(d) Rabinovich, D. *Struct. Bond.* **2006**, *120*, 143-162.

(22) (a) Parkin, G. *New J. Chem.* **2007**, *31*, 1996-2014.
(b) Parkin, G. *Chem. Rev.* **2004**, *104*, 699-767.
(c) Parkin, G. *Chem. Commun.* **2000**, 1971-1985.

(23) (a) Vahrenkamp, H. *Acc. Chem. Res.* **1999**, *32*, 589-596.
(b) Vahrenkamp, H. *Bioinorganic Chemistry – Transition Metals in Biology and their Coordination Chemistry*, Wiley-VCH, Weinheim, **1997**, 540-551.
(c) Vahrenkamp, H. *Dalton Trans.* **2007**, 4751-4759.

(24) Kreider-Mueller, A.; Rong, Y.; Owen, J. S.; Parkin, G. *Dalton Trans.* **2014**, *43*, 10852-10865.

(25) Rajesekharan-Nair, R.; Lutta, S. T.; Kennedy, A. R.; Reglinski, J.; Spicer, M. D. *Acta Cryst.* **2014**, C*70*, 421-427.

(26) (a) Trofimenko, S. *Polyhedron* **2004**, *23*, 197-203.
(b) Parkin, G. *Adv. Inorg. Chem.* **1995**, *42*, 291-393.

(27) (a) Melnick, J. G.; Docrat, A.; Parkin, G. *Chem. Commun.* **2004**, 2870-2871.
(b) Melnick, J. G.; Zhu, G.; Buccella, D.; Parkin, G. *J. Inorg. Biochem.* **2006**, *100*, 1147-1154.

(28) White, J. L.; Tanski, J. M.; Rabinovich, D. *J. Chem. Soc., Dalton Trans*. **2002**, 2987-2991.

(29) Tesmer, M.; Shu, M.; Vahrenkamp, H. *Inorg. Chem.* **2001**, *40*, 4022-4029.

(30) Melnick, J. G.; Parkin, G.*Dalton Trans.* **2006**, 4207-4210.

(31) (a) Melnick, J. G.; Parkin, G. *Science* **2007**, *317*, 225-227.
(b) Melnick, J. G.; Yurkerwich, K.; Parkin, G. *Inorg. Chem* **2009**, *48*, 6763-6772.
(c) Melnick, J. G.; Yurkerwich, K.; Parkin, G. *J. Am. Chem. Soc.* **2010**, *132*, 647-655.

(32) (a) Palmer, J. H.; Parkin, G. *Dalton Trans.* **2014**, *43*, 13874-13882.
(b) Palmer, J. H.; Parkin, G. *J. Mol. Struct.* **2015**, *1081*, 530-535.
(c) Yurkerwich, K.; Yurkerwich, M.; Parkin, G. *Inorg. Chem.* **2011**, *50*, 12284-12295.
(d) Ibrahim, M. M.; Shaban, S. Y. *Inorg. Chim. Acta* **2009**, *362*, 1471-1477.

(33) (a) Tammiku-Taul, J.; Burk, P.; Tuulmets, A. *J. Phys. Chem. A* **2004**, *108*, 133-139.
(b) Henriques, A. M.; Barbosa, A. G. H. *J. Phys. Chem. A* **2011**, *115*, 12259-12270.

(34) Kreider-Mueller, A. R., Ligand Exchange, Hydrides, and Metal-Metal Bonds: An Investigation into the Synthesis, Structure, and Reactivity of Group 12 Metal Complexes in Sulfur and Nitrogen-Rich Environments. Ph.D. Dissertation, Columbia University, New York City, NY, 2014.

(35) Mihalcik, D. J.; White, J. L.; Tanski, J. M.; Zakharov, L. N.; Yap, G. P. A.; Incarvito, C. D.; Rheingold, A. L.; Rabinovich, D. *Dalton Trans.* **2004**, 1626–1634.

(36) Looney, A.; Han, R.; Gorrell, I. B.; Cornebise, M.; Yoon, K.; Parkin, G.; Rheingold, A. L. *Organometallics* **1995**, *14*, 274-288.

(37) (a) da Piedade, M. E. M.; Simões, J. A. M. *J. Organomet. Chem.* **1996**, *518*, 167-180.
(b) Diogo, H. P.; da Piedade, M. E. M.; Simões, J. A. M.; Teixeira, C. *J. Organomet. Chem.* **2001**, *632*, 188-196.

(38) Skinner, H. A. *Adv. Organomet. Chem.* **1964**, *2*, 49-114.

(39) For consistency, the BDE values for Me_2Zn and Me_2Cd are from the same source (reference 38), but we note that a slightly larger BDE has been recently reported for Me_2Zn (44.5 kcal mol^{-1}). See: Haaland, A; Green, J. C.; McGrady, S.; Downs, A.

J.; Gullo, E.; Lyall, M. J.; Timberlake, J.; Tutukin, A. V.; Volden, H. V.; Østby, K.-A. *Dalton Trans.* **2003**, 4356-4366.

(40) Adopting a value of 44.5 kcal mol^{-1} for the average BDE of Me_2Zn (reference 39), the threshold difference is 24.2 kcal mol^{-1} rather than 19.2 kcal mol^{-1}.

(41) Gümrükcüoglü, I. E.; Jeffrey, J.; Lappert, M. F.; Pedley, J. B.; Rai, A. K. *J. Organomet. Chem.* **1988**, *341*, 53-62.

(42) (a) McNally, J. P.; Leong, V. S.; Cooper, N. J. in *Experimental Organometallic Chemistry*, Wayda, A. L.; Darensbourg, M. Y., Eds.; American Chemical Society: Washington, DC, 1987; Chapter 2, pp. 6-23.
(b) Burger, B. J.; Bercaw, J. E. in *Experimental Organometallic Chemistry*; Wayda, A. L.; Darensbourg, M. Y., Eds.; American Chemical Society: Washington, DC, 1987; Chapter 4, pp. 79-98.
(c) Shriver, D. F.; Drezdon, M. A.; *The Manipulation of Air-Sensitive* Compounds, 2nd Edition; Wiley-Interscience: New York, 1986.

(43) Gottlieb, H. E.; Kotlyar, V.; Nudelman, A. *J. Org. Chem*. **1997**, *62*, 7512-7515.

(44) [Tm^{But}]Na may be obtained in both solvated and non-solvated forms (see reference 24). The non-solvated form was used herein. The molecular structure of non-solvated [Tm^{But}]Na has not been determined by X-ray diffraction and the monomeric κ^3-coordination geometry shown in Schemes 2 and 3 is only intended to be illustrative.

CHAPTER 3

Structural Analysis of Transition and Main Group Metal Complexes Featuring 1-methyl-benzimidazole-2-selone, 1-methyl-benzimidazole-2-thione, and 1-*tert*-butyl-imidazole-2-thione Ligands

Table of Contents

3.1 Introduction

1-R-imidazole-2-thiones and 1-R-imidazole-2-selones belong to a class of five-membered heterocyclic nitrogen compounds that feature C=S and C=Se moieties respectively.[1] Although they are often referred to in terms of their tautomeric 2-mercapto-1-R-imidazole and 2-seleno-1-R-imidazole forms, previous reports have shown that the thione and selone are more dominant and stable than the thiol or selenol (Figure 1).[2-4] 1-R-imidazole-2-thiones are well-studied compounds.[5,6] For example, the methyl derivative, methimazole (tapazole), is commonly employed as an antithyroid drug,[2,7-10] while other derivatives are potent multisubstrate inhibitors of β-hydroxylase, octopamine agonists, and CCR2 antagonists.[2,4,11,12] Additionally, 1-R-imidazole-2-thiones, which are considered mimics of the biomolecule ergothioneine,[5,6] serve as effective ligands for a variety of transition and main group metals,[13] and are utilized in the preparation of the *tris*(2-mercaptoimidazolyl)hydroborato ligand, [Tm^R], a tripodal [S_3] donor which serves as a sulfur analogue to the [N_3], [$Tp^{R,R'}$] ligand (Figure 2).[14]

Relative to 1-R-imidazole-2-thiones, 1-R-imidazole-2-selones have received significantly less attention.[15] This disparity is interesting, considering that 1-R-imidazole-2-selones may serve as mimics for the biomolecule selenoneine,[15a,15b] which has been isolated from the blood and tissues of bluefin tuna, and is known to have strong antioxidant properties.[16] Moreover, 2-imidazoleselones have recently been shown to exhibit potential antithyroid activity.[17-19] Exploring the coordination chemistry of 1-R-imidazole-2-selones would allow for further comparison to their sulfur analogues.

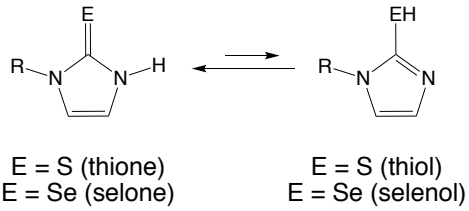

Figure 1. Thione/thiol and selone/selenol tautomerism. The thione/selone is more stable for 2-imidazolethiones and 2-imidazoleselones.

Previously, the Parkin group utilized the benzannulated selone, 1-methyl-1,3-dihydro-2H-benzimidazole-2-selone, H(sebenzim^{Me}),[15a,15b] to study mercury-selenium interactions, thereby showing that H(sebenzim^{Me}) effectively coordinates to mercury centers and is also capable of promoting mercury–carbon bond cleavage. Given the noteworthy reactivity of H(sebenzim^{Me}) towards mercury, and the dearth of metal complexes featuring 1-R-imidazole-2-selones, we felt it appropriate to extend our studies to other metal centers. This chapter details the reactivity of H(sebenzim^{Me}) towards Pd, Ni, Zn, and Cd metal centers, the various coordination modes H(sebenzim^{Me}) adopts, and draws comparisons with the thione counterparts, H(mim$^{Bu^t}$) and H(mbenzim^{Me}).

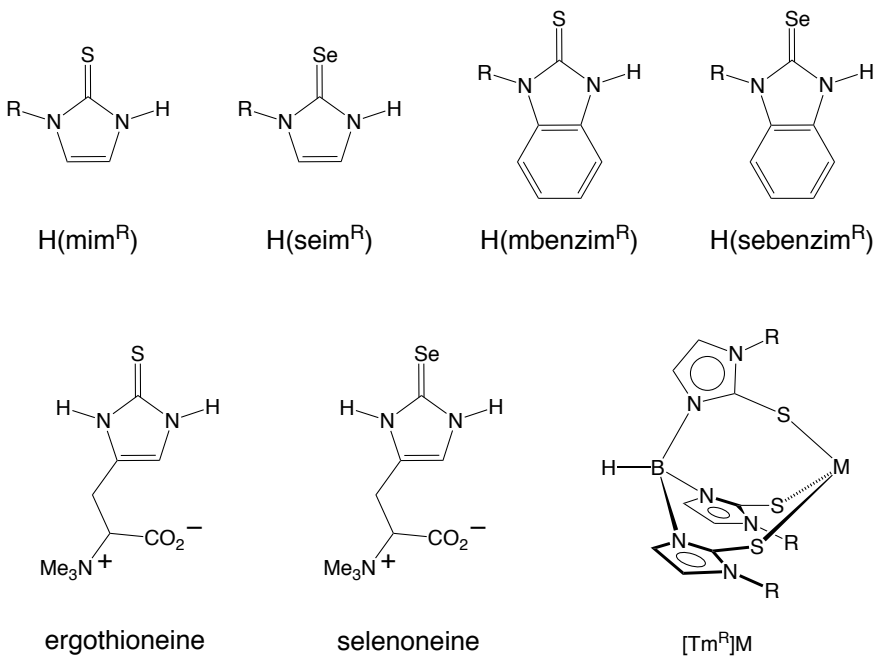

Figure 2. 1-R-imidazole-2-thiones and 1-R-imidazole-2-selones (top), ergothioneine, selenoneine, and [Tm^R] as illustrated in its κ^3-coordination mode (bottom).

3.2 Synthesis and Structural Characterization of Palladium Complexes Featuring H(mim$^{Bu^t}$) and H(sebenzim^{Me}) ligands

3.2.1 Synthesis and Structural Characterization of {[H(mim$^{Bu^t}$)]$_4$Pd}(OAc)$_2$ and [H(sebenzim^{Me})]$_3$Pd(PPh$_3$)Cl$_2$

Previously, it has been demonstrated that the dication, {[H(mim$^{Bu^t}$)]$_4$Pd}$^{2+}$, can be synthesized *via* (*i*) the treatment of $PdCl_2$ with 4 equivalents of H(mim$^{Bu^t}$) to form {[H(mim$^{Bu^t}$)]$_4$Pd}Cl$_2$[20] or (*ii*) the addition of Pd(OAc)$_2$ to {[H(mim$^{Bu^t}$)]$_4$Ni}I$_2$ to form {[H(mim$^{Bu^t}$)]$_4$Pd}I$_2$.[13b] The dication can also be generated by the treatment of Pd(OAc)$_2$ with 4 equivalents of H(mim$^{Bu^t}$) to form {[H(mim$^{Bu^t}$)]$_4$Pd}(OAc)$_2$, which differs by virtue of having two acetate counter ions (Scheme 1).

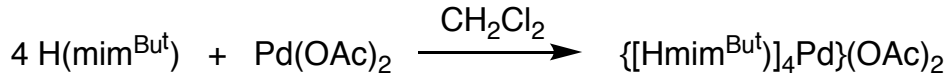

Scheme 1. Formation of $\{[H(mim^{But})]_4Pd\}(OAc)_2$ *via* the treatment of $Pd(OAc)_2$ with 4 equivalent of $H(mim^{But})$.

$\{[H(mim^{But})]_4Pd\}(OAc)_2$ has been characterized by X-ray diffraction (Figure 3), revealing coordination of the $H(mim^{But})$ ligands to Pd *via* an L-type[21] interaction through the thione. Calculated τ_4 and τ_δ indices[22] (Equations 1-3) both give values of 0, thus suggesting an ideal square planar arrangement. However, upon further inspection, while the PdS_4 unit is perfectly planar and the trans sites are exactly 180˚ separated, all the cis S–Pd–S angles do not equal 90˚. Instead, a scissoring distortion[23] is present in which angles of 83.981(19)˚ and 96.020(19)˚ are observed between adjacent $H(mim^{But})$ groups. This discrepancy (of $\tau_4 = \tau_\delta = 0$, indicating an ideal square plane) is due to the inability of τ_4 and τ_δ to account for these distortions, as the indices are only capable of distinguishing whether a 4-coordinate molecule is planar or not. More specifically, in compounds like $\{[H(mim^{But})]_4Pd\}(OAc)_2$ where the two largest angles, α and β, are both equal to 180˚, a value of 0 for both τ_4 and τ_δ is obtained, regardless of the adjacent S–Pd–S angles. Thus, the use of only τ_4 and τ_δ indices is not totally sufficient for describing square planar compounds where the two largest angles are both 180˚, because scissoring or other distortions that do not result in a loss of planarity must be taken into account.

$$\tau_4 = \frac{360° - (\alpha + \beta)}{141°} \qquad (1)$$

$$\tau_\delta = \frac{360° - (\alpha + \beta)}{141°}\delta \qquad (2)$$

$$\delta = \frac{\beta}{\alpha} \qquad (3)$$

The average Pd–S (2.339[9] Å) and C=S (thione) (1.732[2] Å) bonds are very comparable to other $\{[H(mim^{Bu^t})]_4Pd\}^{2+}$ structures [13b,20] and related compounds[24-27] as detailed in Table 1. Two of the adjacent $H(mim^{Bu^t})$ ligands can be considered "up" as they are oriented on the same side of the PdS_4 plane as illustrated in Figure 3. Likewise, the other two ligands can be considered "down" as they are on the opposite side of the PdS_4 plane. This geometry arises partly due to the hydrogen bonding interactions between the N–H's of $H(mim^{Bu^t})$ and the oxygens of the acetate counter ions. The N···O distances are 2.648(3) Å and 2.712(3) Å, which are slightly shorter than the average N···O distances for non-bonded N–H···OAc contacts (2.934 Å) in the Cambridge Structural Database (CSD).[28]

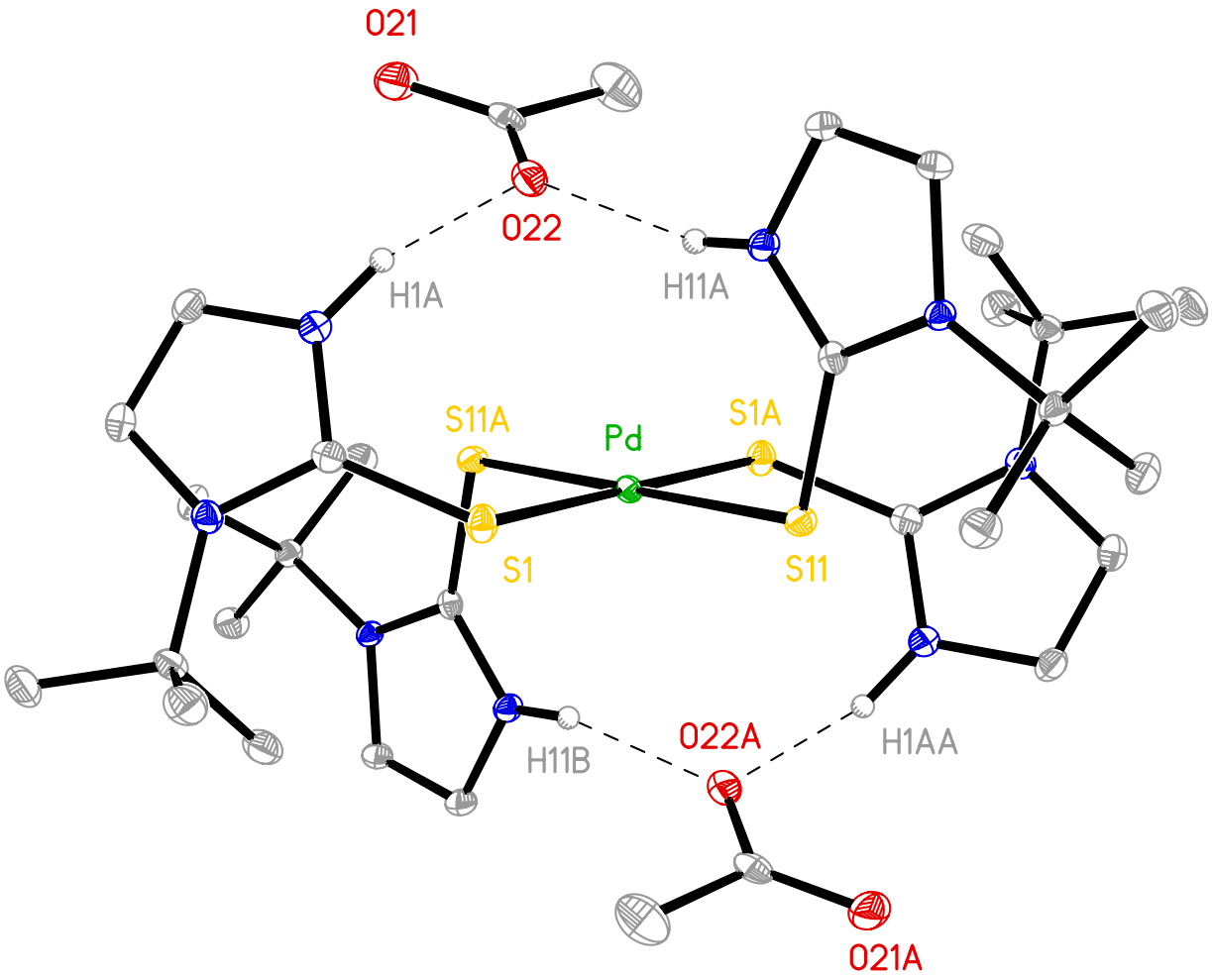

Figure 3. Molecular Structure of {[H(mim^{But})]$_4$Pd}(OAc)$_2$.

Table 1. Bond lengths, angles, and torsion angles for $\{[H(mim^{But})]_4Pd\}^{2+}$ and related compounds.

	Pd–S Avg. /Å	C=S Avg. /Å	S–Pd–S /°[a]	Ref
$\{[H_2(mim)]_4Pd\}Cl_2$	2.3319[4]	1.7277[18]	85.440(16), 94.560(16)	24
$\{[H_2(mim)]_4Pd\}Cl_2$	2.331[2]	1.721[6]	85.6(1), 94.4(1)	25
$\{[H(mim^{Me})]_4Pd\}Cl_2$	2.3407[7]	1.712[3]	87.08(3), 92.92(3)	26
$\{[H(mim^{But})]_4Pd\}Cl_2$	2.323[2]	1.716[5]	87.1(1), 92.9(1)	20
$\{[H(mim^{But})]_4Pd\}I_2$	2.3377[6]	1.726[2]	83.99(2), 96.01(2)	13b
$\{[H(mim^{But})]_4Pd\}(OAc)_2$	2.339[9]	1.732[2]	83.981(19), 96.020(19)	This work
$\{[H_2(mbenzimd)]_4Pd\}Cl_2$[b]	2.379[2] 2.389[2]	1.726[8] 1.725[8]	87.03(7), 92.97(8) 92.91(7), 87.09(7)	27

(a) Adjacent S–Pd–S angles (Note: the two largest angles for all compounds are 180˚).
(b) There are two $\{[H_2(mbenzimd)]_4Pd\}Cl_2$ molecules in the unit cell.

Attempts to synthesize the corresponding $H(sebenzim^{Me})$ compound, $\{[H(sebenzim^{Me})]_4Pd\}(OAc)_2$, proved unsuccessful, as the treatment of $Pd(OAc)_2$ with $H(sebenzim^{Me})$ resulted in intractable mixtures. However, $H(sebenzim^{Me})$ does react with $Pd(PPh_3)_2Cl_2$ to form $\{[H(sebenzim^{Me})]_3Pd(PPh_3)\}Cl_2$ where $H(sebenzim^{Me})$ is datively bound to Pd through the selenium atom.

$$3\ H(sebenzim^{Me}) + Pd(PPh_3)_2Cl_2 \xrightarrow[-PPh_3]{CH_3CN} \{[H(sebenzim^{Me})]_3Pd(PPh_3)\}Cl_2$$

Scheme 2. Synthesis of $\{[H(sebenzim^{Me})]_3Pd(PPh_3)\}Cl_2$ *via* the treatment of $Pd(PPh_3)_2Cl_2$ of with 3 equivalents $H(sebenzim^{Me})$.

{[H(sebenzim^{Me})]$_3$Pd(PPh$_3$)}Cl$_2$ adopts a slightly distorted square planar geometry (τ_4 = 0.16, τ_δ = 0.14) as determined by X-ray diffraction (Figure 4). Whereas the Pd–Se1 (2.4445(4) Å) and Pd–Se3 (2.4421(4) Å) possess very similar bond lengths (Se1 is trans to Se3), the Pd–Se2 (2.4842(4) Å) bond length is slightly longer, which could possibly be attributed to the trans influence of the PPh$_3$ ligand.[29] Although there are not many structurally characterized palladium complexes featuring 2-imidazoleselones,[30] these Pd–Se distances are on the longer side (range from 2.377-2.455 Å in the CSD).[28] In fact, the Pd–Se2 distance is slightly longer than any other Pd–selenourea interaction found in the CSD (2.461 Å).[28] The Cl anions are not coordinated to the Pd center, but, they are positioned on opposite sides of the PdSe$_3$P plane with Pd···Cl1 and Pd···Cl2 distances of 3.5210(9) Å and 4.3555(11) Å respectively (for reference, the average Pd–Cl bond length found in the CSD is 2.338 Å).[28] Given the position of Cl1 and the fact that the sum of the crystallographic van der Waals radii for Pd and Cl is 3.85 Å,[31] it is not unreasonable to suggest that there is a weak interaction between the Palladium center and Cl1. Cl2 is likely too far away for any secondary interaction. Additionally, both Cl anions hydrogen bond to the NH groups of the {[H(sebenzim^{Me})]$_3$Pd(PPh$_3$)}$^+$ cation.

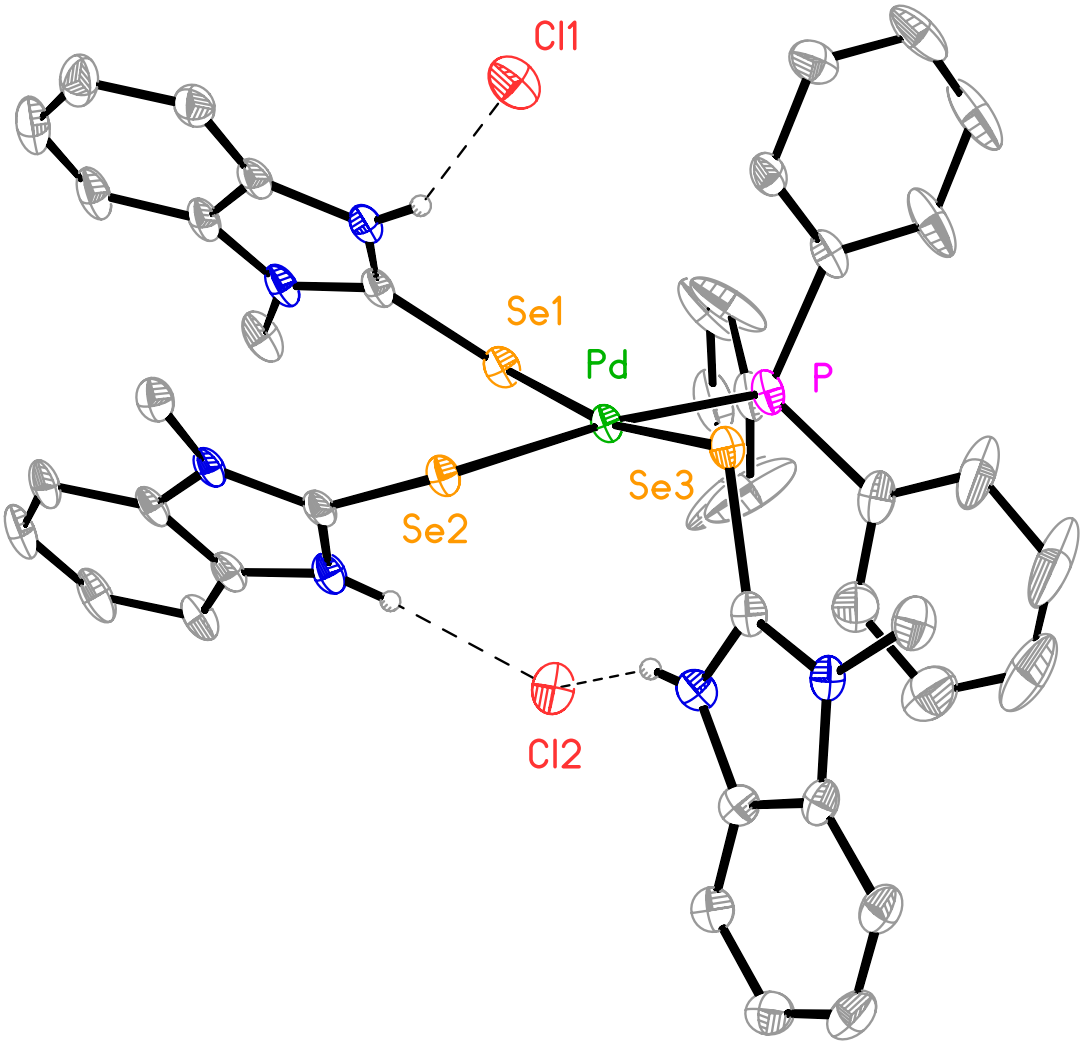

Figure 4. Molecular structure of {[H(sebenzim^{Me})]$_3$Pd(PPh$_3$)}Cl$_2$.

3.2.2 Bridging sebenzim^{Me} Complexes of Palladium: Synthesis and Structural Characterization of [(PPh$_3$)(Cl)Pd(μ-E,N-Ebenzim^{Me})]$_2$ (E = S, Se)

In addition to coordinating metal centers in a dative L-type fashion through the sulfur and selenium, 1-R-imidazole-2-thiones and 1-R-imidazole-2-selones can also be deprotonated, allowing for an LX[21] coordination mode which can result in bridging complexes.[13b,32] In this regard, the deprotonation of H(mbenzim^{Me}) and H(sebenzim^{Me})

with NaH, followed by subsequent treatment with $Pd(PPh_3)_2Cl_2$, results in the formation of the dimers, $[(PPh_3)(Cl)Pd(\mu\text{-}E,N\text{-}Ebenzim^{Me})]_2$ (E = S, Se), as illustrated in Scheme 3.

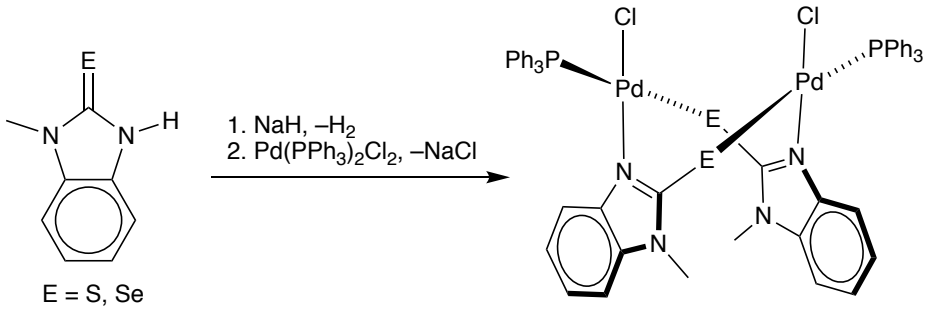

Scheme 3. Synthesis of $[(PPh_3)(Cl)Pd(\mu\text{-}E,N\text{-}Ebenzimid^{Me})]_2$ (E = S, Se).

Both $[(PPh_3)(Cl)Pd(\mu\text{-}S,N\text{-}mbenzim^{Me})]_2$ and $[(PPh_3)(Cl)Pd(\mu\text{-}Se,N\text{-}sebenzim^{Me})]_2$ are isostructural as indicated by X-ray diffraction experiments (Figure 5 and Figure 6). The C2-symmetric dimers bridge through the N and E atoms and are oriented in such a way that the Pd centers achieve a slightly distorted square planar geometry (E = S: $\tau_4 = \tau_\delta = 0.05$; E = Se: $\tau_4 = \tau_\delta = 0.06$). As is expected, the Pd–S bond length (2.3786(5) Å) is shorter than the Pd–Se (2.4713(4) Å) distance. It is also worth noting that the Pd–S and Pd–Se bonds in $[(PPh_3)(Cl)Pd(\mu\text{-}E,N\text{-}Ebenzim^{Me})]_2$ are comparable to the corresponding bonds in $\{[H(mim^{But})]_4Pd\}(OAc)_2$ (2.339[9] Å) and $\{[H(sebenzim^{Me})]_3Pd(PPh_3)\}Cl_2$ (2.4421(4) – 2.4842(4) Å).

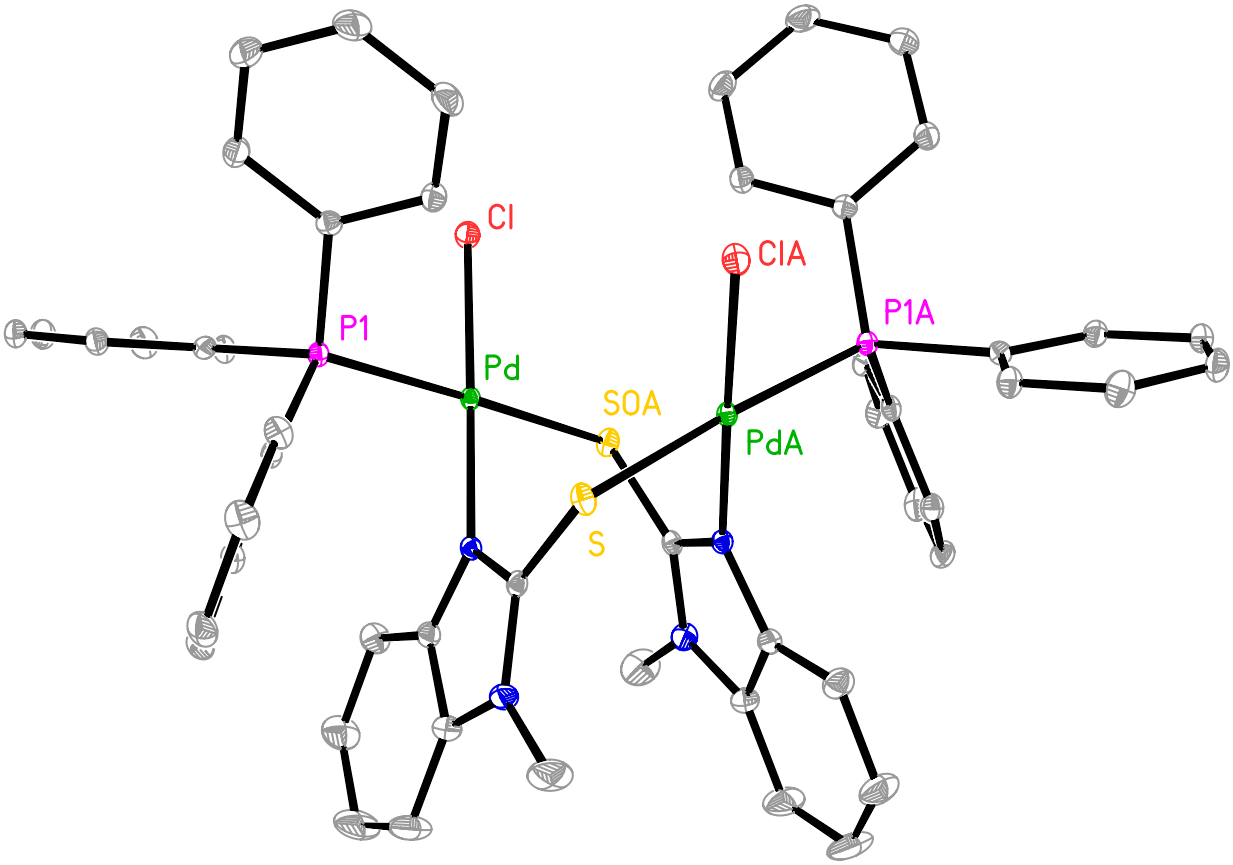

Figure 5. Molecular structure of $[(PPh_3)(Cl)Pd(\mu\text{-}S,N\text{-}mbenzimid^{Me})]_2$.

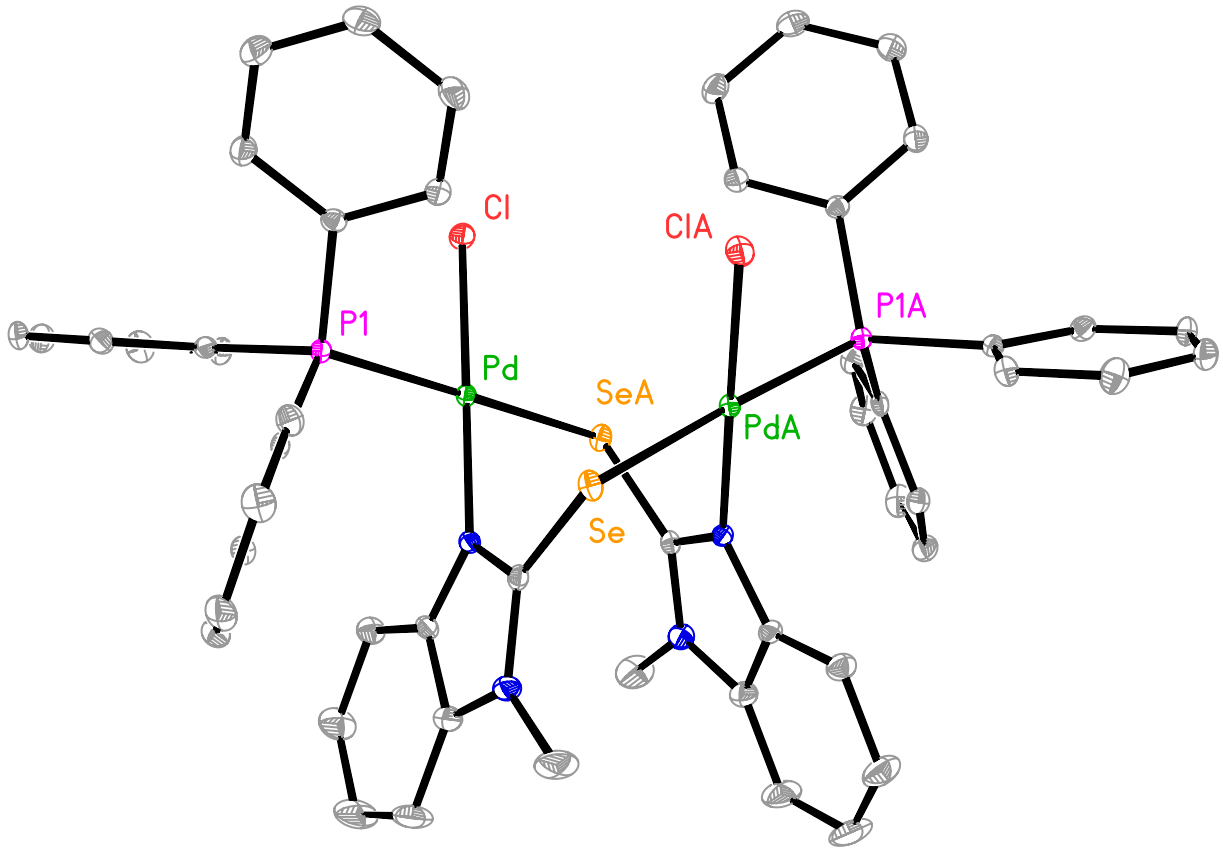

Figure 6. Molecular structure of $[(PPh_3)(Cl)Pd(\mu\text{-Se,N-sebenzim}^{Me})]_2$.

3.3 Synthesis and Structural Characterization of Nickel Complexes Featuring the H(sebenzim^{Me}) Ligand

3.3.1 Reactivity of H(sebenzim^{Me}) Towards NiX_2 (X = Cl, Br, I): Synthesis and Structural Characterization of $[H(sebenzim^{Me})]_4NiCl_2$, $[H(sebenzim^{Me})]_2NiBr_2$, and $\{[H(sebenzim^{Me})]_4NiI\}I$

H(sebenzim^{Me}) is also an effective ligand for nickel, as displayed by its coordination to NiX_2 (X = Cl, Br, I) through the selenium in an L-type[21] fashion. Interestingly, structurally different complexes are obtained depending upon the identity of the halide. More specifically, when $NiCl_2$ is treated with 4 equivalent of H(sebenzim^{Me}), the octahedral complex $[H(sebenzim^{Me})]_4NiCl_2$ is obtained (Figure 7). The Cl ligands are

located trans to one another while the $NiSe_4$ unit forms an almost ideal square plane. Two of the H(sebenzim^{Me}) ligands can be considered "up" as they are on the same side of the $NiSe_4$ plane and have two N–H···Cl hydrogen bonding interactions (2.240(9) Å and 2.28(4) Å), while the other two are "down" (on the opposite side of the $NiSe_4$ plane) and participate in a similar hydrogen bonding arrangement.

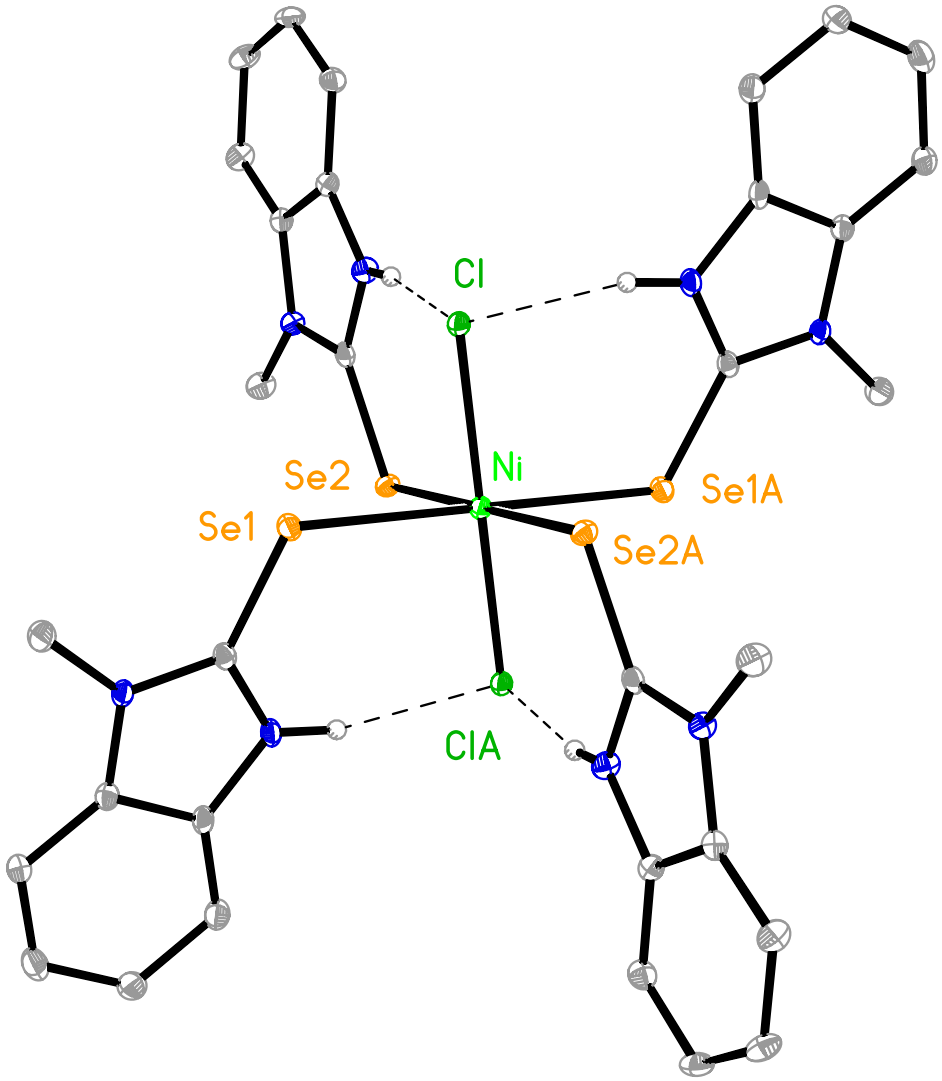

Figure 7. Molecular structure of [H(sebenzim^{Me})]$_4$NiCl$_2$

The reactivity of H(sebenzim^{Me}) towards $NiCl_2$ contrasts the reactivity of the selone towards $NiBr_2$. Specifically, even when $NiBr_2$ is treated with excess H(sebenzim^{Me}), only the 2:1 complex, [H(sebenzim^{Me})]$_2$$NiBr_2$ can be isolated (Figure 8).[33] [H(sebenzim^{Me})]$_2$$NiBr_2$ adopts a slightly distorted tetrahedral geometry (τ_4 = 0.83 and τ_δ = 0.76) and the H(sebenzim^{Me}) ligands are oriented in such a way that the N–H's hydrogen bond to the bromine ligands with a N–H···Br distance of 2.38(4) Å.

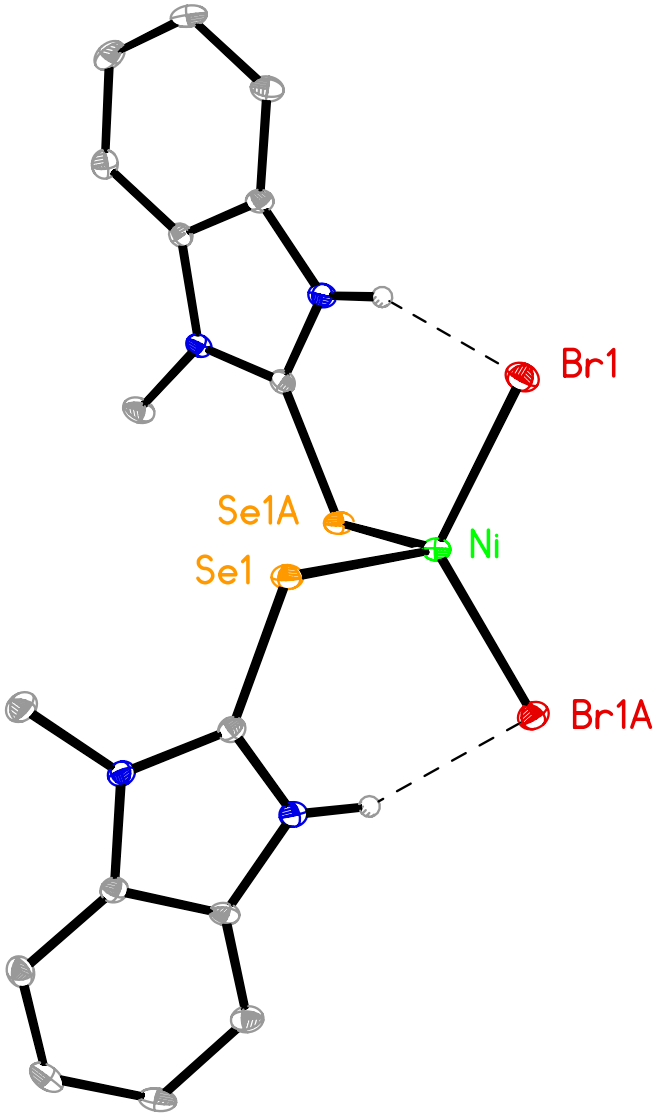

Figure 8. Molecular structure of [H(sebenzim^{Me})]$_2$$NiBr_2$.

Furthermore, a different type of structure is obtained when NiI_2 is treated with H(sebenzim^{Me}). Specifically, 4 equivalents of H(sebenzim^{Me}) react with NiI_2 to form {[H(sebenzim^{Me})]$_4$NiI}I (Figure 9), in which only one of the iodides is still coordinated to the nickel center and the other acts as a counter ion (the Ni–I2 distance is 2.444[2] Å longer than the Ni–I1 distance). {[H(sebenzim^{Me})]$_4$NiI}I adopts a distorted trigonal bipyramidal geometry with a τ_5 parameter of 0.73.[34] Although all four of the N–H's of the H(sebenzim^{Me}) ligands orient themselves toward the non-coordinated I2 anion, only two have considerable hydrogen bonding interactions; the H···I distances in {[H(sebenzim^{Me})]$_4$NiI}I are 2.74(2) Å, 2.797(18) Å, 3.221(18) Å, and 3.550(19) Å. For reference, the average H···I distance for a non-bonded contact in a N–H···I unit found in the CSD[28] is 2.847 Å.

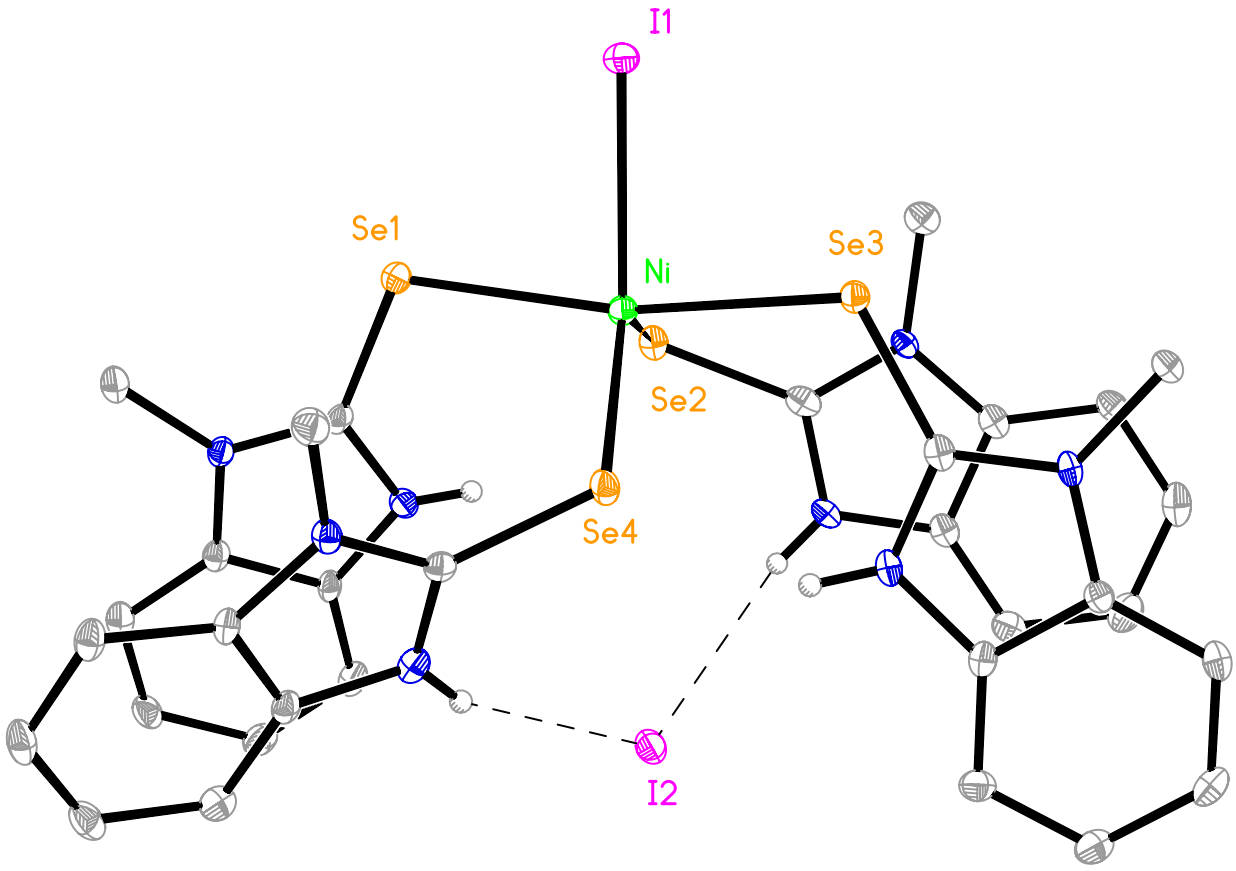

Figure 9. Molecular structure of {[H(sebenzim^{Me})]$_4$NiI}I.

The structural diversity observed in the NiX_2 (Cl, Br, I) series is certainly interesting and serves to demonstrate the wide range of coordination complexes that H(sebenzim^{Me}) is capable of generating. The size of the halide appears to have a significant effect when comparing [H(sebenzim^{Me})]$_4$NiCl$_2$ and {[H(sebenzim^{Me})]$_4$NiI}I, as two coordinated iodide ligands may be too sterically demanding to achieve a $NiSe_4I_2$ octahedral arrangement. For reference, there are no structurally characterized nickel complexes in the CSD[28] that feature an Se_4I_2 coordination environment. With regards to the $NiBr_2$ species, [H(sebenzim^{Me})]$_2$NiBr$_2$, the 2:1 complex preferentially crystallizes, even though NMR evidence suggest that a 3:1 and 4:1 product is possible.

With respect to the bond lengths in this series, [H(sebenzim^{Me})]$_2$NiBr$_2$ displays the shortest Ni–Se bonds (2.3972[5] Å), followed by {[H(sebenzim^{Me})]$_4$NiI}I (2.4909[11] Å) and [H(sebenzim^{Me})]$_4$NiCl$_2$ (2.6108[5] Å). All three of these nickel complexes have comparable Ni–Se bond lengths to other structurally characterized nickel complexes in the CSD[28] that feature 2-imidazoleselones (2.395 Å - 2.593 Å).[35]

Table 2. Selected bond lengths for the [H(sebenzim^{Me})]$_n$NiX$_2$ (X = Cl, Br, I) series.

	Ni–Se Avg. /Å	**Ni–X Avg. /Å**	**C=Se Avg. /Å**
[H(sebenzim^{Me})]$_4$NiCl$_2$	2.6108[5]	2.462(8)	1.843[3]
[H(sebenzim^{Me})]$_2$NiBr$_2$	2.3972(5)	2.3720(4)	1.859(3)
{[H(sebenzim^{Me})]$_4$NiI}I	2.4909[11]	2.6852(12)[a]	1.867[5]

(a) Distance for the covalently bonded I; The other I in {[H(sebenzim^{Me})]$_4$NiI}I is separated from the Ni center by 5.129(2) Å.

3.3.2 Synthesis and Structural Characterization of $Ni_2[\mu\text{-Se,N-sebenzim}^{Me}]_4$

Paddlewheel compounds of nickel featuring H(sebenzim^{Me}) can also be synthesized, and bear a structural resemblance to the paddlewheel complexes synthesized by the Parkin group with H(mim$^{Bu^t}$).[13b] Specifically, the treatment of {[H(sebenzim^{Me})]$_4$NiI}I with NaH results in the formation of $Ni_2[\mu\text{-Se,N-sebenzim}^{Me}]_4$ (Figure 10). Both Ni centers of $Ni_2[\mu\text{-Se,N-sebenzim}^{Me}]_4$ are almost perfectly square planar, and the compound can be designated as the (4,0) isomer[13b] by virtue of each [sebenzim^{Me}]$^-$ ligand bridging with identical orientations. This motif affords two nickel centers within the same molecule that are electronically distinct, one with a {$NiSe_4$} coordination environment, and the other with a {NiN_4} environment. The two square planes are also slightly staggered, as demonstrated by the 28.5° N–Ni–Ni–Se torsion angle (Figure 11). The Ni···Ni distance is 2.6906(8) Å, which is comparable to the Ni–Ni bond length in its elemental form (2.49 Å),[36] suggesting that some degree of Ni–Ni bonding may be present. However, calculations on compounds of this type have revealed that all bonding and anti-bonding Ni–Ni orbitals are filled, thus formally giving a bond order of zero, indicating that there is no net interaction.[13b,37]

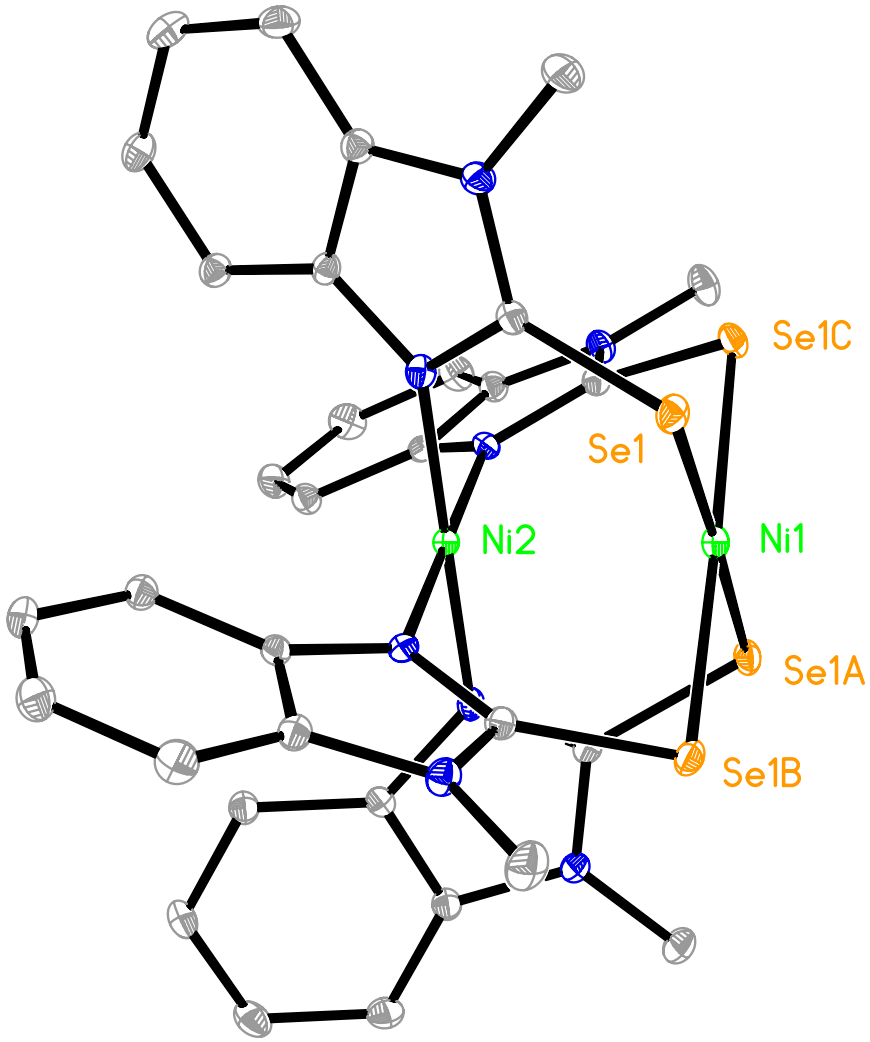

Figure 10. Molecular structure of Ni_2[μ-Se,N-sebenzim^{Me}]$_4$ (side view).

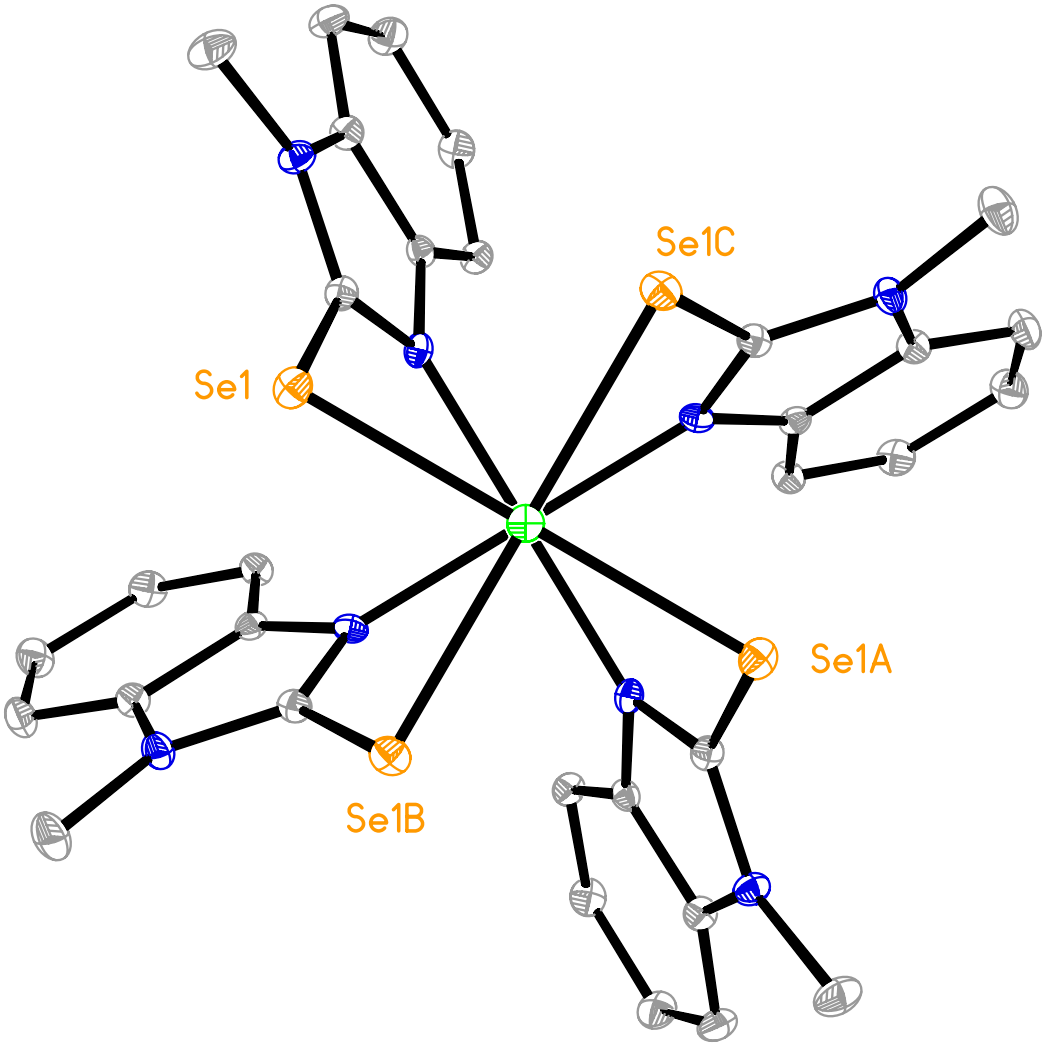

Figure 11. Molecular structure of $Ni_2[\mu\text{-Se,N-sebenzim}^{Me}]_4$ (top-down view).

3.3.3 Synthesis and Structural Characterization of the Nickel Nitrosyl Complexes $[(PPh_3)(NO)Ni(\mu\text{-Se,N-sebenzim}^{Me})]_2$ and $Ni_5(NO)_4(\text{sebenzim}^{Me})_6$

Given that nitric oxide plays an important biological role, interest in transition metal nitrosyl chemistry has received increasing attention.[35b,38] In light of this, we became interested in the reactivity of H(sebenzim^{Me}) towards nickel nitrosyl compounds. To this end, $Ni(PPh_3)_2(NO)Br$ was first treated with H(sebenzim^{Me}), which resulted in no

observable reaction as determined by NMR spectroscopy (Scheme 4). However, upon deprotonating H(sebenzim^{Me}) with NaH to form the sodium salt, followed by addition to Ni(PPh$_3$)$_2$(NO)Br, a complex that is characterized by a broad resonance at 45.4 ppm in the ^{31}P{^{1}H} NMR spectrum is generated.

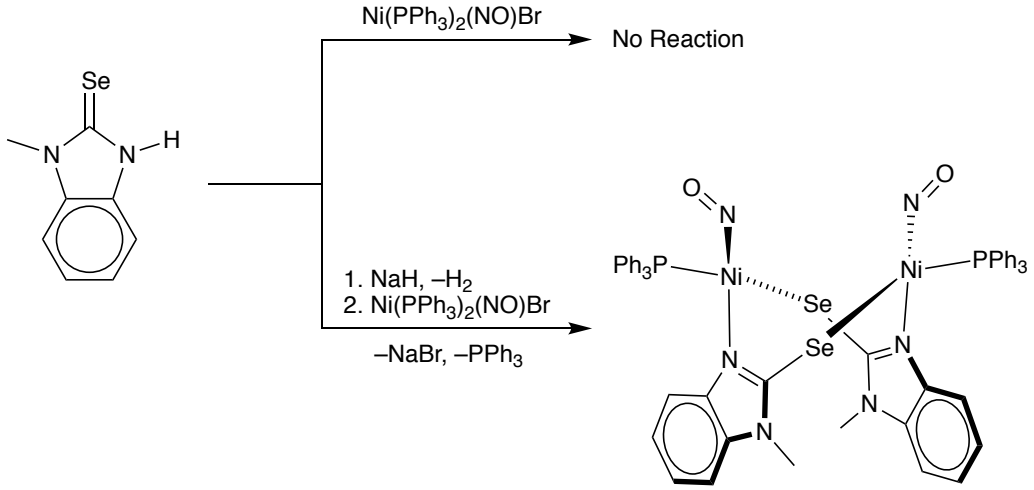

Scheme 4. Reactivity of H(sebenzim^{Me}) towards Ni(PPh$_3$)$_2$(NO)Br.

Single crystal X-ray diffraction reveals that this complex is the dimer, [(PPh$_3$)(NO)Ni(μ-Se,N-sebenzim^{Me})]$_2$ (Figure 12). The [sebenzim^{Me}]$^-$ ligands bridge the two Ni centers which adopt distorted tetrahedral geometries (τ_4= 0.84 and τ_δ = 0.79 for Ni1; τ_4= 0.77 and τ_δ = 0.75 for Ni2) and possess a PPh$_3$ and NO ligand. The Ni–N–O bond angles are 150.0(4)° and 151.5(5)° and possess Ni–O bond lengths of 1.174(6) and 1.171(5) Å suggesting that there is some degree of π donation back to the metal center. Spectroscopically, the N–O stretching frequencies appear at 1716.82 and 1697.68 cm^{-1} in the IR spectrum.

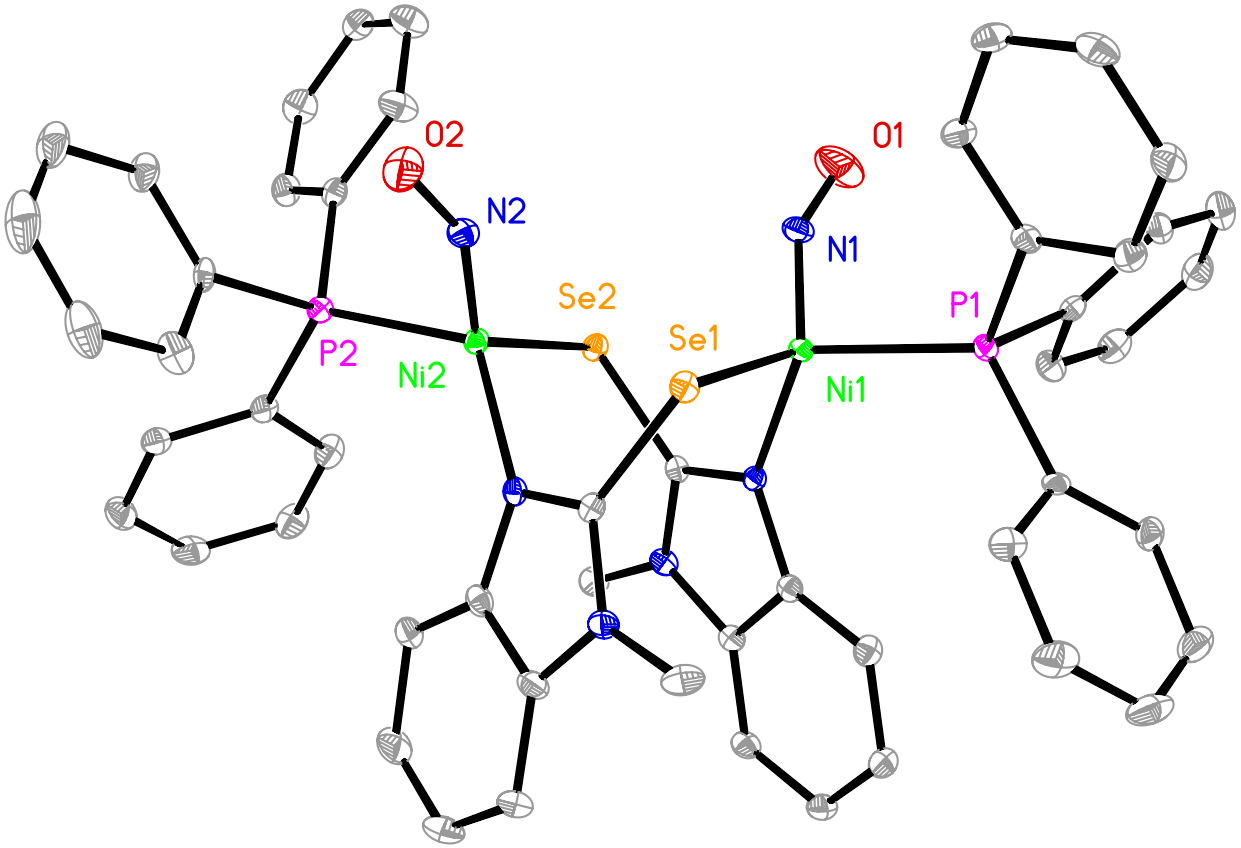

Figure 12. Molecular structure of $[(PPh_3)(NO)Ni(\mu\text{-Se,N-sebenzim}^{Me})]_2$.

3.4 Synthesis and Structural Characterization of Zinc and Cadmium Complexes Featuring the H(sebenzim^{Me}) Ligand

3.4.1 Synthesis and Structural Characterization $[H(sebenzim^{Me})]_2MX_2$ (M = Zn, X = Cl, Br; M = Cd, X = Cl, Br, I)

Previously, the Parkin group investigated the reactivity of H(sebenzim^{Me}) towards mercury compounds, demonstrating that H(sebenzim^{Me}) (*i*) effectively binds mercury halides through the selenium and (*ii*) is capable of protolytically cleaving Hg–C bonds in mercury alkyl complexes.[15a,15b] Given the success of H(sebenzim^{Me}) as a ligand for mercury, and the relative dearth of structurally characterized zinc and cadmium complexes featuring imidazoleselones in the CSD,[15f,28,39] we felt it appropriate to extend

our studies to the lighter group 12 metals. In this regard, H(sebenzim^{Me}) reacts with ZnX_2 (X = Cl, Br) and CdX_2 (X = Cl, Br, I) in a 2:1 stoichiometry to yield $[H(sebenzim^{Me})]_2MX_2$.

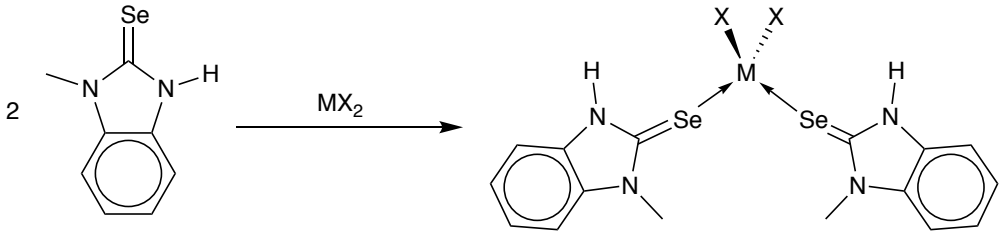

Scheme 5. Synthesis of $[H(sebenzim^{Me})]_2MX_2$ (M = Zn, X =Cl, Br; M = Cd, X = Cl, Br, I).

Structural characterization of the $[H(sebenzim^{Me})]_2MX_2$ series by X-ray diffraction (Figure 13-Figure 17) reveals that each metal center adopts a slightly distorted tetrahedral geometry with τ_4 and τ_δ indices in the range of 0.93–0.95 and 0.88–0.92 respectively (Table 3).[22] In comparison to the previously reported mercury analogues,[15a,15b] the chloride and bromide complexes, $[H(sebenzim^{Me})]_2MX_2$ (M =Zn, Cd; X = Cl, Br), are isostructural with $[H(sebenzim^{Me})]_2HgCl_2$[15a] and possess two intramolecular N–H···X hydrogen bonding moieties. Likewise, $[H(sebenzim^{Me})]_2CdI_2$ is isostructural with the orthorhombic setting of $[H(sebenzim^{Me})]_2HgI_2$,[15b] which possess a different hydrogen bonding pattern in which there is one intramolecular and intermolecular N–H···I moieties.

With regards to the bond lengths of these group 12 complexes, the average Zn–Se bond lengths are shorter than the Cd–Se bond lengths, as expected. However, the average Cd–Se bond lengths are slightly *longer* than the average Hg–Se bond lengths. For example, for the chloride series, $[H(sebenzim^{Me})]_2MCl_2$ (M =Zn, Cd, Hg), the average Zn–Se, Cd–Se, and Hg–Se bond lengths are 2.4708[6] Å, 2.6261[5] Å, and 2.5911[5] Å

respectively (Table 4). Furthermore, the opposite trend is observed for the M–Cl bond lengths, whereby the average Cd–Cl (2.4658[8] Å) bond length is slightly *shorter* than the average Hg–Cl (2.5335[8] Å) bond length (for reference, the average Zn–Cl bond length is 2.2788[9] Å as indicated in Table 4). This anomaly in Cd and Hg having very similar M–Se and M–X bond lengths, despite Hg being below Cd in group 12 on the periodic table, is attributed to the lanthanide contraction.[40] This results in the atomic radii of Cd and Hg being roughly the same size due to poor shielding from a fully filled 4f subshell.

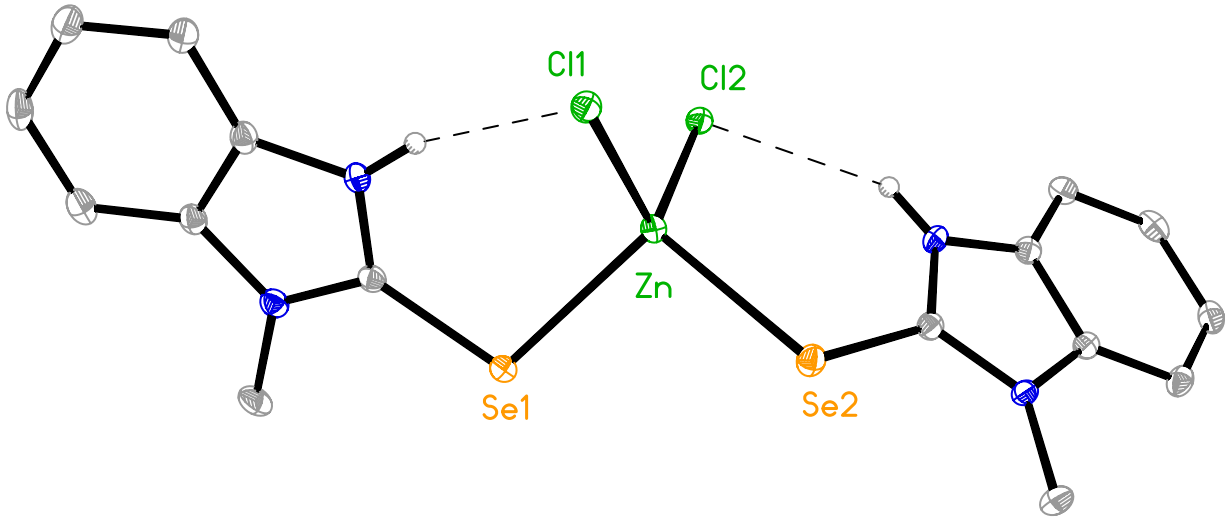

Figure 13. Molecular structure of $[H(sebenzim^{Me})]_2ZnCl_2$.

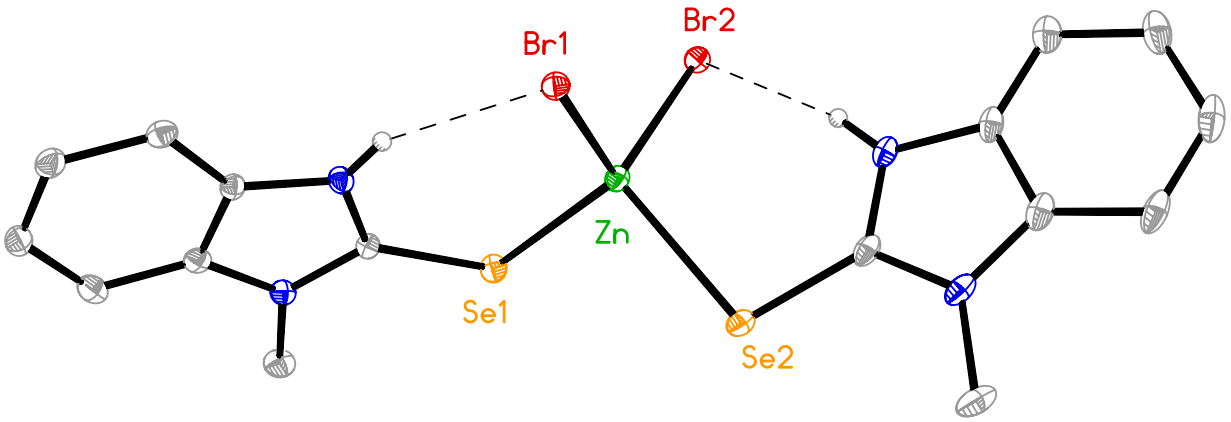

Figure 14. Molecular structure of $[H(sebenzim^{Me})]_2ZnBr_2$.

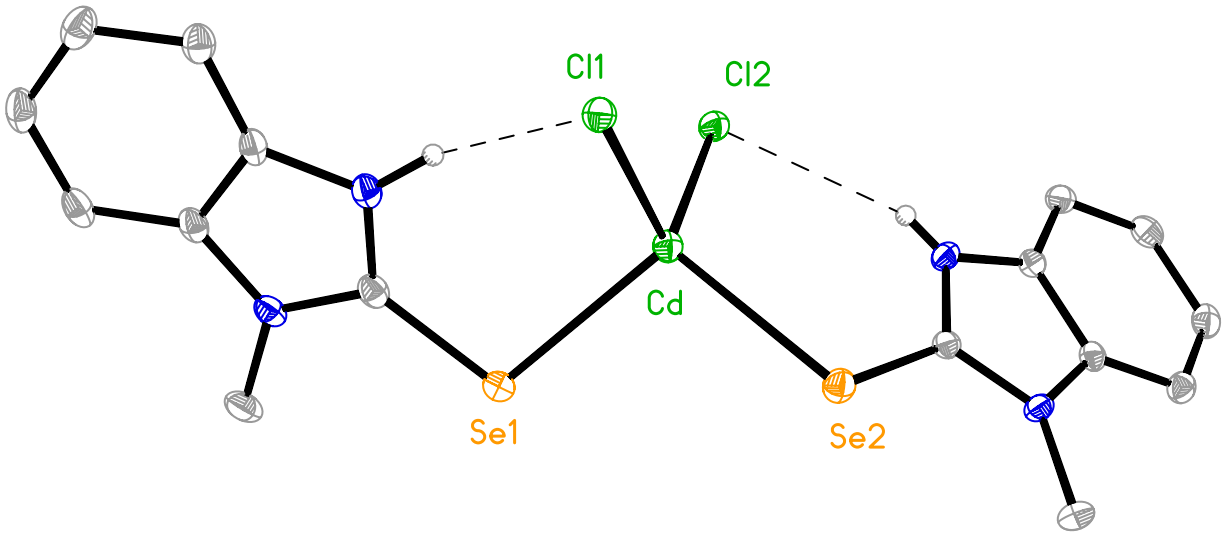

Figure 15. Molecular structure of $[H(sebenzim^{Me})]_2CdCl_2$.

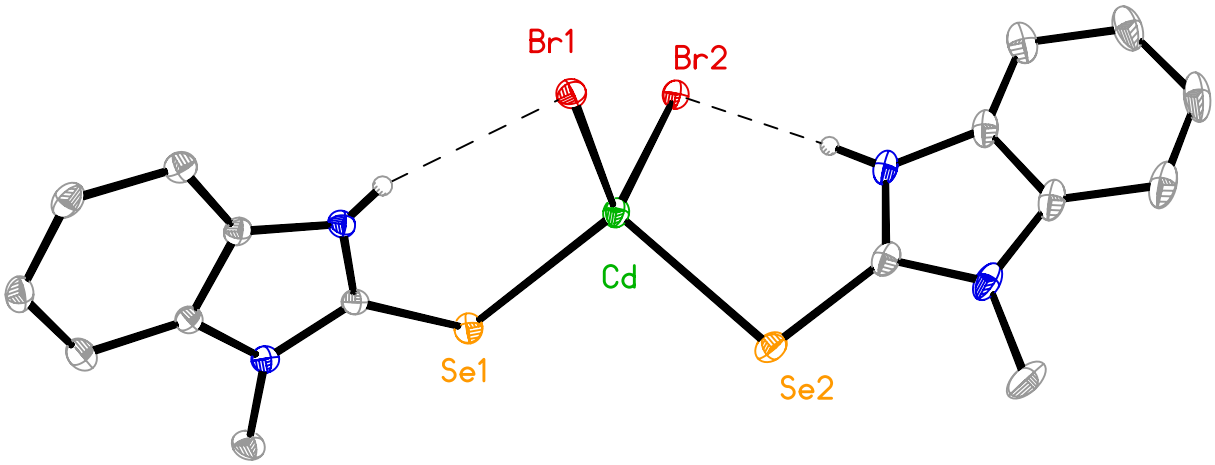

Figure 16. Molecular structure of $[H(sebenzim^{Me})]_2CdBr_2$.

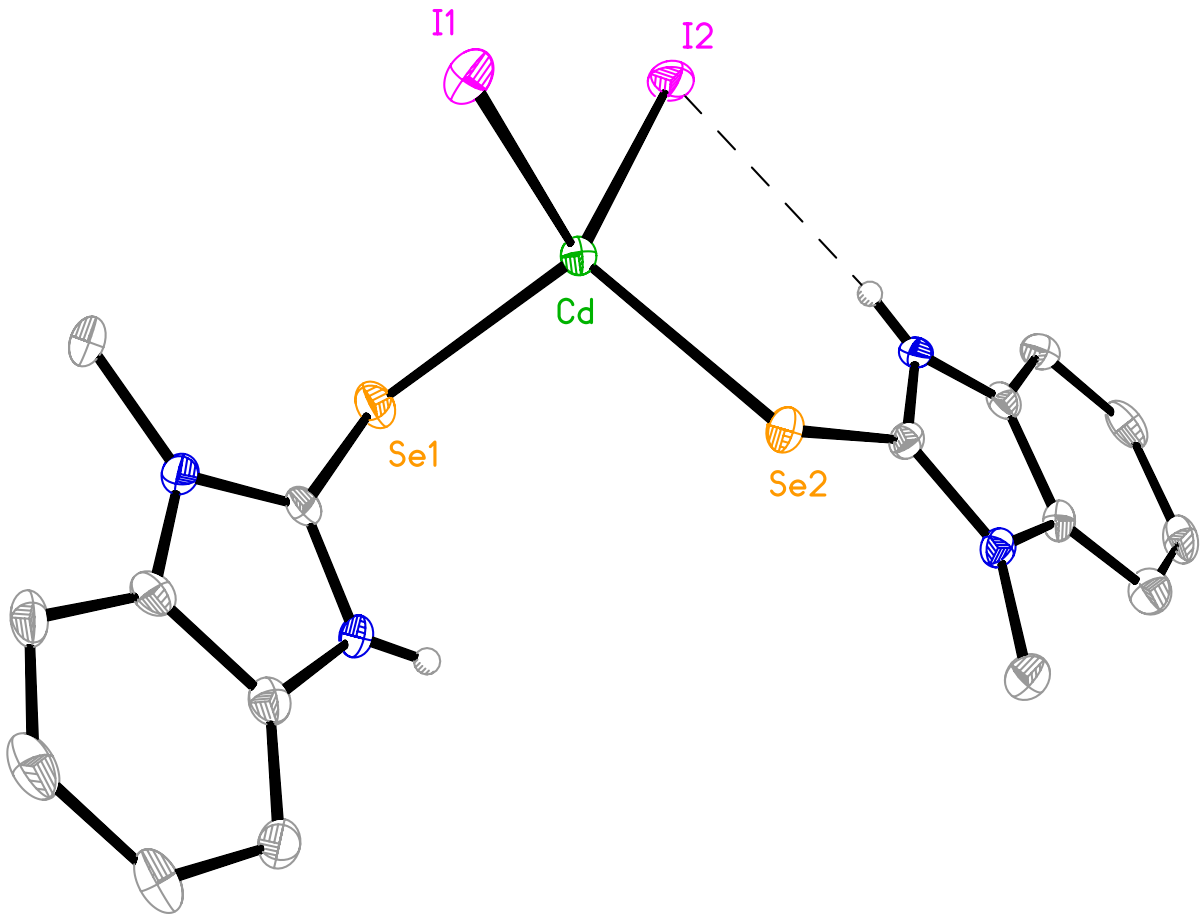

Figure 17. Molecular structure of $[H(sebenzim^{Me})]_2CdI_2$.

Table 3. τ_4 and τ_δ indices for the series $[H(sebenzim^{Me})]_2MX_2$.

	τ_4	τ_δ	**Ref.**
$[H(sebenzim^{Me})]_2ZnCl_2$	0.93	0.90	This work
$[H(sebenzim^{Me})]_2ZnBr_2$	0.93	0.88	This work
$[H(sebenzim^{Me})]_2CdCl_2$	0.94	0.93	This work
$[H(sebenzim^{Me})]_2CdBr_2$	0.95	0.91	This work
$[H(sebenzim^{Me})]_2CdI_2$	0.95	0.92	This work
$[H(sebenzim^{Me})]_2HgCl_2$	0.94	0.92	15a
$[H(sebenzim^{Me})]_2HgI_2$[a]	0.94	0.90	15b

(a) Metrical data is given for the orthorhombic setting of $[H(sebenzim^{Me})]_2HgI_2$.

Table 4. Selected bond lengths for the series $[H(sebenzim^{Me})]_nMX_2$.

	M–Se Avg. /Å	M–X Avg. /Å	Ref
$[H(sebenzim^{Me})]_2ZnCl_2$	2.4708[6]	2.2788[9]	This work
$[H(sebenzim^{Me})]_2ZnBr_2$	2.4787[8]	2.4116[7]	This work
$[H(sebenzim^{Me})]_2CdCl_2$	2.6261[5]	2.4658[8]	This work
$[H(sebenzim^{Me})]_2CdBr_2$	2.6433[9]	2.5956[8]	This work
$[H(sebenzim^{Me})]_2CdI_2$	2.6417[10]	2.7731[8]	This work
$[H(sebenzim^{Me})]_3CdCl_2$[a]	2.6901[8]	2.6788[17]	This work
$[H(sebenzim^{Me})]_4CdCl_2$[a]	2.8111[7]	2.6719(12)	This work
$[H(sebenzim^{Me})]_2HgCl_2$	2.5911[5]	2.5335[8]	15a
$[H(sebenzim^{Me})]_2HgI_2$[b]	2.6273[10]	2.7916[7]	15b
$\{[H(sebenzim^{Me})]_3Hg\}[Cl]$[c]	2.6095[4]	2.7506(9)	15b
$\{[H(sebenzim^{Me})]_4Hg\}[Cl]_2$[d]	2.6627[11]	–	15b

(a) Metrical data for the 3:1 and 4:1 $CdCl_2$ complexes are obtained from the co-crystal, $[H(sebenzim^{Me})]_3CdCl_2 \bullet [H(sebenzim^{Me})]_4CdCl_2$, which is discussed in section 3.4.2 below.
(b) Metrical data is given for the orthorhombic setting of $[H(sebenzim^{Me})]_2HgI_2$.
(c) Only one Cl atom coordinates to the Hg center in $\{[H(sebenzim^{Me})]_3Hg\}[Cl]$
(d) Both Cl atoms do not coordinate to the Hg center in $\{[H(sebenzim^{Me})]_4Hg\}[Cl]_2$

3.4.2 Synthesis and Structural Characterization of $[H(sebenzim^{Me})]_3CdCl_2 \bullet [H(sebenzim^{Me})]_4CdCl_2$

Similar to the corresponding mercury compounds, more than two $H(sebenzim^{Me})$ ligands are capable of coordinating to the same cadmium center. Specifically, when $CdCl_2$ is treated with excess $H(sebenzim^{Me})$, the co-crystal, $[H(sebenzim^{Me})]_3CdCl_2 \bullet [H(sebenzim^{Me})]_4CdCl_2$ is generated (Figure 18). This crystal features two unique Cd centers, one with a 3:1 ligand to Cd ratio in a trigonal bipyramidal arrangement and the other with a 4:1 ligand to Cd ratio in an octahedral arrangement. Several attempts to synthesize the 3:1 and 4:1 complexes separately

proved unsuccessful. In contrast, 3:1 and 4:1 mercury complexes are able to be isolated separately, however, both complexes are not isostructural to either $[H(sebenzim^{Me})]_3CdCl_2$ or $[H(sebenzim^{Me})]_4CdCl_2$. Specifically, the 3:1 complex is best represented as the ion pair, $\{[H(sebenzim^{Me})]_3HgCl\}[Cl]$,[15b] and the 4:1 complex does not have any coordinated chloride ligands, such that it is best represented as $\{[H(sebenzim^{Me})]_4Hg\}[Cl]_2$.[15b]

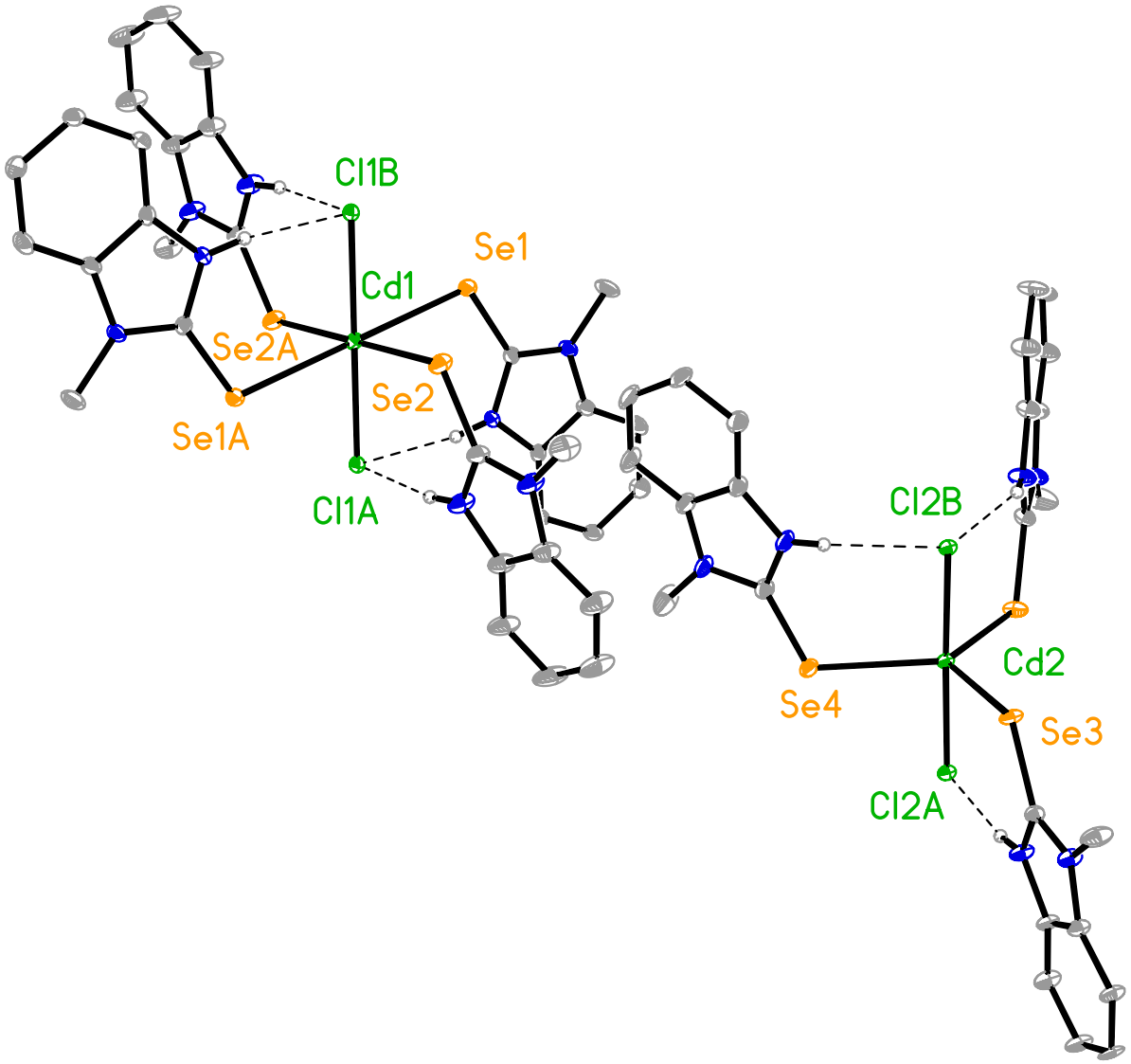

Figure 18. Molecular structure of $[H(sebenzim^{Me})]_3CdCl_2 \bullet [H(sebenzim^{Me})]_4CdCl_2$

Upon comparing the bond lengths, a correlation between the number of coordinated H(sebenzim^{Me}) ligands and the average Cd–Se distance is recognized (Table 4). More specifically, as the number of coordinated H(sebenzim^{Me}) ligands increase, the average Cd–Se distance increases as well, showing a range of 2.6261[5] Å – 2.8111[7] Å for [H(sebenzim^{Me})]$_n$CdCl$_2$ (n = 2, 3, 4). For reference, the average Hg–Se bond lengths do not vary as drastically when the number of H(sebenzim^{Me}) increases in [H(sebenzim^{Me})]$_2$HgCl$_2$, {[H(sebenzim^{Me})]$_3$HgCl}[Cl], and {[H(sebenzim^{Me})]$_4$Hg}[Cl]$_2$ (2.5911[5] Å, 2.6095[4] Å and 2.6627[11] Å respectively). Additionally, the average Cd–Cl distances exhibit a non-monotonic trend with the 3:1 complex, [H(sebenzim^{Me})]$_3$CdCl$_2$, having the longest Cd–Cl bond length (2.6788[17] Å), the 4:1 complex, [H(sebenzim^{Me})]$_4$CdCl$_2$, having the intermediate Cd–Cl bond lengths (2.6719(12) Å), and the 2:1 complex, [H(sebenzim^{Me})]$_2$CdCl$_2$, having the shortest (2.4658[8] Å) as illustrated in Table 4.

3.4.3 Synthesis and Structural Characterization [H(sebenzim^{Me})](benzim^{Me})CdI$_2$

During the synthesis of [H(sebenzim^{Me})]$_2$CdI$_2$, it was noted that the decomposition product, [H(sebenzim^{Me})](benzim^{Me})CdI$_2$, can be formed. Specifically, when H(sebenzim^{Me}) is heated in the presence of CdI$_2$ for prolonged periods, one of the H(sebenzim^{Me}) ligands decomposes to 1-methylbenzimidazole and coordinates to the Cd center through the nitrogen, while the other H(sebenzim^{Me}) ligand remains intact and coordinates through the selenium, as illustrated in Scheme 6 and Figure 19. Accompanying this reaction is the formation of a grey powder, which has been analyzed by powder X-ray diffraction and identified as elemental selenium. This is consistent with the decomposition of H(sebenzim^{Me}) to generate 1-methylbenzimidazole, as elemental selenium would be the expected side product.

[H(sebenzim^{Me})](benzim^{Me})CdI_2 can also be synthesized more directly by treating CdI_2 with an equimolar mixture of H(sebenzim^{Me}) and 1-methylbenzimidazole (Scheme 6).

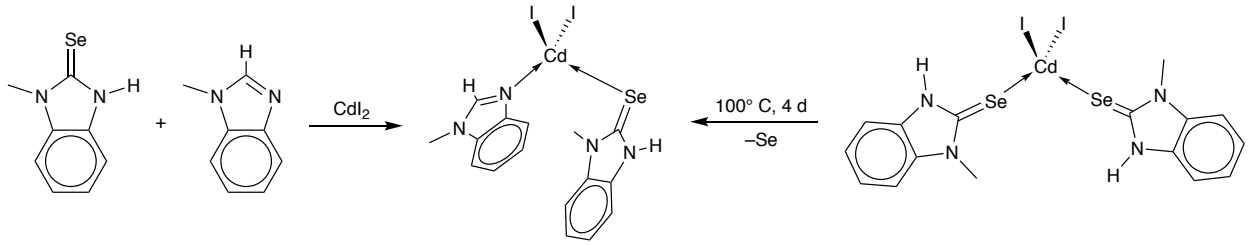

Scheme 6. Synthesis of [H(sebenzim^{Me})](benzim^{Me})CdI_2 by (*i*) the addition of an equimolar mixture of H(sebenzim^{Me}) and 1-methylbenzimidazole to CdI_2, and (*ii*) thermal decomposition of [H(sebenzim^{Me})]$_2CdI_2$.

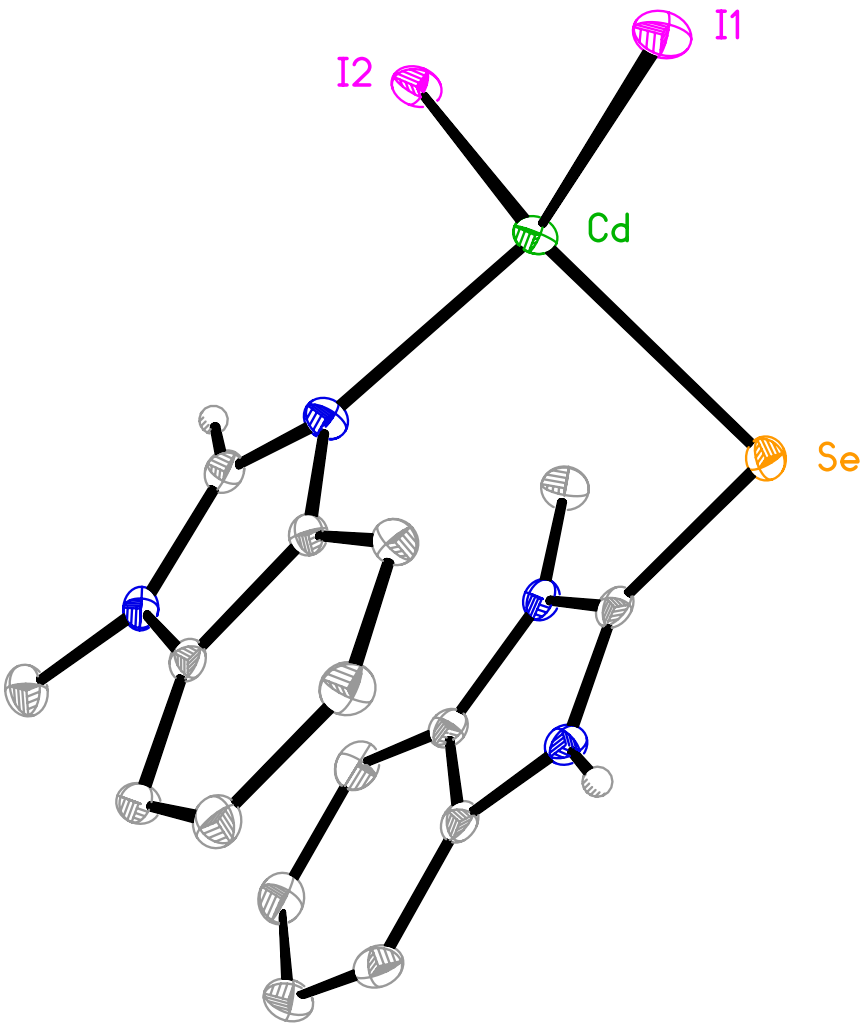

Figure 19. Molecular structure of [H(sebenzim^{Me})](benzim^{Me})CdI_2.

The cadmium center in [H(sebenzim^{Me})](benzim^{Me})CdI_2 adopts a distorted tetrahedral geometry with τ_4 and τ_δ indices of 0.88 and 0.85 respectively. The Cd–Se (2.6747(9) Å) and Cd–I (2.7419(8) Å and 2.7539(7) Å) bond lengths are similar to those found in [H(sebenzim^{Me})]$_2CdI_2$, and the Cd–N bond length (2.249(4) Å) is comparable to the average Cd–$N_{benzimidazole}$ bond length found in the CSD (2.266 Å) for cadmium complexes that also feauture two iodide ligands.[28,41]

3.5 Summary and Conclusions

In summary, a number of metal complexes featuring H(sebenzim^{Me}) have been synthesized and structurally characterized, illustrating the diverse coordination chemistry of H(sebenzim^{Me}). H(sebenzim^{Me}) is able to coordinate metal centers through the selenium atom in a dative fashion (Figure 20a). Depending upon the metal center, up to four H(sebenzim^{Me}) ligands can coordinate the same metal. Additionally, H(sebenzim^{Me}) can be deprotonated to form [sebenzim^{Me}]$^-$, allowing for the potential of an LX coordination mode. In this work, deprotonation of H(sebenzim^{Me}) leads to bridging complexes for the metal compounds investigated (Figure 20b).

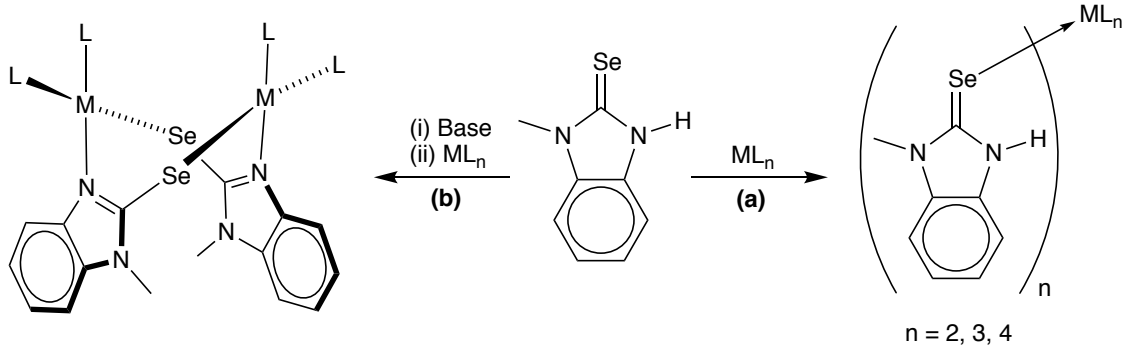

Figure 20. Representative structures of the coordination complexes H(sebenzim^{Me}) forms with the metal compounds investigated in this chapter, (a) dative interaction to the metal center through the selenium atom, (b) deprotonation to form sebenzim^{Me}]$^-$ leading to bridging complexes.

With respect to the metal complexes studied, H(sebenzim^{Me}) reacts with $Pd(PPh_3)_2Cl_2$ to generate $\{[H(sebenzim^{Me})]_3Pd(PPh_3)\}Cl_2$, and upon deprotonation of H(sebenzim^{Me}), the bridging complex, $[(PPh_3)(Cl)Pd(\mu\text{-Se,N-sebenzim}^{Me})]_2$, is formed. H(sebenzim^{Me}) also effectively binds to nickel, producing a series of structurally diverse complexes with NiX_2 (Cl, Br, I). Deprotonation of H(sebenzim^{Me}) also permits access to interesting complexes which include the paddlewheel compound, $Ni_2[\mu\text{-Se,N-sebenzim}^{Me}]_4$, and the nickel nitrosyl compound, $[(PPh_3)(NO)Ni(\mu\text{-Se,N-sebenzim}^{Me})]_2$. Lastly, the

coordination chemistry of H(sebenzim^{Me}) has been expanded to the lighter group 12 metals, Zn and Cd, as displayed by the structural characterization of $[H(sebenzim^{Me})]_2MX_2$ (M = Zn, X = Cl, Br; M = Cd, X = Cl, Br, I), $[H(sebenzim^{Me})]_3CdCl_2 \bullet [H(sebenzim^{Me})]_4CdCl_2$, and $[H(sebenzim^{Me})](benzim^{Me})CdI_2$.

3.6 Experimental Details

3.6.1 General Considerations

All manipulations were performed using a combination of glovebox, high vacuum and Schlenk techniques under a nitrogen or argon atmosphere.[42] Solvents were purified and degassed by standard procedures. NMR spectra were measured on Bruker 300 DRX, Bruker 400 DRX, Bruker 400 Avance III, and Bruker Avance 500 DMX spectrometers. ^{1}H NMR spectra are reported in ppm relative to $SiMe_4$ ($\delta = 0$) and were referenced internally with respect to the protio solvent impurity ($\delta = 7.26$ for $CDCl_3$, $\delta = 7.16$ for C_6D_5H, and $\delta = 1.94$ for CD_2HCN).[43] $^{31}P\{^1H\}$ NMR spectra are reported in ppm relative to 85% H_3PO_4 ($\delta = 0$) and were obtained by using the Ξ/100% value of 40.480742.[44] Coupling constants are reported in hertz. H(sebenzim^{Me}),[15a] H(mim$^{Bu^t}$),[45] and $Ni(PPh_3)_2(NO)Br$[46] were prepared by the corresponding literature procedure. 1-methylbenzimidazole was purchased from Alfa Aesar, $NiCl_2$ and $NiBr_2$ were purchased from Strem Chemicals, and all other chemicals were purchased from Sigma Aldrich and used as supplied. *CAUTION: All cadmium compounds are toxic and appropriate safety precautions must be taken in handling these compounds*.

3.6.2 X-ray Structure Determinations

Single crystal X-ray diffraction data were collected on a Bruker Apex II diffractometer. Crystal data, data collection and refinement parameters are summarized in Table 5. The

structures were solved using direct methods and standard difference map techniques, and were refined by full-matrix least-squares procedures on F^2 with SHELXTL (Versions 2008/4 and 2014/7).[47] X-ray powder diffraction was measured at room temperature on a PANalytical XPert3 Powder diffractometer with Cu radiation, a fixed divergence slit (½ deg.), and a Si zero-diffraction sample holder. Powder data, data collection, and the most intense peaks are summarized in Table 6.

3.6.3 Synthesis of {[H(mim$^{Bu^t}$)]$_4$Pd}(OAc)$_2$

A mixture of Pd(OAc)$_2$ (20.5 mg, 0.094 mmol) and H(mim$^{Bu^t}$) (58.0 mg, 0.371 mmol) was dissolved in dichloromethane (*ca.* 10 mL), producing a dark orange solution which was stirred for 18 hours. The volatile components were then removed *in vacuo* and the resulting orange solid was washed with pentane (2 × 5 mL) and dried *in vacuo* to afford {[H(mim$^{Bu^t}$)]$_4$Pd}(OAc)$_2$ as an orange powder (31.0 mg, 40%). Orange crystals suitable for X-ray diffraction were obtained *via* slow evaporation of a tetrahydrofuran solution. ^{1}H NMR (C_6D_6): 1.51 [s, 36H of C(C$\underline{H}_3$)$_3$], 2.07 [s, 6H of ($C_2\underline{H}_3O_2$)$_2^-$], 5.94 [d, 4 H of imidazole, $^3J_{H\text{-}H}$ = 2.5], 5.99 [d, 4 H of imidazole, $^3J_{H\text{-}H}$ = 2.5], 12.14 [broad s, 4 N-$\underline{H}$].

3.6.4 Synthesis of {[H(sebenzim^{Me})]$_3$Pd(PPh$_3$)}Cl$_2$

A mixture of Pd(PPh$_3$)$_2$Cl$_2$ (48 mg, 0.068 mmol) and H(sebenzim^{Me}) (44 mg, 0.208 mmol) was dissolved in acetonitrile (*ca.* 6 mL) and stirred for 19 hours, resulting in the formation of a red precipitate in an orange solution. The precipitate was isolated by centrifugation, washed with pentane (2 × 5 mL), and dried *in vacuo* to afford {[H(sebenzim^{Me})]$_3$Pd(PPh$_3$)}Cl$_2$ as a red powder (41 mg, 64%). Red crystals suitable for X-ray diffraction were obtained *via* vapor diffusion of diethyl ether into an acetonitrile solution. Anal. calcd. for {[H(sebenzim^{Me})]$_3$Pd(PPh$_3$)}Cl$_2$: C, 47.0%; H, 3.7%; N, 7.8%.

Found: C, 45.7%; H, 3.3%; N, 8.1%. ^{1}H NMR (CD_3CN): 3.59 [s, 9H of C$\underline{H}_3$], 7.27-7.85, [m, 27H of overlapping $C_6\underline{H}_4$ and $C_6\underline{H}_5$], 13.58 [broad s, 3H of N–$\underline{H}$]. No $^{31}P\{^{1}H\}$ NMR resonances observed.

3.6.5 Synthesis of $[(PPh_3)(Cl)Pd(\mu\text{-}S,N\text{-}mbenzim^{Me})]_2$

A solution of H(mbenzim^{Me}) (12 mg, 0.073 mmol) in tetrahydrofuran (3 mL) was treated with NaH (3 mg, 0.125 mmol) and stirred until bubbling ceased (*ca.* 10 min). The mixture was then filtered and the filtrate added to a suspension of $Pd(PPh_3)_2Cl_2$ (52 mg, 0.074 mmol) in tetrahydrofuran (4 mL) and stirred for 4 hours. The resulting orange mixture was filtered, and filtrate pumped to dryness *in vacuo* to leave an orange residue. The residue was then dissolved in benzene (2 mL) and stirred for 14 hours resulting in the formation of an orange precipitate which was isolated by centrifugation, and dried *in vacuo* to afford $[(PPh_3)(Cl)Pd(\mu\text{-}S,N\text{-}mbenzim^{Me})]_2$ as a yellow/orange powder (35 mg, 33%). Yellow crystals suitable for X-ray diffraction were obtained *via* slow evaporation of a benzene solution. Anal. calcd. for $[(PPh_3)(Cl)Pd(\mu\text{-}S,N\text{-}mbenzim^{Me})]_2$: C, 55.0%; H, 3.9%; N, 4.9%. Found: C, 57.4%; H, 3.7%; N, 4.2%. ^{1}H NMR (CD_3CN): 2.65 [s, 6H of C$\underline{H}_3$], 6.44 [d, 2H of $C_6\underline{H}_4$, $^{3}J_{H\text{-}H}$ = 8], 6.93 [t, 2H of $C_6\underline{H}_4$, $^{3}J_{H\text{-}H}$ = 8], 7.08 [t, 2H of $C_6\underline{H}_4$, $^{3}J_{H\text{-}H}$ = 8], 7.19 [m, 12H of $P(C_6\underline{H}_5)_3$], 7.36 [m, 6H of $P(C_6\underline{H}_5)_3$], 7.69 [d, 2H of $C_6\underline{H}_4$, $^{3}J_{H\text{-}H}$ = 8], 7.73 [m, 12H of $P(C_6\underline{H}_5)_3$]. $^{31}P\{^{1}H\}$ NMR (CD_3CN): 26.59 [s, $\underline{P}(C_6H_5)_3$].

3.6.6 Synthesis of $[(PPh_3)(Cl)Pd(\mu\text{-}Se,N\text{-}sebenzim^{Me})]_2$

A mixture of $Pd(PPh_3)_2Cl_2$ (87 mg, 0.124 mmol) and Na(sebenzim^{Me}) (29 mg, 0.124 mmol) was dissolved in benzene (*ca.* 7 mL) and stirred for 24 hours resulting in an orange precipitate. The precipitate was isolated by centrifugation and dried *in vacuo* to afford $[(PPh_3)(Cl)Pd(\mu\text{-}Se,N\text{-}sebenzim^{Me})]_2$ as an orange powder (35 mg, 33%). Orange

crystals suitable for X-ray diffraction were obtained *via* slow evaporation of a benzene solution. Anal. calcd. for $[(PPh_3)(Cl)Pd(\mu\text{-Se,N-sebenzim}^{Me})]_2$: C, 50.8%; H, 3.6%; N, 4.6%. Found: C, 52.6%; H, 3.8%; N, 3.7%. ^{1}H NMR (CD_3CN): 2.62 [s, 6H of C$\underline{H}_3$], 6.48 [d, 2H of $C_6\underline{H}_4$, $^3J_{H\text{-}H}$ = 8], 6.96 [t, 2H of $C_6\underline{H}_4$, $^3J_{H\text{-}H}$ = 8], 7.09 [t, 2H of $C_6\underline{H}_4$, $^3J_{H\text{-}H}$ = 8], 7.19 [m, 12H of $P(C_6\underline{H}_5)_3$], 7.53 [m, 6H of $P(C_6\underline{H}_5)_3$], 7.67 [m, 12H of $P(C_6\underline{H}_5)_3$], 7.72 [d, 2H of $C_6\underline{H}_4$, $^3J_{H\text{-}H}$ = 8]. No $^{31}P\{^1H\}$ NMR resonances observed.

3.6.7 Synthesis of Na(sebenzim^{Me})

A solution of H(sebenzim^{Me}) (60 mg, 0.284 mmol) in tetrahydrofuran (3 mL) was treated with NaH (7 mg, 0.313 mmol) resulting in an effervescent mixture which was stirred for 50 min. The mixture was then filtered and the filtrate pumped *in vacuo* to dryness to yield Na(sebenzim^{Me}) as a white powder (66 mg, 100%). ^{1}H NMR (CD_3CN): 3.69 [s, 3H of C$\underline{H}_3$], 6.94 [m, 2H of $C_6\underline{H}_4$], 7.07 [m, 1H of $C_6\underline{H}_4$], 7.22 [m, 1H of $C_6\underline{H}_4$].

3.6.8 Synthesis of [H(sebenzim^{Me})]$_4$NiCl$_2$

A mixture of $NiCl_2$ (15 mg, 0.116 mmol) and H(sebenzim^{Me}) (98 mg, 0.464 mmol) was suspended in acetonitrile (*ca.* 7 mL) and stirred for 2 days resulting in the formation of an orange/red precipitate in a pale green solution. The precipitate was isolated by centrifugation, washed with diethyl ether (2 × 5 mL), and dried *in vacuo* to afford $[H(sebenzim^{Me})]_4NiCl_2$ as a red powder (30 mg, 26%). Red crystals suitable for X-ray diffraction were obtained *via* slow evaporation of an acetonitrile solution. ^{1}H NMR (CD_3CN): 4.17 [s, 12H of C$\underline{H}_3$], 7.15-7.51, [broad m, 16H of $C_6\underline{H}_4$], 10.34 [broad s, 4H of N–$\underline{H}$].

3.6.9 Synthesis of $[H(sebenzim^{Me})]_2NiBr_2$

A mixture of $NiBr_2$ (26 mg, 0.119 mmol) and $H(sebenzim^{Me})$ (51 mg, 0.242 mmol) was suspended in acetonitrile (*ca.* 7 mL) and stirred for 2 days resulting in the formation of a green solution. The reaction was then filtered to remove any undissolved materials, and the filtrate concentrated *in vacuo* to a small volume (*ca.* 2 mL). Diethyl ether was added (*ca.* 15 mL) resulting in the precipitation of a dark green crystalline material, which was isolated by filtration and dried *in vacuo* to afford $[H(sebenzim^{Me})]_2NiBr_2$ (35 mg, 46%). Red crystals suitable for X-ray diffraction were obtained *via* vapor diffusion of diethyl ether into an acetonitrile solution. Anal. calcd. for $[H(sebenzim^{Me})]_2NiBr_2$: C, 30.0%; H, 2.5%; N, 8.7%. Found: C, 29.6%; H, 2.1%; N, 8.6%. ^{1}H NMR (CD_3CN): 6.52 [s, 6H of $C\underline{H}_3$], 7.04, [s, 4H of $C_6\underline{H}_4$], 7.41, [s, 2H of $C_6\underline{H}_4$], 7.88, [s, 2H of $C_6\underline{H}_4$], 10.77 [broad s, 2H of N–$\underline{H}$].

3.6.10 Synthesis of $\{[H(sebenzim^{Me})]_4NiI\}I$

A mixture of NiI_2 (20 mg, 0.064 mmol) and $H(sebenzim^{Me})$ (54 mg, 0.255 mmol) was suspended in acetonitrile (*ca.* 8 mL) and stirred for 23 hours resulting in the formation of a tan colored solution with a dark precipitate. The mixture was centrifuged and the supernatant pumped to dryness *in vacuo* to afford $\{[H(sebenzim^{Me})]_4NiI\}I$ as a dark red powder (32 mg, 43%). Red crystals suitable for X-ray diffraction were obtained *via* slow evaporation of an acetonitrile solution. Anal. calcd. for $\{[H(sebenzim^{Me})]_4NiI\}I$: C, 33.2%; H, 2.8%; N, 9.7%. Found: C, 34.3%; H, 3.0%; N, 9.9%. ^{1}H NMR (CD_3CN): 3.82 [s, 12H of $C\underline{H}_3$], 7.15-7.41, [m, 16H of $C_6\underline{H}_4$], 10.64 [broad s, 4H of N–$\underline{H}$].

3.6.11 Synthesis of $Ni_2[\mu\text{-}Se,N\text{-}sebenzim^{Me}]_4$

A mixture of NiI_2 (36 mg, 0.115 mmol) and $H(sebenzim^{Me})$ (98 mg, 0.464 mmol) was suspended in acetonitrile (*ca.* 8 mL) and stirred for 2 days resulting in the formation of a

tan colored solution with a dark precipitate. NaH (11 mg, 0.458 mmol) was then added and the reaction stirred for an additional 20 hours producing a green colored precipitate. The precipitate was isolated by centrifugation, washed with diethyl ether (2 × 2 mL), and dried *in vacuo* to afford to $Ni_2[\mu\text{-Se,N-sebenzim}^{Me}]_4$ as a green powder. Dark blue crystals suitable for X-ray diffraction were obtained *via* vapor diffusion of diethyl ether into an acetonitrile solution that had been previously heated to dissolve as much $Ni_2[\mu\text{-Se,N-sebenzim}^{Me}]_4$ as possible. Anal. calcd. for $Ni_2[\mu\text{-Se,N-sebenzim}^{Me}]_4$: C, 40.1%; H, 3.0%; N, 11.7%. Found: C, 38.3%; H, 2.7%; N, 10.9%. ^{1}H NMR (CD_3CN): 3.74 [s, 12H of C$\underline{H}_3$], 7.07-7.38, [m, 16H of $C_6\underline{H}_4$], N–$\underline{H}$ resonance not observed.

3.6.12 Synthesis of $[(PPh_3)(NO)Ni(\mu\text{-Se,N-sebenzim}^{Me})]_2$

A solution of H(sebenzim^{Me}) (15 mg, 0.071 mmol) in tetrahydrofuran (3 mL) was treated with NaH (3 mg, 0.125 mmol) and stirred until bubbling ceased (*ca.* 10 min). This was then filtered and the filtrate added to a solution of $Ni(PPh_3)_2(NO)Br$ (48 mg, 0.069 mmol) in tetrahydrofuran (4 mL) and stirred for 22 hours. The resulting dark green mixture was filtered, and the filtrate pumped to dryness *in vacuo* to leave a dark green residue. The residue was then washed with pentane (2 × 5 mL) and dried *in vacuo* to afford $[(PPh_3)(NO)Ni(\mu\text{-Se,N-sebenzim}^{Me})]_2$ as a green powder (31 mg, 45%). Dark purple crystals suitable for X-ray diffraction were obtained *via* slow evaporation of a tetrahydrofuran solution. ^{1}H NMR (C_6D_6): 2.96 [s, 6H of C$\underline{H}_3$], 6.51 [s, 2H of $C_6\underline{H}_4$, $^3J_{H\text{-}H}$ = 8], 6.89-7.09 [m, 20H of overlapping $C_6\underline{H}_4$ and $C_6\underline{H}_5$], 7.35-7.63 [m, 14H of overlapping $C_6\underline{H}_4$ and $C_6\underline{H}_5$], 8.40 [s, 2H of $C_6\underline{H}_4$, $^3J_{H\text{-}H}$ = 8]. ^{31}P{^{1}H} NMR (C_6D_6): 45.43 [broad s, $\underline{P}(C_6H_5)_3$]. IR (cm^{-1}): 3052 (w), 1717 (m), 1698 (s), 1586 (w), 1480 (w), 1435 (w), 1387 (w), 1342 (w), 1333 (w), 1309 (w), 1282 (w), 1226 (w), 1156 (w), 1096 (w), 1028 (w), 1010 (w), 997 (w), 920 (w), 808 (w), 738 (s), 692 (s), 565 (w), 543 (w), 520 (s), 504 (m), 495 (m).

3.6.13 Synthesis of $[H(sebenzim^{Me})]_2ZnCl_2$

A mixture of $ZnCl_2$ (11 mg, 0.081 mmol) and $H(sebenzim^{Me})$ (35 mg, 0.163 mmol) was suspended in acetonitrile (*ca.* 8 mL) and stirred for 18 hours resulting in the formation of a white precipitate. The precipitate was isolated by decantation, washed with pentane (1 × 2 mL) and dried *in vacuo* to afford $[H(sebenzim^{Me})]_2ZnCl_2$ as a white powder (31 mg, 69%). Colorless crystals suitable for X-ray diffraction were obtained *via* slow evaporation of a chloroform solution. Anal. calcd. for $[H(sebenzim^{Me})]_2ZnCl_2$: C, 34.4%; H, 2.9%; N, 10.0%. Found: C, 34.6%; H, 3.2%; N, 9.9%. ^{1}H NMR (CD_3CN): 3.79 [s, 6H of C$\underline{H}_3$], 7.23-7.43 [m, 8H of $C_6\underline{H}_4$], 11.22 [broad s, 2H of N–$\underline{H}$].

3.6.14 Synthesis of $[H(sebenzim^{Me})]_2ZnBr_2$

A mixture of $ZnBr_2$ (15 mg, 0.067 mmol) and $H(sebenzim^{Me})$ (29 mg, 0.129 mmol) was suspended in acetonitrile (*ca.* 8 mL) and stirred for 18 hours resulting in the formation of a white precipitate. The precipitate was isolated by decantation, washed with pentane (1 × 2 mL) and dried *in vacuo* to afford $[H(sebenzim^{Me})]_2ZnBr_2$ as a white powder (15 mg, 43%). Colorless crystals suitable for X-ray diffraction were obtained *via* slow evaporation of an acetonitrile solution. Anal. calcd. for $[H(sebenzim^{Me})]_2ZnBr_2$: C, 29.7%; H, 2.5%; N, 8.7%. Found: C, 30.0%; H, 2.5%; N, 8.5%. ^{1}H NMR (CD_3CN): 3.79 [s, 6H of C$\underline{H}_3$], 7.25-7.44 [m, 8H of $C_6\underline{H}_4$], 11.25 [broad s, 2H of N–$\underline{H}$].

3.6.15 Synthesis of $[H(sebenzim^{Me})]_2CdCl_2$

A mixture of $CdCl_2$ (22 mg, 0.120 mmol) and $H(sebenzim^{Me})$ (50 mg, 0.237 mmol) was dissolved in acetonitrile (*ca.* 8 mL) and stirred for 18 hours resulting in the formation of a white precipitate. The precipitate was isolated by decantation, washed with pentane (1 × 2 mL) and dried *in vacuo* to afford $[H(sebenzim^{Me})]_2CdCl_2$ as a white powder (55 mg, 76%). Colorless crystals suitable for X-ray diffraction were obtained *via* cooling of a

boiling acetonitrile solution. ^{1}H NMR (CD_3CN): 3.77 [s, 6H of C<u>H</u>$_3$], 7.23-7.46 [m, 8H of C_6<u>H</u>$_4$], 11.49 [broad s, 2H of N–<u>H</u>].

3.6.16 Synthesis of [H(sebenzim^{Me})]$_2$CdBr$_2$

A mixture of $CdBr_2$ (32 mg, 0.118 mmol) and H(sebenzim^{Me}) (50 mg, 0.237 mmol) was dissolved in acetonitrile (*ca.* 8 mL) and stirred for 18 hours resulting in the formation of a white precipitate. The precipitate was isolated by decantation, washed with pentane (1 × 2 mL) and dried *in vacuo* to afford [H(sebenzim^{Me})]$_2$CdBr$_2$ as a white powder (61 mg, 75%). Colorless crystals suitable for X-ray diffraction were obtained *via* vapor diffusion of pentane into a dichloromethane solution. ^{1}H NMR (CD_3CN): 3.79 [s, 6H of C<u>H</u>$_3$], 7.31-7.46 [m, 8H of C_6<u>H</u>$_4$], 11.79 [broad s, 2H of N–<u>H</u>].

3.6.17 Synthesis of [H(sebenzim^{Me})]$_2$CdI$_2$

A mixture of CdI_2 (43 mg, 0.117 mmol) and H(sebenzim^{Me}) (50 mg, 0.237 mmol) was dissolved in acetonitrile (*ca.* 8 mL) to form a colorless solution and was stirred for 18 hours. The reaction was then concentrated *in vacuo* to a small volume (*ca.* 2 mL), and diethyl ether was added (*ca.* 15 mL) resulting in the precipitation of a white solid. The solid was isolated by filtration and dried *in vacuo* to afford [H(sebenzim^{Me})]$_2$CdI$_2$ as a white powder (40 mg, 43%). Colorless crystals suitable for X-ray diffraction were obtained *via* slow evaporation of a dichloromethane solution. Anal. calcd. for [H(sebenzim^{Me})]$_2$CdI$_2$: C, 24.4%; H, 2.1%; N, 7.1%. Found: C, 23.4%; H, 2.6%; N, 6.6%. ^{1}H NMR (CD_3CN): 3.82 [s, 6H of C<u>H</u>$_3$], 7.31-7.48 [m, 8H of C_6<u>H</u>$_4$], 11.32 [broad s, 2H of N–<u>H</u>].

3.6.18 Synthesis of $[H(sebenzim^{Me})]_3CdCl_2 \bullet [H(sebenzim^{Me})]_4CdCl_2$

A mixture of $CdCl_2$ (22 mg, 0.120 mmol) and $H(sebenzim^{Me})$ (100 mg, 0.474 mmol) was dissolved in acetonitrile (*ca.* 8 mL) to form a colorless solution that was stirred for 18 hours at 100°C. Upon cooling, colorless crystals were deposited on the walls of the reaction vessel. When examined under a microscope, large colorless cubic crystals of $[H(sebenzim^{Me})]_3CdCl_2 \bullet [H(sebenzim^{Me})]_4CdCl_2$ suitable for X-ray diffraction were easily identified over the needle shaped crystals of $[H(sebenzim^{Me})]_2CdCl_2$ and were thus analyzed.

3.6.19 Synthesis of $[H(sebenzim^{Me})](benzim^{Me})CdI_2$

(a) A mixture of CdI_2 (35 mg, 0.096 mmol), $H(sebenzim^{Me})$ (20 mg, 0.095 mmol), and 1-methylbenzimidazole (13 mg, 0.098 mmol) was dissolved in acetonitrile (*ca.* 8 mL) to form a colorless solution that was stirred for 18 hours at 100°C. Upon cooling, colorless crystals of $[H(sebenzim^{Me})](benzim^{Me})CdI_2$ suitable for X-ray diffraction were deposited on the walls of the reaction vessel (20 mg, 30%). ^{1}H NMR ($CDCl_3$): 3.85 [s, 3H of $H(sebenzim^{Me})$ $C\underline{H}_3$], 3.90 [s, 3H of $(benzim^{Me})$ $C\underline{H}_3$], 7.29-7.47 [m, 6H of overlapping $C_6\underline{H}_4$], 7.57 [m, 1H of $C_6\underline{H}_4$], 8.11 [d, 1H of $C_6\underline{H}_4$, $^3J_{H\text{-}H} = 8$], 8.40 [s, 1H of $(benzim^{Me})$ $NC\underline{H}N$], 11.96 [broad s, 1H of $N\text{–}\underline{H}$].

(b) A solution of CdI_2 (8 mg, 0.022 mmol) and $H(sebenzim^{Me})$ (20 mg, 0.095 mmol) in CD_3CN (*ca.* 0.7 mL) in an NMR tube equipped with a J. Young valve was heated at 100˚C for 3 days and monitored by ^{1}H NMR spectroscopy, thereby demonstrating the formation of $[H(sebenzim^{Me})](benzim^{Me})CdI_2$. Additionally, upon cooling, colorless crystals suitable for X-ray diffraction were deposited on the walls of the NMR tube corresponding to $[H(sebenzim^{Me})](benzim^{Me})CdI_2$. Accompanied with reaction was the precipitation of elemental selenium which was confirmed by powder X-ray diffraction.

3.7 Crystallographic Data

Table 5. Crystal, intensity collection, and refinement data.

	{[H(mim$^{Bu^t}$)]$_4$Pd}(OAc)$_2$	**{[H(sebenzim^{Me})]$_3$Pd(PPh$_3$)}Cl$_2$**
lattice	Orthorhombic	Triclinic
formula	$C_{40}H_{70}N_8PdS_4$	$C_{42}H_{39}Cl_2N_6PPdSe_3$
formula weight	993.68	1072.94
space group	*Pbca*	*P-1*
a / Å	10.933(4)	12.4523(15)
b / Å	17.724(6)	13.7985(17)
c / Å	24.196(8)	14.8640(18)
α / °	90	66.025(2)
β / °	90	85.743(2)
γ / °	90	83.923(2)
V / Å^3	4689(3)	2319.1(5)
Z	4	2
temperature (K)	130(2)	130(2)
radiation (λ, Å)	0.71073	0.71073
ρ (calcd.) g cm^{-3}	1.408	1.536
μ (Mo Kα), mm^{-1}	0.626	2.939
θ max, deg.	30.572	30.565
no. of data collected	71997	38288
no. of data	7144	14150
no. of parameters	283	548
R_1 [$I > 2\sigma(I)$]	0.0430	0.0412
wR_2 [$I > 2\ \sigma(I)$]	0.0912	0.0857
R_1 [all data]	0.0724	0.0693
wR_2 [all data]	0.0987	0.0925
GOF	1.409	0.997
R_{int}	0.0782	0.0425

Table 5. Crystal, intensity collection, and refinement data.

	[(PPh_3)(Cl)Pd(μ-S,N-mbenzim^{Me})]$_2$	**[(PPh_3)(Cl)Pd(μ-Se,N-sebenzim^{Me})]$_2$**
lattice	Monoclinic	Monoclinic
formula	$C_{76}H_{68}Cl_2N_4P_2Pd_2S_2$	$C_{76}H_{68}Cl_2N_4P_2Pd_2Se_2$
formula weight	1447.10	1540.90
space group	*C2/c*	*C2/c*
a / Å	12.9743(15)	13.025(3)
b / Å	23.556(3)	23.568(5)
c / Å	22.007(3)	22.127(4)
α / °	90	90
β / °	92.203(2)	92.706(3)
γ / °	90	90
V / Å^3	6721.0(13)	6785(2)
Z	4	4
temperature (K)	130(2)	130(2)
radiation (λ, Å)	0.71073	0.71073
ρ (calcd.) g cm^{-3}	1.430	1.508
μ (Mo Kα), mm^{-1}	0.771	1.775
θ max, deg.	30.613	30.530
no. of data collected	54813	55470
no. of data	10294	10386
no. of parameters	398	397
R_1 [$I > 2\sigma(I)$]	0.0331	0.0343
wR_2 [$I > 2\ \sigma(I)$]	0.0655	0.0654
R_1 [all data]	0.0514	0.0582
wR_2 [all data]	0.0707	0.0722
GOF	1.095	1.031
R_{int}	0.0608	0.0708

Table 5. Crystal, intensity collection, and refinement data.

	[H(sebenzim^{Me})]$_4$NiCl$_2$	**[H(sebenzim^{Me})]$_2$NiBr$_2$**
lattice	Triclinic	Monoclinic
formula	$C_{32}H_{32}Cl_2N_8NiSe_4$	$C_{16}H_{16}Br_2N_4NiSe_2$
formula weight	974.10	640.78
space group	*P-1*	*C2/c*
a / Å	9.1990(16)	23.949(3)
b / Å	9.4170(16)	6.1411(7)
c / Å	11.384(2)	15.7686(18)
α / °	96.386(3)	90
β / °	108.454(2)	122.2010(10)
γ / °	98.026(2)	90
V / Å^3	913.5(3)	1962.4(4)
Z	1	4
temperature (K)	130(2)	130(2)
radiation (λ, Å)	0.71073	0.71073
ρ (calcd.) g cm^{-3}	1.771	2.169
μ (Mo Kα), mm^{-1}	4.697	8.778
θ max, deg.	30.570	30.543
no. of data collected	14974	15202
no. of data	5574	3009
no. of parameters	224	119
R_1 [$I > 2\sigma(I)$]	0.0387	0.0321
wR_2 [$I > 2\ \sigma(I)$]	0.0712	0.0805
R_1 [all data]	0.0629	0.0448
wR_2 [all data]	0.0792	0.0856
GOF	1.009	1.223
R_{int}	0.0608	0.0498

Table 5. Crystal, intensity collection, and refinement data.

	{[H(sebenzim^{Me})]$_4$NiI}I	**Ni$_2$[μ-Se,N-sebenzim^{Me}]$_4$**
lattice	Triclinic	Tetragonal
formula	$C_{32}H_{32}I_2N_8NiSe_4$	$C_{32}H_{28}N_8Ni_2Se_4$
formula weight	1157.00	957.88
space group	*P-1*	*P4/n*
a / Å	7.884(3)	13.9990(11)
b / Å	15.135(6)	13.9990(11)
c / Å	15.989(6)	8.2711(7)
α / °	98.648(6)	90
β / °	92.896(6)	90
γ / °	96.180(6)	90
V / Å^3	1870.8(13)	1620.9(3)
Z	2	2
temperature (K)	130(2)	130(2)
radiation (λ, Å)	0.71073	0.71073
ρ (calcd.) g cm^{-3}	2.054	1.963
μ (Mo Kα), mm^{-1}	6.095	5.691
θ max, deg.	30.472	30.530
no. of data collected	30479	25620
no. of data	11314	2486
no. of parameters	444	107
R_1 [$I > 2\sigma(I)$]	0.0460	0.0304
wR_2 [$I > 2\ \sigma(I)$]	0.0677	0.0916
R_1 [all data]	0.0987	0.0410
wR_2 [all data]	0.0784	0.0972
GOF	1.017	1.256
R_{int}	0.0746	0.0368

Table 5. Crystal, intensity collection, and refinement data.

	[(PPh_3)(NO)Ni(μ-Se,N-sebenzim^{Me})]$_2$	**$Ni_5(NO)_4$(sebenzim^{Me})$_6$**
lattice	Triclinic	Monoclinic
formula	$C_{52}H_{44}N_6Ni_2O_2P_2Se_2$	$C_{48}H_{48}N_{16}Ni_5O_4Se_6$
formula weight	1122.21	1752.39
space group	*P-1*	$P2_1/c$
a / Å	9.9597(15)	10.138(5)
b / Å	10.0680(15)	25.968(11)
c / Å	26.724(4)	22.542(10)
α / °	79.835(2)	90
β / °	87.862(2)	92.737(7)
γ / °	64.413(2)	90
V / Å^3	2376.7(6)	5928(4)
Z	2	4
temperature (K)	130(2)	130(2)
radiation (λ, Å)	0.71073	0.71073
ρ (calcd.) g cm^{-3}	1.568	1.964
μ (Mo Kα), mm^{-1}	2.439	5.304
θ max, deg.	30.625	30.670
no. of data collected	38794	95109
no. of data	14382	18216
no. of parameters	597	772
R_1 [$I > 2\sigma(I)$]	0.0692	0.0654
wR_2 [$I > 2\ \sigma(I)$]	0.1670	0.0945
R_1 [all data]	0.1141	0.1743
wR_2 [all data]	0.1827	0.1167
GOF	1.196	0.973
R_{int}	0.0764	0.2863

Table 5. Crystal, intensity collection, and refinement data.

	[H(sebenzim^{Me})]$_2$ZnCl$_2$	**[H(sebenzim^{Me})]$_2$ZnBr$_2$**
lattice	Triclinic	Triclinic
formula	$C_{16}H_{16}Cl_2N_4Se_2Zn$	$C_{16}H_{16}Br_2N_4Se_2Zn$
formula weight	558.52	647.44
space group	*P-1*	*P-1*
a/Å	8.9396(16)	8.743(3)
b/Å	9.1202(17)	9.327(3)
c/Å	14.242(3)	14.755(5)
α/°	72.759(2)	95.538(5)
β/°	87.486(2)	103.703(5)
γ/°	61.394(2)	117.084(4)
V/Å^3	966.9(3)	1011.3(6)
Z	2	2
temperature (K)	130(2)	130(2)
radiation (λ, Å)	0.71073	0.71073
ρ (calcd.) g cm^{-3}	1.918	2.126
μ (Mo Kα), mm^{-1}	5.317	8.771
θ max, deg.	30.795	30.737
no. of data collected	15460	16380
no. of data	5969	6221
no. of parameters	236	236
R_1 [$I > 2\sigma(I)$]	0.0389	0.0340
wR_2 [$I > 2\ \sigma(I)$]	0.1124	0.0855
R_1 [all data]	0.0470	0.0437
wR_2 [all data]	0.1168	0.0904
GOF	1.168	1.008
R_{int}	0.0519	0.0561

Table 5. Crystal, intensity collection, and refinement data.

	[H(sebenzim^{Me})]$_2$CdCl$_2$	**[H(sebenzim^{Me})]$_2$CdBr$_2$**
lattice	Triclinic	Triclinic
formula	$C_{16}H_{16}CdCl_2N_4Se_2$	$C_{16}H_{16}Br_2CdN_4Se_2$
formula weight	605.55	694.47
space group	*P-1*	*P-1*
a/Å	8.8325(8)	8.778(3)
b/Å	9.0143(8)	9.332(3)
c/Å	14.6487(14)	15.073(5)
α/°	73.3470(10)	71.984(4)
β/°	88.3560(10)	75.887(5)
γ/°	62.1770(10)	62.127(4)
V/Å^3	980.59(16)	1030.7(6)
Z	2	2
temperature (K)	130(2)	130(2)
radiation (λ, Å)	0.71073	0.71073
ρ (calcd.) g cm^{-3}	2.051	2.238
μ (Mo Kα), mm^{-1}	5.105	8.474
θ max, deg.	30.780	30.760
no. of data collected	16125	17219
no. of data	6081	6387
no. of parameters	236	236
R_1 [$I > 2\sigma(I)$]	0.0345	0.0267
wR_2 [$I > 2\ \sigma(I)$]	0.0692	0.0626
R_1 [all data]	0.0555	0.0360
wR_2 [all data]	0.0761	0.0661
GOF	1.002	1.018
R_{int}	0.0407	0.0410

Table 5. Crystal, intensity collection, and refinement data.

	[H(sebenzim^{Me})]$_2$CdI$_2$	**[H(sebenzim^{Me})]$_3$CdCl$_2$• [H(sebenzim^{Me})]$_4$CdCl$_2$**
lattice	Orthorhombic	Monoclinic
formula	$C_{16}H_{16}CdI_2N_4Se_2$	$C_{56}H_{56}Cd_2Cl_4N_{14}Se_7$
formula weight	788.45	1844.46
space group	*Pbcn*	$P2_1/m$
a / Å	16.913(5)	9.2219(16)
b / Å	8.507(2)	36.264(6)
c / Å	30.255(8)	9.9324(17)
α / °	90	90
β / °	90	99.103(3)
γ / °	90	90
V / Å^3	4353(2)	3279.8(10)
Z	8	2
temperature (K)	130(2)	130(2)
radiation (λ, Å)	0.71073	0.71073
ρ (calcd.) g cm^{-3}	2.406	1.868
μ (Mo Kα), mm^{-1}	7.191	4.744
θ max, deg.	30.609	30.584
no. of data collected	67842	54035
no. of data	6694	10205
no. of parameters	236	401
R_1 [$I > 2\sigma(I)$]	0.0445	0.0560
wR_2 [$I > 2\ \sigma(I)$]	0.0717	0.0877
R_1 [all data]	0.1189	0.1077
wR_2 [all data]	0.0897	0.0997
GOF	1.030	1.045
R_{int}	0.1750	0.1094

Table 5. Crystal, intensity collection, and refinement data.

	[H(sebenzim^{Me})](benzim^{Me})CdI$_2$
lattice	Orthorhombic
formula	$C_{18}H_{19}CdI_2N_5Se$
formula weight	750.54
space group	$P2_12_12_1$
a / Å	8.627(3)
b / Å	13.279(4)
c / Å	19.861(6)
α / °	90
β / °	90
γ / °	90
V / Å^3	2275.3(11)
Z	4
temperature (K)	130(2)
radiation (λ, Å)	0.71073
ρ (calcd.) g cm^{-3}	2.191
μ (Mo Kα), mm^{-1}	5.286
θ max, deg.	30.624
no. of data collected	37494
no. of data	6985
no. of parameters	252
R_1 [$I > 2\sigma(I)$]	0.0255
wR_2 [$I > 2\ \sigma(I)$]	0.0503
R_1 [all data]	0.0309
wR_2 [all data]	0.0521
GOF	1.020
R_{int}	0.0619

Table 6. Powder data, data collection, and the most intense peaks.

	[H(sebenzim^{Me})](benzim^{Me})CdI$_2$
Anode material	Cu
K-Alpha1 wavelength	1.540598
K-Alpha2 wavelength	1.544426
Ratio K-Alpha2/K-	0.5
Divergence slit, Fixed	0.10mm
Monochromator used	NO
Generator voltage	45
Tube current	40
h k l	0 0 0
Scan axis	Gonio
Scan range min	4.999999999
Scan range max	74.99753695
Scan step size	0.0131303
No. of points	5331
Scan type	CONTINUOUS
Phi	181
Time per step	358.02
Angle	Intensity
23.55965456	35671
29.73088742	34714
29.7440177	34184
23.54652428	33863
23.57278485	33843
29.71775714	32220
29.75714799	31135
23.533394	30563
23.58591513	30454
9.497121816	29354

3.8 References and Notes

(1) Rong, Y.; Al-Harbi, A.; Kriegel, B.; Parkin, G. *Inorg. Chem.* **2013**, *52*, 7172–7182 and references therein.

(2) Palmer, H. J.; Parkin, G. *New J. Chem.* **2014**, *38*, 4071–4082 and references therein.

(3) Landry, V. K.; Minoura, M.; Pang, K.; Buccella, D.; Kelly, B. V.; Parkin, G. *J. Am. Chem. Soc.* **2006**, *128*, 12490–12497.

(4) Hirashima, A.; Morimoto, M.; Ohta, H.; Kuwano, E.; Taniguchi, E.; Eto, M. *Int. J. Mol. Sci.* **2002**, *3*, 56–68.

(5) Figueroa, J. S.; Yurkerwich, K.; Melnick, J.; Buccella, D.; Parkin, G. *Inorg. Chem.* **2007**, *46*, 9234–9244.

(6) (f) Kimani, M. M.; Bayse, C. A.; Brumaghim, J. L. *Dalton Trans.* **2011**, *40*, 3711–3723.

(7) Palmer, J. H.; Parkin, G. *Polyhedron* **2013**, *52*, 658–668.

(8) Cooper, D. S. *New Engl. J. Med.* **2005**, *352*, 905–917.

(9) Fumarola, A.; Di Fiore, A.; Dainelli, M.; Grani, G.; Calvanese, A. *Exp. Clin. Endocrinol. Diabetes* **2010**, 118, 678–684.

(10) Manna, D.; Roy, G.; Mugesh, G. *Acc. Chem. Res.* **2013**, *46*, 2706–2715.

(11) (a) Kruse, L. I.; Kaiser, C.; DeWolf Jr., W. E.; Frazee, J. S.; Ross, S. T.; Wawro, J.; Wise, M.; Flaim, K. E.; Sawyer, J. L.; Erickson, R. W.; Ezekiel, M.; Ohlstein, E. H.; Berkowitz, B. A. *J. Med. Chem.* **1987**, *30*, 486–494.
(b) Kruse, L. I.; Kaiser, C.; DeWolf Jr., W. E.; Frazee, J. S.; Garvey, E.; Hilbert, W. A.; Faulkner, K. E.; Flaim, K. E.; Sawyer, J. L.; Berkowitz, B. A. *J. Med. Chem.* **1986**, *29*, 2465–2472.
(c) Beliaev, A.; Learmonth, D. A.; Soares-da-Silva, P. *J. Med. Chem.* **2006**, *49*, 1191–1197.

(12) (a) Van Lommen, G.; Doyon, J.; Coesemans, E.; Boeckx, S.; Cools, M.; Buntinx, M.; Hermans, B.; VanWauwe, J. *Bioorg. Med. Chem. Lett.* **2005**, *15*, 497–500.
(b) Doyon, J.; Coesemans, E.; Boeckx, S.; Buntinx, M.; Hermans, B.; VanWauwe, J. P.; Gilissen, R.; De Groot, A. H. J.; Corens, D.; Van Lommen, G. *ChemMedChem* **2008**, *3*, 660–669.

(13) (a) White, J. L.; Tanski, J. M.; Churchill, D. G.; Rheingold, A. L.; Rabinovich, D. *Chem. Crystallogr.* **2003**, *33*, 437–445.
(b) Pang, K.; Figueroa, J. S.; Tonks, I. A.; Sattler, W.; Parkin, G. *Inorg. Chim. Acta.*

2009, *362*, 4609–4615.
(c) Cingolani, A.; Effendy; Marchetti, F.; Pettinari, C.; Pettinari, R.; Skelton, B. W.; White, A. H. *Inorg. Chem.* **2002**, *41*, 1151–1161.
(d) Sultana, R.; Lobana, T. S.; Sharma, R.; Castineiras, A.; Akitsu, T.; Yahagi, K.; Aritake, Y. *Inorg. Chim. Acta.* **2010**, *363*, 3432–3441.
(e) Matsunaga, Y.; Fujisawa, K.; Amir, N.; Miyashita, Y.; Okamoto, K.-I. *J. Coord. Chem.* **2005**, *58*, 1047–1061.
(f) Melnick, J. G.; Yurkerwich, K.; Parkin, G. *Inorg. Chem.* **2009**, 48, 6763-6772.
(g) Luqman, A.; Blair, V. L.; Brammananth, R.; Crellin, P. K.; Coppel, R. L.; Andrews, P. C. *Eur. J. Inorg. Chem.* **2016**, 2738-2749.

(14) (a) Garner, M.; Reglinski, J.; Cassidy, L.; Spicer, M. D.; Kennedy, A. R. *Chem. Commun.* **1996**, 1975–1976.
(b) Spicer, M. D.; Reglinski, J. *Eur. J. Inorg, Chem.* **2009**, 1553–1574.
(c) Parkin, G. *New J. Chem.* **2007**, *31*, 1996–2014.

(15) (a) Palmer, J. H.; Parkin, G. *Polyhedron.* **2013**, 658–668.
(b) Palmer, J. H.; Parkin, G. *J. Am. Chem. Soc.* **2015**, *137*, 4503–4516.
(c) Bhabak, K. P.; Mugesh, G. *J. Chem. Sci.* **2011**, *123*, 783–789.
(d) Bhabak, K. P.; Bhowmick, D. *Inorg. Chim. Acta.* **2016**, *450*, 337–345.
(e) Dewhurst, R. D.; Hansen, A. R.; Hill, A. F.; Smith, M. K. *Organometallics* **2006**, *25*, 5843–5846.
(f) $[Tse^R]$ and $[Bse^R]$ ligands have also emerged as the selenium analogues of $[Tm^R]$ and $[Bm^R]$ ligands. See: Landry, V. K.; Buccella, D.; Pang, K.; Parkin G. *Dalton Trans.* **2007**, 866–870.

(16) (a) Yamashita, Y.; Yamashita, M. *J. Biol. Chem.* **2010**, *285*, 18134–18138.
(b) Yadav, S.; Singh, H. B.; Butcher, R. J. *Eur. J. Inorg. Chem.* **2017**, 2968–2979.

(17) (a) Guziec, L. J.; Guziec Jr., F. S. *J. Org. Chem.* **1994**, *59*, 4691–4692.
(b) Taurog, A.; Dorris, M. L.; Guziec, L. J.; Guziec Jr., F. S. *Biochem. Pharm.* **1994**, *48*, 1447–1453.

(18) Roy, G.; Mugesh, G. *J. Am. Chem. Soc.* **2005**, *127*, 15207–15217.

(19) (a) Roy, G.; Mugesh, G. *Phosphorus Sulfur Silicon Relat. Elem.* **2008**, *183*, 908–923.
(b) Roy, G.; Mugesh, G. *Chem. Biodivers.* **2008**, *5*, 414–439.
(c) Roy, G.; Bhabak, K. P.; Mugesh, G. *Crys. Growth Des.* **2011**, *11*, 2279–2286.
(d) Roy, G.; Mugesh, G. *J. Chem. Sci.* **2006**, *118*, 619–625.

(20) Butler, L. M.; Creighton, J. R.; Oughtred, R. E.; Raper, E. S. *Inorg. Chim. Acta* **1983**, *75*, 149–154.

(21) (a) Green, M. L. H. *J. Organomet. Chem.* **1995**, *500*, 127-148.
(b) Parkin, G. in *Comprehensive Organometallic Chemistry III*, Volume 1, Chapter 1.01; Crabtree, R. H. and Mingos, D. M. P. (Eds), Elsevier, Oxford, 2006.
(c) Green, J. C.; Green, M. L. H.; Parkin, G. *Chem Commun.* **2012**, *48*, 11481-

11503.
(d) Green, M. L. H.; Parkin, G. *J. Chem. Educ.* **2014**, *91*, 807-816.

(22) (a) Yang, L.; Powell, D. R.; Houser, R. P. *Dalton Trans.* **2007**, 955–964.
(b) Reineke, M. H.; Sampson, M. D.; Rheingold, A. L.; Kubiak, C. P. *Inorg. Chem.* **2015**, *54*, 3211–3217.

(23) (a) Casanova, D.; Cirera, J.; Llunell, M.; Alemany, P.; Avnir, D.; Alvarez, S. *J. Am. Chem. Soc.* **2004**, *126*, 1755–1763.
(b) Alvarez, S.; Alemany, P.; Casanova, D.; Cirera, J.; Llunell, M.; Avnir, D. *Coord. Chem. Rev.* **2005**, *249*, 1693–1708.
(c) Cirera, J.; Ruiz, E.; Alvarez, S. *Organometallics* **2005**, *24*, 1556–1562.

(24) Lobana, T. S.; Sandhu, A. K.; Mahajan, R. K.; Hundal, G.; Gupta, S. K.; Butcher, R. J.; Castineiras, A. *Polyhedron* **2017**, *127*, 25–35.

(25) Kahn, E. S.; Rheingold, A. L.; Shupack, S. I. *J. Cryst. Spectrosc.* **1993**, *23*, 697–710.

(26) Wagler, J.; Guenther, A. *CSD Communication* **2014**, CCDC 999733.

(27) Talismanova, M. O.; Sidorov, A. A.; Aleksandrov, G. G.; Charushin, V. N.; Kotovskaya, S. K.; Anannikov, V.P. Eremenko, I. L.; Moiseev, I. I. *Izvestiya Rossiiskaya Akademii Nauk Seriya Khimicheskaya* **2008**, 45.

(28) Cambridge Structural Database, CSD version 5.39

(29) Appleton, T. G.; Clark, H. C.; Manzer, L. E. *Coord. Chem. Rev.* **1973**, *10*, 335–422.

(30) (a) Rani, V.; Singh, H. B.; Butcher, R. J. *Eur. J. Inorg. Chem.* **2017**, 3720–3728.
(b) Wang, C.; Tong, Y.; Huang, Y.; Zhang, H.; Yang, Y. *RSC Adv.* **2015**, *5*, 63087–63094.
(c) Sangeeta, Y.; Singh, H. B.; Butcher, R. J. *Eur. J. Inorg. Chem.* **2017**, 2968–2979.
(d) Ghavale, N.; Manjare, S. T.; Singh, H. B.; Butcher, R. J. *Dalton Trans.* **2015**, *44*, 11893–11900.

(31) Batsanov, S. S. *Inorg. Mat.* **2001**, *37*, 871–885.

(32) (a) Serrano, J. L.; Garcia, L.; Perez, J.; Perez, E.; Galiana, J. M.; Garcia, J.; Martinez, M.; Sanchez, G.; da Silva, I. *Dalton Trans*, **2011**, *40*, 156–168.
(b) Ruiz, J.; Florenciano, F.; Lopez, G.; Chaloner, P. A.; Hitchcock, P. B. *Inorg. Chim Acta* **1998**, *281*, 165–173.
(c) Santana, M. D.; Lopez-Banet, L.; Sanchez, G.; Perez, J.; Perez, E.; Garcia, L.; Serrano, J. L.; Espinosa, A. *Dalton Trans.* **2016**, *45*, 8601–8613.
(d) Santana, M. D.; Bueno-Barcia, R.; Garcia, G.; Sanchez, G.; Garcia, J.; Perez, J.; Garcia, L. Serrano, J. L. *Dalton Trans.* **2011**, *40*, 3537–3546.
(e) Ibanez, S.; Vrecko, D. N.; Estevan, F.; Hirva, P.; Sanau, M.; Ubeda, M. *Dalton Trans.* **2014**, *43*, 2961–2970.

(33) Although only the 2:1 complex, $[H(sebenzim^{Me})]_2NiBr_2$, NMRs evidence suggests that 3:1 or even 4:1 complexes can be generated in situ. Attempts to crystallize these complexes have been unsuccessful.

(34) Addison, A. W.; Rao, T. N.; Reedijk, J.; van Rijn, J.; Verschoor, G. C. *J. Chem. Soc. Dalton Trans.* **1984**, 1349–1356.

(35) (a) Blake, A. J.; Casabo, J.; Devillanova, F. A.; Escriche, L.; Garau, A.; Isaia, F.; Lippolis, V.; Kivekas, R.; Muns, V.; Schroder, M.; Sillanpaa, R.; Verani, G. *J. Chem. Soc. Dalton Trans.* **1999**, 1085–1092.
(b) Landry, V. K.; Pang, K.; Quan, S. M.; Parkin G. *Dalton Trans.* **2007**, 820–824.
(c) Landry, V. K.; Parkin G. *Polyhedron* **2007**, *26*, 4751–4757.
(d) Jia, W.-G.; Huang, Y.-B.; Lin, Y.-J.; Wang, G.-L.; Jin, G.-X. *Eur. J. Inorg. Chem.* **2008**, 4063–4073.

(36) L. Pauling, The Nature of the Chemical Bond, third ed., Cornell University Press, Ithaca, NY, 1960.

(37) (a) Cotton, F. A.; Matusz, M.; Poli, R.; Feng, X. *J. Am. Chem. Soc.* **1988**, *110*, 1144–1154.
(b) Berry, J. F.; Bill, E.; Bothe, E.; Cotton, F. A.; Dalal, N. S.; Ibragimov, S. A.; Kaur, N.; Liu, C. Y.; Murillo, C. A.; Nellutla, S.; North, J. M.; Villagran, D. *J. Am. Chem. Soc.* **2007**, *129*, 1393–1401.
(c) Berry, J. F.; Cotton, F. A.; Ibragimov, S. A.; Murillo, C. A.; Wang. X., S. *Inorg. Chem.* **2005**, *44*, 6129–6137.
(d) Xia, B.-H.; Che, C.-M.; Zhou, Z.-Y. *Chem. Eur. J.* **2003**, *9*, 3055–3064.

(38) (a) Mingos D.M.P. (2014) Historical Introduction to Nitrosyl Complexes. In: Mingos D. (eds) Nitrosyl Complexes in Inorganic Chemistry, Biochemistry and Medicine I. Structure and Bonding, vol 153. Springer, Berlin, Heidelberg.
(b) Hayton, T. W.; Legzdins, P.; Sharp, W. B. *Chem. Rev.* **2002**, *102*, 935–991.
(c) McCleverty, J. A. *Chem. Rev.* **2004**, *104*, 403–418.

(39) (a) Williams, D. J.; White, K. M.; Van Derveer, D.; Wilkinson, A. P. *Inorg. Chem. Commun.* **2002**, *5*, 124–126.
(b) Sangeeta, Y.; Singh, H. B.; Butcher, R. J. *Eur. J. Inorg. Chem.* **2017**, 2968–2979.
(c) Babu, C. N.; Srinivas, K.; Prabusankar, G. *Dalton Trans.* **2016**, *45*, 6456–6465.
(d) Minoura, M.; Landry, V. K.; Melnick, J. G.; Pang, K.; Marchio, L.; Parkin, G. *Chem. Commun.* **2006**, 3990–3992.
(e) Williams, D. J.; Mckinney, B. J.; Baker, B.; Gwaltney, K. P.; Van Derveer, D. *J. Chem. Cryst.* **2007**, *37*, 691–694.
(f) Williams, D. J.; White, K. M.; Van Derveer, D.; Wilkinson, A. P. *Inorg. Chem. Commun.* **2002**, *5*, 124–126.

(40) (a) Melnick, J. G.; Yurkerwich, K.; Parkin, G. *J. Am. Chem. Soc.* **2009**, *132*, 647–655.
(b) Bayler, A.; Schier, A.; Bowmaker, G. A.; Schmidbaur, H. *J. Am. Chem. Soc.* **1996**, *118*, 7006–7007.

(c) Tripathi, U. M.; Bauer, A.; Schmidbaur, H. *J. Chem. Soc., Dalton Trans.* **1997**, 2865–2868.
(d) Bruce, M. I.; Williams, M. L.; Patrick, J. M.; Skelton, B. W.; White, A. H. *J. Chem. Soc., Dalton Trans.* **1986**, 2557–2567.
(e) Fujisawa, K.; Imai, S.; Moro-oka, Y. *Chem. Lett.* **1998**, 167–168.
(f) Omary, M. A.; Rawashdeh-Omary, M. A.; Gonser, M. W. A.; Elbjeirami, O.; Grimes, T.; Cundari, T. R.; Diyabalanage, H. V. K.; Gamage, C. S. P.; Dias, H. V. R. *Inorg. Chem.* **2005**, *44*, 8200–8210.

(41) For examples of cadmium complexes that feature two iodide ligands and a Cd–$N_{benzimidazole}$ interaction, see:
(a) Yang, H.-X.; Wang, X.; Xie, C.-X.; Li, X.-F.; Liu, Y.-J. *Acta Crystallogr., Sect. E* **2011**, *67*, m1149–m1151.
(b) Meng, X.-R.; Wu, X.-J.; Li, D.-W.; Hou, H.-W.; Fan, Y.-T. *Polyhedron* **2010**, *29*, 2619–2628.
(c) Chu, W.; Lou, X.; Wang, Z.; Xu, C.; Fan, Y.; Hou, H. *J. Coord. Chem.* **2011**, *64*, 4373–4382.
(d) Wang, Y.-T.; Yan, S.-C.; Tang, G.-M.; Zhao, C.; Li, T.-D.; Cui, Y.-Z. *Inorg. Chim. Acta.* **2011**, *376*, 492–499.
(e) Jiao, C.-H.; Geng, J.-C.; He, C.-H.; Cui, G.-H. *J. Mol. Struct.* **2012**, *1020*, 134–141.

(42) (a) McNally, J. P.; Leong, V. S.; Cooper, N. J. in *Experimental Organometallic Chemistry*, Wayda, A. L.; Darensbourg, M. Y., Eds.; American Chemical Society: Washington, DC, 1987; Chapter 2, pp 6-23.
(b) Burger, B.J.; Bercaw, J. E. in *Experimental Organometallic Chemistry*; Wayda, A. L.; Darensbourg, M. Y., Eds.; American Chemical Society: Washington, DC, 1987; Chapter 4, pp 79-98.
(c) Shriver, D. F.; Drezdzon, M. A.; *The Manipulation of Air-Sensitive Compounds*, 2nd Edition; Wiley-Interscience: New York, 1986.

(43) Fulmer, G. R.; Miller, A. J. M.; Sherden, N. H.; Gottlieb, H. E.; Nudelman, A.; Stoltz, B. M.; Bercaw, J. E.; Goldberg, K. I. *Organometallics* **2010**, *29*, 2176-2179.

(44) (a) Harris, R. K.; Becker, E. D.; De Menezes, S. M. C.; Goodfellow, R.; Granger, P. *Pure Appl. Chem.* **2001**, *73*, 1795-1818.
(b) Harris, R. K.; Becker, E. D.; De Menezes, S. M. C.; Granger, P.; Hoffman, R. E.; Zilm, K. W. *Pure Appl. Chem.* **2008**, *80*, 59-84.

(45) Cassidy, C. S.; Reinhardt, L. A.; Cleland, W. W.; Frey, P. A. *J. Chem. Soc., Perkin Trans.* **1999**, *2*, 635-641.

(46) Soma, S.; Van Stappen, C.; Kiss, M.; Szilagyi, R. K.; Lehnert, N.; Fujisawa, K. *J. Biol. Inorg. Chem.* **2016**, *21*, 757-775.

(47) (a) Sheldrick, G. M. SHELXTL, An Integrated System for Solving, Refining, and Displaying Crystal Structures from Diffraction Data; University of Göttingen, Göttingen, Federal Republic of Germany, 1981.

(b) Sheldrick, G. M. *Acta Cryst.* **2008**, *A64*, 112-122.
(c) Sheldrick, G. M. *Acta Cryst.* **2015**, *A71*, 3–8.

CHAPTER 4

The Flexible Nature of Hexaphenylcarbodiphosphorane

Table of Contents

Reproduced in part from Quinlivan, P. J.; Parkin, G. *Inorg. Chem.* **2017**, *56*, 5493-5497.

4.1 Introduction

Carbodiphosphoranes, $(R_3P)_2C$,[1-4] which were first reported in 1961,[1a] constitute an interesting class of molecules that feature a two-coordinate carbon center. In this regard, carbodiphosphoranes are structurally similar to carbenes. However, whereas the carbon atoms of carbenes are divalent with only one lone-pair and an empty orbital,[5,6] the central carbon atom of carbodiphosphoranes are zerovalent with two lone-pairs (Figure 1), thus classifying them as zerovalent.[7,8] While this unusual electronic arrangement leads to interesting reactivity, it has also, unfortunately, led to much confusion regarding the best classification and representation of carbodiphosphoranes. For example, a variety of incorrectly drawn Lewis structures have appeared in the literature, including depictions with double bonds between the central carbon and phosphorus atoms with no lone-pairs on the carbon.[1,3b,9] Such depictions imply a situation where the phosphorus atoms are hypervalent, and thus disobey the octet rule.

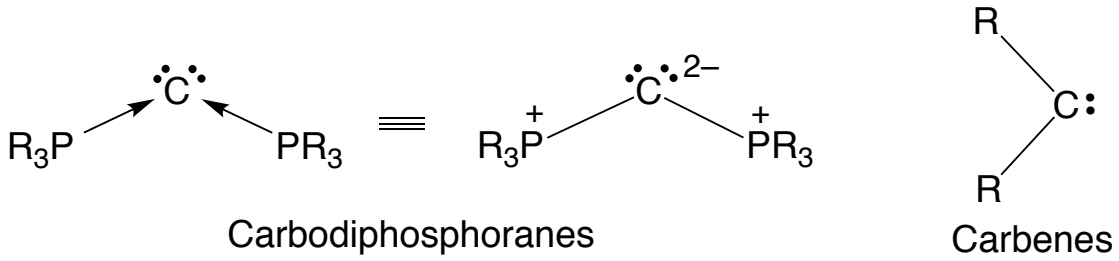

Figure 1. Representations of carbodiphosphoranes and carbenes.

To probe the C–P bonding in carbodiphosphoranes, the hypothetical molecule $(H_3P)_2C$ has been studied *via* natural resonance theory,[10] clearly indicating that the dominant resonance structure (57.67 %) contains single bonds between the phosphorus and carbon atoms and two lone-pairs on the carbon (Figure 2). The six minor resonance structures (totaling 42.33 %), which feature a double bond between one of the

phosphorus and carbon interactions, are also accompanied by the cleavage of a P–H bond. Thus, while there is a certain degree of delocalization over the P–C–P bonds in carbodiphosphoranes, the strict use of only double bonds between phosphorous and carbon *combined* with three P–R single bonds (such that the phosphorus atom has five total bonds) is not an accurate representation. Indeed, natural resonance theory supports that the phosphorus atoms are not hypervalent. Further electronic descriptions of carbodiphosphoranes and related molecules are discussed in detail in this chapter (see section 4.4 and 4.5).

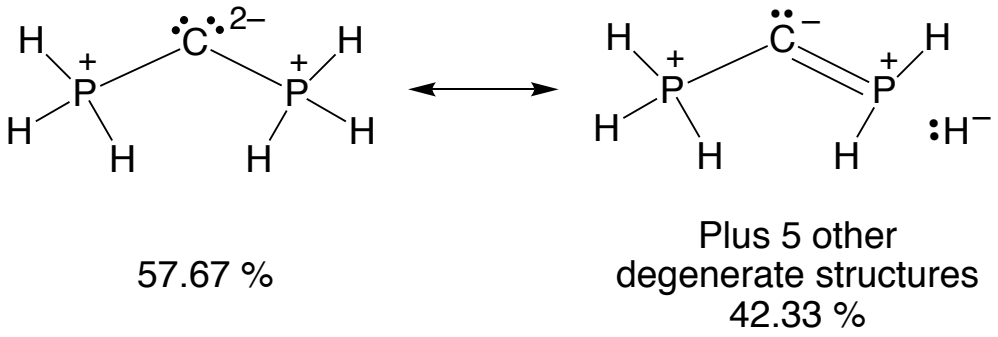

Figure 2. Resonance structures of the hypothetical molecule $(H_3P)_2C$.

Additionally, carbodiphosphoranes are often described in terms of the oxidation state of the carbon atom (oxidation state being defined as: "The charge remaining on an atom when all ligands are removed heterolytically in their closed form, with the electrons being transferred to the more electronegative partner; homonuclear bonds do not contribute to the oxidation number").[6] However, there are inherent ambiguities that arise when assigning formal oxidation states and often the assignments can yield results that are not chemically intuitive. For example, while the oxidation state of phosphorus in PH_3 is –3, the oxidation state of phosphorus in PMe_3 can be either +3 or –3 depending upon the electronegativity scale used. Additionally, the oxidation state of phosphorus in $P(NMe_2)_3$ is +3, despite the obviously similar chemical behavior, and electronic

structure between these three phosphine Lewis bases.[11] Describing atoms in terms of their valence is frequently more informative (valence is defined as: the number of electrons that an atom uses in bonding).[6] As stated above, by virtue of the central carbon atom having two lone-pairs of electrons and two L-type[12] interactions from the phosphines, carbodiphosphoranes are classified as zerovalent.[6] However, there are several instances in the literature where the valence of the central carbon atom of carbodiphosphoranes are incorrectly assigned, as it is often confused with the coordination number of an atom.[3a,b,4a,9c,d,13]

The presence of these lone-pairs is also associated with the fact that such molecules are typically bent in the solid state.[5c,8,14] However, the work completed in this chapter indicates that carbodiphosphoranes are capable of achieving linear conformations, thereby showing that these types of molecules are highly flexible. This chapter details (*i*) the structural characterization of a linear form of hexaphenylcarbodiphosphorane, $(Ph_3P)_2C$, (*ii*) the energetic and electronic profile of $(Ph_3P)_2C$ upon bending the P–C–P bonds, and (*iii*) the comparison of $(Ph_3P)_2C$ towards other isoelectronic molecules.

4.2 Structural Characterization of Linear $(Ph_3P)_2C$

Previous X-ray diffraction studies have demonstrated that carbodiphosphoranes with alkyl or aryl substituents are highly bent, with P–C–P bond angles in the range of 121.8(3)-143.8(6)°.[15-17] For example, two crystalline forms of $(Ph_3P)_2C$ have been structurally characterized, one by Hardy *et al.* which features a 131.7(3)° P–C–P bond angle[16a] and one by Vincent *et al.* which features two independent $(Ph_3P)_2C$ molecules in the unit cell which possess P–C–P bond angles of 130.1(6)° and 143.8(6)°.[16b] The bent nature of $(Ph_3P)_2C$ is also affirmed by computational studies performed by Frenking *et al.*, which result in P–C–P bond angles of 135.0° and 136.9° (BP86/SVP and BP86/TZ2P,

respectively).[3a,3b,4a] It is also worth noting that electron diffraction studies on $(Me_3P)_2C$ in the gas phase indicate a P–C–P bond angle of 147.6(5)˚, but the actual value is considered to be larger because of the "shrinkage effect".[18] Furthermore, a bond angle of 116.7(7)˚ is observed for the cyclic carbodiphosphorane $[(CH_2)_3PPh_2]_2C$.[17b]

In view of these experimental and computational studies, it is noteworthy that a new crystalline form of $(Ph_3P)_2C$ has been obtained which features a *linear* P–C–P moiety (Figure 3). This polymorph was grown by slow evaporation of a benzene solution and consists of the formula $(Ph_3P)_2C{\bullet}2C_6H_6$, which crystallizes in the $R\bar{3}$ space group. Since the molecule resides on a special position in this space group, the possibility exists that the molecule could be disordered such that the P–C–P angle is not *rigorously* linear, but only approximately so. This result is certainly interesting, as simple VSEPR theory predicts that a molecule with a coordination number of two and two lone-pairs, such as H_2O, will possess a bent geometry. It is worth mentioning that this unusual linear arrangement is also observed for the dimethylamido derivative, $[(Me_2N)_3P]_2$,[19] but this serves as the first experimental example of a linear carbodiphosphorane which feature alkyl or aryl substituents.

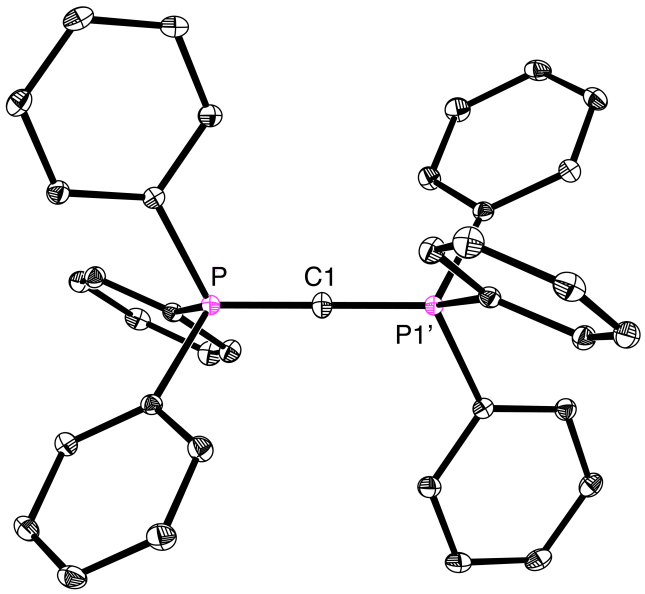

Figure 3. Molecular structure of linear $(Ph_3P)_2C$.

Interestingly, the linear structure of $(Ph_3P)_2C$ also differs from the previously reported structures by the presence of a staggered arrangement of phenyl groups, as illustrated in Figure 4. Indeed, the Ph–P•••P–Ph torsion angle of linear $(Ph_3P)_2C$ is 60.0˚, whereas the known bent forms have average torsion angles of 26.1˚, 6.8˚, and 6.4˚, with the latter two being close to eclipsed.

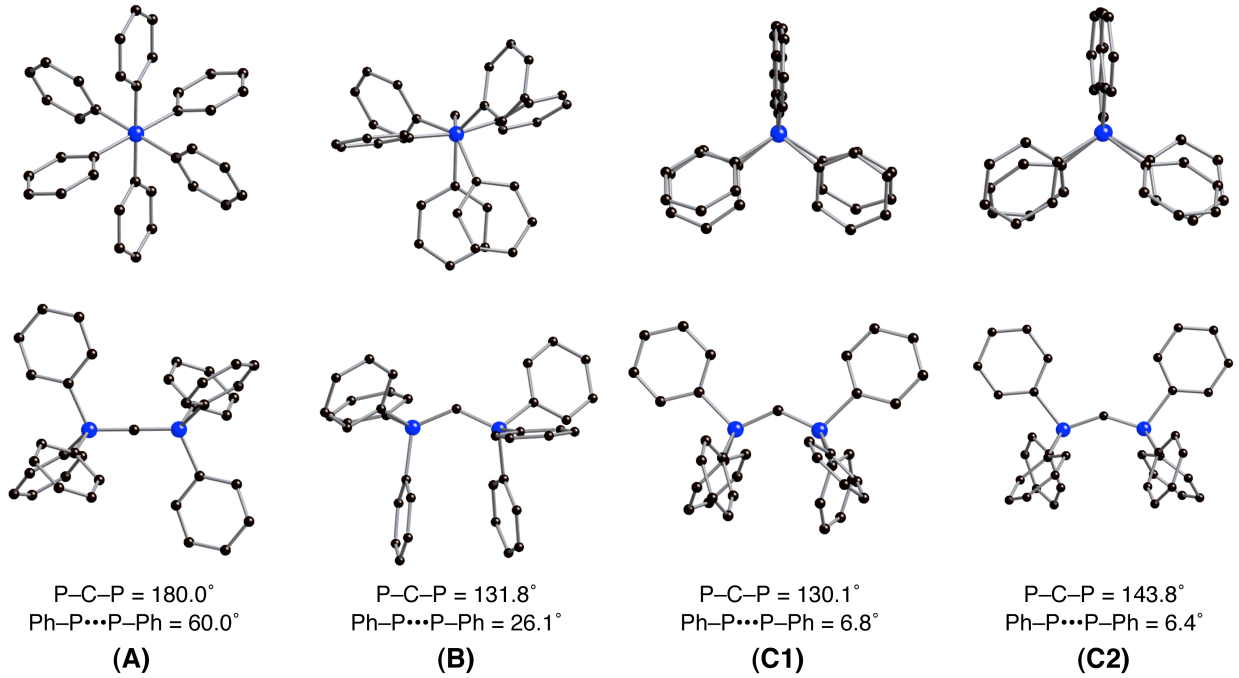

Figure 4. Different crystalline forms of $(Ph_3P)_2C$, which illustrate the staggered and eclipsed extremes (hydrogen atoms omitted for clarity): A (this work), B (ref. 16a), C1 and C2 (ref. 16b).

4.3 Energetic Profile of Bending the P–C–P Bonds in $(Ph_3P)_2C$

Density functional theory (DFT) geometry optimization (B3LYP) on $(Ph_3P)_2C$ with S_6 symmetry reproduces well the experimental linear structure. Additionally, further geometry optimization calculations (B3LYP) on the three previously reported crystallographic bent forms[16] of $(Ph_3P)_2C$ have also been performed. In each case, a bent geometry (137.4-139.5°) is obtained (Table 1) with a conformation similar to that of the respective experimentally determined geometry.[20]

Table 1. Geometry optimized structures of different conformers of $(Ph_3P)_2C$.

	A	**B**	**C1**	**C2**
P–C–P/°	180.0	139.5	138.3	137.4
Ph–P•••P–Ph/°	60.0	19.3	8.5	13.7
E_{rel}/kcal mol^{-1} [a]	0.00	–0.21	–0.32	–0.55

(a) $E_{rel} = E(X) - E(A)$; X = A, B, C1, C2.

Interestingly, despite the fact that the P–C–P angles of the geometry optimized conformers vary considerably from 137.4˚ to 180.0˚, the energies of the molecules only differ by less than 1.0 kcal mol^{-1} (Table 1).[21] Therefore, to examine the sensitivity of the energy of $(Ph_3P)_2C$ with respect to the P–C–P bond angle, a series of geometry optimization calculations in which the P–C–P bond angle is varied incrementally was performed (Figure 5).[22] While there is a minimum energy conformation of approximately 145.0˚, the overall energetic profile of either increasing or decreasing the P–C–P bond angle from 130.0˚ to 180.0˚ is notably shallow. For example, the energy of $(Ph_3P)_2C$ only increases by 0.84 kcal mol^{-1} upon increasing the angle from 145.0˚ to 180.0˚ and by 0.75 kcal mol^{-1} upon decreasing the angle from 145.0˚ to 130.0˚.

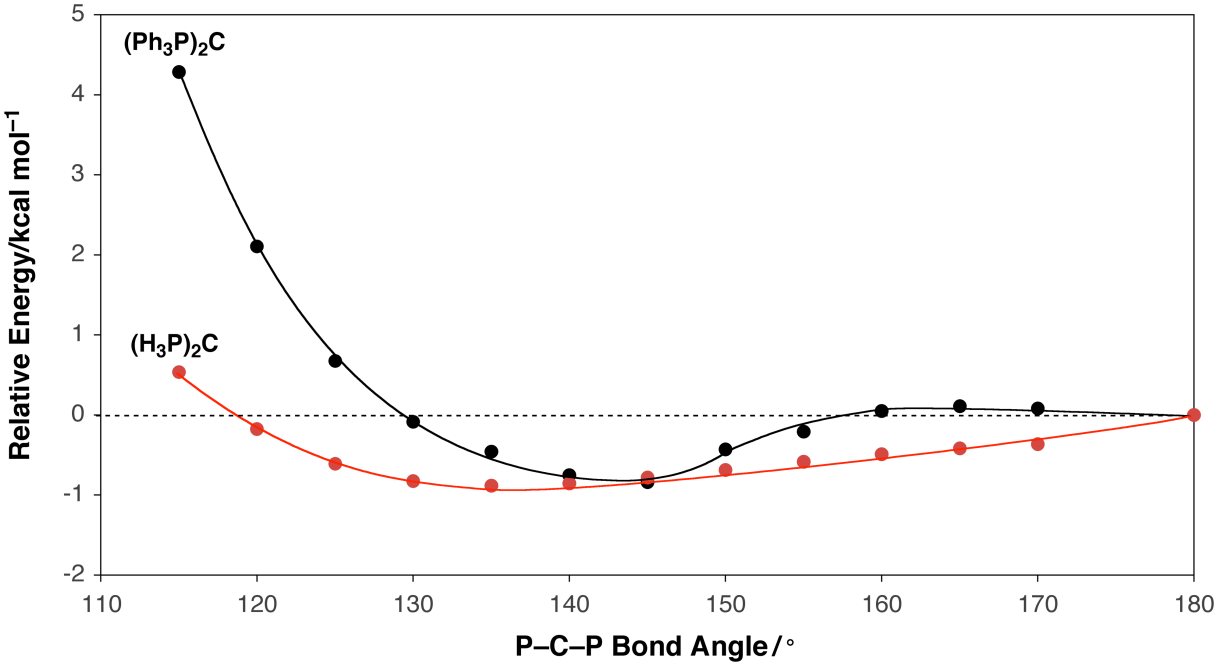

Figure 5. Variation in the energy of $(Ph_3P)_2C$ and $(H_3P)_2C$ as a function of bond angle as determined by DFT.

In addition to studying the flexibility of $(Ph_3P)_2C$, the hypothetical molecule, $(H_3P)_2C$, where each phenyl group is replaced by a hydrogen atom, was also examined. A corresponding series of geometry optimization calculations indicates that $(H_3P)_2C$ also favors a bent geometry, with a P–C–P bond angle of 135.5°. Furthermore, the energy surface for bending the P–C–P bonds of $(H_3P)_2C$ is even more shallow than $(Ph_3P)_2C$, such that the energy of the molecule changes by less than 1.0 kcal mol^{-1} over the range 120.0-180.0°.[23] As such, it is evident from these bending calculations on $(Ph_3P)_2C$ and $(H_3P)_2C$ that packing effects, such as the presence of benzene as a co-crystal in the solid state, would be sufficient enough to perturb the molecular structure.[16a,17]

Moreover, while both $(Ph_3P)_2C$ and $(H_3P)_2C$ have energy minima at approximately 145.0° and 135.0° respectively, the energy of both molecules starts to increase rapidly as the P–C–P angle is further reduced, with $(Ph_3P)_2C$ increasing more sharply. This

behavior is rationalized by virtue of the fact that at small P–C–P bond angles, steric interactions become more significant. Thus, the smallest P–C–P bond angle found in any polymorph of $(Ph_3P)_2C$ is 130.1˚. However, to explain the relatively flat energetic profile of $(Ph_3P)_2C$ in the 145.0-180.0˚ range, the electronics of the molecule appear to have a more profound effect, which is discussed in detail below in section 4.4.

4.4 Natural Localized Molecular Orbitals (NLMOs) of $(Ph_3P)_2C$

Given that steric interactions do not provide a satisfactory explanation for the shallow energetic profile of bending $(Ph_3P)_2C$ in the 145.0-180.0˚ range, it is pertinent to investigate the electronic profile of $(Ph_3P)_2C$. To accomplish this, the Natural Localized Molecular Orbitals (NLMOs) of linear and bent forms of $(Ph_3P)_2C$ were analyzed.[24] The two highest energy NLMOs of $(Ph_3P)_2C$ correspond to carbon lone-pairs that are delocalized to a small extent onto the adjacent phosphorous atoms as illustrated in Figure 6.[20] For example, the two lone-pair orbitals of linear $(Ph_3P)_2C$, which are approximately degenerate, possess 78% carbon and 13% phosphorus character (Table 2). In addition, the application of natural resonance theory[10] demonstrates that while the bonding in $(Ph_3P)_2C$ is highly delocalized, 92.4% of the Lewis structures for the linear form possess two lone-pairs on carbon; likewise, 91.7% of the bent (139.5˚) form possess two lone-pairs on carbon.

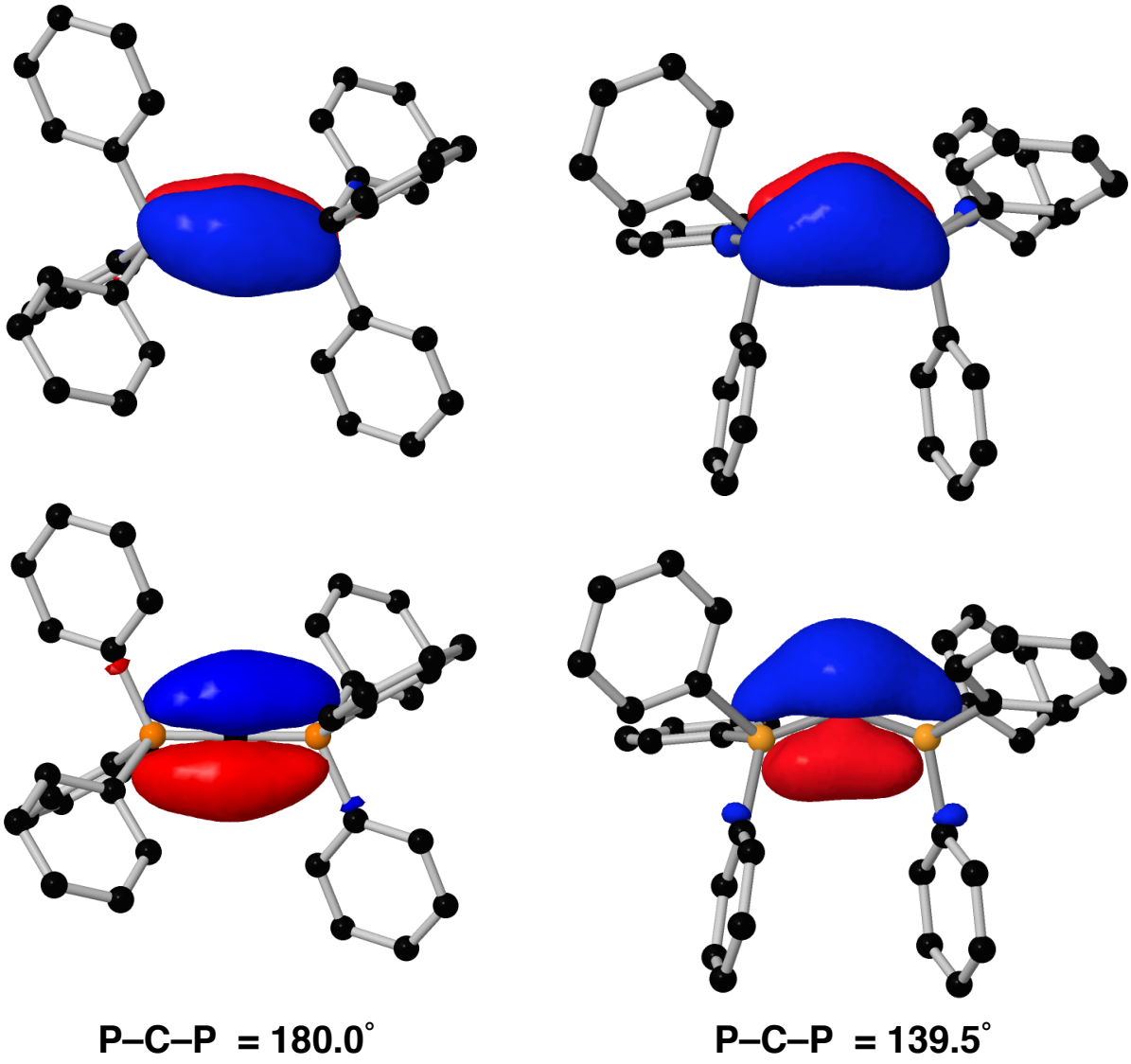

Figure 6. Lone-pair NLMOs of linear (left) and bent (right) forms of $(Ph_3P)_2C$. The σ-type orbital corresponds to the bottom right NLMO and π-type to the top right NLMO.

Table 2. Composition of in-plane (σ-type) and perpendicular (π-type) NLMO lone-pairs of $(Ph_3P)_2C$ as a function of P–C–P bond angle.

P–C–P/°	**in-plane lone-pair (σ-type)**		**perpendicular lone-pair (π-type)**	
	% **C**	% **P**	% **C**	% **P**
180.0	78.0 (0.00 2s, 100.0 2p)	13.2	78.0 (0.00 2s, 100.0 2p)	13.1
170.0	78.0 (0.82 2s, 99.17 2p)	13.1	77.9 (0.05 2s, 99.94 2p)	13.2
160.0	78.3 (3.67 2s, 96.29 2p)	12.9	77.6 (0.02 2s, 99.96 2p)	13.4
150.0	78.7 (8.85 2s, 91.07 2p)	12.3	77.1 (0.11 2s, 99.85 2p)	13.5
140.0	79.5 (15.66 2s, 84.22 2p)	11.6	76.6 (0.13 2s, 99.79 2p)	13.7
130.0	80.4 (24.03 2s, 75.81 2p)	10.9	76.1 (0.09 2s, 99.80 2p)	14.3
120.0	81.6 (35.35 2s, 64.48 2p)	10.3	75.4 (0.04 2s, 99.82 2p)	14.7

Upon further inspection, the carbon component of both the lone-pair NLMOs is 100% 2p in character for the linear geometry, but a significant amount of 2s character becomes incorporated in the in-plane (σ-type) orbital upon bending of the P–C–P bonds.[20] For example, the carbon component of the σ-type NLMO possesses 15.7% 2s character

when the P–C–P bond angle is 140.0° (Table 2). Additionally, this bending is also accompanied by a lowering of the energy of the σ-type NLMO (Figure 7). In contrast to these changes, the perpendicular (π-type) lone-pair orbital incorporates negligible carbon 2s character upon bending of the P–C–P bonds (only 0.13% at 140.0°, Table 2),[20] such that there is little variation in the energy of this NLMO as illustrated in Figure 7 (Note: the terms "σ-type" and "π-type" refer to the symmetry of the lone-pairs with respect to the P–C–P plane).

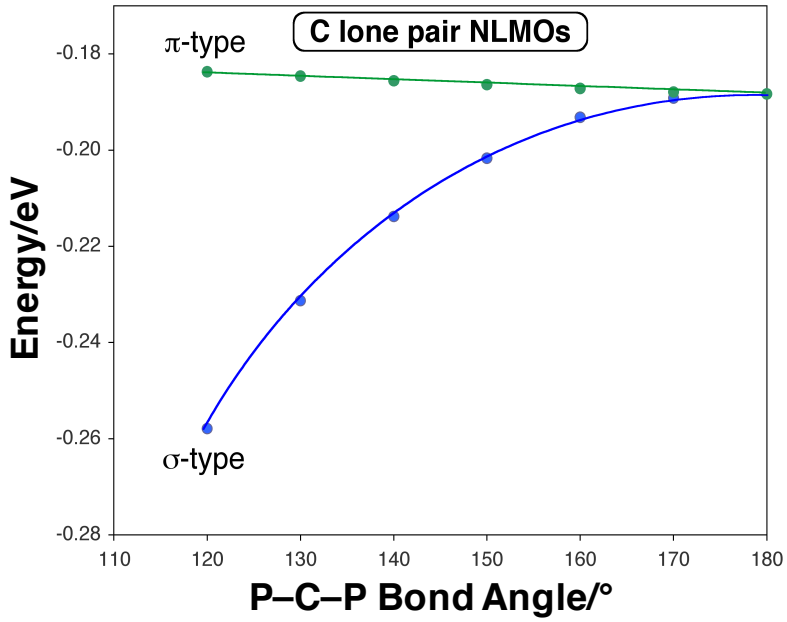

Figure 7. Variation of the lone-pair NLMO energies as a function of the P–C–P bond angle.

It is well-known that the geometry of simple $[AH_2]^{Q\pm}$ molecules is a compromise resulting from the fact that bending of the H–A–H bonds (*i*) stabilizes the $2a_1$ orbital (i.e., a nonbonding np orbital on A in the linear geometry) but (*ii*) destabilizes the bonding $1b_2$ orbital (i.e., the in-phase combination of an np orbital on A and two hydrogen 1s orbitals).[25] Depending upon the occupancies of these orbitals, the molecule

may be either linear (e.g., BeH_2) or bent (H_2O). With respect to $(Ph_3P)_2C$, the stabilization of the σ-type lone-pair NLMO upon bending the molecule is offset by the corresponding destabilization of the two P–C bonding NLMOs (Figure 8), as illustrated in Figure 9.[26] Therefore, the differential behavior of the lone-pair and bonding orbitals upon bending is one component that provides a simple explanation for the flexibility of $(Ph_3P)_2C$.

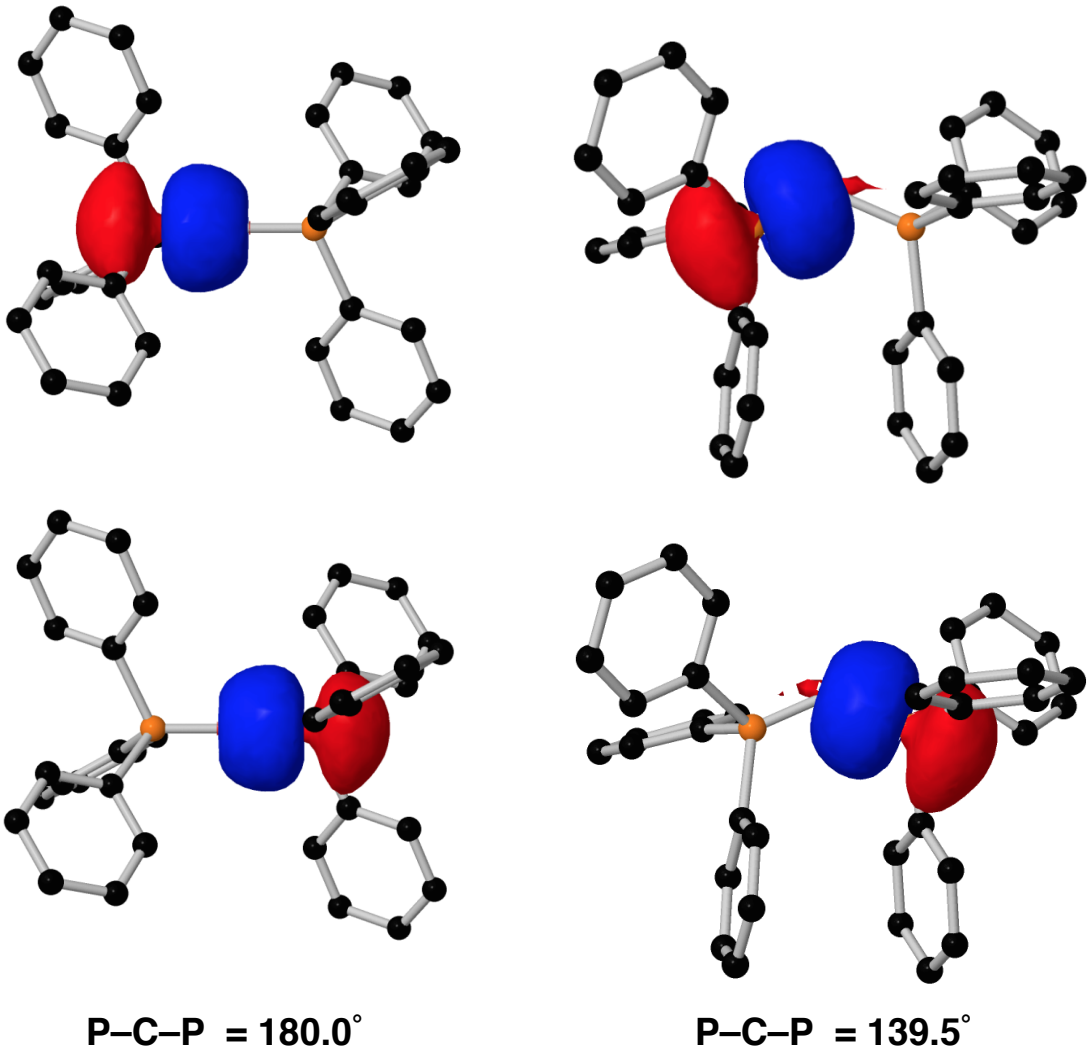

Figure 8. P–C bonding NLMOs of linear (left) and bent (right) forms of $(Ph_3P)_2C$.

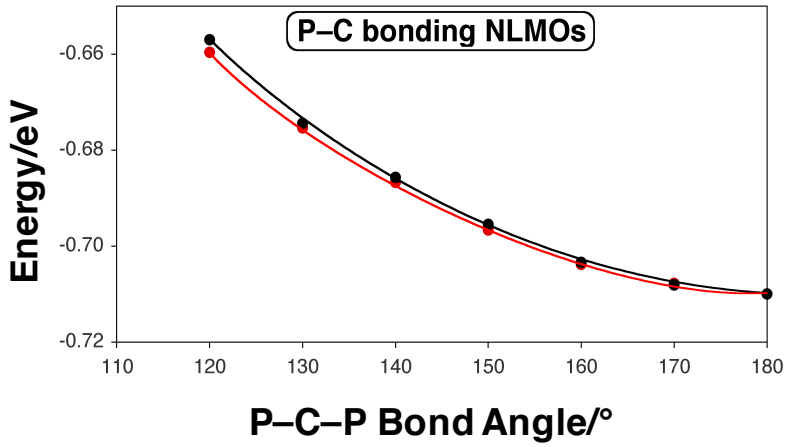

Figure 9. Variation of the P–C bonding NLMO energies as a function of the P–C–P bond angle.

4.5 Comparison of $(Ph_3P)_2C$ to $[(Ph_3P)_2N]^+$ and $(Ph_3Si)_2O$

It is useful to compare the energy surface for bending of the P–C–P bonds of $(Ph_3P)_2C$ with that of relevant isoelectronic compounds. In this regard, the bis(triphenylphosphine)iminium cation, $[(Ph_3P)_2N]^+$ (Figure 10), which is commonly employed as a noncoordinating counterion, has been investigated.[27,28] $[(Ph_3P)_2N]^+$ typically exhibits a bent geometry,[27,29] although linear geometries have also been observed.[30] Specifically, the average P–N–P bond angle in $[(Ph_3P)_2N]^+$ derivatives listed in the Cambridge Structural Database (CSD)[31] is 142.6˚, while only 3.6% have a bond angle greater than or equal to 170˚.

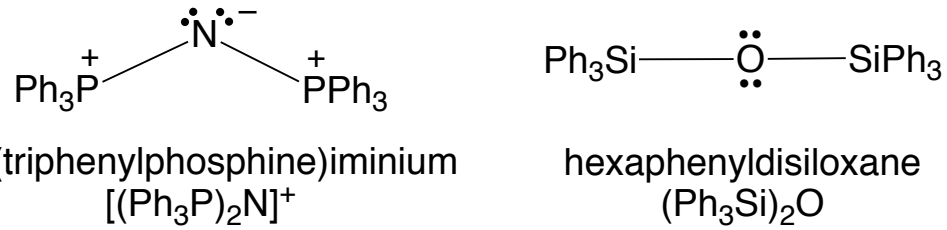

bis(triphenylphosphine)iminium
$[(Ph_3P)_2N]^+$

hexaphenyldisiloxane
$(Ph_3Si)_2O$

Figure 10. Lewis Structure representations of bis(triphenylphosphine)iminium cation, $[(Ph_3P)_2N]^+$, and hexaphenyldisiloxane, $(Ph_3Si)_2O$.

DFT calculations on $[(Ph_3P)_2N]^+$ indicate that a bent geometry is favored, although the energy surface for bending the P–N–P bond is also quite flat as illustrated in Figure 11.[32] For example, the energy of the molecule with an angle of 180.0° is only 0.62 kcal mol^{-1} higher than that of the fully geometry optimized molecule with an angle of 147.2°. Over the range 140-180°, the energy surface for $[(Ph_3P)_2N]^+$ corresponds closely to that of $(Ph_3P)_2C$, but the energy of $[(Ph_3P)_2N]^+$ increases more rapidly than that for $(Ph_3P)_2C$ upon decreasing the angle from 140°. Additionally, the hypothetical molecule, $[(H_3P)_2N]^+$, was investigated and also reveals a flat energy surface, similar to that of $(H_3P)_2C$.[27] The lone-pair NLMOs for $[(Ph_3P)_2N]^+$ are qualitatively similar to those of $(Ph_3P)_2C$, with the principal distinction being that they are more localized on the central atom of the former (Figure 12). For example, the lone-pair orbitals of linear $[(Ph_3P)_2N]^+$ possess 88.2% nitrogen character compared to 78.0% carbon character for $(Ph_3P)_2C$, a change that is in accordance with the electronegativity difference.

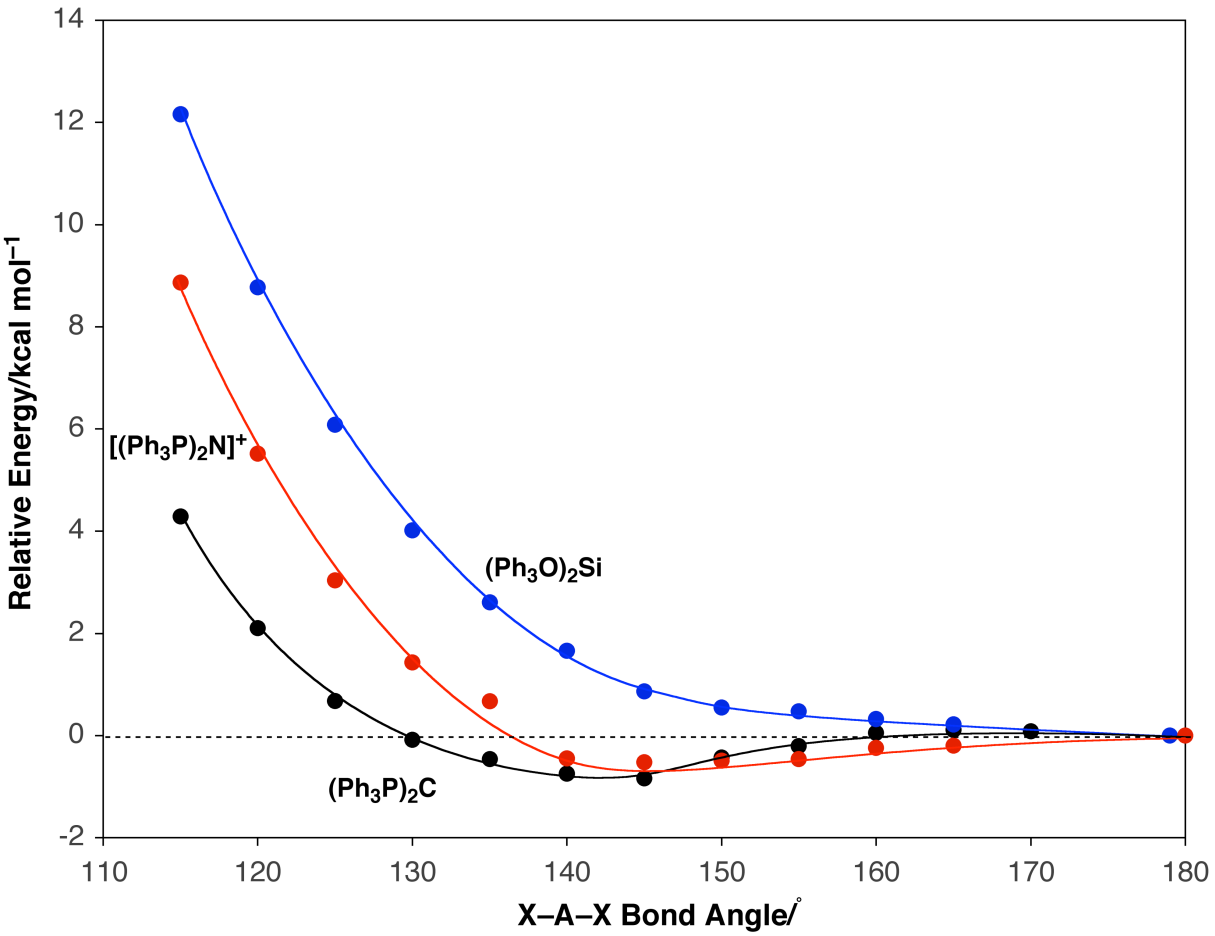

Figure 11. Variation in the energy of $(Ph_3P)_2C$, $[(Ph_3P)_2N]^+$, and $(Ph_3Si)_2O$ as a function of bond angle.

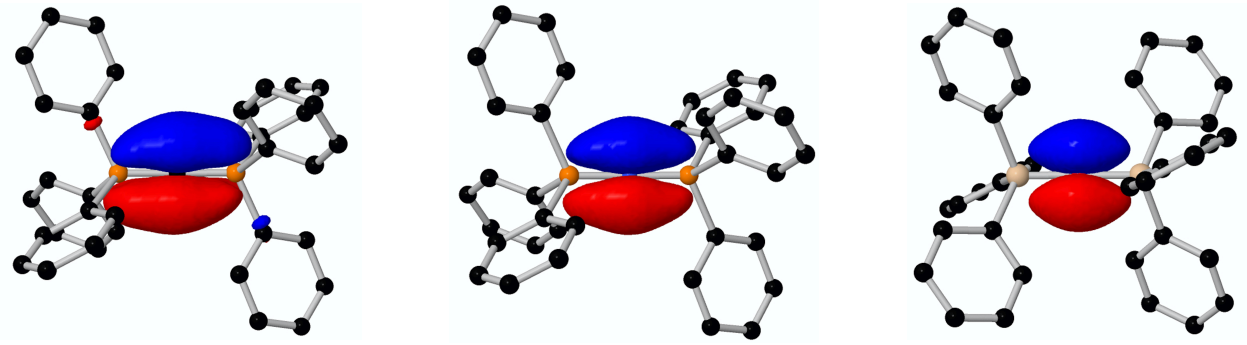

Figure 12. Lone-pair NLMO comparison of linear $(Ph_3P)_2C$, $[(Ph_3P)_2N]^+$, and $(Ph_3Si)_2O$.

For further comparison, the disiloxane, $(Ph_3Si)_2O$, was also investigated. Interestingly, and in contrast to the behavior of $(Ph_3P)_2C$ and $[(Ph_3P)_2N]^+$, the energy surface for bending of the Si–O–Si bonds does not exhibit a minimum, such that the energy of the molecule increases monotonically as the Si–O–Si angle decreases from 180° (Figure 11).[32] This observation is in accord with the fact that only linear structures have been reported for $(Ph_3Si)_2O$ to date. As such, there are 11 structures for $(Ph_3Si)_2O$ listed in the CSD,[31] which correspond to either unsolvated or solvated modifications, and each of these are linear at the oxygen.[33] It is, nevertheless, worth noting that strongly bent disiloxanes are known with other substituents. For example, $[(2,5\text{-}Mes_2C_5H_3)\text{-}Me_2Si]_2O$ has a Si–O–Si angle of 141.9°, while $(Ph_2Bu^tSi)_2O$ has an angle of 152.4°.[34] Additionally, the bis-phosphonium salt, $[(PPh_3)_2O][F_3CSO_3]_2$, also exhibits a bent geometry with a P–O–P bond angle of 164.5°.[35]

The energy surface for bending of the Si–O–Si bonds in $(Ph_3Si)_2O$ is, nevertheless, shallow. For example, $(Ph_3Si)_2O$ with a Si–O–Si angle of 145° is only 0.93 kcal mol^{-1} higher in energy than that for the linear geometry. Additionally, calculations on smaller disiloxanes, $(R_3Si)_2O$ (R = H, Me), also indicate a flat energy surface for bending the Si–O–Si bonds.[36] Continuing the trend in composition of the NLMOs as a function of the electronegativity difference, the lone-pair orbitals of linear $(Ph_3Si)_2O$ possess more oxygen character (94.7%) than do the central atoms in $[(Ph_3P)_2N]^+$ (88.2%) and $(Ph_3P)_2C$ (78.0%) (Figure 12).

As noted above in section 4.4, the different geometries of simple $[AH_2]^{Q\pm}$ molecules is a consequence of the fact that the energies of the lone pair and bonding orbitals do not vary in the same manner upon changing the H–A–H bond angle. That is, upon bending, the lone pair orbital with $2a_1$ symmetry is stabilized but, the bonding orbital with $1b_2$

symmetry is destabilized. An additional complicating feature for non-hydride $[AX_2]^{Q\pm}$ molecules is that the np orbitals on A can also participate in negative hyperconjugative interactions with the X substituents, in which electronic density is formally delocalized into orbitals on X with local σ∗ character.[36] In view of these competing factors, it is, therefore, not surprising that molecules of this class are rather flexible.

4.6 Summary and Conclusions

In summary, crystals of $(Ph_3P)_2C$ obtained from solutions in benzene exhibit a linear P–C–P bond angle as determined by X-ray diffraction, contrasting the highly bent structures that have been previously reported. Geometry optimization calculations reveal that the energetic barrier to bend the P–C–P bonds of $(Ph_3P)_2C$ is very shallow, indicating that small perturbations in the solid state, such as packing effects, may have a profound influence on the molecular structure. Additionally, analysis of the NLMOs of bent and linear forms of $(Ph_3P)_2C$ show that at smaller P–C–P bond angles the σ-type lone-pair orbital decreases in energy, while the P–C bonding NLMOs increase in energy. This differential behavior provides a simple rationalization for the flexible nature of $(Ph_3P)_2C$. Furthermore, computational studies demonstrate that $(Ph_3P)_2C$ has a lower energetic barrier for bending compared to the isoelectronic compounds $[(Ph_3P)_2N]^+$ and $(Ph_3Si)_2O$.

4.7 Experimental Details

4.7.1 General Considerations

All manipulations were performed using a combination of glovebox, high vacuum, and Schlenk techniques under an argon atmosphere.[37] Solvents were purified and degassed

by standard procedures. $(Ph_3P)_2C$[38] was obtained by the literature method. For further spectroscopic characterization of $(Ph_3P)_2C$ see Section 5.2

4.7.2 X-ray Structure Determinations

Yellow crystals of $(Ph_3P)_2C$ suitable for X-ray diffraction were obtained by vapor diffusion of pentane into a solution in benzene. X-ray diffraction data were collected on a Bruker Apex II diffractometer. Crystal data, data collection and refinement parameters are summarized in Table 3. The structure was solved by using direct methods and standard difference map techniques, and was refined by full-matrix least-squares procedures on F^2 with SHELXTL (Version 2014/7).[39]

4.7.3 Computational Details

Calculations were carried out using DFT as implemented in the Jaguar 8.9 (release 15) suite of *ab initio* quantum chemistry programs.[40] Geometry optimizations were performed with the B3LYP density functional using the LACVP** basis sets.[41] NBO, NLMO, and NRT calculations were performed with NBO 6.0[42] as implemented in the Jaguar suite of programs. Cartesian coordinates and energies of the geometry optimized structures are provided in Table 4.

4.8 Crystallographic Data

Table 3. Crystal, intensity collection, and refinement data.

	$(Ph_3P)_2C \cdot 2C_6H_6$
lattice	Trigonal
formula	$C_{49}H_{42}P_2$
formula weight	692.76
space group	*R-3*
a / Å	10.9287(5)
b / Å	10.9287(5)
c / Å	27.4503(14)
α / °	90
β / °	90
γ / °	120
V / Å^3	2839.3(3)
Z	3
temperature (K)	130(2)
radiation (λ, Å)	0.71073
ρ (calcd.) g cm^{-3}	1.215
μ (Mo Kα), mm^{-1}	0.149
θ max, deg.	30.534
no. of data collected	15606
no. of data	1942
no. of parameters	78
R_1 [$I > 2\sigma(I)$]	0.0383
wR_2 [$I > 2\sigma(I)$]	0.1155
R_1 [all data]	0.0462
wR_2 [all data]	0.1213

GOF	1.613
R_{int}	0.0527

4.9 Computational Data

Table 4. Cartesian Coordinates for Geometry Optimized Compounds

$(Ph_3P)_2C$, 180°

-2110.63183085055 Hartrees

atom	x	y	z
P	0	0	1.612801785
C	1.202920981	-1.174849862	2.391788643
C	0	0	0
C	2.391316063	-1.437692615	1.696496058
H	2.550983786	-0.963828848	0.731765274
C	3.116707951	-2.93304721	3.452778776
H	3.856608833	-3.615087652	3.862809858
C	0.978436413	-1.812679694	3.619696731
H	0.055327394	-1.637934081	4.163788822
C	3.344339774	-2.30678892	2.225498146
H	4.262548735	-2.4999441	1.677289613
C	1.9317676	-2.686952168	4.146459409
H	1.744029169	-3.180436902	5.096351423
C	0.415989336	1.629185059	2.391788643
C	0.049420296	2.789786767	1.696496058
H	-0.440791626	2.691131187	0.731765274
C	0.981739419	4.165671867	3.452778776

H	1.202453327	5.147465048	3.862809858
C	1.080608457	1.753690637	3.619696731
H	1.390828827	0.866881969	4.163788822
C	0.325567919	4.049677663	2.225498146
H	0.033740731	4.941447539	1.677289613
C	1.361085037	3.0164359	4.146459409
H	1.882324568	3.100592016	5.096351423
C	-1.618910316	-0.454335197	2.391788643
C	-2.440736359	-1.352094152	1.696496058
H	-2.11019216	-1.727302339	0.731765274
C	-4.09844737	-1.232624657	3.452778776
H	-5.05906216	-1.532377396	3.862809858
C	-2.059044871	0.058989057	3.619696731
H	-1.446156221	0.771052112	4.163788822
C	-3.669907693	-1.742888743	2.225498146
H	-4.296289466	-2.441503439	1.677289613
C	-3.292852636	-0.329483732	4.146459409
H	-3.626353736	0.079844886	5.096351423
P	0	0	-1.612801785
C	-1.202920981	1.174849862	-2.391788643
C	-2.391316063	1.437692615	-1.696496058
H	-2.550983786	0.963828848	-0.731765274
C	-3.116707951	2.93304721	-3.452778776
H	-3.856608833	3.615087652	-3.862809858
C	-0.978436413	1.812679694	-3.619696731
H	-0.055327394	1.637934081	-4.163788822

C	-3.344339774	2.30678892	-2.225498146
H	-4.262548735	2.4999441	-1.677289613
C	-1.9317676	2.686952168	-4.146459409
H	-1.744029169	3.180436902	-5.096351423
C	-0.415989336	-1.629185059	-2.391788643
C	-0.049420296	-2.789786767	-1.696496058
H	0.440791626	-2.691131187	-0.731765274
C	-0.981739419	-4.165671867	-3.452778776
H	-1.202453327	-5.147465048	-3.862809858
C	-1.080608457	-1.753690637	-3.619696731
H	-1.390828827	-0.866881969	-4.163788822
C	-0.325567919	-4.049677663	-2.225498146
H	-0.033740731	-4.941447539	-1.677289613
C	-1.361085037	-3.0164359	-4.146459409
H	-1.882324568	-3.100592016	-5.096351423
C	1.618910316	0.454335197	-2.391788643
C	2.440736359	1.352094152	-1.696496058
H	2.11019216	1.727302339	-0.731765274
C	4.09844737	1.232624657	-3.452778776
H	5.05906216	1.532377396	-3.862809858
C	2.059044871	-0.058989057	-3.619696731
H	1.446156221	-0.771052112	-4.163788822
C	3.669907693	1.742888743	-2.225498146
H	4.296289466	2.441503439	-1.677289613
C	3.292852636	0.329483732	-4.146459409
H	3.626353736	-0.079844886	-5.096351423

$(Ph_3P)_2C$, 170°			
-2110.63169983386 Hartrees			
atom	**x**	**y**	**z**
P	11.22225086	4.99547358	16.67327908
P	14.16951963	5.012304349	15.37750547
C	9.987388107	4.078548945	15.63582101
C	17.4586833	7.111268164	17.92134489
H	18.21393672	7.596767182	18.53337476
C	15.50772328	5.860464059	16.33978704
C	14.32553654	5.728072152	13.67425911
C	10.62709925	8.978039823	17.48681903
H	11.26768488	9.837803959	17.66416745
C	11.14863497	4.106250424	18.30109993
C	15.23463654	5.245898415	12.72211319
H	15.88550577	4.411039369	12.96473993
C	12.69688644	5.144675903	16.02907162
C	14.80869919	3.2820466	15.15491445
C	11.19590072	7.730947374	17.23096225
H	12.2747304	7.607553806	17.18733521
C	13.4751277	6.786946193	13.32986256
H	12.75306677	7.136835364	14.06286566
C	10.38314157	6.613374327	17.00298816
C	9.238575979	9.123658372	17.50729158
H	8.794922621	10.09652462	17.70078416
C	15.33984755	5.963199063	17.72703641

H	14.43296239	5.5660664	18.17502186
C	13.8941275	2.311535094	14.71671654
H	12.86272145	2.599231065	14.52990533
C	11.15432833	2.666936875	20.71130249
H	11.15698887	2.110387891	21.64458217
C	10.10977512	4.176656986	14.24249532
H	10.92025149	4.768447169	13.82516697
C	15.29888455	5.822525617	11.4520378
H	16.00269318	5.436605724	10.71942417
C	14.45550519	6.883329063	11.12118223
H	14.50395369	7.328985743	10.13135504
C	16.65820349	6.403238257	15.75058753
H	16.7965602	6.35168191	14.67499996
C	16.52786218	1.569854862	15.25216797
H	17.55299043	1.28264749	15.47079085
C	10.28790028	4.467394364	19.34636268
H	9.616698025	5.312612341	19.23169637
C	16.31157407	6.579724887	18.51396707
H	16.17087449	6.650195361	19.58923007
C	8.421611469	8.018157038	17.26869412
H	7.340541652	8.128696063	17.27096686
C	8.989805753	6.768070267	17.01641285
H	8.344430856	5.917931893	16.81738676
C	15.61473914	0.615053247	14.80698186
H	15.92634743	-0.41744718	14.6744416
C	16.12907345	2.897849958	15.4244393

H	16.84809536	3.631133877	15.77571785
C	10.29268796	3.750716952	20.54543036
H	9.624501599	4.043799567	21.35083595
C	8.962327076	3.288006066	16.17369378
H	8.8624477	3.184801931	17.24994975
C	13.54278276	7.364156594	12.06235981
H	12.87901135	8.185728475	11.80666398
C	12.01934317	2.304172186	19.67637569
H	12.69707455	1.463946657	19.80181097
C	17.62831007	7.025112388	16.53923592
H	18.51381178	7.447052701	16.07142871
C	8.071651916	2.616619682	15.33308314
H	7.285220848	2.00125092	15.7620204
C	12.02073386	3.022692489	18.48215062
H	12.70756805	2.756109719	17.68331837
C	8.195799332	2.727645951	13.94823573
H	7.504211019	2.202526793	13.29496063
C	9.217497418	3.509458497	13.4042625
H	9.322564659	3.595227002	12.32590643
C	14.29551326	0.988946529	14.538711
H	13.57788748	0.24837777	14.19566229

$(Ph_3P)_2C$, 165°

-2110.63165394868 Hartrees

atom	**x**	**y**	**z**
P	11.22773425	5.024536517	16.67150121

P	14.16527528	5.044282357	15.37866973
C	10.01544145	4.086688455	15.62297749
C	17.50981035	7.095034264	17.88737602
H	18.27787648	7.570605171	18.49129474
C	15.52562305	5.870970255	16.32683167
C	14.33638619	5.732320057	13.66675718
C	10.51728139	8.98136575	17.51337404
H	11.13189875	9.860613026	17.68700353
C	11.17941275	4.113280988	18.28866231
C	15.2400997	5.220234479	12.72540593
H	15.87120841	4.374062643	12.98104277
C	12.69834767	5.245551482	16.03223404
C	14.75891907	3.295414365	15.17418644
C	11.12274675	7.755097297	17.24151695
H	12.20398276	7.665350056	17.18071629
C	13.51105916	6.805352492	13.30704857
H	12.79400446	7.178021961	14.03370377
C	10.34337781	6.613273282	17.01830247
C	9.125329633	9.081541319	17.55476365
H	8.653036897	10.03820688	17.76099281
C	15.35151732	6.020228777	17.70879412
H	14.42692675	5.670169827	18.15968757
C	13.84679555	2.362021702	14.65585019
H	12.84496226	2.68631547	14.38695936
C	11.23861864	2.656320432	20.68822726
H	11.2624172	2.093429012	21.61740559

C	10.11086345	4.232692745	14.23176714
H	10.88947924	4.869840652	13.82061609
C	15.32392606	5.781557948	11.44972952
H	16.02340708	5.373157449	10.72517196
C	14.50534474	6.856807524	11.10302739
H	14.56928172	7.291054676	10.10896669
C	16.70003488	6.352618981	15.73177636
H	16.84463354	6.264191102	14.65954093
C	16.39836698	1.517641693	15.39680436
H	17.391205	1.190748976	15.69446462
C	10.34651495	4.470095222	19.35768294
H	9.675415609	5.318012713	19.26538232
C	16.33974254	6.623487415	18.48559675
H	16.19404601	6.730812401	19.55716578
C	8.341191781	7.951534306	17.32038056
H	7.257223191	8.026840198	17.33881007
C	8.945999951	6.722164718	17.0521129
H	8.325857003	5.852269924	16.85751834
C	15.48898105	0.600455529	14.87239922
H	15.77088703	-0.442702114	14.7577132
C	16.03736676	2.859435147	15.54611283
H	16.75361173	3.563533705	15.95722867
C	10.3781774	3.744875972	20.55140808
H	9.731525515	4.035324399	21.37518026
C	9.030793435	3.241066747	16.15216989
H	8.952283577	3.103161582	17.2263488

C	13.59786691	7.367135692	12.03373587
H	12.95373832	8.200272103	11.76544532
C	12.07539127	2.296882719	19.62909037
H	12.75210867	1.452789929	19.73151297
C	17.68648405	6.961673779	16.50982758
H	18.59050704	7.336745545	16.03752928
C	8.153178343	2.561202024	15.30440203
H	7.397635373	1.903428724	15.72586454
C	12.05070263	3.024053213	18.44059744
H	12.71758602	2.758130285	17.62488239
C	8.250533572	2.719113354	13.92204684
H	7.568920367	2.187664169	13.26350007
C	9.231886875	3.556539505	13.38691723
H	9.315156437	3.67957503	12.31037652
C	14.21088529	1.026155045	14.50102957
H	13.49611082	0.315163482	14.09541703

$(Ph_3P)_2C$, 160°

-2110.63175479250 Hartrees

atom	x	y	z
P	11.23785394	5.072768788	16.67703332
P	14.16438039	5.091710584	15.39529653
C	10.06243198	4.10411865	15.61151568
C	17.59897489	7.045886994	17.86521523
H	18.38918909	7.496588772	18.45925197
C	15.5564801	5.883255691	16.3283231

C	14.34777562	5.745779088	13.67134633
C	10.37355913	9.002948286	17.51127301
H	10.9524173	9.910053397	17.66303201
C	11.2104993	4.131966847	18.27744116
C	15.240852	5.199276594	12.73902642
H	15.86143346	4.350755421	13.01211024
C	12.7039239	5.363708297	16.04669233
C	14.70011161	3.321628252	15.20309915
C	11.02779202	7.802911722	17.23269538
H	12.11011862	7.760235442	17.14529084
C	13.53412717	6.819498549	13.28849385
H	12.82427282	7.21672508	14.0091723
C	10.29659304	6.62526428	17.03584804
C	8.979694243	9.041650959	17.58750394
H	8.46949427	9.977193975	17.7993665
C	15.3827809	6.08902936	17.70280773
H	14.43673442	5.806455844	18.15663852
C	13.78764788	2.432261743	14.61142903
H	12.8211552	2.799189609	14.27639325
C	11.30562119	2.627536668	20.64671935
H	11.34288131	2.045947403	21.56384948
C	10.15060992	4.27560938	14.22249685
H	10.90011958	4.95237356	13.82060097
C	15.32462824	5.726530742	11.44890898
H	16.01445135	5.290452849	10.73122089
C	14.51647836	6.801853684	11.07846826

H	14.57886618	7.208314249	10.07259026
C	16.7602902	6.278790267	15.72798719
H	16.90702237	6.146496895	14.66054292
C	16.24559085	1.473133745	15.51038592
H	17.20241122	1.101905657	15.86803073
C	10.41044101	4.480741822	19.37348549
H	9.749327281	5.33926064	19.313419
C	16.39919671	6.661535246	18.46766298
H	16.25203803	6.812554372	19.5337437
C	8.243087099	7.874390636	17.37920935
H	7.157535033	7.899377984	17.42397007
C	8.896620937	6.671807681	17.10293007
H	8.311620843	5.77361437	16.92846669
C	15.33697815	0.600597143	14.91374901
H	15.58317942	-0.451986315	14.80279575
C	15.93123438	2.827534565	15.65359549
H	16.64742927	3.496356975	16.11971386
C	10.4604207	3.732163144	20.55231114
H	9.838704748	4.016473204	21.39714654
C	9.115186908	3.208569503	16.12677719
H	9.043021982	3.050846844	17.19867405
C	13.62054063	7.347049933	12.00051179
H	12.98402282	8.179843678	11.71356273
C	12.10942378	2.275075173	19.55984845
H	12.77373823	1.41782083	19.62830754
C	17.77492704	6.856863753	16.49347189

H	18.70132786	7.163886201	16.01539593
C	8.268287407	2.503571585	15.26827407
H	7.542487887	1.806850385	15.67937987
C	12.06699869	3.02540698	18.38678153
H	12.70786186	2.760922064	17.5501133
C	8.358863551	2.685900976	13.88860359
H	7.701798089	2.134302383	13.2216909
C	9.302251933	3.574093096	13.36693601
H	9.379963823	3.716680489	12.29238058
C	14.10541874	1.083954141	14.46365694
H	13.39097217	0.408577232	14.00063702

$(Ph_3P)_2C$, 155°

-2110.63216373654 Hartrees

atom	x	y	z
P	11.24150531	5.078705108	16.65874154
P	14.15727634	5.132941875	15.40197216
C	10.08709907	4.126386886	15.55804741
C	17.59856883	7.154770306	17.80383245
H	18.39054125	7.625035893	18.3801418
C	15.55318039	5.941856432	16.31262147
C	14.35281418	5.736893575	13.66180404
C	10.24863547	8.983606419	17.46268212
H	10.78234678	9.92897326	17.51191053
C	11.23878894	4.072299027	18.21335219
C	15.25106152	5.165045092	12.7498173

H	15.86148024	4.316651094	13.0453144
C	12.69703141	5.457687297	16.03992526
C	14.67341454	3.354628102	15.26616514
C	10.93875491	7.813083758	17.14654605
H	12.00443116	7.823518847	16.93353758
C	13.55230492	6.809416938	13.24870425
H	12.8395684	7.227079874	13.95489596
C	10.26363545	6.589364026	17.08105453
C	8.875875641	8.941615545	17.7102098
H	8.337001346	9.853497918	17.95311282
C	15.33044397	6.329091483	17.63900371
H	14.34618992	6.16216157	18.06836965
C	13.87790316	2.499839376	14.48389476
H	13.02991591	2.903184643	13.93681807
C	11.46575929	2.519727035	20.54390916
H	11.55305616	1.91908381	21.44519777
C	10.18952314	4.327284762	14.17470224
H	10.95042496	5.004434259	13.79540112
C	15.351304	5.664901405	11.45002588
H	16.04467406	5.208849346	10.74839894
C	14.55582498	6.738766785	11.04959858
H	14.63188218	7.124381895	10.03651678
C	16.80859402	6.179372901	15.73460419
H	16.99535721	5.903749987	14.70130347
C	16.02545711	1.4429349	15.9117382
H	16.86138065	1.034303702	16.47326289

C	10.79330509	4.568403115	19.4452313
H	10.35609141	5.55980239	19.50481665
C	16.34846557	6.928015875	18.38230904
H	16.16333091	7.221604136	19.41212917
C	8.193515739	7.725664321	17.63760416
H	7.122993215	7.68961551	17.82084086
C	8.882778784	6.55441197	17.3226132
H	8.340052874	5.616155475	17.25703978
C	15.23504274	0.604780009	15.12740019
H	15.45234664	-0.458544847	15.07381934
C	15.74790699	2.810898212	15.9811361
H	16.37048916	3.453134748	16.59542898
C	10.90801528	3.79561727	20.60370403
H	10.55980303	4.194339786	21.55288539
C	9.12133378	3.234683548	16.0455847
H	9.038964247	3.052376466	17.11289936
C	13.65554877	7.309924672	11.95131913
H	13.02904386	8.142160399	11.64159271
C	11.91667677	2.017562481	19.3201526
H	12.35557672	1.024938187	19.2665554
C	17.82485016	6.781991048	16.47722188
H	18.79245461	6.964403162	16.01739201
C	8.270501637	2.562601583	15.16541457
H	7.52973558	1.869386403	15.55523383
C	11.80900901	2.788865971	18.16563856
H	12.17736365	2.396312562	17.22151229

C	8.375309903	2.774649941	13.79084378
H	7.713781727	2.250141752	13.10670727
C	9.33725909	3.658449735	13.29685989
H	9.425065134	3.824740662	12.22649218
C	14.15836546	1.137164622	14.41245936
H	13.53683206	0.489363103	13.80004477

$(Ph_3P)_2C$, 150°

-2110.63251481996 Hartrees

atom	x	y	z
P	11.25286903	5.10925548	16.6550676
P	14.14732947	5.154144778	15.40751462
C	10.12520948	4.134127937	15.54582406
C	17.63318586	7.118246577	17.79266672
H	18.4339223	7.579735592	18.36397762
C	15.56454927	5.930845542	16.31317491
C	14.36314729	5.743850516	13.66470457
C	10.12680306	8.978697608	17.45458006
H	10.62340412	9.944675655	17.49002775
C	11.27905824	4.094210352	18.20297518
C	15.24463887	5.144056954	12.75431201
H	15.82852397	4.277535034	13.05088737
C	12.69775732	5.553877398	16.04181373
C	14.61042722	3.358747206	15.28316508
C	10.8575709	7.834265315	17.13359133
H	11.9185678	7.883639927	16.90347559

C	13.59696657	6.840705583	13.24991699
H	12.89700927	7.28011386	13.9556576
C	10.22939155	6.585167897	17.0851645
C	8.761012944	8.884494335	17.72491113
H	8.190774731	9.775959395	17.97205017
C	15.33995399	6.36649334	17.6240563
H	14.34447705	6.249019053	18.04372615
C	13.81079356	2.524850092	14.48212274
H	12.9893054	2.950423802	13.9119722
C	11.56479946	2.545985496	20.53038336
H	11.67480644	1.947102152	21.43036559
C	10.20535449	4.372023118	14.16661098
H	10.93627066	5.086299915	13.79652883
C	15.36204496	5.640155849	11.4544306
H	16.04207904	5.162742738	10.75396972
C	14.60087121	6.738040575	11.05239344
H	14.6903892	7.120850231	10.03933336
C	16.83435376	6.106280346	15.74438582
H	17.02338522	5.793507993	14.72209652
C	15.89115169	1.408339933	15.96225302
H	16.70208112	0.97807486	16.54387462
C	10.86342357	4.591930208	19.44481302
H	10.42689991	5.583059681	19.51320804
C	16.36935753	6.952738061	18.36172342
H	16.18208886	7.285335987	19.37923082
C	8.125727997	7.642328371	17.67006097

H	7.060658706	7.565294366	17.87147447
C	8.855155585	6.497397094	17.34962946
H	8.348972857	5.537986308	17.29833611
C	15.09663997	0.590463881	15.15999062
H	15.28499263	-0.478400704	15.11195666
C	15.65123452	2.783957845	16.02410714
H	16.27763052	3.4086079	16.65273948
C	11.00703602	3.821414345	20.60135624
H	10.68107818	4.221263982	21.5579604
C	9.197230483	3.19654072	16.02052466
H	9.13096811	2.987305218	17.08386331
C	13.71761536	7.337206847	11.95264651
H	13.11784391	8.188555101	11.64187217
C	11.98601646	2.042148954	19.29689222
H	12.42461731	1.049937672	19.23419622
C	17.86207913	6.69641391	16.48113335
H	18.84063962	6.831687113	16.02827279
C	8.363273213	2.514217348	15.1320781
H	7.652352579	1.785138636	15.51193532
C	11.84868248	2.810948958	18.14360178
H	12.19288079	2.415342041	17.19176827
C	8.44600628	2.7626376	13.76220734
H	7.79723433	2.230420544	13.07183559
C	9.369193151	3.693531758	13.28079073
H	9.439217477	3.889221568	12.21409298
C	14.05342008	1.154006704	14.41932966

H	13.42801943	0.524461219	13.79205641

$(Ph_3P)_2C$, 145°

-2110.63316699004 Hartrees

atom	x	y	z
P	11.26681444	5.134466094	16.65777215
P	14.13302114	5.191744303	15.42180955
C	10.16748912	4.200536233	15.4882789
C	17.69155025	7.214401106	17.63058986
H	18.51205354	7.689780955	18.16135166
C	15.57673375	5.989673471	16.25915447
C	14.33090765	5.704052834	13.65285769
C	10.04946897	8.944516988	17.59035089
H	10.51652824	9.924779659	17.63520275
C	11.30579129	4.039038268	18.15065204
C	15.18568648	5.055006768	12.75046277
H	15.74884056	4.181222507	13.06469596
C	12.70756923	5.653525454	16.08042965
C	14.5700353	3.388508435	15.38405466
C	10.80561841	7.832208546	17.21869487
H	11.85720325	7.91986373	16.95860899
C	13.59428381	6.812818809	13.21500741
H	12.91888995	7.295129711	13.91673733
C	10.21552353	6.565520949	17.15837113
C	8.696494167	8.799858118	17.90003154

H	8.106754434	9.666256468	18.18742644
C	15.36084476	6.583928183	17.50694784
H	14.35446044	6.565559604	17.91673121
C	13.83600713	2.533731935	14.5431922
H	13.09293442	2.948041161	13.86727612
C	11.62537668	2.3840036	20.39807427
H	11.74749236	1.743397931	21.26726607
C	10.28207953	4.487408719	14.12094712
H	11.02234957	5.212831013	13.7945906
C	15.30384731	5.511759011	11.43621379
H	15.96358634	4.996502675	10.7432549
C	14.57174001	6.620971541	11.01150142
H	14.66357443	6.974405067	9.988113636
C	16.86113904	6.022168471	15.69729895
H	17.04359596	5.580472355	14.72241606
C	15.7154569	1.445455653	16.28977438
H	16.4477718	1.026570559	16.97472197
C	10.96444923	4.500240672	19.42880307
H	10.57237964	5.504155786	19.55604786
C	16.41431206	7.191087786	18.19152796
H	16.23655445	7.648389311	19.16120953
C	8.09884957	7.539524893	17.83297966
H	7.043688806	7.423423716	18.06522788
C	8.85358317	6.427155062	17.46168575
H	8.376127864	5.453727582	17.40224065
C	14.987345	0.60635629	15.44657255

H	15.15016773	-0.46750541	15.46939756
C	15.50916301	2.82704981	16.25980698
H	16.08195027	3.468404933	16.9220041
C	11.12361105	3.676374397	20.54521709
H	10.85320528	4.047062754	21.53040326
C	9.226547428	3.247552148	15.90421428
H	9.134348442	2.997385529	16.95669401
C	13.71575174	7.270409642	11.90336985
H	13.14021164	8.132109043	11.57605326
C	11.97402965	1.916978636	19.12834164
H	12.36934649	0.912261734	19.00570058
C	17.91295498	6.631093762	16.38120448
H	18.90460059	6.653784762	15.93737658
C	8.414093121	2.600186484	14.97117947
H	7.69299745	1.859294529	15.3063854
C	11.81878343	2.738177042	18.0138626
H	12.10293601	2.367273369	17.03310694
C	8.531197347	2.898096416	13.61343623
H	7.899141962	2.393059104	12.88801186
C	9.467666793	3.843441053	13.19000827
H	9.565817906	4.077734416	12.13332421
C	14.04514122	1.155745027	14.57205508
H	13.47287103	0.510177967	13.91130355

$(Ph_3P)_2C$, 140°

-2110.63302986930 Hartrees

atom	x	y	z
P	11.2899514	5.164922428	16.67099249
P	14.12632086	5.223414188	15.44787965
C	10.225435	4.227688772	15.46880387
C	17.77145358	7.191825334	17.56897804
H	18.61141038	7.657456793	18.07710183
C	15.60397498	5.99220153	16.25352527
C	14.31481773	5.707057185	13.6682627
C	9.927353548	8.93244638	17.58932163
H	10.35344064	9.931824104	17.6158682
C	11.33718937	4.039678824	18.14141333
C	15.15372084	5.035578965	12.76721138
H	15.71188377	4.161320065	13.08861308
C	12.72288311	5.752778331	16.12137801
C	14.51393531	3.408752032	15.42461073
C	10.72744297	7.848137515	17.22490844
H	11.77174613	7.977553391	16.95318638
C	13.58412868	6.815353212	13.21945732
H	12.92137819	7.315983719	13.92047673
C	10.19254004	6.556023484	17.1849217
C	8.584075502	8.736516691	17.91361505
H	7.960198941	9.580855469	18.19366626
C	15.4124792	6.66562216	17.46433829
H	14.40451887	6.717156866	17.86755139
C	13.79065914	2.569083209	14.55951177
H	13.08350801	2.998541212	13.85547485

C	11.67247807	2.352534835	20.3683195
H	11.7994251	1.700528372	21.22803692
C	10.34319212	4.551954067	14.10983277
H	11.06519133	5.305459738	13.80749072
C	15.26041011	5.467852085	11.44391942
H	15.90698327	4.934071068	10.75253833
C	14.53276285	6.575633385	11.0077869
H	14.61464297	6.909217593	9.976875808
C	16.89145774	5.931611823	15.7003503
H	17.05748529	5.426702019	14.753581
C	15.58019928	1.441632709	16.37464457
H	16.27812885	1.007678521	17.08560436
C	11.02997816	4.491213885	19.43235335
H	10.6575232	5.500191548	19.57832727
C	16.49143129	7.260804268	18.12029092
H	16.33051195	7.781077643	19.06072894
C	8.041619699	7.450107779	17.86828384
H	6.994477517	7.291036463	18.11123281
C	8.839810253	6.365819652	17.50378815
H	8.402152743	5.372920506	17.46018444
C	14.86360617	0.6174417	15.50685977
H	15.00143198	-0.459797342	15.53640578
C	15.4068848	2.827361388	16.33538587
H	15.970035	3.456922002	17.01690471
C	11.1958756	3.652534348	20.53684466
H	10.94936469	4.017929881	21.53023691

C	9.305641561	3.240160426	15.85075503
H	9.208718433	2.961393038	16.89542854
C	13.69386894	7.248626598	11.89829266
H	13.1217058	8.109337492	11.56245849
C	11.98864331	1.895430781	19.086416
H	12.36427536	0.885825408	18.94374335
C	17.96869568	6.527236928	16.35603667
H	18.96183085	6.476049536	15.91790309
C	8.520129432	2.594563355	14.89382706
H	7.816202717	1.82658146	15.20362888
C	11.82534418	2.731308007	17.98311805
H	12.08219233	2.363449578	16.9939808
C	8.641752628	2.928601285	13.54498691
H	8.030968944	2.424403185	12.8009729
C	9.555304253	3.909822483	13.154885
H	9.656877102	4.173537435	12.10547194
C	13.96602031	1.186402773	14.59869714
H	13.40297657	0.552751328	13.9187398

$(Ph_3P)_2C$, 139.5°

-2110.63215164539 Hartrees

atom	**x**	**y**	**z**
P	11.21461883	5.125588204	16.50333759
P	14.11966462	5.277650826	15.4804776
C	9.998672781	4.60979003	15.19642998
C	17.36839237	8.066061455	17.2951056

H	18.11647771	8.722664416	17.73124659
C	15.44158378	6.371748163	16.16977649
C	14.41120121	5.397693723	13.65498793
C	9.811853018	8.706489714	17.93340426
H	10.00567433	9.755889639	17.72809688
C	11.28518967	3.655706771	17.62436729
C	15.3420226	4.611332297	12.96091267
H	15.91504587	3.854345082	13.48665569
C	12.62365487	5.767261924	15.9536629
C	14.68936715	3.565592621	15.8922968
C	10.51587028	7.723289617	17.23927954
H	11.27287877	7.984584601	16.5048734
C	13.66924663	6.35358263	12.94671436
H	12.93536695	6.945666137	13.48686356
C	10.2751355	6.367141763	17.49286915
C	8.864978376	8.345195226	18.89399622
H	8.319434454	9.111728162	19.43766558
C	15.08649971	7.2751066	17.17611473
H	14.04777023	7.303845294	17.49503815
C	14.12161904	2.475714717	15.21205427
H	13.41797966	2.651279568	14.40285702
C	11.60998089	1.44937229	19.33300767
H	11.73392379	0.596366508	19.99462111
C	10.46481234	4.473324489	13.88421221
H	11.50546487	4.697734926	13.67143846
C	15.52614593	4.778605974	11.58701616

H	16.24484956	4.156659206	11.05996146
C	14.78619131	5.735675754	10.89217959
H	14.9295718	5.863886069	9.822725968
C	16.7698322	6.330706255	15.72141659
H	17.05907343	5.646235608	14.92955688
C	15.90883954	2.004463977	17.2977947
H	16.60360374	1.824991604	18.11394904
C	11.89493754	3.806922785	18.88084537
H	12.24837257	4.786145081	19.19162651
C	16.04653511	8.118035221	17.73820954
H	15.76117027	8.816887235	18.52005057
C	8.62773392	6.996501932	19.16110602
H	7.901596599	6.709416829	19.91691882
C	9.328874492	6.010952951	18.46419462
H	9.150727618	4.964776254	18.69496882
C	15.34969199	0.929989591	16.60703137
H	15.60766183	-0.089150688	16.88173432
C	15.58164004	3.314503455	16.94350216
H	16.02545774	4.143070143	17.48593283
C	12.05149376	2.714124986	19.73003436
H	12.51882293	2.84771196	20.70194194
C	8.644410917	4.358288467	15.46409423
H	8.255230978	4.475948888	16.47054114
C	13.85712171	6.523122554	11.57535204
H	13.27566038	7.267866483	11.03861604
C	11.0134501	1.286107827	18.08385141

H	10.67152761	0.304243844	17.76740817
C	17.72857487	7.172078274	16.28410404
H	18.75578282	7.133090816	15.93164822
C	7.783043708	3.960859707	14.44200027
H	6.736521777	3.768135526	14.66269942
C	10.85086467	2.382179797	17.23369628
H	10.38183465	2.242874255	16.26522292
C	8.261804605	3.814049468	13.13816731
H	7.589025281	3.504871254	12.34279462
C	9.6035475	4.073606442	12.8608092
H	9.981623561	3.970797883	11.84715963
C	14.45299108	1.168762943	15.56314755
H	14.01141832	0.335748061	15.02284606

$(Ph_3P)_2C$, 138.3°

-2110.63233485471 Hartrees

atom	x	y	z
C	0	0	0.866158125
C	0.71773241	-2.361843019	-0.845705584
C	0.825021713	-1.971164796	-2.190299493
C	1.798150519	-2.527177038	-3.019151406
C	2.686954178	-3.480497374	-2.516164395
C	2.592424666	-3.872943739	-1.180702539
C	1.615366794	-3.31859864	-0.351138827
C	-0.698528815	-2.640694545	1.68629938
C	-1.360637925	-3.867806944	1.541471531

C	-1.516052227	-4.71718454	2.636821484
C	-1.012395421	-4.348723763	3.886011225
C	-0.355536799	-3.126695571	4.0365523
C	-0.201793583	-2.275024755	2.942086647
C	-2.068147387	-1.552296208	-0.634021533
C	-3.025242523	-0.5719731	-0.340139688
C	-4.272526775	-0.590456468	-0.962762263
C	-4.57845881	-1.589151327	-1.888822995
C	-3.63079609	-2.567391202	-2.192212941
C	-2.381703841	-2.549933602	-1.569283211
H	0.136998965	-1.232789955	-2.593093326
H	1.864104608	-2.215335369	-4.058022599
H	3.446518015	-3.913137103	-3.161203214
H	3.27858316	-4.61510131	-0.781324501
H	1.551935989	-3.632386758	0.686169072
H	-1.766593297	-4.160405169	0.577966866
H	-2.034720874	-5.664476986	2.516281417
H	-1.13644199	-5.01067795	4.73898699
H	0.034446568	-2.834032749	5.007850197
H	0.295798739	-1.313625863	3.035054665
H	-2.773064944	0.208749521	0.371424503
H	-5.004004994	0.177872578	-0.728015996
H	-5.549641083	-1.602613746	-2.37617891
H	-3.861019221	-3.343301086	-2.917576286
H	-1.648318438	-3.30919045	-1.823405211
P	-0.456953165	-1.469453093	0.280075041

P	0.456953165	1.469453093	0.280075041
C	-0.71773241	2.361843019	-0.845705584
C	0.698528815	2.640694545	1.68629938
C	2.068147387	1.552296208	-0.634021533
C	-0.825021713	1.971164796	-2.190299493
C	-1.615366794	3.31859864	-0.351138827
C	1.360637925	3.867806944	1.541471531
C	0.201793583	2.275024755	2.942086647
C	3.025242523	0.5719731	-0.340139688
C	2.381703841	2.549933602	-1.569283211
C	-1.798150519	2.527177038	-3.019151406
H	-0.136998965	1.232789955	-2.593093326
C	-2.592424666	3.872943739	-1.180702539
H	-1.551935989	3.632386758	0.686169072
C	1.516052227	4.71718454	2.636821484
H	1.766593297	4.160405169	0.577966866
C	0.355536799	3.126695571	4.0365523
H	-0.295798739	1.313625863	3.035054665
C	4.272526775	0.590456468	-0.962762263
H	2.773064944	-0.208749521	0.371424503
C	3.63079609	2.567391202	-2.192212941
H	1.648318438	3.30919045	-1.823405211
C	-2.686954178	3.480497374	-2.516164395
H	-1.864104608	2.215335369	-4.058022599
H	-3.27858316	4.61510131	-0.781324501
C	1.012395421	4.348723763	3.886011225

H	2.034720874	5.664476986	2.516281417
H	-0.034446568	2.834032749	5.007850197
C	4.57845881	1.589151327	-1.888822995
H	5.004004994	-0.177872578	-0.728015996
H	3.861019221	3.343301086	-2.917576286
H	-3.446518015	3.913137103	-3.161203214
H	1.13644199	5.01067795	4.73898699
H	5.549641083	1.602613746	-2.37617891

$(Ph_3P)_2C$, 137.4°

-2110.63271120294 Hartrees

atom	x	y	z
C	0	0	0.888484846
C	1.892795514	1.507255604	-0.897171555
C	1.688935773	1.16529423	-2.243861723
C	2.76621349	1.052412648	-3.120672155
C	4.067119389	1.2738963	-2.66380802
C	4.282336256	1.610004431	-1.327435669
C	3.203238603	1.726531139	-0.449443931
C	1.02326883	2.543486856	1.678585467
C	1.240848944	3.919643683	1.521854746
C	1.672567709	4.691137574	2.600235149
C	1.889223284	4.096118386	3.844715966
C	1.669459632	2.727893495	4.00777127
C	1.23623645	1.954848557	2.929794047
C	-0.823758013	2.480465956	-0.567152347

C	-2.163450614	2.234763471	-0.239024262
C	-3.184483259	2.98561645	-0.820532144
C	-2.879089863	3.991698836	-1.738590722
C	-1.548389568	4.241876842	-2.07558116
C	-0.525762288	3.490801446	-1.494243161
H	0.680052787	0.995408799	-2.609477129
H	2.591193112	0.791336951	-4.160864515
H	4.907321112	1.18406137	-3.346742574
H	5.29200055	1.785597983	-0.965838487
H	3.38205839	1.988751295	0.588766295
H	1.066689544	4.395402688	0.56165928
H	1.836345705	5.757393597	2.470047574
H	2.224623368	4.698968074	4.684347365
H	1.833232947	2.26136015	4.975542729
H	1.04994676	0.889058373	3.031353002
H	-2.391980853	1.440787305	0.466003559
H	-4.21938687	2.781832458	-0.559899518
H	-3.674765791	4.574995067	-2.19395521
H	-1.304558321	5.018544733	-2.795608286
H	0.504444517	3.685345172	-1.77649422
P	0.468286552	1.462176682	0.289526908
P	-0.468286552	-1.462176682	0.289526908
C	-1.892795514	-1.507255604	-0.897171555
C	-1.02326883	-2.543486856	1.678585467
C	0.823758013	-2.480465956	-0.567152347
C	-1.688935773	-1.16529423	-2.243861723

C	-3.203238603	-1.726531139	-0.449443931
C	-1.240848944	-3.919643683	1.521854746
C	-1.23623645	-1.954848557	2.929794047
C	2.163450614	-2.234763471	-0.239024262
C	0.525762288	-3.490801446	-1.494243161
C	-2.76621349	-1.052412648	-3.120672155
H	-0.680052787	-0.995408799	-2.609477129
C	-4.282336256	-1.610004431	-1.327435669
H	-3.38205839	-1.988751295	0.588766295
C	-1.672567709	-4.691137574	2.600235149
H	-1.066689544	-4.395402688	0.56165928
C	-1.669459632	-2.727893495	4.00777127
H	-1.04994676	-0.889058373	3.031353002
C	3.184483259	-2.98561645	-0.820532144
H	2.391980853	-1.440787305	0.466003559
C	1.548389568	-4.241876842	-2.07558116
H	-0.504444517	-3.685345172	-1.77649422
C	-4.067119389	-1.2738963	-2.66380802
H	-2.591193112	-0.791336951	-4.160864515
H	-5.29200055	-1.785597983	-0.965838487
C	-1.889223284	-4.096118386	3.844715966
H	-1.836345705	-5.757393597	2.470047574
H	-1.833232947	-2.26136015	4.975542729
C	2.879089863	-3.991698836	-1.738590722
H	4.21938687	-2.781832458	-0.559899518
H	1.304558321	-5.018544733	-2.795608286

H	-4.907321112	-1.18406137	-3.346742574
H	-2.224623368	-4.698968074	4.684347365
H	3.674765791	-4.574995067	-2.19395521

$(Ph_3P)_2C$, 135°

-2110.63256444789 Hartrees

atom	x	y	z
P	11.23535085	5.160885744	16.52324188
P	14.07420308	5.272602993	15.4167739
C	10.02864009	4.450986693	15.30079474
C	17.44610825	7.692233619	17.52274143
H	18.2210351	8.264392434	18.02586653
C	15.44990894	6.21362259	16.22469573
C	14.41695173	5.524940734	13.61383476
C	9.760044674	8.807763046	17.69330855
H	9.976264182	9.846187439	17.45694068
C	11.40628849	3.818876908	17.78221201
C	15.38743197	4.807712782	12.89896889
H	15.9553335	4.021057194	13.38647131
C	12.59434991	5.838710564	15.87925374
C	14.53007301	3.500875048	15.6954845
C	10.50726239	7.791715432	17.09737946
H	11.31607233	8.013895852	16.40646918
C	13.67946827	6.515422911	12.95191799
H	12.91968113	7.054270186	13.51200068
C	10.23987726	6.449599519	17.39181917

C	8.741149038	8.493085235	18.59375206
H	8.161136794	9.284471634	19.06075968
C	15.11400106	7.125123886	17.22996666
H	14.06337807	7.244345831	17.48192122
C	14.02116965	2.511248554	14.83836474
H	13.42925042	2.797429148	13.973526
C	11.93773536	1.810470254	19.67506744
H	12.14022731	1.033983489	20.40771991
C	10.34062442	4.557872314	13.94141749
H	11.27437894	5.034845322	13.65777344
C	15.61414297	5.078498484	11.54864835
H	16.36263939	4.510014599	11.00311559
C	14.87800591	6.070356577	10.89923326
H	15.05530932	6.279246561	9.847736598
C	16.79659971	6.05492864	15.86614824
H	17.0763845	5.360171922	15.08014318
C	15.5228358	1.7550859	17.06145682
H	16.10485266	1.464656581	17.93187009
C	11.80691084	4.151906611	19.08659182
H	11.91346259	5.195914146	19.36688556
C	16.10787605	7.860667955	17.87791059
H	15.83597442	8.566257389	18.65854581
C	8.474173615	7.157654846	18.89965303
H	7.6898631	6.906523843	19.60870008
C	9.218025943	6.140599412	18.30110178
H	9.013403019	5.107460725	18.56520552

C	15.02742877	0.781144066	16.19501846
H	15.2249349	-0.270263467	16.38545637
C	15.27705949	3.106545162	16.81387461
H	15.6717005	3.856350941	17.49207419
C	12.06497247	3.156208709	20.02671066
H	12.36482137	3.430127111	21.03467931
C	8.816393362	3.848958261	15.67270707
H	8.552095759	3.751215433	16.72107231
C	13.90991163	6.788200815	11.60361256
H	13.331399	7.559303958	11.10196199
C	11.55410191	1.46799798	18.37896216
H	11.46038041	0.423118373	18.09609611
C	17.78907748	6.788690579	16.5140384
H	18.83002529	6.657473056	16.23086158
C	7.943476895	3.356964202	14.70345752
H	7.010657546	2.887976992	15.00525963
C	11.28925406	2.464692564	17.43840356
H	10.99103081	2.184428044	16.43363417
C	8.267379132	3.464016186	13.34884993
H	7.586012309	3.079534097	12.59471221
C	9.466651506	4.06607683	12.96988292
H	9.724033312	4.154982394	11.91781314
C	14.27298531	1.162396832	15.08318233
H	13.88203433	0.408582026	14.40497941

$(Ph_3P)_2C$, 130°

-2110.63197021479 Hartrees			
atom	**x**	**y**	**z**
P	11.26819187	5.18736577	16.54773092
P	14.05855667	5.301359145	15.43659749
C	10.1144487	4.417989917	15.30662211
C	17.57288043	7.561532152	17.48388966
H	18.38209155	8.098875895	17.97122126
C	15.48825255	6.173634552	16.22609906
C	14.37766736	5.575575784	13.63122437
C	9.612479992	8.778893341	17.64418094
H	9.791272867	9.823396901	17.40342471
C	11.46105612	3.869231781	17.83138308
C	15.30570689	4.837798081	12.88201202
H	15.85275712	4.019707874	13.34066465
C	12.61273068	5.941304107	15.93934061
C	14.45351485	3.509471114	15.673413
C	10.4172939	7.790257105	17.07810913
H	11.23528108	8.040038132	16.407931
C	13.6669998	6.608038443	13.00505758
H	12.9394218	7.162982679	13.59154369
C	10.19845648	6.440676148	17.37850927
C	8.584114924	8.42963297	18.52065366
H	7.959085913	9.199951179	18.96421997
C	15.21095824	7.114342096	17.22212678
H	14.17042626	7.290290167	17.48287968
C	13.90653282	2.554101978	14.80100203

H	13.31280497	2.875189151	13.95000936
C	11.99712377	1.923001529	19.78545872
H	12.20077477	1.170102298	20.54198956
C	10.43813927	4.542315189	13.95104498
H	11.35175771	5.062081333	13.67807832
C	15.51630806	5.128592341	11.53330573
H	16.23136614	4.543583644	10.96100694
C	14.8068387	6.161845363	10.91949708
H	14.97144703	6.386101566	9.869064468
C	16.82089946	5.938083314	15.85738816
H	17.05561574	5.217812143	15.0796592
C	15.41174785	1.706236669	16.98849907
H	15.99502538	1.380081154	17.84524381
C	11.85005612	4.244598439	19.12796067
H	11.94587084	5.297576673	19.37696269
C	16.24915495	7.805630446	17.84926533
H	16.02301302	8.535575585	18.62208082
C	8.365770766	7.0869647	18.83318558
H	7.57460045	6.809287881	19.52449153
C	9.167425503	6.096981678	18.26457074
H	9.000225592	5.058606619	18.5345171
C	14.8795066	0.766239453	16.10628735
H	15.05028727	-0.294277485	16.27030142
C	15.20100928	3.069125456	16.77434047
H	15.62351816	3.791907911	17.46473819
C	12.11076512	3.279614357	20.09849908

H	12.40124063	3.585734791	21.09989572
C	8.922133333	3.766329956	15.65999035
H	8.647290176	3.655450583	16.70427826
C	13.88159694	6.901069112	11.65833694
H	13.32386553	7.704676547	11.18491971
C	11.62517138	1.539294558	18.49779258
H	11.54288666	0.48581176	18.24497728
C	17.85736992	6.626423192	16.48555751
H	18.8870648	6.435460978	16.19530599
C	8.082190524	3.243431045	14.67795312
H	7.164511288	2.737608226	14.96635285
C	11.35779845	2.505281108	17.52611352
H	11.07033484	2.192722561	16.52798729
C	8.418731794	3.367906423	13.32799155
H	7.762492407	2.960112407	12.56393362
C	9.597418854	4.018943628	12.96651757
H	9.863906419	4.123753362	11.91821564
C	14.1225525	1.19335629	15.01311986
H	13.70231164	0.466440644	14.32320475

$(Ph_3P)_2C$, 125°

-2110.63075900822 Hartrees

atom	x	y	z
P	11.30485782	5.209942462	16.56889336
P	14.03425536	5.314389634	15.43136654
C	10.19987389	4.348141674	15.34360283

C	17.65094222	7.364919817	17.52270319
H	18.48337612	7.855212001	18.02035497
C	15.50600738	6.09808877	16.23842027
C	14.35668266	5.637054871	13.63450567
C	9.540048852	8.77840831	17.57124551
H	9.723642948	9.826406442	17.34991684
C	11.52503161	3.958877558	17.91459245
C	15.25332788	4.891036422	12.85568329
H	15.76908471	4.036269535	13.28267795
C	12.62189096	6.029853493	15.96153807
C	14.3567634	3.500571964	15.59755151
C	10.39212939	7.802184142	17.05399091
H	11.2489875	8.064097033	16.43925549
C	13.68545936	6.718316761	13.04848721
H	12.98165876	7.279465942	13.65758305
C	10.16890378	6.448353119	17.33025518
C	8.45841467	8.412366057	18.37307772
H	7.796181794	9.172826957	18.77800403
C	15.27173056	7.022476974	17.26084325
H	14.240253	7.234569798	17.53028647
C	13.7590766	2.601672799	14.69834344
H	13.16243435	2.977553398	13.87253796
C	12.0813756	2.137952618	19.98118756
H	12.29187526	1.433447795	20.7812104
C	10.44561518	4.571820476	13.98392586
H	11.28309202	5.202853577	13.7009591

C	15.47246013	5.221832751	11.51760808
H	16.16302721	4.630445773	10.92221013
C	14.80266443	6.303617424	10.94408314
H	14.97382006	6.559294342	9.901904385
C	16.82656268	5.818377786	15.85677028
H	17.02855118	5.110612154	15.05863031
C	15.27304445	1.612633024	16.82007811
H	15.86032308	1.231727775	17.6510645
C	11.81102235	4.413825737	19.21245274
H	11.81585557	5.480002827	19.41963975
C	16.34002047	7.652964882	17.90120684
H	16.14706508	8.370132914	18.69464798
C	8.23286014	7.064826379	18.6594602
H	7.397844122	6.77344122	19.29091891
C	9.081919014	6.087899276	18.13986962
H	8.903173036	5.045559695	18.3858972
C	14.68874913	0.728619749	15.91324836
H	14.82345705	-0.343102537	16.03171048
C	15.10830437	2.989665314	16.66468354
H	15.56932998	3.66819713	17.37494985
C	12.08272487	3.510934747	20.23803185
H	12.29293797	3.878402122	21.23883287
C	9.105876998	3.547823528	15.70901649
H	8.894923259	3.353394462	16.75584601
C	13.90839195	7.050912651	11.71237585
H	13.38154963	7.892282747	11.27027711

C	11.81349144	1.676167087	18.69326459
H	11.82082661	0.610255463	18.48300731
C	17.89282267	6.446504832	16.49803935
H	18.91259116	6.221627937	16.19733665
C	8.28666611	2.978139252	14.73507994
H	7.446728529	2.356152135	15.0331418
C	11.53803825	2.579686546	17.66547142
H	11.33807052	2.205363593	16.66743692
C	8.545258655	3.203527914	13.38128892
H	7.906046364	2.758699351	12.62342457
C	9.625709206	4.002293556	13.00792117
H	9.831217604	4.185854434	11.95669404
C	13.92749577	1.226439297	14.85324729
H	13.46759625	0.5437632	14.14379811

$(Ph_3P)_2C$, 120°

-2110.62847848726 Hartrees

atom	x	y	z
P	11.32508884	5.230941926	16.55027171
P	14.00734272	5.33942494	15.43482411
C	10.22929904	4.353049759	15.32381361
C	17.66616658	7.311949905	17.5310377
H	18.5082744	7.783814606	18.03032361
C	15.49643522	6.090812159	16.24339963
C	14.35338668	5.641814716	13.63823646
C	9.449817221	8.732807341	17.58818178

H	9.593523762	9.78710357	17.36706118
C	11.58313736	3.983168323	17.89443017
C	15.24052749	4.871844681	12.87184933
H	15.73270412	4.007906566	13.30794978
C	12.6105557	6.121316304	15.94792526
C	14.29245376	3.521926285	15.61045841
C	10.32643165	7.788014594	17.05407602
H	11.16394292	8.081985553	16.42748212
C	13.71322774	6.735639719	13.04054904
H	13.01610834	7.315530321	13.63975701
C	10.15552806	6.426574838	17.33042468
C	8.394874057	8.327664908	18.40675091
H	7.713585977	9.063707278	18.82511947
C	15.28031563	7.038076488	17.24877727
H	14.25301108	7.285758161	17.50342628
C	13.69246963	2.630364177	14.70527295
H	13.10679379	3.013257072	13.87512616
C	12.15823452	2.191476204	19.98171592
H	12.37605988	1.498306742	20.78973646
C	10.46944438	4.587139114	13.9649061
H	11.29706588	5.231806317	13.68343681
C	15.48027177	5.190580107	11.53455265
H	16.16286827	4.580384455	10.94903719
C	14.84127163	6.284616402	10.94918213
H	15.02839869	6.530903969	9.907505969
C	16.81185098	5.765947737	15.87976544

H	17.00033613	5.040123526	15.09460965
C	15.18078811	1.621549498	16.83535056
H	15.75812026	1.23329784	17.66990701
C	11.93388914	4.457082584	19.16981527
H	11.98142166	5.527018076	19.35083025
C	16.36084083	7.645816578	17.89081886
H	16.18189338	8.380949356	18.67104371
C	8.221327612	6.972335571	18.69274786
H	7.407877738	6.650449837	19.33752766
C	9.095284362	6.026934504	18.15660013
H	8.958327025	4.978766252	18.40472006
C	14.59369595	0.745009074	15.9229404
H	14.71652096	-0.328284707	16.04032139
C	15.03141983	3.000389284	16.6816452
H	15.49481586	3.671984992	17.39672323
C	12.21579522	3.56926557	20.20532449
H	12.47677551	3.951852708	21.18836286
C	9.143349205	3.540694047	15.68694108
H	8.93229697	3.342774525	16.73292927
C	13.95716348	7.056229229	11.7049737
H	13.4543743	7.907326704	11.25358042
C	11.82548821	1.710529609	18.71644007
H	11.7894784	0.640417996	18.53155654
C	17.89025622	6.370983539	16.52279801
H	18.90569411	6.110553812	16.23631911
C	8.329980733	2.965750139	14.71130919

H	7.496548737	2.334302026	15.00777159
C	11.54119154	2.599657362	17.67786451
H	11.29345665	2.209471608	16.69702128
C	8.585121319	3.198905025	13.35824616
H	7.950317115	2.74972941	12.59928698
C	9.655137687	4.012287344	12.98716044
H	9.856608619	4.203724119	11.93660727
C	13.84522717	1.253016388	14.85883974
H	13.3834169	0.576818268	14.14446231

$(Ph_3P)_2C$, 115°

-2110.62500221754 Hartrees

atom	x	y	z
P	11.35177575	5.255161349	16.54467663
P	13.98525019	5.358121815	15.4578295
C	10.28149991	4.376547121	15.29412609
C	17.71975001	7.275105124	17.47515551
H	18.57937131	7.736652888	17.95381807
C	15.50423959	6.081929804	16.23908613
C	14.32933867	5.635256471	13.654552
C	9.330390536	8.672324254	17.59851836
H	9.423695481	9.731646399	17.37431314
C	11.62458583	4.001827178	17.88215106
C	15.18741149	4.835700661	12.88525881
H	15.65426601	3.95753959	13.3206713
C	12.61890742	6.213095392	15.97895631

C	14.23750661	3.534293827	15.6472822
C	10.24389687	7.767424936	17.05682702
H	11.06090664	8.100166533	16.42280993
C	13.72377575	6.74918322	13.0571876
H	13.0492473	7.353459015	13.65822174
C	10.13847777	6.400124314	17.33701782
C	8.303195358	8.221402109	18.42850857
H	7.593023303	8.926526906	18.85212758
C	15.32441142	7.053851751	17.22815734
H	14.30691973	7.332493117	17.49015765
C	13.62999569	2.64323485	14.74701959
H	13.04375849	3.025463019	13.91723697
C	12.18349371	2.228320263	19.98897926
H	12.39548147	1.542131613	20.80445148
C	10.53081206	4.636300302	13.94132551
H	11.35247511	5.295131093	13.67670763
C	15.43203863	5.144611326	11.54642229
H	16.09232639	4.511782637	10.95936281
C	14.8273514	6.258328412	10.96181208
H	15.01857874	6.497085728	9.919144156
C	16.80689453	5.717537805	15.86656973
H	16.96775539	4.972188096	15.09364468
C	15.12425282	1.634840678	16.87380413
H	15.70400878	1.246724546	17.70665876
C	12.02377157	4.485426885	19.13965443
H	12.1160748	5.556147531	19.29751476

C	16.42766021	7.647763083	17.84421657
H	16.27641492	8.402882559	18.6110974
C	8.195622677	6.86037732	18.71956397
H	7.404996406	6.502987745	19.37396444
C	9.107063304	5.95511875	18.17637284
H	9.022488133	4.902591267	18.42963835
C	14.53007791	0.758245765	15.96602838
H	14.65008808	-0.315098545	16.08541199
C	14.97925636	3.013464729	16.71700816
H	15.44811764	3.685704446	17.4278203
C	12.29827598	3.606927038	20.18475188
H	12.59786319	3.997385078	21.15357872
C	9.196522933	3.551683709	15.63232628
H	8.970954528	3.340885506	16.67258105
C	13.97258793	7.059805574	11.7201468
H	13.49666371	7.926842984	11.26994332
C	11.80189693	1.737681123	18.74164538
H	11.72212678	0.666490465	18.57792119
C	17.90781483	6.308730352	16.48376881
H	18.91286248	6.018087052	16.18980438
C	8.398280174	2.985608325	14.63910182
H	7.56579288	2.344597996	14.91710179
C	11.52565209	2.617731656	17.69293922
H	11.24258125	2.218611366	16.72559894
C	8.66538399	3.241758629	13.29253532
H	8.041929777	2.800032857	12.51994908

C	9.73122336	4.07100873	12.94600291
H	9.940826171	4.283256898	11.90108619
C	13.77877079	1.265688316	14.90411691
H	13.31175395	0.589236995	14.19344173

$(H_3P)_2C$, 180°

-724.262642064226 Hartrees

atom	x	y	z
P	0	0	1.603921881
C	0	0	0
P	0	0	-1.603921881
H	1.077111841	-0.621870811	2.308687331
H	0	1.243741622	2.308687331
H	-1.077111841	-0.621870811	2.308687331
H	-1.077111841	0.621870811	-2.308687331
H	0	-1.243741622	-2.308687331
H	1.077111841	0.621870811	-2.308687331

$(H_3P)_2C$, 170°

-724.263224371149 Hartrees

atom	x	y	z
P	11.1952677	5.047557414	16.57950283
P	14.07808848	4.844370743	15.20854024
C	12.58398682	4.998251499	15.77541164
H	10.04636504	5.560965048	15.90837268

H	11.08906347	5.821326053	17.77843399
H	14.33786094	5.266546514	13.87127638
H	14.68414655	3.550572571	15.13121703
H	10.61313588	3.838711267	17.07656842
H	15.16056858	5.527758407	15.84785197

$(H_3P)_2C$, 165°

-724.263306131717 Hartrees

atom	x	y	z
P	11.20368217	5.044022293	16.58457494
P	14.07631454	4.841506131	15.21839661
C	12.56070315	5.02058248	15.72312695
H	10.03168835	5.54898844	15.95139715
H	11.12596882	5.809808978	17.79160254
H	14.37942042	5.253018968	13.88859385
H	14.67193514	3.540878006	15.16703356
H	10.64864428	3.826152674	17.09232484
H	15.14663282	5.517826378	15.88651268

$(H_3P)_2C$, 160°

-724.263425027763 Hartrees

atom	x	y	z
P	11.21397006	5.040572295	16.58868465
P	14.07260539	4.838888023	15.22906739
C	12.53754531	5.041953748	15.67105453

H	10.01970467	5.534637531	15.99327134
H	11.16469814	5.800557638	17.80178835
H	14.41917336	5.242076835	13.90916861
H	14.65613788	3.53144369	15.20097979
H	10.68790395	3.814574367	17.10965047
H	15.13022181	5.505412117	15.92837045

$(H_3P)_2C$, 155°

-724.263575932469 Hartrees

atom	x	y	z
P	11.22627464	5.037036948	16.59184236
P	14.06693385	4.836420304	15.24072659
C	12.51414059	5.063076483	15.61877274
H	10.01153656	5.521687678	16.03550163
H	11.2069455	5.789460797	17.81133654
H	14.45622878	5.229543082	13.93157104
H	14.63918088	3.522945938	15.2377947
H	10.72863703	3.803131242	17.12392357
H	15.11013219	5.494922533	15.97023961

$(H_3P)_2C$, 155°

-724.263575932469 Hartrees

atom	x	y	z
P	11.22627464	5.037036948	16.59184236
P	14.06693385	4.836420304	15.24072659

C	12.51414059	5.063076483	15.61877274
H	10.01153656	5.521687678	16.03550163
H	11.2069455	5.789460797	17.81133654
H	14.45622878	5.229543082	13.93157104
H	14.63918088	3.522945938	15.2377947
H	10.72863703	3.803131242	17.12392357
H	15.11013219	5.494922533	15.97023961

$(H_3P)_2C$, 150°

-724.263736208532 Hartrees

atom	**x**	**y**	**z**
P	11.24064446	5.033433325	16.59399692
P	14.05918344	4.833935486	15.2533127
C	12.49077969	5.084531709	15.56677328
H	10.00717858	5.50964179	16.07747503
H	11.25204536	5.776757082	17.8199315
H	14.49023623	5.215634758	13.95575279
H	14.61960136	3.514744656	15.27626645
H	10.77118479	3.791543851	17.1349468
H	15.08713283	5.485023151	16.01211419

$(H_3P)_2C$, 145°

-724.263890408469 Hartrees

atom	**x**	**y**	**z**
P	11.25700453	5.029322782	16.5951465

P	14.04939075	4.831906332	15.2669679
C	12.46769532	5.105964727	15.51471011
H	10.00642292	5.498965517	16.11972588
H	11.30004907	5.762286808	17.82746206
H	14.52122517	5.199384192	13.9813338
H	14.5979129	3.507900546	15.31831229
H	10.81444532	3.779323484	17.14186527
H	15.06034827	5.478978445	16.05269526

$(H_3P)_2C$, 140°

-724.264004012102 Hartrees

atom	**x**	**y**	**z**
P	11.27547397	5.025231549	16.59518543
P	14.03745557	4.829773041	15.28153311
C	12.44457779	5.127892324	15.46312718
H	10.00859936	5.486750988	16.16153206
H	11.35087252	5.747743886	17.83277027
H	14.55038951	5.183337485	14.00949057
H	14.57249026	3.500818619	15.36039934
H	10.86162012	3.76716961	17.14752329
H	15.03086891	5.47123023	16.09503547

$(H_3P)_2C$, 135.5°

-724.264055720207 Hartrees

atom	**x**	**y**	**z**

P	11.2215397	5.123039862	16.43940389
P	14.0851493	5.283530419	15.46280707
C	12.72192131	5.747197518	16.24156174
H	10.33408147	4.897106487	15.33388299
H	15.15227885	6.203214666	15.59667628
H	14.13216479	5.11100724	14.03842674
H	10.99433595	3.872286606	17.1063735
H	14.79475147	4.084633364	15.80908923
H	10.3715638	5.93594788	17.2262815

$(H_3P)_2C$, 135°

-724.264053483410 Hartrees

atom	**x**	**y**	**z**
P	11.29609991	5.020997472	16.59425347
P	14.02329188	4.827617892	15.29697981
C	12.42174351	5.150303385	15.41184659
H	10.01378462	5.473974211	16.20351657
H	11.40431634	5.73336441	17.83592684
H	14.57780894	5.167151669	14.0401728
H	14.54288257	3.49378722	15.40266264
H	10.91139011	3.754903986	17.15077474
H	14.99793595	5.46338649	16.13820094

$(H_3P)_2C$, 130°

-724.263956608318 Hartrees

atom	x	y	z
P	11.31884122	5.015982408	16.59206959
P	14.00687659	4.825955027	15.31349664
C	12.39937355	5.173786014	15.36107848
H	10.02222381	5.461361632	16.24651559
H	11.46063516	5.715684256	17.8382591
H	14.60260129	5.146000176	14.07188191
H	14.50986708	3.488102059	15.45097396
H	10.96317507	3.740819874	17.14857057
H	14.96155194	5.460230954	16.17904202

$(H_3P)_2C$, 125°

-724.263611402684 Hartrees

atom	x	y	z
P	11.34392229	5.011309224	16.58878584
P	13.98808206	4.824272617	15.33097281
C	12.37689679	5.196334055	15.31037162
H	10.03302449	5.445507119	16.28999749
H	11.52072165	5.701640368	17.83625246
H	14.62749859	5.128068422	14.10819164
H	14.47198941	3.482006699	15.49623314
H	11.02058709	3.728099499	17.14768436
H	14.92065427	5.453729427	16.22446278

$(H_3P)_2C$, 120°

-724.262924836102 Hartrees

atom	x	y	z
P	11.37140514	5.006463614	16.58420943
P	13.96671544	4.822603882	15.3493812
C	12.35477765	5.219702546	15.26031011
H	10.04691341	5.428446178	16.33545981
H	11.5850548	5.686548641	17.83208984
H	14.65166529	5.108111503	14.14785539
H	14.42846746	3.475936205	15.5437417
H	11.0824871	3.714697994	17.1434227
H	14.87528477	5.44727352	16.27122423

$(H_3P)_2C$, 115°

-724.261791459668 Hartrees

atom	x	y	z
P	11.40134026	5.00151653	16.57834546
P	13.94278339	4.821331442	15.36883466
C	12.33277623	5.242347802	15.21043875
H	10.06412779	5.409613305	16.38302856
H	11.65437927	5.671896395	17.82471816
H	14.6753449	5.087189815	14.19171755
H	14.38008212	3.470650268	15.59329286
H	11.14916508	3.701306279	17.13709282
H	14.82424688	5.441871118	16.32010374

$[(Ph_3P)_2N]^+$, 180°			
-2127.20196189954 Hartrees			
atom	**x**	**y**	**z**
P	0	0	1.572248467
C	1.199824256	-1.195684023	2.23209552
N	0	0	0
C	2.431524321	-1.346431008	1.574260912
H	2.645226866	-0.770698069	0.678382534
C	3.107141206	-2.983653663	3.219995974
H	3.847304936	-3.679846862	3.602897406
C	0.928556836	-1.947061501	3.384516158
H	-0.024664185	-1.846104633	3.893743777
C	3.379700251	-2.239262877	2.069450354
H	4.330426477	-2.3552431	1.557942027
C	1.884324922	-2.83723942	3.875436442
H	1.669555008	-3.420161586	4.765814067
C	0.43558061	1.636920297	2.23209552
C	-0.049718703	2.778977336	1.574260912
H	-0.655169327	2.676182699	0.678382534
C	1.030349265	4.182690049	3.219995974
H	1.263188396	5.171787241	3.602897406
C	1.221926304	1.77768456	3.384516158
H	1.611105602	0.901692506	3.893743777
C	0.249408412	4.046537713	2.069450354
H	-0.125512882	4.927880889	1.557942027
C	1.514958953	3.050492961	3.875436442

H	2.127169315	3.155957843	4.765814067
C	-1.635404866	-0.441236275	2.23209552
C	-2.381805618	-1.432546327	1.574260912
H	-1.990057539	-1.90548463	0.678382534
C	-4.137490471	-1.199036386	3.219995974
H	-5.110493332	-1.49194038	3.602897406
C	-2.150483141	0.169376941	3.384516158
H	-1.586441418	0.944412127	3.893743777
C	-3.629108663	-1.807274836	2.069450354
H	-4.204913595	-2.572637789	1.557942027
C	-3.399283875	-0.213253541	3.875436442
H	-3.796724322	0.264203743	4.765814067
P	0	0	-1.572248467
C	-1.199824256	1.195684023	-2.23209552
C	-2.431524321	1.346431008	-1.574260912
H	-2.645226866	0.770698069	-0.678382534
C	-3.107141206	2.983653663	-3.219995974
H	-3.847304936	3.679846862	-3.602897406
C	-0.928556836	1.947061501	-3.384516158
H	0.024664185	1.846104633	-3.893743777
C	-3.379700251	2.239262877	-2.069450354
H	-4.330426477	2.3552431	-1.557942027
C	-1.884324922	2.83723942	-3.875436442
H	-1.669555008	3.420161586	-4.765814067
C	-0.43558061	-1.636920297	-2.23209552
C	0.049718703	-2.778977336	-1.574260912

H	0.655169327	-2.676182699	-0.678382534
C	-1.030349265	-4.182690049	-3.219995974
H	-1.263188396	-5.171787241	-3.602897406
C	-1.221926304	-1.77768456	-3.384516158
H	-1.611105602	-0.901692506	-3.893743777
C	-0.249408412	-4.046537713	-2.069450354
H	0.125512882	-4.927880889	-1.557942027
C	-1.514958953	-3.050492961	-3.875436442
H	-2.127169315	-3.155957843	-4.765814067
C	1.635404866	0.441236275	-2.23209552
C	2.381805618	1.432546327	-1.574260912
H	1.990057539	1.90548463	-0.678382534
C	4.137490471	1.199036386	-3.219995974
H	5.110493332	1.49194038	-3.602897406
C	2.150483141	-0.169376941	-3.384516158
H	1.586441418	-0.944412127	-3.893743777
C	3.629108663	1.807274836	-2.069450354
H	4.204913595	2.572637789	-1.557942027
C	3.399283875	0.213253541	-3.875436442
H	3.796724322	-0.264203743	-4.765814067

$[(Ph_3P)_2N]^+$, 165°

-2127.20227543401 Hartrees

atom	x	y	z
P	11.26302029	5.010455346	16.65358164
P	14.12478993	5.022337542	15.38645902

C	10.1758978	4.015183017	15.58699543
C	17.31014997	7.007751374	18.06390552
H	18.05909155	7.465488719	18.70312299
C	15.38231238	5.833910739	16.41820142
C	14.1908133	5.76165215	13.72625383
C	10.67219974	8.990227506	17.35762616
H	11.29332607	9.856439015	17.5641733
C	11.34205557	4.177819609	18.27075567
C	15.0113381	5.226975334	12.72201075
H	15.59942079	4.334174242	12.91064661
N	12.69449886	5.222386327	16.02358469
C	14.59561044	3.271551592	15.20465922
C	11.2655357	7.74635655	17.15034272
H	12.34534223	7.641112498	17.19072011
C	13.42074746	6.905797031	13.46473979
H	12.77836901	7.314850947	14.23888176
C	10.4647031	6.626115332	16.88190467
C	9.283194661	9.122008007	17.2981201
H	8.823558675	10.09265329	17.45824461
C	15.21057568	5.837424787	17.81130569
H	14.32610924	5.38659204	18.25094239
C	13.69031049	2.396435558	14.57890645
H	12.73205496	2.761892277	14.22098255
C	11.49154517	2.827324794	20.7136688
H	11.54938498	2.302703346	21.66265291
C	10.17626264	4.272953672	14.20539869

H	10.83049263	5.035983132	13.7929416
C	15.06315794	5.837875476	11.46885524
H	15.6958722	5.420048487	10.69185653
C	14.29730558	6.975769305	11.21267719
H	14.33702382	7.446462594	10.23495243
C	16.52122325	6.426025711	15.85333481
H	16.65660493	6.440286919	14.77641484
C	16.15193542	1.438288937	15.49331201
H	17.10751825	1.065856687	15.8495302
C	10.62273167	4.647264761	19.37866698
H	10.00718937	5.537037053	19.29579727
C	16.17475558	6.423023114	18.62916107
H	16.0393566	6.424765578	19.70644257
C	8.483999365	8.009970033	17.02818681
H	7.404695149	8.1140828	16.97428256
C	9.069832424	6.761911174	16.81768431
H	8.443255923	5.903387197	16.59614987
C	15.2514019	0.57406479	14.87148298
H	15.50650467	-0.473396945	14.74135381
C	15.82855737	2.78583286	15.66220262
H	16.53320657	3.452104254	16.14878024
C	10.69995332	3.969586403	20.59629199
H	10.14314153	4.337371454	21.45265662
C	9.33114256	3.025697332	16.10939876
H	9.327808867	2.813550597	17.1736151
C	13.4760463	7.507982636	12.20935466

H	12.87807609	8.391601444	12.00798684
C	12.21182939	2.357044454	19.61251618
H	12.82817242	1.467798624	19.70366722
C	17.48187963	7.009925688	16.67895998
H	18.36054717	7.471501652	16.23913513
C	8.494566844	2.303090623	15.25705943
H	7.843774623	1.535962912	15.66543316
C	12.14019467	3.027345943	18.39377078
H	12.70164222	2.655613234	17.5412819
C	8.49843244	2.561810924	13.88669089
H	7.847480795	1.996858773	13.22623678
C	9.339943764	3.546214047	13.36130275
H	9.342664804	3.747828666	12.29439126
C	14.02040752	1.053465607	14.41532528
H	13.31922736	0.380929545	13.93061055

$[(Ph_3P)_2N]^+$, 160°

-2127.20234997207 Hartrees

atom	**x**	**y**	**z**
P	11.27027222	5.031731927	16.65308269
P	14.11878139	5.048201373	15.38817629
C	10.2110381	4.019035726	15.5723727
C	17.37021251	6.991595534	18.0178339
H	18.13437931	7.44102754	18.64472737
C	15.40285499	5.839579687	16.40344595
C	14.19857181	5.768630046	13.7206934

C	10.56343586	8.988208811	17.38393149
H	11.15973555	9.873626285	17.58203142
C	11.37128609	4.183422477	18.26177192
C	15.01893249	5.217404538	12.7252391
H	15.59474585	4.318501783	12.92307379
N	12.69553871	5.314683664	16.02666291
C	14.543956	3.283339043	15.22097523
C	11.19344038	7.765752674	17.15772887
H	12.27659134	7.695695717	17.1736148
C	13.44490335	6.92066974	13.44703513
H	12.80394537	7.342103207	14.21554895
C	10.4249001	6.620615991	16.90016814
C	9.170105703	9.073926104	17.35399812
H	8.681948574	10.02781539	17.52932774
C	15.21473815	5.921499423	17.79163443
H	14.30178427	5.540567989	18.23867745
C	13.6634513	2.444464741	14.51460847
H	12.75472287	2.846437767	14.07584204
C	11.56783203	2.826811757	20.69875377
H	11.64385701	2.299784557	21.64506857
C	10.18693308	4.313329711	14.19835468
H	10.81011443	5.109080255	13.79989302
C	15.08643258	5.819656695	11.46866333
H	15.71909562	5.389239379	10.69853728
C	14.33653933	6.9653471	11.20031501
H	14.38891279	7.429392034	10.22006748

C	16.57869838	6.342914301	15.82709713
H	16.72773715	6.29830034	14.75281964
C	15.99884941	1.390476426	15.63207025
H	16.90639511	0.981409106	16.06531933
C	10.68113001	4.655068491	19.38744605
H	10.06954779	5.548752921	19.3208213
C	16.19901232	6.495873622	18.59398477
H	16.05078141	6.55867884	19.66769855
C	8.40298166	7.937184307	17.09420033
H	7.319996068	8.005611998	17.06322774
C	9.025177614	6.710342553	16.86495083
H	8.422612049	5.832572328	16.65235264
C	15.12249495	0.562552248	14.93155611
H	15.34776282	-0.49361442	14.81794398
C	15.71392636	2.749086368	15.77938434
H	16.400179	3.386890674	16.32643879
C	10.78192313	3.974540888	20.60167534
H	10.24731692	4.344359555	21.47115518
C	9.404966072	2.989755167	16.07820496
H	9.419729542	2.751510623	17.13682631
C	13.51571419	7.514049176	12.18817546
H	12.93045751	8.403944494	11.97753634
C	12.25901848	2.353833533	19.58034036
H	12.87080891	1.459999252	19.65547052
C	17.55877949	6.915628728	16.63699467
H	18.46586552	7.30829571	16.18805139

C	8.582251138	2.262649068	15.21614996
H	7.960481557	1.465208186	15.61138109
C	12.164259	3.027102319	18.36485079
H	12.70412542	2.652324853	17.49992371
C	8.561751909	2.557239504	13.85329779
H	7.920746078	1.989607619	13.18550925
C	9.364607262	3.582039395	13.34461153
H	9.346991925	3.812034726	12.28364537
C	13.95452334	1.089925773	14.37375183
H	13.27274215	0.446005488	13.82659454

$[(Ph_3P)_2N]^+$, 155°

-2127.20269803135 Hartrees

atom	x	y	z
P	11.27666106	5.056708079	16.64139184
P	14.10708182	5.08012662	15.37877645
C	10.22617588	4.055646282	15.54182963
C	17.38004917	7.036931546	17.97121335
H	18.14904535	7.491023767	18.58887971
C	15.40018847	5.87392375	16.38012703
C	14.21435475	5.748213792	13.69185381
C	10.47805575	8.981461927	17.45224907
H	11.05249377	9.885930996	17.62771247
C	11.41603601	4.159415592	18.22128121
C	15.05132351	5.166386934	12.72782648
H	15.61954461	4.271200692	12.96109754

N	12.68419152	5.411713185	15.99929121
C	14.49811503	3.303231609	15.26203911
C	11.13808914	7.784180683	17.1800953
H	12.22198389	7.751385125	17.13669944
C	13.47167732	6.895071263	13.37194411
H	12.81971213	7.340464673	14.11708019
C	10.3975758	6.615345688	16.95144153
C	9.083098731	9.017732972	17.49668009
H	8.571595475	9.952133765	17.70733993
C	15.18506584	6.047848931	17.75527059
H	14.24609396	5.734782585	18.20062059
C	13.66663662	2.479579248	14.48182315
H	12.82423256	2.902561572	13.94224753
C	11.69142258	2.751079882	20.62199274
H	11.7977535	2.203851974	21.55388866
C	10.19619758	4.379864334	14.17490173
H	10.81618918	5.185608481	13.79237703
C	15.1441962	5.732039607	11.45599399
H	15.78905748	5.277452797	10.71022278
C	14.40405257	6.872455458	11.14145701
H	14.47620673	7.308225944	10.14952636
C	16.6093683	6.291363707	15.80410454
H	16.77965891	6.176940602	14.73820695
C	15.83258017	1.371111672	15.85830252
H	16.67543333	0.941167723	16.39078242
C	10.83419768	4.65254703	19.3979827

H	10.27473643	5.581843287	19.38474362
C	16.17590097	6.627017796	18.5465052
H	16.00658783	6.761046422	19.61057825
C	8.343424589	7.856530979	17.26516382
H	7.258533499	7.886726247	17.29160625
C	8.995495908	6.655268046	16.99042391
H	8.413411324	5.75881787	16.79926442
C	15.00428735	0.558315549	15.08500408
H	15.20184383	-0.507182295	15.01467933
C	15.58352819	2.741659115	15.94945735
H	16.23220496	3.368037822	16.55263868
C	10.97419182	3.946420305	20.59374177
H	10.52236592	4.332998351	21.50210074
C	9.423915899	3.013491301	16.02777708
H	9.443016216	2.751303668	17.08057271
C	13.56798097	7.452067774	12.09828245
H	12.99090178	8.33817019	11.85208105
C	12.27391626	2.255623172	19.45234408
H	12.83172901	1.324307084	19.47333533
C	17.59521031	6.870204809	16.60203488
H	18.52803389	7.196972833	16.15302792
C	8.600198141	2.303446741	15.15255441
H	7.981817224	1.495819387	15.53223479
C	12.1391938	2.953732254	18.25498098
H	12.59363077	2.559078328	17.35091111
C	8.573946026	2.628142274	13.79654414

H	7.931855175	2.073707686	13.11873429
C	9.372670108	3.665685546	13.3079944
H	9.350859531	3.919170063	12.25247614
C	13.92107759	1.113025311	14.39743743
H	13.27777769	0.48107524	13.79276399

$[(Ph_3P)_2N]^+$, 150°

-2127.20274227377 Hartrees

atom	x	y	z
P	11.28740923	5.079224803	16.63460361
P	14.10591138	5.123860086	15.39946262
C	10.26851112	4.091933601	15.49238143
C	17.44311538	7.06295605	17.92912125
H	18.22789876	7.509742375	18.53171635
C	15.42085976	5.916118572	16.374763
C	14.21668792	5.73758106	13.69173883
C	10.34301151	8.974529683	17.44995198
H	10.87782238	9.911560173	17.57124733
C	11.44133608	4.129300496	18.18183521
C	15.05251156	5.122960238	12.74688844
H	15.62194906	4.236883362	13.00983354
N	12.69034344	5.513810698	16.01725063
C	14.45987783	3.336096353	15.32725782
C	11.04803674	7.809152053	17.15084393
H	12.12648623	7.831302915	17.03330782
C	13.47211601	6.871280481	13.33212203

H	12.82153082	7.342262247	14.062546
C	10.358722	6.598870723	16.99130885
C	8.9549417	8.93693316	17.59028223
H	8.408477985	9.846255724	17.82166096
C	15.20542299	6.164523644	17.73842222
H	14.24989726	5.91617438	18.18932242
C	13.66547608	2.521931838	14.49968614
H	12.87987402	2.958314638	13.8898164
C	11.79019785	2.673572944	20.54498865
H	11.92336542	2.107144814	21.46181348
C	10.26778148	4.441460382	14.13144237
H	10.90204705	5.248225264	13.7758192
C	15.14059162	5.641411476	11.45491942
H	15.78384076	5.160499435	10.72442572
C	14.39665553	6.767604174	11.10046684
H	14.46387528	7.165812225	10.0925199
C	16.65226897	6.251634642	15.79171435
H	16.82535947	6.079892502	14.73397653
C	15.68732724	1.377440228	16.05319517
H	16.47581578	0.933624461	16.65321069
C	11.01736374	4.662848012	19.40775611
H	10.54894264	5.640572023	19.44672438
C	16.21680202	6.73505409	18.51074902
H	16.045466	6.926264885	19.56571561
C	8.265601996	7.733411391	17.42787015
H	7.185082935	7.705713145	17.52918217

C	8.961977398	6.56464102	17.12642607
H	8.417323908	5.63537777	16.98852642
C	14.89464699	0.574070044	15.23404351
H	15.06519896	-0.497694212	15.19567955
C	15.47370035	2.756023303	16.10287207
H	16.09495129	3.374335633	16.74210538
C	11.193636	3.933113873	20.58433448
H	10.86132686	4.350090105	21.53006629
C	9.443458021	3.050798192	15.94247374
H	9.436944045	2.769011055	16.99029548
C	13.56320717	7.380962862	12.03819933
H	12.98345519	8.25620485	11.76128003
C	12.21477083	2.137276733	19.32656839
H	12.67627645	1.155038632	19.29441466
C	17.65808632	6.822397677	16.57043587
H	18.60740095	7.084745552	16.113849
C	8.63079223	2.365360235	15.03811495
H	7.995659715	1.558485907	15.39087453
C	12.04348481	2.8586202	18.14786765
H	12.3730655	2.430385304	17.20597181
C	8.636069246	2.713796933	13.68771114
H	8.002111711	2.178580569	12.98719232
C	9.454992795	3.75141961	13.23496353
H	9.456920859	4.02469391	12.18416333
C	13.88352244	1.146974841	14.45761562
H	13.26914197	0.523116478	13.81555343

$[(Ph_3P)_2N]^+$, 147.2°			
-2127.20294445306 Hartrees			
atom	**x**	**y**	**z**
P	11.26576129	5.075599653	16.58373199
P	14.07627676	5.137370416	15.36999799
C	10.22204399	4.096502525	15.45899301
C	17.3063149	7.136393789	17.98472105
H	18.06609231	7.598424076	18.60777662
C	15.35067742	5.951624048	16.37936365
C	14.26048663	5.718167205	13.65859606
C	10.34175685	8.943481246	17.53225146
H	10.87877771	9.879328653	17.65282789
C	11.48604152	4.097533976	18.10584104
C	15.1426241	5.091964611	12.76484345
H	15.69929179	4.210540998	13.06797302
N	12.63101831	5.549992513	15.90693716
C	14.43456522	3.349784532	15.35892771
C	11.03591802	7.789287074	17.17104907
H	12.10746968	7.819172992	17.00355963
C	13.53364014	6.84605277	13.24823997
H	12.8473084	7.324226253	13.94002278
C	10.34398605	6.580200225	17.01323405
C	8.961775059	8.896401142	17.73451045
H	8.423569535	9.797185523	18.01356055
C	15.09075232	6.202528771	17.73485498

H	14.12751036	5.939846126	18.16056766
C	13.68468257	2.513148838	14.51262958
H	12.92906983	2.932249231	13.85461374
C	11.96566229	2.621196462	20.43354527
H	12.14881229	2.046809212	21.33669327
C	10.25980664	4.396222759	14.08751744
H	10.93935442	5.158157657	13.71720018
C	15.29494675	5.594321305	11.47263886
H	15.97445853	5.105309531	10.78150169
C	14.56987986	6.715724052	11.06770003
H	14.68856459	7.102129399	10.05997375
C	16.59273209	6.303533004	15.83027021
H	16.79888132	6.129432535	14.77900819
C	15.63171486	1.414596482	16.1905429
H	16.39128847	0.988792639	16.83898211
C	11.24447816	4.66729844	19.36539483
H	10.86466095	5.680694302	19.44323377
C	16.06987967	6.791850717	18.53344145
H	15.86616185	6.984751148	19.58232001
C	8.269640132	7.69432833	17.57279633
H	7.194988812	7.659470136	17.7223321
C	8.955355576	6.536283638	17.21162503
H	8.408009086	5.608386605	17.07602958
C	14.88362903	0.588819708	15.35189791
H	15.06037126	-0.48260121	15.34646433
C	15.41068549	2.792797494	16.197336

H	15.99752292	3.428802068	16.85147576
C	11.48569639	3.927594117	20.52376294
H	11.29297269	4.372004378	21.49539453
C	9.339801554	3.113264821	15.93170271
H	9.305001072	2.868004265	16.98827787
C	13.68960356	7.339466101	11.95424619
H	13.12429364	8.210663077	11.63770458
C	12.20729289	2.048612561	19.18237937
H	12.57750012	1.030504101	19.11096353
C	17.56588681	6.893760479	16.63484972
H	18.52417109	7.169482161	16.2057843
C	8.508588801	2.43620191	15.03864745
H	7.829894576	1.67371341	15.40834481
C	11.97012605	2.779686015	18.02097129
H	12.15754821	2.323465429	17.05374994
C	8.552321459	2.734917194	13.67681096
H	7.904527462	2.205427401	12.9847542
C	9.427944553	3.714166522	13.20205306
H	9.460354167	3.948299549	12.14233073
C	13.9097605	1.138658568	14.51335357
H	13.3311067	0.497032909	13.85590066

$[(Ph_3P)_2N]^+$, 145°

-2127.20279868164 Hartrees

atom	**x**	**y**	**z**
P	11.29011733	5.097201107	16.60624664

P	14.08677533	5.145142889	15.39000988
C	10.27569045	4.11045743	15.46006763
C	17.42083057	7.090671719	17.92127592
H	18.20347136	7.542084813	18.52327906
C	15.40328276	5.933587098	16.36750849
C	14.23651577	5.72347407	13.67303924
C	10.26360269	8.951897364	17.51466979
H	10.77457492	9.902977197	17.62947377
C	11.49009795	4.12158753	18.12987422
C	15.08354045	5.08636019	12.7536575
H	15.63670552	4.197016045	13.039558
N	12.66778242	5.600769723	15.97046123
C	14.40837501	3.348703882	15.36643545
C	10.99069643	7.813365816	17.16803415
H	12.06213927	7.869852132	17.00689496
C	13.51390646	6.86196161	13.28380754
H	12.85488942	7.349604055	13.99532811
C	10.33238371	6.584882015	17.01794453
C	8.884323764	8.869593199	17.71062941
H	8.320636734	9.758030133	17.97904175
C	15.17077331	6.225755872	17.71935884
H	14.2038277	6.008192542	18.16141324
C	13.65110686	2.529846397	14.50906598
H	12.9104288	2.965582434	13.84502229
C	11.93964473	2.650227384	20.46780846
H	12.11103601	2.077860112	21.37457851

C	10.28999364	4.45211331	14.09739597
H	10.94129505	5.245439811	13.74239636
C	15.2042821	5.586975661	11.45728708
H	15.85623173	5.088684037	10.7464503
C	14.48271363	6.718123211	11.07331657
H	14.57626158	7.102713054	10.06217833
C	16.64945902	6.231514602	15.79534007
H	16.83586001	6.027700699	14.74558325
C	15.55916871	1.384639806	16.19963939
H	16.30470123	0.942031656	16.85313453
C	11.21087897	4.685576236	19.3841856
H	10.81379234	5.69273374	19.45468317
C	16.17993491	6.800386665	18.49171537
H	15.99499589	7.025043995	19.53778392
C	8.225554195	7.647724517	17.55665127
H	7.151469301	7.584965567	17.70158114
C	8.944128915	6.505760319	17.20900723
H	8.422614976	5.562162682	17.08014553
C	14.80312609	0.57578964	15.3508088
H	14.95891116	-0.498757191	15.34187087
C	15.36520416	2.767140594	16.21087214
H	15.95891377	3.388003833	16.87337243
C	11.43691102	3.948702126	20.54727801
H	11.21500364	4.389352353	21.51441282
C	9.426685754	3.088668247	15.91091628
H	9.407064475	2.813875828	16.96043242

C	13.63825809	7.353962658	11.98581406
H	13.07588991	8.233167118	11.68632637
C	12.21918346	2.083190881	19.22208309
H	12.6071483	1.071147789	19.15810164
C	17.65267454	6.807562777	16.5734538
H	18.61312493	7.041497283	16.12462649
C	8.606123567	2.414390135	15.00575537
H	7.95300709	1.622425249	15.35939371
C	11.99721425	2.811783359	18.05616032
H	12.21316033	2.358315416	17.09375625
C	8.626250587	2.755034633	13.65331488
H	7.985422749	2.228893061	12.95216668
C	9.468402422	3.773385506	13.19985903
H	9.481791552	4.040970163	12.14764443
C	13.84865081	1.150439566	14.50597917
H	13.26267745	0.524470995	13.83982919

$[(Ph_3P)_2N]^+$, 140°

-2127.20267748895 Hartrees

atom	**x**	**y**	**z**
P	11.309107	5.112821245	16.61165329
P	14.07532191	5.169582746	15.40425513
C	10.32584703	4.131425421	15.43417769
C	17.4824826	7.076660641	17.86642858
H	18.28231566	7.519420518	18.45223402
C	15.42140363	5.941942938	16.35437984

C	14.22228033	5.720905028	13.67814797
C	10.14642443	8.933479207	17.50855763
H	10.61822962	9.907665129	17.59369661
C	11.52404875	4.113886778	18.12001306
C	15.04548301	5.055057673	12.75701368
H	15.57753451	4.153757221	13.04496587
N	12.67593929	5.690247375	15.99819091
C	14.35678417	3.366585296	15.40416337
C	10.9127804	7.822292334	17.1571595
H	11.9752354	7.922348605	16.96283889
C	13.52817594	6.875680184	13.28444876
H	12.88836929	7.386312716	13.99715739
C	10.30563561	6.564368744	17.04494393
C	8.77861918	8.794640024	17.74694115
H	8.184229396	9.661973767	18.01852659
C	15.19184191	6.320985942	17.68442128
H	14.20996587	6.180340349	18.12388385
C	13.61774326	2.55213494	14.52671267
H	12.91026304	2.993885847	13.83179401
C	11.99578838	2.630799749	20.44589415
H	12.174452	2.053303629	21.34806597
C	10.34038076	4.512591217	14.08222499
H	10.98051871	5.325643669	13.75307358
C	15.16989994	5.542162919	11.45567883
H	15.80324615	5.021423689	10.74404583
C	14.47617316	6.68966266	11.06806637

H	14.57248779	7.064108343	10.05333571
C	16.6872074	6.140833343	15.78214678
H	16.8729057	5.86947699	14.74760205
C	15.44354276	1.390606871	16.29531377
H	16.15788721	0.94177834	16.97874373
C	11.29899991	4.686790112	19.3816147
H	10.93307649	5.70498874	19.46203975
C	16.22260086	6.884675654	18.43629562
H	16.03977161	7.177848089	19.46564793
C	8.170245956	7.542410519	17.63117929
H	7.104600788	7.435096991	17.80920262
C	8.928424357	6.427878867	17.27904093
H	8.444602517	5.460919343	17.17878733
C	14.70421309	0.586395481	15.42686805
H	14.84232678	-0.490604119	15.43224408
C	15.27249561	2.776132014	16.28763585
H	15.85288985	3.393115009	16.96516002
C	11.53612656	3.944594704	20.53847828
H	11.35501895	4.392048072	21.51095912
C	9.487172525	3.086794565	15.85113752
H	9.464354127	2.782085384	16.89212209
C	13.65535096	7.354458606	11.98168507
H	13.11492543	8.246522025	11.67999106
C	12.22222204	2.05548775	19.19340418
H	12.57673571	1.031916494	19.11942231
C	17.7121589	6.706106856	16.53919628

H	18.68828178	6.863103937	16.09046409
C	8.67999044	2.42785707	14.92286282
H	8.03487386	1.618298496	15.25057434
C	11.98962352	2.790202658	18.03289412
H	12.16441972	2.330046911	17.06582976
C	8.701601044	2.807204958	13.58062955
H	8.070703794	2.29342778	12.86141978
C	9.532082821	3.849426699	13.16122804
H	9.546235313	4.148564371	12.11748744
C	13.79125091	1.169325268	14.54274305
H	13.21959616	0.547487624	13.86050067

$[(Ph_3P)_2N]^+$, 135°

-2127.20089301964 Hartrees

atom	x	y	z
P	11.26937052	5.104803412	16.50649943
P	14.03226683	5.222819174	15.39864906
C	10.15504245	4.356195303	15.27474888
C	17.18424278	7.625215354	17.75958716
H	17.92430104	8.193323639	18.31506901
C	15.28207801	6.161154321	16.33046203
C	14.31001375	5.566987221	13.63347951
C	9.952778422	8.850479873	17.48995815
H	10.18266681	9.870473686	17.19771725
C	11.57146093	3.859421114	17.80081434
C	15.26662124	4.859192732	12.88910635

H	15.81241565	4.033741727	13.3349022
N	12.56774205	5.758214621	15.80947263
C	14.37066497	3.452452099	15.64357921
C	10.66607257	7.792824399	16.92657415
H	11.4506762	7.980916377	16.20171658
C	13.60174606	6.618936142	13.03295645
H	12.86184714	7.16563158	13.60864155
C	10.37670248	6.474195243	17.30379357
C	8.948610969	8.599178816	18.42527914
H	8.394918284	9.424391115	18.86263883
C	14.87611594	7.039544435	17.34243338
H	13.819281	7.15703141	17.55704394
C	13.82931933	2.515845582	14.74501336
H	13.23570013	2.8468763	13.89834342
C	12.1432418	1.994690891	19.8071621
H	12.3577189	1.271120545	20.58795315
C	10.45664821	4.474554906	13.91142018
H	11.3612768	4.985664051	13.60033017
C	15.5062362	5.200618931	11.55879481
H	16.24278396	4.646087903	10.98551729
C	14.79722902	6.24576751	10.96475478
H	14.98524862	6.507620792	9.927914149
C	16.64692725	6.02840731	16.02680527
H	16.97477432	5.362782723	15.2339339
C	15.36886094	1.641386959	16.9066516
H	15.96972801	1.302209278	17.74482805

C	12.02454065	4.289553819	19.06046198
H	12.14227903	5.349024854	19.26692166
C	15.82909284	7.767828776	18.05550532
H	15.51103804	8.448731497	18.83910238
C	8.657847751	7.287079782	18.80432332
H	7.882210296	7.089918238	19.53794366
C	9.367742032	6.225198753	18.24768941
H	9.145114834	5.211218138	18.56553132
C	14.83641812	0.717387181	16.00718273
H	15.02557586	-0.343298224	16.14317948
C	15.13907113	3.005743814	16.72898457
H	15.56364489	3.717694877	17.42857396
C	12.3090054	3.358857077	20.05688095
H	12.65069341	3.698022935	21.0299504
C	8.964148207	3.721620857	15.66728735
H	8.709641508	3.623708102	16.71803009
C	13.84518607	6.952680561	11.70148736
H	13.29229773	7.765229387	11.24011587
C	11.69889259	1.561023803	18.55793687
H	11.56964208	0.500948453	18.36290746
C	17.59243195	6.757099534	16.74339235
H	18.64683577	6.650981366	16.50747611
C	8.099954146	3.202480577	14.70661957
H	7.183294102	2.710524323	15.01713976
C	11.41495761	2.486920058	17.55447038
H	11.07051367	2.139566829	16.58679864

C	8.411275876	3.314338659	13.34927779
H	7.734722976	2.90865159	12.60321713
C	9.587224596	3.950567494	12.95383655
H	9.828294589	4.04556588	11.89943926
C	14.06347629	1.155039691	14.92887818
H	13.65152565	0.437258645	14.22606453

$[(Ph_3P)_2N]^+$, 130°

-2127.19968247014 Hartrees

atom	x	y	z
P	11.28581667	5.113849272	16.48013253
P	13.99931688	5.229788788	15.36260314
C	10.14161033	4.311176946	15.3123604
C	17.07927434	7.555867936	17.89452094
H	17.80079761	8.113162425	18.48434049
C	15.22433374	6.118807476	16.37576095
C	14.35497544	5.610833429	13.6187242
C	9.851371862	8.829762828	17.41102511
H	10.01091342	9.846516637	17.06534669
C	11.67890171	3.912846763	17.79168526
C	15.37003804	4.942334894	12.91655881
H	15.92248573	4.132000065	13.38180228
N	12.52040513	5.805287569	15.69185023
C	14.29806167	3.444908745	15.56425499
C	10.57828296	7.784442273	16.84206475
H	11.30358893	7.980054935	16.05968564

C	13.63710728	6.639349127	12.99065173
H	12.85087157	7.152729282	13.53399497
C	10.37989661	6.469897243	17.28760607
C	8.923541218	8.570371255	18.42018749
H	8.359120358	9.38599527	18.86197496
C	14.78519287	7.061904982	17.31369326
H	13.72231026	7.243448303	17.43334832
C	13.76815151	2.552783037	14.61527664
H	13.2027869	2.925824126	13.76696065
C	12.33497282	2.126863902	19.84261801
H	12.58121762	1.43400213	20.64175244
C	10.39149081	4.402247345	13.93659463
H	11.27629527	4.92076162	13.58269581
C	15.65876431	5.300446871	11.60076561
H	16.44018698	4.775943808	11.05945605
C	14.94021453	6.323201897	10.97883544
H	15.16590721	6.597334342	9.952692591
C	16.60097371	5.909376224	16.19086749
H	16.95770918	5.192764504	15.45735226
C	15.24169779	1.572687318	16.77754981
H	15.81674321	1.192366842	17.61614389
C	12.21240222	4.388983866	19.00228786
H	12.35896431	5.453861064	19.15510365
C	15.71377646	7.77553042	18.07252987
H	15.36894575	8.506131146	18.79795883
C	8.723157805	7.262576263	18.86691746

H	8.007126934	7.059754425	19.65745711
C	9.44713799	6.212986135	18.30481553
H	9.295357281	5.203520191	18.6744659
C	14.71881411	0.692257505	15.82991498
H	14.89014557	-0.375645174	15.92848658
C	15.0324654	2.945601516	16.64996895
H	15.44407027	3.622664081	17.39026729
C	12.54019823	3.497121127	20.02054657
H	12.94452044	3.871658271	20.95595549
C	8.97360816	3.673132839	15.76329654
H	8.756320015	3.602278149	16.82455498
C	13.92983747	6.990011507	11.67333584
H	13.36860055	7.78392285	11.19009636
C	11.81128185	1.648084903	18.64142904
H	11.65265662	0.583252947	18.5016112
C	17.52203857	6.624465917	16.95149377
H	18.58508072	6.458189698	16.80678519
C	8.082067349	3.120099408	14.84770809
H	7.182939256	2.626065617	15.20303152
C	11.48601581	2.534658775	17.61520381
H	11.08228648	2.152389454	16.68437159
C	8.342432031	3.203527767	13.47753192
H	7.643960373	2.772863776	12.76639573
C	9.49430625	3.845491772	13.02415836
H	9.693869819	3.920115132	11.95946999
C	13.9778146	1.182475829	14.75164032

H	13.57318377	0.498751035	14.01153627

$[(Ph_3P)_2N]^+$, 125°

-2127.19712411561 Hartrees

atom	x	y	z
P	11.33049664	5.155840214	16.54110822
P	13.99222792	5.257144147	15.41089146
C	10.31278368	4.292249221	15.29736599
C	17.40831069	7.328131672	17.72064988
H	18.20998478	7.819847361	18.26328918
C	15.34696843	6.062255694	16.32277034
C	14.25273883	5.634441608	13.6487652
C	9.720188513	8.803997389	17.47244323
H	9.92877646	9.84432232	17.24215371
C	11.68091345	3.997045567	17.90383157
C	15.112083	4.867823168	12.84588568
H	15.58577816	3.974627281	13.2403694
N	12.59416275	5.951639426	15.88965185
C	14.21286277	3.457113251	15.58809588
C	10.54864076	7.804405035	16.96158176
H	11.3999349	8.057818603	16.33942685
C	13.64089084	6.779182163	13.11440994
H	12.97797703	7.372740141	13.73569155
C	10.28712044	6.460550484	17.25933231
C	8.629757583	8.469419793	18.27509684
H	7.986595508	9.249590396	18.67080303

C	15.04930879	6.908575209	17.39805677
H	14.01398987	7.079493169	17.67211259
C	13.59088202	2.582495621	14.67868871
H	12.97824315	2.972253584	13.87218582
C	12.2721768	2.312155492	20.05973303
H	12.49374963	1.657846165	20.89757523
C	10.50631902	4.594450797	13.94137515
H	11.29269961	5.280945777	13.64643035
C	15.34859348	5.24146663	11.52342327
H	16.00946784	4.641559242	10.90535033
C	14.73408402	6.377748678	10.99543911
H	14.91951291	6.664655134	9.964856996
C	16.68393797	5.862362215	15.94098168
H	16.92791179	5.223310641	15.09771827
C	15.18501853	1.555192445	16.73209292
H	15.80824567	1.157090966	17.52680538
C	12.01650446	4.53860074	19.15745037
H	12.02974491	5.614478444	19.30195549
C	16.08171191	7.537575379	18.09518204
H	15.84742251	8.194289675	18.92741397
C	8.366123823	7.130714851	18.57402812
H	7.5212448	6.867990397	19.20309419
C	9.189637434	6.127777012	18.06921204
H	8.980878544	5.09232705	18.32057865
C	14.56849817	0.692226026	15.82576109
H	14.71461321	-0.380356813	15.91253035

C	15.01004512	2.933744897	16.61749289
H	15.49703788	3.5977771	17.32320565
C	12.31417299	3.698008684	20.22704027
H	12.56678018	4.123907837	21.1931058
C	9.267712611	3.42967593	15.66952192
H	9.091948167	3.191059796	16.71328216
C	13.88055282	7.14456367	11.79073637
H	13.40214676	8.028927944	11.3812954
C	11.9440954	1.768173444	18.81768788
H	11.91401012	0.691137538	18.68460469
C	17.70859963	6.492199074	16.64179492
H	18.74073865	6.335335641	16.34419759
C	8.448139524	2.863503189	14.69539065
H	7.646233436	2.193955016	14.99093611
C	11.65448782	2.603935085	17.73951746
H	11.41467481	2.168384747	16.77636243
C	8.656326976	3.155985712	13.34603428
H	8.01551765	2.712654195	12.58997881
C	9.682947524	4.022609689	12.97126449
H	9.841478534	4.260206775	11.92376667
C	13.76895709	1.206071436	14.80187413
H	13.29381065	0.53604539	14.09190348

$[(Ph_3P)_2N]^+$, 120°

-2127.19317020933 Hartrees

atom	x	y	z

P	11.34319255	5.170680296	16.51251587
P	13.9575591	5.276096847	15.40005125
C	10.31222602	4.294893114	15.28766996
C	17.35597306	7.28894196	17.79055197
H	18.15292197	7.770730343	18.34903206
C	15.30638797	6.045848942	16.35378269
C	14.27915028	5.648013953	13.6458688
C	9.583379862	8.749100928	17.43586984
H	9.705711666	9.788452226	17.14640613
C	11.76118485	4.022396726	17.86606285
C	15.18557076	4.891563934	12.8862278
H	15.66117704	4.011989512	13.3082981
N	12.55712678	6.027468013	15.82063429
C	14.1464925	3.472238663	15.56835672
C	10.42722052	7.778015283	16.89669223
H	11.2067601	8.05422705	16.19511847
C	13.66354889	6.772134476	13.0745601
H	12.96388158	7.35727011	13.66259084
C	10.27750596	6.436303762	17.27195766
C	8.587972562	8.387294883	18.34387091
H	7.93302719	9.145535408	18.76253231
C	14.99922397	6.983214043	17.34733411
H	13.96211894	7.234047249	17.54129579
C	13.55256744	2.614762735	14.62444113
H	12.96837703	3.019486972	13.80473734
C	12.39502554	2.3715305	20.03525413

H	12.63270025	1.730991547	20.87935939
C	10.50812674	4.565752792	13.92598161
H	11.30396869	5.234871933	13.61654796
C	15.46604866	5.255467994	11.57027357
H	16.16334292	4.66318568	10.98565931
C	14.84789938	6.371844767	11.00474991
H	15.06710625	6.650922858	9.978560651
C	16.64927164	5.744570942	16.0710319
H	16.90414169	5.032258009	15.29212998
C	15.07948317	1.546531314	16.70694331
H	15.67641544	1.133122903	17.51399261
C	12.22171799	4.580150306	19.07209274
H	12.31608392	5.656679193	19.1762702
C	16.0249273	7.59979467	18.06467328
H	15.78242822	8.326523414	18.83388333
C	8.436049672	7.050674264	18.7195662
H	7.666717733	6.768151063	19.43163852
C	9.276643619	6.07601816	18.18718069
H	9.159688056	5.043463009	18.50157011
C	14.48919457	0.700894833	15.76707754
H	14.62981124	-0.373601764	15.83933955
C	14.90947279	2.926814977	16.61277859
H	15.3725329	3.574999624	17.34815632
C	12.54156587	3.755877913	20.14775936
H	12.8921824	4.194025743	21.07707752
C	9.249883923	3.462860728	15.67955485

H	9.064256529	3.257864963	16.72869794
C	13.9471704	7.127835639	11.75659986
H	13.4653048	7.996351638	11.31806106
C	11.94311382	1.811879613	18.84005409
H	11.83385388	0.735522027	18.74906798
C	17.66780407	6.363008424	16.79103009
H	18.70430471	6.125825276	16.57096728
C	8.419129454	2.890331215	14.71915515
H	7.603427567	2.244804299	15.03031398
C	11.63290595	2.630347202	17.75409882
H	11.30155004	2.181649238	16.82482607
C	8.63104033	3.149047534	13.36315235
H	7.980140958	2.70206673	12.61771858
C	9.672151154	3.989415208	12.96887039
H	9.831760244	4.203663396	11.91635634
C	13.72283237	1.235648942	14.72879198
H	13.26775085	0.58009416	13.99255515

$[(Ph_3P)_2N]^+$, 115°

-2127.18783860148 Hartrees

atom	x	y	z
P	11.38306638	5.197306551	16.53586519
P	13.94196171	5.284481202	15.4283587
C	10.40342959	4.307201059	15.27741801
C	17.4876125	7.188807635	17.69153297
H	18.31905177	7.64723181	18.2184016

C	15.34893531	6.007642591	16.33449158
C	14.23383845	5.651270281	13.66623729
C	9.454996878	8.701840119	17.41735403
H	9.550628818	9.74786561	17.1425113
C	11.78912139	4.064602394	17.90811373
C	15.06505965	4.851910508	12.86601848
H	15.49433238	3.935520135	13.25778235
N	12.59170083	6.122966916	15.90115768
C	14.08572837	3.472761256	15.59140062
C	10.35942956	7.769236294	16.90895722
H	11.15800869	8.083475903	16.24592542
C	13.6836054	6.828443685	13.13507488
H	13.04398605	7.448558639	13.7547038
C	10.24525736	6.418620266	17.26483486
C	8.433506292	8.29371379	18.27492899
H	7.730819162	9.021930137	18.66849974
C	15.10693364	6.944248681	17.34701695
H	14.08534139	7.218610744	17.58613303
C	13.46748964	2.625663239	14.65437473
H	12.86974106	3.039042079	13.84953461
C	12.37168065	2.461815446	20.12781832
H	12.58932156	1.839644496	20.99079609
C	10.56483106	4.664182738	13.9304886
H	11.31637172	5.394098046	13.65000063
C	15.33246361	5.223715839	11.54916589
H	15.97122281	4.598059527	10.93325297

C	14.77766289	6.391506032	11.02366394
H	14.98710291	6.676887062	9.997208839
C	16.67081894	5.675337007	15.99361261
H	16.87431419	4.964332238	15.19864242
C	15.03286671	1.534977754	16.6970237
H	15.64531689	1.112964569	17.4877858
C	12.19167015	4.650682946	19.12163216
H	12.25797905	5.730720588	19.21136406
C	16.1775518	7.529848092	18.02449335
H	15.98563729	8.256264829	18.8082988
C	8.316297189	6.948470053	18.63158899
H	7.525963133	6.628889796	19.30385774
C	9.217165842	6.012330472	18.12996132
H	9.123614032	4.972363213	18.42787404
C	14.41710398	0.699043203	15.76470622
H	14.55330606	-0.376598753	15.82669986
C	14.86912815	2.916567381	16.61533267
H	15.35272306	3.557524007	17.34380839
C	12.48730693	3.850509691	20.22231198
H	12.79411688	4.310979631	21.15634816
C	9.393099988	3.39697299	15.63192779
H	9.227261388	3.128870387	16.66971173
C	13.953954	7.192048486	11.81682395
H	13.52260162	8.101583101	11.41012421
C	11.97683728	1.874368593	18.92577531
H	11.89291546	0.794748658	18.84822011

C	17.73357937	6.263176958	16.67357677
H	18.75355157	6.003244923	16.407683
C	8.586056727	2.829845102	14.64797633
H	7.811689396	2.12326515	14.93066527
C	11.69380366	2.668521224	17.81487321
H	11.4138365	2.19689101	16.88028399
C	8.767123685	3.172418514	13.30655437
H	8.134798181	2.729204265	12.54326198
C	9.752509066	4.09305757	12.95056069
H	9.88674394	4.374512853	11.91057656
C	13.63182872	1.244919692	14.74679655
H	13.15786657	0.597032887	14.01584076

$(Ph_3Si)_2O$, 180°			
-2044.27529886172 Hartrees			
atom	**x**	**y**	**z**
Si	0	0	1.645355853
C	1.267049447	-1.260173553	2.236971032
O	0	0	0
C	2.500612341	-1.391230036	1.570237049
H	2.713378631	-0.775475719	0.699422661
C	3.207814756	-3.105893483	3.120851199
H	3.954856834	-3.818319394	3.460533678
C	1.032152673	-2.079222833	3.354963114
H	0.084072761	-2.011362018	3.883044614
C	3.460282946	-2.305223504	2.005220502
H	4.404208271	-2.39364771	1.473924189
C	1.992777356	-2.990996629	3.796065754
H	1.789817339	-3.615823774	4.661828885
C	0.457817587	1.727383786	2.236971032
C	-0.045465616	2.86120883	1.570237049
H	-0.685107643	2.737592684	0.699422661
C	1.08587528	4.330995811	3.120851199
H	1.329333178	5.334166184	3.460533678
C	1.284583457	1.933481852	3.354963114
H	1.699854224	1.078490156	3.883044614
C	0.266240643	4.149304687	2.005220502

H	-0.12914441	5.010980101	1.473924189
C	1.593890386	3.221294129	3.796065754
H	2.236486575	3.357939171	4.661828885
C	-1.724867034	-0.467210233	2.236971032
C	-2.455146724	-1.469978794	1.570237049
H	-2.028270988	-1.962116965	0.699422661
C	-4.293690036	-1.225102328	3.120851199
H	-5.284190012	-1.51584679	3.460533678
C	-2.31673613	0.145740982	3.354963114
H	-1.783926984	0.932871863	3.883044614
C	-3.726523589	-1.844081183	2.005220502
H	-4.27506386	-2.617332391	1.473924189
C	-3.586667742	-0.2302975	3.796065754
H	-4.026303914	0.257884603	4.661828885
Si	0	0	-1.645355853
C	-1.267049447	1.260173553	-2.236971032
C	-2.500612341	1.391230036	-1.570237049
H	-2.713378631	0.775475719	-0.699422661
C	-3.207814756	3.105893483	-3.120851199
H	-3.954856834	3.818319394	-3.460533678
C	-1.032152673	2.079222833	-3.354963114
H	-0.084072761	2.011362018	-3.883044614
C	-3.460282946	2.305223504	-2.005220502
H	-4.404208271	2.39364771	-1.473924189
C	-1.992777356	2.990996629	-3.796065754
H	-1.789817339	3.615823774	-4.661828885

C	-0.457817587	-1.727383786	-2.236971032
C	0.045465616	-2.86120883	-1.570237049
H	0.685107643	-2.737592684	-0.699422661
C	-1.08587528	-4.330995811	-3.120851199
H	-1.329333178	-5.334166184	-3.460533678
C	-1.284583457	-1.933481852	-3.354963114
H	-1.699854224	-1.078490156	-3.883044614
C	-0.266240643	-4.149304687	-2.005220502
H	0.12914441	-5.010980101	-1.473924189
C	-1.593890386	-3.221294129	-3.796065754
H	-2.236486575	-3.357939171	-4.661828885
C	1.724867034	0.467210233	-2.236971032
C	2.455146724	1.469978794	-1.570237049
H	2.028270988	1.962116965	-0.699422661
C	4.293690036	1.225102328	-3.120851199
H	5.284190012	1.51584679	-3.460533678
C	2.31673613	-0.145740982	-3.354963114
H	1.783926984	-0.932871863	-3.883044614
C	3.726523589	1.844081183	-2.005220502
H	4.27506386	2.617332391	-1.473924189
C	3.586667742	0.2302975	-3.796065754
H	4.026303914	-0.257884603	-4.661828885

$(Ph_3Si)_2O$, 179°			
-2044.27518759873 Hartrees			
atom	**x**	**y**	**z**
Si	0.006337102	6.433477517	2.76666531
O	0.01163351	6.43659728	4.4125183
C	0.451684272	4.700129965	2.181381476
C	1.280324696	4.482910013	1.066655696
H	1.703023314	5.332155558	0.535330361
C	1.582249726	3.190854297	0.632738879
H	2.226280807	3.045446825	-0.230528485
C	1.064647499	2.087973321	1.311924753
H	1.302490134	1.081515277	0.978050632
C	0.242975006	2.280905288	2.424140246
H	-0.159835349	1.424631972	2.958445088
C	-0.061161972	3.57313765	2.851881494
H	-0.702323979	3.705323944	3.720190637
C	1.279659904	7.685963396	2.169455899
C	1.043890846	8.509476051	1.054583207
H	0.092330133	8.449786013	0.531784033
C	2.008011485	9.41583171	0.610007307
H	1.804272555	10.0438372	-0.25325612
C	3.227647581	9.520854332	1.278384627
H	3.977411253	10.22903398	0.935967297
C	3.480865607	8.716200582	2.390818105
H	4.428284518	8.797279167	2.916824655

C	2.517680334	7.807793322	2.829547761
H	2.73095939	7.189340877	3.698165839
C	-1.718114984	6.909087222	2.181181693
C	-2.331686629	6.274865531	1.086958832
H	-1.813475139	5.470222919	0.571043905
C	-3.604343836	6.652198624	0.654666864
H	-4.061042957	6.147045453	-0.192277674
C	-4.291926869	7.670297593	1.314963747
H	-5.284544572	7.962079291	0.982611335
C	-3.702902442	8.310982447	2.406828091
H	-4.236487051	9.102263347	2.926539034
C	-2.429280032	7.934975825	2.833396186
H	-1.986109746	8.442844513	3.686862202
Si	0.001398987	6.42723994	6.058154326
C	-0.446755229	8.156425368	6.652702526
C	-1.27393313	8.365039632	7.770144224
H	-1.694402358	7.511506103	8.296383407
C	-1.577146903	9.653798283	8.212964437
H	-2.219776346	9.792573196	9.078343725
C	-1.062824621	10.76187168	7.539783287
H	-1.30181356	11.76576388	7.880452832
C	-0.243003288	10.57754664	6.424672551
H	0.157173783	11.43804629	5.89508139
C	0.062668767	9.288501357	5.988166739
H	0.702270766	9.162727267	5.117766557
C	-1.279706079	5.17475347	6.63806562

C	-1.04942776	4.333148536	7.740363613
H	-0.097458691	4.378689712	8.263601405
C	-2.019902512	3.426892089	8.171613139
H	-1.820506274	2.784464405	9.025231816
C	-3.240521875	3.340655244	7.502055669
H	-3.995330996	2.63273542	7.833817828
C	-3.488428688	4.164023024	6.401982259
H	-4.43657537	4.09778634	5.875110271
C	-2.518938227	5.072197551	5.976917467
H	-2.728444114	5.705744968	5.118227895
C	1.720105274	5.944995393	6.655334969
C	2.31919369	6.563746588	7.766214165
H	1.793895954	7.360310616	8.287477498
C	3.586965698	6.181694481	8.208491201
H	4.032669112	6.674782933	9.06838759
C	4.284202032	5.174376717	7.541493388
H	5.273193986	4.87900759	7.881687083
C	3.709283387	4.549140026	6.433224264
H	4.250330785	3.766243392	5.908519844
C	2.440229909	4.929732084	5.997104541
H	2.007495068	4.433179877	5.131872927

$(Ph_3Si)_2O$, 165°

-2044.27484009872 Hartrees

atom	x	y	z
Si	11.16977105	4.912239932	16.61754177

Si	14.14210892	4.97239981	15.2499382
C	9.908014696	4.051229414	15.51842767
C	16.8997584	6.923379001	18.52216362
H	17.53467893	7.382186241	19.27548445
C	15.24978449	5.731088203	16.56951612
C	14.23884691	5.978781471	13.66371852
C	10.40535304	9.007153727	16.40347498
H	10.58935223	9.804741673	15.68850484
C	11.45231769	3.932628784	18.20219987
C	15.39016866	6.710370563	13.32368823
H	16.2388529	6.727101811	14.00337099
O	12.57084687	5.020721385	15.75204104
C	14.62056691	3.177727918	14.94033481
C	10.83674548	7.710285191	16.12532863
H	11.35655522	7.512246454	15.19087815
C	13.15436558	5.999845591	12.76676945
H	12.24767365	5.449392731	13.00603361
C	10.61534442	6.6601521	17.03616746
C	9.738385522	9.280404075	17.59937115
H	9.401603761	10.29050622	17.81699846
C	14.91657284	6.97493373	17.14073496
H	14.00851254	7.487745084	16.83148685
C	15.2720428	2.777766939	13.76059992
H	15.49984802	3.515269016	12.99517355
C	11.8922669	2.498743448	20.59208766
H	12.06231853	1.94602932	21.51228615

C	10.30765655	3.012906434	14.65600297
H	11.35332849	2.717958706	14.61394615
C	15.46121781	7.429730741	12.12979959
H	16.36034566	7.989919365	11.88691765
C	14.37549054	7.436189011	11.25362452
H	14.42784749	7.999017164	10.32541425
C	16.4302234	5.103252837	17.00238685
H	16.70981626	4.138532601	16.58691129
C	14.68273563	0.855780273	15.69103637
H	14.44819798	0.108877873	16.44484313
C	12.43016084	4.346303267	19.12867284
H	13.03063688	5.230087836	18.92630471
C	15.72997038	7.564268984	18.1079961
H	15.45243613	8.52255449	18.53900944
C	9.509211407	8.253995588	18.51571235
H	8.995693781	8.46305933	19.45051325
C	9.947569572	6.958292762	18.23660767
H	9.776145646	6.172108944	18.96789591
C	15.33259012	0.481473174	14.51314834
H	15.60585377	-0.557393085	14.34800529
C	14.33232165	2.189283476	15.9018308
H	13.82625061	2.461228888	16.82531193
C	12.6504498	3.636762955	20.30874767
H	13.41266792	3.971247554	21.00740386
C	8.547899668	4.406443504	15.53651729
H	8.210290841	5.214920699	16.18068176

C	13.22008406	6.721299445	11.57470624
H	12.37053952	6.726911788	10.89688504
C	10.91733855	2.073303438	19.690228
H	10.32541687	1.187593963	19.90572429
C	17.24934389	5.692700955	17.96743089
H	18.15699431	5.188562702	18.28878287
C	7.6190454	3.745933733	14.73113208
H	6.572469381	4.037669832	14.75918827
C	10.70225506	2.783167454	18.50734994
H	9.942967591	2.436389644	17.81132476
C	8.035500035	2.717824695	13.88488134
H	7.313970065	2.20508188	13.25432712
C	9.382348906	2.352746409	13.8472222
H	9.712223482	1.555259845	13.1866021
C	15.62736674	1.444524191	13.54830818
H	16.12952093	1.15737818	12.62817672

$(Ph_3Si)_2O$, 160°

-2044.27467091295 Hartrees

atom	**x**	**y**	**z**
Si	11.16709864	4.923650179	16.59171801
Si	14.12445944	4.979022265	15.22920347
C	9.872782315	4.070140223	15.52587306
C	16.8008183	6.956499709	18.55327674
H	17.41825877	7.42233575	19.31671747
C	15.19623984	5.746184788	16.57376552

C	14.28051392	5.965200534	13.63505052
C	10.38051941	9.016593757	16.45137267
H	10.54352063	9.823997191	15.74234918
C	11.50123026	3.926666269	18.15605235
C	15.45154524	6.675428211	13.31772264
H	16.28213856	6.687421761	14.01954434
O	12.53154939	5.051775581	15.66694869
C	14.6002481	3.177451592	14.9548441
C	10.81280722	7.725805189	16.147563
H	11.31262334	7.541687732	15.19947724
C	13.22054613	5.992586618	12.70963357
H	12.29910269	5.46022782	12.93230648
C	10.61817951	6.663104783	17.04984149
C	9.739234726	9.271056923	17.6652959
H	9.401398455	10.27626042	17.90296261
C	14.85770076	7.001773622	17.11572634
H	13.96293099	7.516712328	16.77335309
C	15.25175168	2.755867004	13.78256536
H	15.48238157	3.479756478	13.00518217
C	12.01624529	2.459304827	20.51082488
H	12.21479824	1.894078033	21.41758317
C	10.24816882	3.050344046	14.6313135
H	11.29418912	2.766803293	14.54411252
C	15.56523024	7.37974349	12.11812814
H	16.47892192	7.923543254	11.89298461
C	14.50326255	7.392253094	11.21332011

H	14.58874362	7.943383699	10.28054326
C	16.35887371	5.116077242	17.04976667
H	16.64205187	4.14273503	16.65760296
C	14.65734568	0.868367936	15.74497439
H	14.42108208	0.135151034	16.51155323
C	12.45315488	4.370235586	19.0958881
H	13.00356958	5.291003565	18.91830617
C	15.6485079	7.599988813	18.0962682
H	15.36698218	8.567210104	18.50407514
C	9.536822676	8.232043014	18.57362264
H	9.043195921	8.426428298	19.5221914
C	9.975950564	6.942451757	18.26862131
H	9.825075109	6.146367496	18.99362913
C	15.30705704	0.472656878	14.57413451
H	15.57855355	-0.569382094	14.42709803
C	14.30963633	2.205909243	15.93290292
H	13.80416374	2.493932454	16.85165541
C	12.71059649	3.644279152	20.25842328
H	13.45178953	4.002988604	20.96753944
C	8.511343585	4.412056454	15.60203647
H	8.191476259	5.206464562	16.27224467
C	13.32891206	6.698745934	11.51170653
H	12.49767013	6.709773704	10.81159348
C	11.06750074	2.003708532	19.59585806
H	10.52419074	1.082206431	19.78795515
C	17.1553833	5.714335674	18.02820464

H	18.04944231	5.208304687	18.38289054
C	7.558148754	3.756301555	14.82174019
H	6.510949912	4.037878502	14.89458717
C	10.81494149	2.730298568	18.43073767
H	10.07554671	2.360824172	17.7251459
C	7.950706123	2.745681365	13.94358032
H	7.209958994	2.236239632	13.33296238
C	9.298267267	2.394066093	13.84829922
H	9.609493123	1.610244688	13.16274998
C	15.60438011	1.418484876	13.59329166
H	16.1070009	1.114820894	12.67876008

$(Ph_3Si)_2O$, 155°

-2044.27443660471 Hartrees

atom	x	y	z
Si	11.16264923	4.931093585	16.56199193
Si	14.10146112	4.982067909	15.20910048
C	9.838762414	4.071577461	15.53792299
C	16.69361751	6.97136022	18.59199648
H	17.29333155	7.44159382	19.3668337
C	15.13552609	5.750445007	16.58202419
C	14.32291682	5.961949265	13.61848115
C	10.3567379	9.021277803	16.47137246
H	10.50257421	9.835000362	15.76583613
C	11.55016022	3.931431642	18.11276429
C	15.52255491	6.637134782	13.33207042

H	16.3349752	6.624395817	14.05484763
O	12.48871053	5.07618123	15.57928283
C	14.57700458	3.176724222	14.95795792
C	10.78989736	7.735190481	16.14959939
H	11.27348797	7.560353403	15.19151967
C	13.28861833	6.02188928	12.6663703
H	12.34614885	5.518135851	12.86597079
C	10.61713868	6.664572928	17.04665668
C	9.736318551	9.263082723	17.69868425
H	9.397629174	10.26464571	17.95023228
C	14.81173018	7.029452414	17.07590919
H	13.94667916	7.559164353	16.68352634
C	15.22322591	2.74316901	13.78695151
H	15.45081973	3.459285347	13.00164506
C	12.14428818	2.45213093	20.44163427
H	12.37351338	1.882350545	21.33830627
C	10.1930531	3.09523508	14.58849278
H	11.24067757	2.850593167	14.43203919
C	15.68822915	7.338125687	12.13663701
H	16.62325636	7.854454552	11.93574496
C	14.65082081	7.382783518	11.20467016
H	14.77667768	7.931379295	10.27497022
C	16.26010924	5.102504306	17.12122191
H	16.53177952	4.111961993	16.7660042
C	14.6402386	0.875935578	15.77171544
H	14.4084953	0.150874804	16.54738011

C	12.46953603	4.41338491	19.0657925
H	12.96330912	5.369169582	18.90912294
C	15.57919335	7.633134286	18.07140538
H	15.30934146	8.6189135	18.44090579
C	9.555705996	8.216026842	18.60238011
H	9.078482149	8.400464466	19.56130975
C	9.995764401	6.931140301	18.27917407
H	9.862682592	6.129055425	19.00102272
C	15.28472152	0.46838369	14.60212056
H	15.55686	-0.574858162	14.46491458
C	14.29187102	2.214978248	15.94717532
H	13.79105619	2.51132412	16.86555581
C	12.76624923	3.681693436	20.21543151
H	13.48167759	4.070936645	20.9348137
C	8.473835367	4.364927343	15.70392637
H	8.168473	5.126147107	16.41807512
C	13.44905463	6.724877361	11.47218786
H	12.63653839	6.761274209	10.75122655
C	11.22753709	1.958194624	19.51371754
H	10.73941118	1.002488007	19.68593641
C	17.03337198	5.705731161	18.11522459
H	17.89824354	5.1858519	18.51890404
C	7.497752505	3.703298414	14.95793511
H	6.448241576	3.946955224	15.10067529
C	10.93529794	2.691207211	18.36200539
H	10.22036921	2.292810977	17.64703473

C	7.869948397	2.735308287	14.02436173
H	7.111134393	2.221007648	13.44055555
C	9.21996169	2.432861704	13.83953298
H	9.515157343	1.6825879	13.11066917
C	15.57599793	1.404130653	13.60986305
H	16.07475033	1.091531919	12.69621159

$(Ph_3Si)_2O$, 150°

-2044.27431549348 Hartrees

atom	x	y	z
Si	11.17777471	5.015373341	16.55709083
Si	14.10799509	5.062591453	15.25151836
C	9.942637087	4.146826454	15.43339818
C	16.90309709	7.067291057	18.45631254
H	17.5523144	7.544591431	19.185448
C	15.21738515	5.827779551	16.56430469
C	14.36422197	5.902161738	13.58688927
C	10.18186076	9.059644064	16.78152322
H	10.34457337	9.943778146	16.17059282
C	11.587277	3.935380277	18.0456858
C	15.62968587	6.362740425	13.18234772
H	16.47988907	6.266358492	13.8538543
O	12.52054475	5.356106044	15.64115396
C	14.44892645	3.213354939	15.1143307
C	10.69965439	7.829162423	16.37658572
H	11.2662598	7.766665249	15.45090947

C	13.28682258	6.06694169	12.6977688
H	12.29571477	5.728651823	12.98825867
C	10.50730047	6.669841911	17.15055166
C	9.456588773	9.155507638	17.97062913
H	9.053019264	10.11357278	18.28738669
C	14.84029467	7.028365947	17.19578413
H	13.88390937	7.486797694	16.9555989
C	14.6608393	2.60142435	13.86524123
H	14.64735109	3.205406887	12.96189752
C	12.2105758	2.350187294	20.29513731
H	12.4507834	1.73951447	21.16156249
C	10.37809754	3.212264024	14.47555821
H	11.43874153	2.998666034	14.36978045
C	15.8158946	6.956941988	11.93387151
H	16.80211287	7.307841385	11.64141206
C	14.73445458	7.106754051	11.06423835
H	14.87714396	7.571694972	10.09221777
C	16.45905323	5.265057092	16.90820572
H	16.77356732	4.331029142	16.44943142
C	14.70958098	1.023368573	16.16125927
H	14.72653059	0.411617104	17.05921879
C	12.41637964	4.425966456	19.07375737
H	12.82774939	5.430201486	19.00650733
C	15.67192894	7.641259238	18.13298403
H	15.36049715	8.566442977	18.61075492
C	9.255500372	8.018386798	18.75328324

H	8.697034305	8.089160936	19.68294612
C	9.77941212	6.789925409	18.34741834
H	9.628496626	5.916775989	18.97760554
C	14.91515564	0.437322469	14.9109393
H	15.09438242	-0.631832523	14.83287291
C	14.48206562	2.395512922	16.2610421
H	14.32595388	2.83215471	17.24392018
C	12.72909043	3.642214534	20.18413881
H	13.37433421	4.039297496	20.963265
C	8.56220395	4.394194068	15.53167964
H	8.19459417	5.121748379	16.25136429
C	13.46858538	6.662141598	11.44884593
H	12.62254776	6.78097693	10.77684931
C	11.38236091	1.84729131	19.29180311
H	10.97491213	0.843136949	19.3747556
C	17.29583922	5.878401758	17.84221435
H	18.25096483	5.424963959	18.09378657
C	7.649282283	3.729035115	14.71213005
H	6.586410845	3.937114924	14.80398698
C	11.07579984	2.632824441	18.17913109
H	10.43213647	2.226159573	17.40387824
C	8.101615058	2.803264146	13.7711336
H	7.392167549	2.286127145	13.13037922
C	9.468597293	2.546515114	13.65334938
H	9.826755089	1.828560585	12.92018522
C	14.89130182	1.228446623	13.76264555

H	15.05376026	0.777554045	12.78712208

$(Ph_3Si)_2O$, 145°

-2044.27380956954 Hartrees

atom	x	y	z
Si	11.18248599	5.035127665	16.53180756
Si	14.08568332	5.078966114	15.24347943
C	9.932265272	4.148128935	15.43783853
C	16.83441227	7.080837745	18.49042545
H	17.473537	7.558897893	19.22793517
C	15.17406735	5.839046837	16.57692145
C	14.40768737	5.894359455	13.57739852
C	10.12144259	9.058587303	16.81541398
H	10.25960828	9.951707939	16.21174506
C	11.64527898	3.953411362	18.00402134
C	15.70459825	6.265616744	13.18013288
H	16.5414649	6.11586055	13.85875171
O	12.48956932	5.419595744	15.57387349
C	14.39866651	3.222825687	15.12440105
C	10.65547682	7.84211119	16.39046324
H	11.21030442	7.798621313	15.45669168
C	13.35118106	6.126742724	12.67822178
H	12.33737947	5.85893773	12.9636558
C	10.49449538	6.671394753	17.1545339
C	9.411116074	9.128916599	18.01502826
H	8.994467646	10.07604453	18.34705982

C	14.80088502	7.053779577	17.18295276
H	13.85688034	7.522120134	16.91479663
C	14.56353756	2.598869764	13.87345998
H	14.53039816	3.196600139	12.96642394
C	12.34261615	2.358835718	20.22520464
H	12.61171957	1.744435908	21.0803468
C	10.35519957	3.227001441	14.46103045
H	11.41585422	3.034346059	14.32020755
C	15.94062397	6.836887182	11.9296257
H	16.95075606	7.117529111	11.64322688
C	14.87901111	7.053269093	11.04960537
H	15.06091371	7.49954263	10.07550081
C	16.40006918	5.26438309	16.95592302
H	16.71252155	4.320701979	16.51586181
C	14.66860967	1.036572434	16.17785621
H	14.70746454	0.431444528	17.07953179
C	12.46203663	4.459275467	19.03455808
H	12.83522899	5.478872129	18.97979986
C	15.61961613	7.667767113	18.13055824
H	15.3108421	8.603974809	18.58806553
C	9.241580621	7.980663727	18.78882602
H	8.695061694	8.031847676	19.72682821
C	9.781667566	6.766037449	18.36299963
H	9.655438222	5.88368047	18.9859403
C	14.8257936	0.439028691	14.92618832
H	14.98980987	-0.632676069	14.85033851

C	14.46005241	2.412203342	16.27515296
H	14.34082967	2.857009856	17.25917422
C	12.81176116	3.670807522	20.13068643
H	13.44744534	4.079984862	20.9113222
C	8.550655335	4.367229714	15.58083108
H	8.191677942	5.083257286	16.31620977
C	13.58319656	6.699033097	11.42658984
H	12.75251626	6.869877026	10.74676404
C	11.52546986	1.840986454	19.22048246
H	11.15533103	0.821613005	19.29114786
C	17.22386929	5.878325185	17.90121091
H	18.16651359	5.414987089	18.18036185
C	7.625494078	3.688745953	14.78675785
H	6.562325066	3.87546823	14.91341325
C	11.18239523	2.630920049	18.12201394
H	10.54861379	2.212219924	17.3450862
C	8.065666586	2.776993324	13.82683116
H	7.346654173	2.249121264	13.20598312
C	9.432784139	2.547676836	13.6645213
H	9.781272639	1.840493388	12.91641665
C	14.77358962	1.222494879	13.77335464
H	14.8989426	0.763213469	12.79632161

$(Ph_3Si)_2O$, 140°

-2044.27254266212 Hartrees

atom	x	y	z

Si	11.19443357	5.055943333	16.50987058
Si	14.06200141	5.089980998	15.23162833
C	9.94118753	4.137612455	15.44510108
C	16.80138438	7.060556769	18.50430943
H	17.43981263	7.533752714	19.24558772
C	15.14323001	5.831224087	16.58113097
C	14.44834504	5.893314739	13.57249567
C	10.05129194	9.054183199	16.83947201
H	10.16831353	9.956402307	16.24486829
C	11.70100891	3.987420129	17.97825464
C	15.77023898	6.182289297	13.18892657
H	16.59008211	5.973173198	13.87272774
O	12.4641674	5.487042759	15.5128136
C	14.33803405	3.227525626	15.11677993
C	10.60948305	7.853752934	16.39983468
H	11.16192918	7.831476845	15.46404254
C	13.41754895	6.200888661	12.66651852
H	12.38635147	5.997602184	12.94210247
C	10.47617556	6.672007478	17.15177723
C	9.343742653	9.096847057	18.04207921
H	8.907925768	10.03128783	18.38545968
C	14.79125267	7.064878132	17.16133511
H	13.8644999	7.552818105	16.86914916
C	14.44895568	2.600477261	13.86106422
H	14.39126916	3.198104196	12.95523511
C	12.42190617	2.419491063	20.21121764

H	12.69987517	1.815581106	21.07102392
C	10.36141778	3.241183909	14.44494497
H	11.42219887	3.085243212	14.26677022
C	16.05418495	6.7468621	11.94554604
H	17.08298729	6.963192163	11.66995833
C	15.01676094	7.038790769	11.05829528
H	15.23599731	7.479752456	10.08944717
C	16.34765059	5.232079296	16.98965642
H	16.64484312	4.275327449	16.56799453
C	14.62428174	1.038808772	16.16093522
H	14.69122291	0.434212945	17.06135369
C	12.50822982	4.513401483	19.00626671
H	12.86420707	5.538563284	18.94569063
C	15.60880311	7.672847525	18.11363894
H	15.31655961	8.623879221	18.55092319
C	9.201702337	7.937029725	18.80434255
H	8.657570907	7.96660881	19.74471286
C	9.766334156	6.738896557	18.36383632
H	9.661449348	5.847829656	18.97825874
C	14.72682087	0.438551898	14.9050935
H	14.87643748	-0.634918763	14.82423564
C	14.433823	2.41674182	16.2646215
H	14.35646903	2.862675391	17.25202223
C	12.87024127	3.737962981	20.10769336
H	13.49881342	4.162773651	20.88572821
C	8.558445204	4.307209228	15.63721681

H	8.200037606	5.003473762	16.39162743
C	13.69744067	6.766565183	11.42148455
H	12.88564575	6.996252488	10.73611696
C	11.61334849	1.881900978	19.20971892
H	11.25874023	0.857529126	19.28752967
C	17.17012284	5.839621133	17.94023199
H	18.09599877	5.357363419	18.24263176
C	7.63054001	3.604027992	14.86814446
H	6.566575238	3.752030651	15.03347417
C	11.25876388	2.658543862	18.10554232
H	10.6316551	2.224450717	17.33182351
C	8.068546831	2.716925444	13.88435865
H	7.347194131	2.169493955	13.28342876
C	9.436357962	2.537246261	13.67329526
H	9.783458195	1.849044796	12.9070111
C	14.63906795	1.221953466	13.7542371
H	14.72253465	0.760827225	12.7736154

$(Ph_3Si)_2O$, 135°

-2044.27102960347 Hartrees

atom	**x**	**y**	**z**
Si	11.20479251	5.06426684	16.47901236
Si	14.03455192	5.092515472	15.21969571
C	9.925898477	4.139296399	15.4501784
C	16.71054232	7.111046789	18.51441691
H	17.33619797	7.597509198	19.25800512

C	15.08486713	5.846757989	16.5860818
C	14.48556345	5.873371045	13.56550615
C	10.02765839	9.046968854	16.87153914
H	10.11844971	9.954757187	16.28079634
C	11.75167725	3.99332718	17.93160104
C	15.82607376	6.090777741	13.19981208
H	16.6249146	5.833638927	13.89215047
O	12.42892374	5.523983451	15.42912831
C	14.30132117	3.226991801	15.12555264
C	10.58720958	7.856161015	16.40798251
H	11.11419529	7.846706506	15.45743479
C	13.48501879	6.241580885	12.64873642
H	12.44117578	6.094351408	12.91147603
C	10.4877122	6.667595389	17.15423345
C	9.352116395	9.072779371	18.09287093
H	8.915305574	9.999691341	18.4549892
C	14.72555735	7.092750325	17.1346604
H	13.80609759	7.577212905	16.81513151
C	14.37756156	2.590957463	13.87111369
H	14.29212095	3.18204228	12.96312067
C	12.48943443	2.423205117	20.15788396
H	12.77384265	1.818572068	21.01508962
C	10.32001701	3.256994136	14.42720716
H	11.3752903	3.115851939	14.20896182
C	16.15643151	6.644752576	11.96333441
H	17.19904463	6.805382151	11.70180974

C	15.14785706	6.997664109	11.06476026
H	15.4034169	7.43063562	10.10119177
C	16.28142374	5.254601607	17.02675259
H	16.58601642	4.290685786	16.62751656
C	14.63213412	1.047087421	16.17487656
H	14.73083841	0.449645786	17.07711002
C	12.54653784	4.525598413	18.96593635
H	12.88512574	5.556810305	18.91392494
C	15.52676516	7.717838596	18.08986149
H	15.22878154	8.678077544	18.5025183
C	9.243186329	7.90565562	18.84958329
H	8.723618781	7.922051917	19.80410056
C	9.809301504	6.717476896	18.38505692
H	9.730537555	5.820747437	18.99498203
C	14.69860998	0.438179224	14.92101986
H	14.85204931	-0.634953801	14.84313608
C	14.43666701	2.424714123	16.2750152
H	14.38638581	2.876788476	17.26102474
C	12.91759383	3.748969161	20.06355523
H	13.53662317	4.179194589	20.84621682
C	8.549096479	4.289971346	15.69354696
H	8.209879133	4.975217411	16.46665535
C	13.81125083	6.796906208	11.41027237
H	13.02204332	7.074308818	10.71622037
C	11.69168996	1.879518579	19.15091354
H	11.35164189	0.849732151	19.22182449

C	17.08734875	5.879063175	17.98044254
H	18.00713461	5.401861077	18.3083147
C	7.602286064	3.582178235	14.95229772
H	6.543336381	3.715840346	15.15739136
C	11.328768	2.657121997	18.05037074
H	10.70959717	2.21841335	17.27306296
C	8.014766511	2.708785644	13.94549701
H	7.278727647	2.15755108	13.36622852
C	9.376091342	2.548101492	13.68345875
H	9.703412549	1.871040783	12.89874562
C	14.57053955	1.212753866	13.76789755
H	14.62639471	0.745308069	12.78834183

$(Ph_3Si)_2O$, 130°

-2044.26878626602 Hartrees

atom	x	y	z
Si	11.20991672	5.052078151	16.42664705
Si	14.00271235	5.094682502	15.19751444
C	9.865336464	4.151684496	15.45712984
C	16.50038796	7.234516883	18.55809728
H	17.0850731	7.747358461	19.3171846
C	14.97803837	5.898459024	16.59236615
C	14.5351133	5.846164787	13.55119046
C	10.08224907	9.040518383	16.91129659
H	10.13797195	9.949506048	16.3181017
C	11.79756777	3.958084282	17.84776589

C	15.89258208	6.059465195	13.25071458
H	16.65451706	5.818164622	13.98889084
O	12.37358544	5.503968532	15.29568953
C	14.30083304	3.23104055	15.1450751
C	10.59898016	7.847229418	16.40625828
H	11.05770158	7.837886586	15.42092678
C	13.58462084	6.19464939	12.57534499
H	12.52832842	6.052594691	12.78645553
C	10.54579494	6.657026237	17.15510738
C	9.495514322	9.067851366	18.17776899
H	9.093510139	9.996993325	18.57298994
C	14.56229226	7.13763898	17.11557554
H	13.63899549	7.58985223	16.76274146
C	14.32178444	2.570481002	13.90095416
H	14.17981769	3.14137553	12.98704133
C	12.54255131	2.348310496	20.04472225
H	12.82864429	1.729031182	20.8909389
C	10.19250107	3.284888239	14.39790803
H	11.23266547	3.144572243	14.11539322
C	16.28734912	6.5893334	12.02233253
H	17.3425266	6.74626654	11.81417453
C	15.32803403	6.922557371	11.06368479
H	15.63359347	7.336741312	10.10667072
C	16.18098987	5.352415606	17.0747838
H	16.532338	4.396913634	16.69434325
C	14.73282496	1.079526797	16.21594672

H	14.89254977	0.502943266	17.12309639
C	12.57614219	4.478156701	18.90059464
H	12.89752164	5.51536844	18.87671786
C	15.31175207	7.79740336	18.08958867
H	14.9688326	8.750688021	18.48284089
C	9.430614842	7.898912179	18.93643681
H	8.979638739	7.915472109	19.92527856
C	9.95369733	6.708182945	18.42983805
H	9.910659888	5.810629805	19.04174603
C	14.7418833	0.445946184	14.97285694
H	14.91221189	-0.625534068	14.90764517
C	14.5136204	2.454696993	16.30004203
H	14.50184951	2.923741244	17.27908376
C	12.95057586	3.682259175	19.98350332
H	13.55576967	4.104628251	20.78117294
C	8.505576951	4.303601561	15.78265498
H	8.21562637	4.976810675	16.58592113
C	13.97531296	6.726009989	11.34433908
H	13.22258304	6.988476055	10.60541031
C	11.76119755	1.815810357	19.01905454
H	11.43572853	0.779874751	19.06384585
C	16.93513543	6.011845955	18.04703815
H	17.85983872	5.568610836	18.40741507
C	7.512633872	3.612500458	15.08682464
H	6.468624819	3.748559048	15.35681532
C	11.39463713	2.612883845	17.93410263

H	10.7858325	2.182453841	17.14424017
C	7.85900147	2.752696961	14.04341681
H	7.087173733	2.214312497	13.50009948
C	9.20244342	2.591277516	13.70004776
H	9.480161739	1.925757523	12.88683929
C	14.53406016	1.194276148	13.81378854
H	14.54462637	0.708032946	12.84187288

$(Ph_3Si)_2O$, 125°

-2044.26549473390 Hartrees

atom	**x**	**y**	**z**
Si	11.21900432	5.059873983	16.39771481
Si	13.96713709	5.09022842	15.20105743
C	9.843732299	4.16233262	15.46833057
C	16.40866722	7.314985232	18.54611626
H	16.98514159	7.850610996	19.29558479
C	14.90812755	5.919821346	16.60438145
C	14.56975287	5.814446542	13.56655321
C	10.06417224	9.036545542	16.90362132
H	10.08853112	9.941945211	16.30293683
C	11.83637822	3.956711039	17.7992599
C	15.9422395	5.971968733	13.30290342
H	16.67391434	5.700127113	14.06079661
O	12.33438913	5.521445986	15.21411795
C	14.26620141	3.225480086	15.16424213
C	10.58123318	7.847004567	16.39038754

H	11.00856057	7.836986594	15.39106205
C	13.65963269	6.200028395	12.56684043
H	12.59350716	6.100757769	12.75067413
C	10.56811075	6.660998546	17.14791731
C	9.516788757	9.064659461	18.18754965
H	9.114348959	9.990835529	18.58921399
C	14.47819687	7.166385894	17.09764484
H	13.55396493	7.603199405	16.72901314
C	14.24145784	2.560655923	13.92202955
H	14.0516127	3.126237059	13.01333471
C	12.58999065	2.320382205	19.97361403
H	12.88009741	1.690794724	20.81077252
C	10.12373923	3.384195557	14.33046292
H	11.14383449	3.315529682	13.96222802
C	16.39056952	6.484695437	12.08632143
H	17.45613391	6.598838591	11.90507004
C	15.47037036	6.855481631	11.10393282
H	15.8176091	7.256421911	10.15530446
C	16.11548529	5.397785125	17.10294209
H	16.48144508	4.440102108	16.74259924
C	14.78663456	1.085192266	16.21786745
H	14.99940229	0.514484714	17.11775585
C	12.59636591	4.47084453	18.86828782
H	12.89973852	5.513431565	18.86624628
C	15.21650151	7.854873711	18.0604
H	14.86232348	8.813363465	18.43026469

C	9.491332014	7.899981132	18.95484054
H	9.070685211	7.916714121	19.95693123
C	10.0143607	6.712738305	18.43963931
H	10.00098345	5.818863286	19.05826352
C	14.74881569	0.447590655	14.97761245
H	14.93593228	-0.620704652	14.90688448
C	14.54499857	2.456343827	16.309437
H	14.56535035	2.926548338	17.28760548
C	12.97498556	3.661908782	19.93998216
H	13.56569048	4.080292583	20.75043506
C	8.508133261	4.226544706	15.90502901
H	8.252245826	4.831784293	16.7715945
C	14.10403977	6.714240628	11.34701923
H	13.38319158	7.00646834	10.58771895
C	11.82646122	1.793112866	18.93181428
H	11.51900014	0.751018878	18.95469802
C	16.8584065	6.086289419	18.06328732
H	17.7870649	5.661538664	18.43542213
C	7.49478479	3.53510636	15.24027121
H	6.470253224	3.602073736	15.59692055
C	11.4549979	2.603321811	17.85865155
H	10.85970944	2.176891873	17.05650869
C	7.795287773	2.762743153	14.11693368
H	7.007352598	2.223906256	13.59771934
C	9.113066999	2.690034484	13.66286776
H	9.35481451	2.093572015	12.78696556

C	14.47222581	1.188184649	13.82798734
H	14.44539138	0.69943865	12.85766924

$(Ph_3Si)_2O$, 120°

-2044.26120952341 Hartrees

atom	x	y	z
Si	11.25940965	5.063692251	16.36435837
Si	13.95314374	5.096023562	15.18800827
C	9.85712193	4.171347281	15.47309299
C	16.27813551	7.398905511	18.56656674
H	16.82559708	7.949273236	19.32710493
C	14.848849	5.961873555	16.60024717
C	14.61736221	5.767798825	13.55089581
C	10.01731899	9.010031766	16.88941074
H	9.998809605	9.911872094	16.28312466
C	11.8897583	3.952090095	17.75389016
C	15.99580882	5.76753604	13.26908362
H	16.70026084	5.388743007	14.00680504
O	12.31949797	5.547519736	15.12877579
C	14.24282236	3.229835258	15.19992937
C	10.5628766	7.835092413	16.37233767
H	10.96794311	7.83222627	15.36375646
C	13.74982421	6.279695764	12.57046035
H	12.68137431	6.301109738	12.76534317
C	10.60511227	6.654168348	17.13668122
C	9.495253578	9.028090866	18.18405903

H	9.06942065	9.942577601	18.58841179
C	14.37846951	7.197197632	17.08373018
H	13.44938228	7.609076401	16.70028797
C	14.1377563	2.530441938	13.98159183
H	13.88540604	3.069342299	13.07185119
C	12.58714626	2.302568919	19.93798539
H	12.85379482	1.668486912	20.77962522
C	10.00717557	3.702812323	14.15717068
H	10.94566022	3.865947564	13.63567435
C	16.48862395	6.252328848	12.058237
H	17.55832725	6.242283857	11.86574779
C	15.6089089	6.752708559	11.09541615
H	15.99087301	7.131579771	10.15128983
C	16.06315428	5.474998228	17.11837247
H	16.46342219	4.528674495	16.76501526
C	14.84426639	1.122351386	16.275273
H	15.11918612	0.577778139	17.17460774
C	12.61847412	4.460525311	18.84697228
H	12.91707394	5.50411431	18.86129415
C	15.08095424	7.90590222	18.05890756
H	14.69344285	8.854079615	18.42189818
C	9.523688611	7.867810378	18.95766643
H	9.121631129	7.876210052	19.96754595
C	10.07504326	6.695433341	18.43846996
H	10.1009931	5.804867959	19.0612291
C	14.72650407	0.450101882	15.05860402

H	14.91419129	-0.619189825	15.00527108
C	14.5995565	2.494117493	16.34482075
H	14.67448183	2.989896061	17.30736286
C	12.96891464	3.645365806	19.92385282
H	13.53347047	4.060528252	20.75440562
C	8.621969871	3.953841366	16.1113583
H	8.464782251	4.315535525	17.12523618
C	14.2383236	6.766022397	11.35535324
H	13.54744333	7.156610134	10.61255302
C	11.85664914	1.779884028	18.87049314
H	11.55270073	0.736535765	18.87680699
C	16.7701875	6.183386548	18.09087177
H	17.703656	5.78421385	18.47906558
C	7.581800347	3.287239578	15.46571225
H	6.636176648	3.13141561	15.97841591
C	11.51329076	2.596327101	17.79305517
H	10.94183161	2.172737497	16.97278258
C	7.755209223	2.822415781	14.16050134
H	6.945907607	2.301649161	13.6554696
C	8.96907605	3.03277388	13.50695979
H	9.107947904	2.676409055	12.48954694
C	14.36720771	1.156745383	13.91031783
H	14.27537893	0.640299162	12.95854692

$(Ph_3Si)_2O$, 115°

-2044.25581201749 Hartrees

atom	x	y	z
Si	11.27994318	5.06173499	16.336281
Si	13.9160977	5.083190892	15.18232797
C	9.854246267	4.14043918	15.50899501
C	16.18063576	7.418091153	18.58080608
H	16.71787332	7.977893597	19.34156039
C	14.77632363	5.955497188	16.61365964
C	14.65691595	5.759053492	13.57802731
C	10.0228052	9.010184023	16.82009961
H	9.989940937	9.901663099	16.19938587
C	11.94240076	3.975414329	17.73301052
C	16.04453169	5.725248091	13.34732538
H	16.71010517	5.314851235	14.10412453
O	12.28138843	5.542183525	15.03862172
C	14.19378947	3.214271476	15.17548823
C	10.57106379	7.830973497	16.31549435
H	10.96396869	7.81463041	15.30224761
C	13.84159937	6.310977381	12.5749576
H	12.7675132	6.359076723	12.73046705
C	10.63210983	6.662201416	17.09766578
C	9.516188027	9.045345876	18.12033749
H	9.088235717	9.96292187	18.51513923
C	14.31765264	7.211838364	17.05290793
H	13.40794729	7.631975532	16.63423444
C	14.03748563	2.534094257	13.95134828
H	13.74695687	3.087341396	13.06171292

C	12.63899241	2.356563309	19.94128072
H	12.90468638	1.734774076	20.79218787
C	9.908414126	3.777413774	14.1529499
H	10.79014884	4.027291705	13.57035052
C	16.59583371	6.215517945	12.16431395
H	17.67134684	6.178588499	12.01190653
C	15.76713765	6.756291357	11.17852737
H	16.19444864	7.139953174	10.25614102
C	15.96978226	5.462702732	17.17414492
H	16.36684233	4.50416393	16.85216085
C	14.84121769	1.089243889	16.1891322
H	15.1537402	0.530605589	17.06724511
C	12.64037381	4.50708542	18.83534896
H	12.91429501	5.557045233	18.84843216
C	15.00697812	7.932537469	18.02868717
H	14.62731357	8.89647539	18.35641777
C	9.561502228	7.897451152	18.9113237
H	9.170331274	7.91859039	19.92521155
C	10.11488929	6.720797712	18.40421442
H	10.15162269	5.84034041	19.0404746
C	14.67165694	0.436872149	14.96814199
H	14.85691794	-0.631082407	14.88922612
C	14.59750564	2.45926819	16.29151723
H	14.70753289	2.938000686	17.25860806
C	12.99022788	3.707221003	19.92383086
H	13.53041337	4.141311766	20.76073235

C	8.690585848	3.812951156	16.23034308
H	8.608723133	4.085362239	17.28048859
C	14.3888344	6.803460131	11.38759187
H	13.7373239	7.225586106	10.62674591
C	11.9395677	1.810006549	18.86513361
H	11.65954875	0.760133548	18.8731793
C	16.66343915	6.183416247	18.14721043
H	17.58027889	5.778823466	18.56784555
C	7.628220807	3.144177383	15.62481325
H	6.739648857	2.902424416	16.20211257
C	11.59707159	2.610837867	17.77606667
H	11.05009752	2.168625139	16.94926196
C	7.70663049	2.785933733	14.27748474
H	6.880150356	2.262898802	13.80378411
C	8.847879138	3.104583592	13.54269032
H	8.913092036	2.83049162	12.49295714
C	14.26287308	1.161995692	13.84843263
H	14.12923223	0.661224671	12.89340501

4.10 References and Notes

(1) (a) Ramirez, F.; Hansen, B.; Desai, N. B.; McKelvie, N. *J. Am. Chem. Soc.* **1961**, *83*, 3539-3540.
(b) Gasser, O.; Schmidbaur, H. *J. Am. Chem. Soc.* **1975**, *97*, 6281-6282.

(2) (a) Schmidbaur, H. "Carbodiphosphorane" *Nachr. Chem. Tech. Lab.* **1979**, *27*, 620-622.
(b) Schmidbaur, H.; Schier, A. *Angew. Chem. Int. Edit.* **2013**, *52*, 176-186.
(c) Kolodiazhnyi, O. I. *Tetrahedron* **1996**, *52*, 1855-1929.

(3) (a) Frenking, G.; Tonner, R. *Pure Appl. Chem.* **2009**, *81*, 597-614.
(b) Tonner, R.; Frenking, G. *Chem. Eur. J.* **2008**, *14*, 3260-3272.
(c) Frenking, G.; Tonner, R.; Klein, S.; Takagi, N.; Shimizu, T.; Krapp, A.; Pandey, K. K.; Parameswaran, P. *Chem. Soc. Rev.* **2014**, *43*, 5106-5139.

(4) (a) Tonner, R.; Oexler, F.; Neumuller, B.; Petz, W.; Frenking, G. *Angew. Chem. Int. Edit.* **2006**, *45*, 8038-8042.
(b) Schmidbaur, H. *Angew. Chem. Int. Edit.* **2007**, *46*, 2984-2985.
(c) Frenking, G.; Neumuller, B.; Petz, W.; Tonner, R.; Oxler, F. *Angew. Chem. Int. Edit.* **2007**, *46*, 2986-2987.

(5) (a) de Fremont, P.; Marion, N.; Nolan, S. P. *Coord. Chem. Rev.* **2009**, *253*, 862-892.
(b) Crabtree, R. H. *Coord. Chem. Rev.* **2013**, *257*, 755−766.
(c) Dyker, A.; Bertrand, G. *Nat. Chem.* **2009**, *1*, 265−266.
(d) Martin, D.; Melaimi, M.; Soleilhavoup, M.; Bertrand, G. *Organometallics* **2011**, *30*, 5304−5313.

(6) Parkin G. *J. Chem. Educ.* **2006**, *83*, 791-799.

(7) (a) Kaska, W. C.; Mitchell, D. K.; Reichelderfer, R. F. *J. Organomet. Chem.* **1973**, *47*, 391-402.
(b) Kaska, W. C. *Coord. Chem. Rev.* **1983**, *48*, 1-58.
(c) Kaska, W. C.; Ostoja Starzwski, K. A. Transition metal complexes with ylides In *Ylides and imines of phosphorus*; Johnson, A. W., Ed.; Kaska, W. C., Ostoja Starzewski, K. A., Dixon, D. A., Special Contributors; Wiley: New York, 1993.

(8) Alcarazo, M.; Lehmann, C. W.; Anoop, A.; Thiel, W.; Furstner, A. "Coordination chemistry at carbon" *Nat. Chem.* **2009**, *1*, 295-301.

(9) (a) Petz, W. *Coord. Chem. Rev.* **2015**, *291*, 1-27.
(b) Schmidbaur, H.; Zybill, C. E.; Neugebaur, D. *Angew. Chem. Int. Ed. Engl.* **1982**, *21* 310-311.
(c) Kaufhold, O.; Hahn, F. E. *Angew. Chem. Int. Ed.* **2008**, *47* 4057-4061.
(d) Petz, W.; Frenking, G. *Top. Organomet. Chem.* **2010**, *30*, 49-92.

(e) Kubo, K.; Jones, N. D.; Ferguson, M. J.; McDonald, R.; Cavell, R. G. *J. Am. Chem. Soc.* **2005**, *127*, 5314-5315.

(10) Glendening, E. D.; Weinhold, F. *J Comput. Chem.* **1998**, *19*, 593-609.

(11) Ellis, B. D.; Macdonald, C. L. B. *Coord. Chem. Rev.* **2007**, *251*, 936-973.

(12) (a) Green, M. L. H. *J. Organomet. Chem.* **1995**, *500*, 127-148.
(b) Parkin, G. in *Comprehensive Organometallic Chemistry III*, Volume 1, Chapter 1.01; Crabtree, R. H. and Mingos, D. M. P. (Eds), Elsevier, Oxford, 2006.
(c) Green, J. C.; Green, M. L. H.; Parkin, G. *Chem Commun.* **2012**, *48*, 11481-11503.
(d) Green, M. L. H.; Parkin, G. *J. Chem. Educ.* **2014**, *91*, 807-816.

(13) Morosaki, T.; Suzuki, T.; Fujii, T. *Organometallics* **2016**, *35*, 2715-2721.(14) Petz, W.; Kuzu, I.; Frenking, G.; Andrada, D. M.; Neumuller, B.; Fritz, M.; Munzer, J. E. *Chem. Eur. J.* **2016**, *22*, 8536-8546.

(15) Alcarazo, M.; Radkowski, K.; Mehler, G.; Goddard, R.; Fürstner, A. *Chem. Commun*. **2013**, *49*, 3140−3142.

(16) (a) Hardy, G. E.; Kaska, W. C.; Chandra, B. P.; Zink, J. I. *J. Am. Chem. Soc.* **1981**, *103*, 1074−1079.
(b) Vincent, A. T.; Wheatley, P. J. *J. Chem. Soc., Dalton Trans.* **1972**, 617−622.

(17) (a) Schmidbaur, H.; Hasslberger, G.; Deschler, U.; Schubert, U.; Kappenstein, C.; Frank, A. *Angew. Chem., Int. Ed. Engl.* **1979**, *18*, 408−409.
(b) Schubert, U.; Kappenstein, C.; Milewskimahrla, B.; Schmidbaur, H. *Chem. Ber.* **1981**, *114*, 3070−3078.

(18) Ebsworth, E. A. V.; Fraser, T. E.; Rankin, D. W. H.; Gasser, O.; Schmidbaur, H. *Chem. Ber.* **1977**, *110*, 3508−3516.

(19) Appel, R.; Baumeister, U.; Knoch, F. *Chem. Ber.* **1983**, *116*, 2275−2284.

(20) For other calculations on $(Ph_3P)_2C$, see ref. 3 and 4a.

(21) Previous calculations have shown that linear and bent forms have similar energies, but conformational differences were not discussed. See ref. 3.

(22) The data for $(Ph_3P)_2C$ in Figure 5 and Figure 7 correspond to geometries derived initially from conformation B in Figure 4. Other conformations were also considered and were observed to have similar energies.

(23) For other calculations on $(H_3P)_2C$ see ref. 3b and:
(a) Petz, W.; Weller, F.; Uddin, J.; Frenking, G. *Organometallics* **1999**, *18*, 619−626.
(b) Albright, T. A.; Hofmann, P.; Rossi, A. R. *Z Naturforsch, B: J Chem. Sci.* **1980**,

35b, 343−351.
(c) Carroll, P. J.; Titus, D. D. *J. Chem. Soc., Dalton Trans.* **1977**, 824−829.

(24) Examining NLMOs for this type of study is appropriate because NLMOs take into account mixing between bonding and antibonding orbitals, and therefore give an improved electronic picture for delocalized structures such as $(Ph_3P)_2C$. See:
(a) Reed, A. E.; Weinhold, F. *J. Chem. Phys.* **1985**, *83*, 1736-1740
(b) Glendening, E. D.; Landis, C. R.; Weinhold, F. *J. Comput. Chem.* **2013**, *34*, 1429-1437.

(25) Albright, T. A.; Burdett, J. K.; Whangbo, M.-H. *Orbital Interactions in Chemistry*, 2nd ed.; John Wiley & Sons, Inc.; New York, 2013.

(26) As would be expected, the two P–C bonding NLMOs possess more phosphorus character than do the lone pairs. For example, the P–C bonding NLMOs of the linear form possess an average of 37.5% phosphorus character, which increases to 40.7% for a P–C–P angle of 120˚.

(27) Lewis, G. R.; Dance, I. *J. Chem. Soc. Dalton Trans.* **2000**, 299-306.

(28) Despite the widespread use of $[(Ph_3P)_2N]^+$ as a counterion, there are examples in which it associates with varying degrees with a metal center and may also undergo reaction. See, for example:
(a) Sussman, V. J.; Ellis, J. E. *Chem. Commun.* **2008**, 5642-5644.
(b) Bauzá, A.; Frontera, A.; Mooibroek, T. J.; Reedijk, J. *CrystEngComm* **2015**, *17*, 3768-3771.
(c) Tilset, M.; Zlota, A. A.; Folting, K.; Caulton, K. G. *J. Am. Chem. Soc.* **1993**, *115*, 4113-4119.
(d) Darensbourg, M.; Barros, H.; Borman, C. *J. Am. Chem. Soc.* **1977**, *99*, 1647-1648.
(e) Ragaini, F.; Sironi, A.; Fumagalli, A. *Chem. Commun.* **2000**, 2117-2118.
(f) Bolli, C.; Gellhaar, J.; Jenne, C.; Kessler, M.; Scherer, H.; Seeger, H.; Uzun, R. *Dalton Trans.* **2014**, *43*, 4326-4334.

(29) Churchill, M. R.; Lake, C. H.; Wang, P.; Atwood, J. D. *J. Chem. Crystallogr.* **1994**, *24*, 473-476 and references cited therein.

(30) (a) Wilson, R. D.; Bau, R. *J. Am. Chem. Soc.* **1974**, *96*, 7601-7602.
(b) Kirtley, S. W.; Chanton, J. P.; Love, R. A.; Tipton, D. L.; Sorrell, T. N.; Bau, R. *J. Am. Chem. Soc.* **1980**, *102*, 3451-3460.
(c) Haiduc, I.; Cea-Olivares, R.; Hernández-Ortega, S.; Silvestru, C. *Polyhedron* **1995**, *14*, 2041-2046.

(31) Cambridge Structural Database, CSD version 5.39

(32) The energy surfaces for $[(Ph_3P)_2N]^+$ and $(Ph_3Si)_2O$ correspond to conformations that are similar to those of $(Ph_3P)_2C$.

(33) (a) Hönle, W.; Manríquez, V.; von Schnering, H. G. *Acta Crystallogr.* **1990**, *C46*, 1982-1984.
(b) Purdy, A. P.; Smoot, E.; Butcher, R. J.; Kerr, A. *Acta Cryst.* 2012, *E68*, o588.
(c) Percino, J.; Pacheco, J. A.; Soriano-Moro, G.; Ceron, M.; Castro, M. E.; Chapela, V. M.; Bonilla-Cruz, J.; Lara-Ceniceros, T. E.; Flores-Guerrero, M.; Saldivar-Guerra, E. *RSC Adv.* **2015**, *5*, 79829-79844.
(d) Prince, P. D.; Bearpark, M. J.; McGrady, G. S.; Steed, J. W. *Dalton Trans.* **2008**, 271-282.

(34) (a) Karle, I. L.; Karle, J. M.; Nielsen, C. J. *Acta Cryst.* **1986**, *C42*, 64-67.
(b) Pietschnig, R.; Merz, M. *Organometallics* **2004**, *23*, 1373-1377.

(35) (a) You, S.-L.; Razavi, H.; Kelly, J. W. *Angew. Chem. Int. Ed.* **2003**, *42*, 83-85.

(36) (a) Cypryk, M.; Gostynski, B. *J. Mol. Model.* **2016**, *22*, 35.
(b) Weinhold, F.; West, R. *Organometallics* **2011**, *30*, 5815-5824.
(c) Csonka, G. I.; Reffy, J. *Chem. Phys. Lett.* **1994**, *229*, 191-197.
(d) Zhang, Y.; Li, Z. H.; Truhlar, D. G. *J. Chem. Theory Comput.* **2007**, *3*, 593-604.
(e) Shambayati, S.; Blake, J. F.; Wierschke, S. G.; Jorgensen, W. L.; Schreiber, S. L. *J. Am. Chem. Soc.* **1990**, *112*, 697-703.

(37) (a) McNally, J. P.; Leong, V. S.; Cooper, N. J. in *Experimental Organometallic Chemistry*, Wayda, A. L.; Darensbourg, M. Y., Eds.; American Chemical Society: Washington, DC, 1987; Chapter 2, pp 6-23.
(b) Burger, B.J.; Bercaw, J. E. in *Experimental Organometallic Chemistry*; Wayda, A. L.; Darensbourg, M. Y., Eds.; American Chemical Society: Washington, DC, 1987; Chapter 4, pp 79-98.
(c) Shriver, D. F.; Drezdzon, M. A.; *The Manipulation of Air-Sensitive Compounds*, 2nd Edition; Wiley-Interscience: New York, 1986.

(38) Appel, R.; Knoll, F.; Scholer, H.; Wihler, H. *Angew. Chem. Int. Edit. Engl.* **1976**, *11*, 702-703.

(39) (a) Sheldrick, G. M. SHELXTL, An Integrated System for Solving, Refining, and Displaying Crystal Structures from Diffraction Data; University of Göttingen, Göttingen, Federal Republic of Germany, 1981.
(b) Sheldrick, G. M. *Acta Cryst.* **2008**, *A64*, 112-122.
(c) Sheldrick, G. M. *Acta Cryst.* **2015**, *A71*, 3-8.

(40) (a) Jaguar, version 8.9, Schrodinger, Inc., New York, NY, 2015.
(b) Bochevarov, A. D.; Harder, E.; Hughes, T. F.; Greenwood, J. R.; Braden, D. A.; Philipp, D. M.; Rinaldo, D.; Halls, M. D.; Zhang, J.; Friesner, R. A. *Int. J. Quantum Chem.* **2013**, *113*, 2110–2142.

(41) (a) Becke, A. D. *J. Chem. Phys.* **1993**, *98*, 5648-5652.
(b) Becke, A. D. *Phys. Rev. A* **1988**, *38*, 3098-3100.
(c) Lee, C. T.; Yang, W. T.; Parr, R. G. *Phys. Rev. B* **1988**, *37*, 785-789.

(d) Vosko, S. H.; Wilk, L.; Nusair, M. *Can. J. Phys.* **1980**, *58*, 1200-1211.
(e) Slater, J. C. *Quantum Theory of Molecules and Solids, Vol. 4: The Self-Consistent Field for Molecules and Solids*; McGraw-Hill: New York, 1974.

(42) NBO 6.0. Glendening, E. D.; Badenhoop, J. K.; Reed, A. E.; Carpenter, J. E.; Bohmann, J. A.; Morales, C. M.; Landis, C. R.; Weinhold, F. (Theoretical Chemistry Institute, University of Wisconsin, Madison, WI, 2013); http://nbo6.chem.wisc.edu/.

CHAPTER 5

Synthesis, Structural Characterization, and Reactivity of Main Group and Transition Metal Complexes supported by Hexaphenylcarbodiphosphorane

Table of Contents

5.1 Introduction

In addition to their flexible nature,[1] carbodiphosphoranes,[2-6] which feature a two-coordinate carbon center with *two* lone-pairs of electrons, are also effective ligands for a variety metals and nonmetals.[7-9] While carbodiphosphoranes are similar to carbenes by virtue of both being effective σ–donors,[5a,b,10,11] there are several cases where the reactivity varies due to the different electronic structures of carbodiphosphoranes and carbenes, which will be discussed below.

This chapter outlines *i*) a literature summary of the general reactivity of carbodiphosphoranes towards a variety of substrates, *ii*) a detailed spectroscopic characterization of $(Ph_3P)_2C$, and *iii*) the reactivity of $(Ph_3P)_2C$ towards main group and transition metal alkyl and aryl complexes.

5.2 General Reactivity Patterns of Carbodiphosphoranes

There are several ways carbodiphosphoranes can react, the most common of which is to coordinate to a metal or nonmetal in an L-type[12] fashion to form a simple Lewis acid/base adduct (Scheme 1a).[8b,13-26] In this coordination mode, the σ-type lone-pair donates both electrons to form a dative bond and the π-type lone pair is maintained on the central carbon.[27] Also, because there are two lone pairs, it is possible to coordinate two metals (Scheme 1b).[28] However, in order to coordinate two metal centers, the reagents used must be appropriately sized, as bulky reagents will only lead to coordination of one metal center; thus, metal reagents such as AuCl or CuCl are well suited for carbodiphosphoranes to coordinate two metals. Furthermore, if the Lewis acid and carbodiphosphorane are sufficiently bulky, a frustrated Lewis acid/base pair can be formed, as demonstrated by $(Ph_3P)_2C$ and $(C_6F_5)_3B$.[29] Additionally, due to the

presence of second lone pair, it is also possible to have π-donation to form a double bond (Scheme 1c) if a vacant orbital is available on the substrate, [9a,30,31] as demonstrated by the cation $[(Ph_3P)_2C{=}BH_2]^+$.[32]

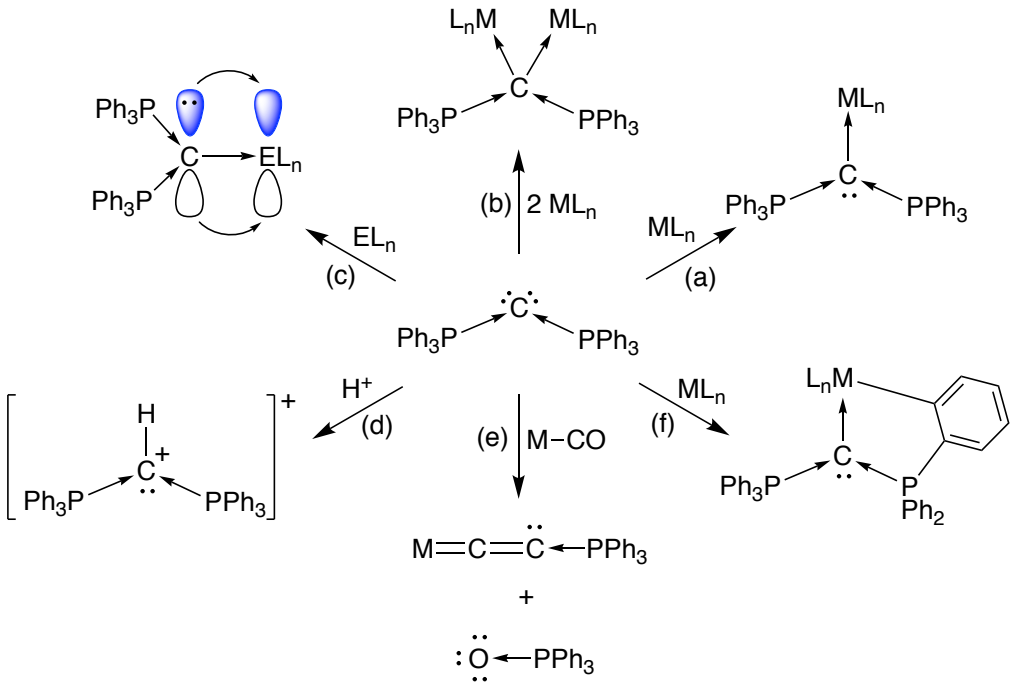

Scheme 1. Representative reactions of carbodiphosphoranes. (a) simple Lewis acid/base adduct, (b), coordination of two metals, (c) π-donation to form a double bond, (d) protonation, (e)Wittig-type reaction with metal carbonyls, (f) ortho metalation.

Carbodiphosphoranes are also susceptible to protonation (Scheme 1d). As pointed out in the seminal reported synthesis, [2a] the basicity of $(Ph_3P)_2C$ (to form $[HC(PPh_3)_2]^+$) is comparable to KOH, such that it can be considered a strong base.[5c,6a,33] Due to the presence of the additional lone-pair, it is also possible to doubly protonate $(Ph_3P)_2C$, forming the dication $[H_2C(PPh_3)_2]^{2+}$. However, $[HC(PPh_3)_2]^+$ is not as basic as $(Ph_3P)_2C$.[5c,6a,8c] The reactivity of the protonated species has also recently been investigated, and $[HC(PPh_3)_2]^+$ is capable of coordinating metal centers, as well as acting

as a counterion.[18,34,35] It should also be noted that $(Ph_3P)_2C$ will readily react with H_2O to yield $(Ph_3P)(Ph_2OP)CH$ and C_6H_6 as illustrated in Scheme 2.[2,36]

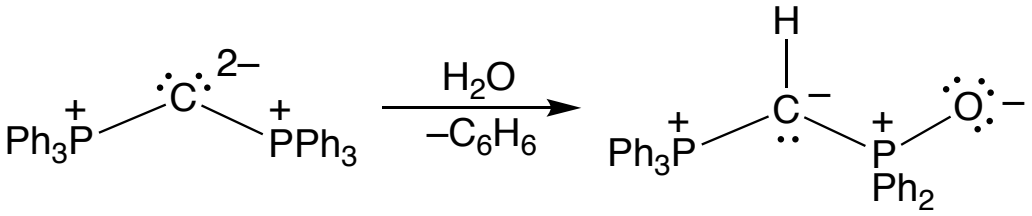

Scheme 2. Reactivity of $(Ph_3P)_2C$ towards H_2O.

It is also possible for carbodiphosphoranes to undergo a Wittig-type reaction with metal carbonyls. For example, rather than simply coordinate to the metal center of a $M(CO)_n$ complex, $(Ph_3P)_2C$ reacts with one of the CO ligands to form Ph_3PO and the M=C=C–PPh_3 fragment as illustrated in Scheme 1e.[37,38] A notable exception to this is the reactivity of $(Ph_3P)_2C$ towards $Ni(CO)_4$ which forms $[(Ph_3P)_2C]Ni(CO)_3$ and $[(Ph_3P)_2C]Ni(CO)_2$.[39]

Interestingly, carbodiphosphoranes with phenyl groups are also capable of undergoing ortho metalation to achieve a bidentate coordination mode (Scheme 1f).[40] This is typically observed with noble transition metals that also possess ligands (such as methyl or halides) that are susceptible to reductive elimination with the resulting M–H intermediate that is formed. A double ortho metalation to form a C_3-pincer ligand has also been observed.[40a,41] For example, $(Ph_3P)_2C$ reacts with $Me_2Pt(SMe_2)_2$ to yield $[\kappa^3$-(C,C,C)-$(Ph_2(C_6H_4)P)_2C]Pt(SMe_2)$.[40a]

Beyond carbodiphosphoranes that feature the same R-group for each phosphine, such as $(Ph_3P)_2C$ or $(Me_3P)_2C$, carbodiphosphoranes and carbodiphosphorane-like complexes have been modified to include various groups, such as sulfoxides.[42] Additionally,

carbodiphosphoranes have been modified to incorporate donor atoms,[43] such as $(Ph_3P)C(Ph_2Py)$[28b] and $(dppm)_2C$[44], which can provide a chelating coordination environment. The growing interest in the field of carbodiphosphoranes will certainly lead to even more interesting variations, leading to new areas of coordination chemistry.

5.3 Synthesis and Spectroscopic Characterization of $(Ph_3P)_2C$

$(Ph_3P)_2C$ can be synthesized via a two-step process developed by Appel *et. al.* as illustrated in Scheme 3.[45,46] Specifically, a solution of PPh_3 in CH_2Cl_2 is treated with CCl_4 and stirred for 6 hours. The resulting suspension that is formed is then treated with 1,2-epoxybutane to yield the intermediate salt $[(PPh_3)–C(Cl)–(PPh_3)]Cl$. Subsequent treatment of the tri-coordinate intermediate salt with $P[(NMe_2)]_3$ results in the production of $(Ph_3P)_2C$. $(Ph_3P)_2C$ possesses a strong yellow color and reacts vigorously with moisture, and so care must be taken to ensure all solvents are purified properly and $(Ph_3P)_2C$ is only handled under inert atmospheres.

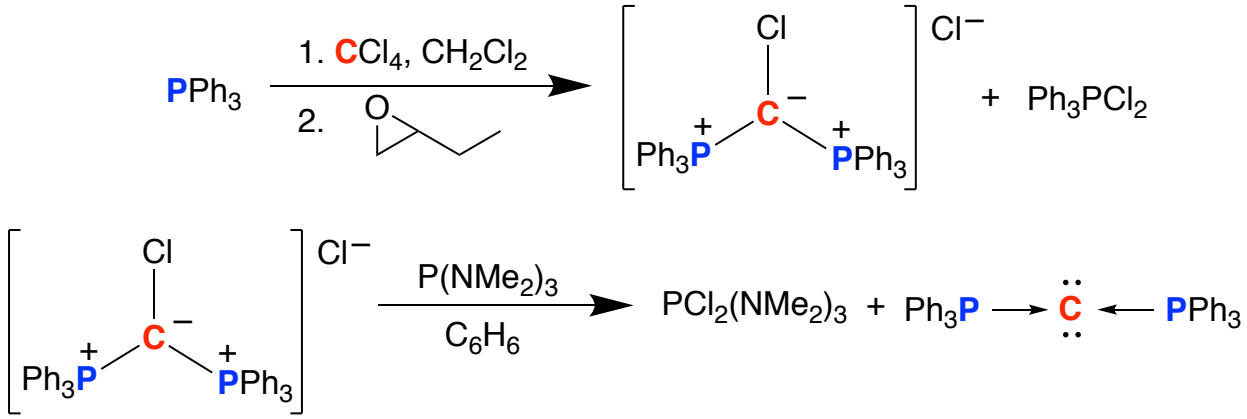

Scheme 3. Synthesis of $(Ph_3P)_2C$.

Interestingly, despite the fact $(Ph_3P)_2C$ was first synthesized in 1961,[2] the NMR spectroscopic data has only recently been documented in the literature,[47] after our research was in progress. Regardless, it still warrants discussion as this seemingly simple molecule possess complex spectroscopic features.

In the $^{13}C\{^1H\}$ NMR spectrum of $(Ph_3P)_2C$, the central carbon atom resonance appears as a triplet at 12.88 ppm ($^1J_{C(central)–P}$ = 126 Hz) corresponding to an A_2X pattern (Figure 1)[48] that is consistent with coupling to two magnetically equivalent, spin ½, phosphorus atoms. Interestingly, upon initial inspection, the ipso carbon signal has the appearance of a "quintet" with a chemical shift of 138.14 ppm (Figure 1). However, this multiplet arises as a result of virtual coupling. That is, in addition to the large $^1J_{C(ipso)–P}$ and small $^3J_{C(ipso)–P}$ couplings, both phosphorus atoms are also strongly coupled ($^2J_{P–P}$), leading to the formation of an AA'X signal.

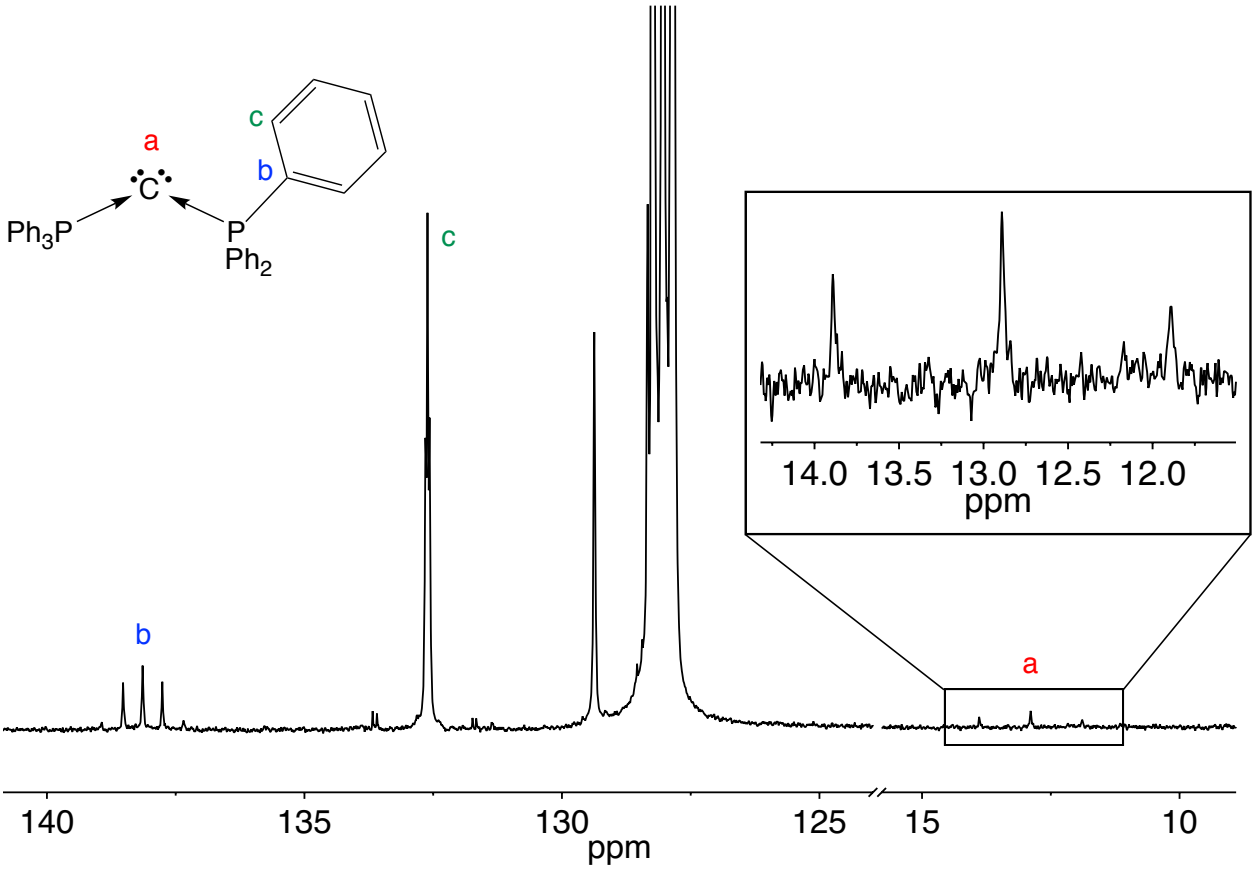

Figure 1. $^{13}C\{^{1}H\}$ NMR spectrum of $(Ph_3P)_2C$, (a) central carbon signal, (b) *ipso*-carbon siganal, (c) *ortho*-carbon signal.

To demonstrate how this multiplet arises, the AA'X spin system was simulated (Figure 2). If no coupling between the phosphorus atoms is present, ($^{2}J_{P-P} = 0$ Hz), a simple doublet would be observed (bottom spectra of Figure 2). However, as the $^{2}J_{P-P}$ coupling constant is increased, the appearance of the "inner peak" and "outer peaks" begin to emerge.[49] The ipso carbon peak is best simulated with the following parameters: $^{2}J_{P-P}$ = 90 Hz, $^{1}J_{C(ipso)-P} = 88$ Hz, and $^{3}J_{C(ipso)-P} = 7$ Hz as illustrated in Figure 3.[50]

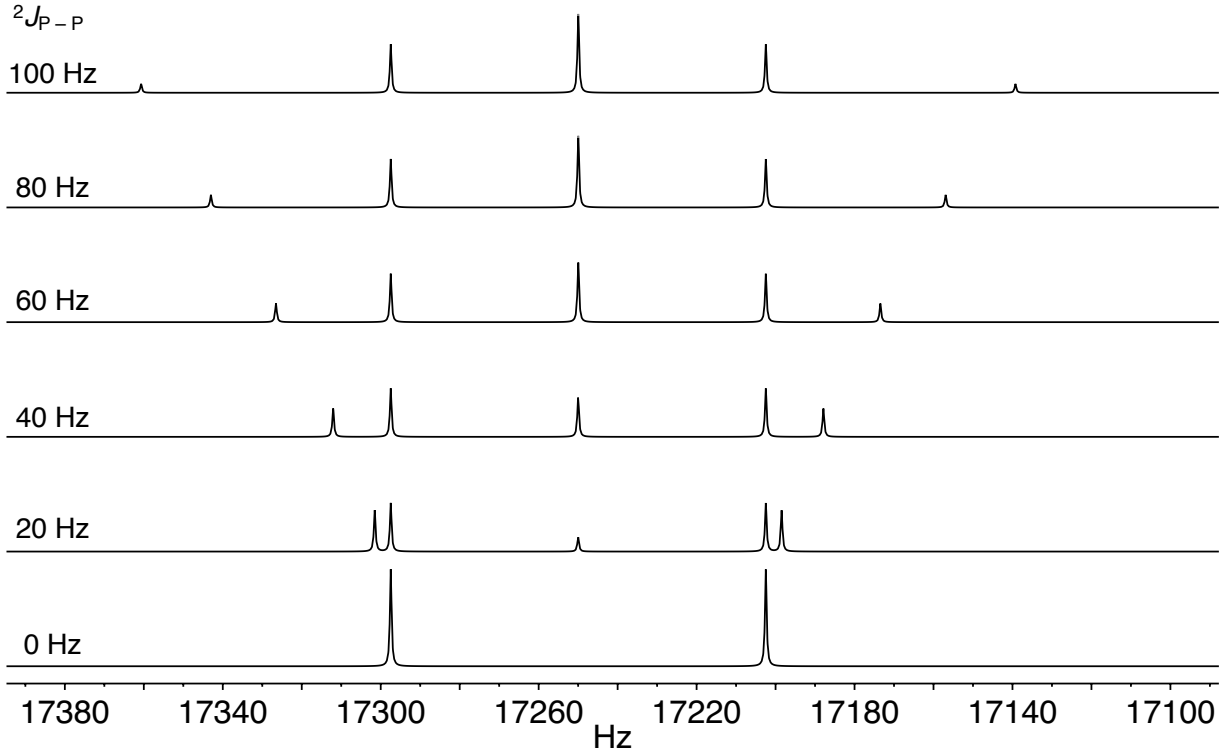

Figure 2. Spin simulation of AA′X multiplet (corresponds to the ipso-^{13}C NMR signal for $(Ph_3P)_2C$). $^2J_{A-X}$ is held constant at 95 Hz and $^2J_{A-A'}$ is incrementally increased from 0 Hz to 100 Hz.

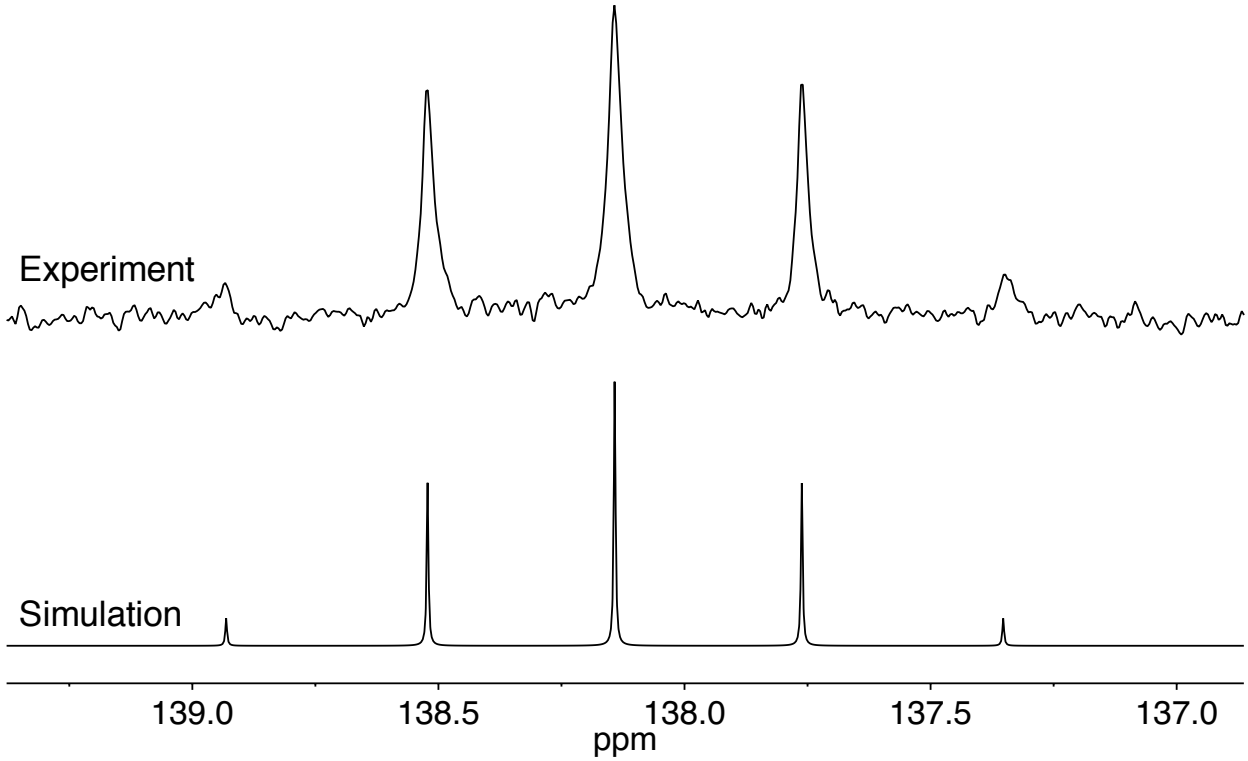

Figure 3. Simulated and experimental $^{13}C\{^{1}H\}$ NMR signal for the ipso-carbon of $(Ph_3P)_2C$. $^{2}J_{P-P}$ = 90 Hz, $^{1}J_{C(ipso)-P}$ = 88 Hz, and $^{3}J_{C(ipso)-P}$ = 7 Hz.

Additionally, the ^{13}C-ortho signal appears as a virtual triplet in the $^{13}C\{^{1}H\}$ NMR spectrum at 132.61 ppm (Figure 1). The $^{2}J_{C(ortho)-P}$ is much smaller than $^{1}J_{C(ipso)-P}$ and is reproduced well with the following parameters: $^{2}J_{C(ortho)-P}$ = 10 Hz and $^{2}J_{P-P}$ = 90 Hz. Also, the meta and para signals appear at 129.40 and 127.79 ppm.[51] It is also worth noting that a similar $^{2}J_{P-P}$ coupling constant of 85 Hz is observed for the pyridine substituted carbodiphosphorane, $(Ph_3P)C(Ph_2Py)$,[28b] which can be measured directly since the phosphorus atoms have different chemical shifts.

In addition to the singlet at –4.05 ppm[52] that is observed for the chemically equivalent phosphorus atoms in the $^{31}P\{^{1}H\}$ NMR spectrum of $(Ph_3P)_2C$, two sets of ^{13}C-satellite

signals also appear (Figure 4). The first corresponds to the A_2X pattern derived from ^{31}P-coupling to the isotopomer with ^{13}C located in the central position, and the second consists of an AA'X pattern where the ^{31}P-coupling is to the isotopomer with a ^{13}C-atom substituted at the ipso-position (Figure 4). Statistically, the AA'X pattern is more likely to occur than the A_2X pattern (i.e., there are six ipso carbons vs. one central carbon), and thus, the AA'X pattern is more intense. The ^{13}C-satellite A_2X and AA'X patterns are reproduced well *via* spin simulation using all the above parameters ($^2J_{P-P}$ = 90 Hz, $^1J_{C(ipso)-P}$ = 88 Hz, $^3J_{C(ipso)-P}$ = 7 Hz, and $^1J_{C(central)-P}$ = 126 Hz).[53] For further discussion of ^{31}P and ^{13}C couplings, see reference 47.

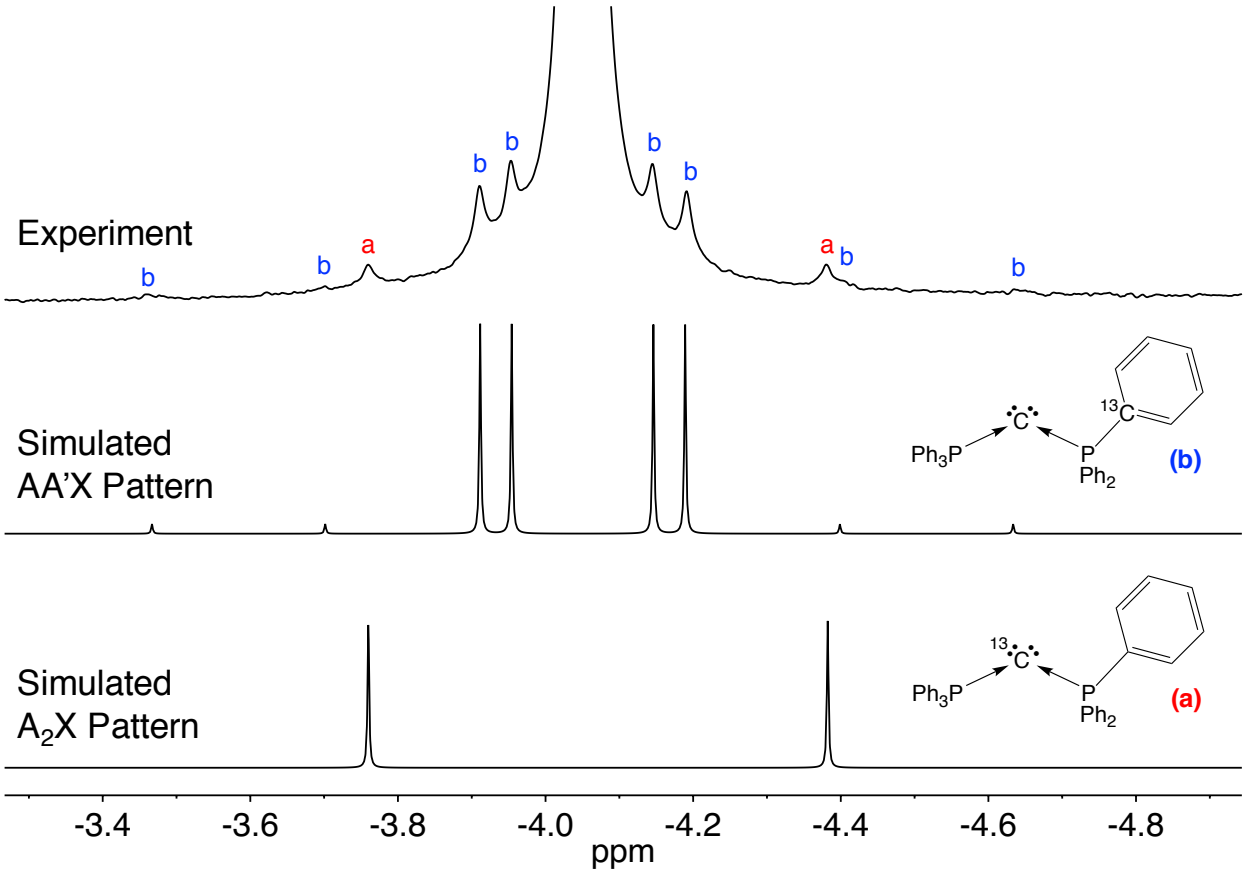

Figure 4. $^{31}P\{^1H\}$ NMR spectrum of $(Ph_3P)_2C$ (top), simulated AA'X pattern derived from ^{31}P-coupling to the ipso-^{13}C isotopomer (b) (middle), simulated A_2X pattern derived from ^{31}P-coupling to the central ^{13}C isotopomer (a) (bottom).

5.4 Reactivity of $(Ph_3P)_2C$ Towards Main Group Alkyl Complexes

There are several examples of main group metal complexes that feature $(Ph_3P)_2C$ as a ligand. However, the reactivity of $(Ph_3P)_2C$ towards main group *alkyl* metal complexes still remains relatively unexplored. Therefore, in order to expand the scope of $(Ph_3P)_2C$ with regards to its coordination chemistry, the reactivity of $(Ph_3P)_2C$ towards Me_3Al, Me_3Ga, Me_2Zn, Me_2Cd, MeHgI, Me_2Mg, and $Mg[N(TMS)_2]_2$ was investigated.

5.4.1 Synthesis and Characterization of $[(Ph_3P)_2C]EMe_3$ (E = Al, Ga)

Although the synthesis and molecular structure of $[(Ph_3P)_2C]InMe_3$ has previously been reported,[24] lighter group 13 analogues have not. In this regard, $[(Ph_3P)_2C]EMe_3$ (Al, Ga) are synthesized *via* the treatment of Me_3Al or Me_3Ga with $(Ph_3P)_2C$ to form the corresponding Lewis acid/base adduct (Scheme 4). The molecular structure of both $[(Ph_3P)_2C]AlMe_3$ and $[(Ph_3P)_2C]GaMe_3$ have been determined by X-ray diffraction (Figure 5 and Figure 6), thus allowing for a more detailed study of the group 13 adducts.

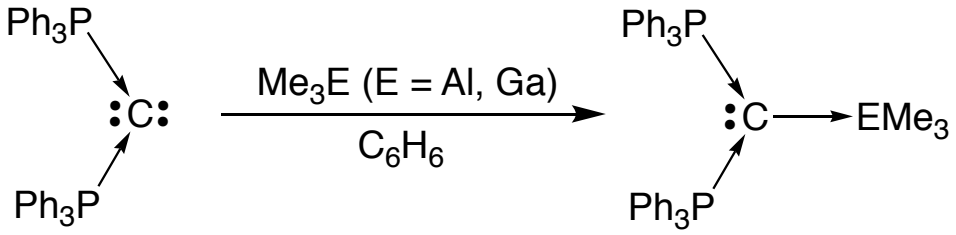

Scheme 4. Synthesis of $[(Ph_3P)_2C]EMe_3$ (Al, Ga) via treatment of Me_3E with $(Ph_3P)_2C$.

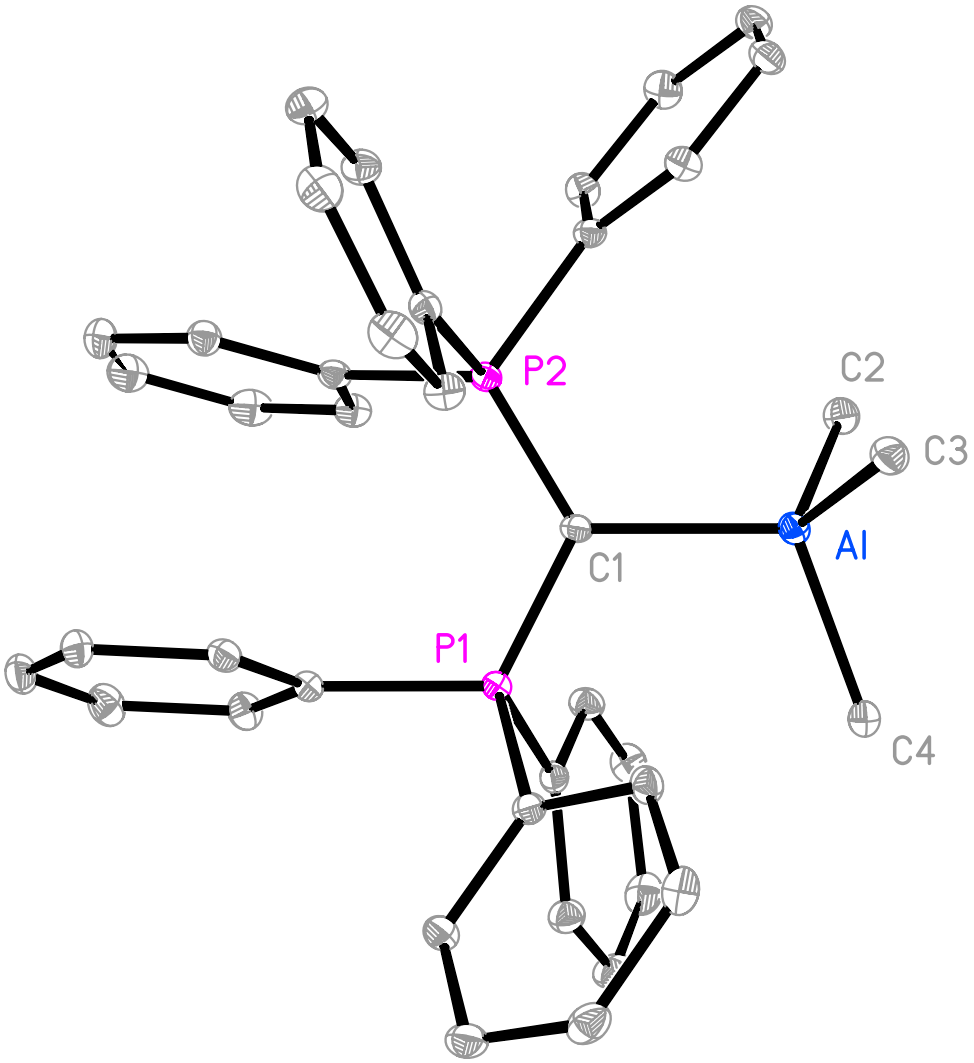

Figure 5. Molecular structure of $[(Ph_3P)_2C]AlMe_3$.

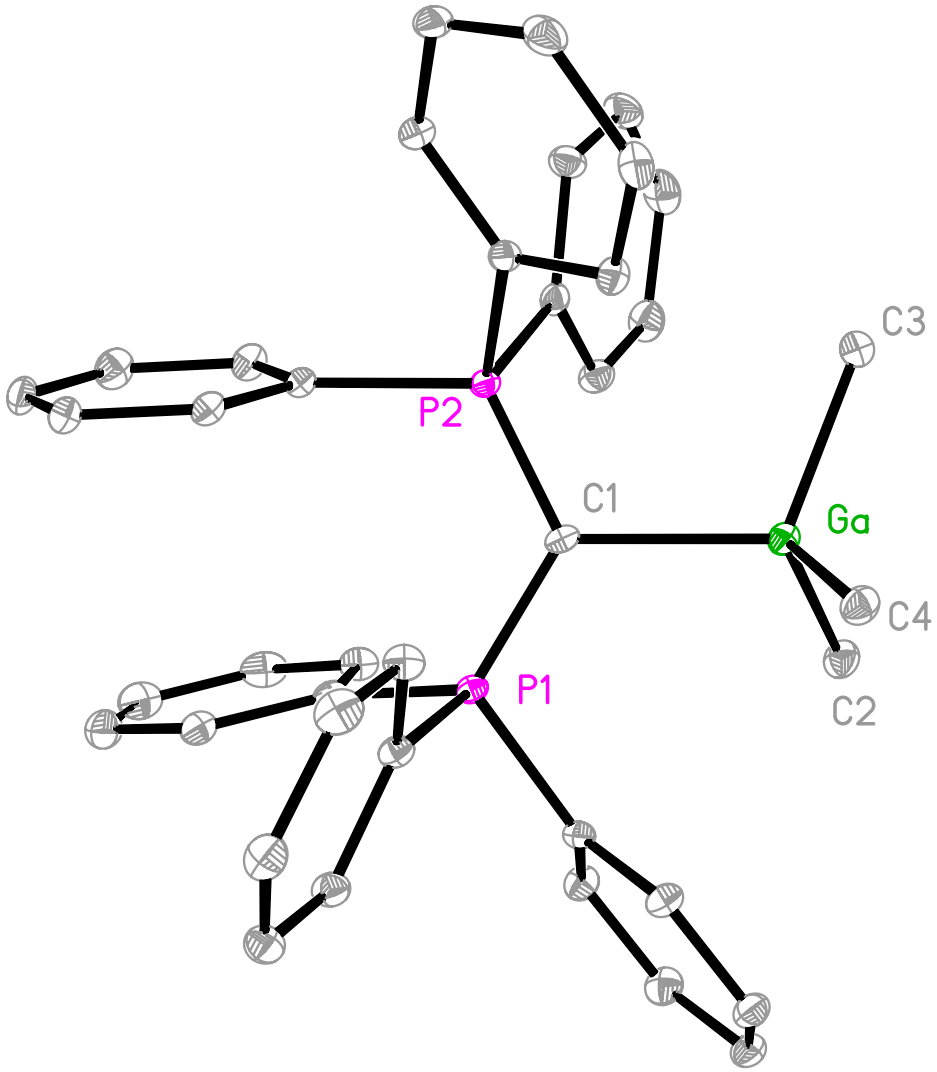

Figure 6. Molecular structure of $[(Ph_3P)_2C]GaMe_3$.

Similar to $[(Ph_3P)_2C]InMe_3$, both $[(Ph_3P)_2C]AlMe_3$ and $[(Ph_3P)_2C]GaMe_3$ possess tetrahedral metal centers with τ_4 and τ_δ parameters[54] in the range of 0.95-0.97 and 0.92-0.96 respectively (Table 1). A dative bond is formed with $(Ph_3P)_2C$ acting as the Lewis base, which donates its σ-type lone-pair to the empty orbital on Me_3E, while the π-type lone pair remains localized on the central carbon.[27] As such, all three complexes are isostructural.

Upon inspection of the bond lengths, the $(Ph_3P)_2C$–Al (2.0957(17) Å) and $(Ph_3P)_2C$–Ga (2.135(2) Å) distances are very similar, with the latter only being 0.0393 Å longer. While the C–Ga bond length is *slightly* longer than the C–Al bond length, the magnitude of the difference between the bond lengths is certainly smaller than one would expect for going down a group. For example, the difference between C–B and C–Al bond lengths is 0.37 Å on the basis of covalent radii.[55] Furthermore, the $(Ph_3P)_2C$–In bond length (2.332(3) Å) is longer than the $(Ph_3P)_2C$–Ga bond length by 0.197 Å. This *apparent* discrepancy in Al and Ga bond lengths is attributed to the scandide contraction,[56] which results in the atomic radii of Al and Ga to be roughly the same size due to poor shielding from a fully filled 3d subshell.

Comparison of $[(Ph_3P)_2C]EMe_3$ (E = Al, Ga) to the related halide compounds, $[(Ph_3P)_2C]AlBr_3$,[24] $[(Ph_3P)_2C]GaCl_3$,[19] and $[(Ph_2P–(CH_2)_3–PPh_2)C]GaCl_3$[19] reveals similar $(Ph_3P)_2C$–E bond distances, although the values for the halide compounds are consistently slightly shorter. This could in part be rationalized by the X ligands (Cl and Br) being more electronegative/electron withdrawing, thus increasing the amount of σ-donation from $(Ph_3P)_2C$ to the metal center. See Table 1 for selected, bond lengths, angles, and τ_4/τ_δ parameters.

Table 1. Selected bond lengths, angles, and τ_4/τ_δ parameters for $[(Ph_3P)_2C]EMe_3$ (Al, Ga, In) and related compounds.

	C[a]–E /Å	**E–X[b] Avg. /Å**	**P–C–P /°**	**τ_4**	**τ_δ**	**Ref**
$[(Ph_3P)_2C]AlMe_3$	2.0957(17)	2.006(17)	122.36(9)	0.97	0.96	This work
$[(Ph_3P)_2C]GaMe_3$	2.135(2)	2.021(2)	122.87(13)	0.97	0.95	This work
$[(Ph_3P)_2C]InMe_3$	2.332(3)	2.207(3)	124.2(2)	0.95	0.92	24
$[(Ph_3P)_2C]AlBr_3$	1.969(3)	2.326(1)	119.5(2)	0.93	0.92	24
$[(Ph_3P)_2C]GaCl_3$	1.981(1)	2.2062(4)	122.46(7)	0.93	0.92	19
$[(Ph_2P–(CH_2)_3–PPh_2)C]GaCl_3$	1.947(1)	2.2147(4)	116.70(8)	0.91	0.88	19

(a) Central C of $(Ph_3P)_2C$.
(b) X = Me, Cl, or Br

$[(Ph_3P)_2C]AlMe_3$ and $[(Ph_3P)_2C]GaMe_3$ are characterized by ^1H NMR spectroscopic signals at –0.56 ppm and 0.21 ppm, respectively, which are attributed to the methyl protons. In addition, $[(Ph_3P)_2C]AlMe_3$ and $[(Ph_3P)_2C]GaMe_3$ exhibit a singlet in the $^{31}P\{^1H\}$ NMR spectra at 19.69 ppm and 20.29 ppm, respectively.

5.4.2 Reactivity of $[(Ph_3P)_2C$ towards Me_2Zn and Me_2Cd

In contrast to the reactivity of $(Ph_3P)_2C$ towards Me_3E (E = Al, Ga), $(Ph_3P)_2C$ does not bind effectively to Me_2M (M = Zn, Cd). For example, whereas the Lewis acid/base adducts, $[(Ph_3P)_2C]AlMe_3$ and $[(Ph_3P)_2C]GaMe_3$, can be formed, isolated, and characterized, no coordination complexes of $(Ph_3P)_2C$ and Me_2M could be isolated. Rather, a weak reversible association is observed *via* NMR spectroscopy.

More specifically, when $(Ph_3P)_2C$ is treated with excess Me_2Zn in C_6D_6, a singlet at 11.59 ppm is observed in the $^{31}P\{^1H\}$ NMR spectrum, which is tentatively assigned as the 1:1 adduct $[(Ph_3P)_2C]ZnMe_2$ (Figure 7). However, upon lyophilizing the solution and redissolving in C_6D_6, the singlet in the $^{31}P\{^1H\}$ NMR spectrum appears to "shift" to 5.68 ppm. Further cycles of lyophilizing/redissolving in C_6D_6 results in an even more upfield shift of the singlet, approaching the chemical shift value of free $(Ph_3P)_2C$ in the $^{31}P\{^1H\}$ NMR spectrum (–4.05 ppm) as illustrated in Figure 7.[57] Similar behavior is observed for the $(Ph_3P)_2C/Me_2Cd$ system, although the chemical shift values do not vary as significantly as the $(Ph_3P)_2C/Me_2Zn$ system.

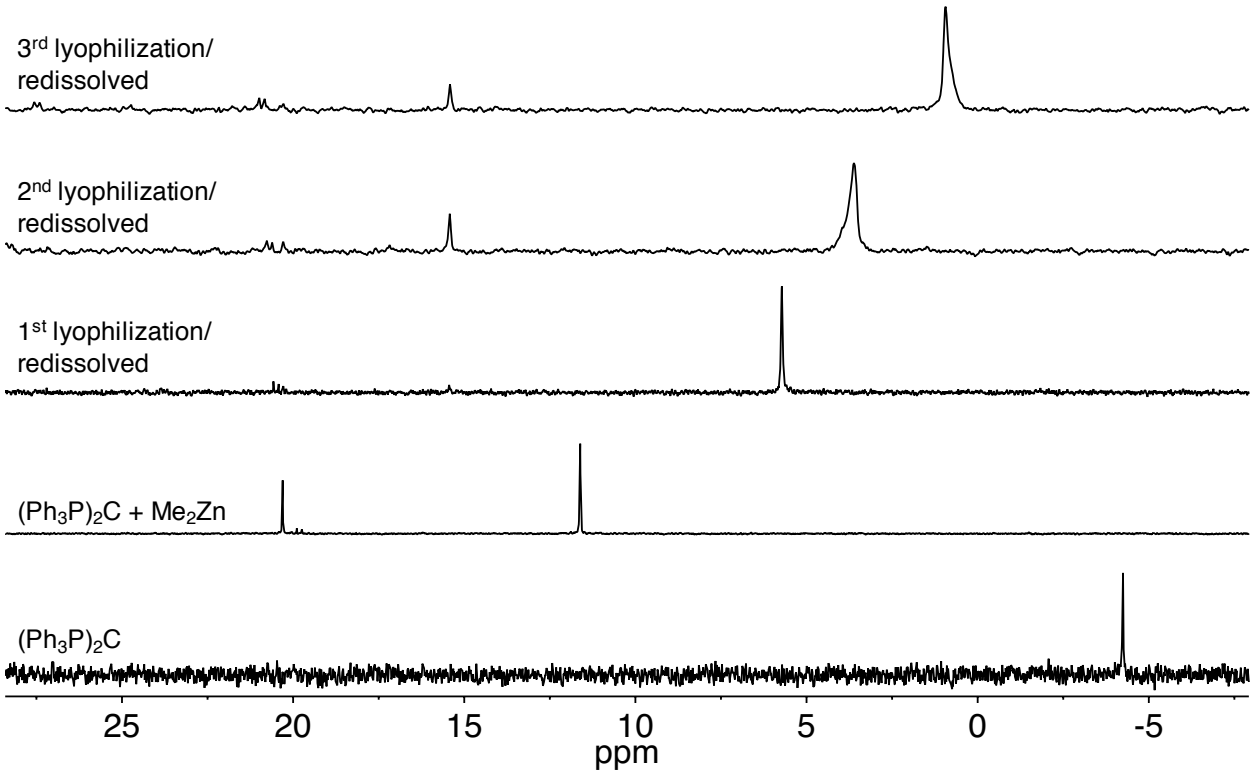

Figure 7. Stacked ^1H NMR spectra of $(Ph_3P)_2C$, $(Ph_3P)_2C$ treated with Me_2Zn, and successive lyophilization/redissolving cycles.

Furthermore, this variable chemical shift behavior is also observed for titration of a solution of $(Ph_3P)_2C$ with Me_2Zn. For example, addition of 0.1 equivalents of Me_2Zn to a solution of $(Ph_3P)_2C$ in C_6D_6 results in a small downfield shift of the $^{31}P\{^1H\}$ NMR signal from –4.05 ppm to –3.48 ppm. Increasing amounts of Me_2Zn results in even more significant downfield shifts, with the singlet appearing at 11.43 ppm when 7 equivalents are added.[57] Thus, as a result of these lyophilization/redissolution and titration experiments, it appears that $(Ph_3P)_2C$ has a relatively low affinity for Me_2Zn and Me_2Cd, and only forms weak reversible associations with the metal compounds, which is in equilibrium with free $(Ph_3P)_2C$ and bound $(Ph_3P)_2C$ in $[(Ph_3P)_2C]ZnMe_2$.[58]

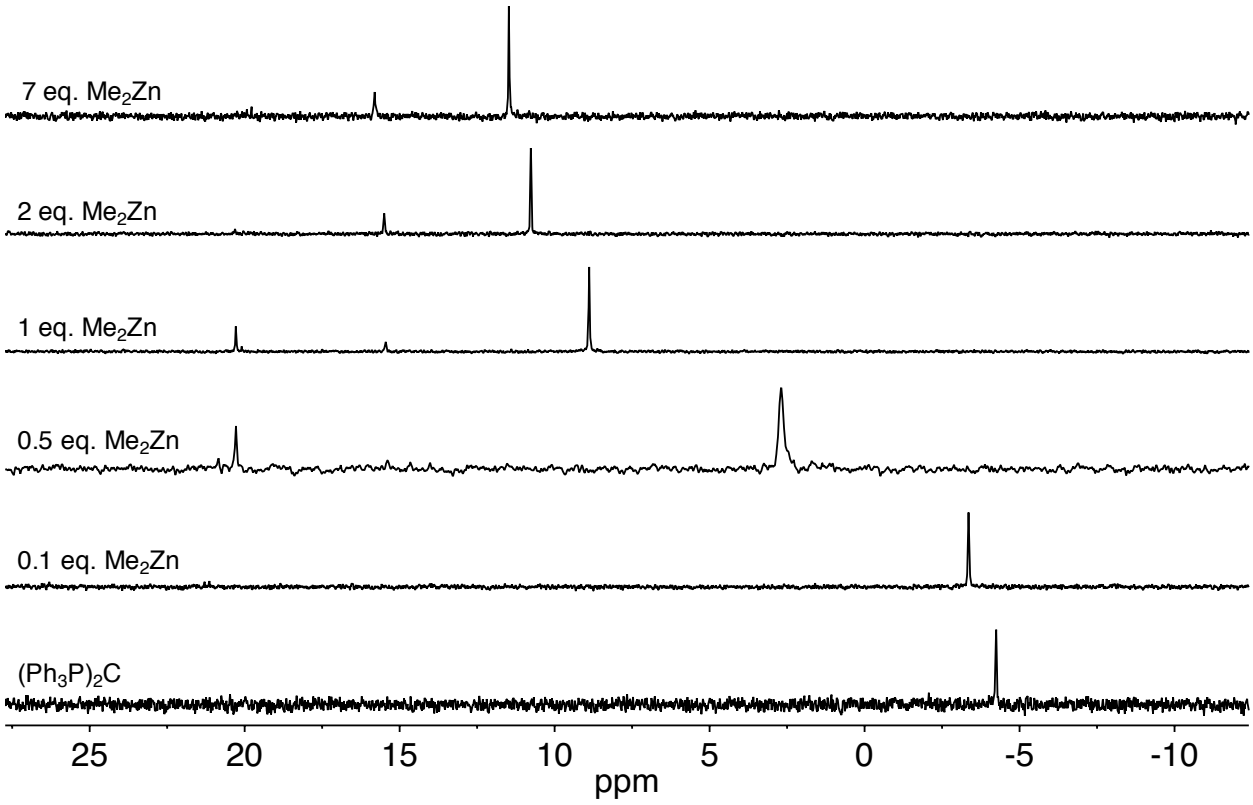

Figure 8. ^1H NMR titration of $(Ph_3P)_2C$ with Me_2Zn.

The lower binding affinity of $(Ph_3P)_2C$ towards Me_2M (Zn, Cd) versus Me_3E (E = Al, Ga, In) is also supported by computational studies as indicated in Table 2. For example, the formation of $[(Ph_3P)_2C]AlMe_3$, $[(Ph_3P)_2C]GaMe_3$, and $[(Ph_3P)_2C]InMe_3$ is thermodynamically more favorable by 6.18, 0.85, and 2.13 kcal mol^{-1} respectively than the formation of $[(Ph_3P)_2C]ZnMe_2$. Additionally, the formation of $[(Ph_3P)_2C]CdMe_2$ is even *less* favorable than the formation of $[(Ph_3P)_2C]ZnMe_2$ by 4.24 kcal mol^{-1}. The stronger affinity of $(Ph_3P)_2C$ towards Me_3E (E = Al, Ga) versus Me_2M (Zn, Cd) could also in part be explained by the stronger Lewis acidity of Me_3E than Me_2M, and observation that is in accord with previous reports.[59]

Table 2. Relative energy of formation (E_{rel}) for $[(Ph_3P)_2C]EMe_3$ (E = Al, Ga, In) and $[(Ph_3P)_2C]MMe_2$ (M = Zn, Cd).

	E_{rel} / kcal mol^{-1} [a]
$[(Ph_3P)_2C]AlMe_3$ (1)	–10.42
$[(Ph_3P)_2C]GaMe_3$ (2)	–5.09
$[(Ph_3P)_2C]InMe_3$ (3)	–6.37
$[(Ph_3P)_2C]ZnMe_2$ (4)	–4.24
$[(Ph_3P)_2C]CdMe_2$ (5)	0

(a) $E_{rel} = E(X) - E(5)$; X = 1, 2, 3, 4, 5.

5.4.3 Synthesis and Characterization of {[(Ph$_3$P)$_2$C]HgMe}I

The reactivity of $(Ph_3P)_2C$ towards mercury complexes has not been investigated thoroughly in the literature. To date only one structurally characterized coordination complex has been reported, namely $\{[(Ph_3P)_2C]_2Hg\}[Hg_2I_6]$.[21] Thus, it is noteworthy that the coordination chemistry of $(Ph_3P)_2C$ can be extended to alkyl mercury complexes.

More specifically, when MeHgI is treated with $(Ph_3P)_2C$ in C_6H_6, the salt {[$(Ph_3P)_2C$]HgMe}I, is precipitated (Scheme 5).

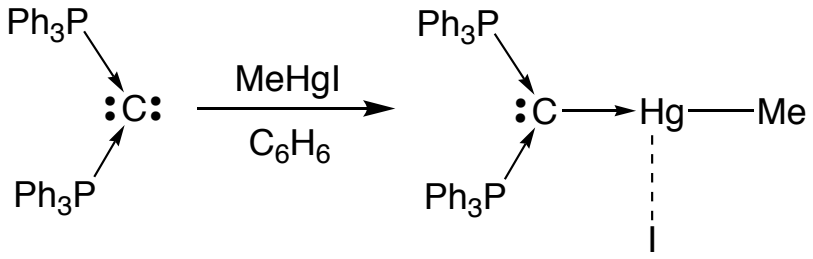

Scheme 5. Synthesis of {[$(Ph_3P)_2C$]HgMe}I *via* treatment of MeHgI with $(Ph_3P)_2C$.

The molecular structure of {[$(Ph_3P)_2C$]HgMe}I has been determined by X-ray diffraction (Figure 9) revealing that the mercury center adopts a roughly linear geometry, with a C–Hg–Me bond angle of 169.7(3)˚. The $(Ph_3P)_2C$–Hg bond length (2.121(7) Å) is slightly longer, but comparable to the $(Ph_3P)_2C$–Hg bond lengths in {[$(Ph_3P)_2C]_2Hg$}[Hg_2I_6] (2.057(6 and 2.082(7) Å). A secondary interaction is also observed between the Hg center and the iodide, having a Hg···I distance of 3.309 Å. This distance is certainly longer than the sum of the covalent radii for a Hg–I bond (2.71 Å),[55] but is well within the sum of the crystallographic van der Waals radii (4.15 Å).[60] For reference, the average Hg–I bond length found in the CSD is 2.784 Å.[61] The related compound, [MeHgTab]I, which features the 4-(trimethylammonio)benzenethiolate ligand (Tab) coordinated to methylmercury, has also been structurally characterized. Similar to {[$(Ph_3P)_2C$]HgMe}I, [MeHgTab]I contains a linear Hg center (S–Hg–Me = 175.6(3)˚) and an iodide counter-ion with a weak secondary interaction with a Hg···I distance of 3.3819(3) Å. Linear geometries for mercury complexes are common due to the strong preference of mercury to be two-coordinate, which results in the ability of the mercury center to partake in secondary interactions.[62,63] The preference of linear, two-coordinate mercury centers

has been attributed to relativistic effects,[64] although other explanations and factors have been suggested.[65,66]

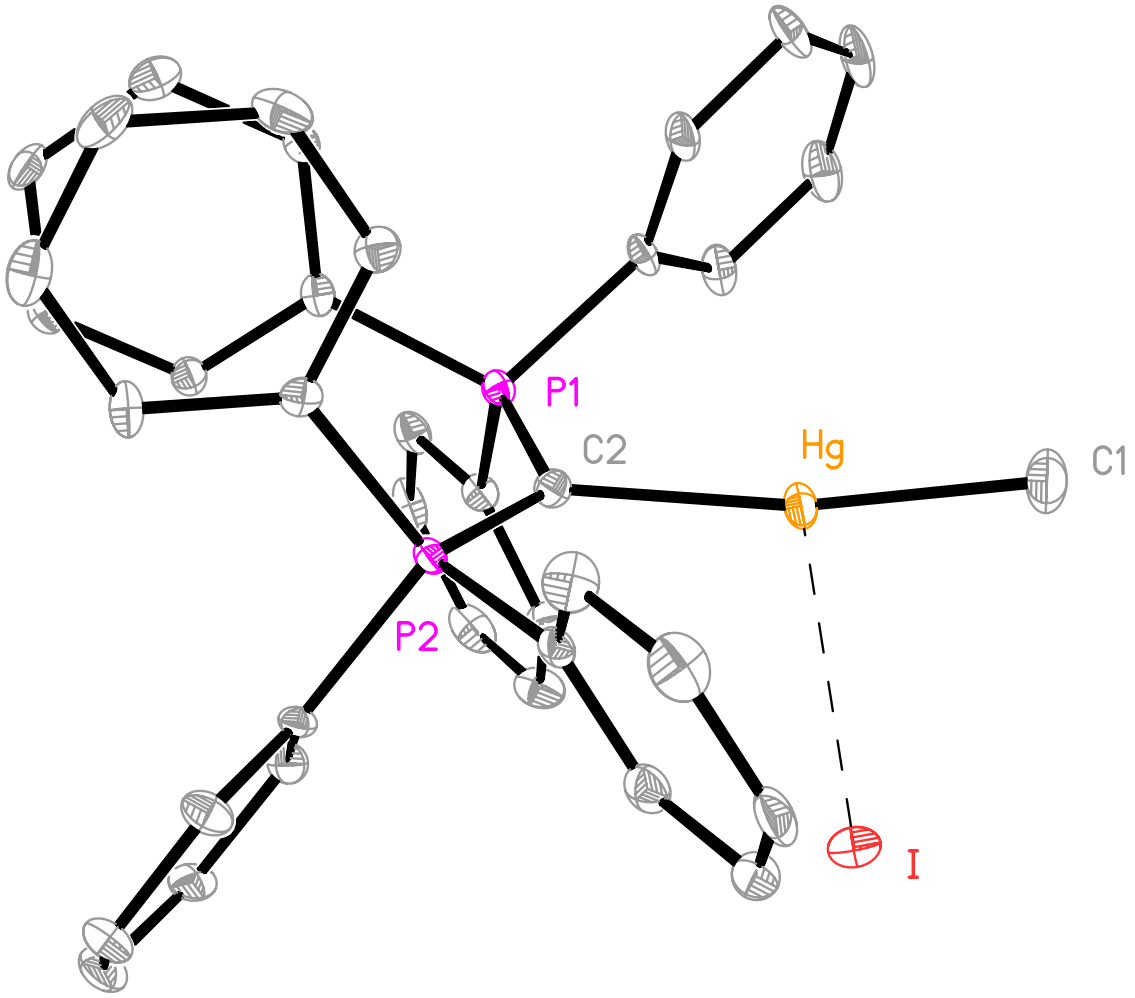

Figure 9. Molecular structure of {[$(Ph_3P)_2C$]HgMe}I.

{[$(Ph_3P)_2C$]HgMe}I is characterized by a singlet at 0.017 ppm in the ^{1}H NMR spectrum corresponding to the methyl protons. Due to the presence of the magnetically active ^{199}Hg nucleus (16.9% abundant, spin = ½),[66] satellite peaks are also observed flanking the methyl peak, having a $^{2}J_{Hg-H}$ of 151 Hz.[67] Additionally, a signal at –409.01 ppm is observed for {[$(Ph_3P)_2C$]HgMe}I in the $^{199}Hg\{^{1}H\}$ NMR spectrum. Furthermore, a singlet

is observed in the $^{31}P\{^{1}H\}$ NMR spectrum at 20.26 ppm which is consistent with both phosphorous atoms being chemically equivalent.

5.4.4 Synthesis and Characterization of $\{[\kappa^2\text{-}(C,C)\text{-}(Ph_3PCPPh_2(C_6H_4))]Mg(\mu\text{-}Me)\}_2$ and $[\kappa^2\text{-}(C,C)\text{-}(Ph_3PCPPh_2(C_6H_4))]MgN(TMS)_2$

The reactivity of $(Ph_3P)_2C$ towards the magnesium reagents, Me_2Mg and $Mg[N(TMS)_2]_2$, was also investigated. Interestingly, while both reactions yield ortho metalated products, structurally different complexes are obtained. Specifically, when $(Ph_3P)_2C$ is treated with Me_2Mg in C_6H_6 and heated at 80˚C for 1 hour, the ortho metalated dimer, $\{[\kappa^2\text{-}(C,C)\text{-}(Ph_3PCPPh_2(C_6H_4))]Mg(\mu\text{-}Me)\}_2$, is obtained, whereas, when $(Ph_3P)_2C$ is treated with $Mg[N(TMS)_2]_2$ and heated at 80˚C for 1 day, the ortho metalated monomer, $[\kappa^2\text{-}(C,C)\text{-}(Ph_3PCPPh_2(C_6H_4))]MgN(TMS)_2$, is isolated (Scheme 6).

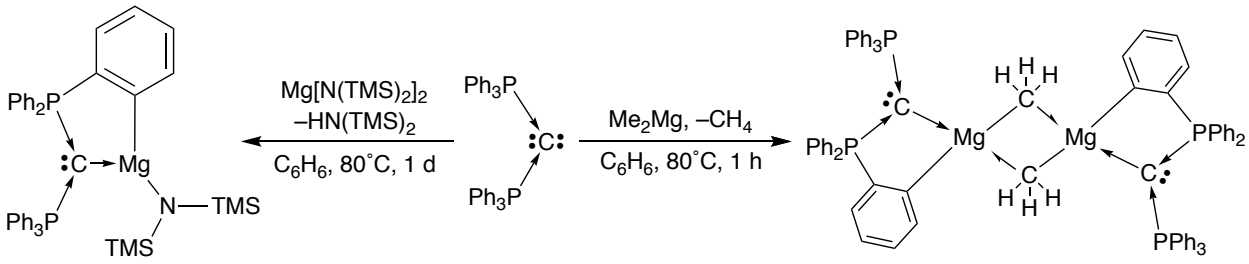

Scheme 6. Synthesis of $\{[\kappa^2\text{-}(C,C)\text{-}(Ph_3PCPPh_2(C_6H_4))]Mg(\mu\text{-}Me)\}_2$ and $[\kappa^2\text{-}(C,C)\text{-}(Ph_3PCPPh_2(C_6H_4))]MgN(TMS)_2$ via treatment of $(Ph_3P)_2C$ with Me_2Mg and $Mg[N(TMS)_2]_2$ respectively.

Both compounds have been structurally characterized by X-ray diffraction as illustrated in Figure 10 and Figure 11. The dimer, $\{[\kappa^2\text{-}(C,C)\text{-}(Ph_3PCPPh_2(C_6H_4))]Mg(\mu\text{-}Me)\}_2$, features two slightly distorted tetrahedral Mg centers ($\tau_4 = 0.87$ and $\tau_\delta = 0.82$)[54] that possess a $\{C_4\}$ coordination environment and are bridged by the methyl ligands. Each Mg is further coordinated in a bidentate fashion by $(Ph_3P)_2C$ through the central carbon in a dative L-type[12] manner and through the ortho-carbon of one of the phenyl rings *via*

ortho metalation. In contrast, [κ^2-(C,C)-($Ph_3PCPPh_2(C_6H_4)$)]$MgN(TMS)_2$ does not form a dimer, but the trigonal Mg center is also cyclometalated by $(Ph_3P)_2C$. In both compounds, the π-type lone pair remains localized on the central carbon.[27] In regards to the bond lengths, both {[κ^2-(C,C)-($Ph_3PCPPh_2(C_6H_4)$)]Mg(μ-Me)}$_2$ and [κ^2-(C,C)-($Ph_3PCPPh_2(C_6H_4)$)]$MgN(TMS)_2$ have similar $C_{(central)}$–Mg (2.183(2) and 2.162(3) Å) and $C_{(ortho)}$–Mg (2.145(2) and 2.135(3) Å) bond distances respectively. Furthermore, the P–C–P bond angles of {[κ^2-(C,C)-($Ph_3PCPPh_2(C_6H_4)$)]Mg(μ-Me)}$_2$ and [κ^2-(C,C)-($Ph_3PCPPh_2(C_6H_4)$)]$MgN(TMS)_2$ are also very similar as well (125.72(12)° and 124.15(15)° respectively). Additionally, the Mg–C bond lengths (2.248(3) and 2.280(3) Å) and Mg–C–Mg bond angle (75.00(9)°) of the bridging methyl groups are within the ranges for other structurally characterized bridging methyl groups of magnesium dimers found in the CSD (1.977–2.378 Å and 67.946–96.123°).[61]

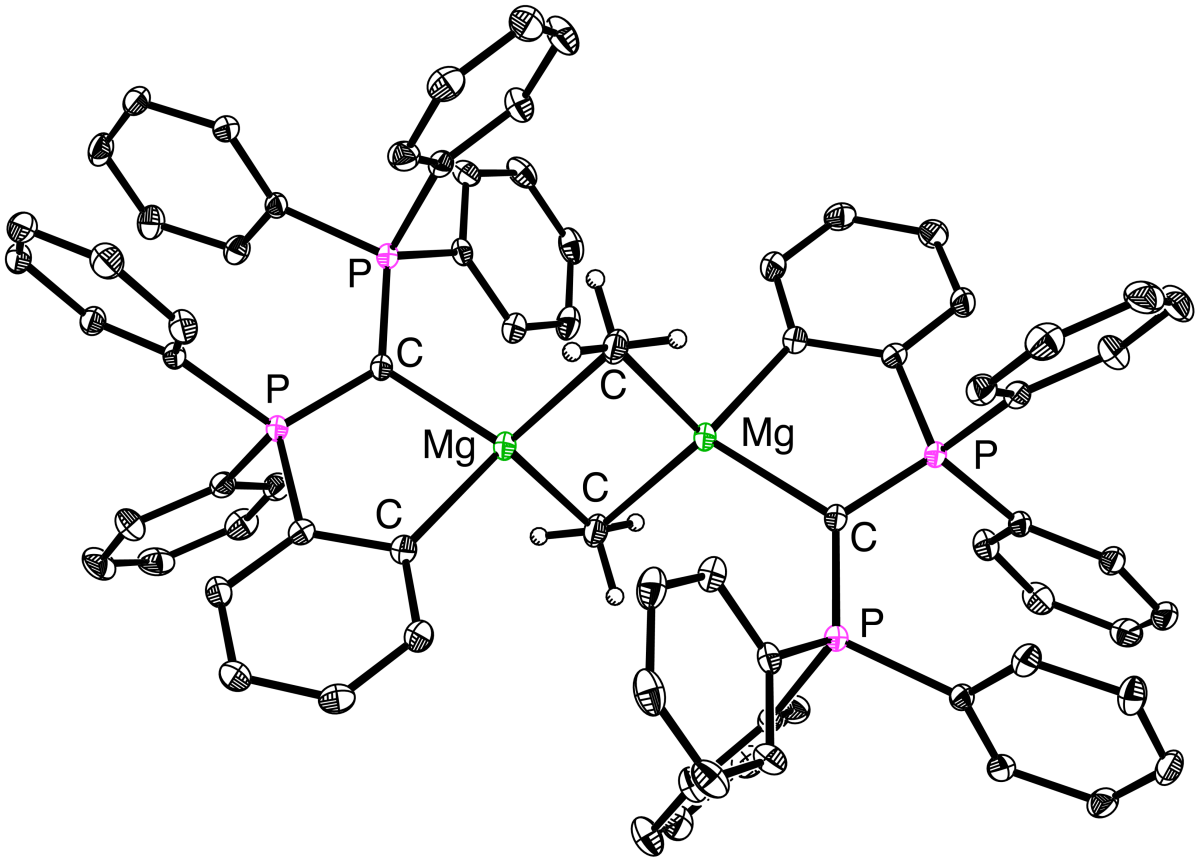

Figure 10. Molecular structure of {[κ^2-(C,C)-($Ph_3PCPPh_2(C_6H_4)$)]Mg(μ-Me)}$_2$.

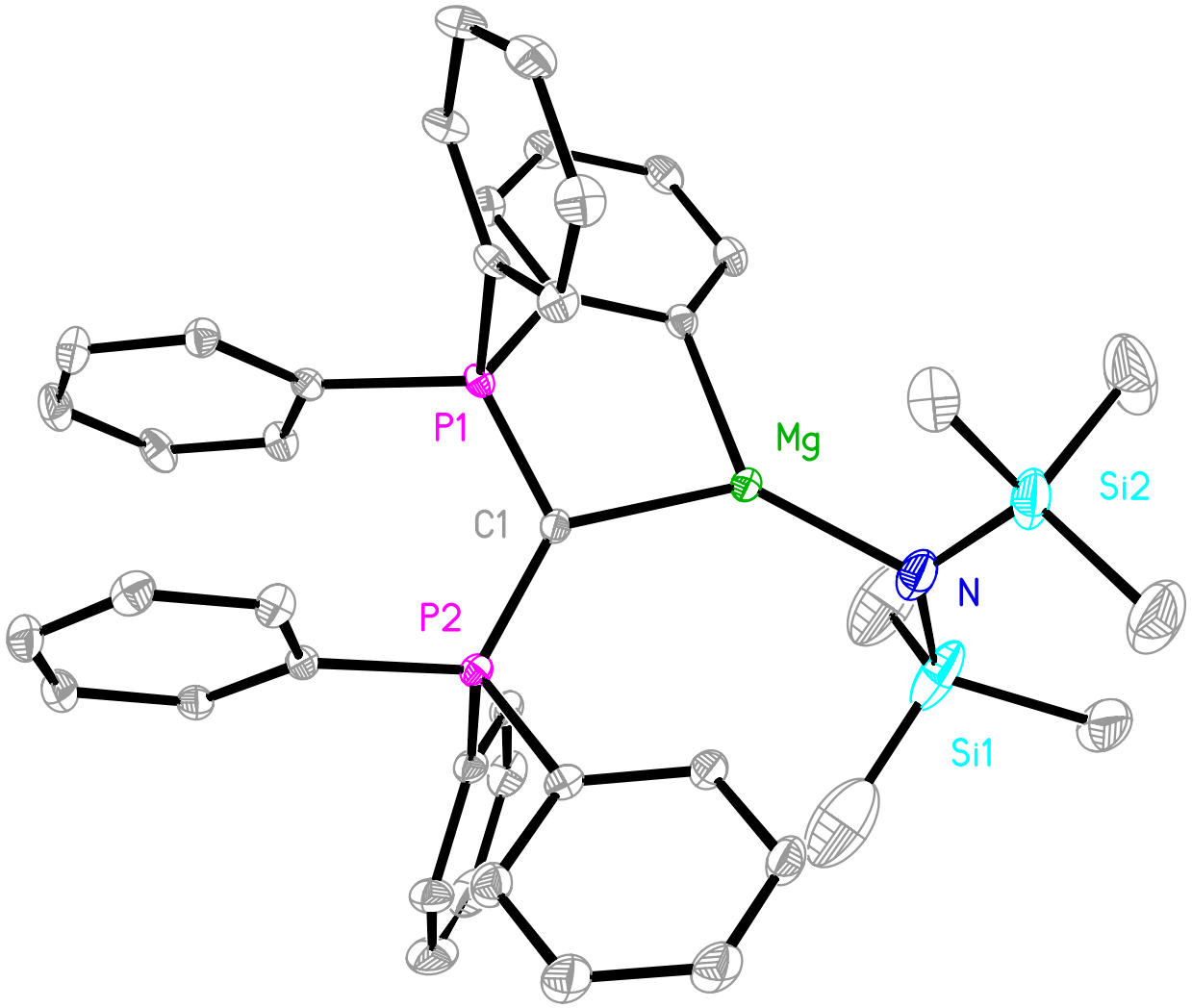

Figure 11. Molecular structure of $[\kappa^2\text{-}(C,C)\text{-}(Ph_3PCPPh_2(C_6H_4))]MgN(TMS)_2$.

The proposed mechanism for the formation of $\{[\kappa^2\text{-}(C,C)\text{-}(Ph_3PCPPh_2(C_6H_4))]Mg(\mu\text{-}Me)\}_2$ proceeds *via* initial coordination of $(Ph_3P)_2C$ to Me_2Mg to form the corresponding Lewis acid/base adduct, $[(Ph_3P)_2C]MgMe_2$. Next, a metathesis step occurs which forms the ortho metalated fragment, $\{[\kappa^2\text{-}(C,C)\text{-}(Ph_3PCPPh_2(C_6H_4))]MgMe\}$, and an equivalent of CH_4. The resulting $\{[\kappa^2\text{-}(C,C)\text{-}(Ph_3PCPPh_2(C_6H_4))]MgMe\}$ fragment then dimerizes to form $\{[\kappa^2\text{-}(C,C)\text{-}(Ph_3PCPPh_2(C_6H_4))]Mg(\mu\text{-}Me)\}_2$. $[\kappa^2\text{-}(C,C)\text{-}(Ph_3PCPPh_2(C_6H_4))]MgN(TMS)_2$ is proposed to be formed by a similar mechanism,

which involves initial coordination of $(Ph_3P)_2C$ to $Mg[N(TMS)_2]_2$ to form $[(Ph_3P)_2C]Mg[N(TMS)_2]_2$. This then undergoes a metathesis step to release $HN(TMS)_2$ and form $[\kappa^2\text{-}(C,C)\text{-}(Ph_3PCPPh_2(C_6H_4))]MgN(TMS)_2$. $[\kappa^2\text{-}(C,C)\text{-}(Ph_3PCPPh_2(C_6H_4))]MgN(TMS)_2$ does not dimerize likely due to the steric demands of the $[N(TMS)_2]^-$ ligand.

Consistent with two chemically inequivalent phosphorus atoms, $\{[\kappa^2\text{-}(C,C)\text{-}(Ph_3PCPPh_2(C_6H_4))]Mg(\mu\text{-}Me)\}_2$ is characterized by two sets of doublets in the ^{31}P NMR spectrum at 12.86 ppm and 17.65 ppm that each have a coupling constant of 24 Hz. Similarly, $[\kappa^2\text{-}(C,C)\text{-}(Ph_3PCPPh_2(C_6H_4))]MgN(TMS)_2$ also displays two doublets in the ^{31}P NMR spectrum at 14.96 ppm and 19.38 ppm with coupling constants of 21 Hz. In the ^1H NMR spectrum of $\{[\kappa^2\text{-}(C,C)\text{-}(Ph_3PCPPh_2(C_6H_4))]Mg(\mu\text{-}Me)\}_2$, the bridging methyl protons are observed as a broad singlet at –0.67 ppm. Correspondingly, the hydrogens of the $[N(TMS)_2]^-$ ligand of $[\kappa^2\text{-}(C,C)\text{-}(Ph_3PCPPh_2(C_6H_4))]MgN(TMS)_2$ are observed as a singlet at 0.71 ppm.

The formation of these ortho metalated complexes is significant because, to date, only noble transition metal complexes have been observed to undergo cyclometalation,[40,41] making $\{[\kappa^2\text{-}(C,C)\text{-}(Ph_3PCPPh_2(C_6H_4))]Mg(\mu\text{-}Me)\}_2$ and $[\kappa^2\text{-}(C,C)\text{-}(Ph_3PCPPh_2(C_6H_4))]MgN(TMS)_2$ the first examples of main group metals to feature this coordination mode. The concomitant formation of CH_4 and $HN(TMS)_2$ provides a driving force for the synthesis of these complexes.

5.5 Reactivity of $(Ph_3P)_2C$ Towards Transition Metal Complexes

Although several coordination complexes of $(Ph_3P)_2C$ have been synthesized thus far (see section 5.2), there are still some transition metals that have not been explored.

Therefore, to expand the coordination chemistry of carbodiphosphoranes to some of these under-represented metals, the reactivity of $(Ph_3P)_2C$ towards palladium, cobalt, iridium, and ruthenium complexes was investigated and described below.

5.5.1 Synthesis and Characterization of [κ^2-(C,C)-($Ph_3PCPPh_2(C_6H_4)$)]Pd(π-cinnamyl) and [$(Ph_3P)_2CH$][(π-cinnamyl)$PdCl_2$]

The reactivity of carbodiphosphoranes towards palladium is relatively unexplored. For example, the only reported palladium complex that features $(Ph_3P)_2C$ is [κ^2-(C,C)-($Ph_3PCPPh_2(C_6H_4)$)]Pd(allyl).[40b] Additionally, the chelating phosphine, $(dppm)_2C$, can be utilized to synthesize the palladium complexes, $[(dppm)_2C]PdCl$[68] and [PdAu(Cl)2(C(dppm)2)]Cl.[69] Therefore, it is significant that the reactivity of $(Ph_3P)_2C$ towards [Pd(π-cinnamyl)Cl]$_2$ was investigated.

When [Pd(π-cinnamyl)Cl]$_2$ is treated with $(Ph_3P)_2C$, the ortho metalated product, [κ^2-(C,C)-($Ph_3PCPPh_2(C_6H_4)$)]Pd(π-cinnamyl), is obtained (Scheme 7). Accompanying the ortho metalation of $(Ph_3P)_2C$ is the generation of one equivalent of HCl, which will protonate any unreacted $(Ph_3P)_2C$ in a side reaction to ultimately form [$(Ph_3P)_2CH$][(π-cinnamyl)$PdCl_2$] as illustrated in Scheme 7. The formation of HCl is proposed to occur *via* a reductive elimination step from a transient Pd–H species. Therefore, in order for this reaction to go to completion, two equivalents of $(Ph_3P)_2C$ must be used.

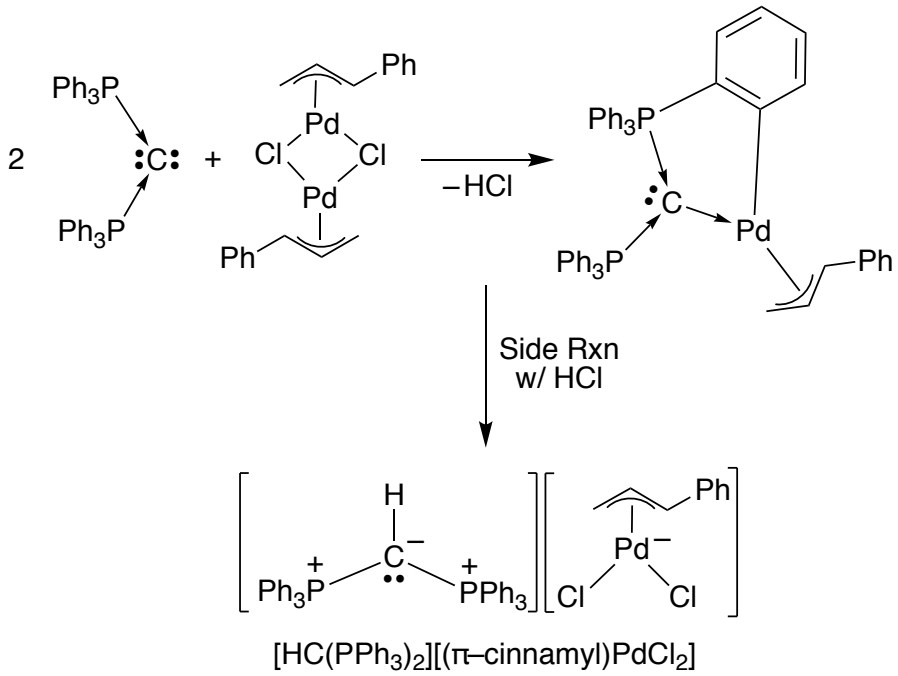

Scheme 7. Synthesis of [κ^2-(C,C)-($Ph_3PCPh_2(C_6H_4)$)]Pd(π-cinnamyl) and [$(Ph_3P)_2CH$][(π-cinnamyl)$PdCl_2$].

Both the cyclometalated product, [κ^2-(C,C)-($Ph_3PCPPh_2(C_6H_4)$)]Pd(π-cinnamyl), and protonated side product, [$(Ph_3P)_2CH$][(π-cinnamyl)$PdCl_2$], have been structurally characterized by X-ray diffraction (Figure 12 and Figure 13). [κ^2-(C,C)-($Ph_3PCPPh_2(C_6H_4)$)]Pd(π-cinnamyl) features a {C_5} coordination environment resulting from coordination of the central and ortho carbon of $(Ph_3P)_2C$ and the [C_3] unit of the π-cinnamyl ligand. [κ^2-(C,C)-($Ph_3PCPPh_2(C_6H_4)$)]Pd(π-cinnamyl) is isostructural with the related compound, [κ^2-(C,C)-($Ph_3PCPPh_2(C_6H_4)$)]Pd(allyl), and, as expected, the $C_{(central)}$–Pd (2.103(2) Å) and $C_{(ortho)}$–Pd (2.063(3) Å) bond distances are similar ($C_{(central)}$–Pd = 2.126(7) Å and $C_{(ortho)}$–Pd = 2.056(7) Å for [κ^2-(C,C)-($Ph_3PCPPh_2(C_6H_4)$)]Pd(allyl)). Furthermore, the average Pd–π-cinnamyl (2.183(3) Å) and Pd–allyl (2.178 Å) bond distances are also approximately the same. With respect to the protonated side product, the average π-cinnamyl [C_3] distance (2.116(2) Å) is slightly shorter than the average π-cinnamyl [C_3] distance (2.183(3) Å) for [κ^2-(C,C)-($Ph_3PCPPh_2(C_6H_4)$)]Pd(π-cinnamyl). It is

significant that $[(Ph_3P)_2CH][(\pi\text{-cinnamyl})PdCl_2]$ is characterized by X-ray diffraction, as the proposed protonated side product in the synthesis of $[\kappa^2\text{-}(C,C)\text{-}(Ph_3PCPPh_2(C_6H_4))]Pd(allyl)$ is $[(Ph_3P)_2CH]Cl$.[40b]

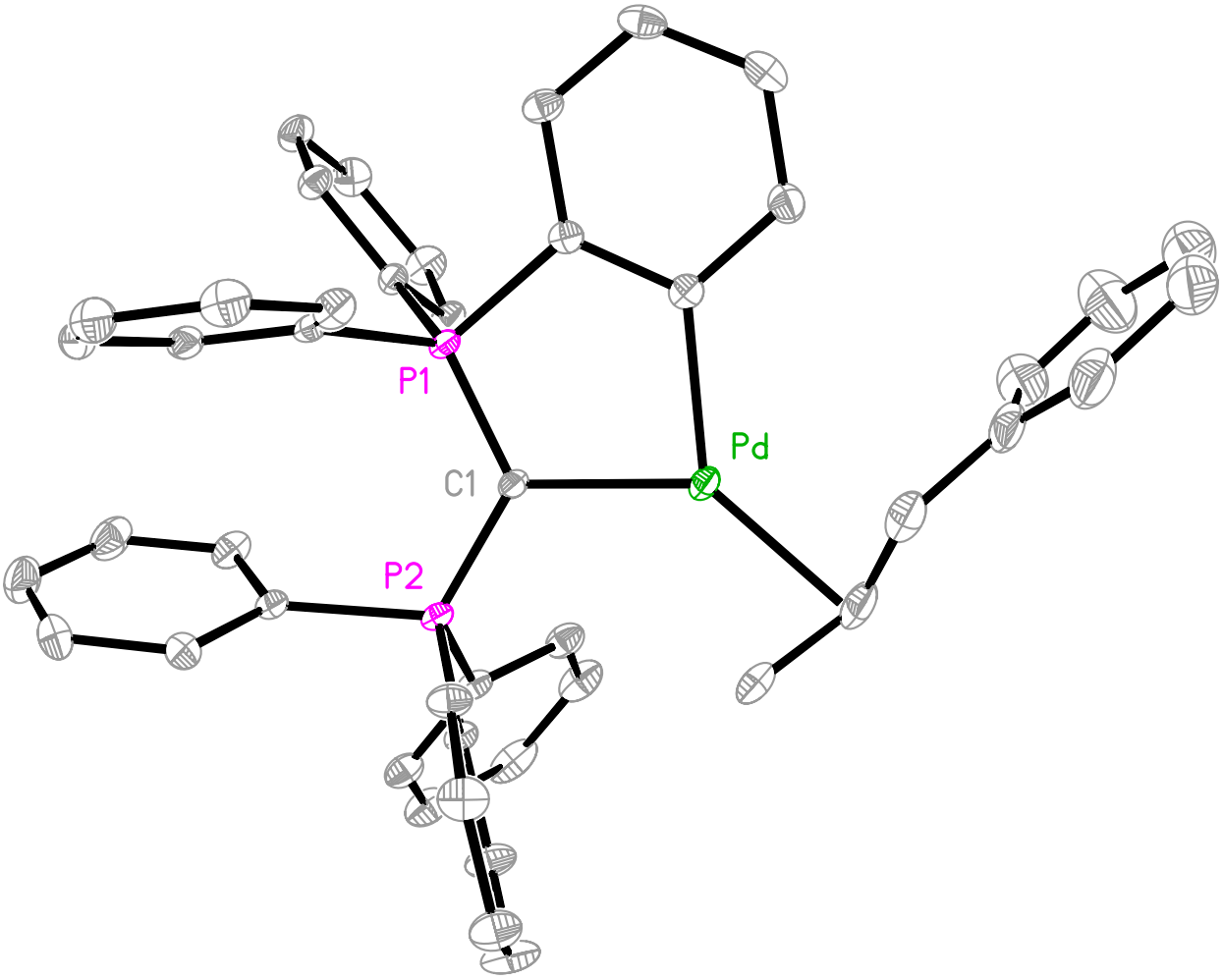

Figure 12. Molecular structure of $[\kappa^2\text{-}(C,C)\text{-}(Ph_3PCPPh_2(C_6H_4))]Pd(\pi\text{-cinnamyl})$.

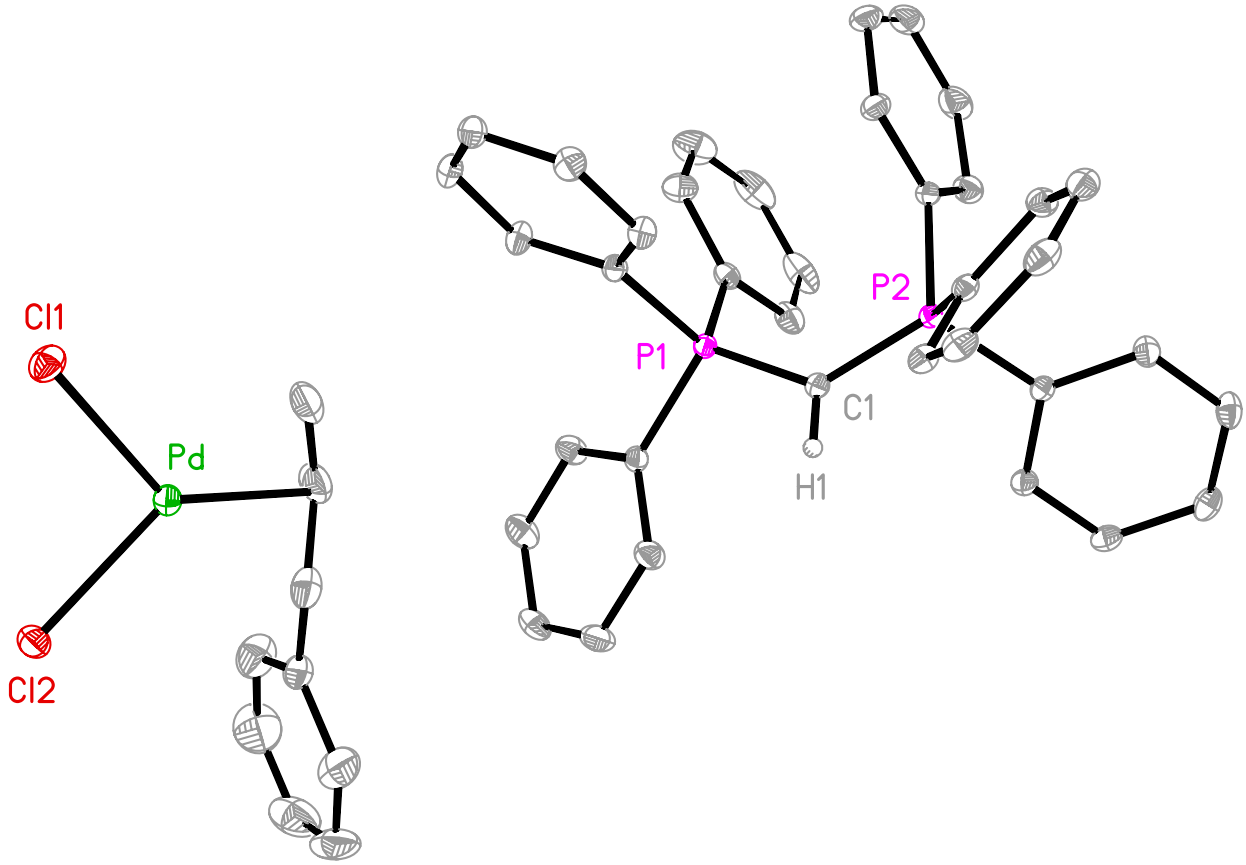

Figure 13. Molecular structure of $[(Ph_3P)_2CH][(\pi\text{-cinnamyl})PdCl_2]$.

$[\kappa^2\text{-}(C,C)\text{-}(Ph_3PCPPh_2(C_6H_4))]Pd(\pi\text{-cinnamyl})$ is characterized by two doublets in the ^{31}P NMR spectrum at 9.13 ppm and 37.04 ppm, each with a coupling constant of 52 Hz. This pattern is consistent with ortho metalation because both of the phosphorus atoms are chemically inequivalent.

5.5.2 Synthesis and Characterization of $[\kappa^2\text{-}(C,C)\text{-}(Ph_3PCPPh_2(C_6H_4))]Co[N(TMS)_2]$

To date, the coordination chemistry of carbodiphosphoranes towards cobalt complexes remains under-developed. Specifically, there are no structurally characterized cobalt complexes which feature carbodiphosphorane ligands. For example, only the reactivity of $(Ph_3P)_2C$ towards $Co_2(CO)_8$ has been explored, and this yields the protonated

compound, $\{[(Ph_3P)_2CH]Co(CO)_4\}\{Co(CO)_4\}$,[70] when the reaction is carried out in THF (it is thought the H^+ atom abstraction comes from adventitious water in the solvent). In contrast, if the reaction is performed in toluene, the Wittig-type product, $[(Ph_3PCC)Co(CO)_n]^x$, is formed which ultimately decomposes to the tetra-nuclear cluster $[Co_4(CO)_{10}(PPh_3)(\mu_4\text{-}CCPPh_3)]$.[70,71] Therefore, it is significant that the reactivity of $(Ph_3P)_2C$ towards $\{Co[N(TMS)_2]_2\}_2$ has been investigated.

More specifically, when $\{Co[N(TMS)_2]_2\}_2$ is treated with $(Ph_3P)_2C$, the ortho metalated product, $[\kappa^2\text{-}(C,C)\text{-}(Ph_3PCPPh_2(C_6H_4))]Co[N(TMS)_2]$, is produced, along with the formation of one equivalent of $HN(TMS)_2$ (Scheme 8).

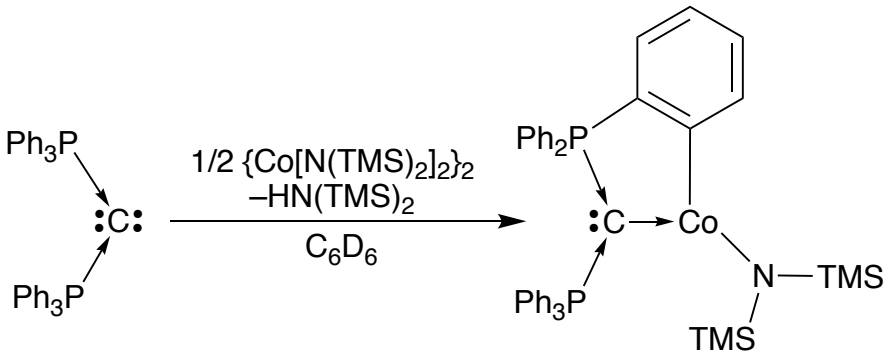

Scheme 8. Synthesis of $[\kappa^2\text{-}(C,C)\text{-}(Ph_3PCPPh_2(C_6H_4))]Co[N(TMS)_2]$ via treatment of $\{Co[N(TMS)_2]_2\}_2$ with $(Ph_3P)_2C$.

$[\kappa^2\text{-}(C,C)\text{-}(Ph_3PCPPh_2(C_6H_4))]Co[N(TMS)_2]$ has been structurally characterized by X-ray diffraction (Figure 14). The $C_{(central)}$–Co and $C_{(ortho)}$–Co bond distances are 2.057(3) and 2.064(3) Å. These bond lengths are shorter than the isostructural magnesium compound, $[\kappa^2\text{-}(C,C)\text{-}(Ph_3PCPPh_2(C_6H_4))]Mg[N(TMS)_2]$, (2.162(3) and 2.135(3) Å from section 5.4.4) in accord with the difference in covalent radii of the metal centers (Mg = 1.41 Å, low spin Co = 1.26 Å).[55]

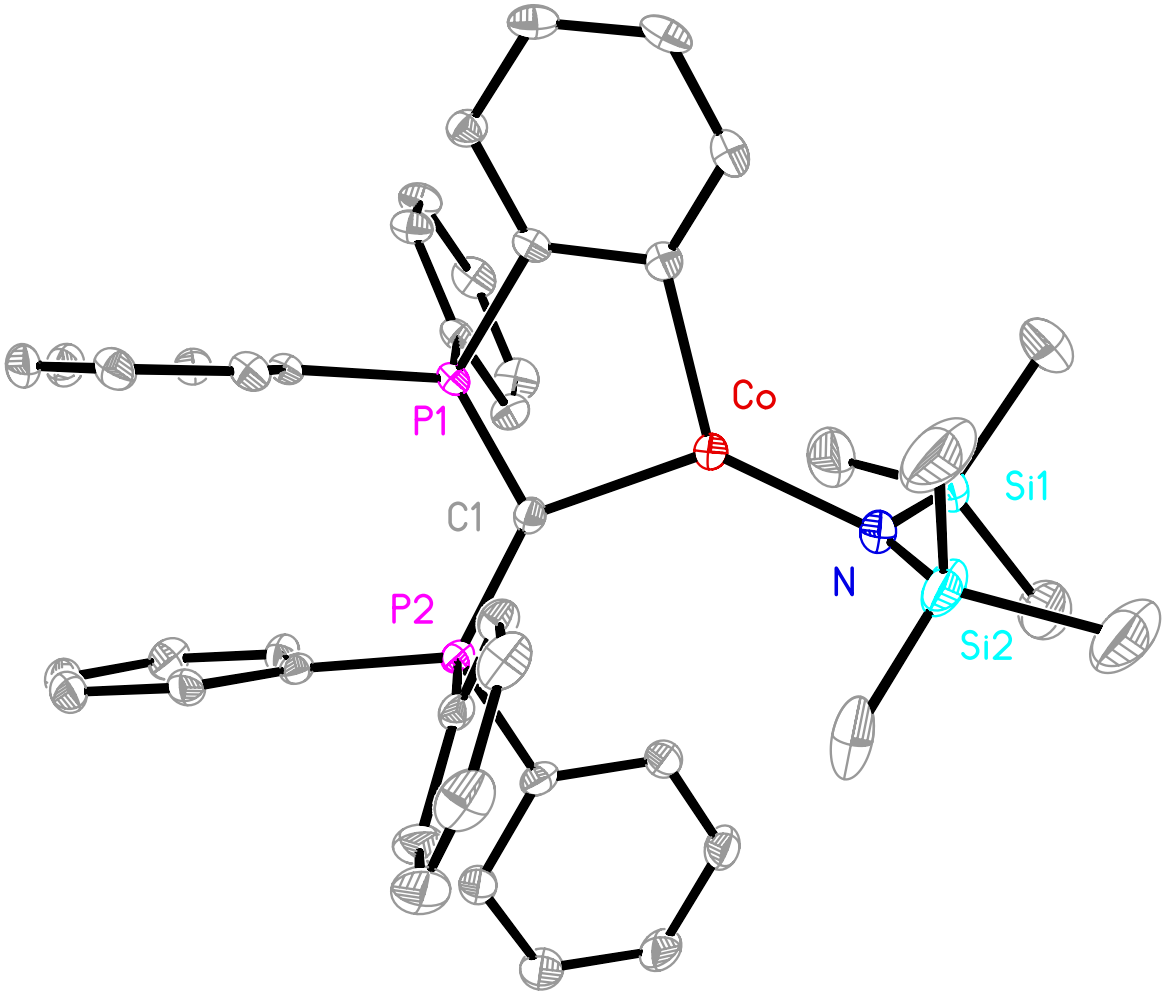

Figure 14. Molecular structure of [κ^2-(C,C)-($Ph_3PCPPh_2(C_6H_4)$)]Co[$N(TMS)_2$].

Due to the Co(II) metal center possessing an odd number of electrons, [κ^2-(C,C)-($Ph_3PCPPh_2(C_6H_4)$)]Mg[$N(TMS)_2$] is paramagnetic. Thus, the ^{1}H NMR is comprised of broad peaks at –17.81, –9.28, –2.25, 2.29, 7.07, and 7.90 ppm. Additionally, a signal at 16.75 ppm is observed in the ^{31}P NMR spectrum.

5.5.3 Reactivity of $(Ph_3P)_2C$ towards $[Ir(COD)Cl_2]_2$

The reactivity of $(Ph_3P)_2C$ towards iridium also deserves attention, as there are no structurally characterized complexes of iridium that feature $(Ph_3P)_2C$ as a ligand.

Therefore, the coordination chemistry of $(Ph_3P)_2C$ towards iridium was investigated. Similar to the reactivity of $(Ph_3P)_2C$ with $[Rh(COD)Cl]_2$ to yield $[\kappa^2$-(C,C)-$(Ph_3PCPPh_2(C_6H_4))]Rh(COD)$,[40a] $(Ph_3P)_2C$ reacts with $[Ir(COD)Cl]_2$ to form the ortho metalated complex, $[\kappa^2$-(C,C)-$(Ph_3PCPPh_2(C_6H_4))]Ir(COD)$, and protonated compound, $[(Ph_3P)_2CH]Cl$ (Scheme 9). The proposed mechanism by which the above occurs involves (*i*) initial coordination of $(Ph_3P)_2C$ to break apart the bridging metal centers to form $[(Ph_3P)_2C]Ir(COD)(Cl)$, followed by (*ii*) ortho metalation of one of the phenyl rings to form a transient Ir–H species, and (*iii*) reductive elimination to form one equivalent of HCl, which will protonate free $(Ph_3P)_2C$. Due to this reductive elimination step, in order for this reaction to go to completion, a 2:1 $(Ph_3P)_2C$ to Ir ratio must be used. A similar mechanism has been proposed for the formation of $[\kappa^2$-(C,C)-$(Ph_3PCPPh_2(C_6H_4))]Rh(COD)$.[40a]

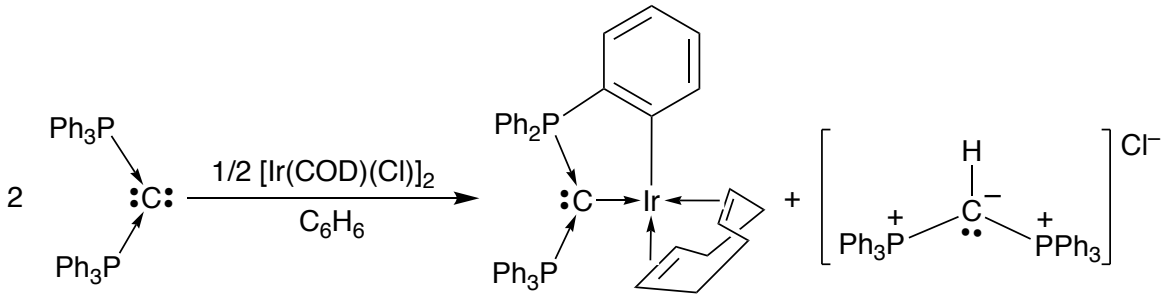

Scheme 9. Synthesis of $[\kappa^2$-(C,C)-$(Ph_3PCPPh_2(C_6H_4))]Ir(COD)$ and $[(Ph_3P)_2CH][Cl]$ *via* treatment of $[Ir(COD)Cl]_2$ with $(Ph_3P)_2C$.

This mechanism is supported by NMR spectroscopic evidence. For example, when $(Ph_3P)_2C$ is treated with $[Ir(COD)Cl]_2$, a singlet at 14.16 ppm in the ^{31}P NMR spectrum is initially observed, which corresponds to $[(Ph_3P)_2C]Ir(COD)(Cl)$. As the reaction proceeds, two sets of doublets begin to appear at 12.81 and 30.97 ppm, with coupling constants of 59 Hz, which correspond to the ortho metalated complex, $[\kappa^2$-(C,C)-

($Ph_3PCPPh_2(C_6H_4)$)]Ir(COD). A singlet at 20.09 ppm is also observed, which is assigned to the protonated complex [$(Ph_3P)_2CH$]Cl (Figure 15).

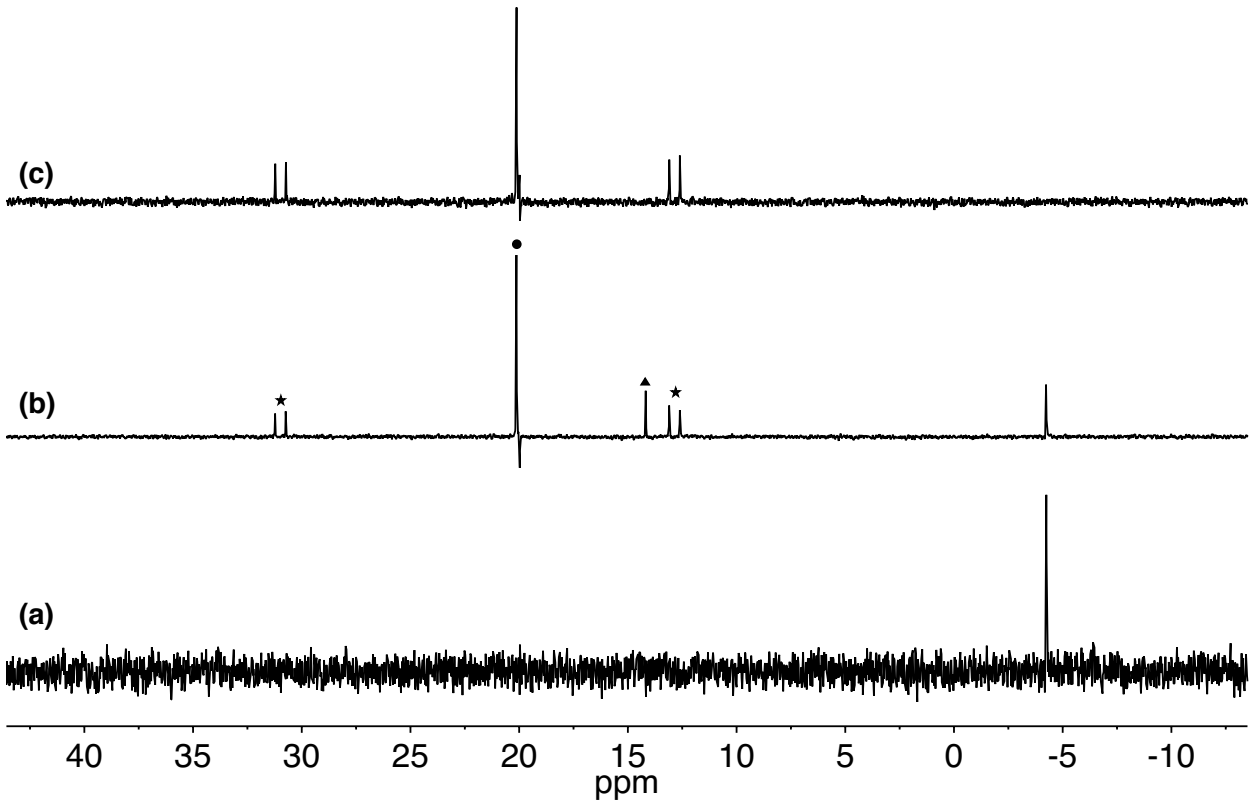

Figure 15. $^{31}P\{^1H\}$ NMR spectra of $[Ir(COD)Cl]_2$ upon treated with $(Ph_3P)_2C$. (a) free $(Ph_3P)_2C$, (b) mixture of $(Ph_3P)_2C$ and $[Ir(COD)Cl]_2$ after 10 minutes, (c) mixture of $(Ph_3P)_2C$ and $[Ir(COD)Cl]_2$ after 24 hours (Key: ★ = [κ^2-(C,C)-($Ph_3PCPPh_2(C_6H_4)$)]Ir(COD), ▲ = initial coordination complex, ● = [$(Ph_3P)_2CH$]Cl).

The geometry optimized structure of the proposed cyclometalated complex, [κ^2-(C,C)-($Ph_3PCPPh_2(C_6H_4)$)]Ir(COD), has been determined (Figure 16). The $C_{(central)}$–Ir and $C_{(ipso)}$–Ir bond lengths are 2.141 Å and 2.083 Å respectively. For reference, the average C–Ir bond length listed in the CSD[61] is 2.120 Å. Also, the P–C–P bond angle is 122.4˚.

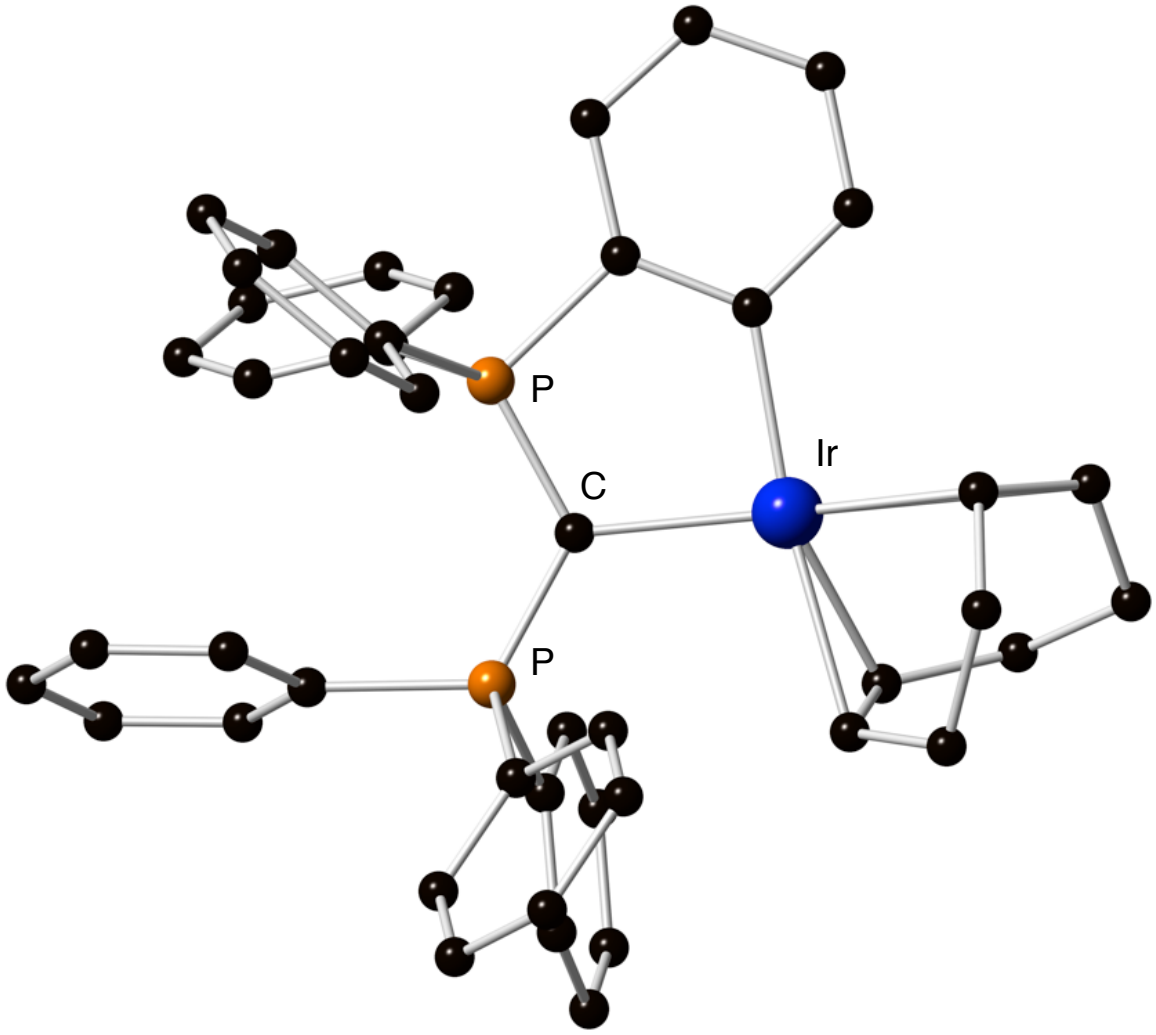

Figure 16. Geometry optimized structure of [κ^2-(C,C)-($Ph_3PCPPh_2(C_6H_4)$)]Ir(COD).

5.5.4 Synthesis, Characterization, and Protonation of [κ^2-(C,C)-($Ph_3PCPh_2(C_6H_4)$)]Ru(mesitylene)(Cl)

With respect to ruthenium, to date, only theoretical investigations into the use of carbodiphosphoranes versus NHC's as ligands for Grubb's catalysts have been explored.[72] Thus, to fill this void in the literature, the reactivity of $(Ph_3P)_2C$ towards $[Ru(mesitylene)Cl_2]_2$ was studied.

$(Ph_3P)_2C$ reacts with the ruthenium dimer, $[Ru(mesitylene)Cl_2]_2$, to yield the ortho metalated complex, $[\kappa^2\text{-}(C,C)\text{-}(Ph_3PCPPh_2(C_6H_4))]Ru(mesitylene)(Cl)$ as illustrated in Scheme 10. Similar to the other ortho metalated transition metal complexes in section 5.5.1 and 5.5.3, HCl is generated during the course of the reaction, such that the protonated compound, $[(Ph_3P)_2CH]Cl$, is formed as a side product. Thus, 2:1 ratio of $(Ph_3P)_2C$ to Ru must be used for the reaction to go to completion. $[\kappa^2\text{-}(C,C)\text{-}(Ph_3PCPPh_2(C_6H_4))]Ru(mesitylene)(Cl)$ is characterized by two doublets in the $^{31}P\{^1H\}$ NMR spectrum at 21.28 and 26.26 ppm, both with a coupling constant of 20 Hz.

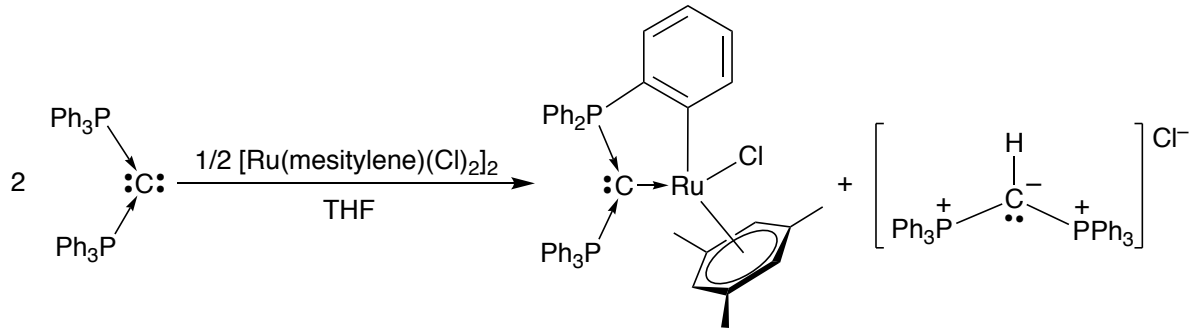

Scheme 10. Synthesis of $[\kappa^2\text{-}(C,C)\text{-}(Ph_3PCPPh_2(C_6H_4))]Ru(mesitylene)(Cl)$ via treatment of $[Ru(mesitylene)Cl_2]_2$ with $(Ph_3P)_2C$.

To study its susceptibility towards protonation, $[\kappa^2\text{-}(C,C)\text{-}(Ph_3PCPPh_2(C_6H_4))]Ru(mesitylene)(Cl)$ was treated with the strong acid 1,2,3,4,5-pentacarbomethoxycyclopentadiene (PCCP). Upon treatment, the NMR data are most consistent with protonation to generate $\{[\kappa^2\text{-}(C,C)\text{-}(Ph_3PCHPPh_2(C_6H_4))]Ru(mesitylene)(Cl)\}^+$, as identified by a new signal 4.74 ppm in the ^1H NMR. This signal appears as a doublet of doublets and is consistent with coupling to two chemically equivalent phosphorous atoms. Furthermore, two doublets are observed in the $^{31}P\{^1H\}$ NMR due to the chemically inequivalent phosphorus atoms, but the signals display second-order effects by virtue of the chemical shift frequencies

having similar values (21.75 and 22.15 ppm). Similar behavior is also observed for the compound [(dppm)$_2$C]NiCl, which forms {[(dppm)$_2$CH]NiCl}$^+$ upon treatment of HBF_4•OEt_2 and is characterized by a triplet at 4.37 ppm in the ^{1}H NMR.[44d]

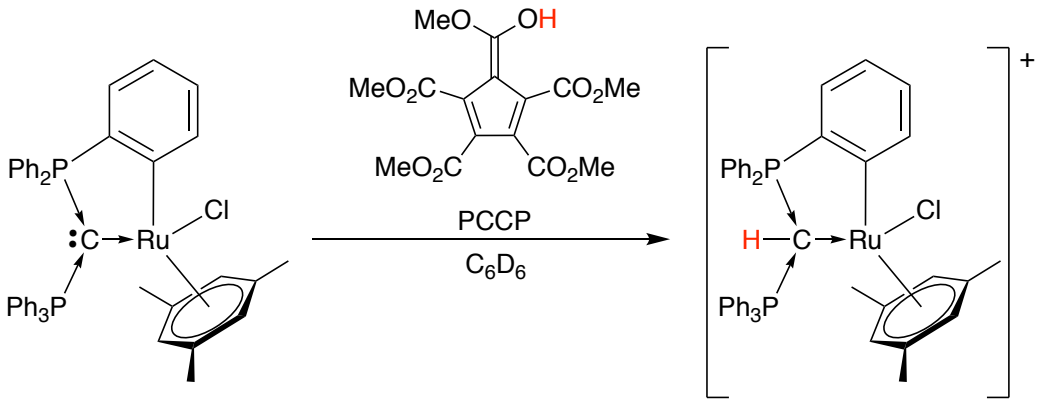

Scheme 11. Protonation of [κ^2-(C,C)-($Ph_3PCPPh_2(C_6H_4)$)]Ru(mesitylene)(Cl) with PCCP to form {[κ^2-(C,C)-($Ph_3PCHPPh_2(C_6H_4)$)]Ru(mesitylene)(Cl)}$^+$.

5.6 Summary and Conclusions

In summary, the first part of this chapter has outlined the reactivity of $(Ph_3P)_2C$ towards Lewis acids. The most common way $(Ph_3P)_2C$ reacts is to form a Lewis acid/base adduct in which the σ-lone pair donates its electrons to form a dative interaction. Additionally, because there are two lone pairs, $(Ph_3P)_2C$ can accommodate up to two metal centers, if the metals and ligands are of suitable steric size. Furthermore, if vacant orbitals are present on the coordinated metal/nonmetal, π-lone pair donation from $(Ph_3P)_2C$ is possible. $(Ph_3P)_2C$ is also susceptible to protonation and is also capable of forming ortho metalated complexes.

In the second part of this chapter, the NMR spectroscopic features of $(Ph_3P)_2C$ was discussed. For such a simple looking molecule, $(Ph_3P)_2C$ possess some complex features. Strong coupling between the phosphorus atoms of $(Ph_3P)_2C$ gives rise to a virtual

multiplet in the $^{13}C\{^1H\}$ NMR spectrum for the ipso-carbon that is consistent with an AA'X pattern (with A/A' corresponding to the phosphorus atoms and X corresponding to the ipso-carbon atom). Additionally, the central carbon atom appears as a triplet in the $^{13}C\{^1H\}$ NMR, consistent with an A_2X type pattern (A_2 corresponding to the phosphorus atoms and X corresponding to the central carbon). The ^{13}C-satellite peaks of the $^{31}P\{^1H\}$ NMR spectrum also exhibit the two AA'X and A_2X patterns which correspond to ^{31}P-coupling to the isotopomer with a ^{13}C-atom substituted at the ipso-position and ^{31}P-coupling to the central ^{13}C-atom isotopomer of $(Ph_3P)_2C$ respectively.

Lastly, the reactivity of $(Ph_3P)_2C$ towards main group alkyl metal complexes and transition metal complexes was discussed. $(Ph_3P)_2C$ reacts with Me_3Al, Me_3Ga, and MeHgI to form the corresponding Lewis acid/base compounds. However, $(Ph_3P)_2C$ only coordinates weakly to Me_2Zn and Me_2Cd such that coordination complexes cannot be isolated. $(Ph_3P)_2C$ also coordinates to Me_2Mg and $Mg[N(TMS)_2]_2$, but the simple Lewis acid/base complexes are not formed. Rather, the ortho metalated dimer and monomer, $\{[\kappa^2\text{-}(C,C)\text{-}(Ph_3PCPPh_2(C_6H_4))]Mg(\mu\text{-}Me)\}_2$ and $[\kappa^2\text{-}(C,C)\text{-}(Ph_3PCPPh_2(C_6H_4))]MgN(TMS)_2$, are respectively formed and serve as the first example of main group metal complexes undergoing ortho metalation of $(Ph_3P)_2C$. The coordination chemistry of $(Ph_3P)_2C$ has also been extended to the transition metals palladium, cobalt, iridium, and ruthenium, and, in each case, ortho metalated complexes are obtained.

5.7 Experimental Details

5.7.1 General Considerations

All manipulations were performed using a combination of glovebox, high vacuum and Schlenk techniques under a nitrogen or argon atmosphere.[73] Solvents were purified and

degassed by standard procedures. NMR spectra were measured on Bruker 300 DRX, Bruker 400 DRX, and Bruker Avance 500 DMX spectrometers. ^{1}H NMR spectra are reported in ppm relative to $SiMe_4$ ($\delta = 0$) and were referenced internally with respect to the protio solvent impurity ($\delta = 7.16$ for C_6D_5H and $\delta = 1.94$ for CD_2HCN).[74] ^{13}C NMR spectra are reported in ppm relative to $SiMe_4$ ($\delta = 0$) and were referenced internally with respect to the solvent ($\delta = 128.06$ for C_6D_6 and $\delta = 118.26$ for CD_3CN).[74] ^{31}P{^{1}H} NMR spectra are reported in ppm relative to 85% H_3PO_4 ($\delta = 0$) and were obtained by using the Ξ/100% value of 40.480742.[75] Coupling constants are reported in hertz. $(Ph_3P)_2C$,[45] Me2Mg,[76] $Mg[N(TMS)_2]_2$,[77] and $\{Co[N(TMS)_2]_2\}_2$[78] have been reported and were prepared by the corresponding literature method. PCCP was generously donated from the Tristan Lambert Lab at Columbia University. Other chemicals were obtained from Strem [Me_3Al, Me_3Ga, Me_2Zn, Me_2Cd] and Sigma-Aldrich [MeHgI, [Pd(π-cinnamyl)Cl]$_2$, [Ir(COD)Cl]$_2$, [Ru(mesitylene)Cl_2]$_2$.

5.7.2 X-ray Structure Determinations

X-ray diffraction data were collected on a Bruker Apex II diffractometer. Crystal data, data collection and refinement parameters are summarized in Table 3. The structures were solved by using direct methods and standard difference map techniques, and were refined by full-matrix least-squares procedures on F^2 with SHELXTL (Version 2014/7).[79]

5.7.3 Computational Details

Calculations were carried out using DFT as implemented in the Jaguar 8.9 (release 15) suite of *ab initio* quantum chemistry programs.[80] Geometry optimizations were performed with the B3LYP density functional using the LACVP** basis sets.[81] NBO calculations were performed with NBO 6.0[82] as implemented in the Jaguar suite of

programs. Cartesian coordinates and energies of the geometry optimized structures are provided in Table 4-Table 18.

5.7.4 Synthesis of $[(Ph_3P)_2C]AlMe_3$

A solution of $(Ph_3P)_2C$ (12 mg, 0.022 mmol) in benzene (1 mL) was treated with Me_3Al (10 mg, 0.139 mmol) to form a colorless solution which was left undisturbed in a vial for 2 days. During this time, colorless crystals were deposited on the walls of the vial which were then collected *via* decantation and washed with pentane (1 × 2 mL) to afford $[(Ph_3P)_2C]AlMe_3$ (5 mg, 36%). The colorless crystals obtained were suitable for X-ray diffraction. Anal. calcd. for $[(Ph_3P)_2C]AlMe_3$: C, 78.9%; H, 6.5%. Found: C, 77.9%; H, 6.4%. ^{1}H NMR (C_6D_6): –0.56 [s, 9H of C$\underline{H}_3$], 6.89 [m, 18H of $C_6\underline{H}_5$], 7.70 [m, 12H of $C_6\underline{H}_5$]. $^{31}P\{^1H\}$ NMR (C_6D_6): 19.69 [s, $[(Ph_3\underline{P})_2C]AlMe_3$].

5.7.5 Synthesis of $[(Ph_3P)_2C]GaMe_3$

A solution of $(Ph_3P)_2C$ (10 mg, 0.019 mmol) in C_6D_6 (0.7 mL) was treated with Me_3Ga (6 mg, 0.052 mmol) to form a colorless solution and was stirred for 1 hour. After this time, colorless crystals were crashed out and collected *via* decantation from the reaction by setting up a vapor diffusion with pentane as a counter solvent to yield $[(Ph_3P)_2C]GaMe_3$ (2 mg, 16%). The colorless crystals obtained were suitable for X-ray diffraction. ^{1}H NMR (C_6D_6): 0.21 [s, 9H of C$\underline{H}_3$], 7.03 [m, 18H of $C_6\underline{H}_5$], 7.41 [m, 12H of $C_6\underline{H}_5$]. $^{31}P\{^1H\}$ NMR (C_6D_6): 20.26 [s, $[(Ph_3\underline{P})_2C]GaMe_3$].

5.7.6 Reactivity of $(Ph_3P)_2C$ towards Me_2Zn

(a) A solution of $(Ph_3P)_2C$ (9 mg, 0.017 mmol) in C_6D_6 (0.7 mL) was treated with Me_2Zn (3 mg, 0.031 mmol) to form a colorless solution which was transferred to an NMR tube equipped with a J. Young valve and analyzed by ^{1}H and $^{31}P\{^1H\}$ NMR spectroscopy. The

reaction was then lyophilized and redissolved in C_6D_6 several times and analyzed by ^1H and $^{31}P\{^1H\}$ NMR spectroscopy each time thereby demonstrating that $(Ph_3P)_2C$ weakly coordinates to Me_2Zn due to the signals shifting after each lyophilization/redissolution cycle.

(b) A solution of $(Ph_3P)_2C$ (5 mg, 0.009 mmol) in C_6D_6 (0.7 mL) in an NMR tube equipped with a J. Young valve was titrated with increasing amounts of Me_2Zn (0.1 equivalents – 7 equivalents). The solution was analyzed by ^1H and $^{31}P\{^1H\}$ NMR spectroscopy there by demonstrating that $(Ph_3P)_2C$ weakly coordinates to Me_2Zn due to the signals shifting after each addition.

5.7.7 Reactivity of $(Ph_3P)_2C$ towards Me_2Cd

A solution of $(Ph_3P)_2C$ (9 mg, 0.017 mmol) in C_6D_6 (0.7 mL) was treated with Me_2Cd (3 mg, 0.021 mmol) to form a colorless solution which was transferred to an NMR tube equipped with a J. Young valve and analyzed by ^1H and $^{31}P\{^1H\}$ NMR spectroscopy. The reaction was then lyophilized and redissolved in C_6D_6 several times and analyzed by ^1H and $^{31}P\{^1H\}$ NMR spectroscopy each time thereby demonstrating that $(Ph_3P)_2C$ weakly coordinates to Me_2Cd due to the signals shifting after each lyophilization/redissolution cycle.

5.7.8 Synthesis of $\{[(Ph_3P)_2C]HgMe\}I$

A solution of MeHgI (11 mg, 0.032 mmol) in benzene (2 mL) was treated with $(Ph_3P)_2C$ (17 mg, 0.032 mmol) resulting in the immediate precipitation of colorless crystals. The reaction was allowed to sit for 16 hours in a vial and was occasionally shaken until the formation of crystals appeared to cease. The crystals were isolated by decantation and washed with benzene (2 × 2 mL) and pentane (1 × 2 mL) to yield $\{[(Ph_3P)_2C]HgMe\}I$ (25

mg, 89%). The colorless crystals obtained were suitable for X-ray diffraction. Anal. calcd. for $[(Ph_3P)_2C]AlMe_3$: C, 59.1%; H, 3.8%. Found: C, 55.1%; H, 3.8%. ^{1}H NMR (CD_3CN): 0.02 [s, 3H of C<u>H</u>$_3$], 7.42 [m, 12H of C_6<u>H</u>$_5$], 7.58 [m, 18H of C_6<u>H</u>$_5$]. $^{31}P\{^1H\}$ NMR (CD_3CN): 20.32 [s, {[(Ph_3<u>P</u>)$_2$C]HgMe}I]. $^{199}Hg\{^1H\}$ NMR (CD_3CN): –408.03 [s, {[$(Ph_3P)_2$C]<u>Hg</u>Me}I].

5.7.9 Synthesis of $\{[\kappa^2\text{-}(C,C)\text{-}(Ph_3PCPPh_2(C_6H_4))]Mg(\mu\text{-}Me)\}_2$

An ampoule charged with a mixture of $(Ph_3P)_2C$ (48 mg, 0.089 mmol) and Me_2Mg (26 mg, 0.481 mmol) in benzene (8 mL) was heated at 80˚C for 4.5 hours which slowly turns from being yellow in color to white. After this time, the reaction was filtered, and the volatile components of the filtrate were removed *in vacuo* and to yield $\{[\kappa^2\text{-}(C,C)\text{-}(Ph_3PCPPh_2(C_6H_4))]Mg(\mu\text{-}Me)\}_2$ as a white powder (37 mg, 57%). Colorless crystals suitable for X-ray diffraction were obtained *via* vapor diffusion of pentane into benzene solution. ^{1}H NMR (C_6D_6): –0.67 [broad s, 6H of bridging C<u>H</u>$_3$], 6.78–7.03 [m, 15H of C_6<u>H</u>$_5$], 7.09 [m, 1H of C_6<u>H</u>$_4$], 7.34 [m, 2H of C_6<u>H</u>$_4$], 7.47–7.62 [m, 10H of C_6<u>H</u>$_5$], 8.55 [m, 1H of C_6<u>H</u>$_4$]. $^{31}P\{^1H\}$ NMR (C_6D_6): 13.11 [d, 1P of $\{[\kappa^2\text{-}(C,C)\text{-}(Ph_3$<u>P</u>$CPPh_2(C_6H_4))]Mg(\mu\text{-}Me)\}_2$, $^2J_{P\text{-}P}$ = 20], 17.81 [d, 1P of $\{[\kappa^2\text{-}(C,C)\text{-}(Ph_3PC$<u>P</u>$Ph_2(C_6H_4))]Mg(\mu\text{-}Me)\}_2$, $^2J_{P\text{-}P}$ = 20].

5.7.10 Synthesis of $[\kappa^2\text{-}(C,C)\text{-}(Ph_3PCPPh_2(C_6H_4))]MgN(TMS)_2$

A solution of $(Ph_3P)_2C$ (11 mg, 0.021 mmol) in C_6D_6 (0.7 mL) was treated with $Mg[N(TMS)_2]_2$ (23 mg, 0.067 mmol) to form a colorless solution which was transferred to an NMR tube equipped with a J. Young valve and was heated at 60˚C for 1 day. After this time, colorless crystals were crashed out and collected *via* decantation from the reaction by setting up a vapor diffusion with pentane as a counter solvent to yield $[\kappa^2\text{-}(C,C)\text{-}(Ph_3PCPPh_2(C_6H_4))]MgN(TMS)_2$ (5 mg, 34%). The colorless crystals obtained were suitable for X-ray diffraction. ^{1}H NMR (C_6D_6): 0.30 [s, 18H of C<u>H</u>$_3$], 6.76 [m, 4H of C_6<u>H</u>$_5$],

6.83–6.98 [m, 10H of $C_6\underline{H}_5$], 7.03 [m, 3H of $C_6\underline{H}_5$], 7.21–7.36 [m, 3H of $C_6\underline{H}_4$], 7.38–7.54 [m, 8H of $C_6\underline{H}_4$], 8.47 [d, 1H of $C_6\underline{H}_4$, $^3J_{H\text{-}H}$ = 7 Hz]. $^{31}P\{^1H\}$ NMR (C_6D_6): 14.92 [d, 1P of [κ^2-(C,C)-($Ph_3\underline{P}CPh_2(C_6H_4)$)]$MgN(TMS)_2$, $^2J_{P\text{-}P}$ = 22], 19.38 [d, 1P of [κ^2-(C,C)-($Ph_3PC\underline{P}Ph_2(C_6H_4)$)]$MgN(TMS)_2$, $^2J_{P\text{-}P}$ = 22].

5.7.11 Synthesis of [κ^2-(C,C)-($Ph_3PCPPh_2(C_6H_4)$)]Pd(π-cinnamyl) and crystallization of [$(Ph_3P)_2CH$][(π-cinnamyl)$PdCl_2$]

A solution of [Pd(π-cinnamyl)Cl]$_2$ (13 mg, 0.025 mmol) in benzene (6 mL) was treated with $(Ph_3P)_2C$ (27 mg, 0.050 mmol) and stirred for 20 hours resulting in the formation of an orange precipitate in a yellow solution. The reaction was then filtered, and the volatile components of the filtrate were removed *in vacuo* to yield a yellow residue. The residue was then extracted with diethyl ether (2 × 5 mL) and the combined extracts were pumped to dryness *in vacuo* to afford [κ^2-(C,C)-($Ph_3PCPPh_2(C_6H_4)$)]Pd(π-cinnamyl) as a yellow powder (15 mg, 38%). Yellow crystals suitable for X-ray diffraction were obtained *via* slow evaporation of a tetrahydrofuran solution. ^1H NMR (C_6D_6): 1.95 [d, 1H of π-cinnamyl $C_3\underline{H}_4$, $^3J_{H\text{-}H}$ = 13 Hz], 2.37 [d, 1H of π-cinnamyl $C_3\underline{H}_4$, $^3J_{H\text{-}H}$ = 8 Hz], 4.35 [d, 1H of π-cinnamyl $C_3\underline{H}_4$, $^3J_{H\text{-}H}$ = 12 Hz], 5.58 [m, 1H of π-cinnamyl $C_3\underline{H}_4$], 6.74–7.13 [m, 16H of $C_6\underline{H}_5$], 7.23 [m, 3H of $C_6\underline{H}_5$], 7.43–7.58 [m, 7H of $C_6\underline{H}_5$], 7.69 [m, 2H of $C_6\underline{H}_5$], 7.82 [m, 7H of $C_6\underline{H}_5$]. $^{31}P\{^1H\}$ NMR (C_6D_6): 9.14 [d, 1P of [κ^2-(C,C)-($Ph_3\underline{P}CPPh_2(C_6H_4)$)]Pd(π-cinnamyl), $^2J_{P\text{-}P}$ = 52], 37.05 [d, 1P of [κ^2-(C,C)-($Ph_3PC\underline{P}Ph_2(C_6H_4)$)] Pd(π-cinnamyl), $^2J_{P\text{-}P}$ = 52]. Crystals suitable for X-ray diffraction of the protonated side product, [$(Ph_3P)_2CH$][(π-cinnamyl)$PdCl_2$], were obtained *via* slow evaporation of the filtrate from the reaction mixture yield orange crystals, which are clear and distinct from the yellow crystal of [κ^2-(C,C)-($Ph_3PCPPh_2(C_6H_4)$)]Pd(π-cinnamyl).

5.7.12 Synthesis of [κ^2-(C,C)-($Ph_3PCPPh_2(C_6H_4)$)]Co[$N(TMS)_2$]

A solution of $\{Co[N(TMS)_2]_2\}_2$ (8 mg, 0.011 mmol) in C_6D_6 (0.7 mL) was treated with $(Ph_3P)_2C$ (6 mg, 0.011 mmol) to form a green solution and was transferred to an NMR tube equipped with a J. Young valve. After 24 hours, the reaction mixture was allowed to slowly evaporate producing green crystals which were collected *via* decantation to afford [κ^2-(C,C)-($Ph_3PCPPh_2(C_6H_4)$)]Co[$N(TMS)_2$] (3 mg, 38%). The green crystals obtained were suitable for X-ray diffraction. ^{1}H NMR (C_6D_6): –17.83 [broad s], –9.28 [broad s], –5.76 [broad s], –2.25 [broad s], 2.29 [broad s], 3.28 [s], 3.92 [s], 4.45 [s], 7.07 [broad s], 7.90 [broad s]. $^{31}P\{^1H\}$ NMR (C_6D_6): 16.76 [s].

5.7.13 Generation of [κ^2-(C,C)-($Ph_3PCPPh_2(C_6H_4)$)]Ir(COD)

A solution of $[Ir(COD)Cl]_2$ (5 mg, 0.007 mmol) in C_6D_6 (0.7 mL) was treated with $(Ph_3P)_2C$ (16 mg, 0.030 mmol) to form a yellow/orange solution and was transferred to an NMR tube equipped with a J. Young valve. The reaction was monitored by NMR spectroscopy over the course of 3 days thereby demonstrating the formation of [κ^2-(C,C)-($Ph_3PCPPh_2(C_6H_4)$)]Ir(COD) {$^{31}P\{^1H\}$ NMR (C_6D_6): 12.81 [d, 1P of [κ^2-(C,C)-($Ph_3\underline{P}CPPh_2(C_6H_4)$)]Ir(COD), $^2J_{P\text{-}P}$ = 59], 30.98 [d, 1P of [κ^2-(C,C)-($Ph_3PC\underline{P}Ph_2(C_6H_4)$)]Ir(COD), $^2J_{P\text{-}P}$ = 59]}, $[(Ph_3P)_2CH]Cl$ {$^{31}P\{^1H\}$ NMR (C_6D_6): 20.11 [s, 2P of $[(Ph_3\underline{P})_2CH]Cl$]}, and $[(Ph_3P)_2C]Ir(COD)(Cl)$ {$^{31}P\{^1H\}$ NMR (C_6D_6): 14.15 [s, 2P of $[(Ph_3P)_2C]Ir(COD)(Cl)$}.

5.7.14 Synthesis of [κ^2-(C,C)-($Ph_3PCPPh_2(C_6H_4)$)]Ru(mesitylene)(Cl)

A solution of $[Ru(mesitylene)Cl_2]_2$ (8 mg, 0.014 mmol) in THF (8 mL) was treated with $(Ph_3P)_2C$ (31 mg, 0.058 mmol) and stirred for 3 days resulting in the formation of brown colored solution with a lighter colored precipitate. After this time, the reaction was filtered, and the filtrate was pumped to dryness *in vacuo* to yield a brown oily residue.

The residue was dissolved in benzene (1 mL) and lyophilized to afford [κ^2-(C,C)-($Ph_3PCPPh_2(C_6H_4)$)]Ru(mesitylene)(Cl) as fluffy tan powder (10 mg, 43%). ^{1}H NMR (C_6D_6): 1.36 [broad s, 9H of mesitylene C$\underline{H}_3$], 6.90–7.14 [m, 20 aromatic H's], 7.75 [m, 8 aromatic H's], 8.12 [m, 4 aromatic H's. $^{31}P\{^1H\}$ NMR (C_6D_6): 21.31 [d, 1P of [κ^2-(C,C)-($Ph_3\underline{P}CPPh_2(C_6H_4)$)]Ru(mesitylene)(Cl), $^2J_{P\text{-}P}$ = 19], 26.23 [d, 1P of [κ^2-(C,C)-($Ph_3PC\underline{P}Ph_2(C_6H_4)$)]Ru(mesitylene)(Cl), $^2J_{P\text{-}P}$ = 19].

5.7.15 Protonation of [κ^2-(C,C)-($Ph_3PCPPh_2(C_6H_4)$)]Ru(mesitylene)(Cl)

A solution of [κ^2-(C,C)-($Ph_3PCPPh_2(C_6H_4)$)]Ru(mesitylene)(Cl) (2 mg, 0.003 mmol) in C_6D_6 (0.7 mL) was treated with PCCP (1 mg, 0.003 mmol) to form a colorless solution and was transferred to an NMR tube equipped with a J. Young valve. The reaction was monitored by NMR spectroscopy thereby showing the formation of {[κ^2-(C,C)-($Ph_3PCHPPh_2(C_6H_4)$)]Ru(mesitylene)(Cl)}$^+$. ^{1}H NMR (C_6D_6): 1.35 [broad s, 9H of mesitylene C$\underline{H}_3$], 3.63 [s, 15H of PCCP C$\underline{H}_3$], 4.74 [dd, 1H of ($Ph_3PC\underline{H}PPh_2(C_6H_4)$), $^2J_{H\text{-}P}$ = 12 and 17 Hz], 6.93–7.14 [m, 20 aromatic H's], 7.48 [m, 8 aromatic H's], 8.10 [m, 4 aromatic H's. $^{31}P\{^1H\}$ NMR (C_6D_6): 21.76 [ab quartet, 1P of {[κ^2-(C,C)-($Ph_3\underline{P}CHPPh_2(C_6H_4)$)]Ru(mesitylene)(Cl)}$^+$, $^2J_{P\text{-}P}$ = 14], 22.16 [d, {[κ^2-(C,C)-($Ph_3PCH\underline{P}Ph_2(C_6H_4)$)]Ru(mesitylene)(Cl)}$^+$, $^2J_{P\text{-}P}$ = 14].

5.8 Crystallographic Data

Table 3. Crystal, intensity collection, and refinement data.

	$[(Ph_3P)_2C]AlMe_3$	**$[(Ph_3P)_2C]GaMe_3$**
lattice	Monoclinic	Monoclinic
formula	$C_{40}H_{39}AlP_2$	$C_{40}H_{39}GaP_2$
formula weight	608.63	651.37
space group	$P2_1/c$	$P2_1/c$
a/Å	16.072(2)	16.0714(6)
b/Å	11.5121(17)	11.5306(4)
c/Å	18.600(3)	18.5845(7)
α/°	90	90
β/°	109.899(2)	109.8387(5)
γ/°	90	90
V/Å^3	3235.9(8)	3239.6(2)
Z	4	4
temperature (K)	130(2)	130(2)
radiation (λ, Å)	0.71073	0.71073
ρ (calcd.) g cm^{-3}	1.249	1.336
μ (Mo Kα), mm^{-1}	0.190	0.976
θ max, deg.	30.610	30.622
no. of data collected	52477	52562
no. of data	9961	9984
no. of parameters	391	391
R_1 [$I > 2\sigma(I)$]	0.0476	0.0466
wR_2 [$I > 2\ \sigma(I)$]	0.1226	0.1559
R_1 [all data]	0.0719	0.0549
wR_2 [all data]	0.1330	0.1584
GOF	1.229	1.932
R_{int}	0.0594	0.0384

Table 3. Crystal, intensity collection, and refinement data.

	{[(Ph$_3$P)$_2$C]HgMe}I	**{[κ^2-(C,C)-(Ph$_3$PCPPh$_2$(C$_6$H$_4$))]Mg(μ-Me)}$_2$•2C$_6$H$_6$**
lattice	Triclinic	Monoclinic
formula	$C_{44}H_{39}HgIP_2$	$C_{100}H_{88}Mg_2P_4$
formula weight	957.18	1462.20
space group	*P–1*	$P2_1/c$
a / Å	9.7589(13)	14.655(6)
b / Å	10.7621(15)	10.248(5)
c / Å	18.482(3)	26.929(12)
α / °	85.570(2)	90
β / °	87.893(2)	98.887(7)
γ / °	79.353(2)	90
V / Å^3	1901.5(5)	3996(3)
Z	2	2
temperature (K)	130(2)	130(2)
radiation (λ, Å)	0.71073	0.71073
ρ (calcd.) g cm^{-3}	1.672	1.215
μ (Mo Kα), mm^{-1}	4.973	0.159
θ max, deg.	27.102	30.580
no. of data collected	24594	64258
no. of data	8407	12221
no. of parameters	434	490
R_1 [$I > 2\sigma(I)$]	0.0494	0.0607
wR_2 [$I > 2\ \sigma(I)$]	0.0947	0.1423
R_1 [all data]	0.0871	0.1206
wR_2 [all data]	0.1067	0.1675
GOF	1.019	1.090
R_{int}	0.0816	0.1023

Table 3. Crystal, intensity collection, and refinement data.

	[κ²-(C,C)-($Ph_3PCPPh_2(C_6H_4)$)]MgN(TMS)$_2$	**[κ²-(C,C)-($Ph_3PCPPh_2(C_6H_4)$)]Pd(π-cinnamyl)•C_6H_6**
lattice	Triclinic	Monoclinic
formula	$C_{43}H_{47}MgNP_2Si_2$	$C_{49}H_{41}PdP_2$
formula weight	720.24	798.16
space group	*P–1*	$P2_1/c$
a / Å	10.927(2)	10.6668(5)
b / Å	13.208(2)	14.6748(7)
c / Å	14.974(3)	24.7212(13)
α / °	87.327(3)	90
β / °	83.015(3)	93.5620(10)
γ / °	73.912(3)	90
V / Å^3	2060.9(7)	3862.2(3)
Z	2	4
temperature (K)	130(2)	130(2)
radiation (λ, Å)	0.71073	0.71073
ρ (calcd.) g cm^{-3}	1.161	1.373
μ (Mo Kα), mm^{-1}	0.208	0.597
θ max, deg.	30.539	30.539
no. of data collected	32418	62442
no. of data	12471	11799
no. of parameters	452	469
R_1 [$I > 2\sigma(I)$]	0.0820	0.0441
wR_2 [$I > 2\ \sigma(I)$]	0.2369	0.1111
R_1 [all data]	0.1102	0.0685
wR_2 [all data]	0.2479	0.1211
GOF	1.864	1.208
R_{int}	0.0386	0.0714

Table 3. Crystal, intensity collection, and refinement data.

	[$(Ph_3P)_2CH$][(π-cinnamyl)$PdCl_2$])•C_6H_6	**[κ^2-(C,C)-($Ph_3PCPPh_2(C_6H_4)$)]Co[$N(TMS)_2$]**
lattice	Triclinic	Triclinic
formula	$C_{52}H_{46}Cl_2P_2Pd$	$C_{43}H_{47}CoNP_2Si_2$
formula weight	910.13	754.86
space group	*P–1*	*P–1*
a / Å	11.1448(6)	10.8977(4)
b / Å	14.6776(8)	13.0738(5)
c / Å	14.8081(8)	15.0695(5)
α / °	107.2210(10)	87.4400(10)
β / °	106.0170(10)	83.0190(10)
γ / °	97.8080(10)	74.2830(10)
V / Å^3	2160.5(2)	2051.27(13)
Z	2	2
temperature (K)	160(2)	130(2)
radiation (λ, Å)	0.71073	0.71073
ρ (calcd.) g cm^{-3}	1.399	1.222
μ (Mo Kα), mm^{-1}	0.663	0.584
θ max, deg.	30.832	30.737
no. of data collected	35806	34331
no. of data	13339	12694
no. of parameters	518	452
R_1 [$I > 2\sigma(I)$]	0.0380	0.0696
wR_2 [$I > 2\ \sigma(I)$]	0.1100	0.2065
R_1 [all data]	0.0441	0.1008
wR_2 [all data]	0.1135	0.2204
GOF	1.476	1.417
R_{int}	0.0439	0.0385

5.9 Computational Data

Table 4. Cartesian Coordinates for Geometry Optimized Compounds

$[(Ph_3P)_2C]AlMe_3$			
-2472.85909245198 Hartrees			
atom	**x**	**y**	**z**
Al	8.946690318	3.271702779	13.28157703
P	8.334344153	4.964713738	10.5217366
P	7.128469626	6.111904878	13.00756383
C	8.074338308	4.935380822	12.21355485
C	10.14153776	4.005571008	14.72367221
H	10.75108727	3.185342585	15.13154684
H	9.618962115	4.457027526	15.57446328
H	10.85788242	4.756061432	14.35706044
C	7.423538467	2.111174488	13.96718267
H	7.348922581	2.133776731	15.06301751
H	7.600411768	1.059379263	13.69863335
H	6.420115963	2.356149465	13.58731114
C	10.0643786	2.165098583	12.01433837
H	10.23641625	1.211056659	12.5373097
H	11.05692775	2.586360084	11.81507921
H	9.636304553	1.895841993	11.04051132
C	10.12344755	4.843756807	10.09474628
C	11.05614792	5.341284373	11.01241862
H	10.71132609	5.680000977	11.98305158
C	12.41472418	5.359663318	10.69877187
H	13.12873669	5.740066281	11.4234297

C	12.85548569	4.8736617	9.468100392
H	13.91442433	4.881669801	9.225548475
C	11.93312408	4.362600483	8.554628687
H	12.27122541	3.967579003	7.600734816
C	10.57388007	4.347212187	8.863908629
H	9.87311622	3.932497719	8.148392876
C	7.793390529	6.458240498	9.568872108
C	8.711994006	7.457516852	9.217345122
H	9.754693249	7.358429054	9.497951816
C	8.297221918	8.579012501	8.499586428
H	9.022024012	9.342605404	8.232326106
C	6.962922746	8.716755256	8.120318509
H	6.643781408	9.587323309	7.554141737
C	6.039621143	7.729934832	8.466912586
H	4.998349677	7.827949339	8.172946535
C	6.450370314	6.608401396	9.185708135
H	5.722680658	5.844751201	9.438059215
C	7.495167874	3.604598474	9.588652377
C	6.994926426	2.500739425	10.29134193
H	7.099670291	2.455269996	11.36966943
C	6.358790266	1.461368311	9.611054766
H	5.979642304	0.611191501	10.17061694
C	6.211427651	1.513131155	8.225530511
H	5.715007514	0.703227034	7.69823752
C	6.69716335	2.613534616	7.518113635
H	6.575832927	2.667283998	6.43973685

C	7.331747204	3.654747402	8.193848215
H	7.679438068	4.515900537	7.632014463
C	7.600018708	7.860645889	12.62687798
C	8.956765482	8.199021556	12.76908424
H	9.668575502	7.439527852	13.07720777
C	9.398151341	9.495289247	12.51208113
H	10.44885979	9.741639252	12.63751734
C	8.493585831	10.47014352	12.08742261
H	8.836913163	11.47991678	11.8803212
C	7.150765247	10.13820149	11.91933112
H	6.444250197	10.88660492	11.57160509
C	6.703700328	8.843699809	12.19051915
H	5.657685043	8.603088107	12.04263306
C	5.287705765	6.036244957	12.7750064
C	4.736614801	5.04901229	11.95241493
H	5.394131867	4.347059259	11.44974369
C	3.351191271	4.944060814	11.79823133
H	2.93923849	4.168403295	11.15862316
C	2.503131005	5.823017534	12.47011038
H	1.426455441	5.74301636	12.35076012
C	3.044260276	6.797255852	13.31348194
H	2.389167172	7.473802512	13.85511208
C	4.424553499	6.897608926	13.47328655
H	4.829843004	7.640512435	14.15387376
C	7.216214846	6.002228525	14.84523084
C	7.906149142	6.93708987	15.62748713

H	8.43948703	7.757332642	15.16305854
C	7.910320152	6.829268458	17.01862355
H	8.452517668	7.562187429	17.60938642
C	7.225777179	5.789773334	17.64632714
H	7.233028551	5.70587475	18.72934747
C	6.527021562	4.860469537	16.87388777
H	5.988646147	4.046718534	17.35090956
C	6.515411796	4.968397713	15.48490254
H	5.965222098	4.239653716	14.9017054

Table 5. Cartesian Coordinates for Geometry Optimized Compounds

Me_3Al			
-362.200078676821 Hartrees			
atom	**x**	**y**	**z**
Al	8.937411076	2.924699516	13.41361796
C	9.826803569	4.045916302	14.77315322
H	9.98324834	3.482194706	15.70312217
H	9.208330999	4.910718621	15.04720713
H	10.80399292	4.426519185	14.45653474
C	7.104219296	2.264893221	13.72908484
H	6.739991401	2.455089206	14.7445377
H	7.023959908	1.185949388	13.54377415
H	6.395965917	2.742276088	13.03766224
C	9.879054629	2.465350319	11.74097253
H	10.77078986	1.857865342	11.94789549
H	10.24130948	3.363949921	11.22459234

H	9.261676961	1.903403351	11.03164581

Table 6. Cartesian Coordinates for Geometry Optimized Compounds

$[(Ph_3P)_2C]GaMe_3$

-2232.46664123747 Hartrees

atom	x	y	z
Ga	8.88943668	3.183774808	13.2967597
P	8.345157492	4.986692247	10.50385676
P	7.127744634	6.118049432	12.99113493
C	8.070706084	4.949734242	12.18976069
C	10.06834489	3.917695071	14.77013407
H	10.6979223	3.107322181	15.16450424
H	9.518966047	4.336039569	15.61968807
H	10.75749118	4.697368332	14.41682517
C	7.262942313	2.103945953	13.92040615
H	7.195907963	2.068107789	15.01558527
H	7.344125096	1.061742809	13.58174336
H	6.292116788	2.471420996	13.55936381
C	9.994360772	2.063009845	12.00825527
H	10.12608382	1.081242117	12.48685178
H	10.99906546	2.465787099	11.83795436
H	9.557994282	1.864337069	11.02261581
C	10.14352597	4.845492981	10.10838015
C	11.0638795	5.280662195	11.0696916
H	10.69912972	5.588019591	12.0444946
C	12.43194201	5.275936697	10.79363681

H	13.13383366	5.608206984	11.55351762
C	12.8964968	4.829722128	9.556016518
H	13.96170505	4.820022881	9.34226988
C	11.98543739	4.379453015	8.598850397
H	12.33900824	4.014177167	7.638406648
C	10.61778964	4.386594321	8.871044441
H	9.928163002	4.018069754	8.11981659
C	7.816416678	6.482397127	9.540502912
C	8.74104277	7.464233758	9.157812368
H	9.787497093	7.355891278	9.422818136
C	8.329492125	8.580795663	8.427897843
H	9.061154782	9.329580531	8.136977794
C	6.990888462	8.732685504	8.066578083
H	6.673808892	9.598558728	7.491867796
C	6.06140212	7.762429223	8.446076714
H	5.016109395	7.868667487	8.168358853
C	6.469543653	6.646771158	9.175653893
H	5.734288263	5.89829921	9.45182769
C	7.504434271	3.632522063	9.557558815
C	6.965675769	2.541193924	10.25165811
H	7.048546783	2.495078009	11.33173714
C	6.317302023	1.515519433	9.562063064
H	5.907035023	0.676163805	10.11661701
C	6.196686709	1.567090575	8.173931954
H	5.690358887	0.767946718	7.63900765
C	6.721507135	2.654513678	7.473779203

H	6.620196002	2.709130161	6.393039123
C	7.366530289	3.683024077	8.159877834
H	7.739751289	4.536564197	7.602346246
C	7.54280213	7.878058503	12.58477803
C	8.894910472	8.253948106	12.66125191
H	9.643662202	7.509698065	12.91562369
C	9.285259798	9.566946089	12.40523635
H	10.33407982	9.841513157	12.47961101
C	8.33246519	10.52223088	12.04685129
H	8.635333625	11.54546972	11.84163444
C	6.992498051	10.15354184	11.94128322
H	6.247246673	10.88673156	11.64471534
C	6.597418748	8.842010465	12.2116254
H	5.55152391	8.573890788	12.11647206
C	5.283353418	5.999495955	12.80501653
C	4.737217699	5.032677858	11.95521553
H	5.399409115	4.368615883	11.40957968
C	3.35221431	4.895079265	11.83085156
H	2.943908822	4.134260795	11.17115968
C	2.499418497	5.721117453	12.56030531
H	1.422107148	5.613909503	12.46619054
C	3.033987659	6.677754728	13.42739768
H	2.373840459	7.313234945	14.0116933
C	4.41494226	6.810293154	13.55657721
H	4.817628431	7.538033727	14.25549286
C	7.256807354	6.040769199	14.82953638

C	7.979332165	6.981636482	15.57573357
H	8.515701855	7.782143255	15.07994419
C	8.009950637	6.908770966	16.96962
H	8.575722097	7.647626689	17.53056262
C	7.319679664	5.89840313	17.63762566
H	7.345307405	5.842908554	18.72232881
C	6.590361031	4.962068364	16.9023751
H	6.046733489	4.170724176	17.41058586
C	6.552215681	5.035502939	15.51159585
H	5.977495101	4.301553025	14.95889021

Table 7. Cartesian Coordinates for Geometry Optimized Compounds

Me_3Ga			
-121.816112967257 Hartrees			
atom	**x**	**y**	**z**
Ga	8.937435481	2.92514893	13.41342272
C	9.833084775	4.053744081	14.78544511
H	9.984108997	3.488918602	15.71450826
H	9.214067462	4.919224563	15.0525051
H	10.81033226	4.427703973	14.46464827
C	7.090181696	2.25846037	13.73069747
H	6.732528024	2.452194468	14.74679716
H	7.016164047	1.179776641	13.54703348
H	6.384153354	2.735404119	13.03814445
C	9.886781291	2.461998349	11.72794688
H	10.7754316	1.852518062	11.9374048

H	10.24824541	3.361875881	11.21519584
H	9.262919558	1.902916051	11.0236225

Table 8. Cartesian Coordinates for Geometry Optimized Compounds

$[(Ph_3P)_2C]InMe_3$			
-2232.26816129136 Hartrees			
atom	**x**	**y**	**z**
In	9.022682201	3.136642889	13.36501729
P	8.276537516	5.009724547	10.47836538
P	7.062797533	6.146681576	12.96789706
C	7.998494806	4.981518063	12.16091767
C	10.29948834	4.097253018	14.86453715
H	10.95478488	3.350463747	15.3328355
H	9.735689901	4.581981627	15.66800645
H	10.95889076	4.857347674	14.42437199
C	7.325839253	1.914707859	14.09540123
H	7.192436385	1.990787295	15.18178091
H	7.512517594	0.855121604	13.87470179
H	6.357150188	2.162123763	13.63910811
C	10.1717987	1.970927405	11.89234539
H	10.35317158	0.978435211	12.32851701
H	11.15206165	2.407052414	11.67130809
H	9.670326875	1.800449212	10.93295018
C	10.07431743	4.858231796	10.07792229
C	11.00307013	5.342568116	11.00772414
H	10.64917006	5.698335722	11.96977147

C	12.36809611	5.333121169	10.71722547
H	13.07612948	5.704411359	11.45294536
C	12.82203428	4.832759787	9.496307748
H	13.88500292	4.818379226	9.271873722
C	11.90329369	4.334745952	8.570814905
H	12.24874647	3.926920958	7.624669683
C	10.53850089	4.346811685	8.857402149
H	9.842685192	3.940952765	8.131391156
C	7.761366378	6.500617449	9.500745933
C	8.692806409	7.483138159	9.134712348
H	9.736126851	7.370735411	9.410134992
C	8.291960586	8.605310232	8.40784971
H	9.028864403	9.353829074	8.12951744
C	6.957544089	8.762860087	8.033055675
H	6.649092891	9.63302772	7.460117782
C	6.021738638	7.792173891	8.395607264
H	4.979913105	7.902729027	8.106872015
C	6.418878822	6.670731943	9.122978804
H	5.678995316	5.922414018	9.387315185
C	7.440234492	3.641363349	9.551583259
C	6.939949543	2.543220763	10.26404829
H	7.035892949	2.513048366	11.34405273
C	6.30920704	1.493702068	9.594304692
H	5.930064092	0.648747108	10.16226357
C	6.165846496	1.529947874	8.20768501
H	5.672727575	0.712805775	7.687927305

C	6.650769239	2.624220303	7.489650506
H	6.532062803	2.665439409	6.410153383
C	7.281371686	3.674724655	8.155812402
H	7.629920499	4.530039716	7.584913391
C	7.532033466	7.901120348	12.60545501
C	8.888828481	8.239209784	12.75054401
H	9.599172683	7.480391955	13.06516738
C	9.332321551	9.533966464	12.48976765
H	10.38323396	9.779728776	12.61729351
C	8.429629532	10.5081396	12.05850965
H	8.77477112	11.51679889	11.8475631
C	7.08624068	10.17749317	11.89015144
H	6.38098567	10.92611671	11.53932352
C	6.637000572	8.884065968	12.16513185
H	5.589979046	8.64414716	12.01883146
C	5.21710296	6.075090115	12.75043205
C	4.658521059	5.104425557	11.91273791
H	5.312133203	4.414986641	11.38748983
C	3.271775563	4.9981338	11.77258898
H	2.854345483	4.234874484	11.12137483
C	2.428403439	5.859296522	12.4732124
H	1.350338891	5.777501858	12.36553086
C	2.97673231	6.81825634	13.32994823
H	2.325815039	7.481391965	13.89350606
C	4.359120829	6.919529896	13.47581805
H	4.770430674	7.650599566	14.16644818

C	7.161186364	6.009712662	14.80499194
C	7.800431542	6.964276317	15.6074976
H	8.291237232	7.820221472	15.15931513
C	7.80820724	6.828910736	16.99726053
H	8.311231205	7.577054216	17.60384126
C	7.177676889	5.74299142	17.60306099
H	7.187693438	5.638345338	18.68441806
C	6.529428537	4.793472901	16.81070911
H	6.032920338	3.943694851	17.27039201
C	6.514165717	4.928047736	15.42386678
H	6.002198519	4.183169321	14.82537571

Table 9. Cartesian Coordinates for Geometry Optimized Compounds

Me_3In			
-121.615604007729 Hartrees			
atom	**x**	**y**	**z**
In	8.937510919	2.924993271	13.41356267
C	9.90846291	4.151717406	14.90796344
H	10.06179857	3.585654955	15.83448572
H	9.29035548	5.018363719	15.16910389
H	10.88431515	4.521759346	14.5796849
C	6.927619464	2.199744409	13.75380633
H	6.577656908	2.395069499	14.7718558
H	6.857970683	1.121125815	13.57356842
H	6.222694824	2.679379801	13.06400658
C	9.973321295	2.422514629	11.58198004

H	10.85779195	1.809256638	11.79175676
H	10.33079651	3.323437547	11.07035572
H	9.342525537	1.866424276	10.88203766

Table 10. Cartesian Coordinates for Geometry Optimized Compounds

$[(Ph_3P)_2C]ZnMe_2$			
-2256.04896087612 Hartrees			
atom	**x**	**y**	**z**
Zn	7.353840163	5.623917053	3.326146196
P	6.188687104	3.195084195	5.465700208
P	6.72894401	2.326217564	2.632448749
C	6.808129996	3.414815787	3.912018178
C	5.338539981	4.722436407	6.052750904
C	5.378621833	5.14947493	7.388447784
H	5.955185096	4.596519649	8.122469303
C	4.691440658	6.298121262	7.781707142
H	4.738343278	6.622614243	8.817785492
C	3.955426346	7.03384725	6.850514017
H	3.42626555	7.930997213	7.159650507
C	3.911652635	6.616044814	5.519723727
H	3.350703287	7.185831033	4.78434433
C	4.599449764	5.467816427	5.1216098
H	4.580548985	5.15607603	4.082462183
C	7.472903953	2.878855306	6.757515653
C	8.778327322	3.323028552	6.50484168
H	8.994700819	3.820341709	5.564345509

C	9.782929353	3.132302329	7.454304714
H	10.78965571	3.48587616	7.248944658
C	9.497197585	2.49182394	8.661068306
H	10.28208412	2.338785289	9.397117217
C	8.19973516	2.047367681	8.920860312
H	7.971668852	1.5458868	9.857850552
C	7.190654875	2.242083999	7.976628579
H	6.186671395	1.887596234	8.189145571
C	4.951975171	1.847743404	5.7588062
C	3.577279069	2.123531896	5.77799986
H	3.226903935	3.14570945	5.678878068
C	2.649786648	1.092123943	5.929399411
H	1.588053306	1.32315682	5.945645039
C	3.081395031	-0.22692751	6.067177299
H	2.357834699	-1.028116733	6.192452636
C	4.447799511	-0.513461881	6.046364614
H	4.792975665	-1.538268933	6.155380926
C	5.376947761	0.514622179	5.891155434
H	6.43550909	0.275800098	5.879831491
C	7.558494853	0.673764827	2.820266201
C	7.433678102	-0.338817792	1.8556229
H	6.779758216	-0.200308601	0.999680622
C	8.147448656	-1.52928065	1.98417489
H	8.035425984	-2.308541671	1.234832844
C	9.008582903	-1.718020983	3.067591235
H	9.56619335	-2.645789246	3.164498669

C	9.157625639	-0.707806211	4.017086094
H	9.836687166	-0.841440276	4.854993994
C	8.438466892	0.482885709	3.892071103
H	8.568442535	1.27591401	4.622242417
C	7.665080398	2.986823279	1.193377872
C	7.249115047	2.803907382	-0.132141555
H	6.299180512	2.324949119	-0.346233038
C	8.044473747	3.251111986	-1.189125497
H	7.703211694	3.112921789	-2.211580637
C	9.266050807	3.876472045	-0.937230142
H	9.881083397	4.226232791	-1.761557681
C	9.693467197	4.048535644	0.380792154
H	10.64400568	4.531381253	0.58940639
C	8.90224112	3.602465806	1.439173828
H	9.243866732	3.736901307	2.461463123
C	5.035552439	1.949599677	1.99663801
C	4.384837226	0.731024363	2.237271837
H	4.908240135	-0.080310808	2.731460061
C	3.051852393	0.551852895	1.859756535
H	2.562829371	-0.398228712	2.058253676
C	2.351173209	1.583907486	1.236718723
H	1.315527503	1.441428597	0.940255611
C	2.987042358	2.806906718	1.006226789
H	2.44781351	3.62098353	0.529208282
C	4.313844265	2.994106132	1.390299668
H	4.788671864	3.957659239	1.226432462

C	6.078410832	6.400813138	1.867548586
H	6.209954913	7.488758409	1.784019231
H	5.010589297	6.229822369	2.064375469
H	6.293058611	5.982929155	0.873795384
C	9.023589439	6.291027131	4.379599736
H	8.842066995	6.361947194	5.460758281
H	9.314579204	7.294446051	4.040030685
H	9.906429227	5.647225087	4.247976126

Table 11. Cartesian Coordinates for Geometry Optimized Compounds

Me_2Zn			
-145.399789689958 Hartrees			
atom	**x**	**y**	**z**
Zn	7.644800803	5.745152972	3.308120429
C	8.271439186	4.749055382	1.659082211
H	8.809935952	5.412297206	0.973139872
H	7.426568485	4.31920752	1.109525679
H	8.946575058	3.92780633	1.924443126
C	7.014901719	6.740396657	4.956544071
H	6.55094055	6.059876943	5.679129722
H	6.274379266	7.505783267	4.699010838
H	7.848392563	7.241713459	5.460983753

Table 12. Cartesian Coordinates for Geometry Optimized Compounds

$(Ph_3P)_2C(ZnMe_2)_2$

-2401.44427006478 Hartrees			
atom	**x**	**y**	**z**
Zn	7.26637336	5.800043761	3.695938981
P	6.604942964	3.035345703	5.556406342
P	6.906060141	2.435875227	2.594361121
C	7.370766646	3.271716568	4.030439676
C	5.291373013	4.273605629	5.969701426
C	5.007457177	4.606469679	7.302981832
H	5.570509575	4.150058258	8.111278184
C	4.010557318	5.534624939	7.602792624
H	3.807470737	5.787692683	8.639760603
C	3.285078314	6.145637095	6.577259607
H	2.514242134	6.873859136	6.813164023
C	3.563103847	5.822612286	5.249196031
H	3.012051039	6.296814604	4.442075958
C	4.561731003	4.894513381	4.946555968
H	4.770847166	4.661537438	3.908194491
C	7.81119198	3.221313149	6.940792294
C	8.745840332	4.268707796	6.894750634
H	8.73549615	4.974307092	6.072061074
C	9.673357506	4.434291767	7.924328472
H	10.38951712	5.248552339	7.86527488
C	9.677946641	3.566532983	9.016356231
H	10.40271808	3.695249304	9.815225213
C	8.73990322	2.535308524	9.078583325
H	8.729819136	1.856438027	9.926990941

C	7.811074324	2.361884484	8.051010824
H	7.094946371	1.551035618	8.119085145
C	5.793989577	1.412670108	5.908670225
C	4.422530453	1.309321618	6.188002593
H	3.804839681	2.201060829	6.219891607
C	3.843604836	0.063305087	6.441113207
H	2.780372984	0.000440785	6.657093259
C	4.625514565	-1.091528201	6.427064461
H	4.174322365	-2.059171593	6.628330722
C	5.992356695	-0.996455354	6.154764483
H	6.610075418	-1.889602346	6.138055185
C	6.573487368	0.243572358	5.895058302
H	7.635566331	0.303916961	5.682627988
C	6.947561528	0.575693664	2.610616417
C	5.850382505	-0.237121071	2.291493617
H	4.893087625	0.203001221	2.039290483
C	5.976261186	-1.629009332	2.28319246
H	5.112492855	-2.240783417	2.036173992
C	7.198849404	-2.229576758	2.579501761
H	7.295182593	-3.311893971	2.56568746
C	8.30173869	-1.426815654	2.882847451
H	9.263697717	-1.878396091	3.109064743
C	8.177841162	-0.039029039	2.898023634
H	9.042950403	0.565782068	3.147560799
C	8.091028941	2.774544139	1.226042768
C	8.074083343	1.943791716	0.091124434

H	7.37770938	1.113531391	0.032821683
C	8.953210581	2.168906385	-0.965489511
H	8.923686627	1.518080141	-1.835097399
C	9.873777679	3.218513617	-0.90257538
H	10.56418004	3.389059814	-1.723856283
C	9.902474829	4.041197048	0.221737829
H	10.61521102	4.85762406	0.289161398
C	9.012273827	3.825398337	1.277209399
H	9.049332108	4.475716451	2.13941277
C	5.234900136	2.792859702	1.871437903
C	4.082271205	2.468021406	2.608649072
H	4.171806884	2.004453563	3.586685225
C	2.810035935	2.719208377	2.095697646
H	1.933531423	2.454306522	2.681053438
C	2.664484349	3.307541925	0.83750665
H	1.674277079	3.506888959	0.437414315
C	3.800904687	3.63954565	0.101019397
H	3.700829096	4.105787376	-0.875206433
C	5.076054196	3.38328056	0.610060206
H	5.944498117	3.656114575	0.022368562
C	6.499817871	6.284783238	1.826589718
H	6.645746087	7.365192432	1.687795475
H	5.421030445	6.095805608	1.751657128
H	6.978153891	5.783033119	0.97914377
C	7.780657918	7.025639837	5.291530464
H	7.288076036	6.793772715	6.242802334

H	7.448142516	8.030742552	4.994392668
H	8.859661906	7.096024267	5.477026288
Zn	9.8396754	3.0936751	4.422576769
C	10.81656325	4.877219849	3.971520458
H	11.45080243	5.168278935	4.820660312
H	10.18119591	5.743931029	3.749158274
H	11.48798489	4.735167037	3.113386111
C	10.53656221	1.231199215	5.039893236
H	9.803198035	0.546105915	5.482672462
H	11.29942232	1.418081622	5.808914204
H	11.04451495	0.68471708	4.232089467

Table 13. Cartesian Coordinates for Geometry Optimized Compounds

$[(Ph_3P)_2C]CdMe_2$			
-2238.49909550795 Hartrees			
atom	**x**	**y**	**z**
Cd	7.428983371	5.850705084	3.265912071
P	6.164632251	3.144771299	5.485105201
P	6.720296892	2.262218798	2.658433175
C	6.79655992	3.338605812	3.93998345
C	5.323727307	4.688698214	6.052452827
C	5.373263082	5.139271556	7.379576174
H	5.9483428	4.594100179	8.120744535
C	4.696684253	6.300317715	7.755523399
H	4.750934959	6.64299117	8.785407458
C	3.961419558	7.024265052	6.815108373

H	3.439779514	7.930344993	7.110626165
C	3.907712467	6.582775529	5.492145968
H	3.345667471	7.14253436	4.749861374
C	4.58607139	5.423233637	5.111797234
H	4.558177058	5.08969699	4.079374869
C	7.439436937	2.830301109	6.790361447
C	8.753283546	3.245647079	6.533323248
H	8.97902301	3.723362637	5.584837528
C	9.753718618	3.046555287	7.485109018
H	10.7675038	3.377024976	7.27599606
C	9.454697459	2.42526617	8.69855636
H	10.23632396	2.264241575	9.436380224
C	8.148987221	2.008974401	8.962622571
H	7.911457248	1.521108699	9.904417957
C	7.144129083	2.212678151	8.015817405
H	6.133441834	1.878537941	8.230000937
C	4.912821588	1.812395203	5.795749261
C	3.540790686	2.098011698	5.831006669
H	3.196666428	3.122932895	5.738626128
C	2.606947182	1.072932394	5.988837489
H	1.547152971	1.311837076	6.01594768
C	3.029504623	-0.249620742	6.117726072
H	2.301176517	-1.045851809	6.246706084
C	4.393319419	-0.546273366	6.08079505
H	4.731893595	-1.574186806	6.181331039
C	5.328004157	0.475156195	5.918110473

H	6.384627418	0.227764156	5.891550223
C	7.573551352	0.615534351	2.814036947
C	7.503435354	-0.357536349	1.80417452
H	6.88310998	-0.191483012	0.928098228
C	8.231028438	-1.541427838	1.911315693
H	8.162982789	-2.289420098	1.125632699
C	9.05118344	-1.76285475	3.020147838
H	9.620687713	-2.685016482	3.100156963
C	9.144635147	-0.792330198	4.016662517
H	9.791985648	-0.951639101	4.87497632
C	8.411542046	0.392028732	3.912217315
H	8.50050684	1.156987441	4.677985088
C	7.636764155	2.938996216	1.21172578
C	7.19065698	2.801675411	-0.108678867
H	6.229809544	2.342556406	-0.316799723
C	7.971107961	3.268485145	-1.16807009
H	7.608391741	3.166929514	-2.187480727
C	9.206514948	3.866417523	-0.921662304
H	9.810804518	4.230394432	-1.748107871
C	9.664714758	3.994121721	0.390860612
H	10.62831643	4.453964096	0.591918567
C	8.887028855	3.530440793	1.451228445
H	9.249087518	3.626164545	2.470848358
C	5.029863209	1.867380229	2.023923076
C	4.414030497	0.621992968	2.210678859
H	4.961939883	-0.195100942	2.667604835

C	3.086725254	0.421355845	1.823731874
H	2.624789441	-0.550051842	1.979460805
C	2.357389222	1.458439653	1.243560595
H	1.326763581	1.299020292	0.938292415
C	2.958470928	2.707535361	1.066122463
H	2.397285122	3.525156533	0.621471864
C	4.278980614	2.915104207	1.460664605
H	4.727584438	3.896720648	1.33357783
C	5.906050323	6.495187508	1.720167704
H	5.960076258	7.574601663	1.532882991
H	4.873166935	6.270799803	2.01524891
H	6.094390393	5.991370174	0.763804754
C	9.285583323	6.305815228	4.470573668
H	9.079072321	6.300353513	5.547163547
H	9.69197069	7.29238321	4.218454468
H	10.07934563	5.570087173	4.284908093

Table 14. Cartesian Coordinates for Geometry Optimized Compounds

Me_2Cd			
-127.856682219457 Hartrees			
atom	**x**	**y**	**z**
Cd	7.601170959	5.634045195	3.358673225
C	8.285461756	4.546330353	1.560969014
H	8.820763453	5.218468177	0.883509592
H	7.43459667	4.12093337	1.020326005
H	8.959570619	3.729930426	1.837216311

C	6.915211341	6.719246726	5.157278915
H	6.454089715	6.029975789	5.871198848
H	6.176257033	7.480599098	4.890001368
H	7.755306683	7.214703316	5.653179246

Table 15. Cartesian Coordinates for Geometry Optimized Compounds

{[$(Ph_3P)_2C$]HgMe}I -2204.73212186768 Hartrees			
atom	**x**	**y**	**z**
Hg	7.776570581	5.491820484	3.375049977
I	10.72796596	5.102240001	4.055793989
P	6.044080033	3.176845813	5.503580321
P	6.657540578	2.216215266	2.66873534
C	7.074700224	7.476605292	2.514399257
H	6.266527766	7.311117448	1.798928391
H	7.927537739	7.94379706	2.020437844
H	6.726738427	8.106245182	3.335499392
C	6.663355153	3.341971614	3.933255605
C	5.466859405	4.818621988	6.111912919
C	5.644420509	5.223254542	7.442749799
H	6.159488635	4.57680365	8.145261347
C	5.174684951	6.465812225	7.870410878
H	5.330082957	6.771309011	8.901400486
C	4.519607862	7.316539859	6.979145129
H	4.160454005	8.285624303	7.313853129
C	4.337366161	6.920831095	5.652717061

H	3.836581717	7.579863809	4.949217802
C	4.810904548	5.68191746	5.220552662
H	4.689034005	5.384542553	4.183632587
C	7.232628861	2.616920362	6.801560415
C	8.594639985	2.905617789	6.631055018
H	8.94708407	3.420237429	5.740808761
C	9.519888026	2.527326662	7.604402918
H	10.56932945	2.764395392	7.454146515
C	9.098117053	1.852978282	8.75080777
H	9.821059853	1.553492651	9.505206145
C	7.743845652	1.561253434	8.927471657
H	7.409995231	1.034041066	9.817487535
C	6.81305227	1.942830372	7.960885408
H	5.763614536	1.708348835	8.109754873
C	4.603923406	2.039119621	5.741999821
C	3.31041034	2.525016643	5.976002579
H	3.137715436	3.593062996	6.060050354
C	2.236088339	1.643113857	6.109296293
H	1.240126051	2.036203901	6.295036207
C	2.437903776	0.266821065	6.010654239
H	1.601068186	-0.417916198	6.116524597
C	3.72361997	-0.226534203	5.777930335
H	3.892060567	-1.29733047	5.701438106
C	4.798445288	0.650686493	5.646319882
H	5.792397727	0.248091368	5.473054544
C	7.749314417	0.725668655	2.786115138

C	8.066538096	-0.029293261	1.643328709
H	7.679415795	0.26400519	0.671512582
C	8.891878641	-1.147833706	1.741965872
H	9.130752855	-1.72224336	0.850952786
C	9.422509609	-1.520613227	2.979226023
H	10.07238664	-2.38837526	3.053251614
C	9.13110733	-0.765043174	4.113440774
H	9.559603556	-1.033855733	5.074965055
C	8.301861253	0.354634423	4.016625838
H	8.114523025	0.959057747	4.896892141
C	7.288908103	3.003120449	1.130882791
C	6.450850287	3.345701444	0.061461605
H	5.388774512	3.129122111	0.106934006
C	6.979810858	3.962621432	-1.073653095
H	6.322342659	4.222799901	-1.898611932
C	8.343602763	4.244629237	-1.149219298
H	8.751777954	4.72775575	-2.032727867
C	9.184677818	3.905120092	-0.088290996
H	10.24664341	4.127392223	-0.131663422
C	8.664779735	3.28024093	1.044506009
H	9.334958517	3.02468465	1.860186485
C	4.989700125	1.543953655	2.219157717
C	4.759112696	0.209560055	1.855150195
H	5.57438446	-0.505437555	1.853835728
C	3.478113196	-0.21762717	1.500947263
H	3.31752522	-1.256749373	1.225713981

C	2.409588939	0.678947842	1.502089818
H	1.414072994	0.344185501	1.22390045
C	2.627242563	2.007810367	1.871225949
H	1.800809921	2.713249483	1.883483413
C	3.904436303	2.434749763	2.232136958
H	4.066416407	3.464395061	2.536622059

Table 16. Cartesian Coordinates for Geometry Optimized Compounds

$\{[\kappa^2\text{-}(C,C)\text{-}(Ph_3PCPPh_2(C_6H_4))]Mg(\mu\text{-}Me)\}_2$			
-4700.14341688905 Hartrees			
atom	**x**	**y**	**z**
Mg	1.331476498	0.072677691	0.379871564
P	3.984630598	-0.161721939	2.110675737
P	1.68205364	1.002816644	3.716606154
C	-0.002068852	1.821016509	-0.18016766
C	2.368348944	0.305041623	2.346565548
C	4.304855138	-0.464789433	0.328281161
C	3.228776441	-0.352250771	-0.575801153
C	3.561715111	-0.601360751	-1.926359636
H	2.784628861	-0.530528909	-2.686670511
C	4.851043396	-0.934197063	-2.343702567
H	5.055113577	-1.113038315	-3.398281037
C	5.887310245	-1.041335773	-1.410086055
H	6.894461578	-1.301839716	-1.725491973
C	5.612079617	-0.808489279	-0.066821107
H	6.417925842	-0.885512493	0.659180845

C	5.290653194	1.049684191	2.609088601
C	5.631623751	2.062014905	1.696253833
H	5.189227441	2.060452012	0.704696109
C	6.544806167	3.054863327	2.045814205
H	6.80289745	3.82682202	1.325837525
C	7.134938193	3.050662017	3.311175068
H	7.850763614	3.82208942	3.582064225
C	6.801452557	2.052170693	4.225349277
H	7.251374837	2.044870619	5.214286928
C	5.883549148	1.059155727	3.879297514
H	5.629425685	0.295305151	4.605945871
C	4.467944857	-1.739868224	2.956715578
C	5.797475935	-2.125631992	3.186476299
H	6.613421604	-1.456197392	2.934113046
C	6.086506717	-3.36507745	3.757382099
H	7.120757045	-3.646835258	3.936409026
C	5.054078105	-4.240072403	4.098306106
H	5.282380254	-5.205311573	4.542052739
C	3.729295517	-3.868850619	3.867912672
H	2.919306609	-4.544660387	4.128540201
C	3.439538146	-2.626535143	3.303255663
H	2.4100208	-2.328599616	3.128807963
C	1.014169547	2.692683856	3.383323219
C	-0.213378999	3.160308109	3.869554734
H	-0.859250814	2.507270167	4.445847909
C	-0.627492095	4.465422271	3.59681643

H	-1.589583177	4.81142768	3.964186892
C	0.183299792	5.317821912	2.848112959
H	-0.142687955	6.332472309	2.636213657
C	1.406930404	4.85804496	2.357589871
H	2.037335994	5.512942798	1.762468683
C	1.814748535	3.550056451	2.613485386
H	2.751951465	3.181075757	2.206779153
C	2.713818399	1.248995667	5.234687203
C	3.129432159	2.515301182	5.663838153
H	2.854015301	3.398441331	5.098157597
C	3.895848313	2.652525933	6.822928716
H	4.208978935	3.641789728	7.145140191
C	4.252537324	1.528914209	7.566191505
H	4.842641214	1.638590368	8.472003319
C	3.844804318	0.260611502	7.144675139
H	4.116686062	-0.619732139	7.720525366
C	3.080645446	0.120743457	5.988042026
H	2.764225606	-0.869112949	5.673001244
C	0.269904257	0.045526116	4.431553673
C	-0.229874375	0.333315782	5.712887011
H	0.199123157	1.141797169	6.297285828
C	-1.262837391	-0.428984167	6.255270072
H	-1.63873183	-0.197793547	7.248248577
C	-1.805017802	-1.491792998	5.52962875
H	-2.607225326	-2.087975797	5.955576885
C	-1.312403286	-1.785585675	4.259138351

H	-1.729853945	-2.608182648	3.685998012
C	-0.279265231	-1.021123922	3.712813978
H	0.104172431	-1.255071675	2.726542183
H	-0.781105575	2.175139505	-0.874625255
H	-0.232877037	2.328781272	0.76535706
H	0.913929609	2.305216916	-0.558729545
Mg	-1.331476498	-0.072677691	-0.379871564
P	-3.984630598	0.161721939	-2.110675737
P	-1.68205364	-1.002816644	-3.716606154
C	0.002068852	-1.821016509	0.18016766
C	-2.368348944	-0.305041623	-2.346565548
C	-4.304855138	0.464789433	-0.328281161
C	-3.228776441	0.352250771	0.575801153
C	-3.561715111	0.601360751	1.926359636
H	-2.784628861	0.530528909	2.686670511
C	-4.851043396	0.934197063	2.343702567
H	-5.055113577	1.113038315	3.398281037
C	-5.887310245	1.041335773	1.410086055
H	-6.894461578	1.301839716	1.725491973
C	-5.612079617	0.808489279	0.066821107
H	-6.417925842	0.885512493	-0.659180845
C	-5.290653194	-1.049684191	-2.609088601
C	-5.631623751	-2.062014905	-1.696253833
H	-5.189227441	-2.060452012	-0.704696109
C	-6.544806167	-3.054863327	-2.045814205
H	-6.80289745	-3.82682202	-1.325837525

C	-7.134938193	-3.050662017	-3.311175068
H	-7.850763614	-3.82208942	-3.582064225
C	-6.801452557	-2.052170693	-4.225349277
H	-7.251374837	-2.044870619	-5.214286928
C	-5.883549148	-1.059155727	-3.879297514
H	-5.629425685	-0.295305151	-4.605945871
C	-4.467944857	1.739868224	-2.956715578
C	-5.797475935	2.125631992	-3.186476299
H	-6.613421604	1.456197392	-2.934113046
C	-6.086506717	3.36507745	-3.757382099
H	-7.120757045	3.646835258	-3.936409026
C	-5.054078105	4.240072403	-4.098306106
H	-5.282380254	5.205311573	-4.542052739
C	-3.729295517	3.868850619	-3.867912672
H	-2.919306609	4.544660387	-4.128540201
C	-3.439538146	2.626535143	-3.303255663
H	-2.4100208	2.328599616	-3.128807963
C	-1.014169547	-2.692683856	-3.383323219
C	0.213378999	-3.160308109	-3.869554734
H	0.859250814	-2.507270167	-4.445847909
C	0.627492095	-4.465422271	-3.59681643
H	1.589583177	-4.81142768	-3.964186892
C	-0.183299792	-5.317821912	-2.848112959
H	0.142687955	-6.332472309	-2.636213657
C	-1.406930404	-4.85804496	-2.357589871
H	-2.037335994	-5.512942798	-1.762468683

C	-1.814748535	-3.550056451	-2.613485386
H	-2.751951465	-3.181075757	-2.206779153
C	-2.713818399	-1.248995667	-5.234687203
C	-3.129432159	-2.515301182	-5.663838153
H	-2.854015301	-3.398441331	-5.098157597
C	-3.895848313	-2.652525933	-6.822928716
H	-4.208978935	-3.641789728	-7.145140191
C	-4.252537324	-1.528914209	-7.566191505
H	-4.842641214	-1.638590368	-8.472003319
C	-3.844804318	-0.260611502	-7.144675139
H	-4.116686062	0.619732139	-7.720525366
C	-3.080645446	-0.120743457	-5.988042026
H	-2.764225606	0.869112949	-5.673001244
C	-0.269904257	-0.045526116	-4.431553673
C	0.229874375	-0.333315782	-5.712887011
H	-0.199123157	-1.141797169	-6.297285828
C	1.262837391	0.428984167	-6.255270072
H	1.63873183	0.197793547	-7.248248577
C	1.805017802	1.491792998	-5.52962875
H	2.607225326	2.087975797	-5.955576885
C	1.312403286	1.785585675	-4.259138351
H	1.729853945	2.608182648	-3.685998012
C	0.279265231	1.021123922	-3.712813978
H	-0.104172431	1.255071675	-2.726542183
H	0.781105575	-2.175139505	0.874625255
H	0.232877037	-2.328781272	-0.76535706

H	-0.913929609	-2.305216916	0.558729545

Table 17. Cartesian Coordinates for Geometry Optimized Compounds

$[\kappa^2$-(C,C)-$(Ph_3PCPPh_2(C_6H_4))]Co[N(TMS)_2]$			
-3128.50105582726 Hartrees			
atom	**x**	**y**	**z**
Co	6.520731835	9.9916379	4.278937647
P	6.011399148	6.982291165	4.522407928
P	8.507413203	7.844029912	2.962289464
Si	4.945090093	12.37148022	3.113024425
Si	7.278775496	12.91511169	5.076851658
N	6.281528389	11.87309969	4.10902648
C	7.036481129	8.126877162	3.765337303
C	5.085417315	7.965519743	5.717399029
C	5.372815236	9.346714976	5.638628034
C	4.705439977	10.17266096	6.569050403
H	4.882666733	11.24262284	6.553736854
C	3.802844681	9.646456473	7.495999984
H	3.305106568	10.31318187	8.197384727
C	3.516665089	8.276161355	7.526124233
H	2.803573458	7.876095282	8.241704632
C	4.159063551	7.430309299	6.625952392
H	3.948637286	6.362919991	6.639572483
C	4.754020269	6.186239389	3.424785911
C	4.367946212	6.86345796	2.25878411
H	4.867328841	7.793130836	1.998845993

C	3.352015756	6.355936671	1.447639414
H	3.063261539	6.893899236	0.548654364
C	2.706702647	5.165685103	1.790254371
H	1.916669334	4.769496639	1.158246142
C	3.07890499	4.490384397	2.953882818
H	2.579907486	3.565253224	3.230650352
C	4.092579686	4.997353346	3.769078226
H	4.370611639	4.456593009	4.668480322
C	6.767873412	5.57093523	5.441891038
C	7.147136673	4.385069761	4.791814829
H	6.929437378	4.245756688	3.737796184
C	7.801685814	3.372616436	5.49319837
H	8.08690433	2.460059983	4.976672485
C	8.087063147	3.528508236	6.850220526
H	8.594005739	2.73685653	7.395551369
C	7.716932959	4.704104174	7.504684161
H	7.931150785	4.830367916	8.562620968
C	7.063115363	5.719508029	6.807119695
H	6.769332911	6.626727609	7.326276807
C	8.793227668	9.033004412	1.5846129
C	8.901317275	10.40005077	1.887288158
C	9.068818311	11.34073921	0.871899148
H	9.136665691	12.39367571	1.128845162
C	9.144072154	10.93120061	-0.460825096
H	9.275594452	11.66431351	-1.251666369
C	9.052013479	9.573993045	-0.769522438

H	9.116171708	9.243058082	-1.802747638
C	8.878284496	8.629211616	0.244187053
H	8.813757565	7.578825328	-0.017844013
C	11.27921762	8.306324244	3.436747217
H	11.38483228	8.380214118	2.357805762
C	12.40232424	8.452288046	4.250531913
H	13.37404647	8.635588936	3.799914022
C	12.27741431	8.372188832	5.640192443
H	13.15255637	8.491233854	6.27297955
C	11.02400331	8.149806615	6.211494992
H	10.91844478	8.09751884	7.291631352
C	9.89727548	8.004165688	5.399229552
H	8.91688071	7.851883163	5.839419464
C	8.704147554	6.17682665	2.204912097
C	9.821323049	5.365217975	2.446923631
H	10.61559578	5.712450982	3.09847974
C	9.917270484	4.101841666	1.860664389
H	10.78677829	3.481884391	2.061740621
C	8.903681883	3.634779993	1.024173786
H	8.981552885	2.651137046	0.568792042
C	7.786610456	4.435513136	0.775682785
H	6.990715562	4.079051649	0.127570908
C	7.68514697	5.696059159	1.363304888
H	6.806000602	6.303560017	1.175258051
C	5.365581347	13.91137724	2.071021705
H	4.520648631	14.1867004	1.427538808

H	6.22887472	13.7249731	1.421563908
H	5.600705347	14.78409351	2.691206282
C	4.452499478	11.00700041	1.882560031
H	3.665730725	11.36484412	1.205779764
H	4.064093162	10.1240978	2.402456103
H	5.304255091	10.69067381	1.26925787
C	3.380347947	12.77925374	4.117389265
H	2.544079504	13.04581216	3.458559486
H	3.541868299	13.61849774	4.80331157
H	3.069618483	11.91713121	4.71827998
C	8.229720205	11.91609505	6.388029232
H	8.856727534	11.13563617	5.940432312
H	7.545381538	11.42440005	7.088315151
H	8.888566493	12.57324963	6.970239724
C	6.299202712	14.25318536	6.015879473
H	5.553722462	13.80808477	6.685478762
H	5.765515479	14.9261896	5.334995185
H	6.966609145	14.87095678	6.629923854
C	8.584648326	13.82689433	4.028591341
H	9.29499133	13.12347173	3.577307404
H	9.165643079	14.52932057	4.639527995
H	8.122183837	14.39771179	3.215826635
H	8.84736304	10.74078862	2.916707245
C	10.01697053	8.073009067	4.006577882

Table 18. Cartesian Coordinates for Geometry Optimized Compounds

$[\kappa^2$-(C,C)-($Ph_3PCPPh_2(C_6H_4)$)]Ir(COD)			
-2526.77725177818 Hartrees			
atom	**x**	**y**	**z**
Ir	-0.376665607	2.967579491	11.53472613
P	0.640205556	6.045838874	11.31433102
P	-2.127002094	5.571456253	10.17053488
C	-0.688178594	4.997473755	10.92853208
C	0.032681267	0.095577811	12.47503774
H	1.090319703	-0.115802331	12.62522653
C	-0.50264845	1.349897282	13.0087903
H	0.102859082	1.686729008	13.8558828
C	-1.988344006	1.325715792	13.43442058
H	-2.168294071	2.226579837	14.03396841
H	-2.192001253	0.468905975	14.09582649
C	-2.975968422	1.324128093	12.2440301
H	-3.247424604	0.297273231	11.96960819
H	-3.914287582	1.802683552	12.54912162
C	-2.420920519	2.064131658	11.0333156
H	-3.083112206	2.819512632	10.62262892
C	-1.425629643	1.585390072	10.1619103
H	-1.390190679	2.077421177	9.190909673
C	-0.80211533	0.197282887	10.07554454
H	0.192433981	0.311693617	9.623136976
H	-1.395969135	-0.381536733	9.348794596
C	-0.658844505	-0.644073469	11.37196101
H	-1.655899262	-0.978551765	11.68881343

H	-0.105043738	-1.556959162	11.11950156
C	1.841829341	4.990409285	12.14379349
C	1.443073474	3.641582869	12.29276416
C	2.406734974	2.815939007	12.92123531
H	2.186304876	1.762511476	13.0657557
C	3.641085066	3.294348147	13.35852757
H	4.346177082	2.611329513	13.82871349
C	3.980643421	4.643826797	13.20945793
H	4.937096662	5.019631023	13.56269235
C	3.06884457	5.498057574	12.59882448
H	3.315523316	6.550128112	12.47259558
C	1.516957872	6.803435223	9.880157723
C	1.16934088	8.051762312	9.34029269
H	0.393258589	8.652633957	9.802288897
C	1.818349423	8.534677055	8.203444348
H	1.541083825	9.505178947	7.80078098
C	2.81295682	7.776617192	7.585033551
H	3.317426631	8.155854265	6.700254608
C	3.156922251	6.528745972	8.107410442
H	3.931856953	5.932738826	7.632850024
C	2.516757781	6.044930803	9.247108302
H	2.797764025	5.078976269	9.655220263
C	0.331739296	7.42924588	12.50064894
C	1.1134395	8.594136053	12.54431729
H	1.887855688	8.761910483	11.80312797
C	0.903570033	9.552125528	13.53826854

H	1.51509685	10.45061183	13.55366426
C	-0.079713953	9.357977871	14.50878904
H	-0.239168617	10.1038368	15.2825655
C	-0.85067716	8.193496992	14.48343436
H	-1.611960054	8.026649541	15.24079399
C	-0.646235148	7.236857718	13.48932971
H	-1.244016471	6.330516089	13.47710355
C	-2.216039511	7.329891642	9.59249158
C	-2.074529303	7.669531198	8.237959193
H	-1.933523631	6.893297603	7.493721534
C	-2.116133824	9.004477131	7.831745434
H	-2.010781355	9.245482307	6.777309085
C	-2.292676073	10.02297017	8.768881011
H	-2.324682022	11.0613932	8.450867486
C	-2.437073578	9.695605219	10.1200967
H	-2.581880387	10.47837122	10.8597449
C	-2.405053015	8.363293964	10.5287508
H	-2.527971044	8.129586127	11.58111998
C	-3.618526613	5.491787597	11.26102513
C	-3.528452623	4.853515688	12.50366305
H	-2.595646634	4.366295057	12.77691239
C	-4.625205508	4.835428293	13.36660475
H	-4.541704623	4.338213742	14.3292258
C	-5.820156968	5.452675063	12.99737721
H	-6.672538302	5.439123842	13.67139701
C	-5.916570374	6.09597487	11.7620933

H	-6.841269086	6.588330199	11.47323795
C	-4.820726788	6.123030481	10.90041144
H	-4.898227512	6.657944105	9.958243226
C	-2.494699013	4.61726389	8.636008401
C	-3.792719683	4.30409981	8.209977075
H	-4.648005539	4.55225217	8.829530494
C	-3.996105904	3.653252865	6.991925902
H	-5.006733604	3.40557104	6.678716752
C	-2.910124205	3.31816741	6.181843691
H	-3.072089364	2.813965032	5.233215406
C	-1.614119018	3.621869997	6.603687342
H	-0.761444075	3.352130217	5.986563039
C	-1.405018758	4.259483113	7.82728382
H	-0.396684731	4.465124567	8.175131101

5.10 References and Notes

(1) See Chapter 4 for a detailed discussion of bent and linear forms of carbodiphosphoranes.

(2) Ramirez, F.; Hansen, B.; Desai, N. B.; McKelvie, N. *J. Am. Chem. Soc.* **1961**, *83*, 3539-3540.

(3) Gasser, O.; Schmidbaur, H. *J. Am. Chem. Soc.* **1975**, *97*, 6281-6282.

(4) (a) Schmidbaur, H. *Nachr. Chem. Tech. Lab.* **1979**, *27*, 620-622.
(b) Schmidbaur, H.; Schier, A. *Angew. Chem. Int. Edit.* **2013**, *52*, 176-186.
(c) Kolodiazhnyi, O. I. *Tetrahedron* **1996**, *52*, 1855-1929.

(5) (a) Frenking, G.; Tonner, R. *Pure Appl. Chem.* **2009**, *81*, 597-614.
(b) Tonner, R.; Frenking, G. *Chem. Eur. J.* **2008**, *14*, 3260-3272.
(c) Frenking, G.; Tonner, R.; Klein, S.; Takagi, N.; Shimizu, T.; Krapp, A.; Pandey, K. K.; Parameswaran, P. *Chem. Soc. Rev.* **2014**, *43*, 5106-5139.

(6) (a) Tonner, R.; Oexler, F.; Neumuller, B.; Petz, W.; Frenking, G. *Angew. Chem. Int. Edit.* **2006**, *45*, 8038-8042.
(b) Schmidbaur, H. *Angew. Chem. Int. Edit.* **2007**, *46*, 2984-2985.
(c) Frenking, G.; Neumuller, B.; Petz, W.; Tonner, R.; Oxler, F. *Angew. Chem. Int. Edit.* **2007**, *46*, 2986-2987.

(7) (a) Kaska, W. C.; Mitchell, D. K.; Reichelderfer, R. F. *J. Organomet. Chem.* **1973**, *47*, 391-402.
(b) Kaska, W. C. *Coord. Chem. Rev.* **1983**, *48*, 1-58.
(c) Kaska, W. C.; Ostoja Starzwski, K. A. Transition metal complexes with ylides In *Ylides and imines of phosphorus*; Johnson, A. W., Ed.; Kaska, W. C., Ostoja Starzewski, K. A., Dixon, D. A., Special Contributors; Wiley: New York, 1993.

(8) (a) Petz, W. *Coord. Chem. Rev.* **2015**, *291*, 1-27.
(b) Schmidbaur, H.; Zybill, C. E.; Neugebaur, D. *Angew. Chem. Int. Ed. Engl.* **1982**, *21* 310-311.
(c) Petz, W.; Frenking, G. *Top. Organomet. Chem.* **2010**, *30*, 49-92.

(9) (a) Frenking, G.; Hermann, M.; Andrada, D., M.; Holzmann, N. *Chem. Soc. Rev.* **2016**, *45*, 1129-1144.
(b) Matthews, C. N.; Birum, B. H. *Acc. Chem. Res.* **1969**, *2*, 373-379.
(c) Varshavsky, Y. S. *Metalloorganicheskaya Khimiya* **1988**, *1*, 249-259.

(10) Kaufhold, O.; Hahn, F. E. *Angew. Chem. Int. Ed.* **2008**, *47*, 4057-4061.

(11) Petz, W.; Oxler, F.; Neumuller, B.; Tonner, R.; Frenking, G. *Eur. J. Inorg. Chem.* **2009**, 4507-4517.

(12) (a) Green, M. L. H. *J. Organomet. Chem.* **1995**, *500*, 127-148.
(b) Parkin, G. in *Comprehensive Organometallic Chemistry III*, Volume 1, Chapter 1.01; Crabtree, R. H. and Mingos, D. M. P. (Eds), Elsevier, Oxford, 2006.
(c) Green, J. C.; Green, M. L. H.; Parkin, G. *Chem Commun.* **2012**, *48*, 11481-11503.
(d) Green, M. L. H.; Parkin, G. *J. Chem. Educ.* **2014**, *91*, 807-816.

(13) Schmidbaur, H.; Zybill, C.; Neugebaur, D.; Muller, G. *Z. Naturforsch.* **1985**, 1293-1300.

(14) Pranckevicius, C.; Iovan, D. A.; Stephan, D. W. *Dalton Trans.* **2016**, *45*, 16820-16825.

(15) Petz, W.; Kutschera, C.; Heitbaum, M.; Frenking, G.; Tonner, R.; Neumuller, B. *Inorg. Chem.* **2005**, *44*, 1263-1274.

(16) Muller, G.; Kruger, C.; Zybill, C.; Schmidbaur, H. *Acta Cryst.* **1986**, *C42*, 1141-1144.

(17) Khan, S.; Gopakumar, G.; Thiel, W.; Alcarazo, M. *Angew. Chem. Int. Ed.* **2013**, *52*, 5644-5647.

(18) Petz, W.; Neumuller, B. *Eur. J. Inorg. Chem.* **2011**, 4889-4895.

(19) El-Hellani, A.; Monot, J.; Tang, S.; Guillot, R.; Bour, C.; Gandon, V. *Inorg. Chem.* **2013**, *52*, 11493-11502.

(20) Petz, W.; Oxler, F.; Neumuller, B. *J. Organomet. Chem.* **2009**, *694*, 4094-4099.

(21) Petz, W.; Neumuller, B.; Klein, S.; Frenking, G. *Organometallics* **2011**, *30*, 3330-3339.

(22) Zybill, C.; Muller, G. *Organometallics* **1987**, *6*, 2489-2494.

(23) Peters, K.; von Schnering, H. G. *Organometallics* **1994**, *13*, 2560-2562.

(24) Petz, W.; Kutschera, C.; Tschan, S.; Weller, F.; Neumuller, B. *Z. Anorg. Allg. Chem.* **2003**, *629*, 1235-1244.

(25) Petz, W.; Dehnicke, K.; Holzmann, N.; Frenking, G.; Neumuller, B. *Z. Anorg. Allg. Chem.* **2011**, *637*, 1702-1710.

(26) Kuzu, I.; Kneusels, N. H.; Bauer, M.; Neumuller, B.; Tonner, R. *Z. Anorg. Allg. Chem.* **2014**, *640*, 417-422.

(27) The terms "σ-type" and "π-type" refer to the symmetry of the lone-pairs with respect to the P–C–P plane.

(28) (a) Vicente, J.; Singhal, A. R. *Organometallics.* **2002**, *21,* 5887-5900.
(b) Alcarazo, M.; Radkowski, K.; Mehler, G.; Goddard, R.; Furstner, A. *Chem. Commun.* **2013**, *49,* 3140-3142.
(c) Schmidbaur, H.; Gasser, O. *Angew. Chem. Int. Ed. Engl.* **1976**, *15,* 502-503.

(29) Alcarazo, M.; Gomez, C.; Holle, S.; Goddard, R. *Angew. Chem. Int. Ed.* **2010**, *49,* 5788-5791.

(30) Hermann, M.; Frenking G. *Chem. Eur. J.* **2017**, *23,* 3347-3356.

(31) Munzer, J. E.; Ona-Burgos, P.; Arrabal-Campos, F. M.; Neumuller, B.; Tonner, R.; Fernandez, I.; Kuzu, I. *Eur. J. Inorg. Chem.* **2016**, 3852-3858.

(32) Ines, B.; Patil, M.; Carreras, J.; Goddard, R.; Thiel, W.; Alcarazo, M. *Angew. Chem. Int. Ed.* **2011**, *50,* 8400-8403.

(33) Petz, W.; Kuzu, I.; Frenking, G.; Andrada, D. M.; Neumuller, B.; Fritz, M.; Munzer, J. E. *Chem. Eur. J.* **2016**, *22*, 8536-8546.

(34) Petz, W.; Oxler, F.; Neumuller, B. *Z. Anorg. Allg. Chem.* **2008**, *634,* 223-224.

(35) Ganguly, R.; Jevtovic, V. *Acta Cryst.* **2017**, *E73,* 1259-1263.

(36) Petz, W.; Neumuller, B. *Z. Anorg. Allg. Chem.* **2016**, *642,* 275-281.

(37) Petz, W.; Wenck, K.; Neumuller, B. *Z. Naturforsch.* **2007**, *62b,* 413-418.

(38) Goldberg, S. Z.; Duesler, E. N.; Raymond, K. N. *Inorg. Chem.* **1972**, *11,* 1397-1401.

(39) Petz, W.; Weller, F.; Uddin, J.; Frenking, G. *Organometallics* **1999**, *18,* 619-626.

(40) (a) Kubo, K.; Jones, N. D.; Ferguson, M. J.; McDonald, R.; Cavell, R. G. *J. Am. Chem. Soc.* **2005**, *127*, 5314-5315.
(b) Marrot, S.; Kato, T.; Gornitzka, H.; Baceiredo. *Angew. Chem. Int. Ed.* **2006**, *45*, 2598-2601.
(c) Petz, W.; Kutschera, C.; Neumuller, B. *Organometallics* **2005**, *24*, 5038-5043.

(41) (a) Petz, W.; Neumuller, B. *Polyhedron* **2011**, *30*, 1779-1784.
(b) Kubo, K.; Okitsu, H.; Miwa, H.; Kume, S.; Cavell, R. G.; Mizuta, T. *Organometallics* **2017**, *36*, 266-274.

(42) Gonzalez, M. L.; Bousquet, L.; Hameury, S.; Toledano, C. A.; Satton-Merceron, N.; Branchadell, V.; Maerten, E.; Baceiredo, A. *Chem. Eur. J.* **2018**, *24*, 2570-2574.

(43) (a) Yogendra, S.; Schulz, S.; Hennersdorf, F.; Kumar, S.; Fischer, R.; Weigand, J. J. *Organometallics* **2018**, *37*, 748-754.
(b) Barthes, C.; Bijani, C.; Lugan, N.; Canac, Yves. *Organometallics* **2018**, *37*, 673-678.

(44) (a) Reitsamer, C.; Stallinger, S.; Schuh, W.; Kopacka, H.; Wurst, K.; Obendorf, D.; Peringer, P. *Dalton Trans.* **2012**, *41*, 3503-3514.
(b) Reitsamer, C.; Hackl, I.; Schuh, W.; Kopacka, H.; Wurst, K.; Peringer, P. *J. Organomet. Chem.* **2017**, *830*, 150-154.
(c) Reitsamer, C.; Hackl, I.; Partl, G.; Schuh, W.; Kopacka, H.; Wurst, K.; Peringer, P. *Acta Cryst.* **2018**, *E74*, 620-624.
(d) Maser, L.; Herritsch, J.; Langer, R. *Dalton Trans.* **2018**, DOI: 10.1039/c7dt04930g.

(45) (a) Appel, R.; Knoll, F.; Michel, W.; Morbach, W.; Wihler, H.-D.; Veltmann, H. *Chem. Ber.* **1976**, *109*, 58-70.
(b) Appel, R.; Knoll, F.; Scholer, H.; Wihler, H.-D. *J. Angew. Chem. Int. Ed. Engl.* **1976**, *15*, 702-703.
(c) El-Hellani, A.; Bour, C.; Gandon, V. *Adv. Synth. Catal.* **2011**, *353*, 1865-1870.

(46) It should be noted that additional routes to $(Ph_3P)_2C$ have been reported. See reference 2 and:
(a) Zybill, C.; Muller, G. *Organometallics* **1987**, *6*, 2489-2494.
(b) Driscoll, J. S.; Grisley Jr., D. W.; Pustinger, J. V.; Harris, J. E.; Matthews, C. N. *J. Org. Chem.* **1964**, *29*, 2427-2431.
(c) Birum, G. H.; Matthews, C. N. *J. Am. Chem. Soc.* **1966**, *88*, 4198-4203.

(47) Gruber, M.; Bauer, W.; Maid, H.; Scholl, K.; Tykwinski, R. R. *Inorg. Chim. Acta* **2017**, *468*, 152-158.

(48) A value of 130 Hz is reported for $^{1}J_{C(central)–P}$ in $(Ph_3P)_2C$ in reference 47.

(49) For simplicity the small $^{3}J_{C(ipso)–P}$ coupling is ignored in this example.

(50) Values of $^{2}J_{P–P}$ = 94 Hz, $^{1}J_{C(ipso)–P}$ = 85 Hz, and $^{3}J_{C(ipso)–P}$ = 10 Hz are reported for $(Ph_3P)_2C$ in reference 47.

(51) Note: One of the meta/para peaks is overlapping with the C_6D_6 solvent peak, however a strong cross peak is observed in the HSQC at 127.79 ppm (^{13}C shift) and 7.00 ppm (^{1}H shift).

(52) The $\delta(^{31}P)$ peak is reported at –2.79 ppm in reference 47.

(53) An upfield isotopomer shift of 0.021 ppm is observed for the A_2X ^{13}C-satellite peaks, i.e. the ^{31}P-coupling to the central ^{13}C isotopomer.

(54) (a) Yang, L.; Powell, D. R.; Houser, R. P. *Dalton Trans.* **2007**, 955–964.
(b) Reineke, M. H.; Sampson, M. D.; Rheingold, A. L.; Kubiak, C. P. *Inorg. Chem.* **2015**, *54*, 3211–3217.

(55) Cordero, B.; Gomez, V.; Platero-Prats, A. E.; Reves, M.; Echeverria, J.; Cremades, E.; Barragan, F.; Alvarez, S. *Dalton Trans.* **2008**, 2832-2838.

(56) The scandide contraction is also referred to as the d-block contraction. See, for example:
(a) G. Wulfsberg, Inorganic Chemistry, University Science Books, Sausalito, California, 2000, p. 35;
(b) R.B. King (Ed.), Encyclopedia of Inorganic Chemistry, vol. 4, Wiley, New York, 1994, p. 1943.

(57) Additional singlets are also observed at 15.41 ppm and 20.26 ppm are observed during the lyophilization/redissolution and titration experiments which are tentatively assigned as the 2:1 adduct $(Ph_3P)_2C(ZnMe_2)_2$ and dimer $\{[(Ph_3P)_2C]Zn(Me)(\mu\text{-}Me)\}_2$.

(58) As indicated in reference 57, other bound forms of $(Ph_3P)_2C$ that could possibly be in an equilibrium mixture include the 2:1 adduct $(Ph_3P)_2C(ZnMe_2)_2$ and dimer $\{[(Ph_3P)_2C]Zn(Me)(\mu\text{-}Me)\}_2$.

(59) (a) Brand, S.; Pahl, J.; Elsen, H.; Harder, S. *Eur. J. Inorg. Chem.* **2017**, 4187-4195.
(b) Zheng, A.; Liu, S.-B.; Deng, F. *Chem. Rev.* **2017**, *117*, 12475-12531.
(c) Beckett, M. A.; Brassington, D. S.; Coles, S. J.; Hursthouse, M. B. *Inorg. Chem. Commun.* **2000**, *3*, 530-533.
(d) Beckett, M. A.; Brassington, D. S.; Light, M. E.; Hursthouse, M. B. *J. Chem. Soc. Dalton Trans.* **2001**, 1768-1772.
(e) Gutmann, V. *Coord. Chem. Rev.* **1976**, *18*, 225-255.
(f) Kuran, W.; Pasynkiewicz, S.; Florjanczyk, Z. *Die Makromolekulare Chemie.* **1972**, *154*, 71-79.
(g) Kuran, W.; Florjanczyk, Z. *J. Polym. Sci.* **1978**, *16*, 861-866.

(60) Batsanov, S. S.; *Inorg. Mater.* **2001**, *37*, 871–885.

(61) Cambridge Structural Database, CSD version 5.39

(62) Rabenstein, D. L. *Acc. Chem. Res.* **1978**, *11*, 100–107.

(63) Casas, J. S.; Garcia-Tasende, M. S.; Sordo, J. *Coord. Chem. Rev.* **1999**, *193-195*, 283–3593.

(64) Kaupp, M.; von Schnering, H. G. *Inorg. Chem.* **1994**, *33*, 2555–2564.

(65) Tossell, J. A.; Vaughan, D. J. *Inorg. Chem.* **1981**, *20*, 3333–3340.

(66) Yurkerwich, K.; Quinlivan, P. J.; Rong, Y.; Parkin, G. *Polyhedron* **2016**, *103*, 307–314

(67) For reference, the $^2J_{Hg-H}$ coupling constant for MeHgOH is 203 Hz. See: Robert, J. M.; Rabenstein, D. L. *Anal. Chem.* **1991**, *63*, 2674–2679.

(68) (a) Reitsamer, C.; Stallinger, S.; Schuh, W.; Kopacka, H.; Wurst, K.; Obendorf, D.; Peringer, P. *Dalton Trans.* **2012**, *41*, 3503–3514.
(b) Reitsamer, C.; Schuh, W.; Kopacka, H.; Wurst, K.; Ellmerer, E. P.; Peringer, P. *Dalton Trans.* **2011**, *30*, 4220–4223.

(69) Reitsamer, C.; Schuh, W.; Kopacka, H.; Wurst, K.; Peringer, P. *Organometallics* **2009**, *28*, 6617–6620.

(70) Petz, W.; Wenck, K.; Neumuller, B. *Z. Naturforsch.* **2007**, *62b*, 413–418.

(71) Additionally, the CS_2 adduct, $(Ph_3P)_2C\text{-}CS_2$, has been used as a ligand to synthesize the cobalt compound $[Co(S_2CC(PPh_3)_2)_3][Co(CO)_4]_3$ which feature coordination to the cobalt center through the sulfur atoms. See: Petz, W.; Neumuller, B.; Hehl, J. *Z. Anorg. Allg. Chem.* **2006**, *632*, 2232–2237.

(72) Tonner, R.; Frenking, G. *Chem. Commun.* **2008**, 1584–1586.

(73) (a) McNally, J. P.; Leong, V. S.; Cooper, N. J. in *Experimental Organometallic Chemistry*, Wayda, A. L.; Darensbourg, M. Y., Eds.; American Chemical Society: Washington, DC, 1987; Chapter 2, pp 6-23.
(b) Burger, B.J.; Bercaw, J. E. in *Experimental Organometallic Chemistry*; Wayda, A. L.; Darensbourg, M. Y., Eds.; American Chemical Society: Washington, DC, 1987; Chapter 4, pp 79-98.
(c) Shriver, D. F.; Drezdzon, M. A.; *The Manipulation of Air-Sensitive Compounds*, 2nd Edition; Wiley-Interscience: New York, 1986.

(74) Fulmer, G. R.; Miller, A. J. M.; Sherden, N. H.; Gottlieb, H. E.; Nudelman, A.; Stoltz, B. M.; Bercaw, J. E.; Goldberg, K. I. *Organometallics* **2010**, *29*, 2176-2179.

(75) (a) Harris, R. K.; Becker, E. D.; De Menezes, S. M. C.; Goodfellow, R.; Granger, P. *Pure Appl. Chem.* **2001**, *73*, 1795-1818.
(b) Harris, R. K.; Becker, E. D.; De Menezes, S. M. C.; Granger, P.; Hoffman, R. E.; Zilm, K. W. *Pure Appl. Chem.* **2008**, *80*, 59-84.

(76) Yousef, R. I.; Walfort, B.; Ruffer, T.; Wagner, C.; Schmidt, H.; Herzog, R.; Steinborn, D. *J. Organomet. Chem.* **2005**, *690*, 1178-1191.

(77) Henderson, K. W.; Allan, J. F.; Kennedy, A. R. *Chem. Commun.* **1997**, 1149-1150.

(78) Bryan, A. M.; Long, G. J.; Grandjean, F.; Power, P. P. *Inorg. Chem.* **2013**, *52*, 12152-12160.

(79) (a) Sheldrick, G. M. SHELXTL, An Integrated System for Solving, Refining, and Displaying Crystal Structures from Diffraction Data; University of Göttingen, Göttingen, Federal Republic of Germany, 1981.
(b) Sheldrick, G. M. *Acta Cryst.* **2008**, *A64*, 112-122.
(c) Sheldrick, G. M. *Acta Cryst.* **2015**, *A71*, 3-8.

(80) (a) Jaguar, version 8.9, Schrodinger, Inc., New York, NY, 2015.
(b) Bochevarov, A. D.; Harder, E.; Hughes, T. F.; Greenwood, J. R.; Braden, D. A.; Philipp, D. M.; Rinaldo, D.; Halls, M. D.; Zhang, J.; Friesner, R. A. *Int. J. Quantum Chem.* **2013**, *113*, 2110–2142.

(81) (a) Becke, A. D. *J. Chem. Phys.* **1993**, *98*, 5648-5652.
(b) Becke, A. D. *Phys. Rev. A* **1988**, *38*, 3098-3100.
(c) Lee, C. T.; Yang, W. T.; Parr, R. G. *Phys. Rev. B* **1988**, *37*, 785-789.
(d) Vosko, S. H.; Wilk, L.; Nusair, M. *Can. J. Phys.* **1980**, *58*, 1200-1211.
(e) Slater, J. C. *Quantum Theory of Molecules and Solids, Vol. 4: The Self-Consistent Field for Molecules and Solids*; McGraw-Hill: New York, 1974.

(82) NBO 6.0. Glendening, E. D.; Badenhoop, J. K.; Reed, A. E.; Carpenter, J. E.; Bohmann, J. A.; Morales, C. M.; Landis, C. R.; Weinhold, F. (Theoretical Chemistry Institute, University of Wisconsin, Madison, WI, 2013); http://nbo6.chem.wisc.edu/.

CHAPTER 6

Synthesis, Structural Characterization, and Reactivity of Transition Metal Complexes Featuring Nitron as a Ligand

Table of Contents

6.1 Introduction

Since the report of the first structurally characterized *N*-heterocyclic carbene (NHC) by Arduengo and co-workers in 1991,[1] the field of NHC chemistry has seen tremendous growth and development, progressing from basic structural characterizations and laboratory curiosities, to being applied in synthesis and catalysis.[2] A particularly prominent NHC is 1,3,4-triphenyl-1,2,4-triazol-5-ylidene, which is commonly referred to as "Enders carbene" (Figure 1).[3] Due to its remarkable utility in organocatalysis, Enders carbene became the first NHC to be commercially available;[4] however, several derivatives still remain expensive, exceeding hundreds of US dollars per gram in some cases.[5] It has now recently been shown that the low cost analytical reagent nitron,[6,7] which has been commercially available since 1905[8] as a reagent for the quantitative determination of nitrate, perchlorate,[8,9] and some metal ions,[10] exhibits reactivity in solution that is typical of an NHC.[11] This NHC-like behavior is attributed to the presence of the carbenic tautomer of nitron when placed in solution, as illustrated in Figure 1,[11] and is both structurally[6c] and electronically similar to Enders carbene, as reflected by the identical Tolman electronic parameter (TEP) of 2057 cm^{-1}.[11b,12] As such, nitron has been demonstrated to server as an effective ligand for Rh, Cu, Ag, and Au.[11,13] In view of its low cost and commercial availability, and the fact that its coordination chemistry is in its infancy, the reactivity of nitron towards other metal centers was explored.

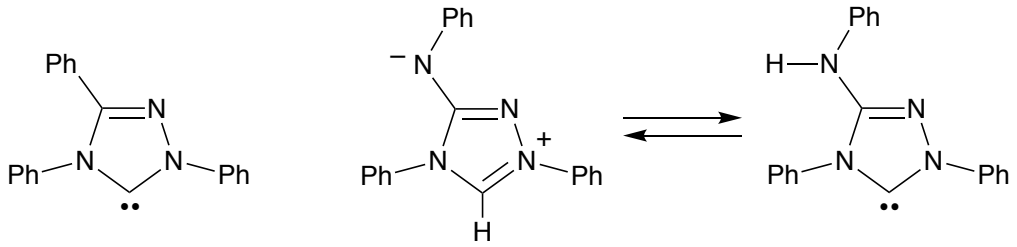

Figure 1. Structure of Enders carbene and tautomeric forms of nitron.

This chapter outlines (*i*) the synthesis and structural characterization of nickel, palladium, and iridium complexes that feature nitron as a ligand, and (*ii*) the ability of the corresponding iridium complexes to serve as catalysts for the dehydrogenation of formic acid and the hydrosilylation of aldehydes.

6.2 Synthesis and Structural Characterization of (nitron)$_2$NiBr$_2$ and (nitron)$_2$PdCl$_2$

To further explore the coordination chemistry of nitron, its reactivity towards $NiBr_2$ and $PdCl_2$ was investigated. Two equivalents of nitron reacts with both $NiBr_2$ and $PdCl_2$ to form the isostructural complexes (nitron)$_2$NiBr$_2$ and (nitron)$_2$PdCl$_2$, respectively (Scheme 1).

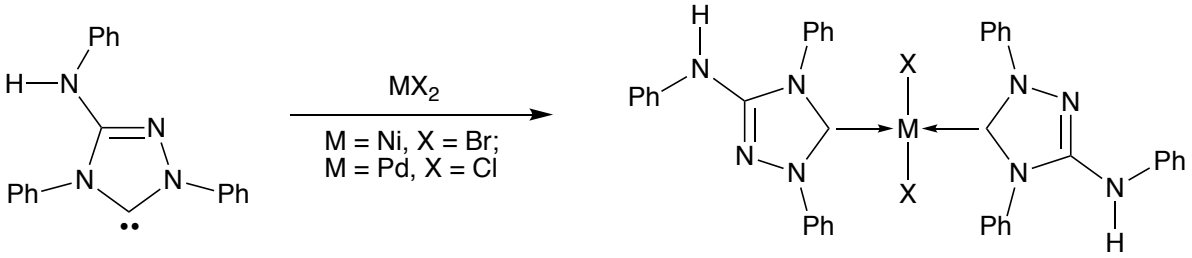

Scheme 1. Synthesis of (nitron)$_2$NiBr$_2$ and (nitron)$_2$PdCl$_2$ *via* treatment of nitron with $NiCl_2$ and $PdCl_2$ respectively.

Both $(nitron)_2NiBr_2$ and $(nitron)_2PdCl_2$ have been structurally characterized by X-ray diffraction (Figure 2 and Figure 3). Both metal centers possess a square planar arrangement with the nitron ligands positioned *trans* to one another. As discussed in Section 3.2.1 of Chapter 3, due to the symmetry of the molecule, the two largest angles (C1–Ni–C1A and Br–Ni–BrA) are both 180˚ which results in τ_4 and τ_δ values equal to 0, indicating a perfect square planar compound.[14] However, slight scissoring distortions[15] are present with C–M–X bond angles that deviate from 90˚ (C1–Ni–Br = 93.14(9)˚ and C1–Ni–BrA = 86.86(9)˚ for $(nitron)_2NiBr_2$ and C1–Pd–Cl = 92.52(5)˚; C1–Pd–ClA = 87.48(5)˚ for $(nitron)_2PdCl_2$). In regards to the bond lengths, the Ni–C (1.894(3) Å) distances are expectedly shorter than the Pd–C (2.0142(14) Å) distances. Additionally, the Ni–C and Pd–C bond lengths in $(nitron)_2NiBr_2$ and $(nitron)_2PdCl_2$ are very similar to the average Ni–C and Pd–C bond distances for typical NHC complexes listed in the Cambridge Structural Database (CSD)[16] (Ni–C average = 1.901 Å and Pd–C average = 2.000 Å).

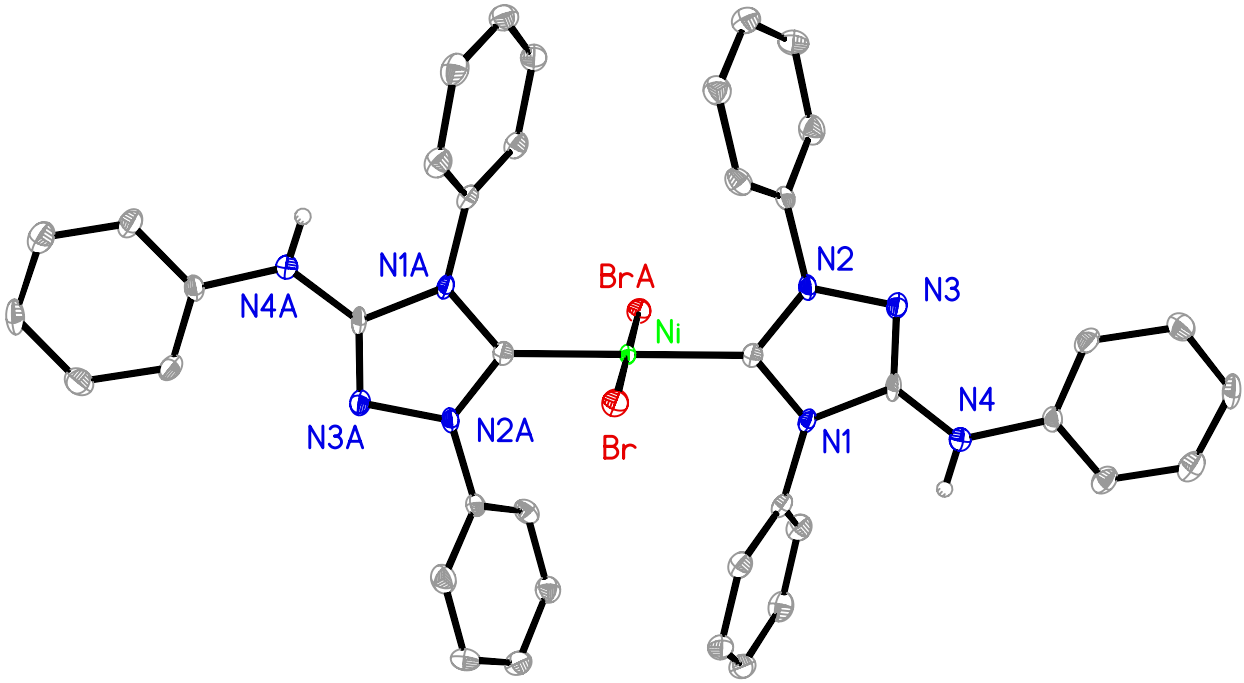

Figure 2. Molecular structure of (nitron)$_2$NiBr$_2$.

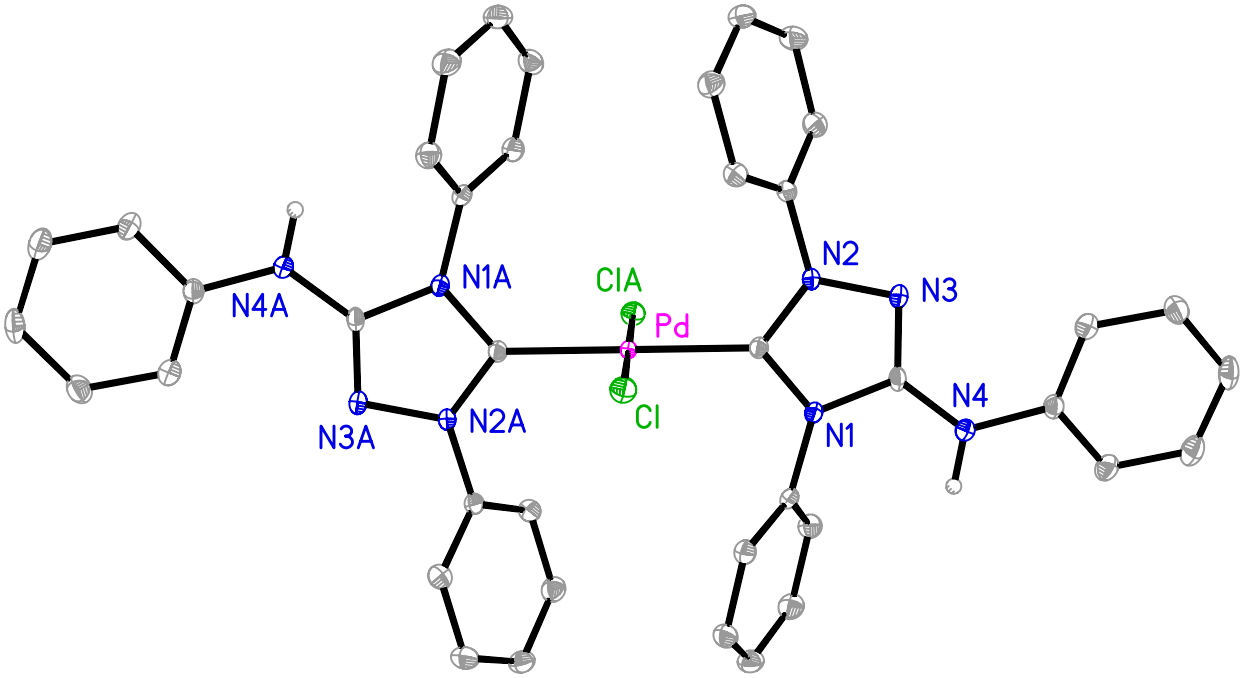

Figure 3. Molecular structure of (nitron)$_2$PdCl$_2$.

6.3 Synthesis, Characterization, and Reactivity of Iridium Complexes featuring Nitron as a Ligand

6.3.1 Synthesis and Structural Characterization of (nitron)Ir(COD)(Cl)

Nitron is also an effective ligand for iridium. When the bridging dimer, $[Ir(COD)Cl]_2$, is treated with nitron in acetonitrile, (nitron)Ir(COD)(Cl) is isolated as illustrated in Scheme 2.

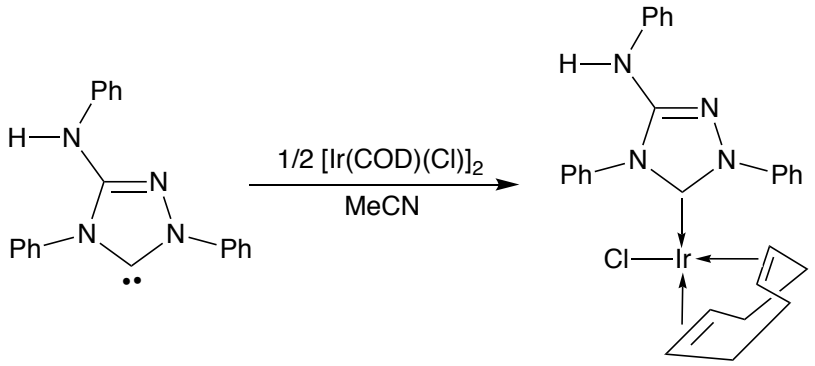

Scheme 2. Synthesis of (nitron)Ir(COD)(Cl) *via* treatment of $[Ir(COD)Cl]_2$ with nitron.

(nitron)Ir(COD)(Cl) has been structurally characterized by X-ray diffraction (Figure 4). The C1–Ir bond length is 2.013(4) Å, which is comparable to the average Ir–$C_{(NHC)}$ bond length (2.040 Å) found in the CSD.[16] Additionally, the Ir–$C_{(COD)}$ distances range from 2.088(4)–2.178(4) Å, which are in the range (1.918–2.238 Å) for other structurally characterized Ir complexes in the CSD that feature η^4-(C_4)-COD ligands.[16,17] Spectroscopically, the N–H hydrogen resonance of the nitron ligand in (nitron)Ir(COD)(Cl) appears at 5.78 ppm in CD_3CN in the ^1H NMR spectrum.

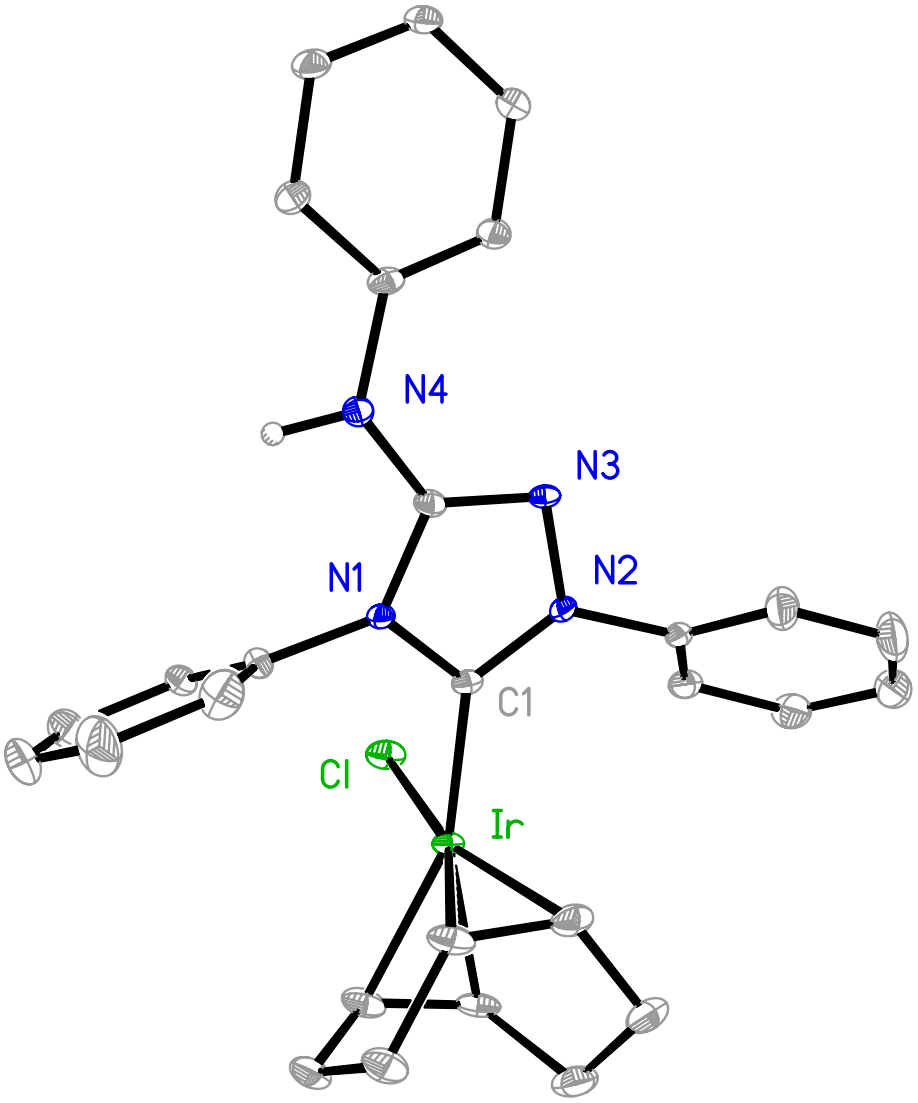

Figure 4. Molecular structure of (nitron)Ir(COD)(Cl).

6.3.2 Reactivity of (nitron)Ir(COD)(Cl): Synthesis and Characterization of {[κ^2-(C,C)-(nitron)]Ir(PMe_3)$_2$(cycloocta-4-enyl)(MeCN)}[Cl], (nitron)Ir(CO)$_2$(Cl), and (nitron)Ir(CO)(PPh_3)(Cl)

(nitron)Ir(COD)(Cl) affords a good platform with which to explore the reactivity of an iridium complex supported by nitron towards Lewis bases. In this regard, when (nitron)Ir(COD)(Cl) is treated with PMe_3 and recrystallized from MeCN, {[κ^2-(C,C)-(nitron)]Ir(PMe_3)$_2$(cycloocta-4-enyl)(MeCN)}[Cl] is obtained (Scheme 3).

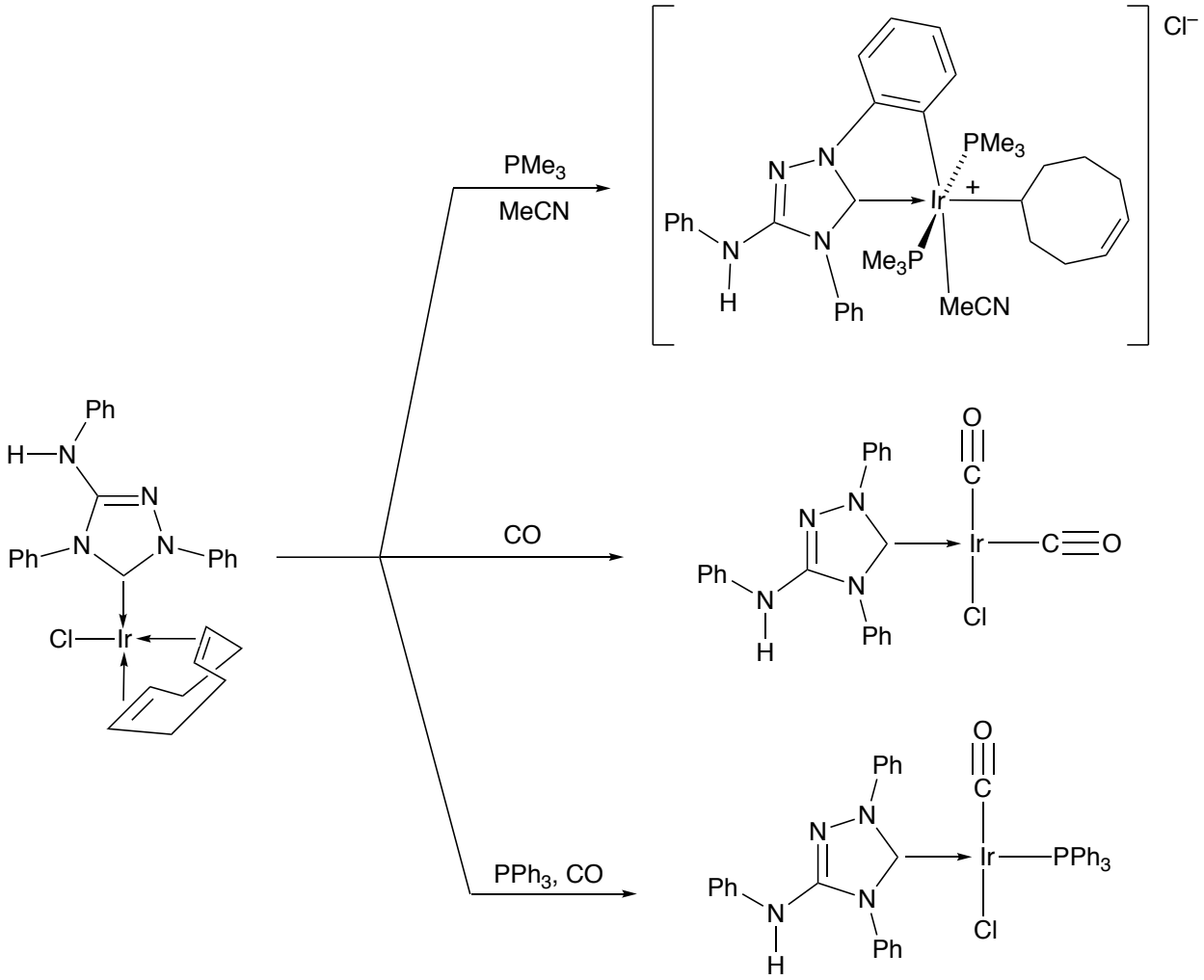

Scheme 3. Synthesis of {[κ^2-(C,C)-(nitron)]Ir(PMe_3)$_2$(cycloocta-4-enyl)(MeCN)}[Cl], (nitron)Ir(CO)$_2$(Cl), and (nitron)Ir(CO)(PPh_3).

{[κ^2-(C,C)-(nitron)]Ir(PMe_3)$_2$(cycloocta-4-enyl)(MeCN)}[Cl], which has been structurally characterized by X-ray diffraction (Figure 5), features an octahedral Ir(III) metal center, that has been formally oxidized from Ir(I) in (nitron)Ir(COD)(Cl). The nitron ligand exhibits a κ^2-cooridination mode in which one of the phenyl rings ortho metalates the Ir center, in addition to coordination through the carbenic carbon atom. Perhaps the most interesting aspect about the structure of {[κ^2-(C,C)-(nitron)]Ir(PMe_3)$_2$(cycloocta-4-enyl)(MeCN)}[Cl], is the nature of the cycloocta-4-enyl ligand. Specifically, the

cycloocta-4-enyl ligand only coordinates to the Ir center *via* an Ir–C σ-bond, such that the alkene functionality remains uncoordinated. This is unusual for iridium complexes featuring cycloocta-4-enyl ligands, as there are only 3 examples in the CSD[16] which feature this coordination mode.[18,19] The lack of alkene coordination in {[κ^2-(C,C)-(nitron)]Ir(PMe_3)$_2$(cycloocta-4-enyl)(MeCN)}[Cl] can be attributed to steric and electronic saturation around the Ir center. Furthermore, {[κ^2-(C,C)-(nitron)]Ir(PMe_3)$_2$(cycloocta-4-enyl)(MeCN)}[Cl] possesses two PMe_3 ligands, one MeCN ligand which results from solvent coordination, and a Cl counterion. Spectroscopically, {[κ^2-(C,C)-(nitron)]Ir(PMe_3)$_2$(cycloocta-4-enyl)(MeCN)}[Cl] is characterized by a $^{31}P\{^1H\}$ NMR signal at –41.48 ppm

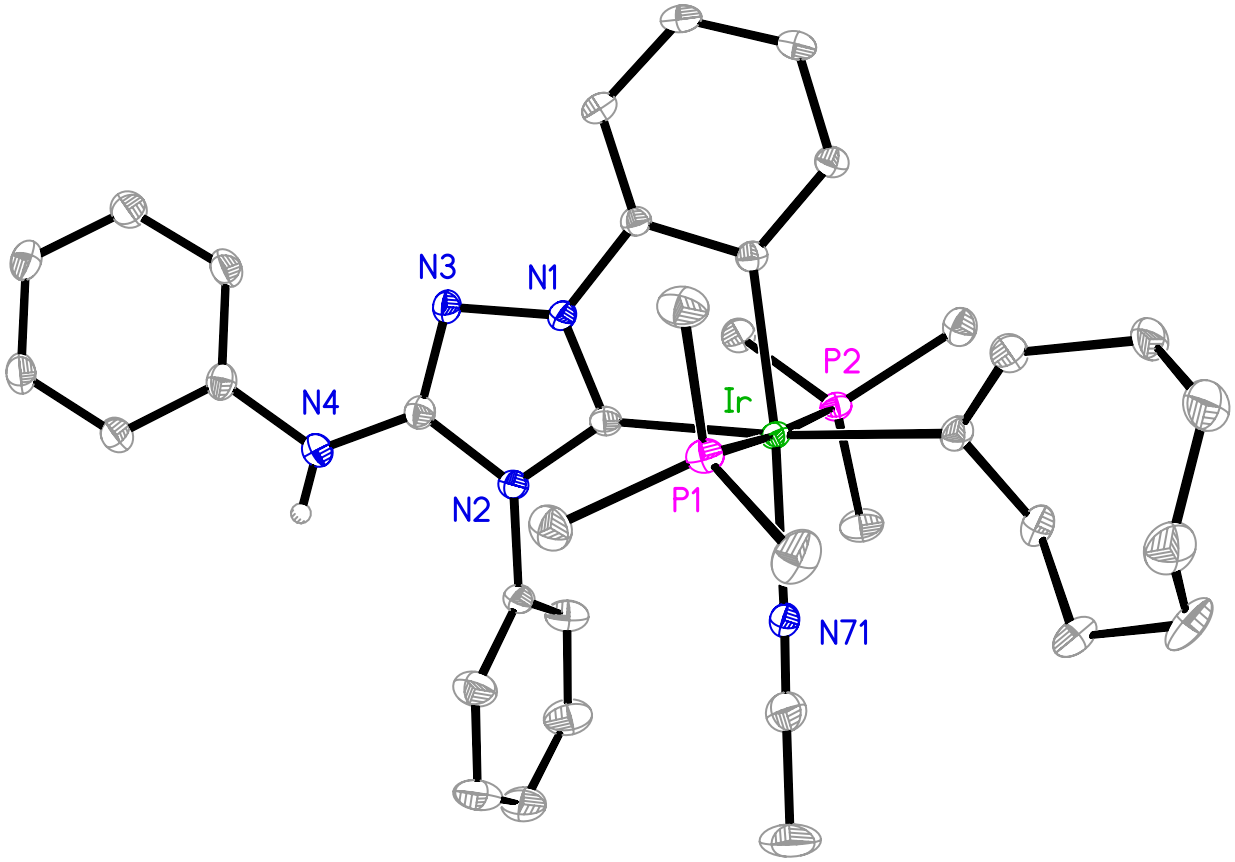

Figure 5. Molecular structure of {[κ^2-(C,C)-(nitron)]Ir(PMe_3)$_2$(cycloocta-4-enyl)(MeCN)}[Cl] (the Cl anion is omitted for clarity).

When (nitron)Ir(COD)(Cl) is treated with CO, (nitron)Ir(CO)$_2$(Cl) is obtained as illustrated in Scheme 3. (nitron)Ir(CO)$_2$(Cl) has been structurally characterized by X-ray diffraction (Figure 6), thereby showing that the Ir metal center possess an approximately square planar geometry ($\tau_4 = \tau_\delta = 0.04$)[20] with the CO ligands positioned *cis* to one another. The CO ligand *trans* to nitron has a slightly longer Ir–C bond length than the CO ligand *trans* to the Cl ligand (Ir–C1 = 1.892(3) Å, Ir–C2 = 1.843(3) Å). Furthermore, the CO ligand *trans* to nitron has a slightly longer C–O bond length (C1–O1 = 1.135(3) Å) than the CO ligand *trans* to the chloride (C2–O2 = 1.119(4) Å). Additionally, the Ir–$C_{(nitron)}$ bond length in (nitron)Ir(CO)$_2$(Cl) (2.064(2) Å) is slightly

longer than the Ir–$C_{(nitron)}$ bond length in (nitron)Ir(COD)(Cl) (2.013(4) Å), as indicated in Table 1.

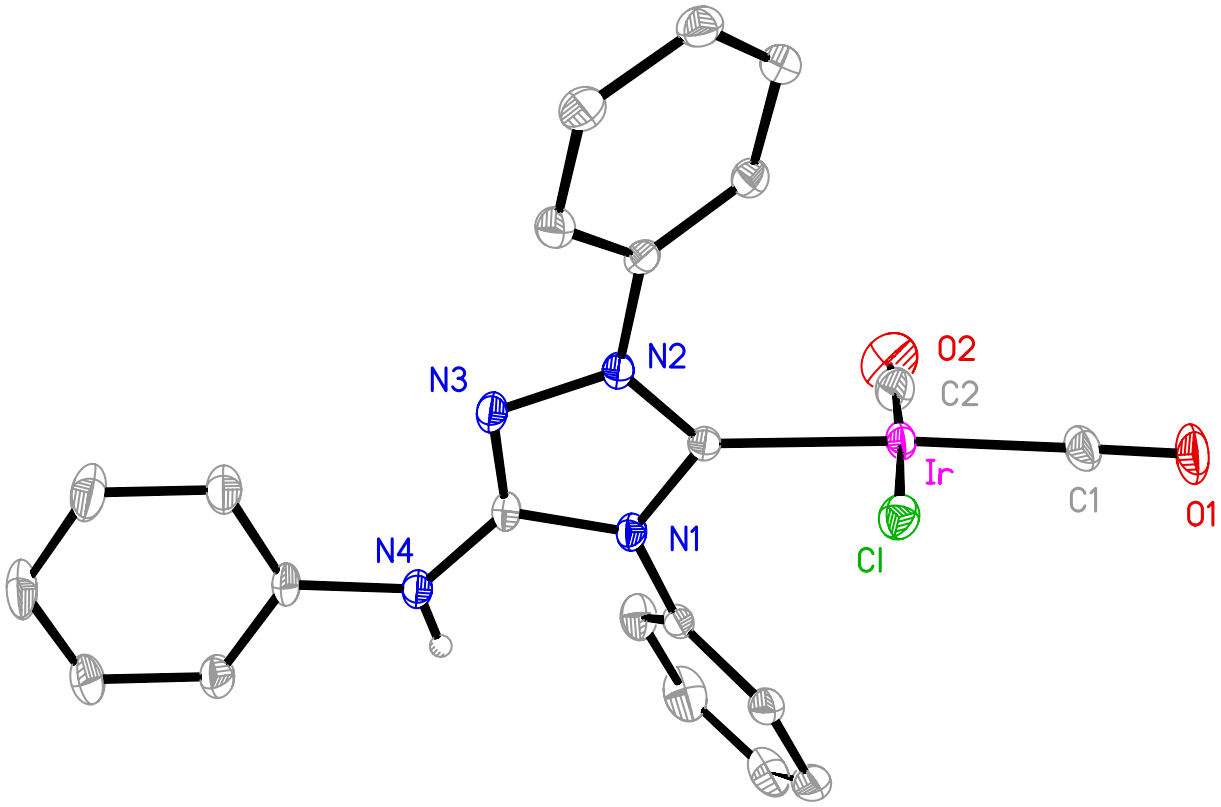

Figure 6. Molecular structure of (nitron)Ir$(CO)_2$(Cl).

Spectroscopically, the N–H hydrogen resonance of the nitron ligand in (nitron)Ir$(CO)_2$(Cl) appears at 5.37 ppm, which is shifted upfield from the N–H hydrogen resonance of (nitron)Ir(COD)(Cl) (5.78 ppm). Additionally, the ν(CO) stretching frequencies appear at 2066 cm^{-1} and 1981 cm^{-1} in the IR spectrum, in the range of typical terminal metal carbonyl stretches.

Additionally, when (nitron)Ir(COD)(Cl) is treated with PPh_3, followed by the addition of CO, (nitron)Ir(CO)(PPh_3)(Cl) is obtained (Scheme 3). (nitron)Ir(CO)(PPh_3)(Cl) has

been structurally characterized by X-ray diffraction (Figure 7), and, similar to (nitron)Ir(CO)$_2$(Cl), the Ir metal center possess an approximately square planar geometry ($\tau_4 = \tau_\delta = 0.07$),[20] with the nitron ligand *trans* to PPh_3. The Ir–$C_{(nitron)}$ bond length (2.047(3) Å) in (nitron)Ir(CO)(PPh_3)(Cl) is intermediate to the Ir–$C_{(nitron)}$ bond lengths in (nitron)Ir(COD)(Cl) (2.013(4) Å) and (nitron)Ir(CO)$_2$(Cl) (2.064(2) Å) (Table 1). With regards to the carbonyl ligand, the Ir–C1 bond length is intermediate (1.850(4) Å) to the two Ir–$C_{(CO)}$ bond lengths in (nitron)Ir(CO)$_2$(Cl) (1.892(3) and 1.843(3) Å), but the C1–O bond length (1.092(4) Å) is shorter than both the corresponding bonds in (nitron)Ir(CO)$_2$(Cl) (1.119(4) and 1.135(3) Å). For reference, the closely related compound, commonly referred to as Vaska's complex, (PPh_3)$_2$Ir(CO)(Cl), features an Ir–$C_{(CO)}$ bond length of 1.791(13) Å and a C–O bond length of 1.161(18) Å[21] as summarized in Table 1.

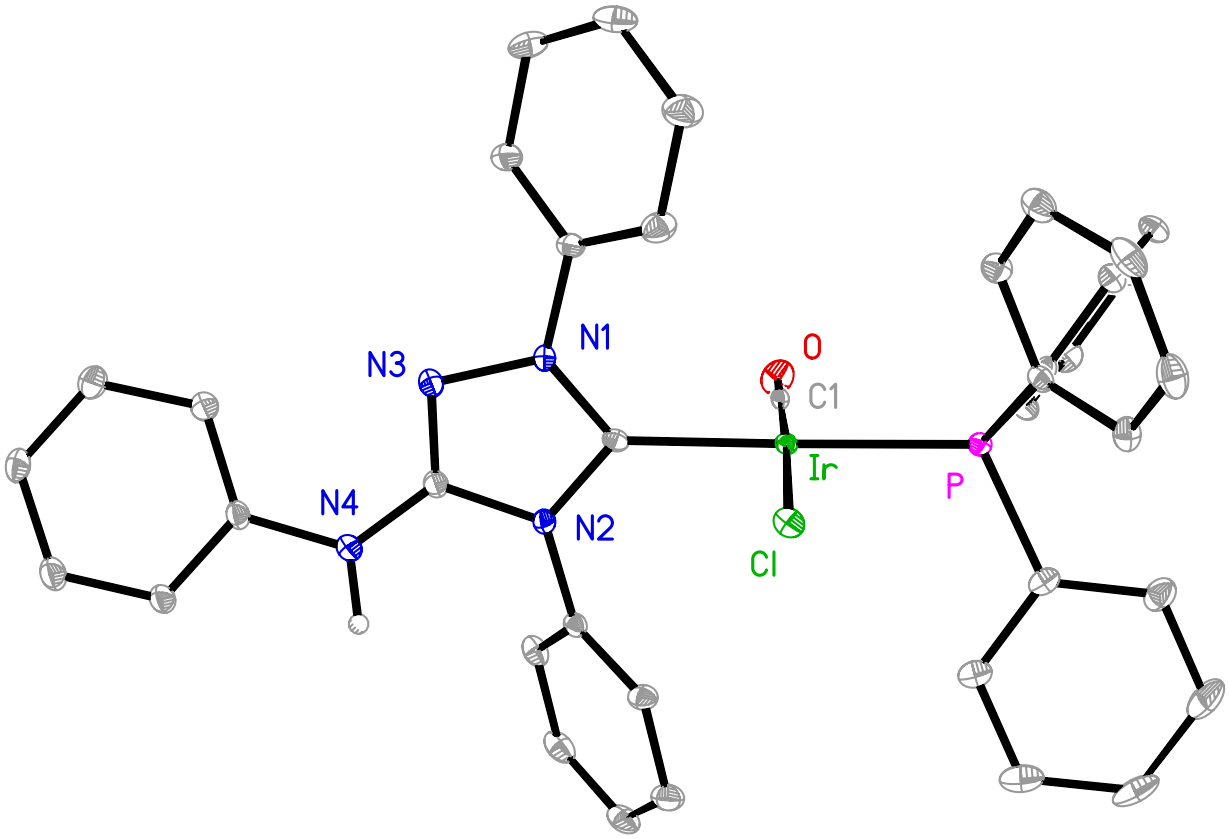

Figure 7. Molecular structure of (nitron)Ir(CO)(PPh_3)(Cl).

Spectroscopically, (nitron)Ir(CO)(PPh_3)(Cl) is characterized by a singlet at 24.1 ppm in the $^{31}P\{^1H\}$ NMR spectrum. Additionally, the CO stretching frequency is observed at 1947 cm^{-1} in the IR spectrum.

Table 1. Selected bond distances for iridium complexes featuring nitron and related complexes.

Compound	Ir–$C_{(nitron)}$ /Å	Ir–$C_{(CO)}$ /Å	$C_{(CO)}$–O /Å	ν(CO) /cm^{-1}	Ref
(nitron)Ir(COD)(Cl)	2.013(4)	–	–	–	this work
(nitron)Ir$(CO)_2$(Cl)	2.064(2)	1.892(3), 1.843(3)	1.135(3), 1.119(4)	2066, 1981	this work
(nitron)Ir(CO)(PPh_3)(Cl)	2.047(3)	1.850(4)	1.092(4)	1947	this work
$(PPh_3)_2$Ir(CO)(Cl) (Vaska's complex)	–	1.791(13)	1.161(18)	1960	21
{[κ^2-(C,C)-(nitron)]Ir$(PMe_3)_2$(cyclo octa-4-enyl)(MeCN)}[Cl]	2.058(3)	–	–	–	this work

6.4 Reactivity of (nitron)Ir$(CO)_2$(Cl) and (nitron)Ir(CO)(PPh_3)(Cl)

6.4.1 Dehydrogenation of Formic Acid

To keep up with the ever-growing demand for energy, it is pertinent to develop new, alternative, and clean energy sources that are more sustainable than traditional fossil fuels, which pose potential hazards to Earth's environment.[22] To this end, hydrogen has become an attractive source of energy; however, storing the gas poses several challenges.[23] Recently, interest has focused on using formic acid as a chemical hydrogen transportation medium,[24,25,26] as its decomposition yields hydrogen and carbon dioxide, the latter of which could potentially be trapped[27] and recycled[28] to store more hydrogen. The dehydrogenation of formic acid has been carried out by both heterogeneous[29,30] and homogeneous catalysts.[31-41] More recently in the Parkin lab, Dr.

Michelle Neary has shown that a variety of Mo and Ni complexes are capable of catalyzing this transformation.[42] Therefore, it is significant that both (nitron)Ir(CO)$_2$(Cl) and (nitron)Ir(CO)(PPh$_3$)(Cl) are also capable of catalyzing the dehydrogenation of formic acid (Scheme 4).

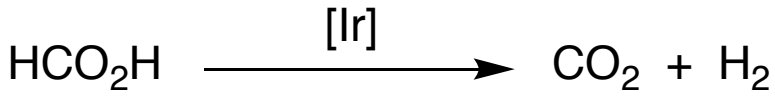

Scheme 4. Formic acid dehydrogenation reaction {[Ir] = (nitron)Ir(CO)$_2$(Cl) or (nitron)Ir(CO)(PPh$_3$)(Cl)}.

More specifically, when (nitron)Ir(CO)$_2$(Cl) and (nitron)Ir(CO)(PPh$_3$)(Cl) are treated with formic acid in C_6D_6 and heated at 80˚ C, the formation of H_2 and CO_2 are observed. Additionally, at room temperature, the conversion of formic acid to H_2 and CO_2 is observed, but the reaction is much slower. It should also be noted that after converting 10 equivalents of formic acid to H_2 and CO_2 over the course of 24 hours, (nitron)Ir(CO)(PPh$_3$)(Cl) begins to decompose, whereas (nitron)Ir(CO)$_2$(Cl) appears to remain intact as discerned by NMR spectroscopy.

6.4.2 Hydrosilylation of Aldehydes

The catalytic hydrosilylation of carbonyl compounds to afford alkoxysilanes is not only of interest in terms of providing a means to reduce a substrate to an alcohol,[43] but is also of interest as alkoxysilanes have applications in organic synthesis[44] and materials chemistry.[45] In this regard, it is significant that (nitron)Ir(CO)$_2$(Cl) is capable of effecting the hydrosilylation of benzaldehyde. Specifically, (nitron)Ir(CO)$_2$(Cl) catalyzes the double insertion of PhCHO into two of the Si–H bonds of $PhSiH_3$ when heated at 60˚C for 1 hour to afford $PhSiH(OCH_2Ph)_2$. This corresponds to a TOF of 20 h^{-1} per Si–H bond. The mechanism of this reaction is not known, but an Ir–H species is proposed to

be the catalytic intermediate. An independent NMR spectroscopic study indicates that treatment of (nitron)Ir(CO)$_2$(Cl) with PhSiH$_3$ results in the generation of an Ir–H species *inter alia*.

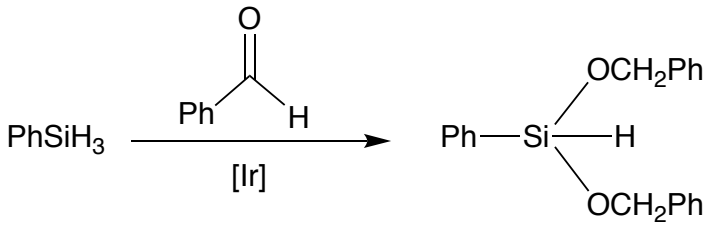

Scheme 5. Hydrosilylation of benzaldehyde {[Ir] = (nitron)Ir(CO)$_2$(Cl)}.

6.5 Summary and Conclusions

In summary, the coordination chemistry of nitron, which has been used as an analytical reagent for the better part of the past century, has been extended to Ni, Pd, and Ir. In solution, nitron behaves similarly to traditional NHC complexes, which coordinate to metal complexes through the central carbon atom. With regards to the metal complexes synthesized in this chapter, two equivalents of nitron react with NiBr$_2$ and PdCl$_2$ to yield the isostructural complexes, (nitron)$_2$NiBr$_2$ and (nitron)$_2$PdCl$_2$. Furthermore, nitron is also an effective ligand for iridium, as demonstrated by the synthesis of (nitron)Ir(COD)(Cl). (nitron)Ir(COD)(Cl) also reacts with a variety of Lewis bases as indicated by the isolation of {[κ^2-(C,C)-(nitron)]Ir(PMe$_3$)$_2$(cycloocta-4-enyl)(MeCN)}[Cl], (nitron)Ir(CO)$_2$(Cl), and (nitron)Ir(CO)(PPh$_3$). Additionally, (nitron)Ir(CO)$_2$(Cl) and (nitron)Ir(CO)(PPh$_3$) are capable of catalyzing the dehydrogenation of formic acid, and (nitron)Ir(CO)$_2$(Cl) has been demonstrated to be an effective catalyst for the hydrosilylation of benzaldehyde.

6.6 Experimental Details

6.6.1 General Considerations

All manipulations were performed using a combination of glovebox, high vacuum and Schlenk techniques under a nitrogen or argon atmosphere.[46] Solvents were purified and degassed by standard procedures. NMR spectra were measured on Bruker 300 DRX, Bruker 400 DRX, and Bruker Avance 500 DMX spectrometers. ^{1}H NMR spectra are reported in ppm relative to $SiMe_4$ ($\delta = 0$) and were referenced internally with respect to the protio solvent impurity ($\delta = 7.16$ for C_6D_5H and $\delta = 1.94$ for CD_2HCN).[47] ^{13}C NMR spectra are reported in ppm relative to $SiMe_4$ ($\delta = 0$) and were referenced internally with respect to the solvent ($\delta = 128.06$ for C_6D_6 and $\delta = 118.26$ for CD_3CN).[47] $^{31}P\{^{1}H\}$ NMR spectra are reported in ppm relative to 85% H_3PO_4 ($\delta = 0$) and were obtained by using the $\Xi/100\%$ value of 40.480742.[48] Coupling constants are reported in hertz. Infrared spectra were recorded on a Perkin Elmer Spectrum Two spectrometer, and are reported in reciprocal centimeters. All chemicals were obtained from Sigam-Aldrich, with the exception of $PhSiH_3$ which was obtained from Acros Organics, and used as supplied.

6.6.2 X-ray Structure Determinations

X-ray diffraction data were collected on a Bruker Apex II diffractometer. Crystal data, data collection and refinement parameters are summarized in Table 2. The structures were solved by using direct methods and standard difference map techniques, and were refined by full-matrix least-squares procedures on F^2 with SHELXTL (Version 2014/7).[49]

6.6.3 Synthesis of (nitron)$_2$NiBr$_2$

A mixture of $NiBr_2$ (11 mg, 0.050 mmol) and nitron (34 mg, 0.109 mmol) was dissolved in CD_3CN (1 mL), transferred to an NMR tube equipped with a J. Young valve, and heated at 80˚C for 24 hours. After this time, a pale red/pink precipitate had formed, which was isolated *via* decantation, washed with diethyl ether (1 × 2 mL), and dried *in vacuo* to afford (nitron)$_2$NiBr$_2$ as a pale red/pink powder (15 mg, 36%). Red crystals suitable for X-ray diffraction were obtained by heating a concentrated solution of (nitron)$_2$NiBr$_2$ in acetonitrile which was then allowed to cool slowly. ^{1}H NMR (CD_3CN): 6.75 [t, 1H of nitron, $^3J_{H\text{-}H}$ = 7 Hz], 7.19 [t, 2H of nitron, $^3J_{H\text{-}H}$ = 8 Hz], 7.42-7.64 [m, 8H of nitron], 7.84 [d, 2H of nitron, $^3J_{H\text{-}H}$ = 8 Hz], 7.91 [d, 2H of nitron, $^3J_{H\text{-}H}$ = 8 Hz], 9.36 [broad s, 1H of nitron N–H].

6.6.4 Synthesis of (nitron)$_2$PdCl$_2$

A mixture of $PdCl_2$ (5 mg, 0.028 mmol) and nitron (18 mg, 0.058 mmol) was dissolved in CD_3CN (1 mL), transferred to an NMR tube equipped with a J. Young valve, and heated at 80˚C for 24 hours. After this time, a dark green solution had formed along with the formation of green crystals on the walls of the NMR tube. The crystals were isolated by decantation, washed with diethyl ether (1 × 2 mL), and dried *in vacuo* to afford (nitron)$_2$PdCl$_2$ (7 mg, 31%). The green crystals obtained from the reaction were suitable for X-ray diffraction. ^{1}H NMR (CD_3CN): 7.04 [t, 1H of nitron, $^3J_{H\text{-}H}$ = 8 Hz], 7.20-7.70 [m, 10H of nitron], 8.36 [d, 2H of nitron, $^3J_{H\text{-}H}$ = 8 Hz], 8.74 [d, 2H of nitron, $^3J_{H\text{-}H}$ = 8 Hz], 10.10 [broad s, 1H of nitron N–H].

6.6.5 Synthesis of (nitron)Ir(COD)(Cl)

A suspension of [Ir(COD)Cl]$_2$ (245 mg, 365 mmol) in acetonitrile (10 mL) was treated with nitron (228 mg, 730 mmol) and stirred for 21 hours resulting in the formation of a

yellow precipitate in a dark brown solution. The precipitate was isolated *via* centrifugation, washed with diethyl ether (1 × 2 mL), and dried *in vacuo* to afford (nitron)Ir(COD)(Cl) as a yellow powder (302 mg, 64%). Yellow crystals suitable for X-ray diffraction were obtained *via* slow evaporation of an acetonitrile solution. ^{1}H NMR (C_6D_6): 1.16-1.68 [m, 6H of COD], 1.78-2.08 [m, 2H of COD], 2.43 [m, 1H of COD], 2.80 [m, 1H of COD], 4.97 [m, 2H of COD], 5.79 [s, 1H of nitron N–H], 6.80 [t, 1H of nitron, $^{3}J_{H\text{-}H}$ = 8 Hz], 7.01-7.24 [m, 10H of nitron], 7.61 [d, 2H of nitron, $^{3}J_{H\text{-}H}$ = 8 Hz], 8.88 [d, 2H of nitron, $^{3}J_{H\text{-}H}$ = 8 Hz]. IR (cm^{-1}): 3289 (w), 2882 (w), 2833 (w), 1630 (m), 1596 (m), 1489 (m), 1452 (w), 1369 (m), 1320 (w), 1233 (w), 1170 (w), 971 (m), 751 (s), 693 (s), 506 (m).

6.6.6 Synthesis of {[κ^2-(C,C)-(nitron)]Ir(PMe$_3$)$_2$(cycloocta-4-enyl)(MeCN)}[Cl]

A solution of (nitron)Ir(COD)(Cl) (15 mg, 0.023 mmol) in C_6D_6 (0.7 mL) in an NMR tube equipped with a J. Young valve was treated with PMe_3 (11 μL, 0.115 mmol) *via* vapor transfer resulting in the formation of a yellow solution. The NMR tube was occasionally shaken over the course of 1 day, after which time the volatile components were removed *via* lyophilization to afford a pale-yellow powder. This crude powder was recrystallized from acetonitrile to yield {[κ^2-(C,C)-(nitron)]Ir(PMe_3)$_2$(cycloocta-4-enyl)(MeCN)}[Cl] as yellow crystals (5 mg, 26%) suitable for X-ray diffraction. ^{1}H NMR (CD_3CN): 1.07 [m, 6H of COD], 1.57 [m, 18H of PMe_3], 2.12-2.63 [m, 4H of COD], 3.29 [s, 3H of MeCN], 7.01-8.04 [m, 15H of nitron], 9.73 [broad s, 1H of nitron N–H]. ^{31}P{^{1}H} NMR (CD_3CN): –41.48 [s, $\underline{P}Me_3$].

6.6.7 Synthesis of (nitron)Ir(CO)$_2$(Cl)

A solution of (nitron)Ir(COD)(Cl) (20 mg, 0.031 mmol) in C_6D_6 (0.7 mL) in an NMR tube equipped with a J. Young valve was degassed *via* a freeze-pump-thaw cycle and then exposed to CO (1 atm). The solution immediately turned a paler yellow color and was

occasionally shaken for 1 hr. The volatile components were then removed *via* lyophilization to afford a pale-yellow powder, which was washed with pentane (1 × 2 mL), and dried *in vacuo* to afford (nitron)Ir(CO)$_2$(Cl) (13 mg, 67%). Crystals suitable for X-ray diffraction were obtained *via* slow evaporation of a benzene solution. ^{1}H NMR (C_6D_6): 5.37 [s, 1H of nitron N–H], 6.79 [t, 1H of nitron, $^3J_{H\text{-}H}$ = 8 Hz], 6.89-7.20 [m, 12H of nitron], 8.39 [d, 2H of nitron, $^3J_{H\text{-}H}$ = 8 Hz]. IR (cm^{-1}): 3306 (w), 3067 (w), 2066 (vs, [ν(CO)]), 1980 (vs [ν(CO)]), 1622 (m), 1602 (m), 1586 (m), 1546 (m), 1494 (m), 1455 (w), 1211 (w), 984 (w), 748 (s), 688 (s), 501 (m).

6.6.8 Synthesis of (nitron)Ir(CO)(PPh$_3$)(Cl)

A solution of (nitron)Ir(COD)(Cl) (11 mg, 0.017 mmol) in C_6D_6 (0.7 mL) was treated with PPh_3 (5 mg, 0.019 mmol) and transferred to an NMR tube equipped with a J. Young valve which was degassed *via* a freeze-pump-thaw cycle and then exposed to CO (1 atm). The solution immediately turned a paler yellow color and was shaken for 5 minutes. After this time, the volatile components were removed *via* lyophilization to afford a pale-yellow powder, which was washed with pentane (1 × 2 mL) and dried *in vacuo* to afford (nitron)Ir(CO)(PPh_3)(Cl) (4 mg, 29%). Crystals suitable for X-ray diffraction were obtained *via* slow evaporation of a benzene solution. ^{1}H NMR (C_6D_6): 5.61 [s, 1H of nitron N–H], 6.82-7.58 [m, 15H of nitron], 7.06 [m, 9H of PPh_3], 7.78 [m, 6H of PPh_3], 8.99 [d, 2H of nitron, $^3J_{H\text{-}H}$ = 8 Hz]. ^{31}P{^{1}H} NMR (CD_3CN): 24.310 [s, $\underline{P}Ph_3$]. IR (cm^{-1}): 3053 (w), 1947 (s, [ν(CO)]), 1617 (m), 1601 (m), 1585 (m), 1543 (m), 1495 (m), 1435 (m), 1095 (w), 747 (m), 689 (s), 530 (m), 511 (m).

6.6.9 Reactivity of (nitron)Ir(CO)$_2$(Cl) Towards Formic Acid

(a) A solution of (nitron)Ir(CO)$_2$(Cl) (6 mg, 0.010 mmol) in C_6D_6 (0.7 mL) in an NMR tube equipped with a J. Young valve was treated with formic acid (4.5 mg, 0.098 mmol)

and heated at 80˚C. The reaction was monitored *via* NMR spectroscopy, thereby demonstrating the formation of H_2 and CO_2.

(b) A solution of (nitron)Ir(CO)$_2$(Cl) (4 mg, 0.007 mmol) in C_6D_6 (0.7 mL) in an NMR tube equipped with a J. Young valve was treated with formic acid (3.5 mg, 0.076 mmol). The reaction was monitored at room temperature *via* NMR spectroscopy, thereby demonstrating the formation of H_2 and CO_2.

6.6.10 Reactivity of (nitron)Ir(CO)(PPh$_3$)(Cl) Towards Formic Acid

(a) A solution of (nitron)Ir(CO)(PPh$_3$)(Cl) (4.5 mg, 0.005 mmol) in C_6D_6 (0.7 mL) in an NMR tube equipped with a J. Young valve was treated with formic acid (3.1 mg, 0.067 mmol) and heated at 80˚C. The reaction was monitored *via* NMR spectroscopy, thereby demonstrating the formation of H_2 and CO_2.

(b) A solution of (nitron)Ir(CO)(PPh$_3$)(Cl) (3 mg, 0.004 mmol) in C_6D_6 (0.7 mL) in an NMR tube equipped with a J. Young valve was treated with formic acid (3 mg, 0.065 mmol). The reaction was monitored at room temperature *via* NMR spectroscopy, thereby demonstrating the formation of H_2 and CO_2.

6.6.11 Hydrosilylation of Benzaldehyde by PhSiH$_3$ catalyzed by (nitron)Ir(CO)$_2$(Cl)

A solution of (nitron)Ir(CO)$_2$(Cl) (2.1 mg, 0.004 mmol), benzaldehyde (12.6 mg, 0.119 mmol), and $PhSiH_3$ (3.8 mg, 0.035 mmol) in C_6D_6 (0.7 mL) in an NMR tube equipped with a J. Young valve was heated at 60˚C. The reaction was monitored by ^{1}H NMR spectroscopy, thereby demonstrating the formation of PhSiH(OCH$_2$Ph)$_2$ after 1 hr.

6.7 Crystallographic Data

Table 2. Crystal, intensity collection, and refinement data.

	(nitron)$_2$NiBr$_2$	**(nitron)$_2$PdCl$_2$**
lattice	Monoclinic	Monoclinic
formula	$C_{40}H_{32}Br_2N_8Ni$	$C_{40}H_{32}Cl_2N_8Pd$
formula weight	843.26	802.03
space group	$P2_1/c$	$P2_1/c$
a / Å	9.9112(5)	9.8550(4)
b / Å	22.8862(11)	22.9116(10)
c / Å	7.9848(4)	7.8638(4)
α / °	90	90
β / °	105.2260(10)	102.6799(6)
γ / °	90	90
V / Å^3	1747.61(15)	1732.29(14)
Z	2	2
temperature (K)	170(2)	170(2)
radiation (λ, Å)	0.71073	0.71073
ρ (calcd.) g cm^{-3}	1.602	1.538
μ (Mo Kα), mm^{-1}	2.885	0.733
θ max, deg.	30.523	30.648
no. of data collected	28218	28315
no. of data	5347	5339
no. of parameters	236	236
R_1 [$I > 2\sigma(I)$]	0.0554	0.0315
wR_2 [$I > 2\ \sigma(I)$]	0.1191	0.0848
R_1 [all data]	0.0691	0.0370
wR_2 [all data]	0.1206	0.0866
GOF	2.406	1.588
R_{int}	0.0366	0.0493

Table 2. Crystal, intensity collection, and refinement data.

	(nitron)Ir(COD)(Cl)	**{[κ²-(C,C)-(nitron)]Ir(PMe_3)$_2$(cycloocta-4-enyl)(MeCN)}[Cl]**
lattice	Monoclinic	Monoclinic
formula	$C_{30}H_{31}ClIrN_5$	$C_{38}H_{51}ClIrN_6P_2$
formula weight	689.25	881.43
space group	$P2_1/c$	$C2/c$
a / Å	10.4055(8)	29.422(2)
b / Å	34.794(3)	11.6424(9)
c / Å	7.7242(6)	22.6899(17)
α / °	90	90
β / °	93.9570(10)	90.1080(10)
γ / °	90	90
V / Å^3	2789.9(4)	7772.3(10)
Z	4	8
temperature (K)	170(2)	160(2)
radiation (λ, Å)	0.71073	0.71073
ρ (calcd.) g cm^{-3}	1.641	1.507
μ (Mo Kα), mm^{-1}	4.909	3.622
θ max, deg.	30.562	30.507
no. of data collected	44585	62825
no. of data	8535	11882
no. of parameters	339	445
R_1 [$I > 2\sigma(I)$]	0.0480	0.0294
wR_2 [$I > 2\ \sigma(I)$]	0.1125	0.0714
R_1 [all data]	0.0518	0.0409
wR_2 [all data]	0.1135	0.0751
GOF	1.803	1.158
R_{int}	0.0658	0.0479

Table 2. Crystal, intensity collection, and refinement data.

	(nitron)Ir(CO)$_2$(Cl)	**(nitron)Ir(CO)(PPh$_3$)(Cl)**
lattice	Triclinic	Triclinic
formula	$C_{31}H_{25}ClIrN_4O_2$	$C_{45}H_{37}ClIrN_4OP$
formula weight	713.20	6908.40
space group	*P-1*	*P-1*
a / Å	10.1756(7)	9.7234(4)
b / Å	10.5897(8)	12.1313(5)
c / Å	14.2908(10)	17.7587(8)
α / °	74.5490(10)	71.3220(10)
β / °	85.3990(10)	86.0480(10)
γ / °	76.2920(10)	74.0520(10)
V / Å^3	1441.75(18)	1907.65(14)
Z	2	2
temperature (K)	160(2)	129(2)
radiation (λ, Å)	0.71073	0.71073
ρ (calcd.) g cm^{-3}	1.643	1.581
μ (Mo Kα), mm^{-1}	4.757	3.653
θ max, deg.	30.589	30.778
no. of data collected	23491	31842
no. of data	8817	11815
no. of parameters	356	482
R_1 [$I > 2\sigma(I)$]	0.0243	0.0336
wR_2 [$I > 2\ \sigma(I)$]	0.0563	0.0685
R_1 [all data]	0.0297	0.0449
wR_2 [all data]	0.0583	0.0721
GOF	1.063	1.012
R_{int}	0.0274	0.0462

6.8 References and Notes

(1) Arduengo III, A. J.; Harlow, R. L.; Kline, M. *J. Am. Chem. Soc.* **1991**, *113,* 361-363.

(2) (a) Hopkinson, M. N.; Richter, C.; Schedler, M.; Glorius, F. *Nature* **2014**, *51,* 485-496.
(b) Hock, S. J.; Schaper, L.-A.; Hermann, W. A.; Kuhn, F. E. *Chem. Soc. Rev.* **2013**, *42,* 5073-5089.
(c) Siemeling, U. *Eur. J. Inorg. Chem.* **2012**, 3523-3536.
(d) Diez-Gonzalez, S., Ed. *N-Heterocyclic Carbenes*; Royal Society of Chemistry: Cambridge, U. K., 2011.
(e) Cavell, K. J.; McGuinness, D. S. *Coord. Chem. Rev.* **2004**, *248,* 671-681.
(f) Cesar, V.; Bellemin-Laponnaz, S.; Gade, L. H. *Chem. Soc. Rev.* **2004**, *33,* 619-636.
(g) Tskhovrebov, A. G.; Solari, E.; Wodrich, M. D.; Scopelliti, R. Severin, K. *Angew. Chem. Int. Ed.* **2012**, *51,* 232-234.
(h) Navarro, O.; Viciu, M. S. *Annu. Rep. Prog. Chem., Sect. B* **2010**, *106,* 243-259.
(i) Berthon-Gelloz, G.; Siegler, M. A.; Spek, A. L.; Tinant, B.; Reek, J. N. H.; Marko, I. E. *Dalton Trans.* **2010**, *39,* 1444-1446.
(j) Schmidt, A.; Wiechmann, S.; Otto, C. F. Advances in Heterocyclic Chemistry from Heterocyclic Chemistry in the 21st Century: A Tribute to Alan Katritzky, **2016**, *119*, 143-172.
(k) Zhao, C.; Guo D.; Munkerup, K.; Huang, K.-W.; Li, F.; Wang, J. *Nature Comm.* **2018**, *9,* 1-10.

(3) Enders, D.; Breuer, K.; Raabe, G.; Runsink, J.; Teles, J. H.; Melder, J.-P.; Ebel, K.; Brode, S. *Angew. Chem. Int. Ed.* **1995**, *34,* 1021-1023.

(4) (a) Fevre, M.; Pinaud, J.; Gnanou, Y.; Vignolle, J.; Taton, D. *Chem. Soc. Rev.* **2013**, *42,* 2142-2172.
(b) Enders, D.; Niemeir, O.; Henseler, A. *Chem. Soc. Rev.* **2007**, *107,* 5606-5655.
(c) Enders, D.; Balensiefer, T. *Acc. Chem. Res.* **2004**, *37*, 534-541.

(5) For example, 1,3,4-Triphenyl-4,5-dihydro-1H-1,2,4-triazol-5-ylidene from Acros Organics (363940010) is listed as $454.98/gram on Fisher Scientific's website, https://www.fishersci.com/shop/products/1-3-4-triphenyl-4-5-dihydro-1h-1-2-4-triazol-5-ylidene-acros-organics-1g-glass-bottle/ac363940010

(6) (a) Szabo, J.; Greiner, J.; Maas, G. *Beilstein J. Org. Chem.* **2017**, *13,* 579-588.
(b) Baker, W.; Ollis, W. D.*Q. Rev., Chem. Soc.* **1957**, *11,* 15-29.
(c) Cannon, J. R.; Raston, C. L.; White, A. H.*Aust. J. Chem.* **1980**, *18,* 2237-2247.

(7) Nitron can be purchased from Alfa Aesar at a price of $8.32/gram, https://www.fishersci.com/shop/products/nitron-95-3/p-7023844#?keyword=nitron

(8) Busch, M. *Ber. Dtsch. Chem. Ges.* **1905**, *38,* 861-866.

(9) Gutbier, A. *Ber. Dtsch. Chem. Ges.* **1905**, *38,* 861-866.

(10) *The Merck Index*, 10th ed.; Merck & Co, Inc.: Rahway, NJ, U.S.A., 1983.

(11) (a) Farber, C.; Leibold, M.; Bruhn, C.; Maurer, M.; Siemeling. *Chem. Commun.* **2012**, *48,* 227-229.
(b) Hitzel, S.; Farber, C.; Bruhn, C.; Siemeling, U. *Organometallics* **2014**, *33,* 425-428.
(c) Thie, C.; Hitzel, S.; Wallbaum, L.; Bruhn, C.; Siemeling, U. *J. Organomet. Chem.* **2016**, *821,* 112-121.

(12) (a) Pidlypnyi, N.; Namyslo, J. C.; Drafz, M. H. H.; Nieger, M.; Schmidt, A. *J. Org. Chem.* **2013**, *78,* 1070-1079.
(b) Cesar, V.; Tourneux, J.-C.; Vujkovic, N.; Brousses, R.; Lugan, N.; Lavigne, G. *Chem. Commun.* **2012**, *42,* 2349-2351.

(13) Additionally, nitron is capable of reacting in similar ways to traditional NHC compounds, which include reacting with sulfur to yield the corresponding thione, and also reacting with CS_2 to form the adduct.

(14) (a) Yang, L.; Powell, D. R.; Houser, R. P. *Dalton Trans.* **2007**, 955–964.
(b) Reineke, M. H.; Sampson, M. D.; Rheingold, A. L.; Kubiak, C. P. *Inorg. Chem.* **2015**, *54*, 3211–3217.

(15) (a) Casanova, D.; Cirera, J.; Llunell, M.; Alemany, P.; Avnir, D.; Alvarez, S. *J. Am. Chem. Soc.* **2004**, *126*, 1755–1763.
(b) Alvarez, S.; Alemany, P.; Casanova, D.; Cirera, J.; Llunell, M.; Avnir, D. *Coord. Chem. Rev.* **2005**, *249,* 1693–1708.
(c) Cirera, J.; Ruiz, E.; Alvarez, S. *Organometallics* **2005**, *24*, 1556–1562.

(16) Cambridge Structural Database, CSD version 5.39.

(17) For examples of structurally characterized iridium complexes that feature an NHC and COD ligand, see:
(a) Sun, J.-F.; Chen, F.; Dougan, B. A.; Xu, H.-J.; Cheng, Y.; Li, Y.-Z.; Chen, X.-T.; Xue, Z.-L. *J. Organomet. Chem.* **2009**, *694*, 2096–2105.
(b) Tennyson, A. G.; Rosen, E. L.; Collins, M. S.; Lynch, V. M.; Bielawski, C. W. *Inorg. Chem.* **2009**, *48*, 6924–6933.
(c) Romanenko, I.; Gajan, D.; Sayah, R.; Crozet, D. Jeanneau, E.; Lucas, C.; Leroux, L.; Veyre, L.; Lesage, A.; Emsley, L.; Lacote, E.; Thieuleux, C. *Angew. Chem., Int. Ed.* **2015**, *54*, 12937–12941.

(18) (a) Tsoureas, N.; Haddow, M. F.; Hamilton, A.; Owen, G. R. *Chem. Commun.* **2009**, 2538–2540.
(b) Tsoureas, N.; Hamilton, A.; Haddow, M. F.; Harvey, J. N.; Orpen, A. G.; Owen, G. R. *Organometallics* **2013**, *32*, 2840–2856.

(19) For examples of iridium complexes that feature cycloocta-4-enyl coordinating through an Ir–C σ-bond and the alkene, see:
(a) Fernandez, M. J.; Esteruelas, M. A.; Oro, L. A.; Apreda, M.-C.; Foces, C. F.; Cano, F. H. *Organometallics* **1987**, *6*, 1751–1757.
(b) Bresciani-Pahor, N.; Calligaris, M.; Nardin, G.; Delise, P. *J. Chem. Soc., Dalton Trans.* **1976**, 762–765.
(c) Nguyen, D. H.; Greger, I.; Perez-Torrente, J. J.; Jimenez, M. V.; Modrego, F. J.; Lahoz, F. J.; Oro, L. A. *Organometallics* **2013**, *32*, 6903–6917.

(20) (a) Yang, L.; Powell, D. R.; Houser, R. P. *Dalton Trans.* **2007**, 955–964.
(b) Reineke, M. H.; Sampson, M. D.; Rheingold, A. L.; Kubiak, C. P. *Inorg. Chem.* **2015**, *54*, 3211–3217.

(21) Structural data for Vaska's complex taken from: Churchill, M. R.; Fettinger, J. C.; Buttrey, L. A.; Barkan, M. D.; Thompson, J. S. *J. Organomet. Chem.* **1988**, *340*, 257–266.
IR spectral data taken from: Rahlm, M.; Ahmed, K. J. *Inorg. Chem.* **1994**, *33*, 3003–3004.

(22) Jacobson, M. Z. *Energy Environ. Sci.* **2009**, *2*, 148-173.

(23) Schlapbach, L.; Züttel, A. *Nature* **2001**, *414*, 353-358.

(24) (a) Singh, A. K.; Singh, S.; Kumar, A. *Catal. Sci. Technol.* **2016**, *6*, 12-40.
(b) Grasemann, M.; Laurenczy, G. *Energy Environ. Sci.* **2012**, *5*, 8171-8181.
(c) Enthaler, S.; von Langermann, J.; Schmidt, T. *Energy Environ. Sci.* **2010**, *3*, 1207-1217.
(d) Enthaler, S. *ChemSusChem* **2008**, *1*, 801-804.
(e) Joó, F. *ChemSusChem* **2008**, *1*, 805-808.

(25) Wang, W.-H.; Himeda, Y.; Muckerman, J. T.; Fujita, E. *Adv. Inorg. Chem.* **2014**, *66*, 189-222.

(26) (a) Loges, B.; Boddien, A.; Gärtner, F.; Junge, H.; Beller, M. *Top. Catal.* **2010**, *53*, 902-914.
(b) Laurenczy, G. *Chimia* **2011**, *65*, 663-666.

(27) Sumida, K.; Rogow, D. L.; Mason, J. A.; McDonald, T. M.; Bloch, E. D.; Herm, Z. R.; Bae, T.-H.; Long, J. R. *Chem. Rev.* **2012**, *112*, 724–781.

(28) (a) Behr, A.; Nowakowski, K. *Adv. Inorg. Chem.* **2014**, *66*, 223-258.
(b) He, M.; Sun, Y.; Han, B. *Angew. Chem. Int. Ed. Engl.* **2013**, *52*, 9620–9633.
(c) Appel, A. M.; Bercaw, J. E.; Bocarsly, A. B.; Dobbek, H.; Dubois, D. L.; Dupuis, M.; Ferry, J. G.; Fujita, E.; Hille, R.; Kenis, P. J. A.; Kerfeld, C. A.; Morris, R. H.; Peden, C. H. F.; Portis, A. R.; Ragsdale, S. W.; Rauchfuss, T. B.; Reek, J. N. H.; Seefeldt, L. C.; Thauer, R. K.; Waldrop, G. L. *Chem. Rev.* **2013**, *113*, 6621–6658.

(29) Ting, S.-W.; Hu, C.; Pulleri, J. K.; Chan, K.-Y. *Ind. Eng. Chem. Res.* **2012**, *51*, 4861–4867 and references therein.

(30) (a) Kuehnel, M. F.; Wakerley, D. W.; Orchard, K. L.; Reisner, E. *Angew. Chem. Int. Ed.* **2015**, *54*, 9627–9631.
(b) Mori, K.; Tanaka, H.; Dojo, M.; Yoshizawa, K.; Yamashita, H. *Chem. Eur. J.* **2015**, *21*, 12085–12092.

(31) Vogt, M.; Nerush, A.; Diskin-Posner, Y.; Ben-David, Y.; Milstein, D. *Chem. Sci.* **2014**, *5*, 2043-2051.

(32) (a) Coffey, R. S. *Chem. Commun.* **1967**, 923-924.
(b) Gao, Y.; Kuncheria, J.; Yap, G. P. A.; Puddephatt, R. J. *Chem. Commun.* **1998**, 2365-2366.
(c) Man, M. L.; Zhou, Z.; Ng, S. M.; Lau, C. P. *Dalton Trans.* **2003**, *2*, 3727-3735.
(d) Boddien, A.; Loges, B.; Junge, H.; Beller, M. *ChemSusChem* **2008**, *1*, 751-758.
(e) Fellay, C.; Yan, N.; Dyson, P. J.; Laurenczy, G. *Chem. Eur. J.* **2009**, *15*, 3752-3760.
(f) Fukuzumi, S.; Kobayashi, T.; Suenobu, T. *J. Am. Chem. Soc.* **2010**, *132*, 1496-1497.
(g) Savourey, S.; Lefèvre, G.; Berthet, J.-C.; Thuéry, P.; Genre, C.; Cantat, T. *Angew. Chem. Int. Ed. Engl.* **2014**, *53*, 10466 –10470.

(33) Fukuzumi, S.; Kobayashi, T.; Suenobu, T. *ChemSusChem* **2008**, *1*, 827-834.

(34) (a) Himeda, Y. *Green Chem.* **2009**, *11*, 2018-2022.
(b) Maenaka, Y.; Suenobu, T.; Fukuzumi, S. *Energy Environ. Sci.* **2012**, *5*, 7360-7367.
(c) Miller, A. J. M.; Heinekey, D. M.; Mayer, J. M.; Goldberg, K. I. *Angew. Chem. Int. Ed. Engl.* **2013**, *52*, 3981-3984.
(d) Manaka, Y.; Wang, W.-H.; Suna, Y.; Kambayashi, H.; Muckerman, J. T.; Fujita, E.; Himeda, Y. *Catal. Sci. Technol.* **2014**, *4*, 34-37.
(e) Wang, Z.; Lu, S.-M.; Li, J.; Wang, J.; Li, C. *Chem. Eur. J.* **2015**, *21*, 12592–12595.

(35) Broggi, J.; Jurčík, V.; Songis, O.; Poater, A.; Cavallo, L.; Slawin, A. M. Z.; Cazin, C. S. J. *J. Am. Chem. Soc.* **2013**, *135*, 4588-4591.

(36) (a) Bianchini, C.; Peruzzini, M.; Polo, A.; Vacca, A.; Zanobini, F. *Gazz. Chim. Ital.* **1991**, *121*, 543-549.
(b) Boddien, A.; Mellmann, D.; Gärtner, F.; Jackstell, R.; Junge, H.; Dyson, P. J.; Laurenczy, G.; Ludwig, R.; Beller, M. *Science.* **2011**, *333*, 1733–1736.
(c) Zell, T.; Butschke, B.; Ben-David, Y.; Milstein, D. *Chem. Eur. J.* **2013**, *19*, 8068–8072.
(d) Federsel, C.; Boddien, A.; Jackstell, R.; Jennerjahn, R.; Dyson, P. J.; Scopelliti, R.; Laurenczy, G.; Beller, M. *Angew. Chem. Int. Ed.* **2010**, *49*, 9777-9780.
(e) Boddien, A.; Loges, B.; Gärtner, F.; Torborg, C.; Fumino, K.; Junge, H.; Ludwig, R.; Beller, M. *J. Am. Chem. Soc.* **2010**, *132*, 8924-8934.

(f) Boddien, A.; Gärtner, F.; Mellmann, D.; Sponholz, P.; Junge, H.; Laurenczy, G.; Beller, M. *Chimia* **2011**, *65*, 214–218.

(37) Shin, J. H.; Churchill, D. G.; Parkin, G. *J. Organomet. Chem.* **2002**, *642*, 9-15.

(38) Kudrik, E. V.; Makarov, S. V.; Ageeva, E. S.; Dereven'kov, I. A. *Macroheterocycles* **2009**, *2*, 69-70.

(39) Enthaler, S.; Brück, A.; Kammer, A.; Junge, H.; Irran, E.; Gülak, S. *ChemCatChem* **2015**, *7*, 65-69.

(40) Chauvier, C.; Tlili, A.; Das Neves Gomes, C.; Thuéry, P.; Cantat, T. *Chem. Sci.* **2015**, *6*, 2938–2942.

(41) Myers, T. W.; Berben, L. A. *Chem. Sci.* **2014**, *5*, 2771-2777.

(42) (a) Neary, M. C.; Parkin, G. *Chem. Sci.* **2015**, *6*, 1859-1865.
(b) Neary, M. C.; Parkin, G. *Dalton Trans.* **2016**, *45*, 14645-14650.(43) See, for example: Junge, K.; Schroder, K.; Beller, M. "Homogeneous catalysis using iron complexes: recent developments in selective reductions" *Chem. Commun.* **2011**, *47*, 4849-4859.

(44) (a) Luo, F.; Pan, C.; Cheng, J. "The application of trialkoxysilane as transmetallation reagent in organic synthesis" *Curr. Org. Chem.* **2011**, *15*, 2816-2829.
(b) Nakao, Y.; Hiyama, T. "Silicon-based cross-coupling reaction: an environmentally benign version" *Chem. Soc. Rev.* **2011**, *40*, 4893-4901.
(c) Denmark, S. E.; Sweis, R. F. "Design and implementation of new, silicon-based, cross-coupling reactions: Importance of silicon-oxygen bonds" *Acc. Chem. Res.* **2002**, *35*, 835-846.
(d) Denmark, S. E.; Sweis, R. F. "Cross-coupling reactions of organosilicon compounds: New concepts and recent advances" *Chem. Pharm. Bull.* **2002**, *50*, 1531-1541.

(45) (a) Trewyn, B. G.; Slowing, I. I.; Giri, S.; Chen, H.-T.; Lin, V. S.-Y. "Synthesis and functionalization of a mesoporous silica nanoparticle based on the sol-gel process and applications in controlled release" *Acc. Chem. Res*. **2007**, *40*, 846–853.
(b) Kuo, S.-W.; Chang, F.-C. "POSS related polymer nanocomposites" *Prog. Polym. Sci.* **2011**, *36*, 1649-1696.
(c) Szwarc-Rzepka, K.; Ciesielczyk, F.; Jesionowski, T. "Preparation and physicochemical properties of functionalized silica/octamethacryl-silsesquioxane hybrid systems" *J. Nanomater.* **2013**, 15 #674237, doi:10.1155/2013/674237.

(46) (a) McNally, J. P.; Leong, V. S.; Cooper, N. J. in *Experimental Organometallic Chemistry*, Wayda, A. L.; Darensbourg, M. Y., Eds.; American Chemical Society: Washington, DC, 1987; Chapter 2, pp 6-23.

(b) Burger, B.J.; Bercaw, J. E. in *Experimental Organometallic Chemistry*; Wayda, A. L.; Darensbourg, M. Y., Eds.; American Chemical Society: Washington, DC, 1987; Chapter 4, pp 79-98.
(c) Shriver, D. F.; Drezdzon, M. A.; *The Manipulation of Air-Sensitive Compounds*, 2nd Edition; Wiley-Interscience: New York, 1986.

(47) Fulmer, G. R.; Miller, A. J. M.; Sherden, N. H.; Gottlieb, H. E.; Nudelman, A.; Stoltz, B. M.; Bercaw, J. E.; Goldberg, K. I. *Organometallics* **2010**, *29*, 2176-2179.

(48) (a) Harris, R. K.; Becker, E. D.; De Menezes, S. M. C.; Goodfellow, R.; Granger, P. *Pure Appl. Chem.* **2001**, *73*, 1795-1818.
(b) Harris, R. K.; Becker, E. D.; De Menezes, S. M. C.; Granger, P.; Hoffman, R. E.; Zilm, K. W. *Pure Appl. Chem.* **2008**, *80*, 59-84.

(49) (a) Sheldrick, G. M. SHELXTL, An Integrated System for Solving, Refining, and Displaying Crystal Structures from Diffraction Data; University of Göttingen, Göttingen, Federal Republic of Germany, 1981.
(b) Sheldrick, G. M. *Acta Cryst.* **2008**, *A64*, 112-122.
(c) Sheldrick, G. M. *Acta Cryst.* **2015**, *A71*, 3-8.